UC Berkeley
UC Berkeley Electronic Theses and Dissertations

Title

Organic Catalysis with Metal-Dinitrosyl Complexes and Synthetic Biomimetic Supramolecular Nanovessels

Permalink

https://escholarship.org/uc/item/6z25n2h0

Author

Zhao, Chen

Publication Date

2014

Peer reviewed|Thesis/dissertation

eScholarship.org Powered by the California Digital Library
University of California

Organic Catalysis with Metal-Dinitrosyl Complexes and Synthetic Biomimetic Supramolecular Nanovessels

by

Chen Zhao

A dissertation submitted in partial satisfaction of the

requirements for the degree of

Doctor of Philosophy

in

Chemistry

in the

GRADUATE DIVISION

of the

UNIVERSITY OF CALIFORNIA, BERKELEY

Committee in charge:

Professor Robert G. Bergman, Co-Chair
Professor F. Dean Toste, Co-Chair
Professor Kenneth N. Raymond
Professor Wenjun Zhang

Spring 2014

Abstract

Organic Catalysis with Metal-Dinitrosyl Complexes and Synthetic Biomimetic Supramolecular Nanovessels

by

Chen Zhao

Doctor of Philosophy in Chemistry

University of California, Berkeley

Professor F. Dean Toste, Co-Chair

Professor Robert G. Bergman, Co-Chair

The work described in this dissertation explores the field of organic catalysis with metal-dinitrosyl complexes and synthetic supramolecular nanovessels. Part I (Chapters 1-3) presents the development of both stoichiometric and catalytic vinylic C–H functionalization reactions of unactivated alkenes mediated by cobalt and ruthenium dinitrosyl complexes. Part II (Chapters 4-7) describes the design and synthesis of terephthalamide-based supramolecular M_4L_6 nanovessels and their application in organic catalysis.

Part I – Metal-Dinitrosyl Mediated Vinylic C–H Functionalization

Chapter 1 contains a brief literature review of C–H activation and functionalization reactions mediated by transition-metal complexes. Of the examples presented, the cobalt dinitrosyl mediated intermolecular vinylic C–H functionalization reaction offers an approach for the activation of simple alkenyl C–H bonds that takes advantage of the ligand-based reactivity of such cobalt complexes. The difficulties of isolating the reactive cobalt dinitrosyl species and achieving catalytic turnover for functionalization, as well as extension toward other metals, are also presented to provide a context in which Chapters 2 and 3 can be viewed.

Chapter 2 describes the development of a one-pot cobalt-dinitrosyl mediated inter- and intramolecular vinylic C–H functionalization reaction of unactivated and alkyl-substituted alkenes. Enantioselective intramolecular cobalt-dinitrosyl mediated *5-exo-trig* and *6-endo-trig* cyclization reactions are also described. Although catalytic turnovers can be achieved with such complexes for vinylic C–H functionalization, generality of the methodology and broader substrate scope remain elusive.

Chapter 3 presents the application of a ruthenium-dinitrosyl complex in the context of vinylic C–H functionalization reaction of simple alkenes. The recently discovered ruthenium-dinitrosyl complex proves to be stable for isolation and characterization, an improvement over the cobalt system, but also proves to be less reactive as a catalyst for vinylic C–H functionalization. The challenges associated with the development of metal-dinitrosyl catalyzed C–H functionalization and its outlook are also discussed.

Part II – Synthesis of Terephthalamide-based Ga_4L_6 Supramolecular Nanovessels and their Application in Enantioselective and Stereospecific Organic Catalysis

Chapter 4 introduces the field of supramolecular chemistry with a main focus on the synthesis and chemistry of enantiopure host complexes. Examples of asymmetric organic reactions catalyzed by chiral host assemblies are also presented to provide a platform from which Chapters 5-7 can be viewed.

Chapter 5 describes the design, synthesis and characterization of enantiopure supramolecular Ga_4L_6 nanovessels that are based on terephthalamide (TAM)-derived ligands. The synthesis of achiral TAM-based ligands and their corresponding racemic host-guest complexes are also presented.

Chapter 6 summarizes the development of an enantioselective ring-opening reaction of *meso*-episulfonium catalyzed by the enantiopure host assembly presented in Chapter 5. Additionally, the application of this new cluster as a chiral host catalyst for the Aza-Cope rearrangement and the Prins-like cyclization reactions are also discussed.

Chapter 7 describes the development of a stereospecific reaction catalyzed by both racemic and enantiopure supramolecular Ga_4L_6 host assemblies. The host assemblies are capable of catalyzing the substitution reaction at a secondary benzylic carbon center to give products with overall stereochemical retention, while reaction of the same substrates in bulk solution gives products with inversion. Such ability of a biomimetic synthetic host assembly to reverse the stereochemical outcome of a nucleophilic substitution reaction is unprecedented in the field of supramolecular catalysis.

I dedicate this dissertation to my family.

Table of Contents

Abstract 1
List of Figures vi
List of Schemes viii
List of tables x
Acknowledgements xi

Chapter 1. C–H Activation and Functionalization Reactions Mediated by Transition Metal Complexes 1
  1.1. Introduction to C-H Activation and Functionalization Reactions 1
  1.2. Step-wise Cobalt-Dinitrosyl Mediated Vinylic C–H Functionalization 3
  References 7

Chapter 2. The Development of a Stoichiometric and Catalytic Vinylic C-H Functionalization Reaction Mediated by a Cobalt Dinitrosyl Complex 9
  2.1 Introduction 9
  2.2. Results and Discussion 10
    2.2.1. Step-wise *5-exo-trig* and *6-exo-trig* Cyclization Reactions Mediated by Cobalt-dinitrosyl Complex [CpCo(NO)$_2$] 10
    2.2.2. The Development of One-Pot C–H Functionalization Reaction Mediated by Stoichiometric Amounts of Cobalt Complex **5** 12
    2.2.3. The Development of C–H Functionalization Reaction Catalyzed by Complex **5** 14
  2.3. Conclusion 16
  2.4. Experimental 17
    2.4.1. General Information. 17
    2.4.2. Synthesis of Cobalt Dinitrosoalkane Complex **5** 18
    2.4.3. Substrate Synthesis 18
    2.4.4. Stepwise C-H Functionalization of **4a** and **4b** 25
    2.4.5. One-pot Reactions 29
    2.4.6. Intramolecular C–H Functionalization of **4i** Catalyzed by Complex 5 32
  2.5. References 33
  2.6. ^{1}H and ^{13}C NMR Spectra 34

Chapter 3. The Application of a Ruthenium Dinitrosyl Complex to the Vinylic C-H Functionalization Reaction of Simple Alkenes and A Comparison of the Cobalt and Ruthenium Systems 68

3.1. Introduction ... 68

3.2. Results and Discussion ... 70

3.2.1. Development of C-H Functionalization Reaction Mediated by Ruthenium Complex 1 ... 70

3.2.2. Comparison of Cobalt and Ruthenium Dinitrosyl Systems ... 74

3.3. Conclusion ... 77

3.4. Experimental ... 78

3.4.1. General Information. ... 78

3.4.2. Synthesis of Ruthenium Dinitrosyl **1** ... 78

3.4.3. Substrates Synthesis (**7c-f**) ... 79

3.4.4. Synthesis of Ruthenium Dinitrosoalkane Complexes **8a-f** ... 82

3.4.5. Ruthenium Dinitrosyl Mediated C–H Functionalization ... 84

3.4.6. “Delayed” Alkene Binding with Ruthenium Complex **1** ... 87

3.5. References ... 88

3.6. ^{1}H and ^{13}C NMR Spectra ... 89

Chapter 4. Enantiopure Supramolecular Host Assemblies and their Application to Asymmetric Organic Catalysis ... 103

4.1. Introduction ... 103

4.2. Chiral Supramolecular Host Complexes ... 104

4.3. Asymmetric Organic Reactions Mediated and Catalyzed by Chiral Nanovessels ... 107

4.4. References ... 110

Chapter 5. The Synthesis of Terephthalamide-based Diastereo- and Enantiopure Ga_4L_6 Supramolecular Nanovessels ... 111

5.1. Introduction ... 111

5.2. Results and Discussion ... 112

5.2.1. Synthesis and Characterization of Enantiopure Ga_4L_6 Supramolecular Host Complex ... 112

5.2.2. Synthesis and Characterization of Racemic and Terephthalamide-based Ga_4L_6 Host-Guest Complexes ... 117

5.3. Conclusion ... 119

5.4. Experimental ... 120

5.4.1. General Methods. ... 120

5.4.2. Synthesis of chiral ligand **(*R*)-5** ... 120

5.4.3. Synthesis of Complex **6** ... 123

5.4.4. Mass Spectrum of ΔΔΔΔ-**6** 124
5.4.5. Encapsulation of PEt_4^+ by Assembly **6** to give **7** 124
5.4.6. Synthesis of Chiral Salts **(*R*)-8** 125
5.4.7. Host-guest chemistry of ΔΔΔΔ-**6** and ΛΛΛΛ-**6** individually with chiral salts ***(R)*-8** and **(*S*)-8** 125
5.4.8. ^{1}H and ^{13}C NMR Spectra 126
5.4.9. X-ray Crystallography Information for **6** 134
5.5. References 136

Chapter 6. Asymmetric Organic Transformations Catalyzed by a Diastereo- and Enantiopure Supramolecular Host Complex 137
6.1. Introduction 137
6.2. Results and Discussion 138
6.2.1. Asymmetric Ring-Opening Reaction of an Episulfonium Ion 138
6.2.2. Enantioselective Prins-like Carbonyl-Ene Cyclization Reaction 140
6.2.3. Enantioselective Aza-Cope Rearrangement Reaction 142
6.3. Conclusion 144
6.4. Experimental 145
6.4.1. Synthesis of ompound **3** 145
6.4.2. Asymmetric ring opening of an episulfonium ion generated from **3** catalyzed by complex **1** 148
6.4.3. Stacked ^{1}H NMR spectra of reaction between **3** and host **1** to give **4** as monitored by ^{1}H NMR spectroscopy 148
6.4.4. Reaction of **3**, complex **5** and Me_4NCl 151
6.4.5. Enantioslective monoterpene-like cyclization catalyzed by complex **1** 152
6.4.6. Rate comparison for the cyclization of **7a** catalyzed by complex **1** and complex **5**. 154
6.4.7. Enantioselective Aza-cope rearrangement reactions catalyzed by complex **6** 154
6.5. References 156

Chapter 7. Nucleophilic Substitution Catalyzed by a Supramolecular Cavity Proceeds with Retention of Absolute Stereochemistry 157
7.1 Introduction 157
7.2. Results and Discussion 158
7.3. Conclusion 163
7.4. Experimental 164
7.4.1. General Information. 164

7.4.2. Synthesis of enantiopure **(*S*)-3** 164
7.4.3. Synthesis of enantioenriched benzyl chloride **7** 165
7.4.4. Synthesis of enantiopure ammonium tosylate **8** 165
7.4.5. Synthesis of racemic **10** 166
7.4.6. ^{1}H and ^{13}C NMR, and Chiral GC Spectra 167
7.4.7. Independently synthesized enantiopure **(*S*)-3** from **(*S*)-6** 172
7.4.8. Solvolysis of **(*S*)-3** in methanol catalyzed by a phosphoric acid 174
7.4.9. Host-catalyzed substitution reaction of **(*S*)-3** 176
7.4.10. Host-catalyzed substitution reaction of **(*R*)-7** 178
7.4.11. Encapsulation of **(*R*)-8** by host complex **1** 180
7.5. References 181
7.6. Additional Chiral GC Spectra 183

List of Figures

Chapter 2

Figure 2.1. Proposed Catalytic Cycle for Cobalt-Dinitrosyl Mediated C–H Functionalization ... 16

Chapter 3

Figure 3.1. Possible Isomers of $[CpCo(NO)_2]$ ... 74

Figure 3.2. (a) Selected Limiting Valence Bond Description of $[CpCo(NO)_2]$ and (b) Diradical Mechanism for Alkene Binding ... 76

Chapter 4

Figure 4.1. Supramolecular host complex **1** catalyzed Diels-Alders reaction of ... 104

Figure 4.2. (A) Schematic representation of Ga_4L_6 supramolecular assembly **2** (B) The homochiral ΛΛΛΛ and ΔΔΔΔ enantiomers of assembly **2**. ... 105

Figure 4.3. (A) Resolution of assembly **2** using (*S*)-nicotinium salt. (B) Ion-exchange of [(*S*)-Nic ⊂ ΛΛΛΛ-**2**] with NMe_4Cl to give [NMe_4 ⊂ ΛΛΛΛ-**2**] ... 105

Figure 4.4. (A) Synthesis of enantiopure tetrahedron **3** with 1,1-biphenyl-derived chiral ligands and Fe or Ga atoms. (B) Enantioselective association of one enantiomer of a chiral alcohol that results in the enantiopure co-crystallization of 2-butanol. ... 106

Figure 4.5. (A) Synthesis of homochiral hexanuclear iridium assemblies. ... 106

Figure 4.6. (A) The synthesis of an enantiopure tetrahedral cluster ΔΔΔΔ-**5**. ... 107

Figure 4.7. (A) Schematic representation of an enantiopure octahedral assembly. (B) Application of 6 as a chiral reaction pocket for the enantioselective [2+2] photoaddition of fluoranthene and maleimide. ... 108

Figure 4.8. Enantioselective Aza-Cope rearrangement reaction catalyzed by enantiopure host **5**. ... 109

Chapter 5

Figure 5.1. Supramolecular Ga_4L_6 assembly (left) Schematic view of **1** ... 111

Figure 5.2. ^{1}H NMR Spectra of 6-$K_{12}Ga_4(R)$-5_6 ... 114

Figure 5.3. ^{1}H NMR Spectra of **7** ... 114

Figure 5.4. CD and UV-Vis Absorption Spectra of ΔΔΔΔ-**6** and ΛΛΛΛ-**6** ... 115

Figure 5.5. CD Absorption Spectra of ΔΔΔΔ-[NEt_4 ⊂ **6**] and ΛΛΛΛ-[NEt_4 ⊂ **6**] (left) and ΔΔΔΔ-[*S*-nic ⊂ **6**] and ΛΛΛΛ-[*S*-nic ⊂ **6**] ... 115

Figure 5.6. X-Ray Structure of ΔΔΔΔ-**6** 116

Figure 5.7. ^{1}H NMR spectra (encapsulation region) of complexes from host-guest chemistry of ΔΔΔΔ-**6** and ΛΛΛΛ-**6** individually with chiral ammonium salts **(*S*)-8** and **(*R*)-8** 117

Figure 5.8 ^{1}H NMR Spectrum of **14b** 118

Figure 5.9. ^{1}H NMR Spectrum of **14b** 118

Figure 5.10. ^{1}H NMR spectra of "empty" **14b** and its encapsulation of NEt_4 cation 119

Chapter 6

Figure 6.1. (left) Schematic representation of ΔΔΔΔ-**1** (right) X-ray crystal structure of ΔΔΔΔ-**1** 137

Figure 6.2. Proposed catalytic cycle for the asymmetric ring-opening reaction of 140

Figure 6.3. Proposed catalytic cycle for the Prins-like cyclization of carbonyl-ene substrates mediated by supramolecular nanovessel 1 142

Figure 6.4. (A) ^{1}H NMR spectrum showing encapsulation of **9a**. (B) Rate acceleration of 1 catalyzed Aza-Cope rearrangement of **9a** compared to reactions with ΔΔΔΔ–[($NEt_4 \subset 1$] and with no catalyst 143

Figure 6.5. Rearrangement of **9c** to **10c** catalyzed by host **1** as monitored by ^{1}H NMR spectroscopy 144

Chapter 7

Figure 7.1. (A) Schematic representations of the Ga_4L_6 assemblies **1** and **2** with only one ligand shown for clarity. (B) X-ray crystal structure of ΛΛΛΛ-1. (C) X-ray crystal structure of ΔΔΔΔ-**2** 157

Figure 7.2. (A) Substitution reaction of racemic **3** catalyzed by host ΔΔΔΔ-**2**. (B) Catalyst controlled divergent stereospecific substitutions of **(*S*)-3** 159

Figure 7.3. Stereoretentive substitution reactions of **(*S*)-3** and **(*R*)-3** catalyzed by supramolecular Ga_4L_6 hosts **1**, ΛΛΛΛ-**2**, and ΔΔΔΔ-**2** 160

Figure 7.4. (A) Nucleophilic substitution of racemic benzyl chloride **7** catalyzed by ΔΔΔΔ-2. (B) Retentive substitution of enantioenriched 7 catalyzed by either ΛΛΛΛ-**2** or ΔΔΔΔ-**2** 161

Figure 7.5. A proposed intermediate showing a transient carbocation interacting with only one of the six naphthalene walls through cation-π interactions (where X represents the leaving group). 162

List of Schemes

Chapter 1

Scheme 1.1. General Classes of C–H Activation Mechanisms 1

Scheme 1.2. Rh(I) catalyzed vinylic C–H activation of conjugated alkenes................................ 2

Scheme 1.3. Nickel-catalyzed direct conjugate addition of simple alkenes to eneones 2

Scheme 1.4. Intermolecular C–H Functionalization of Cobalt Dinitrosoalkane Complexes 4

Scheme 1.5. Retrocycloaddition of functionalized cobalt complexes 4

Scheme 1.6. Cobalt-Mediated [3 + 2] Annulation Reaction of Alkene with Cyclohexenone........ 5

Scheme 1.7. Enantioselective vinylic C–H functionalization of norbornene 5

Scheme 1.8. Cobalt dinitrosyl mediated enantioselective synthesis of C_2-symmetric ligands....... 6

Chapter 2

Scheme 2.1. Synthetic Entry Points to [CpCo(NO)$_2$] 9

Scheme 2.2. Intramolecular vinylic C–H functionalization of alkenes mediated by [CpCo(NO)$_2$] 10

Scheme 2.3. Cycloaddition of 4a-c to [CpCo(NO)$_2$] 10

Scheme 2.4. Reaction conditions for the cyclization of complex 6a to give complex 7 and/or 8a 11

Scheme 2.5. Cyclization of cobalt complex 6b... 11

Scheme 2.6. (a) One-Pot Intermolecular C–H Functionalization Reaction Mediated by 5;......... 14

Chapter 3

Scheme 3.1. Alkene Binding Reaction of Complex 1, Norbornadiene and TMEDA 68

Scheme 3.2. Scope of Binding Reaction Between 1 and Simple Alkenes 69

Scheme 3.3. Isomerization and O-Alkylation of Oxime Complex 4 70

Scheme 3.4. Alkene Exchange Reactions Between Complex 3 and Norbornadiene 70

Scheme 3.5. Synthesis of Ruthenium Dinitrosoalkane Complexes 8a-f from Substrates 7a-f..... 71

Scheme 3.6. Ruthenium Dinitrosyl Mediated Intramolecular *6-exo-trig* 72

Scheme 3.7. Ruthenium-Dinitrosyl Mediated *6-exo-dig* Conjugate Addition to Ynone Functionality 73

Scheme 3.8. Ruthenium Complex 1 Mediated One-Pot Intramolecular C–H Functionalization. 73

Chapter 5

Scheme 5.1. Ligand Design for the Diastereoselective Assembly of an Enatiopure Cluster 112

Scheme 5.2. Synthesis of Ligand (*R*)-5 113

Scheme 5.3. Synthesis of Supramolecular Assembly 6 and its Encapsulation of PEt_4 Cation... 113

Scheme 5.4. Synthesis of chiral and racemic terephthalamide-based Ga_4L_6 clusters 117

Chapter 6

Scheme 6.1. Thiourea catalyzed ring-opening of an episulfonium ion generated from 2 138

Scheme 6.2. Synthesis of substrate 3 138

Scheme 6.3. (A) Reaction of 3 to 4 catalyzed by 1, (B) ^1H NMR spectrum of an observed intermediate, (C) Schematic representation of complex 5 139

Scheme 6.4. Substrate scope of the asymmetric ring-opening reaction of 139

Scheme 6.5. (A) Divergent reaction pathways for the carbonyl-ene cyclization catalyzed by complex 5 and reaction in bulk acidic solution (B) Cyclization of 6a catalyzed by 5 to give mostly *trans* product 7a 141

Scheme 6.6. Substrate scope of the ΔΔΔΔ-1 catalyzed enantioselective Aza-Cope rearrangement reaction 144

List of tables

Chapter 2

Table 2.1. Reaction optimization of 4a to 8a mediated by complex 5 12

Table 2.2. Substrate scope of the one-pot C–H functionalization reaction mediated by 5 13

Table 2.3. Complex 5 Catalyzed Intramolecular C–H Functionalization of 4a 15

Chapter 6

Table 6.1. Enantioselective and chemoselective Prins-like carbonyl-ene cyclization catalyzed by ΔΔΔΔ-1 141

Acknowledgements

I'd like to first and foremost thank my advisors Professors Robert G. Bergman, F. Dean Toste, and Kenneth N. Raymond for their guidance and support over the past five years. Although different in styles, Bob, Dean, and Ken have been the best combination of advisors that any graduate student could hope for. As a team, their extensive knowledge and interests in science and technology have been tremendously educational. More importantly, they have helped me to not only become a much better scientist but also a better person.

I am extremely grateful to my co-workers spanning over the three research groups. Professor Mark R. Crimmin, whom I was extremely lucky to have worked with during my first two years of graduate school, taught me everything I know about organometallic chemistry, both from the textbooks and in the labs. Dr. Jerome Volkman taught me how to think critically when reading a paper and, most importantly, how to properly open and drink a beer. I would also like to thank Dr. Elana Arceo-Rebollo for all the "fresh-air" breaks when neither of our chemistry was working. Additionally, I thank all the past and current Toste group members, in particular postdocs such as Dr. Osamu Kanno, Dr. Matthew Campell, Dr. Vivek Rauyinar, Dr. Hosea Nelson, and many others, who helped to pick me up when I was discouraged by the latest result; and former graduate students such as Jeff Wu, Yiming Wang, Aaron Lackner, and Mika Shiramizu for helping me through every step of graduate school. I am also very grateful to have joined the Raymond group during my fourth year and to have worked next to the Raymond group members since then. Lastly, I thank all the past and current members of the "ClusterFolks" group, Dr. Kristen Clary (Burford), Dr. Tommy Sun, Billy Hart-Cooper, Dr. Kaking Yan, Dr. Derek Dalton, Rebecca Triano, Cindy Hong, David Kaphan and Professor (soon to be) Michael Nippe, for all stimulating research conversations and making every working just as fun as the day before.

I would like to thank my fellow classmates and group mates, Miles Johnson, Hunter Shunatona, Thomas Giannetti, Tiffany Pham, and David Tatum because graduate school would have been much more difficult without them. I thank Justin Lomont, Aaron Harrison, Katherine Mackenzie, Olivia Lee, and Stephanie Jones for enduring my constant complaining. I also thank Bao Tran, Allen Chen, Andrew B. Lee, and Kevin Luu for their encouragement and support since high school.

During the first quarter of my second year of undergraduate studies at U.C. San Diego, I took an introductory organic chemistry class with Professor Charles Perrin that forever changed my career. I thank Professor Perrin for his support and encouragement throughout the years, and I will forever be grateful to him for guiding me to Berkeley. I would also like to thank Brandon Morinaka for helping me get started in a chemistry lab and for always being critical of my work.

I thank Maggie for always putting up with me, cooking for me, cleaning after me while kicking-ass in her research at the same time. Most importantly, I thank her for her understanding, patience, and love over the years, and I am extremely happy and proud to call her my Dr. Wife.

Last but not least, I thank my parents, Junzi and Ping. 17 years ago, they gave up their lives completely and took a huge leap of faith by bringing me to the United States to give me the chance to have a better life. The love and support they have provided me are indescribable, and I hope that someday I will become half the parents and the people they are. I am who I am today because of them, and I am forever grateful to call them Ba and Ma.

Chapter 1. C–H Activation and Functionalization Reactions Mediated by Transition Metal Complexes

1.1. Introduction to C-H Activation and Functionalization Reactions

The field of transition metal catalyzed carbon-hydrogen (C–H) bond activation and functionalization reactions has undergone intensive development over the past few decades.[1-7] The ability to selectively activate and functionalize inert C–H bonds has provided powerful new methods for the synthesis of complex molecules.[8-11] Of paramount importance to this synthetic revolution has been the work of a number of groups to elucidate the intimate mechanism of catalyst capable of C–H activation and functionalization.[12-18]

The majority of C–H bond activation reactions can be organized into two general classes, namely "inner-sphere" and "outer-sphere" pathways; these classifications were introduced by Sanford and co-workers in 2006 (Scheme 1.1).[17] The "inner-sphere" mechanism can be thought of as the direct cleavage of a *sp*^{2} or *sp*^{3} C–H bond by a transition metal to generate a metal-alkyl or metal-aryl complex via oxidative addition, σ-bond metathesis or coordination/deprotonation pathway. On the other hand, reactions that proceed by the "outer-sphere" mechanism generally involve the initial formation of a high oxidation organometallic complexes, such as [M]=Y, where Y is an activated ligand (imido, oxo or carbene), followed by reaction between the C–H bond with the ligand Y rather than with the metal center. This latter functionalization step can proceed by either direct insertion or hydrogen atom abstraction followed by radical recombination. These classifications are not exhaustive, and the numerous modes of C–H activation by transition metals are continuing to be studied. Incorporation of the organometallic products of C–H activation in cycles has led to catalytic protocols for carbon-carbon and carbon-heteroatom bond formation from the C–H functional group.

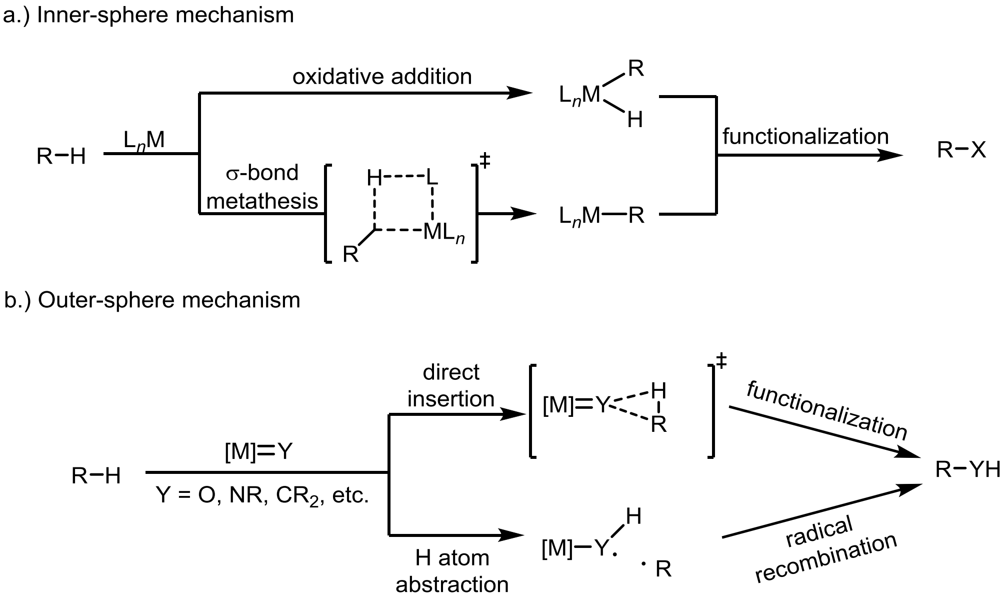
a.) Inner-sphere mechanism
R–H
L$_n$M
oxidative addition
L$_n$M(R)(H)
σ-bond metathesis
‡
L$_n$M—R
functionalization
R–X
b.) Outer-sphere mechanism
R–H
[M]=Y
Y = O, NR, CR$_2$, etc.
direct insertion
‡
functionalization
R–YH
H atom abstraction
[M]–Y(H) · R
radical recombination

Scheme 1.1. General Classes of C–H Activation Mechanisms

Despite fast growth of this field, the activation of vinylic C–H bonds to generate metal-vinyl complexes or alkenyl anion synthons directly from the corresponding alkene is underexplored. In 1995, the Trost group reported the ruthenium catalyzed alkylation reaction with alkenes of conjugated enones and enals via directed vinylic C–H bond activation.[19] Rh(I) catalyzed vinylic C–H activation of alkenes conjugated with imine and ketoxime directing groups have also been reported by both the Bergman and Ellman groups,[20] as well as the Cheng group.[21]

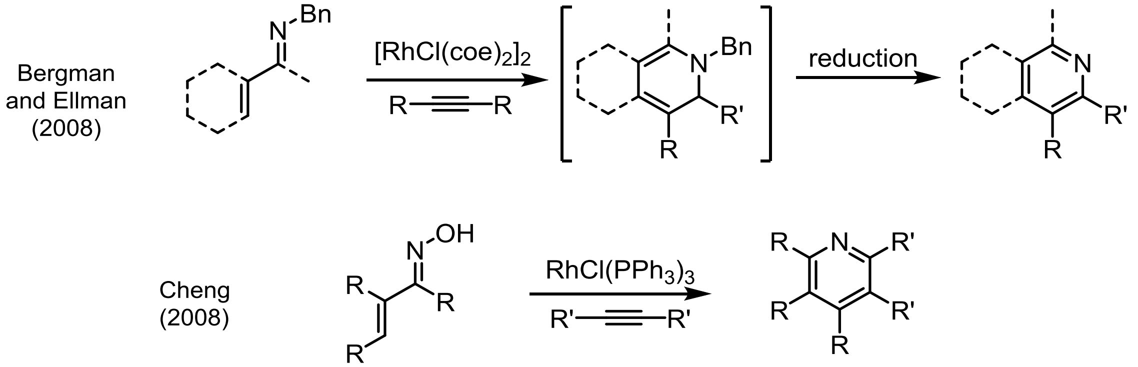

Scheme 1.2. Rh(I) catalyzed vinylic C–H activation of conjugated alkenes

In recent years, researchers have developed alternative approaches for generating alkenyl anion equivalents that could act as nucleophiles toward functionalization with both internal and external electrophiles. The *in situ* functionalization of unsaturated carbon–carbon bonds with catalytic quantities of a transition metal complex has emerged as a powerful method for the generation of transient alkyl, allyl and vinyl organometallics. Several atom-efficient addition reactions of simple alkenes, allenes and alkynes to aldehydes, imines, ketones, dicarbonyls and Michael acceptors have been reported. For example, Krische and co-workers have demonstrated that rhodium and iridium catalysts can be used for reductive coupling of unsaturated hydrocarbons with carbonyls under an atmosphere of H_2.[22-26] Similarly, Montgomery, Jamison, Sato and others have also shown that Ni(0) complexes, in the presence of trialkylphosphine, triarylphosphine or N-heterocyclic carbene ligands and a stoichiometric reductant such as triethylborane, a dialkylzinc, or trialkylsilane, catalyze C–C bond forming reactions between alkynes or allenes and aldehydes, imines, epoxides and Michael acceptors (Scheme 1.3).[27-34]

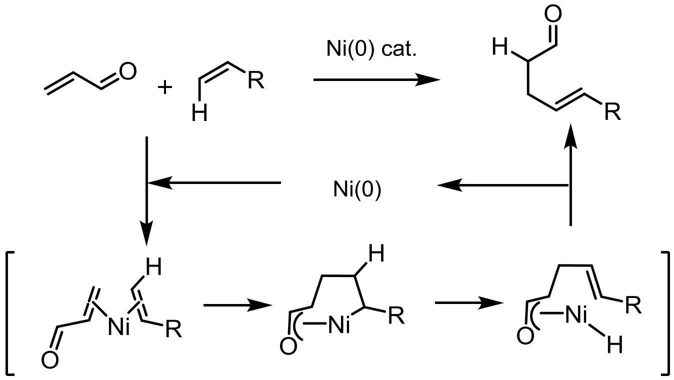

Scheme 1.3. Nickel-catalyzed direct conjugate addition of simple alkenes to eneones

Nevertheless, these advances have their limitations. In order to achieve the delivery of a vinyl anion fragment, more highly unsaturated substrates are required, namely alkynes, ene-ynes, diynes and allenes. In many cases, stoichiometric amounts of reducing agents are required. Depending on the stereospecificity of the intermediate reaction steps, along with the stereointegrity of the organometallic species and the potential of the catalyst to effect off-cycle alkene isomerization, the stereo- and regiochemistry of the olefin moiety in the organic products are potentially difficult to control.

1.2. Step-wise Cobalt-Dinitrosyl Mediated Vinylic C–H Functionalization

Reported by Brunner and Loskot in 1968,[35-37] $CpCo(CO)_2$ reacted with nitric oxide (NO) in the presence of strained alkenes to afford cobalt dinitrosoalkane complexes (eq. 1). This discovery led to detailed scope and mechanistic studies by the Bergman group in the 1980s, in which cobalt dinitrosyl complex $CpCo(NO)_2$ **1** was proposed to be the active species that reacts with a wide range of olefins to afford the corresponding dinitrosoalkane complexes.[38-40] They also demonstrated that alkene binding to cobalt dinitrosyl complex **1** is reversible and stereospecific (eq 2), allowing olefin exchange of one cobalt dinitrosoalkane complex with an external alkene to form a different complex under either thermal or photochemical conditions.

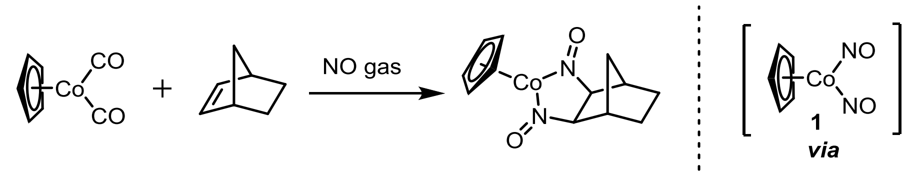

(eq 1)

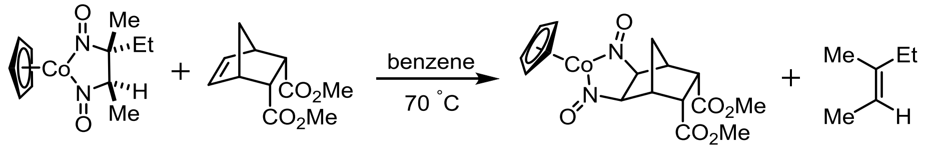

(eq 2)

During the reduction of cobalt dinitrosoalkane complex **2** with $LiAlH_4$, a mixture of *cis* and *trans* diamines were obtained (eq. 3). This observation suggested that deprotonation of the C–H bond alpha to the dinitroso groups could have occurred during the reduction process, which would then lead to epimerization at that carbon atom *via* an enolate-like intermediate and eventually to a mixture of *cis* and *trans* diamines. If such hypothesis holds true, cobalt dinitrosoalkane complexes possessing alpha C–H bonds, such as **2**, should act as nucleophiles in the presence of base toward electrophiles to give more functionalized cobalt complexes.

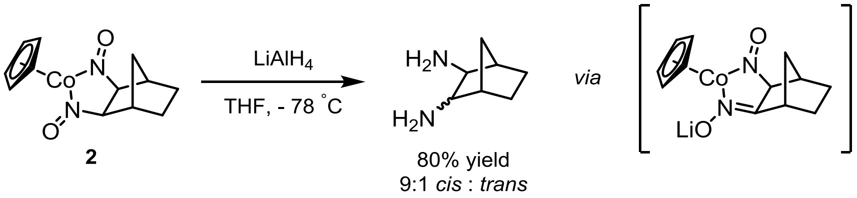

(eq 3)

In 2009, the Toste and Bergman groups demonstrated that cobalt dinitrosyl complex **1** can indeed mediate the vinylic C–H functionalization reaction of simple alkenes in a stepwise fashion.[41] After the initial binding of the substrate alkene, a cobalt dinitrosoalkane complex such as **2** can react with enone electrophiles in the presence of strong bases and Lewis acid to afford the desired functionalized cobalt dintirosoalkane complexes (Scheme 1.4). Alkene exchange with substrate olefin would then provide the overall vinylic C–H functionalized organic products (Scheme 1.5). Overall, the net reaction represents a direct vinylic C–H functionalization of simple alkenes in the absence of any directing groups.

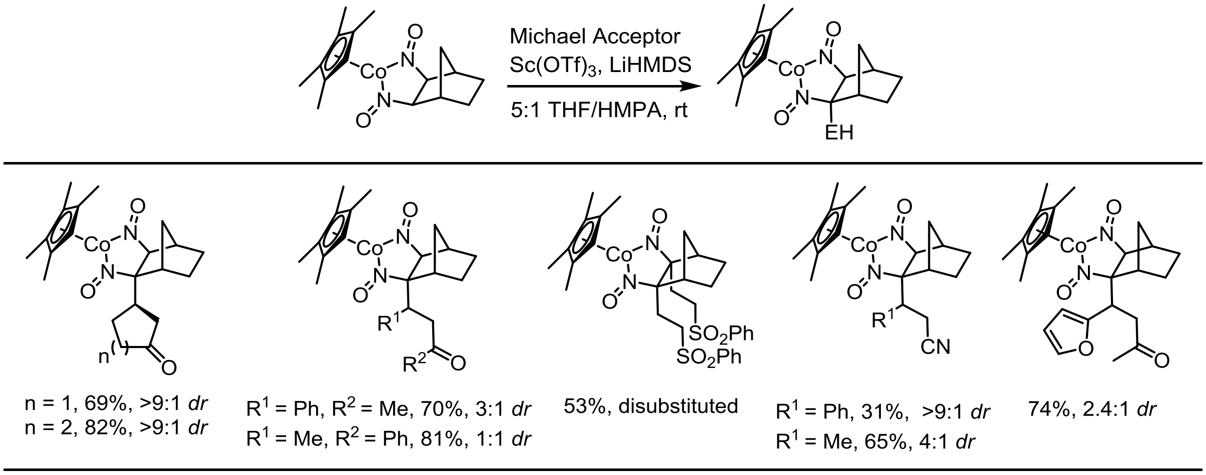
Michael Acceptor
Sc(OTf)3, LiHMDS
5:1 THF/HMPA, rt
EH
n = 1, 69%, >9:1 dr
n = 2, 82%, >9:1 dr
R1 = Ph, R2 = Me, 70%, 3:1 dr
R1 = Me, R2 = Ph, 81%, 1:1 dr
53%, disubstituted
R1 = Ph, 31%, >9:1 dr
R1 = Me, 65%, 4:1 dr
74%, 2.4:1 dr

Scheme 1.4. Intermolecular C–H Functionalization of Cobalt Dinitrosoalkane Complexes

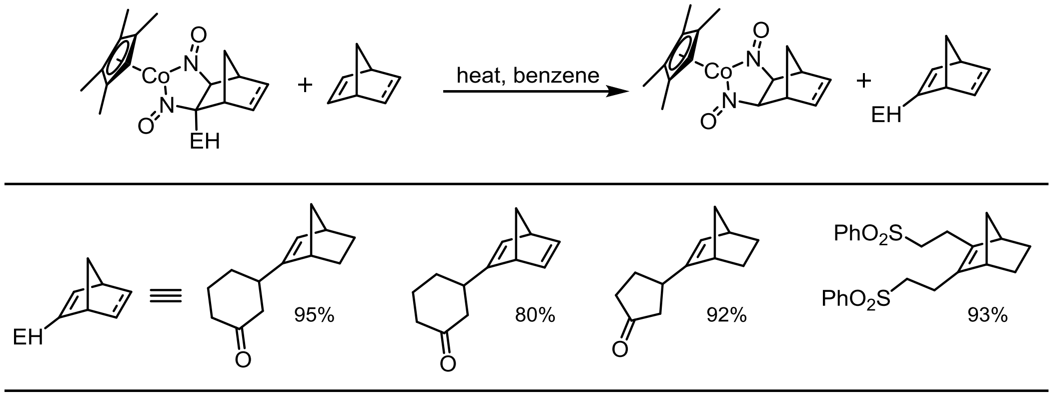
heat, benzene
EH
95%
80%
92%
PhO2S
PhO2S
93%

Scheme 1.5. Retrocycloaddition of functionalized cobalt complexes

Many cobalt dinitrosoalkane complexes were also shown to participate in a [3+2] annulation reaction.[42] For example, complex **3** reacted with cyclohexenone in the presence of Sc(OTf)$_3$ and LiHMDS to give complex **4** in 58% yield (Scheme 1.6). Subsequent reduction of **4** gave the tricyclic diamine **5** in 79% yield. Simple alkene exchange between **4** and norbornadiene also furnished tetrasubstituted alkene product **6** in 72% yield.

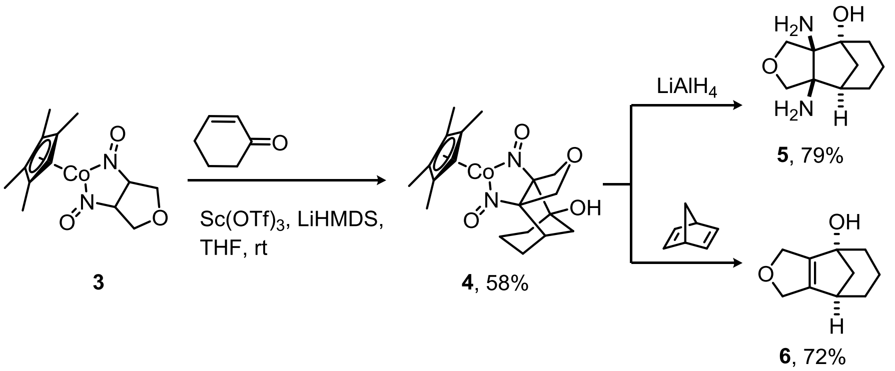

Scheme 1.6. Cobalt-Mediated [3 + 2] Annulation Reaction of Alkene with Cyclohexenone

Additionally, the enantioselective intermolecular C–H functionalization of alkenes with enones could also be achieved with the use of stoichiometric amount of a chiral base mixture (Scheme 1.7).[43] When **7** was treated with a premixed solution containing NaHDMS and cinchona alkaloid salt **8** at – 58 °C in THF, Michael addition followed by alkene exchange proceeded to give **9** in good yield with excellent diastereoselectivity (99% de) and enantioselectivity (83% ee).

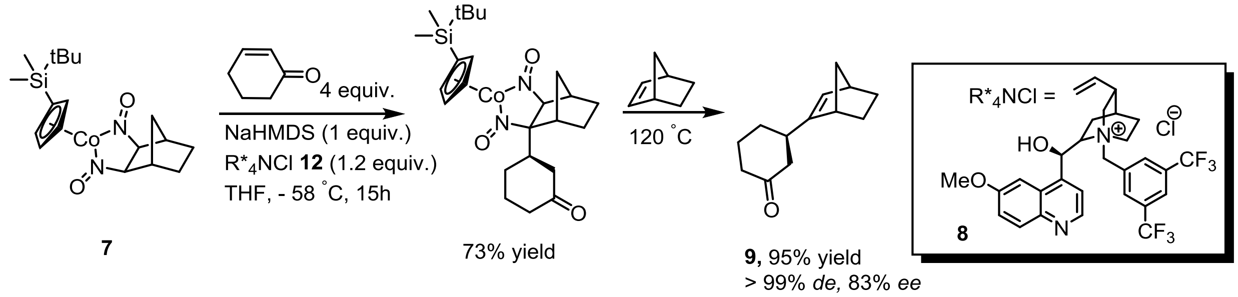

Scheme 1.7. Enantioselective vinylic C–H functionalization of norbornene

This methodology was applied to the synthesis of C_2- and C_1-symmetric dienes, which have been shown to be effective ligands for asymmetric organic transformations mediated by transition metals, via two sequential enantioselective C–H activation/Michael addition events (Scheme 1.8). Following the first alkylation of **10**, complexes **11a-c** can undergo a thermally promoted migration to produce complexes **12a-c**. Following a second iteration of the sequence of C–H functionalization and alkene exchange, C_2-symmetric chiral dienes **13a-c** were obtained in moderate to good yields over the two steps with high enantiomeric excess (90-96 % e.e.).[43]

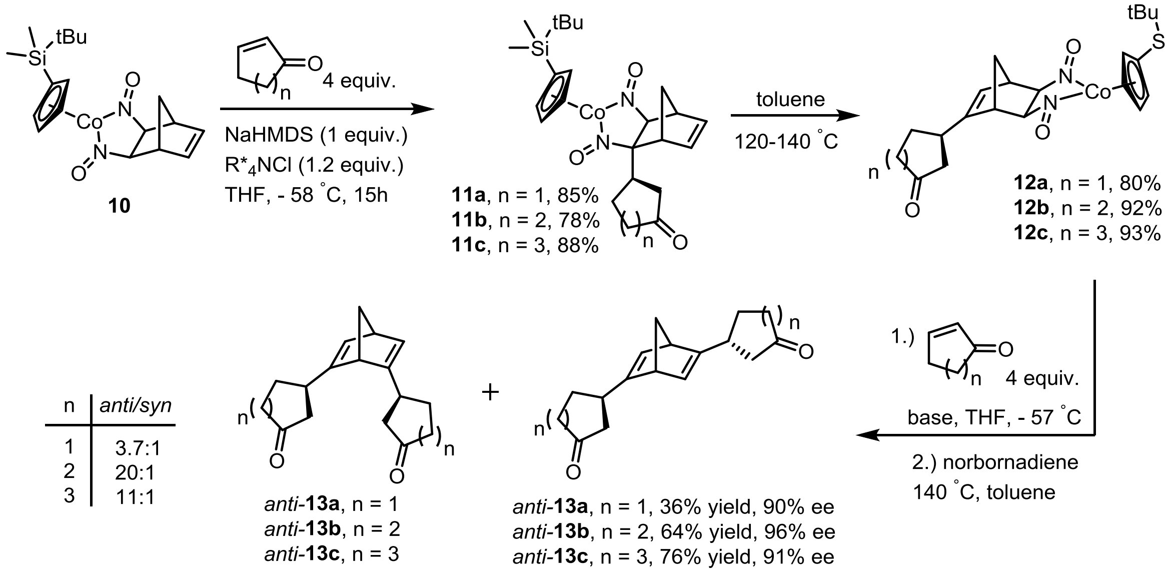
tBu
Si
Co
N
O
10
4 equiv.
n
NaHMDS (1 equiv.)
R*$_4$NCl (1.2 equiv.)
THF, - 58 °C, 15h
11a, n = 1, 85%
11b, n = 2, 78%
11c, n = 3, 88%
toluene
120-140 °C
12a, n = 1, 80%
12b, n = 2, 92%
12c, n = 3, 93%
1.)
4 equiv.
base, THF, - 57 °C
2.) norbornadiene
140 °C, toluene
+
anti-**13a**, n = 1
anti-**13b**, n = 2
anti-**13c**, n = 3
anti-**13a**, n = 1, 36% yield, 90% ee
anti-**13b**, n = 2, 64% yield, 96% ee
anti-**13c**, n = 3, 76% yield, 91% ee

n	*anti/syn*
1	3.7:1
2	20:1
3	11:1

Scheme 1.8. Cobalt dinitrosyl mediated enantioselective synthesis of C_2-symmetric ligands

As just described, the intermolecular and step-wise vinylic C-H functionalization reaction mediated by a stoichiometric amount of cobalt dinitrosyl complexes has been investigated thoroughly. The development of a catalytic variant of the vinylic C-H functionalization reaction of nobornene has thus far yielded promising preliminary results (eq 4). If a one-pot or a more general catalytic variant of this unique ligand-based vinylic C–H functionalization reaction can be developed, it would not only serve as a useful synthetic tool for organic synthesis, but could offer a new paradigm for future methodology development of C–H functionalization reactions that will make significant contribution to this important field of chemical research.

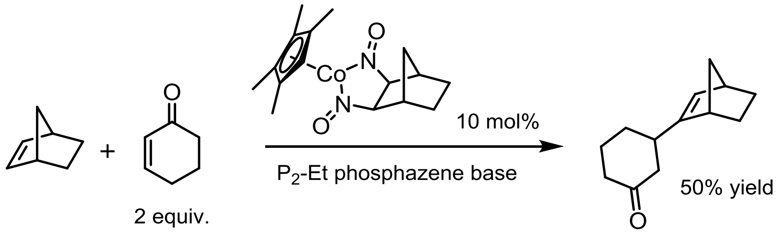
+
O
2 equiv.
Co
N
O
10 mol%
P$_2$-Et phosphazene base
50% yield

(eq 4)

References

(1) Shilov, A. E.; Shul'pin, G. B. *Chem. Rev.* **1997**, *97*, 2879-2932.
(2) Crabtree, R. H. *Chem. Rev.* **2010**, *110*, 575-575.
(3) Colby, D. A.; Bergman, R. G.; Ellman, J. A. *Chem. Rev.* **2009**, *110*, 624-655.
(4) Bellina, F.; Rossi, R. *Chem. Rev.* **2009**, *110*, 1082-1146.
(5) Lyons, T. W.; Sanford, M. S. *Chem. Rev.* **2010**, *110*, 1147-1169.
(6) Wencel-Delord, J.; Droge, T.; Liu, F.; Glorius, F. *Chem. Soc. Rev.* **2011**, *40*, 4740-4761.
(7) Colby, D. A.; Tsai, A. S.; Bergman, R. G.; Ellman, J. A. *Accts. Chem. Res.* **2011**, *45*, 814-825.
(8) Giri, R.; Shi, B.-F.; Engle, K. M.; Maugel, N.; Yu, J.-Q. *Chem. Soc. Rev.* **2009**, *38*, 3242-3272.
(9) Gutekunst, W. R.; Baran, P. S. *Chem. Soc. Rev.* **2011**, *40*, 1976-1991.
(10) Davies, H. M. L.; Du Bois, J.; Yu, J.-Q. *Chem. Soc. Rev.* **2011**, *40*, 1855-1856.
(11) Collet, F.; Lescot, C.; Dauban, P. *Chem. Soc. Rev.* **2011**, *40*, 1926-1936.
(12) Janowicz, A. H.; Bergman, R. G. *J. Am. Chem. Soc.* **1983**, *105*, 3929-3939.
(13) Lenges, C. P.; Brookhart, M. *J. Am. Chem. Soc.* **1999**, *121*, 6616-6623.
(14) Jun, C.-H.; Moon, C. W.; Lee, D.-Y. *Chemistry – A European Journal* **2002**, *8*, 2422-2428.
(15) Matsubara, T.; Koga, N.; Musaev, D. G.; Morokuma, K. *Organometallics* **2000**, *19*, 2318-2329.
(16) Labinger, J. A.; Bercaw, J. E. *Nature* **2002**, *417*, 507-514.
(17) Dick, A. R.; Sanford, M. S. *Tetrahedron* **2006**, *62*, 2439-2463.
(18) Doyle, M. P.; Duffy, R.; Ratnikov, M.; Zhou, L. *Chem. Rev.* **2009**, *110*, 704-724.
(19) Trost, B. M.; Imi, K.; Davies, I. W. *J. Am. Chem. Soc.* **1995**, *117*, 5371-5372.
(20) Colby, D. A.; Bergman, R. G.; Ellman, J. A. *J. Am. Chem. Soc.* **2006**, *128*, 5604-5605.
(21) Parthasarathy, K.; Jeganmohan, M.; Cheng, C.-H. *Organic Letters* **2007**, *10*, 325-328.
(22) Huddleston, R. R.; Jang, H.-Y.; Krische, M. J. *J. Am. Chem. Soc.* **2003**, *125*, 11488-11489.
(23) Huddleston, R. R.; Krische, M. J. *Organic Letters* **2003**, *5*, 1143-1146.
(24) Jang, H.-Y.; Huddleston, R. R.; Krische, M. J. *J. Am. Chem. Soc.* **2002**, *124*, 15156-15157.
(25) Ngai, M.-Y.; Barchuk, A.; Krische, M. J. *J. Am. Chem. Soc.* **2007**, *129*, 12644-12645.
(26) Smejkal, T.; Han, H.; Breit, B.; Krische, M. J. *J. Am. Chem. Soc.* **2009**, *131*, 10366-10367.
(27) Ho, C.-Y.; Ng, S.-S.; Jamison, T. F. *J. Am. Chem. Soc.* **2006**, *128*, 5362-5363.
(28) Matsubara, R.; Jamison, T. F. *J. Am. Chem. Soc.* **2010**, *132*, 6880-6881.
(29) McCarren, P. R.; Liu, P.; Cheong, P. H.-Y.; Jamison, T. F.; Houk, K. N. *J. Am. Chem. Soc.* **2009**, *131*, 6654-6655.
(30) Herath, A.; Thompson, B. B.; Montgomery, J. *J. Am. Chem. Soc.* **2007**, *129*, 8712-8713.
(31) Herath, A.; Montgomery, J. *J. Am. Chem. Soc.* **2008**, *130*, 8132-8133.
(32) Savchenko, A. V.; Montgomery, J. *The Journal of Organic Chemistry* **1996**, *61*, 1562-1563.
(33) Ikeda, S.-i.; Sato, Y. *J. Am. Chem. Soc.* **1994**, *116*, 5975-5976.
(34) Ohashi, M.; Kishizaki, O.; Ikeda, H.; Ogoshi, S. *J. Am. Chem. Soc.* **2009**, *131*, 9160-9161.
(35) Brunner, H.; Loskot, S. *Angew. Chem., Int. Ed.* **1971**, *10*, 515-516.
(36) Brunner, H.; Loskot, S. *J. Organomet. Chem.* **1973**, *61*, 401-414.
(37) Brunner, H. *J. Organomet. Chem.* **1968**, *12*, 517-522.
(38) Becker, P. N.; White, M. A.; Bergman, R. G. *J. Am. Chem. Soc.* **1980**, *102*, 5676-5677.
(39) Becker, P. N.; Bergman, R. G. *J. Am. Chem. Soc.* **1983**, *105*, 2985-2995.
(40) Becker, P. N.; Bergman, R. G. *Organometallics* **1983**, *2*, 787-796.

(41) Schomaker, J. M.; Boyd, W. C.; Stewart, I. C.; Toste, F. D.; Bergman, R. G. *J. Am. Chem. Soc.* **2008**, *130*, 3777-3779.
(42) Schomaker, J. M.; Toste, F. D.; Bergman, R. G. *Organic Letters* **2009**, *11*, 3698-3700.
(43) Boyd, W. C.; Crimmin, M. R.; Rosebrugh, L. E.; Schomaker, J. M.; Bergman, R. G.; Toste, F. D. *J. Am. Chem. Soc.* **2010**, *132*, 16365-16367.

Chapter 2. The Development of a Stoichiometric and Catalytic Vinylic C-H Functionalization Reaction Mediated by a Cobalt Dinitrosyl Complex

Portions of this chapter have been previously published in:
Chen Zhao, F. Dean Toste and Robert G. Bergman. "Direct Michael Addition of Alkenes via a Cobalt-Dinitrosyl Mediated Vinylic C–H Functionalization Reaction," *J. Am. Chem. Soc.* **2011**, *133*, 10787-10789.

2.1 Introduction

Initially reported in the early 1970's,[1-3] the cyclopentadienylcobalt dinitrosyl complex [CpCo(NO)$_2$] (**1**) is a reactive intermediate that has been studied by *in situ* spectroscopic techniques[4-6] and computational chemistry.[7] As depicted in Scheme 2.1, four different synthetic methods have been developed for the generation of [CpCo(NO)$_2$] (**1**). These include (i) the reaction of CpCo(CO)$_2$ with nitric oxide (NO) gas[1-3] (ii) the reversible reaction of the cobalt dimer **2** with NO[4-6] (iii) the salt-metathesis of [(κ^2-TMEDA)Co(NO)$_2$][BPh$_4$] (**3**) with group 1 cyclopentadienyl salts,[8] and (iv) the thermal or UV-light promoted retrocycloaddition of alkenes from cobalt dinitrosoalkane complexes. Although it has been detected spectroscopically, attempts to isolate the reactive cobalt dinitrosyl complex **1** by tuning both the electronic and steric properties of the Cp ligand have, to date, proved unsuccessful.[1-3,7,8] In the absence of a suitable alkene trap, [CpCo(NO)$_2$] decomposes to a complex mixture including **2**.

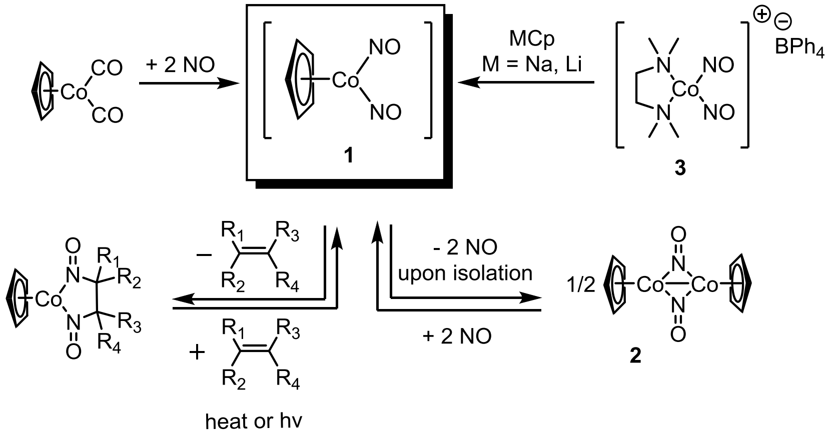

Scheme 2.1. Synthetic Entry Points to [CpCo(NO)$_2$]

As presented in Chapter 1, the step-wise intermolecular C–H functionalization of cobalt dinitrosoalkane complexes can be achieved with the use of stoichiometric amounts of both Lewis acid and base.[9,10] Attempts at rendering the overall reaction in one-pot with either stoichiometric or catalytic amounts of [CpCo(NO)$_2$] source have been limited due to the high temperature require for the release/retrocycloaddition of the product from the cobalt fragment, the instability of [CpCo(NO)$_2$] under such strongly basic reaction conditions, and the need for substrate-bound cobalt complex as the precatalyst. Thus, we sought to investigate the possibility of an intramolecular system with the goal of developing a one-pot vinylic C–H functionalization reaction of simple alkenes mediated by [CpCo(NO)$_2$] (**1**) as illustrated in Scheme 2.2.

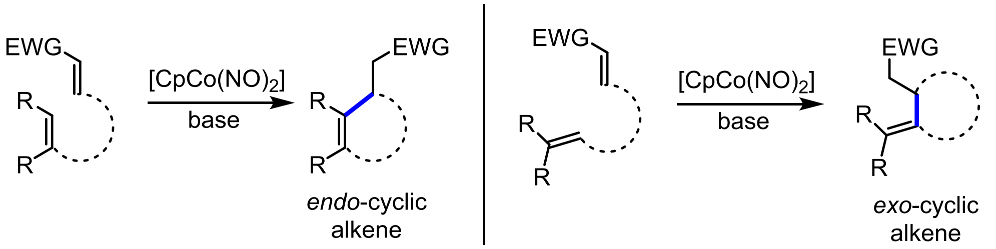
EWG
R
R
[CpCo(NO)2]
base
EWG
R
R
endo-cyclic alkene
EWG
R
R
[CpCo(NO)2]
base
EWG
R
R
exo-cyclic alkene

Scheme 2.2. Intramolecular vinylic C–H functionalization of alkenes mediated by [CpCo(NO)$_2$]

2.2. Results and Discussion

2.2.1. Step-wise *5-exo-trig* and *6-exo-trig* Cyclization Reactions Mediated by Cobalt-dinitrosyl Complex [CpCo(NO)$_2$]

We began our studies by first examining the step-wise chemistry of our proposed intramolecular system with model substrates **4a-c**. Initially, alkene exchange reaction conditions were employed for the synthesis of substrate-bound complexes **5a-c.** Isolation and purification were achieved by flash chromatography on silica gel to give the desired dinitrosoalkane complexes in good yields (Table 1). Although 10 equivalents of the substrates were generally required, the mild reaction conditions of this alkene exchange procedure allowed for the recovery of the unreacted organic substrates with no decomposition.

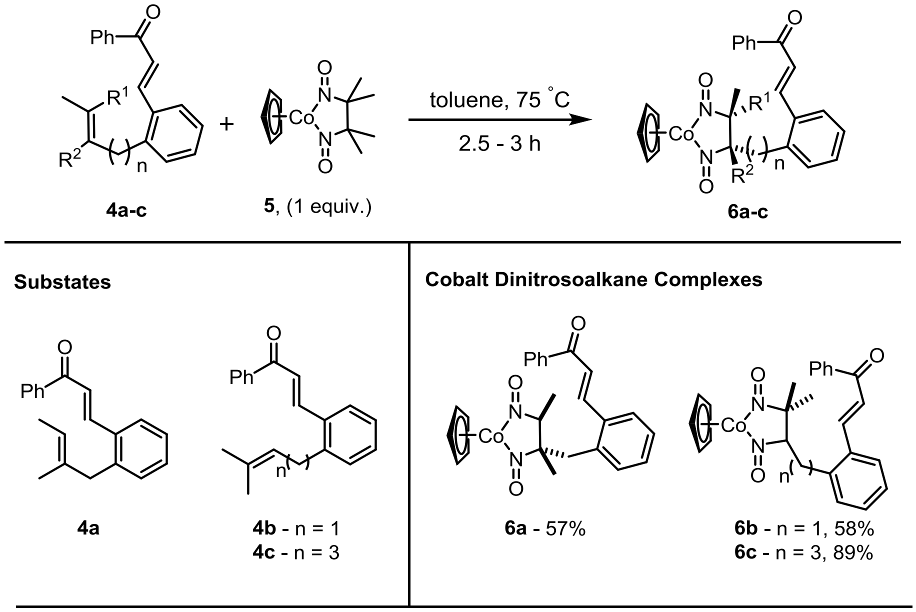
Ph
O
R1
R2
n
4a-c
+
Co
N
O
N
O
5, (1 equiv.)
toluene, 75 °C
2.5 - 3 h
6a-c
Substates
4a
4b - n = 1
4c - n = 3
Cobalt Dinitrosoalkane Complexes
6a - 57%
6b - n = 1, 58%
6c - n = 3, 89%

Scheme 2.3. Cycloaddition of **4a-c** to [CpCo(NO)$_2$]

Upon treatment with catalytic amount (10 mol%) of Verkade's base, complex **6a** cyclized in a *6-exo-trig* fashion under the same reaction conditions to give both the cobalt complex **7** and the desired organic product **8a**. While repeating the cyclization at –78 °C had no effect on this product distribution, when **6a** was heated in the presence of base, compound **8a** was obtained exclusively in 81% yield. Furthermore, when complex **7** was heated with 10 mol% of Verkade's base at 75 °C, **8a** was also obtained in 83% yield (Scheme 2.4). The lability of [CpCo(NO)$_2$] fragment in **7** has precedent in our previous studies, and cobalt dinitrosoalkane complexes of cyclohexene have previously only been generated and studied *in situ* due to their thermal instability. Further support was provided by a control experiment in which heating of complex **7** in THF for 30 min at 75 °C gave **8a** in 93% yield.

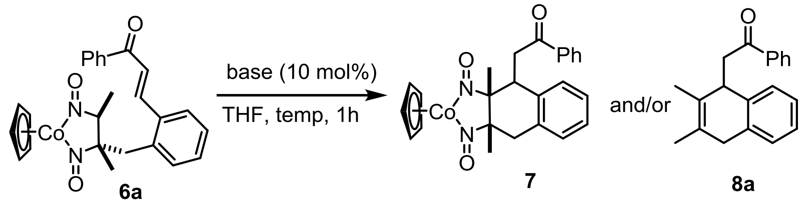

entry	base	temp (°C)	yield of **7**	yield of **8a**
1	Verkade's	- 78	25%	26%
2	Verkade's	25	25%	25%
3	Verkade's	75	0%	80%
4	*t*BuOK	75	0%	81%

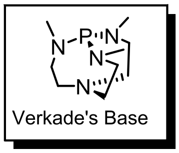

Scheme 2.4. Reaction conditions for the cyclization of complex **6a** to give complex **7** and/or **8a**

On the other hand, complex **6b** cyclized in a *5-exo-trig* fashion to give only the desired complex **9** in 57% yield. Repeating the cyclization reaction of **6b** at 75 °C gave slightly higher yield of complex **9** (65% yield) but no retrocycloaddition of **10** was observed. However, in the presence of added norbornene, complex **9** reacted to afford the desired product **10** in high yield.

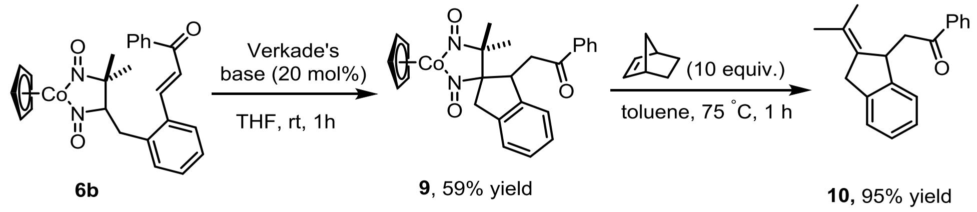

Scheme 2.5. Cyclization of cobalt complex **6b**

Inspired by the high enantioselectivity obtained from the intermolecular C-H functionalization reaction,[11] we were interested to see whether the chiral base mixture resulting from cinchona alkaloid **12** would affect the enantioselective cyclization of cobalt complex **6b**. Indeed, reaction between **6b** and a premixed THF solution containing both NaHMDS and chiral salt **12** at – 10 °C for 1h led to the desired cyclized cobalt complex **9** in 57% yield. Following alkene exchange of complex **9** with norbornene, **10** was obtained in 57% ee. However, control experiment between enantioenriched cobalt complex **9** and the chiral base mixture at room temperature for 3 hours led to erosion in the enantiomeric excess of product **10** (3% ee), suggesting that the C–C bond forming step may be reversible, with racemization of the product occurring at longer reaction times. While attempts to trap the intermediate enolate to prevent the racemization process were not successful, the cobalt-dinitrosyl mediated vinylic C–H functionalization was shown to proceed enantioselectively in the presence of a chiral base mixture in both the inter- and intramolecular systems.

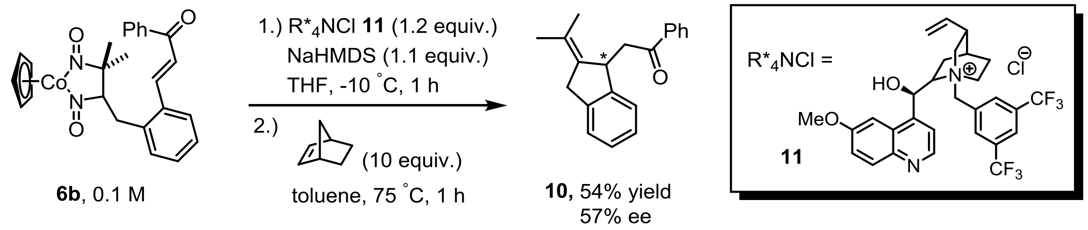

(eq 2)

2.2.2. The Development of One-Pot C–H Functionalization Reaction Mediated by Stoichiometric Amounts of Cobalt Complex 5

After thorough investigation of the stepwise cobalt dinitrosyl mediated intramolecular C–H functionalization reaction, we sought to develop a one-pot procedure for the overall transformation. Initial attempts to promote the cyclization of **4a** with a stoichiometric amount of cobalt complex **5** and a catalytic amount of Verkade's base gave **8a** in 55% yield (Table 2.1, entry 1). By increasing the concentration of **4a** and employing 20 mol% of P_1-*t*Bu phosphazene base, **8** was obtained in 85% yield over 24h (Table 2.1, entry 6). Control experiments between **4a** and 20 mol% of either Verkade's or P_1-*t*Bu phosphazene base at 75 °C for 72h gave no desired product and only recovered **4a**.

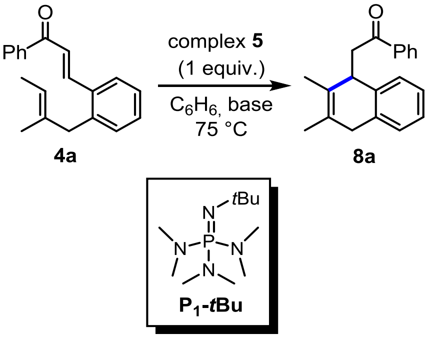

entry	conc. of **4a**	base	mol%	time	yield
1	0.1	Verkade's	10	53	55%
2	0.2	Verkade's	10	72	70%
3	0.33	Verkade's	10	53	78%
4	0.33	LiCp	15	48	46%
5	0.33	P_1-*t*Bu	15	24	75%
6	**0.33**	**P_1-*t*Bu**	**20**	**24**	**85%**
7	0.33	P_1-*t*Bu	25	24	72%

Table 2.1. Reaction optimization of **4a** to **8a** **m**ediated by complex **5**

The scope of the one-pot C–H functionalization reaction mediated by stoichiometric amount of cobalt complex **5** was next surveyed (Table 2.2). A variety of Michael acceptors can be utilized to give the corresponding tetra-alkyl-substituted alkene products in moderate to good yields (entries 1 – 6). Initially reported in the intermolecular system, *α,β*-unsaturated esters were ineffective as electrophiles for functionalization of cobalt dinitrosoalkane complexes; however, substrate **4d** cyclized to give the desired product in good yield. Although substrate **4h** was synthesized as a mixture of *cis* and *trans* isomers in a 2:3 ratio, it cyclized in the presence of complex **5** and P_1-*t*Bu phosphazene base to give **8f** in good yield. Cyclic alkenyl group containing molecules, such as **4i** and **4j**, also reacted to give the desired tricyclic products. The cyclopentenyl group of substrate **4i** proves to be advantageous since strained alkenes bind [CpCo(NO)$_2$] much more effectively than simple and unstrained olefins. This argument is further exemplified by the low yield obtained with substrate **4j**. Ynone-containing substrate **4l** also cyclized in the presence of cobalt complex and P$_1$-*t*Bu phosphazene base to give highly conjugated product **8j** in good yield.

entry	substrates			products	yield[b]
1[a]	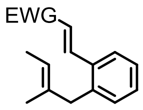	EWG = 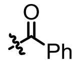	**4a**	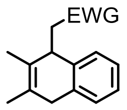	**8a** - 85%
2[c]		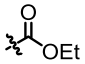	**4d**		**8b** - 75%[c]
3[c]		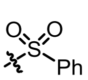	**4e**		**8c** - 83%[c] (61%)[a]
4		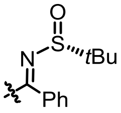	**4f**		**8d** - 83% 3:1 *dr*
5		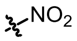	**4g**		**8e** - 68%[d]
6[c]	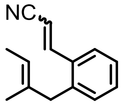	2:3 *cis:trans*	**4h**	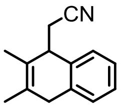	**8f** - 74%[d]
7	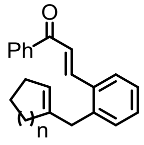	n = 1 n = 2	**4i** **4j**	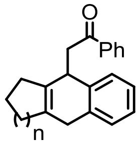	**8g** - 91%[d] **8h** - 19%
8	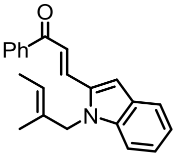		**4k**	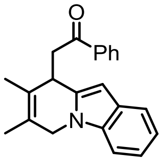	**8i** - 77%
9	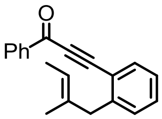		**4l**	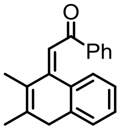	**8j** - 78%[d] (46%)[a]

[a] General condition: 1.2 equiv of **5**, P$_1$-*t*Bu (20 mol%), 75 °C, 24h, benzene (0.33 M). [b] Yields are deteremined by ^{1}H NMR spectroscopy with trimethoxybenzene as internal standrad. [c] P$_1$-*t*Bu (100 mol%), second equiv of **5** added after 12h of heating, followed by additional heating for 24h. [d] 1.2 equiv of **5**, P$_1$-*t*Bu (10 mol%), 24h. [e] 2 equiv of enone, 1.2 equiv of **5**, P$_1$-*t*Bu (10 mol%), 95 °C, 24 h. [f] Isolated yields.

Table 2.2. Substrate scope of the one-pot C–H functionalization reaction mediated by **5**

Intermolecular functionalization of norbornene with both cylopentenone and cyclohexenone can also be achieved in one step to give the corresponding coupled products, **9a** and **9b**, in good yields with high diastereoselectivity (Scheme 2.6a). The highly basic and less nucleophilic P_1-*t*Bu phosphazene base proves to be vital for the successful intermolecular couplings shown in Scheme 2.6a since the use of Verkade's or other phosphazene bases provided low yields of the desired product due to Baylis–Hillman type dimerization of the enones.

a.) Intermolecular one-pot functionalization

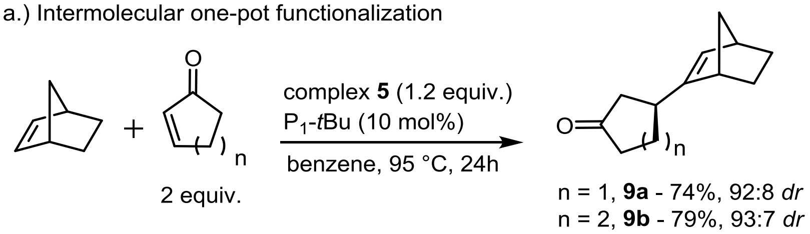
O
+
n
2 equiv.
complex **5** (1.2 equiv.)
P_1-*t*Bu (10 mol%)
benzene, 95 °C, 24h
O
n
n = 1, **9a** - 74%, 92:8 *dr*
n = 2, **9b** - 79%, 93:7 *dr*

b.) Baylis-Hillman type dimerization of enones

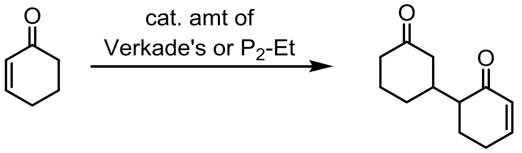

Scheme 2.6. (a) One-Pot Intermolecular C–H Functionalization Reaction Mediated by **5**; (b) Baylis-Hillman Type Dimerization of Cyclohexenone

2.2.3. The Development of C–H Functionalization Reaction Catalyzed by Cobalt Complex 5

While cobalt is an affordable and readily available transition metal, rendering the reactions outlined in Scheme 2.2 catalytic in cobalt dinitrosyl complex [$CpCo(NO)_2$] (**1**) would further improve upon the chemistry of this class of ligand-based C–H functionalization reaction. As discussed in Chapter 1, intermolecular functionalization of norbornene with cyclohexenone proceeded to give 50% yield of the desired product with 10 mol% of a cobalt complex as the precatalyst. We hypothesized that the formation of the cyclohexene-containing product **8a** from the cyclization of substrate **4a** might provide facile retrocycloaddition of **8a** from the cobalt fragment and allow for fast trapping of the reactive catalyst by another equivalent of the substrate **4a**, allowing turnover of the [$CpCo(NO)_2$] catalyst. However, reaction between substrate **4a**, 20 mol% of cobalt complex **5** and 10 mol% of P_1-*t*Bu proceeded at 75 °C over 24 h to give only 19% yield of the desired product **8a**. When tetramethylethylene was used as an additive in either catalytic or stoichiometric amounts or as the solvent, no improved catalytic turnover was obtained. Attempts to carry out the catalytic reaction under an atmosphere of nitric oxide gas in order to prevent any buildup of the catalytically inactive cobalt dimer **2** led to low production of **8a** and decomposition of the organic components over 48h. A variety of bases were also tested in the functionalization/cyclization reaction of **4a** in the presence of 20 mol% of cobalt complex **5**, but no improved results were obtained (see Experimental section of this Chapter for more details).

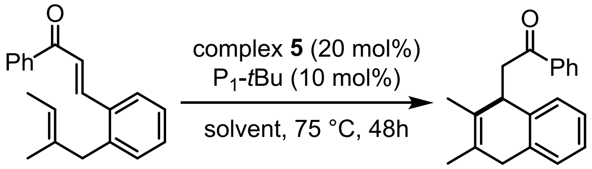

4a **8a**

entry	solvent	additive	yield (%)
1	THF	none	20
2	toluene	none	22
3	benzene	none	21
4	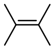	none	trace
5	benzene	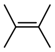 20 mol%	21
6	THF	$NO_{(g)}$	16

Table 2.3. Complex **5** Catalyzed Intramolecular C–H Functionalization of **4a**

As mentioned above, the cyclopentenyl moiety of substrate **4i** proves to be advantageous in its cyclization reaction mediated by stoichiometric amount of cobalt complex **5** due to the strained nature of the substituent, providing the desired in product with the highest yield of all the substrates examined. Although based-mediated decomposition of [CpCo(NO)$_2$] and the formation of dimer **2** have thus far limited catalytic turnover, substrate **4i** cyclized to give 60% yield of **8g** in the presence of 20 mol% of precatalyst **5** and 10 mol% P$_1$-*t*Bu phosphazene base.

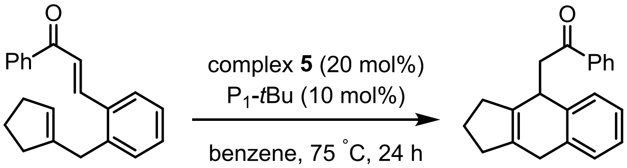

4i, 0.33 M **8g**, 60% yield

(eq 3)

Based on our step-wise and stoichiometric studies, we propose a catalytic cycle for the intramolecular vinylic C-H functionalization reaction mediated by [CpCo(NO)$_2$] that involves substrate binding, deprotonation and cyclization, and retrocycloaddition as shown in Figure 2.1.

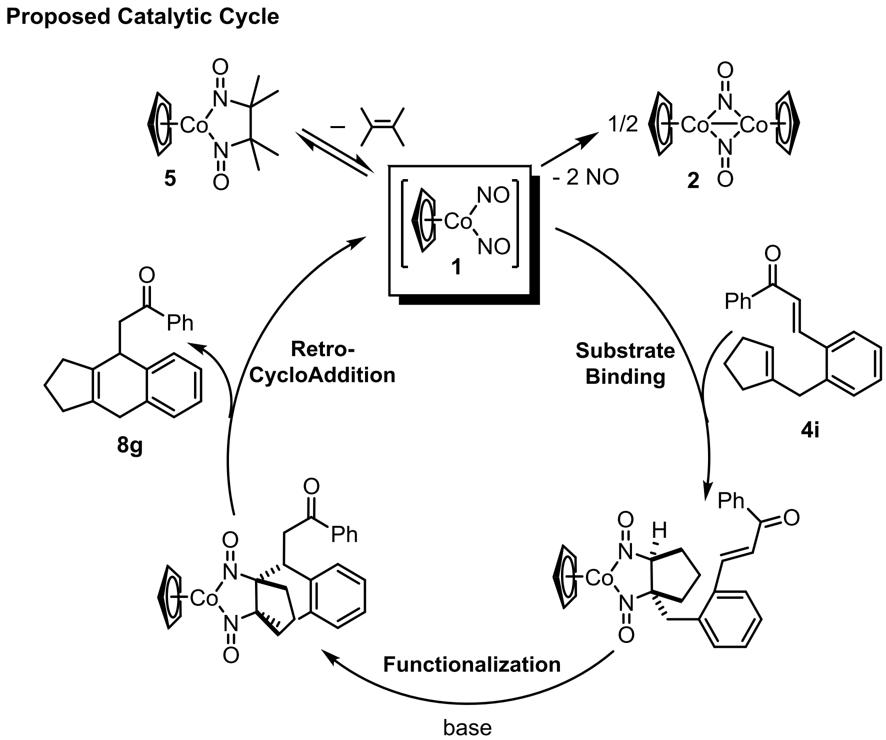
Proposed Catalytic Cycle
5
–
1/2
- 2 NO
2
NO
Co
NO
1
Retro-
CycloAddition
Substrate
Binding
Ph
8g
4i
Ph
H
Functionalization
base

Figure 2.1. Proposed Catalytic Cycle for Cobalt-Dinitrosyl Mediated C–H Functionalization

2.3. Conclusion

We have developed a simple, one-pot C–H functionalization reaction of alkenes mediated by complex **5**. This methodology allows for the chemoselective generation of nucleophiles directly from vinylic C–H bonds, which can add to a variety of internal, and some external Michael acceptors in a 1,4-fashion. This strategy also give rise to tri- and tetra-alkyl-substituted alkene products, where the olefin is γ,δ-unsaturated with respect to the electron-withdrawing functional groups. Lastly, the application of a chiral base mixture to the enantioselective intramolecular C–H functionalization can also be achieved to give the overall product in good yield and moderate enantiomeric excess. Although additional work is necessary to further improve the catalytic capability of cobalt dinitrosyl complex for vinylic C–H functionalization of simple alkenes, this ligand-based vinylic C–H functionalization reaction can provide chemists with a new tool for organic synthesis.

2.4. Experimental

2.4.1. General Information.

Unless otherwise noted, all reagents were obtained commercially and used without further purification. All air- and moisture-sensitive compounds were manipulated using standard Schlenk techniques. Reactions were carried out under a nitrogen atmosphere in glassware that was either oven-dried at 150 ºC overnight or flame-dried under nitrogen immediately prior to use. Pentane, hexane, diethyl ether, benzene, toluene, tetrahydrofuran and methylene chloride were dried and purified by passage through a column of activated alumina (type A2, 12 x 32, UOP LLC) under a stream of dry nitrogen. Unless otherwise specified, all other reagents were purchased from Acros, Aldrich or Fisher and were used without further purification.

Reaction solutions were magnetically stirred with the exception of those reactions performed in sealed NMR tubes. The majority of experiments were monitored by thin layer chromatography (TLC) using 0.25 mm pre-coated silica gel plates from Silicycle (TLGR10011B-323) containing a fluorescent indicator for visualization by UV light. Various stains were used to visualize reaction products, including *p*-anisaldehyde, $KMnO_4$ and phosphomolybdic acid in ethanol. Flash chromatography was performed using MP Biomedicals SiliTech silica gel 32-63D, 60 Å.

A specially designed gas cabinet was built by the College of Chemistry at University of California, Berkeley for the storage and use of nitric oxide gas cylinders. This set-up allows for direct connection between gas cylinders and manifolds for safe and controlled manipulation of harmful gases. For more details of this set-up, please contact the corresponding authors.

All NMR spectra were obtained at ambient temperature using Bruker AVQ-400, AVB-400 or DRX-500 spectrometers. ^1H NMR chemical shifts are reported relative to residual solvent peaks (7.26 ppm for $CDCl_3$, 7.16 ppm for C_6D_6). ^{13}C NMR chemical shifts were also reported with reference to residual solvent peaks (77.23 ppm for $CDCl_3$, 128.06 ppm for C_6D_6). Infrared (IR) spectra were recorded on a Nicolet Avatar FT-IR spectrometer. Low-resolution mass spectral data were obtained on an Agilent 6890N/5973 GC/MS equipped with a J&W Scientific DB-5MS capillary column (30 m x 0.25 mm, 0.50 micron). Both low- and high-resolution mass spectral data were obtained from the Micromass/Analytical Facility operated by the College of Chemistry, University of California, Berkeley.

2.4.2. Synthesis of Cobalt Dinitrosoalkane Complex 5

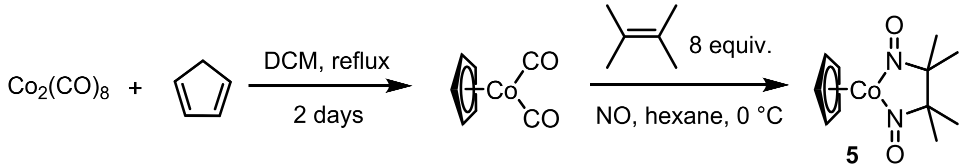

A 500 mL oven-dried round-bottom flask was cooled under a stream of nitrogen, followed by addition of 250 mL of dichloromethane. The solvent was purged with nitrogen for 10 min and kept under a steady stream of nitrogen. Cyclopentadiene monomer, freshly "cracked" from dicyclopentadiene, (3.30 g, 50.0 mmol, 2 equiv) and dicobalt octacarbonyl (8.55 g, 25.0 mmol, 1 equiv) were added quickly to the flask. A reflux condenser was then fitted to the flask, which was covered with aluminum foil, and the dark red solution was heated to reflux for 48 h. The reaction mixture was cooled and dichloromethane was carefully removed under vacuum at ambient temperature. The dark red-black residue was then distilled under reduced pressure through a 6" Vigreaux column. The product distilled as a dark red-orange liquid (3.36 g, 18.7 mmol, 75% yield) and was stored inside a –40 °C refrigerator inside the glove box.

An oven-dried three-neck flask was loaded with 40 mL of hexane, $CpCo(CO)_2$ (1.00 g, 5.55 mmol, 1 equiv) and tetramethylethylene (3.84 g, 45.6 mmol, 8 equiv) inside a dry-box. The flask was then transferred out of the box and subsequent procedures were done on the bench. The reaction flask was cooled to 0 °C and put under an atmosphere of argon, before nitric oxide gas was bubbled slowly through the solution at a rate of approximately 1 bubble/sec through a manifold. A dark brown solid gradually precipitated from the dark red solution as the reaction progressed (e.g. 1-2 h). The reaction progress was closely monitored by TLC until no starting $CpCo(CO)_2$ was seen (generally 1 h for reaction utilizing less than 1.00 g of $CpCo(CO)_2$). The NO addition was stopped and argon was bubbled through the reaction mixture for 10 min to ensure that any traces of NO gas were removed. The solvent was removed *in vacuo*, and the residue was loaded onto a silica gel column packed with hexanes. The column was eluted with hexanes until the excess tetramethylethylene and $[CpCo(CO)_2]$ were removed. The polarity of the mobile phase was then increased to 10% EtOAc in hexane to afford complex **5** (1.18 g, 4.44 mmol, 80% yield) as a dark red-black solid. ^1H NMR: (400 MHz, $CDCl_3$): δ (ppm) 4.92 (s, 5H), 1.14 (s, 12H). ^{13}C NMR (100 MHz, $CDCl_3$): δ (ppm) 94.1, 89.9, 24.5. IR [neat, ν_{max} (cm^{-1})]: 1444, 1417, 1360, 1342, 1183, 1119, 1009, 807 cm^{-1}. HRMS (*m/z*): calculated for $C_{11}H_{17}CoN_2O_2$ 268.0617, found 268.0619.

2.4.3. Substrate Synthesis

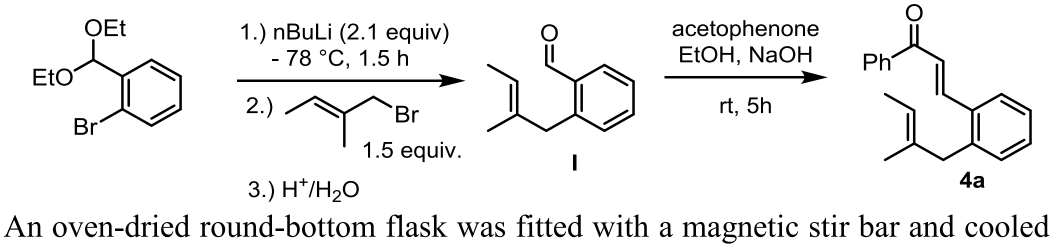

An oven-dried round-bottom flask was fitted with a magnetic stir bar and cooled under a stream of nitrogen. 2-bromobenzaldehyde diethyl acetal (3.80 g, 15.0 mmol, 1 equiv) was dissolved in THF (60 mL) and cooled to -78 °C. After 15 min, nBuLi (2.5 M, 12.8 mL, 32.0 mmol, 2.1 equiv) was added to the solution, and the resulting mixture was stirred at -78 °C for 1 h. (*E*)-1-bromo-2-methylbut-2-ene (3.31 g, 22.5 mmol, 1.5 equiv) was then added and the resulting reaction mixture was warmed to room temperature slowly and stirred for 14 h. The reaction was quenched by addition of 1 M aq. HCl solution (20 mL). The resulting mixture was extracted with diethyl ether (3 x 20 mL). The combined organic layer was washed with brine, dried with $MgSO_4$ and concentrated *in vacuo.* The crude residue was then purified by silica chromatography (3% EtOAc in hexane) to give the desired aldehyde **I** (2.14 g, 12.3 mmol, 82% yield) as a pale yellow oil: ^{1}H NMR (500 MHz, $CDCl_3$): δ (ppm) 10.28 (s, 1H), 7.87 (d, 1H, *J* = 7.5 Hz), 7.50 (t, 1H, *J* = 7.5 Hz), 7.37 (t, 1H, *J* = 8.5 Hz), 7.25 (d, 1H, *J* = 8.5 Hz), 5.05 (q, 1H, *J* = 6.5 Hz), 3.70 (s, 1H), 1.63 (s, 3H), 1.58 (d, 3H, *J* = 6.5 Hz). ^{13}C NMR (125 MHz, $CDCl_3$): δ (ppm) 192.3, 143.0, 135.5, 134.6, 133.9, 131.7, 130.0, 126.9, 121.5, 41.6, 16.5, 13.6. IR [neat, ν_{max} (cm^{-1})]: 2918, 2857, 1697, 1599, 1573, 1450, 1207, 1025, 752 cm^{-1}. HRMS (*m/z*): calculated for $C_{12}H_{14}O$ 174.1045, found 174.1038.

Aldehyde **I** (1.03 g, 5.91 mmol, 1 equiv) and acetophenone (1.10 g, 9.17 mmol, 1.5 equiv) were dissolved in 25 mL of absolute EtOH, followed by addition of 2 M aq. NaOH solution (1 mL) at 25 °C. After stirring for 5 h, the mixture was neutralized by addition of 1M aq. HCl solution. The resulting mixture was extracted with diethyl ether (3 x 20mL). The combined organic layer was washed with brine, dried with $MgSO_4$ and concentrated *in vacuo*. The residue was purified by silica chromatography (3% EtOAc in hexane) to yield the desired compound **4a** (1.57 g, 5.7 mmol, 95%) as a yellow oil: ^{1}H NMR (500 MHz, $CDCl_3$): δ (ppm) 8.08 (d, 1H, *J* = 15.5 Hz), 7.99 (d, 2H, *J* = 7.5 Hz), 7.72 (d, 1H, *J* = 8.0 Hz), 7.58 (t, 1H, *J* = 7.5 Hz), 7.50 (t, 2H, *J* = 7.5 Hz), 7.38 (d, 1H, *J* = 15.5 Hz), 7.33 (t, 1H, *J* = 7.0 Hz), 7.29 (d, 1H, *J* = 7.5 Hz), 7.22 (d, 1H, *J* = 7.0 Hz), 5.07 (q, 1H, *J* = 6.0 Hz), 3.45 (s, 2H), 1.62 (s, 3H), 1.57 (d, 3H, *J* = 6.0 Hz). ^{13}C NMR (125 MHz, $CDCl_3$): δ (ppm) 191.2, 143.2, 140.5, 138.5, 134.7, 134.6, 132.8, 131.2, 130.34, 128.8, 128.8, 126.9, 126.7, 123.7, 121.3, 43.1, 16.4, 13.7. IR [neat, ν_{max} (cm^{-1})]: 2916, 1663, 1640, 1578, 1479, 1447, 1330, 1282, 1214, 1179, 1016, 749, 693 cm^{-1}. HRMS (*m/z*): calculated for $C_{20}H_{20}O$ 276.1514, found 276.1513.

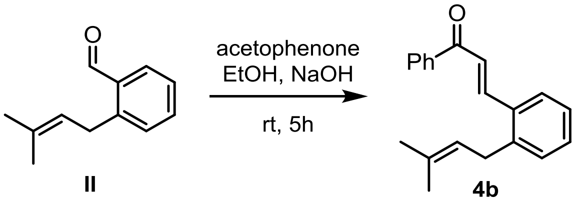

To a solution of aldehyde **II** (870 mg, 5 mmol, 1 equiv.), synthesized according to literature procedure,[12] and acetophenone (900 mg, 7.5 mmol, 1.5 equiv.) in ethanol (10 mL) was added 2M aq. NaOH solution (0.25 mL, 0.5 mmol, 10 mol%) at room temperature. The reaction was followed by TLC with 10% ethyl acetate in hexane as the eluting solvent. After 5 hours, the reaction mixture was neutralized by addition of 2M aq. HCl solution. The resulting mixture was extracted with diethyl ether (3 x 20 mL). The combined organic layers were washed with brine, dried with anhydrous $MgSO_4$ and concentrated *in vacuo*. The residue was purified by flash chromatography on silica (3-5% EtOAc in hexanes) to give **4b** in 85 yield. ^{1}H NMR (500 MHz, $CDCl_3$): δ (ppm) 8.12 (d, 1H, *J* = 15.5 Hz), 8.02 (d, 2H, *J* = 8.0 Hz), 7.71 (d, 1H, *J* = 8.0 Hz), 7.59 (t, 1H, *J* = 7.5 Hz), 7.50 (t, 2H, *J* = 8.0 Hz), 7.43 (d, 1H, *J* = 15.5 Hz), 7.35 (t, 1H, *J* = 7.0 Hz), 7.26 (t, 2H, *J* = 8.0 Hz), 5.21 (t, 1H, *J* = 7.5 Hz), 3.49 (d, 2H, *J* = 7.0 Hz), 1.72 (s, 6H). ^{13}C NMR (125 MHz, $CDCl_3$): δ (ppm) 190.9, 142.9, 142.2, 138.5, 133.9, 133.1, 132.9, 130.6, 130.1, 128.8, 128.7, 126.9, 126.7, 123.7, 122.7, 32.55, 25.9, 18.1. IR [neat, ν_{max} (cm^{-1})]: 2973, 2911, 1662, 1603, 1482, 1447, 1328 cm^{-1}. HRMS (*m/z*): calculated for $[C_{20}H_{20}O]^+$, 276.1514; observed, 276.1516.

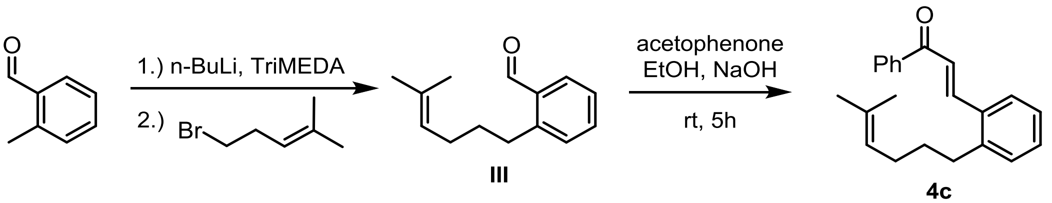

4c

An oven dried flask was fitted with an addition funnel and cooled under nitrogen. THF (24 mL) and *N,N,N'*-trimethyl ethylene-diamine (TriMEDA, 0.94 g, 9.1 mmol, 1.1 equiv.) were added to the flask and chilled to –20 °C, at which time 1.1 equiv. of *n*-BuLi (3.64 mL, 2.5M in hexane, 9.1 mmol) was added dropwise. After 15 minutes, 2-methylbenzaldehyde (1.00 g, 8.4 mmol, 1 equiv.) was added, followed 15 minutes later by 3 more equiv. of *n*-BuLi (11 mL, 2.5M in hexane, 24 mmol). The reaction mixture (0.3M with respect to 2-methylbenzaldehyde) turned dark orange and was stirred at –20 °C for 1.5 h. The reaction flask was then cooled to –65 °C followed by dropwise addition of 5-bromo-2-methyl-2-pentene (3.3 g, 20 mmol, 2.5 equiv.). The solution turned pale yellow upon being warmed slowly to room temperature. The reaction was quenched by pouring the reaction mixture into cold, stirred 1M HCl. The mixture was then extracted with diethyl ether (3 x 20 mL), and the combined organic layers were washed with brine, dried with $MgSO_4$ and concentrated *in vacuo*. The residue was then purified by reduced pressure distillation to give aldehyde **III** in 76% yield.

To a solution of aldehyde **III** (1.68 g, 8.3 mmol, 1 equiv.) and acetophenone (1.24 g, 10.3 mmol, 1.2 equiv.) in ethanol (16 mL) was added 2M aq. NaOH solution (0.8 mL, 1.6 mmol, 18 mol%) at room temperature. The reaction was followed by TLC with 10% ethyl acetate in hexane as the eluting solvent. After 5 hours, the reaction mixture was neutralized by addition of 2M aq. HCl solution. The resulting mixture was extracted with diethyl ether (3 x 20 mL). The combined organic layers were washed with brine, dried with anhydrous $MgSO_4$ and concentrated *in vacuo*. The residue was purified by flash chromatography on silica (3-5% EtOAc in hexanes) to give **4c** in 92% yield. ^{1}H NMR (400MHz, $CDCl_3$): δ (ppm) 8.14 (d, 1H, *J* = 15.5 Hz), 8.03 (d, 2H, *J* = 7.5 Hz), 7.71 (d, 1H, *J* = 8.0 Hz), 7.59 (t, 1H, *J* = 7.6 Hz), 7.53 (t, 2H, *J* = 8.0 Hz), 7.49 (d, 1H, *J* = 15.5 Hz), 7.35 (t, 1H, *J* = 6 Hz), 7.22-7.33 (m, 2H), 5.13 (t, 1H, *J* = 7.5 Hz), 2.79 (t, 2H, *J* = 7.6 Hz), 2.04 (q, 2H, *J* = 7.6 Hz), 1.69 (s, 3H), 1.63, (q, 2H, *J* = 7.5 Hz). ^{13}C NMR (100MHz, $CDCl_3$): δ (ppm) 190.7, 143.3, 138.5, 133.6, 132.9, 132.3, 130.4, 130.3, 128.8, 128.7, 126.74, 126.5, 124.1, 123.5, 33.1, 31.9, 27.9, 25.9, 17.9. IR [neat, ν_{max} (cm^{-1})]: 2926, 2855, 1662, 1592, 1481, 1446, 1329, 1212, 1178 cm^{-1}. HRMS (*m/z*): calculated for $[C_{22}H_{24}O]^+$, 304.1827; observed, 304.1824.

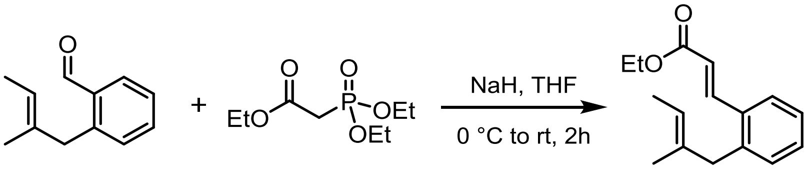

4d

Substrate **2b**: To a THF (5 mL) solution/suspension containing sodium hydride (95%, 31.2 mg, 1.30 mmol, 1.3 equiv) was added ethyl-(diethoxy-phosphoryl) acetate (270 mg, 1.20 mmol, 1.2 equiv) at 0 °C and the resulting mixture was stirred for 30 min. Aldehyde **I** (174 mg, 1.00 mmol, 1 equiv) was then added as a solution in THF (2 mL) and the resulting mixture was stirred at 0 °C for 30 min before being warmed to 25 °C and stirred for 1 h. The reaction was quenched with saturated aqueous NH_4Cl (10 mL) and the reaction mixture was extracted with diethyl ether (3 x 20 mL). The combined organic layers were washed with brine (20 mL), dried with $MgSO_4$ and concentrated *in vacuo*. The crude residue was then purified by silica chromatography (3% EtOAc in hexane) to give **2b** (228 mg, 0.93 mmol, 93% yield, >98% *trans* isomer) as a pale yellow oil: ^{1}H NMR (500 MHz, $CDCl_3$): δ (ppm) 8.00 (d, 1H, *J* = 15.5 Hz), 7.56 (d, 1H, *J* = 8.0 Hz), 7.30 (t, 1H, *J* = 7.0 Hz), 7.23 (t, 1H, *J* = 7.5 Hz), 7.18 (d, 1H, *J* = 7.5 Hz), 6.32 (d, 1H, *J* = 15.5 Hz), 5.13 (q, 1H, *J* = 6.5 Hz), 4.25 (q, 2H, *J* = 7.0 Hz), 3.42 (s, 2H), 1.61 (d, 3H, *J* = 6.5 Hz), 1.54 (s, 3H), 1.34 (t, 3H, *J* = 7.0 Hz); ^{13}C NMR (125 MHz, $CDCl_3$): δ (ppm) 167.2, 142.8, 139.9, 134.6, 134.1, 131.0, 130.0, 126.8, 126.7, 121.32, 119.4, 60.6, 43.1, 16.2, 14.5, 13.7. IR [neat, ν_{max} (cm^{-1})]: 2924, 1713, 1634, 1310, 1173, 1036, 980, 763 cm^{-1}. HRMS (*m/z*): calculated for $C_{16}H_{20}O_2$ 244.1463, found 244.1466.

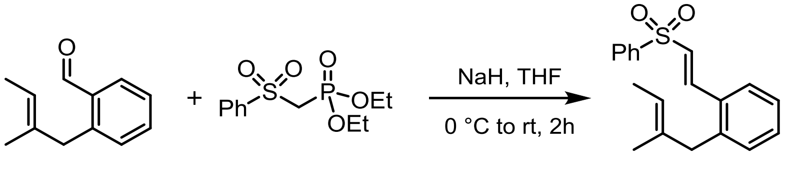

4e

Substrate **2c**: To a THF (10 mL) solution/suspension containing sodium hydride (95%, 62.5 mg, 2.60 mmol, 1.3 equiv) was added diethyl (phenylsulfonyl)-ethylphosphonate (652 mg, 2.40 mmol, 1.2 equiv) at 0 °C and the resulting mixture was stirred for 30 min. Aldehyde **I** (348 mg, 2.00 mmol, 1 equiv) was then added as a solution in THF (4 mL) and the resulting solution was stirred at 0 °C for 30 min before being warmed to 25 °C and stirred for 1 h. The reaction was quenched with saturated aqueous NH_4Cl (10 mL) and extracted with diethyl ether (3 x 20 mL). The combined organic layers were washed with brine (20 mL), dried with $MgSO_4$ and concentrated *in vacuo*. The crude residue was then purified by silica chromatography (5% EtOAc in hexane), followed by recrystallization from absolute ethanol to give **2c** (556 mg, 1.78 mmol, 89% yield) as a white solid: ^{1}H NMR (500 MHz, $CDCl_3$): δ (ppm) 7.96 (d, 1H, *J* = 15.5 Hz), 7.92 (d, 2H, *J* = 7.5 Hz), 7.61 (t, 1H, *J* = 7.5 Hz), 7.54 (t, 2H, *J* = 7.5 Hz), 7.45 (d, 1H, *J* = 7.5 Hz), 7.33 (t, 1H, *J* = 7.5 Hz), 7.21 (m, 2H), 6.73 (d, 1H, *J* = 15.5 Hz), 5.08 (q, 1H, *J* = 6.5 Hz), 3.43 (s, 2H), 1.58 (s, 3H) 1.55 (d, 3H, *J* = 6.5 Hz); ^{13}C NMR (125 MHz, $CDCl_3$): δ (ppm) 141.1, 140.9, 140.5, 134.6, 133.5, 132.0, 129.5, 128.2, 127.9, 127.1, 121.6, 115.2, 43.3, 16.3, 13.7. IR [neat, ν_{max} (cm^{-1})]: 1479, 1446, 1305, 1145, 1085, 1069, 748 cm^{-1}. HRMS (*m/z*): calculated for $C_{19}H_{20}O_2S$ 312.1184, found 312.1175.

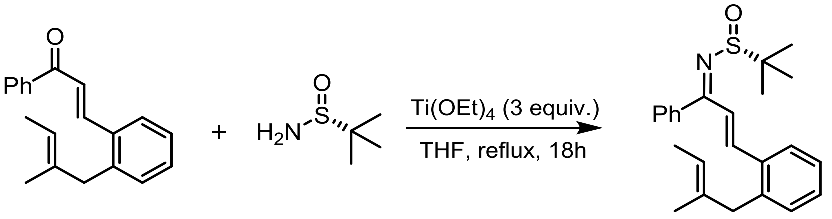

4f

Substrate **2d**: A flame-dried round bottom flask was fitted with a magnetic stir bar and cooled under a stream of nitrogen. The flask was charged with a THF solution (4 mL) containing **2a** (520 mg, 1.88 mmol, 1.2 equiv), (*R*)-(+)-2-methyl-2-propanesulfinamide (190 mg, 1.57 mmol, 1 equiv) and $Ti(OEt)_4$ (1.43 g, 6.28 mmol, 4 equiv). The resulting mixture was then heated to reflux and the reaction progress was monitored by TLC. After 18 h, the reaction was quenched with 5 mL of saturated aqueous $NaHCO_3$ and the resulting mixture was filtered through Celite with ethyl acetate. The aqueous layer was separated and extracted with ethyl acetate. The combined organic layers were washed with brine, dried with $MgSO_4$, filtered and concentrated *in vacuo*. The crude residue was purified by silica chromatography (5-10% EtOAc in hexane) to give **2d** (362 mg, 0.95 mmol, 61% yield) as a yellow oil: ^{1}H NMR (500 MHz, C_6D_6): δ (ppm) 8.62 (d, 1H, J = 16.0 Hz), 7.88 (d, 1H, J = 7.0 Hz), 7.56 (br d, 2H), 7.22 (d, 1H, J = 16.0 Hz), 7.11 (m, 3 H), 7.01 (t, 1H, J = 7.0 Hz), 6.97 (t, 1H, J = 7.0 Hz), 6.91 (d, 1H, J = 7.0 Hz), 4.76 (br q, 1H), 3.00 (s, 2H), 1.35 (d, 3H, J = 6.0 Hz), 1.31 (s, 3H), 1.29 (s, 9H); ^{13}C NMR (125 MHz, C_6D_6): δ (ppm) 175.3, 141.9, 140.2, 139.6, 135.7, 135.1, 131.6, 130.5, 130.2, 129.7, 128.9, 127.7, 127.4, 124.1, 121.1, 58.7, 43.7, 23.4, 16.4, 13.8. IR [neat, ν_{max} (cm^{-1})]: 2920, 1614, 1541, 1443, 1301, 1072, 753, 703 cm^{-1}. HRMS (*m/z*): calculated for $C_{24}H_{30}NOS$ 380.2043, found 380.2046.

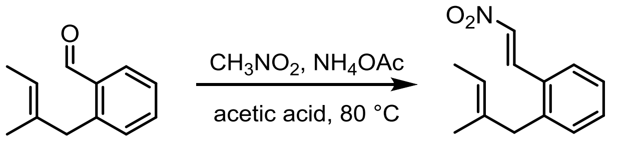

4g

Substrate **2e**: Aldehyde **I** (174 mg, 1.00 mmol, 1 equiv) and NH_4OAc (7.7 mg, 0.1 mmol, 10 mol%) were dissolved in nitromethane (1 mL) before glacial acetic acid (1 mL) was added. The resulting mixture was then heated to 80 °C. After 5 h, the mixture was quenched with 2 mL of water and the resulting mixture was extracted with diethyl ether (3 x 10 mL). The combined organic layer was then washed with brine, dried with $MgSO_4$, filtered and concentrated *in vacuo*. The residue was purified by silica chromatography (3% EtOAc in hexane) to give **2e** as a yellow oil in 73% yield: ^{1}H NMR (500 MHz, $CDCl_3$): 8.33 (d, 1H, J = 16.5 Hz), 7.51 (d, 1H, J = 8.0 Hz), 7.46 (d, 1H, J = 16.5 Hz), 7.42 (t, 1H, J = 8.0 Hz), 7.25-7.30 (m, 3H), 5.13 (q, 1H, J = 7.0 Hz), 3.44 (s, 2H), 1.58 (d, 3H, J = 7.0 Hz), 1.55 (s, 3H) ^{13}C NMR (125 MHz, $CDCl_3$): δ (ppm) 141.5, 137.7, 137.3, 134.4, 131.9, 131.7, 129.6, 127.5, 127.3, 121.9, 43.5, 16.3, 13.7. IR [neat, ν_{max} (cm^{-1})]: 2921, 1631, 1516, 1339, 1256, 1214, 964, 761 cm^{-1}. HRMS (*m/z*): calculated for $C_{13}H_{15}NO_2$ 217.1103, observed, 217.1097.

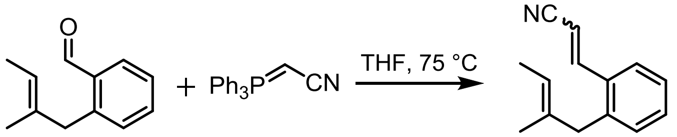

4h

Aldehyde **I** (174 mg, 1.00 mmol, 1 equiv) and (triphenylphosphoranyliden)-acetonitrile (362 mg, 1.20 mmol, 1.2 equiv) were dissolved in THF (2 mL) and heated to 75 °C. After 14 h, the solvent was removed *in vacuo* and the residue was purified by silica chromatography (2% EtOAc in hexane) to give the desired compound **4h** (146 mg, 0.74 mmol, 74%) as a mixture of *cis* and *trans* (2:3) isomers: ^{1}H NMR (400 MHz, $CDCl_3$): δ (ppm) 7.92 (d, 1H, J = 7.6 Hz, *cis* isomer), 7.64 (d, 1H, J = 16.5 Hz, *trans* isomer), 7.44 (d, 1H, J = 7.7 Hz, *trans* isomer), 7.39 (d, 1H, J = 12.0 Hz, *cis* isomer), 7.35-7.16 (m, *cis* and *trans* signals overlap), 5.74 (d, 1H, J = 16.5 Hz, *trans* isomer), 5.45 (d, 1H, J = 12.0 Hz, *cis* isomer), 5.03-4.96 (q and q, *cis* and *trans* signals overlap), 3.33 (s, 2H, *trans* isomer), 3.29 (s, 2H, *cis* isomer), 1.57 (s, 3H, *cis* and *trans* signals overlap), 1.55 (, 2, 3H, *cis* and *trans* signals overlap); ^{13}C NMR (100 MHz, $CDCl_3$): δ (ppm) 148.9 (*trans*), 148.1 (*cis*), 139.3 (*trans*), 139.2 (*cis*), 134.3 (*trans*), 134.1 (*cis*), 133.3 (*trans*), 133.1 (*cis*), 131.4 (*trans*), 130.9 (*trans*), 130.8 (*cis*), 130.6 (*cis*), 128.1 (*cis*), 127.1 (*trans*), 126.9 (*cis*), 125.8 (*trans*), 121.4 (*trans*), 121.2 (*cis*), 118.6 (*trans*), 117.3 (*cis*), 97.2 (*trans*), 96.9 (*cis*), 43.2 (*cis*), 42.9 (*trans*), 16.4 (*trans*), 16.3 (*cis*), 13.6 (*trans*), 13.5 (*cis*); (IR [neat, ν_{max} (cm^{-1})]: 2915, 2859, 2216, 1614, 1598, 1482, 1449, 963, 750 cm^{-1}. HRMS (*m/z*): calculated for *cis* isomer: $C_{14}H_{15}N$ 197.1204, found 197.1203; calculated for *trans* isomer: $C_{14}H_{15}N$ 197.1204, found 197.1201.

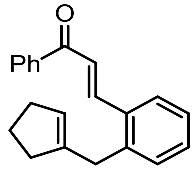

4i Compound **4i** was synthesized following the procedure outlined for **4a** with 1-bromomethylcyclopentene as the allylic bromide to give the desired compound in 75% yield over two steps as yellow oil: ^{1}H NMR (400 MHz, $CDCl_3$): δ (ppm) 8.07 (d, 1H, *J* = 15.6 Hz), 7.98 (d, 2H, *J* = 7.2 Hz), 7.72 (d, 1H, *J* = 6.8 Hz), 7.59 (t, 1H, *J* = 7.2 Hz), 7.50 (t, 2H, *J* = 7.2 Hz), 7.39 (d, 1H, *J* = 15.6 Hz), 7.35 (d, 1H, *J* = 6.0 Hz), 7.34-7.22 (m, 3H), 5.16 (br t, 1H), 3.52 (s, 2H), 2.28-2.24 (m, 4H), 1.86 (quintet, 2H, *J* = 7.6 Hz). ^{13}C NMR (100 MHz, $CDCl_3$): δ (ppm) 191.2, 143.4, 143.1, 140.6, 138.4, 134.1, 132.9, 131.0, 130.4, 128.8, 128.7, 126.9, 126.7, 126.4, 123.7, 35.8, 35.5, 32.6, 23.6. IR [neat, ν_{max} (cm^{-1})]: 2844, 1662, 1592, 1446, 1213, 1034, 751, 693 cm^{-1}. HRMS (*m/z*): calculated for $C_{21}H_{20}O$ 288.1514, found 288.1519.

Aldehyde precursor for **4i**: ^{1}H NMR (400 MHz, $CDCl_3$): δ (ppm) 10.26, (s, 1H), 7.87 (d, 1H, *J* = 7.6 Hz), 7.52 (t, 1H, *J* = 6.8 Hz), 7.37 (t, 1H, *J* = 7.2 Hz), 7.27 (d, 1H, *J* = 6.8 Hz), 5.12 (br t, 1H), 3.77, (s, 2H), 2.27 (t, 4H, *J* = 7.2 Hz), 1.87 (quintet, 2H, *J* = 7.2 Hz). ^{13}C NMR (100 MHz, $CDCl_3$): δ (ppm) 192.1, 144.0, 142.8, 134.1, 133.9, 131.4, 129.9, 126.8, 126.4, 35.4, 34.3, 32.5, 23.4. IR [neat, ν_{max} (cm^{-1})]: 2846, 1695, 1599, 1258, 1015 cm^{-1}. HRMS (*m/z*): calculated for $C_{13}H_{14}O$ 186.1045, found 186.1042.

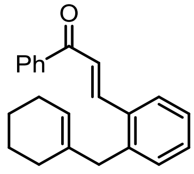

4j Compound **4j** was synthesized following the procedure outlined for **4a** with 1-bromomethylcyclohexene as the allylic bromide to give the desired compound in 68% yield over two steps as a pale yellow oil: ^{1}H NMR (400 MHz, $CDCl_3$): δ (ppm) 8.08 (d, 1H, *J* = 15.6 Hz), 7.99 (d, 2H, *J* = 8.0 Hz), 7.71 (d, 1H, *J* = 8.0 Hz), 7.59 (t, 1H, *J* = 7.2 Hz), 7.51 (t, 2H, *J* = 7.2 Hz), 7.39 (d, 1H, *J* = 15.6 Hz), 7.33 (d, 1H, *J* = 7.2 Hz), 7.30-7.22 (m, 3H), 5.25 (br t, 1H), 3.40 (s, 2H), 1.96-1.91 (m, 4 H), 1.63-1.52 (m, 4H). ^{13}C NMR (100 MHz, $CDCl_3$): δ (ppm) 191.3, 143.4, 140.5, 138.5, 136.8, 134.5, 132.8, 131.3, 130.3, 128.8, 128.5, 126.8, 126.7, 123.8, 123.7, 41.8, 28.9, 25.5, 23.1, 22.5. IR [neat, ν_{max} (cm^{-1})]: 2926, 1662, 1604, 1593, 1446, 1329, 1214, 1016, 979, 749, 693 cm^{-1}. HRMS (*m/z*): calculated for $C_{22}H_{22}O$ 302.1671, found 302.1676.

Aldehyde precursor for **4j**: ^{1}H NMR (400 MHz, $CDCl_3$): δ (ppm) 10.28 (s, 1H), 7.87 (d, 1H, *J* = 8.0 Hz), 7.51 (t, 1H, *J* = 8.0 Hz), 7.36 (t, 1H, *J* = 7.6 Hz), 7.26 (d, 1H, *J* = 7.2 Hz), 5.21 (br t, 1H), 3.65 (s, 2H), 1.96-1.94 (m, 4H), 1.65-1.50 (m, 4H); ^{13}C NMR (100 MHz, $CDCl_3$): δ (ppm) 192.3, 142.9, 137.7, 134.6, 133.9, 131.7, 129.8, 126.9, 124.0, 40.4, 29.0, 25.5, 23.1, 22.5. IR [neat, ν_{max} (cm^{-1})]: 2927, 2855, 1694, 1599, 1448, 1208, 751 cm^{-1}. HRMS (*m/z*): calculated for $C_{14}H_{16}O$ 200.1201, found 200.1204.

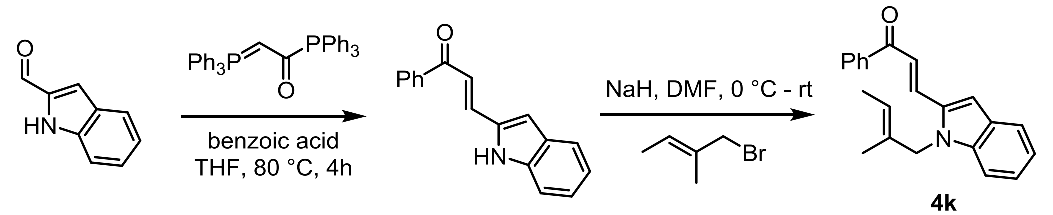

4k

Indole-2-carboxaldehyde (145 mg, 1.00 mmol, 1 equiv), the ylide (570 mg, 1.50 mmol, 1.5 equiv) and benzoic acid (146 mg, 1.20 mmol, 1.2 equiv) were dissolved in 2 mL of THF and loaded into a scintillation vial and sealed. The mixture was heated to 80 °C and the reaction progress was followed by TLC. After 4 h, solvent was evaporated *in vacuo* and the residue was purified by silica chromatography (10% EtOAc in hexane) to yield the desired enone (235 mg, 0.95 mmol, 95% yield) as a yellow solid.

To a DMF (2 mL) solution/suspension containing sodium hydride (24 mg, 1.0 mmol, 1.2 equiv) was added the enone (196 mg, 0.83 mmol, 1 equiv) at 0 °C and the resulting solution was stirred for 1 h. The allylic bromide (179 mg, 1.20 mmol, 1.2 equiv) was then added at 0 °C. The mixture was warmed to 25 °C and the reaction progress was followed by TLC. After 1.5 h, the reaction was quenched with 5 mL of water and extracted with diethyl ether (3 x 20 mL). The combined organic layers were washed with brine (20 mL), dried with $MgSO_4$ and concentrated *in vacuo*. The crude residue was then purified by chromatography (5% EtOAc in hexane) to give the desired product **4k** as a yellow oil (168 mg, 0.53 mmol, 64% yield), as well as the C3- and N-di-allylated side product (no yield was determined).

Substrate **4k**: ^{1}H NMR (400 MHz, $CDCl_3$): δ (ppm) 8.04 (d, 2H, *J* = 7.6 Hz), 7.92 (d, 1H, *J* = 15.2 Hz), 7.65 (d, 1H, *J* = 8.0 Hz), 7.60 (t, 2H, *J* = 8.0 Hz), 7.52 (t, 2H, *J* = 8.0 Hz), 7.32-7.24 (m, 2 H), 7.16 (s, 1H), 7.14 (t, 1H, *J* = 7.6 Hz), 5.12 (q, 1H, *J* = 6.4 Hz), 4.77 (s, 2H), 1.61 (s, 3H), 1.57 (d, 3H, *J* = 6.4 Hz). ^{13}C NMR (100 MHz, $CDCl_3$): δ (ppm) 189.9, 139.5, 138.5, 136.0, 133.2, 132.9, 131.4, 128.8, 128.6, 127.7, 124.1, 121.9, 121.7, 120.9, 120.8, 110.4, 104.4, 50.5, 14.2, 13.3. IR [neat, ν_{max} (cm^{-1})]: 2924, 1655, 1588, 1447, 1350, 1284, 1219, 1016, 774, cm^{-1}. HRMS (*m/z*): calculated for $C_{22}H_{21}NO$ 315.1623, found 315.1623.

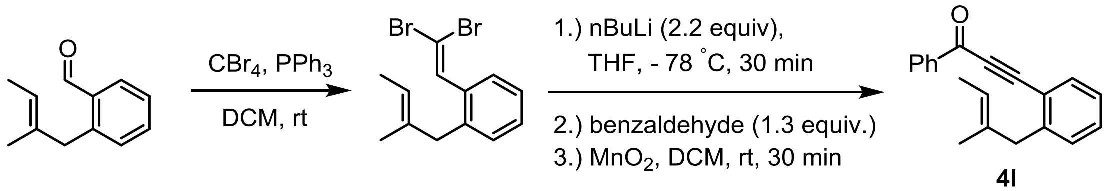

4l

Aldehyde **I** (1.0 g, 5.74 mmol, 1 equiv.) and CBr_4 (2.28 g, 6.86 mmol, 1.2 equiv.) were dissolved in dichloromethane (20 mL) and cooled to 0 °C. To this solution was then added triphenylphosphine (3.0 g, 11.5 mmol, 2 equiv.) as a DCM solution (10 mL) dropwise at 0 °C. The resulting solution was then warmed to room temperature and the reaction progress was followed by TLC. After 2 h, the reaction was quenched by dilution with petroleum ether (40 mL) and the resulting heterogeneous solution was filtered through a silica plug. The filtrate was then concentrated and the crude residue was purified by silica chromatography to give the dibromide (1.47 g, 4.46 mmol) as a pale yellow oil in 78% yield.

The dibromide (736 mg, 2.23 mmol, 1 equiv.) was dissolved in THF (10 mL) and cooled to – 78 °C, followed by addition of nBuLi (2.5 M solution in hexane, 1.9 mL, 4.48 mmol, 2.1 equiv.) and the resulting solution was stirred for 1 hour. Benzaldehyde (354 mg, 3.35 mmol, 1.5 equiv.) was then added and the cold bath was removed. After 1 hour, the reaction mixture was diluted with 0.1 M HCl solution (10 mL) and the resulting mixture was extracted with diethyl ether (3x20 mL). The organic layers were combined, washed with brine, dried with $MgSO_4$ and filtered. Solvent was then removed and the resulting residue was dissolved in DCM (10 mL), followed by addition of MnO_2 (2 g, 23 mmol, 10 equiv.). The resulting heterogeneous solution was stirred for 30 minuntes at room temperature and then filtered. The resulting solution was then concentrated *in vacuo* and the residue was purified by silica chromatography (2% to 5% EtOAc in hexanes) to give the desired compound **4l** in 75% yield as a pale yellow oil. ^{1}H NMR (500 MHz, $CDCl_3$) δ(ppm) 8.22 (d, *J* = 7.7 Hz, 2H), 7.65 (m, 2H), 7.52 (t, *J* = 7.7 Hz, 2H), 7.41 (t, *J* = 7.6 Hz, 1H), 7.30 – 7.24 (m, 3H), 5.24 (q, *J* = 6.7 Hz, 1H), 3.60 (s, 2H), 1.64 (s, 3H), 1.58 (d, *J* = 6.7 Hz, 3H). ^{13}C NMR (125 MHz, $CDCl_3$) δ (ppm) 178.0, 144.4, 137.1, 134.0, 133.9, 130.8, 129.7, 129.6, 128.7, 128.1, 126.3, 121.3, 120.3, 92.4, 90.4, 44.1, 16.1, 13.6. IR [neat, νmax (cm^{-1})]: 2191, 1638, 1597, 1448, 1315, 1286, 1213, 1009, 698. HRMS (m/z): calculated for $C_{20}H_{18}O$, 274.1358 found 274.1353.

2.4.4. Stepwise C-H Functionalization of 4a and 4b

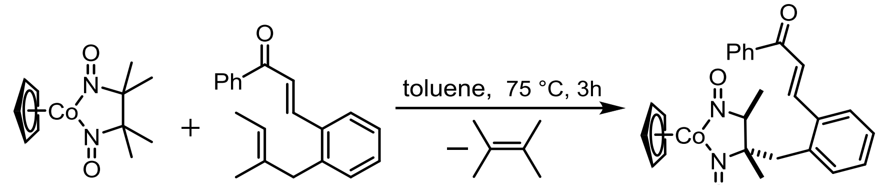

5 **4a** **6a**

An oven-dried round bottom flask was fitted with a septum and cooled under nitrogen. A toluene solution (2 mL) containing complex **5** (58.0 mg, 0.18 mmol, 1 equiv) and **4a** (515 mg, 1.86 mmol, 10 equiv.) were then added to the flask. A nitrogen needle inlet and a needle outlet were then pierced through the septum as a way to “bleed-out” tetramethylethylene during the reaction. The reaction flask was then immersed in a 75 °C oil bath. The reaction progress was monitored by TLC, with 10% ethyl acetate in hexane as the eluting solvent. Heating was stopped upon significant observation of cobalt complex decomposition on TLC, as an immovable dark brown spot (e.g. 2.5-3 h). The reaction mixture was allowed to cool to room temperature before loading the entire mixture directly onto a silica gel column packed with hexane. The desired product was isolated with 10% ethyl acetate in hexane as the eluting solvent. Complex **6a** (58.2 mg, 0.120 mmol, 65% yield) was isolated as a purple, crystalline solid and was used immediately due to instability of the adduct: ^{1}H NMR (400 MHz, $CDCl_3$): δ (ppm) 8.05-7.93 (m, 3H), 7.66 (t, 1H, *J* = 8.0 Hz), 7.60 (d, 1H, *J* = 8.0 Hz), 7.52 (t, 2H, *J* = 8.0 Hz), 7.44 (d, 1H, *J* = 16 Hz), 7.30-7.26 (m, 2H), 7.10 (d, 1H, *J* = 8.0 Hz), 4.87 (s, 5H), 3.29 (d, 1H, *J* = 16 Hz), 3.05 (d, 1H, *J* = 16 Hz), 2.87 (q, 1H, *J* = 8.0 Hz), 1.20 (s, 3H), 1.09 (d, 3H, *J* = 8.0 Hz). ^{13}C NMR (100 MHz, $CDCl_3$): δ (ppm) 190.1, 142.4, 138.2, 136.4, 135.2, 133.2, 132.7, 130.0, 128.9, 128.8, 127.8, 127.0, 124.2, 92.9, 90.4, 90.2, 41.4, 22.2, 17.1. IR [neat, ν_{max} (cm^{-1})]: 2922, 1661, 1603, 1424, 1406, 1371, 1356, 1261, 1213, 1180, 1114, 1051, 1016 cm^{-1}. HRMS (*m*/*z*): calculated for $C_{25}H_{24}O_3N_2Co$ [M-H] 459.1113, found 459.1119.

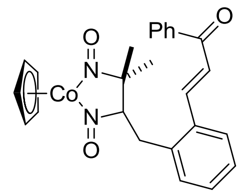

Complex **6b** was synthesized according to procedure for **6a** and isolated as a dark brown solid in 58% yield. ^{1}H NMR (400MHz, $CDCl_3$): δ (ppm) 8.05-7.93 (m, 3H), 7.66 (t, 1H, J = 8.0 Hz), 7.60 (d, 1H, J = 8.0 Hz), 7.52 (t, 2H, J = 8.0 Hz), 7.44 (d, 1H, J = 16 Hz), 7.30-7.26 (m, 2H), 7.10 (d, 1H, J = 8.0 Hz), 4.87 (s, 5H), 3.29 (d, 1H, J = 16 Hz), 3.29 (d, 1H, J = 8.0 Hz), 3.05 (d, 1H, J = 8.0 Hz), 2.87 (q, 1H, J = 8.0 Hz), 1.20 (s, 3H), 1.09 (d, 3H, J = 8.0 Hz). ^{13}C NMR (100MHz, $CDCl_3$): δ (ppm) 190.1, 142.4, 138.2, 136.4, 135.2, 133.2, 132.7, 130.0, 128.9, 128.8, 127.8, 127.0, 124.2, 92.9, 90.4, 90.2, 41.4, 22.2, 17.1. IR [neat, ν_{max} (cm^{-1})]: 2922, 1661, 1603, 1424, 1406, 1371, 1356, 1261, 1213, 1180, 1114, 1051, 1016 cm^{-1}. HRMS (*m*/*z*): calculated for $[C_{25}H_{25}O_3N_2Co–H]^+$, 459.1113; observed, 459.1119.

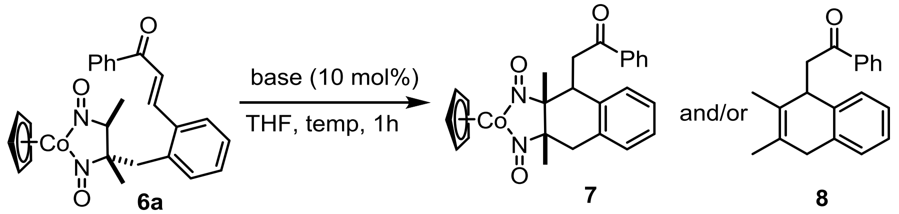

Cobalt complex **6a** was dissolved in THF to make a 0.2 M solution in the dry-box and the resulting solution was loaded into a Schlenk tube. The base (10 mol%), either Verkade's base or *t*BuOK, was dissolved in THF to make a 0.02 M solution and combined with the complex to make an overall 0.1 M solution with respect to **3**. The Schlenk tube was then sealed with a Teflon screw cap and transferred out of the box. The solution was either stirred at room temperature or heated to 75 °C for 1 h.

For reactions at –78 °C, cobalt complex **6a** was dissolved in THF to make a 0.2 M solution inside a glove box, loaded into a Schlenk tube and sealed. In a separate Schlenk tube, the base (10 mol%) was dissolved in THF to make a 0.02 M solution and sealed. Both flasks were transferred outside the box to the bench. The cobalt complex **3** solution was cooled to –78 °C in a dry ice-acetone bath. The base solution was then transferred to the solution of **3** via cannulation technique under a stream of nitrogen to make an overall 0.1 M solution with respect to **3**, and the combined mixture was stirred at – 78 °C for 1 h.

All reactions were monitored by TLC by taking aliquots of the reaction mixtures under a stream of nitrogen. The reactions were quenched by filtering the reaction mixtures through a plug of silica packed with hexane and eluted with ethyl acetate. Solvents were removed *in vacuo.* The residues were purified by silica chromatography (5-10% EtOAC in hexane) to afford the desired products; complex **4** is more polar than **5a.**

Cobalt complex **7:** isolated as a purple, crystalline solid and is rather unstable. ^{1}H NMR (500 MHz, $CDCl_3$): δ (ppm) 7.97, (d, 2H, J = 7.2 Hz), 7.59 (t, 1H, J = 7.2 Hz), 7.49 (t, 2H, J = 7.2 Hz), 7.11-7.01 (m, 3H), 6.89 (d, 1H, J = 6.8 Hz), 4.73 (s, 5H), 3.64-3.58 (m, 2H), 3.34 (dd, 1H, J = 10.4, 8.0 Hz), 3.27 (d, 1H, J = 15.2 Hz), 2.80 (d, 1H, J = 15.2 Hz), 1.33 (s, 3H), 1.30 (s, 3H). ^{13}C NMR (125 MHz, $CDCl_3$): δ (ppm) 198.0, 137.6, 137.1, 134.9, 133.5, 128.9, 128.3, 128.2, 127.1, 126.2, 95.5, 95.2, 90.1, 44.4, 41.7, 37.1, 25.8, 22.7. IR [neat, ν_{max} (cm^{-1})]: 2923, 2851, 1685, 1419, 1372, 1351, 1260, 1211, 807, 749 cm^{-1}. HRMS (*m*/*z*): calculated for $[C_{25}H_{26}O_3N_2Co]^+$ 461.1270, found 461.1276.

Compound **8:** isolated as a pale yellow oil: ^{1}H NMR (500 MHz, $CDCl_3$): δ (ppm) 7.82 (d, 2H, *J* = 8.0 Hz), 7.50 (t, 1H, *J* = 7.5 Hz), 7.38 (t, 2H, *J* = 7.5 Hz), 7.18 (d, 1H, *J* = 7.5 Hz), 3.98 (m, 1H), 3.44 (d, 1H, *J* = 20.0 Hz), 3.17-3.10 (m, 3H), 1.80 (s, 3H), 1.79 (s, 3H). ^{13}C NMR (125 MHz, $CDCl_3$): δ (ppm) 199.9, 139.7, 135.9, 133.0, 128.6, 128.4, 128.3, 127.9, 127.7, 126.9, 126.1, 115.2, 44.9, 43.5, 36.9, 19.3, 17.9. IR [neat, ν_{max} (cm^{-1})]: 2913, 2856, 1730, 1682, 1596, 1579, 1490, 1447, 1344, 1261, 1216, 746, 689 cm^{-1}. HRMS (*m*/*z*): no parent ion was observed, only $[M\text{-}H_2]^+$ and $[M\text{-}C_8H_8O]^+$ were observed.

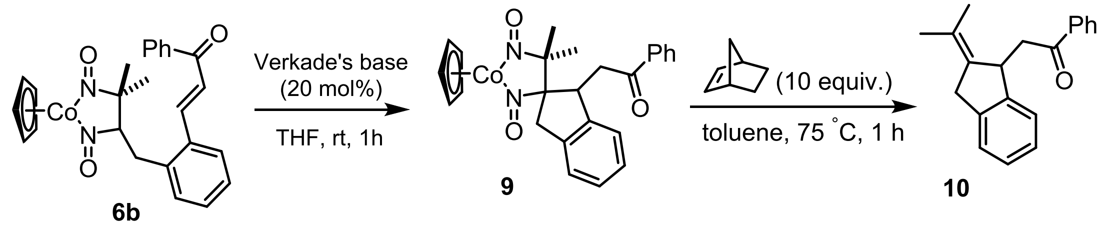

In a vial inside the glove-box, complex **6b** (46 mg, 0.10 mmol, 1 equiv.) and Verkade's base (4.32 mg, 0.02 mmol, 20 mol%) were dissolved in THF (1.0 mL). The resulting solution was sealed and taken out to the bench. The reaction progress was followed by TLC, (15% EtOAc in hexanes). After 1 h, solvent was removed, and the resulting residue was purified by silica chromatography (15% EtOAc in hexanes) to give cobalt complex **9** (26 mg, 0.057 mmol) as a dark brown solid in 59% yield. ^{1}H NMR (500MHz, $CDCl_3$): δ (ppm) 7.93 (d, 2H, *J* = 7.5 Hz), 7.59 (t, 1H, *J* = 7.5 Hz), 7.49 (t, 2H, *J* = 8.0 Hz), 7.15 (d, 2H, *J* = 7.5 Hz), 7.04 (t, 1H, *J* = 8.0 Hz), 6.85 (d, 1H, *J* = 7.5 Hz), 4.87 (s, 5H), 4.00 (dd, 1H, *J* = 8.75, 3.5 Hz), 3.69 (d, 1H, *J* = 16.5 Hz), 3.49 (dd, 1H, *J* = 18.0, 3.5 Hz), 3.14 (dd, 1H, *J* = 9.0, 9.0 Hz), 2.93 (d, 1H, *J* = 16.5 Hz), 1.25 (s, 3H), 1.24 (s, 3H). ^{13}C NMR (125MHz, $CDCl_3$): δ (ppm) 197.8, 142.9, 139.7, 137.2, 133.6, 128.9, 128.2, 127.5, 127.1, 123.6, 123.5, 105.4, 95.2, 90.0, 45.7, 41.3, 37.2, 30.4, 21.1. IR [neat, vmax (cm^{-1})]: 2978, 1683, 1596, 1429, 1385, 1355, 1303, 1144 cm^{-1}. HRMS (m/z): calculated for $[C_{25}H_{25}O_3N_2Co]^+$, 460.1192; observed, 460.1201.

Complex **9** (26 mg, 0.057 mmol, 1 equiv.) and norbornene (53 mg, 0.57 mmol, 10 equiv.) were dissolved in toluene (1.0 mL) and the resulting solution was loaded into a vial, sealed and then heated at 75 °C for 1 h. The solvent was then removed and the resulting residue was purified by silica chromatography to give **10** (15 mg, 0.054 mmol) in 95% yield as a white solid. ^{1}H NMR (500MHz, $CDCl_3$): δ (ppm) 7.91 (d, 2H, J = 7.5 Hz), 7.53 (t, 1H, J = 7.5 Hz), 7.42 (t, 2H, J = 8.0 Hz), 7.24 (d, 1H, J = 8.0 Hz), 7.14 (t, 1H, J = 7.0 Hz), 7.07 (t, 1H, J = 7.5 Hz), 4.62 (dd, 1H, J = 6.0, 4.0 Hz), 3.64 (dd, 2H, J = 20.5, 10.0 Hz), 3.29 (dd, 1H, J = 17.0, 9.0 Hz), 3.23 (dd, 1H, J = 17.0, 4.0 Hz), 1.75 (s, 3H), 1.73 (s, 3H). ^{13}C NMR (125MHz, $CDCl_3$): δ (ppm) 199.4, 146.8, 141.8, 137.5, 135.8, 133.1, 128.7, 128.3, 126.9, 126.6, 125.3, 124.9, 124.7, 46.0, 43.3, 36.6, 21.5, 20.8. IR [neat, vmax (cm^{-1})]: 2909, 2866, 1683, 1596, 1478, 1459, 1402, 1346 cm^{-1}. HRMS (m/z): calculated for $[C_{20}H_{20}ONa]^+$, 299.1406; observed, 299.1398.

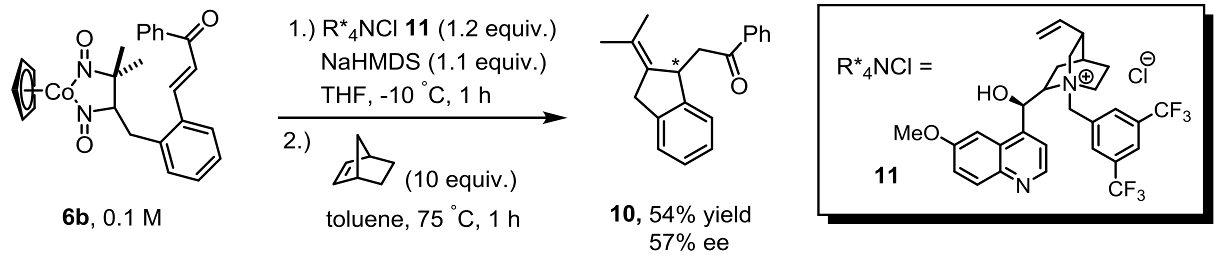

To a flame-dried microwave tube was added complex **6a** (35 mg, 0.076 mmol, 1 equiv.) in THF (0.5 mL) inside a glovebox, sealed and cooled to – 10 °C. To a different flame-dried microwave tube was added the cinchona alkaloid salt (49 mg, 0.084 mmol, 1.1 equiv.) in THF (0.3 mL), followed by addition of NaHMDS (17 mg, 0.091 mmol, 1.2 equiv.), where upon addition an instant color change occurred, from pale yellow to dark purple. This tube was then sealed inside the box, brought to the bench and the chiral base solution was added to the solution containing **6a** in one portion at – 10 °C (0.1 M solution). The resulting mixture was stirred at – 10 °C and the progress of the reaction was monitored by TLC. After 1h, **6a** appeared to be consumed. Solvent was then removed, and the crude residue was purified by silica chromatography to yield enantioenriched complex **9** (20 mg, 0.043 mmol) in 57% yield.

Complex **9** (20 mg, 0.043 mmol, 1 equiv.) and norbornene (40 mg, 0.43 mmol, 10 equiv.) were dissolved in toluene (1.0 mL) and the resulting solution was loaded into a vial, sealed and then heated at 75 °C for 1 h. The solvent was then removed and the resulting residue was purified by silica chromatography to give **10** (11 mg, 0.041 mmol) in 95% yield as a white solid. Its spectroscopic data are in agreement with previously isolated racemic compound **10**. Enantiomeric excess was determined by HPLC analysis: (Chiralpak **AD-H column**, 99:01 hexanes/isopropanol 1.0 mL/minute, 57% ee.)

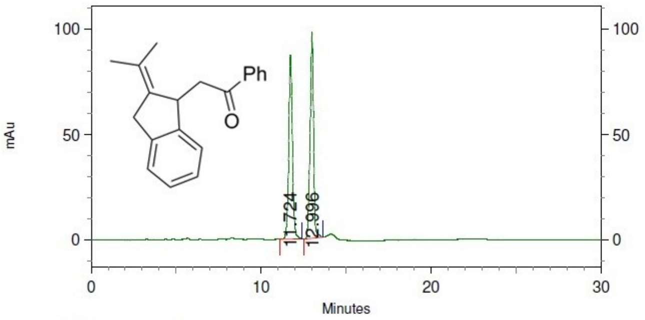

```
3: 244 nm, 4
nm Results
 Retention Time           Area   Area Percent    Lambda Max
         11.724        1325200         49.085           266
         12.996        1374614         50.915           267
```

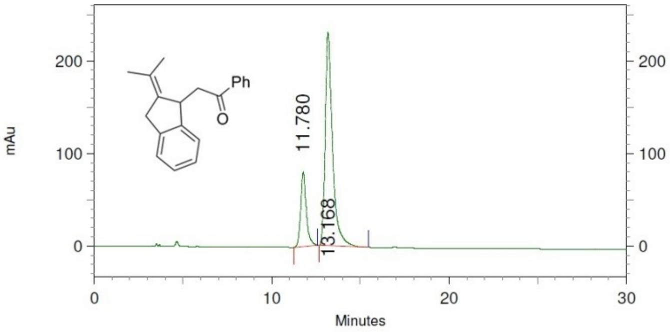

```
3: 244 nm, 4
nm Results
 Retention Time           Area   Area Percent    Lambda Max
         11.780        1754293         21.155           266
         13.168        6538179         78.845           267
```

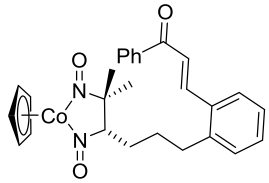

Complex 6**c** was synthesized according to procedure for complex **6a** and isolated as a dark brown solid in 89% yield. ^{1}H NMR (400MHz, CDCl$_3$): δ (ppm) 8.10 (d, 1H, *J* = 16.0 Hz), 8.04 (d, 2H, *J* = 8.0 Hz), 7.7 (d, 1H, *J* = 8.0 Hz), 7.59 (t, 1H, *J* = 8.0 Hz), 7.51 (t, 2H, *J* = 8.0 Hz), 7.43 (d, 1H, *J* = 16.0 Hz), 7.34 (t, 1H, *J* = 8.0 Hz), 7.26 (t, 1H, *J* = 8.0 Hz), 7.21 (d, 1H, *J* = 8.0 Hz), 4.88 (s, 5H), 2.80-2.75 (m, 3H), 1.72-1.65 (m, 3H), 1.63-1.59 (m, 1H), 1.27 (s, 3H), 1.21 (s, 3H). ^{13}C NMR (100MHz, CDCl$_3$): δ (ppm) 190.4, 142.2, 138.4, 133.7, 133.1, 130.6, 130.3, 128.9, 128.7, 126.9, 123.6, 97.6, 90.3, 89.9, 33.2, 31.1, 28.9, 28.3, 21.9. IR [neat, νmax (cm^{-1})]: 2927, 1661, 1591, 1447, 1355, 1214, 1179, 1033 cm^{-1}. HRMS (m/z): calculated for [$C_{27}H_{29}O_3N_2Co$]+, 488.1505; observed, 488.1517.

2.4.5. One-pot Reactions

General procedure 1: In a dry-box, cobalt complex **1** (32.0 mg, 0.12 mmol, 1.2 equiv), substrate (0.1 mmol, 1 equiv), and P$_1$-*t*Bu phosphazene base (4.68 mg, 0.02 mmol, 20 mol%) were dissolved in 0.3 mL of benzene, loaded into a microwave tube and sealed. The mixture was heated to 75 °C in an oil bath and stirred for 24 h. The microwave tube was then opened to air and the reaction mixture was filtered through a plug of silica with 20% EtOAc in hexane as the eluent. Solvent was evaporated *in vacuo* to give the crude mixture. Yields were determined by ^{1}H NMR analysis of the crude mixture with 1,3,5-trimethoxybenzene as the internal standard.

General procedure 2: In a dry-box, cobalt complex **1** (32.0 mg, 0.12 mmol, 1.2 equiv), substrate (0.1 mmol, 1 equiv), and P$_1$-*t*Bu phosphazene base (23.4 mg, 0.10 mmol, 1 equiv) were dissolved in 0.3 mL of benzene, loaded into a microwave tube and sealed. The mixture was heated to 75 °C in an oil bath and stirred for 12 h. An additional equivalent of **1** (27.0 mg, 0.10 mmol, 1 equiv) was then added to the reaction mixture in a dry-box, and the microwave tube was resealed and heated to 75 °C for another 24 h. The microwave tube was opened to air and the reaction mixture was filtered through a plug of silica with 20% EtOAc in hexane as the eluent. Solvent was evaporated *in vacuo* to give the crude mixture. Yields were determined by ^{1}H NMR analysis of the crude mixture with 1,3,5-trimethoxybenzene as the internal standard.

General procedure 3: In a dry-box, cobalt complex **1** (32.0 mg, 0.12 mmol, 1.2 equiv), norbornene (9.40 mg, 0.10 mmol, 1 equiv), enone (0.20 mmol, 2 equiv) and P$_1$-*t*Bu phosphazene base (2.34 mg, 0.01 mmol, 10 mol%) were dissolved in 0.3 mL of benzene, loaded into a microwave tube and sealed. The mixture was heated to 95 °C in an oil bath and stirred for 24 h. The microwave tube was then opened to air and the reaction mixture was filtered through a plug of silica with 20% EtOAc in hexane as the eluent. Solvent was evaporated *in vacuo* to give the crude residue, which was then purified by silica chromatography to give the desired product.

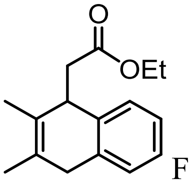

Following general procedure 2: compound **8b** and substrate **4d** were inseparable, therefore for characterization purposes, 2 additional equivalents of cobalt complex **1** were used to convert all of **4d** to the product. Compound **8b** was obtained as a pale yellow oil: ^{1}H NMR (500 MHz, CDCl$_3$): δ (ppm) 7.18-7.13 (m, 4H), 4.17 (q, 2H, *J* = 6.5 Hz), 3.80 (br t, 1H), 3.53 (d, 1H, *J* = 18.5 Hz), 3.25 (d, 1H, *J* = 19.5 Hz), 2.70 (dd, 1H, *J* = 13.8, 4.5 Hz), 2.48 (dd, 1H, *J* =

14.0, 8.5 Hz), 1.99 (s, 3H), 1.96 (s, 3H), 1.38 (t, 3H, J = 6.5 Hz). ^{13}C NMR (125 MHz, CDCl$_3$): δ (ppm) 172.7, 139.0, 136.0, 127.7, 127.6, 127.5, 127.0, 126.2, 126.0, 60.5, 44.3, 40.9, 36.8, 19.3, 17.7, 14.4. IR [neat, $\nu_{\max}$ (cm^{-1})]: 2921, 1732, 1457, 1262, 1154, 1039, 754 cm^{-1}. Low-resolution GC-MS shows [M-H$_2$], and a high-resolution mass spectrum could not be obtained.

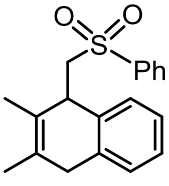

Following general procedure 2: compound **8c** was isolated by silica chromatography (0.5% to 1% EtOAc in hexane) as a white solid: ^{1}H NMR (500 MHz, CDCl$_3$): δ (ppm) 7.85 (d, 2H, J = 7.5 Hz), 7.59 (t, 1H, J = 7.5 Hz), 7.50 (t, 2H, J = 7.5 Hz), 7.32 (t, 1H, J = 5.0 Hz), 7.14-7.11 (m, 3H), 3.93 (br t, 1H), 3.34 (d, 1H, J = 19.5 Hz), 3.23 (d, 2H, J = 5.5 Hz), 3.11 (d, 1H, J = 20.0 Hz), 1.80 (s, 3H), 1.76 (s, 3H). ^{13}C NMR (100 MHz, CDCl$_3$): δ (ppm) 140.7, 137.5, 136.2, 133.6, 129.4, 128.9, 128.4, 127.9, 127.6, 127.0, 126.7, 126.3, 115.2, 61.3, 41.8, 36.9, 19.4, 17.6. IR [neat, $\nu_{\max}$ (cm^{-1})]: 2916, 1446, 1319, 1305, 1145, 1086, 756, 688 cm^{-1}. HRMS (m/z): calculated for [$C_{19}H_{20}O_2SNa$]$^+$ 335.1076, found 335.1079.

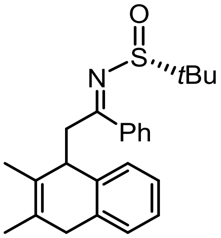

Following general procedure 1, the reaction gave two diastereomers of **8d** in 2.8:1 ratio. The two diastereomers were separated by chromatography (1% EtOAc in hexane).

Major diastereomer: ^{1}H NMR (500 MHz, CDCl$_3$): δ (ppm) 7.81 (d, 2H, J = 7.2 Hz), 7.49-7.40 (m, 3H), 7.15-7.08 (m, 2H), 6.98 (t, 1H, J = 7.2 Hz), 6.78 (d, 1H, J = 7.2 Hz), 3.67-3.61 (m, 3H), 3.28 (dd, 1H, J = 12.2, 4.7 Hz), 3,14 (d, 1H, J = 19.7 Hz), 1.86 (s, 3H), 1.79 (s, 3H), 1.18 (s, 9H). ^{13}C NMR (125 MHz, CDCl$_3$): δ (ppm) 178.7, 138.5, 138.1, 137.0, 131.5, 128.7, 128.5, 128.3, 128.1, 127.8, 127.6, 127.4, 126.3, 125.7, 57.6, 47.0, 37.0, 29.9, 22.9, 19.4, 18.1. IR [neat, $\nu_{\max}$ (cm^{-1})]: 2921, 1601, 1567, 1445, 1360, 1283, 1180, 1073, 752, 691 cm^{-1}. HRMS (m/z): calculated for [$C_{24}H_{30}NOS$]$^+$ 380.2043, found 380.2047.

Minor diastereomer: ^{1}H NMR (500 MHz, CDCl$_3$): δ (ppm) 7.64 (d, 2H, J = 7.2 Hz), 7.42 (t, 1H, J = 7.2 Hz), 7.33 (t, 2H, J = 7.7 Hz), 7.19-7.01 (m, 4H), 3.79 (t, 1H, J = 7.1 Hz), 3.71-3.66 (m, 1H), 3.59 (d, 1H, J = 19.7 Hz), 3.14 (dd, 2H, J = 19.8, 5.2 Hz), 1.74 (s, 6H), 1.29 (s, 9H). ^{13}C NMR (125 MHz, CDCl$_3$): δ (ppm) 178.3, 139.2, 139.0, 136.6, 131.3, 128.5, 128.4, 128.2, 127.7, 127.6, 127.3, 126.2, 126.1, 58.2, 47.2, 37.0, 29.9, 23.1, 19.3, 18.5. IR [neat, $\nu_{\max}$ (cm^{-1})]: 2921, 2858, 1589, 1566, 1445, 1282, 1075, 753, 690 cm^{-1}. HRMS (m/z): calculated for [$C_{24}H_{29}NOSNa$]$^+$ 402.1862, found 402.1867.

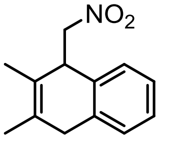

Following general procedure 1 with only 10 mol% of P$_1$-*t*Bu phosphazene base, compound **8e** was isolated by preparative TLC (1% EtOAc in hexane) as a pale yellow oil: ^{1}H NMR (500 MHz, CDCl$_3$): δ (ppm) 7.28-7.18 (m, 3H), 7.10 (d, 1H, J = 7.2 Hz), 4.46 (d, 1H, J = 6.5 Hz), 4.25 (t, 1H, J = 9.1 Hz), 4.01 (br t, 1H), 3.42 (d, 1H, J = 20.4 Hz), 3.19 (d, 1H, J = 20.4 Hz), 1.88 (s, 3H), 1.83 (s, 3H). ^{13}C NMR (125 MHz, CDCl$_3$): δ (ppm) 135.9, 134.9, 130.6, 128.0, 127.4 (overlapping peaks), 126.6, 123.5, 79.3, 46.9, 36.7, 19.5, 17.8. IR [neat, ν_{max} (cm^{-1})]: 2916, 2849, 1548, 1374, 908, 752, 728 cm^{-1}. HRMS (*m*/*z*): calculated for $C_{13}H_{15}NO_2$ 217.1102, found 217.1097.

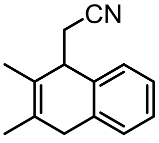

Following general procedure 2, compound **8f** was isolated by silica chromatography (5% EtOAc in hexane) as a pale yellow oil: ^{1}H NMR (400 MHz, CDCl$_3$): δ (ppm) 7.18-7.26 (m, 4H), 3.50-3.60 (m, 2H), 3.17 (d, 1H, *J* = 20.8 Hz), 2.59 (m, 2H), 1.87 (s, 3H), 1.84 (s, 3H); ^{13}C NMR (100 MHz, CDCl$_3$): δ (ppm) 136.3, 135.9, 129.4, 128.1, 127.6, 127.1, 126.5, 124.8, 118.7, 43.9, 36.7, 24.8, 19.4, 17.7. IR [neat, ν_{max} (cm^{-1})]: 2917, 2246, 1494, 1457, 1421, 755, 736 cm^{-1}. HRMS (*m*/*z*): calculated for $C_{14}H_{15}N$ 197.1204, found 197.1207.

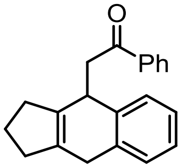

Following general procedure 1, compound **8g** was isolated by silica chromatography (1-2% EtOAc in hexane) as a pale yellow oil: ^{1}H NMR (400 MHz, CDCl$_3$): δ (ppm) 7.87 (d, 2H, *J* = 8.0 Hz), 7.53 (t, 1H, *J* = 7.4 Hz), 7.41 (t, 2H, *J* = 7.4 Hz), 7.25 (m, 1H), 7.12-7.18 (m, 3H), 4.25 (br t, 1H), 3.43 (d, 1H, *J* = 24.4 Hz), 3.26-3.45 (m, 2H), 3.18 (dd, 1H, *J* = 16.4, 5.6 Hz), 2.34-2.43 (m, 4 H), 1.89 (m, 2H). ^{13}C NMR (100 MHz, CDCl$_3$): δ (ppm) 199.6, 139.5, 137.6, 136.0, 135.3, 134.3, 133.1, 128.9, 128.7 (overlapping peaks), 128.4, 126.4, 126.2, 46.7, 37.2, 35.9, 34.8, 31.4, 22.5. IR [neat, ν_{max} (cm^{-1})]: 2889, 2841, 1683, 1447, 1265, 1208, 751, 689. HRMS (*m*/*z*): calculated for $C_{21}H_{20}O$ 288.1513, found 288.1491.

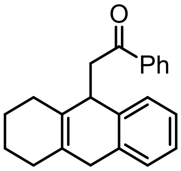

Following general procedure 1, compound **8h** was isolated by preparative TLC (0.5% EtOAc in hexane) as a pale yellow oil: ^{1}H NMR (400 MHz, CDCl$_3$): δ (ppm) 7.82 (d, 2H, *J* = 7.2 Hz), 7.49 (t, 1H, *J* = 7.6 Hz), 7.39 (t, 2H, *J* = 7.6 Hz), 7.19 (d, 1H, *J* = 7.2 Hz), 7.14-7.06 (m, 3H), 3.89 (br t, 1H), 3.39 (d, 1H, *J* = 19.6 Hz), 3.15-2,98 (m, 3H), 2.13-2.01 (m, 4H), 1.66-1.55 (m, 4H). ^{13}C NMR (100 MHz, CDCl$_3$): δ (ppm) 200.1, 139.9, 137.6, 135.9, 133.1, 131.1, 129.2, 128.6, 128.4, 128.1, 127.9, 126.1, 126.0, 45.2, 42.6, 35.9, 29.9, 23.3, 23.1, 22.9. IR [neat, ν_{max} (cm^{-1})]: 2922, 2850, 1682, 1447, 1261, 906, 728 cm^{-1}. HRMS (*m*/*z*): calculated for $C_{22}H_{22}O$ 302.1671, found 302.1671.

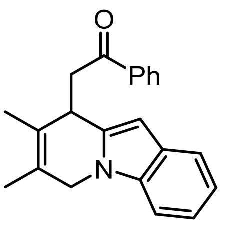

Following general procedure 1, compound **8i** was isolated by silica chromatography (0.5-1% EtOAc in hexane) as a pale yellow oil: ^{1}H NMR (500 MHz, CDCl$_3$): δ (ppm): 7.86 (d, 2H, *J* = 7.6 Hz), 7.51 (d, 2H, *J* = 7.0 Hz), 7.39 (t, 2H, *J* = 7.5 Hz), 7.27 (t, 1H, *J* = 8.0 Hz), 7.15 (t, 1H, *J* = 7.4 Hz), 7.07 (t, 1H, *J* = 7.4 Hz), 6.24 (s, 1H), 4.47 (s, 2H), 4.36 (br t, 1H), 3.35 (dd, 1H, *J* = 17.0, 8.3 Hz), 3.28 (br dd, 1H, *J* = 14.0 Hz), 1.88 (s, 6H). ^{13}C NMR (100

MHz, $CDCl_3$): δ (ppm) 198.8, 138.7, 137.3, 135.3, 1332, 128.7, 128.6, 128.3, 125.9, 122.4, 120.5, 120.2, 119.8, 108.9, 97.1, 46.5, 45.1, 35.9, 17.5, 17.3. IR [neat, ν_{max} (cm^{-1})]: 2917, 1684, 1596, 1455, 1333, 1265, 1207, 748, 689 cm^{-1}. HRMS (*m/z*): calculated for $C_{22}H_{21}NO$ 315.1623, found 315.1622.

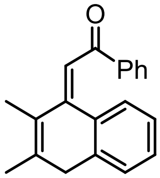

Following general procedure 1, compound **8j** was isolated by chromatography (0.5-1% EtOAc in hexane) as a white solid in 76% yield. ^{1}H NMR (500 MHz, CD_2Cl_2): δ (ppm) 8.14 (d, 2H, *J* = 7.0 Hz), 7.75 (d, 1H, *J* = 7.5 Hz), 7.65 (t, 2H, *J* = 7.0 Hz), 7.63 (s, 1H), 7.55 (t, 2H, *J* = 7.5 Hz), 7.35 (m, 2H), 4.85 (s, 2H), 2.47 (s, 3H), 2.30 (s, 3H). ^{13}C NMR (125 MHz, CD_2Cl_2): δ (ppm) 197.6, 137.7, 136.1, 135.6, 133.8, 132.8, 132.1, 129.4, 129.3, 128.7, 128.4, 127.9, 125.9, 125.3, 123.9, 39.6, 21.9, 16.9. IR [neat, ν_{max} (cm^{-1})]: 2922, 1727, 1672, 1273, 1211, 742. HRMS (*m/z*): calculated for $C_{20}H_{18}O$ 274.1358, found 274.1360.

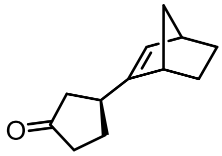

Following general procedure 3, compound **9a** was isolated by silica chromatography (5% EtOAc in hexane) as a pale yellow oil and exhibits spectroscopic properties consistent with previously reported data.[1]

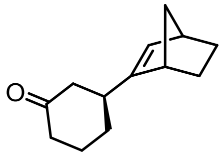

Following general procedure 3, compound **9b** was isolated by silica chromatography (5% EtOAc in hexane) as a pale yellow oil and exhibits spectroscopic properties consistent with previously reported data.[1]

2.4.6. Intramolecular C–H Functionalization of 4i Catalyzed by Complex 5

In a dry-box, cobalt complex **5** (5.3 mg, 0.02 mmol, 20 mol%), substrate **4i** (29.0 mg, 0.1 mmol, 1 equiv), and P_1-*t*Bu phosphazene base (2.34 mg, 0.01 mmol, 10 mol%) were dissolved in 0.3 mL of benzene, loaded into a microwave tube and sealed. The mixture was heated to 75 °C in an oil bath and stirred for 24 h. The microwave tube was then opened to air and the reaction mixture was filtered through a plug of silica with 20% EtOAc in hexane as the eluent. Solvent was evaporated *in vacuo* to give the crude mixture. Yields were determined by ^{1}H NMR analysis of the crude mixture with 1,3,5-trimethoxybenzene as the internal standard.

2.5. References

(1) Brunner, H. *J. Organomet. Chem.* **1968**, *12*, 517-522.
(2) Brunner, H.; Loskot, S. *J. Organomet. Chem.* **1973**, *61*, 401-414.
(3) Brunner, H.; Loskot, S. *Angew. Chem., Int. Ed.* **1971**, *10*, 515-516.
(4) Becker, P. N.; Bergman, R. G. *J. Am. Chem. Soc.* **1983**, *105*, 2985-2995.
(5) Becker, P. N.; Bergman, R. G. *Organometallics* **1983**, *2*, 787-796.
(6) Becker, P. N.; White, M. A.; Bergman, R. G. *J. Am. Chem. Soc.* **1980**, *102*, 5676-5677.
(7) Tomson, N. C.; Crimmin, M. R.; Petrenko, T.; Rosebrugh, L. E.; Sproules, S.; Boyd, W. C.; Bergman, R. G.; DeBeer, S.; Toste, F. D.; Wieghardt, K. *J. Am. Chem. Soc.* **2011**, *133*, 18785-18801.
(8) Crimmin, M. R.; Rosebrugh, L. E.; Tomson, N. C.; Weyhermüller, T.; Bergman, R. G.; Toste, F. D.; Wieghardt, K. *J. Organomet. Chem.* **2011**, *696*, 3974-3981.
(9) Schomaker, J. M.; Boyd, W. C.; Stewart, I. C.; Toste, F. D.; Bergman, R. G. *J. Am. Chem. Soc.* **2008**, *130*, 3777-3779.
(10) Schomaker, J. M.; Toste, F. D.; Bergman, R. G. *Organic Letters* **2009**, *11*, 3698-3700.
(11) Boyd, W. C.; Crimmin, M. R.; Rosebrugh, L. E.; Schomaker, J. M.; Bergman, R. G.; Toste, F. D. *J. Am. Chem. Soc.* **2010**, *132*, 16365-16367.
(12) Padwa, A.; Lipka, H.; Watterson, S. H.; Murphree, S. S. *The Journal of Organic Chemistry* **2003**, *68*, 6238-6250.

2.6. Appendix – ^{1}H and ^{13}C NMR Spectra

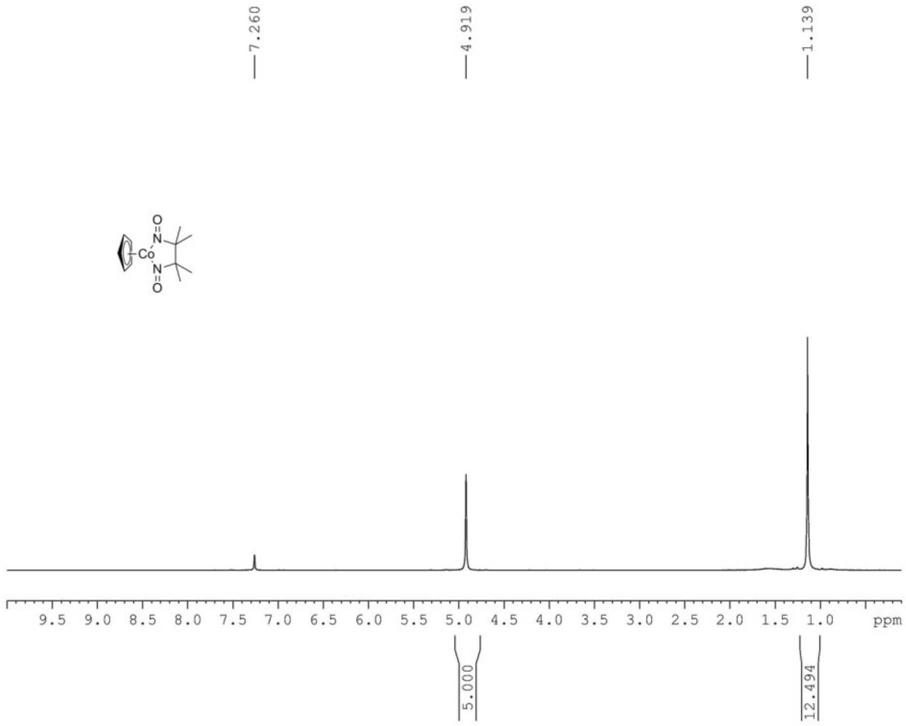

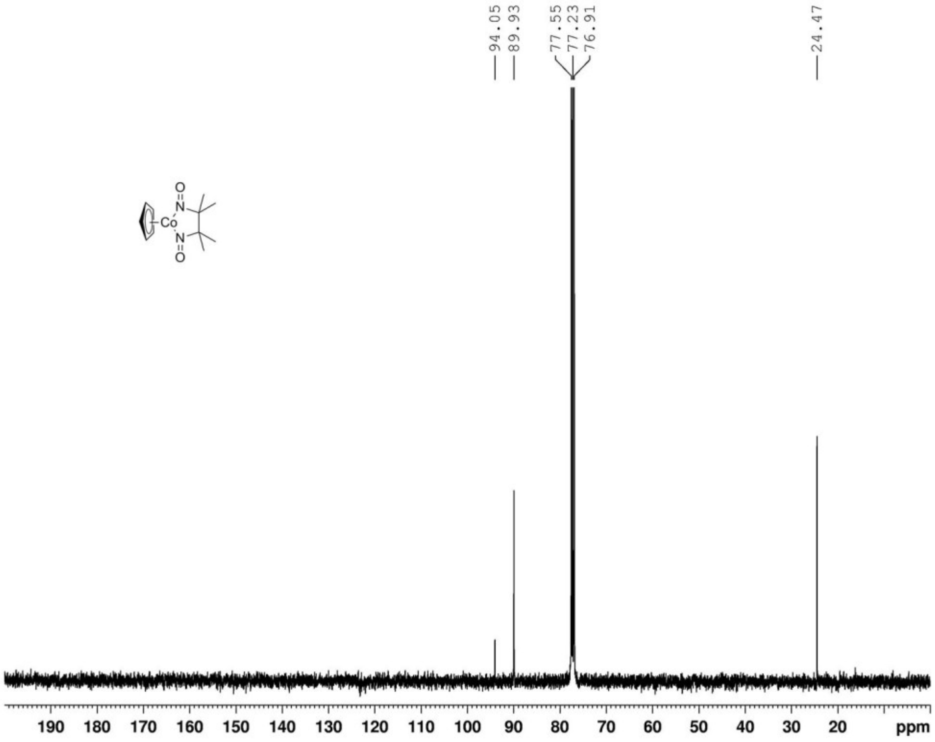

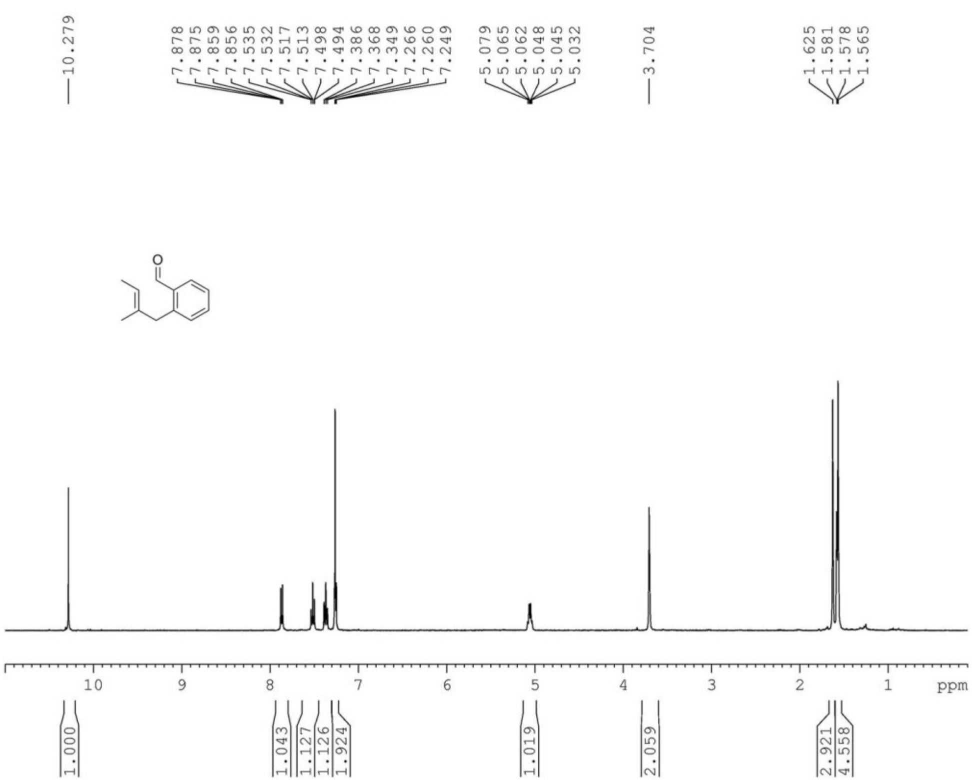
10.279
7.878
7.875
7.859
7.856
7.535
7.532
7.517
7.513
7.498
7.494
7.386
7.368
7.349
7.266
7.260
7.249
5.079
5.065
5.062
5.048
5.045
5.032
3.704
1.625
1.581
1.578
1.565
O
10
9
8
7
6
5
4
3
2
1
ppm
1.000
1.043
1.127
1.126
1.924
1.019
2.059
2.921
4.558

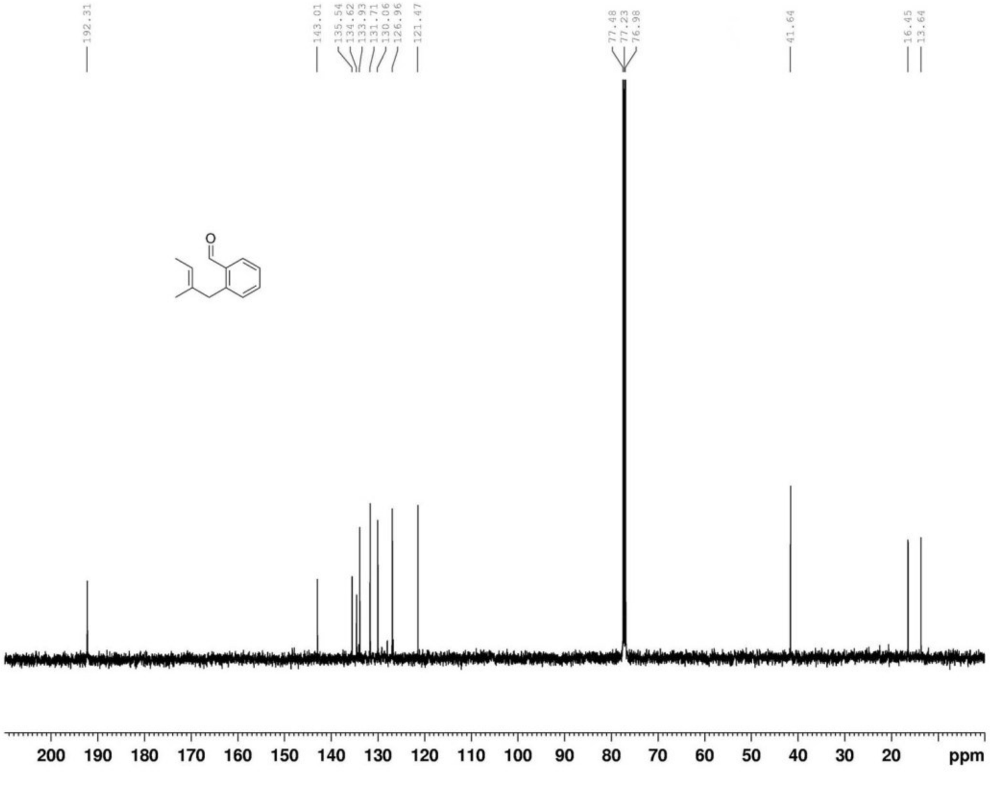
192.31
143.01
135.54
134.62
133.93
131.71
130.06
126.96
121.47
77.48
77.23
76.98
41.64
16.45
13.64
O
200
190
180
170
160
150
140
130
120
110
100
90
80
70
60
50
40
30
20
ppm

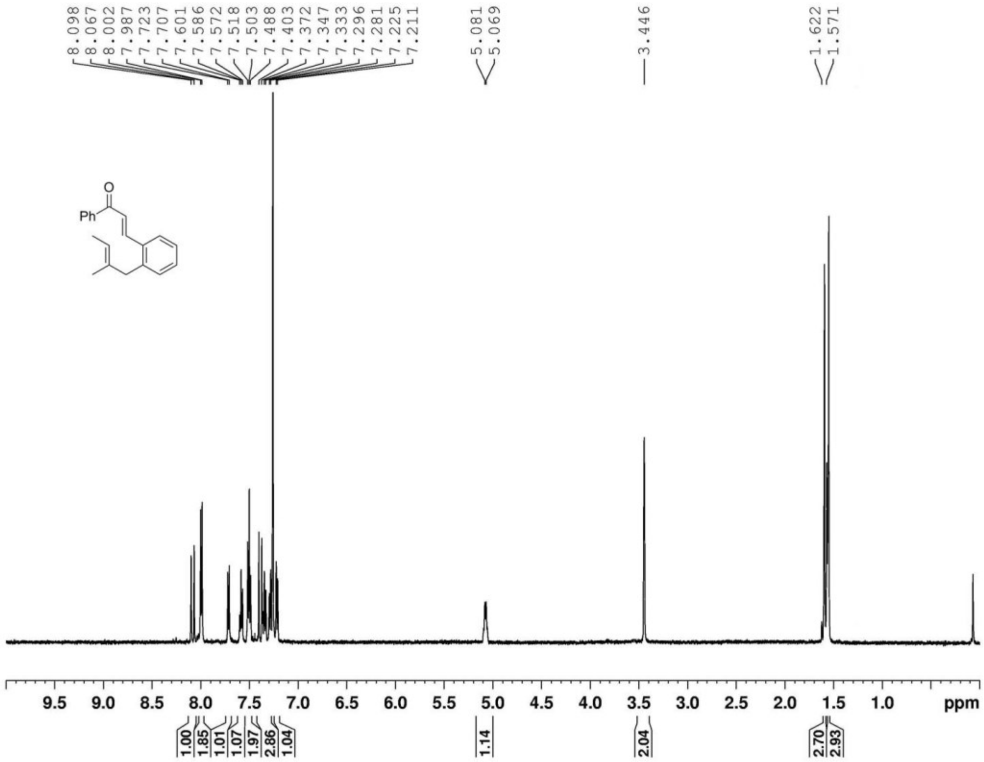
8.098
8.067
8.002
7.987
7.723
7.707
7.601
7.586
7.572
7.518
7.503
7.488
7.403
7.372
7.347
7.333
7.296
7.281
7.225
7.211
5.081
5.069
3.446
1.622
1.571
O
Ph
9.5
9.0
8.5
8.0
7.5
7.0
6.5
6.0
5.5
5.0
4.5
4.0
3.5
3.0
2.5
2.0
1.5
1.0
ppm
1.00
1.85
1.01
1.07
1.97
2.86
1.04
1.14
2.04
2.70
2.93

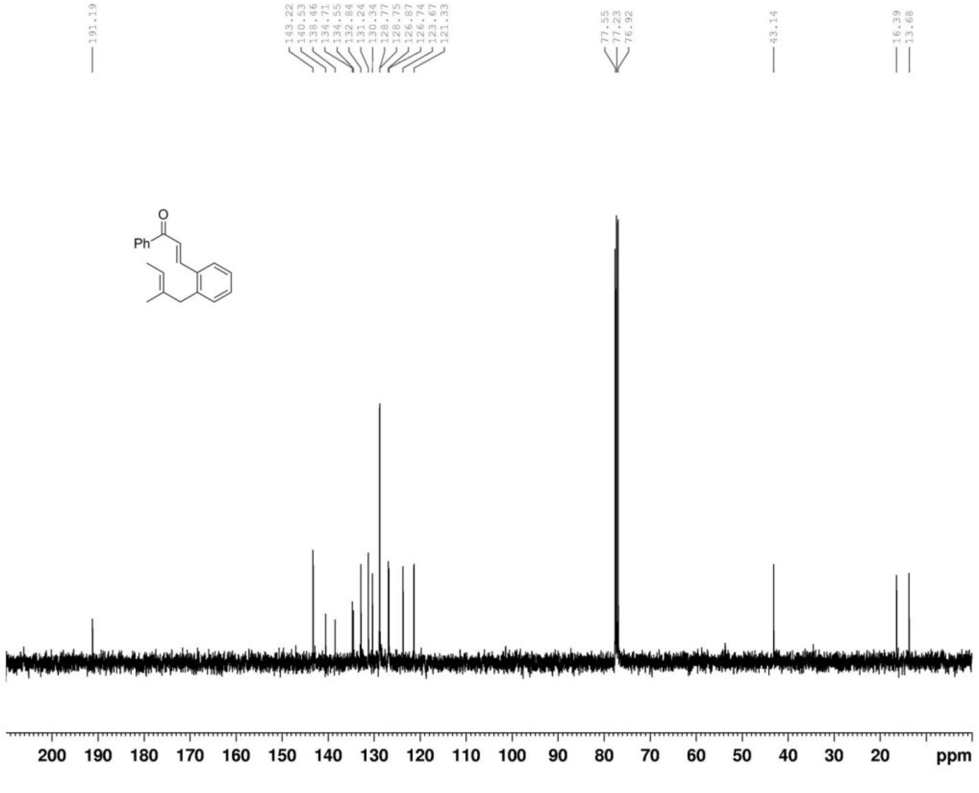
191.19
143.22
140.53
138.46
134.71
134.55
132.84
131.24
130.34
128.77
128.75
126.87
126.74
123.67
121.33
77.55
77.23
76.92
43.14
16.39
13.68
O
Ph
200
190
180
170
160
150
140
130
120
110
100
90
80
70
60
50
40
30
20
ppm

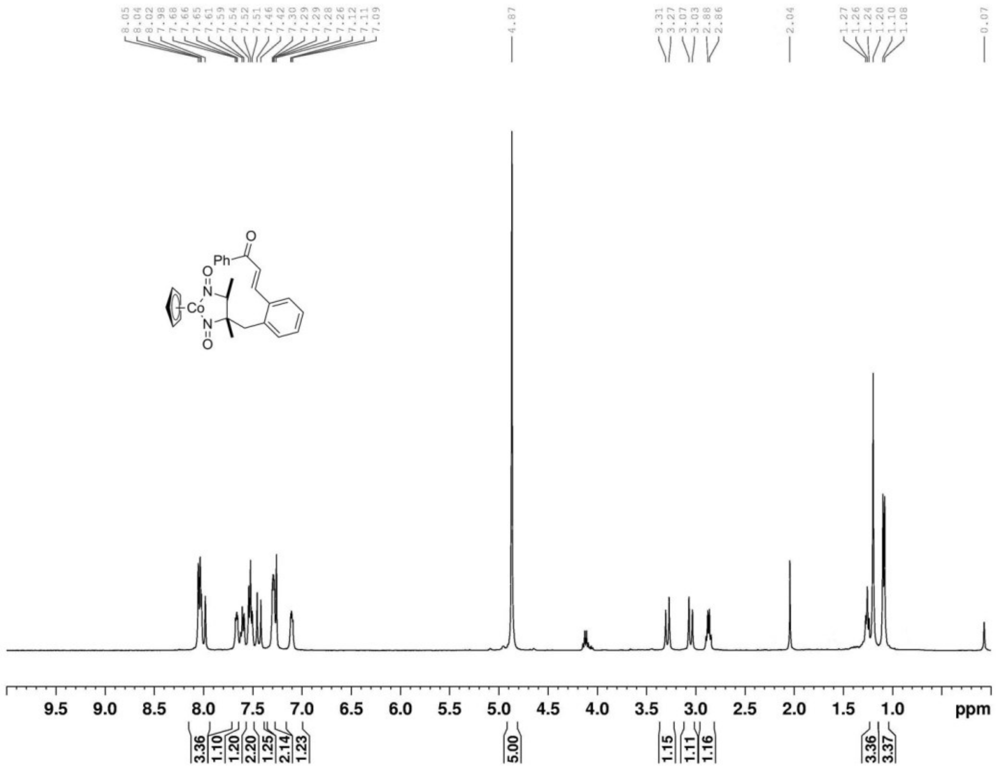
8.05
8.04
8.02
7.98
7.68
7.66
7.65
7.61
7.59
7.54
7.52
7.51
7.46
7.42
7.30
7.29
7.28
7.26
7.12
7.11
7.09
4.87
3.31
3.27
3.07
3.03
2.88
2.86
2.04
1.27
1.26
1.24
1.20
1.10
1.08
0.07
Ph
O
N
Co
9.5
9.0
8.5
8.0
7.5
7.0
6.5
6.0
5.5
5.0
4.5
4.0
3.5
3.0
2.5
2.0
1.5
1.0
ppm
3.36
1.10
1.20
2.20
1.25
2.14
1.23
5.00
1.15
1.11
1.16
3.36
3.37

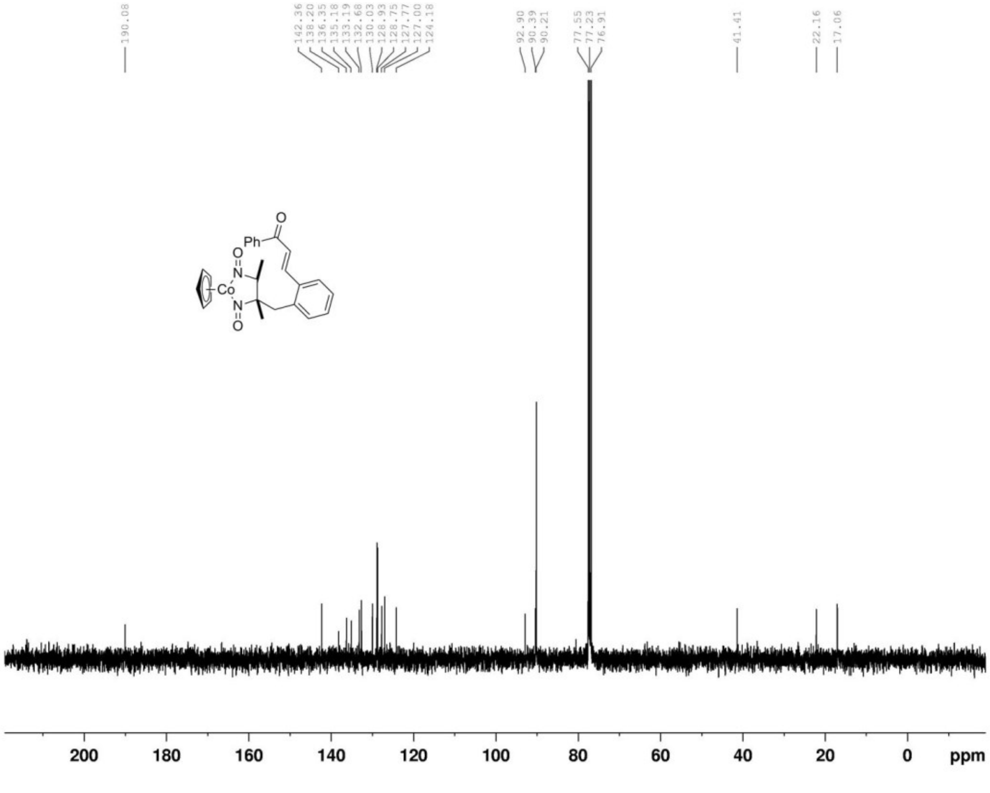
190.08
142.36
138.20
136.35
135.18
133.19
132.68
130.03
128.93
128.75
127.77
127.00
124.18
92.90
90.39
90.21
77.55
77.23
76.91
41.41
22.16
17.06
Ph
O
N
Co
200
180
160
140
120
100
80
60
40
20
0
ppm

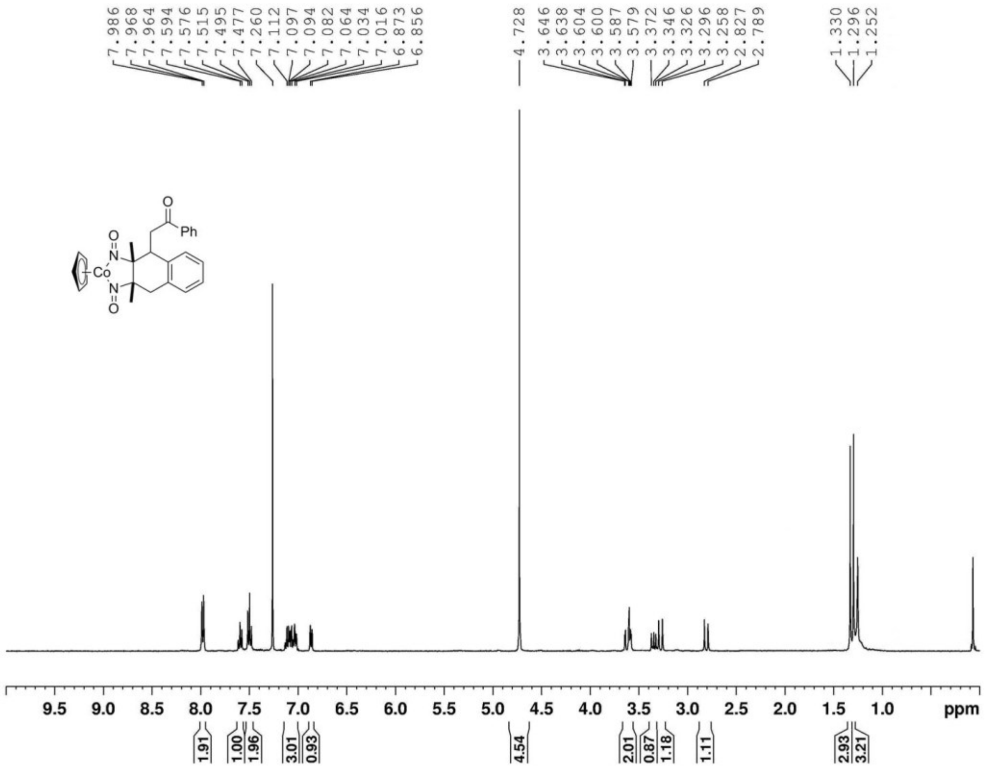
7.986
7.968
7.964
7.594
7.576
7.515
7.495
7.477
7.260
7.112
7.097
7.094
7.082
7.064
7.034
7.016
6.873
6.856
4.728
3.646
3.638
3.604
3.600
3.587
3.579
3.372
3.346
3.326
3.296
3.258
2.827
2.789
1.330
1.296
1.252
O
Ph
O
N
Co
N
O
9.5
9.0
8.5
8.0
7.5
7.0
6.5
6.0
5.5
5.0
4.5
4.0
3.5
3.0
2.5
2.0
1.5
1.0
ppm
1.91
1.00
1.96
3.01
0.93
4.54
2.01
0.87
1.18
1.11
2.93
3.21

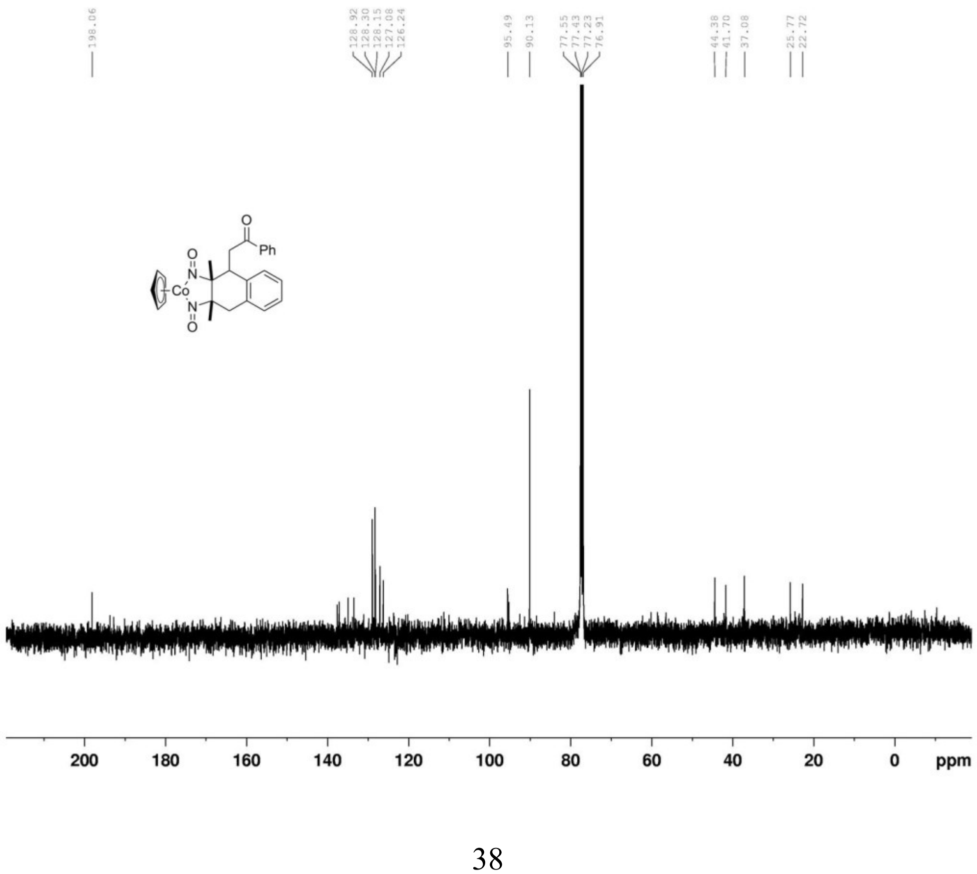
198.06
128.92
128.30
128.15
127.08
126.24
95.49
90.13
77.55
77.43
77.23
76.91
44.38
41.70
37.08
25.77
22.72
O
Ph
O
N
Co
N
O
200
180
160
140
120
100
80
60
40
20
0
ppm

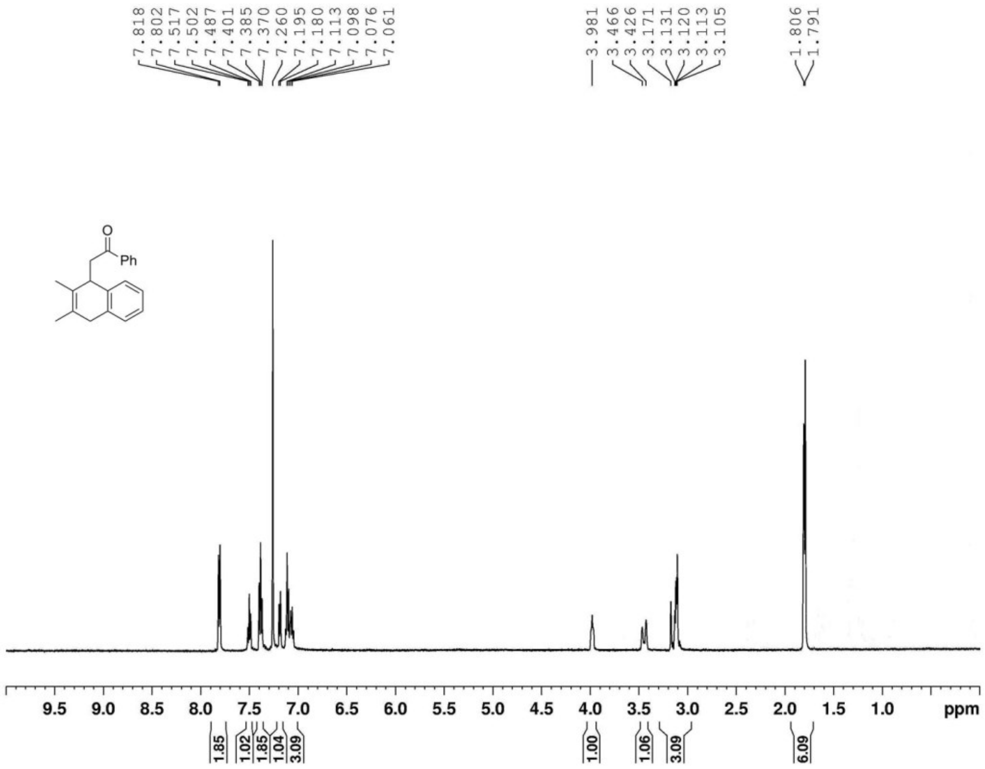
7.818
7.802
7.517
7.502
7.487
7.401
7.385
7.370
7.260
7.195
7.180
7.113
7.098
7.076
7.061
3.981
3.466
3.426
3.171
3.131
3.120
3.113
3.105
1.806
1.791
O
Ph
9.5
9.0
8.5
8.0
7.5
7.0
6.5
6.0
5.5
5.0
4.5
4.0
3.5
3.0
2.5
2.0
1.5
1.0
ppm
1.85
1.02
1.85
1.04
3.09
1.00
1.06
3.09
6.09

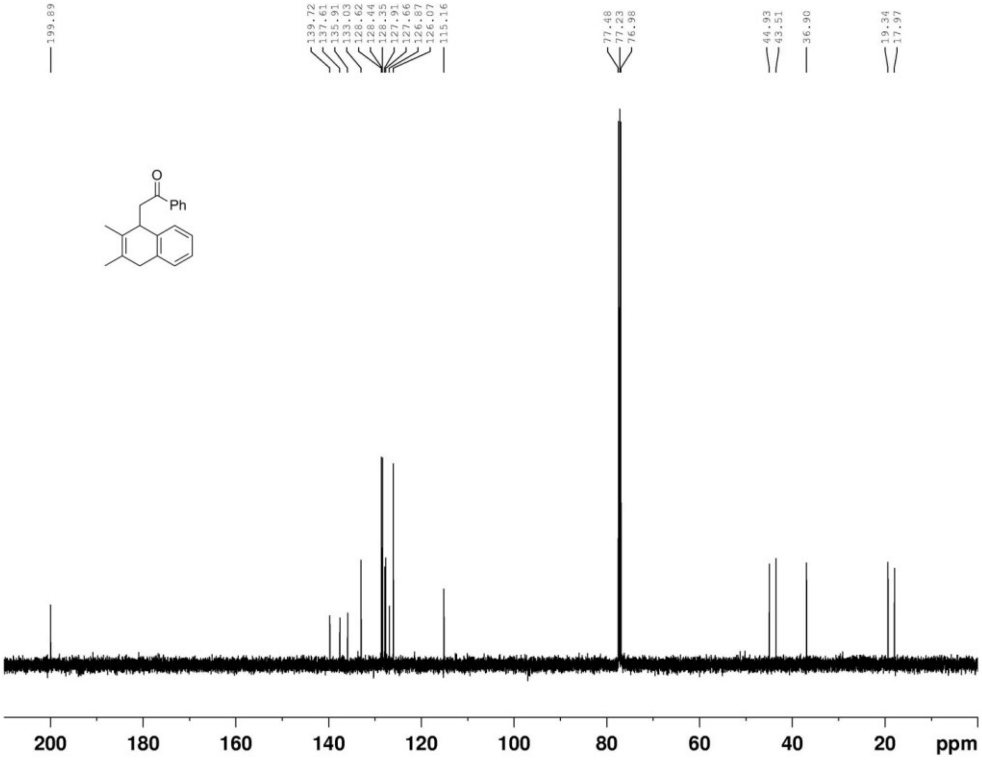
199.89
139.72
137.61
135.91
133.03
128.62
128.44
128.35
127.91
127.66
126.87
126.07
115.16
77.48
77.23
76.98
44.93
43.51
36.90
19.34
17.97
O
Ph
200
180
160
140
120
100
80
60
40
20
ppm

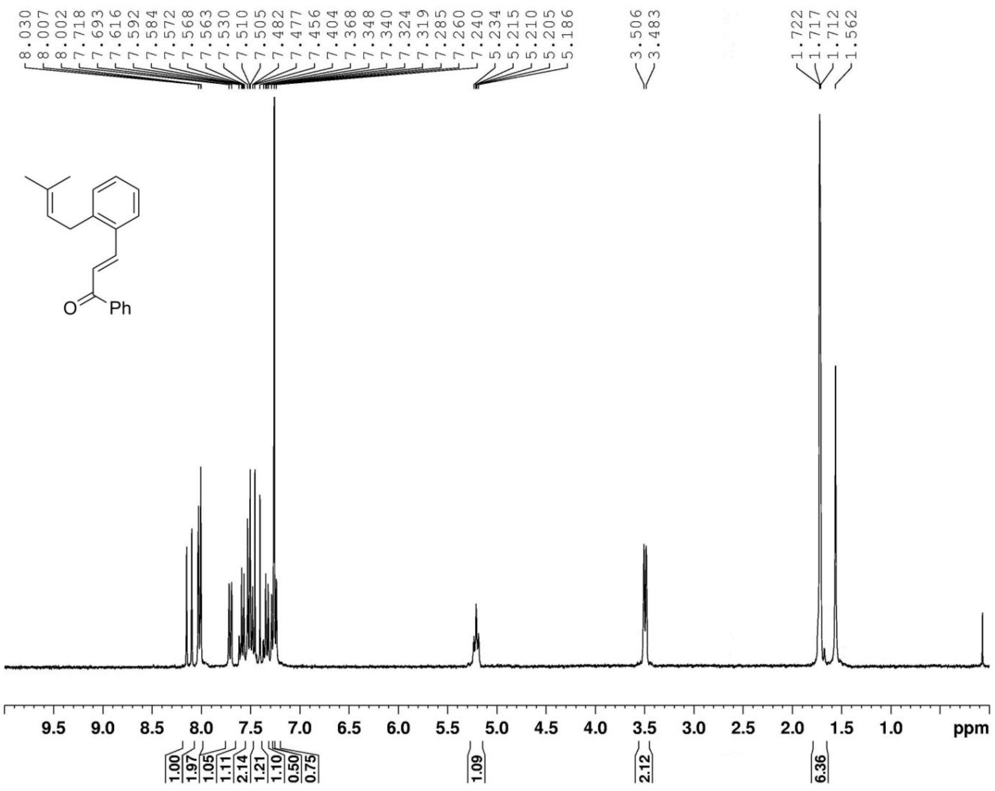
8.030
8.007
8.002
7.718
7.693
7.616
7.592
7.584
7.572
7.568
7.563
7.530
7.510
7.505
7.482
7.477
7.456
7.404
7.368
7.348
7.340
7.324
7.319
7.285
7.260
7.240
5.234
5.215
5.210
5.205
5.186
3.506
3.483
1.722
1.717
1.712
1.562
O
Ph
9.5 9.0 8.5 8.0 7.5 7.0 6.5 6.0 5.5 5.0 4.5 4.0 3.5 3.0 2.5 2.0 1.5 1.0 ppm
1.00
1.97
1.05
1.11
2.14
1.21
1.10
0.50
0.75
1.09
2.12
6.36

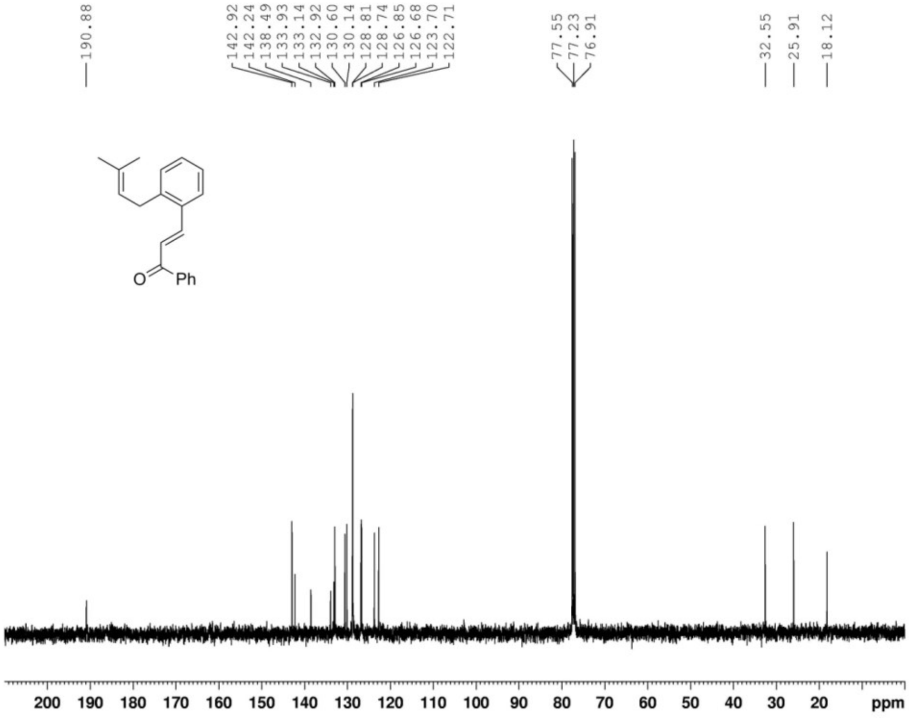
190.88
142.92
142.24
138.49
133.93
133.14
132.92
130.60
130.14
128.81
128.74
126.85
126.68
123.70
122.71
77.55
77.23
76.91
32.55
25.91
18.12
O
Ph
200 190 180 170 160 150 140 130 120 110 100 90 80 70 60 50 40 30 20 ppm

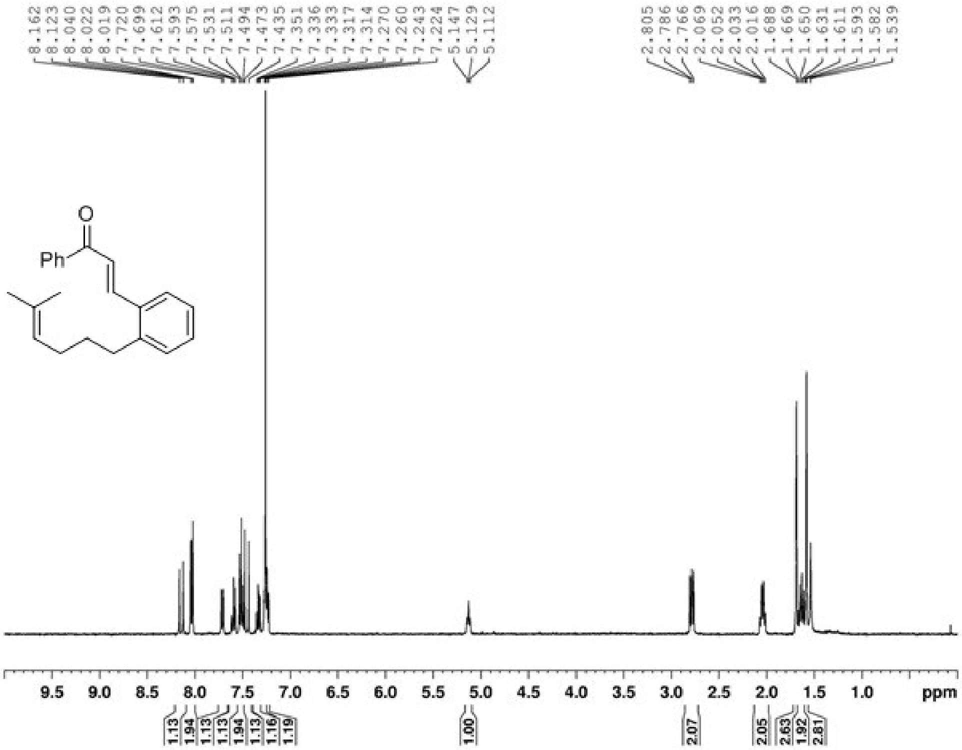
8.162 8.123 8.040 8.022 8.019 7.720 7.699 7.612 7.593 7.575 7.531 7.511 7.494 7.473 7.435 7.351 7.336 7.333 7.317 7.314 7.270 7.260 7.243 7.224 5.147 5.129 5.112
2.805 2.786 2.766 2.069 2.052 2.033 2.016 1.688 1.669 1.650 1.631 1.611 1.593 1.582 1.539
O
Ph
9.5 9.0 8.5 8.0 7.5 7.0 6.5 6.0 5.5 5.0 4.5 4.0 3.5 3.0 2.5 2.0 1.5 1.0 ppm
1.13 1.94 1.13 1.13 1.94 1.13 1.16 1.19
1.00
2.07
2.05 2.63 1.92 2.81

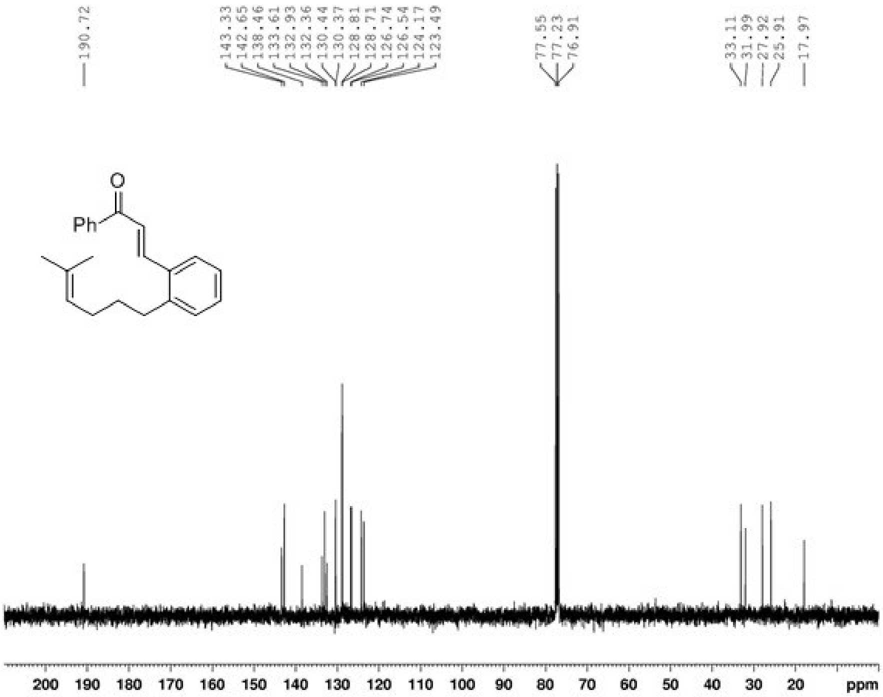
190.72
143.33 142.65 138.46 133.61 132.93 132.36 130.44 130.37 128.81 128.71 126.74 126.54 124.17 123.49
77.55 77.23 76.91
33.11 31.99 27.92 25.91 17.97
O
Ph
200 190 180 170 160 150 140 130 120 110 100 90 80 70 60 50 40 30 20 ppm

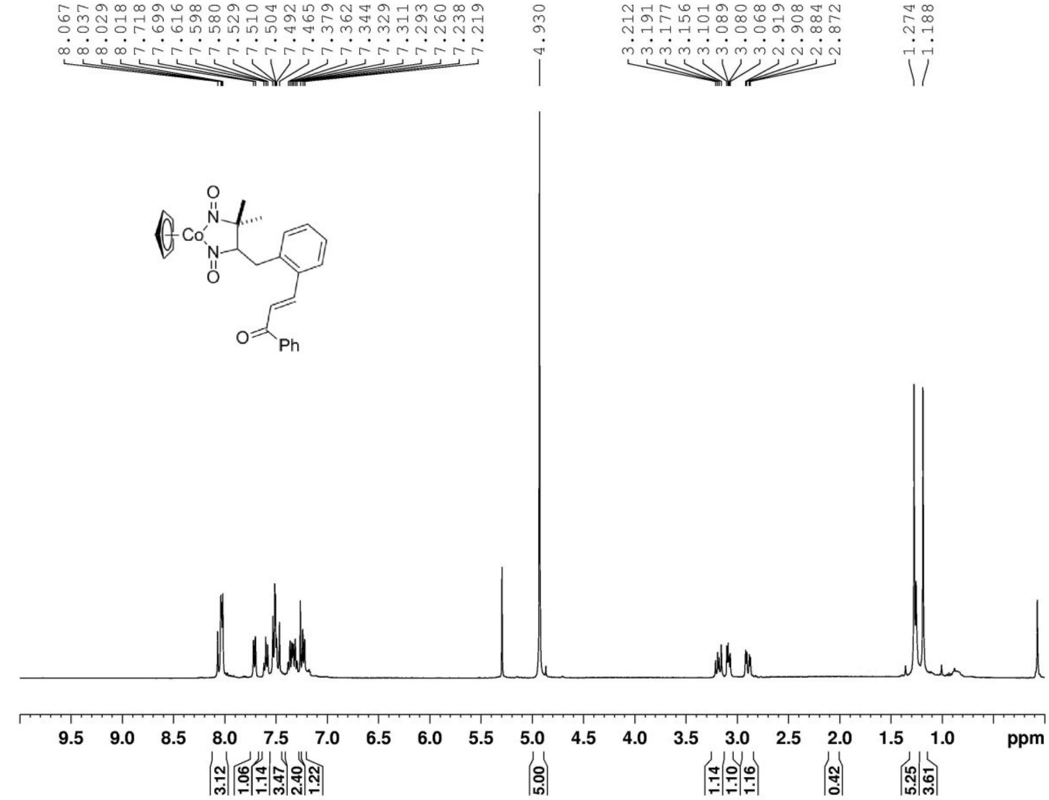
8.067
8.037
8.029
8.018
7.718
7.699
7.616
7.598
7.580
7.529
7.510
7.504
7.492
7.465
7.379
7.362
7.344
7.329
7.311
7.293
7.260
7.238
7.219
4.930
3.212
3.191
3.177
3.156
3.101
3.089
3.080
3.068
2.919
2.908
2.884
2.872
1.274
1.188
O
N
Co
N
O
O
Ph
9.5
9.0
8.5
8.0
7.5
7.0
6.5
6.0
5.5
5.0
4.5
4.0
3.5
3.0
2.5
2.0
1.5
1.0
ppm
3.12
1.06
1.14
3.47
2.40
1.22
5.00
1.14
1.10
1.16
0.42
5.25
3.61

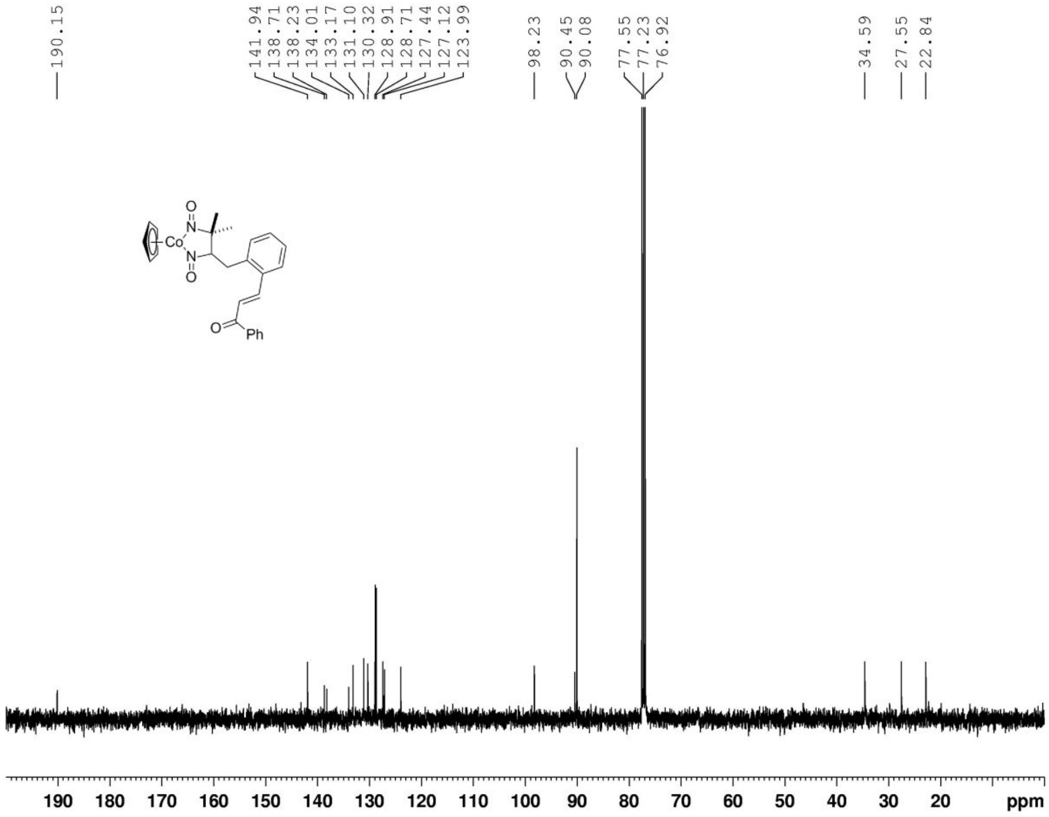
190.15
141.94
138.71
138.23
134.01
133.17
131.10
130.32
128.91
128.71
127.44
127.12
123.99
98.23
90.45
90.08
77.55
77.23
76.92
34.59
27.55
22.84
O
N
Co
N
O
O
Ph
190
180
170
160
150
140
130
120
110
100
90
80
70
60
50
40
30
20
ppm

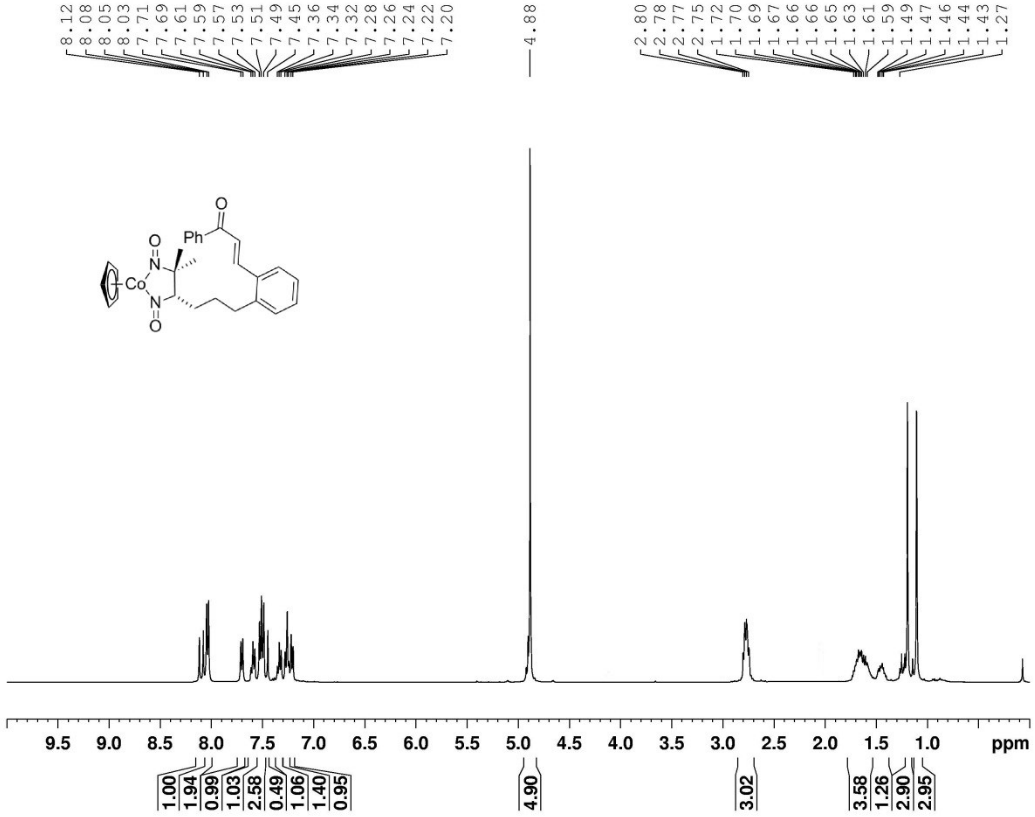
8.12
8.08
8.05
8.03
7.71
7.69
7.61
7.59
7.57
7.53
7.51
7.49
7.45
7.36
7.34
7.32
7.28
7.26
7.24
7.22
7.20
4.88
2.80
2.78
2.77
2.75
1.72
1.70
1.69
1.67
1.66
1.66
1.65
1.63
1.61
1.59
1.49
1.47
1.46
1.44
1.43
1.27
O
Ph
O
N
Co
N
O
9.5
9.0
8.5
8.0
7.5
7.0
6.5
6.0
5.5
5.0
4.5
4.0
3.5
3.0
2.5
2.0
1.5
1.0
ppm
1.00
1.94
0.99
1.03
2.58
0.49
1.06
1.40
0.95
4.90
3.02
3.58
1.26
2.90
2.95

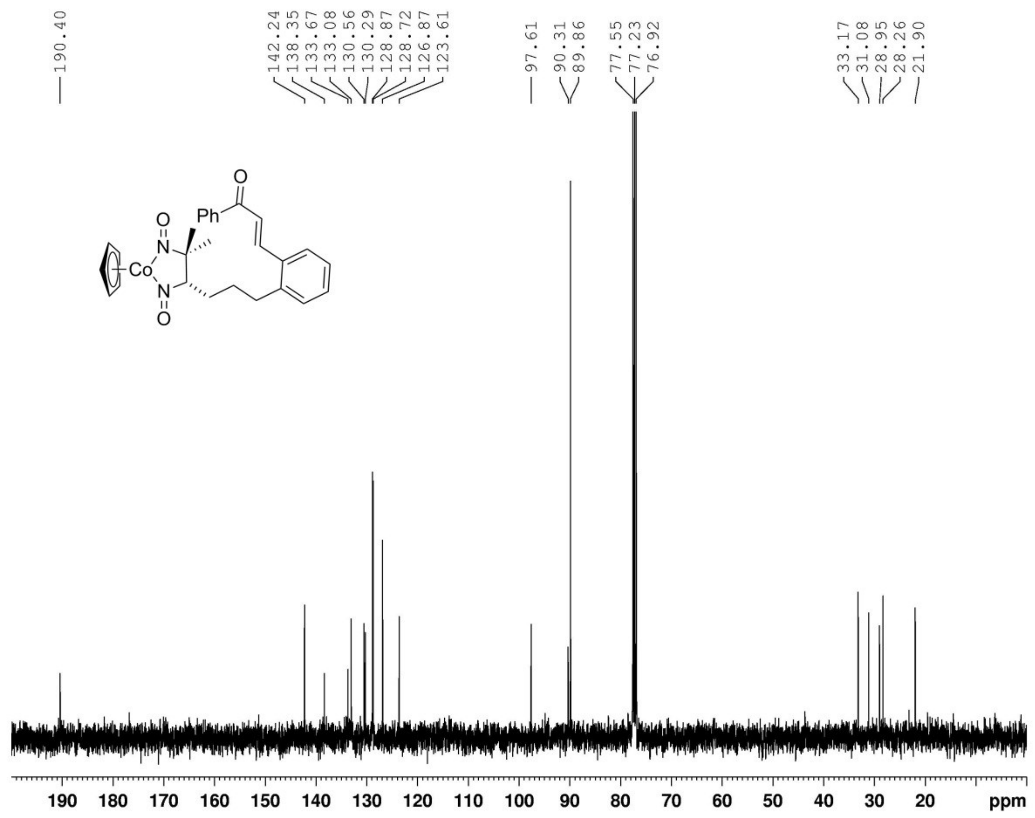
190.40
142.24
138.35
133.67
133.08
130.56
130.29
128.87
128.72
126.87
123.61
97.61
90.31
89.86
77.55
77.23
76.92
33.17
31.08
28.95
28.26
21.90
O
Ph
O
N
Co
N
O
190
180
170
160
150
140
130
120
110
100
90
80
70
60
50
40
30
20
ppm

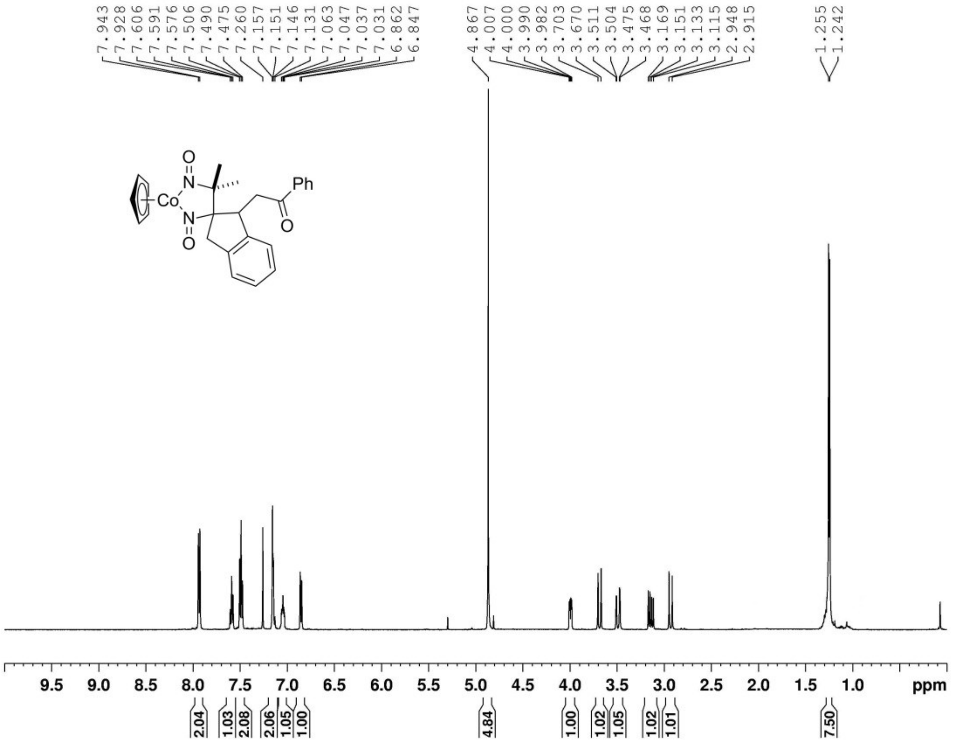
7.943
7.928
7.606
7.591
7.576
7.506
7.490
7.475
7.260
7.157
7.151
7.146
7.131
7.063
7.047
7.037
7.031
6.862
6.847
4.867
4.007
4.000
3.990
3.982
3.703
3.670
3.511
3.504
3.475
3.468
3.169
3.151
3.133
3.115
2.948
2.915
1.255
1.242
Co
N
O
N
O
Ph
O
9.5
9.0
8.5
8.0
7.5
7.0
6.5
6.0
5.5
5.0
4.5
4.0
3.5
3.0
2.5
2.0
1.5
1.0
ppm
2.04
1.03
2.08
2.06
1.05
1.00
4.84
1.00
1.02
1.05
1.02
1.01
7.50

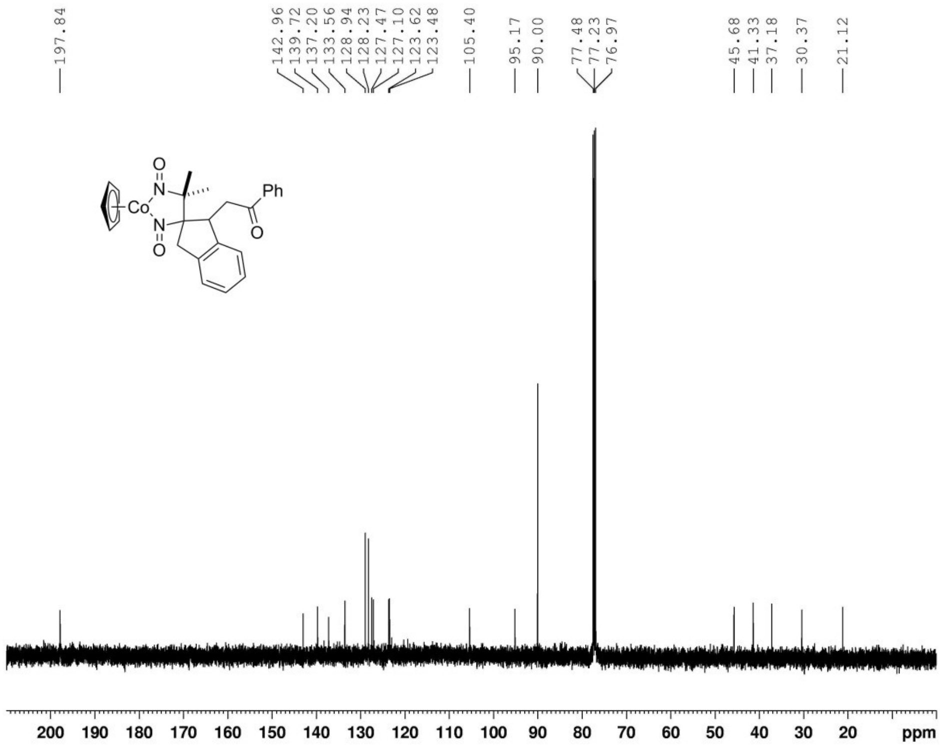
197.84
142.96
139.72
137.20
133.56
128.94
128.23
127.47
127.10
123.62
123.48
105.40
95.17
90.00
77.48
77.23
76.97
45.68
41.33
37.18
30.37
21.12
Co
N
O
N
O
Ph
O
200
190
180
170
160
150
140
130
120
110
100
90
80
70
60
50
40
30
20
ppm

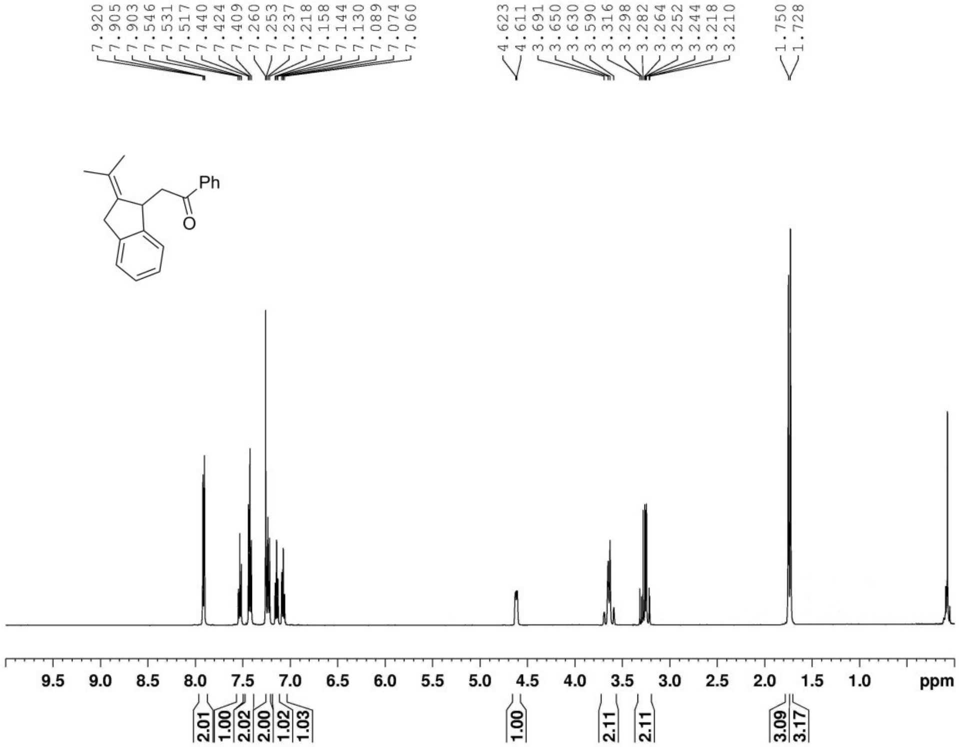
7.920
7.905
7.903
7.546
7.531
7.517
7.440
7.424
7.409
7.260
7.253
7.237
7.218
7.158
7.144
7.130
7.089
7.074
7.060
4.623
4.611
3.691
3.650
3.630
3.590
3.316
3.298
3.282
3.264
3.252
3.244
3.218
3.210
1.750
1.728
Ph
O
9.5
9.0
8.5
8.0
7.5
7.0
6.5
6.0
5.5
5.0
4.5
4.0
3.5
3.0
2.5
2.0
1.5
1.0
ppm
2.01
1.00
2.02
2.00
1.02
1.03
1.00
2.11
2.11
3.09
3.17

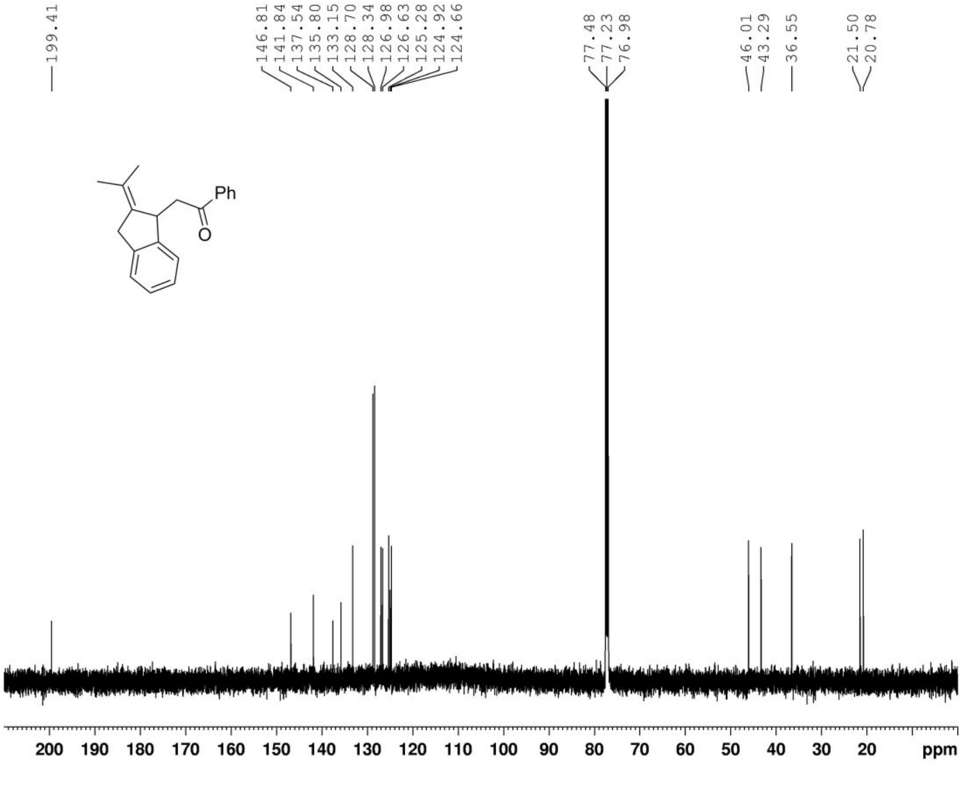
199.41
146.81
141.84
137.54
135.80
133.15
128.70
128.34
126.98
126.63
125.28
124.92
124.66
77.48
77.23
76.98
46.01
43.29
36.55
21.50
20.78
Ph
O
200
190
180
170
160
150
140
130
120
110
100
90
80
70
60
50
40
30
20
ppm

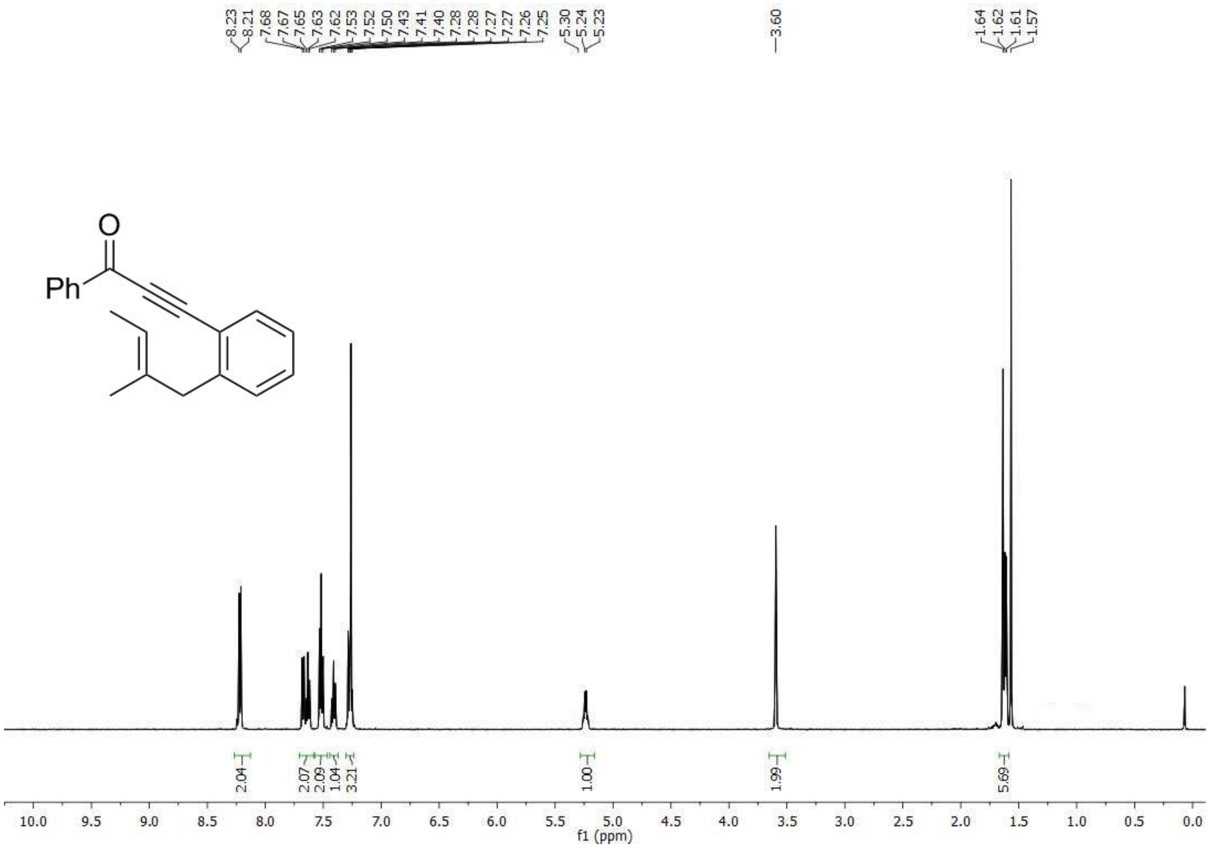
8.23
8.21
7.68
7.67
7.65
7.63
7.62
7.53
7.52
7.50
7.43
7.41
7.40
7.28
7.28
7.27
7.27
7.26
7.25
5.30
5.24
5.23
3.60
1.64
1.62
1.61
1.57
O
Ph
2.04
2.07
2.09
1.04
3.21
1.00
1.99
5.69
10.0
9.5
9.0
8.5
8.0
7.5
7.0
6.5
6.0
5.5
5.0
4.5
4.0
3.5
3.0
2.5
2.0
1.5
1.0
0.5
0.0
f1 (ppm)

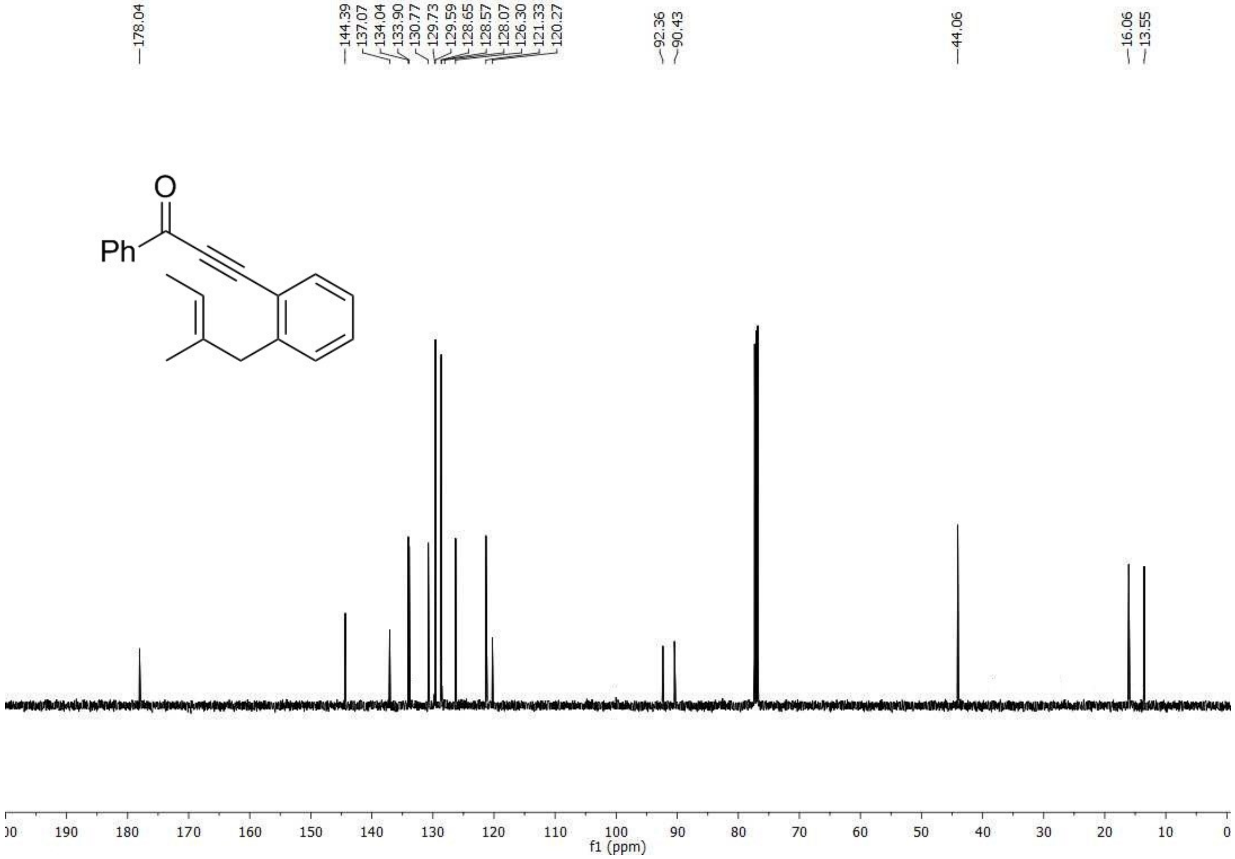
178.04
144.39
137.07
134.04
133.90
130.77
129.73
129.59
128.65
128.57
128.07
126.30
121.33
120.27
92.36
90.43
44.06
16.06
13.55
O
Ph
00
190
180
170
160
150
140
130
120
110
100
90
80
70
60
50
40
30
20
10
0
f1 (ppm)

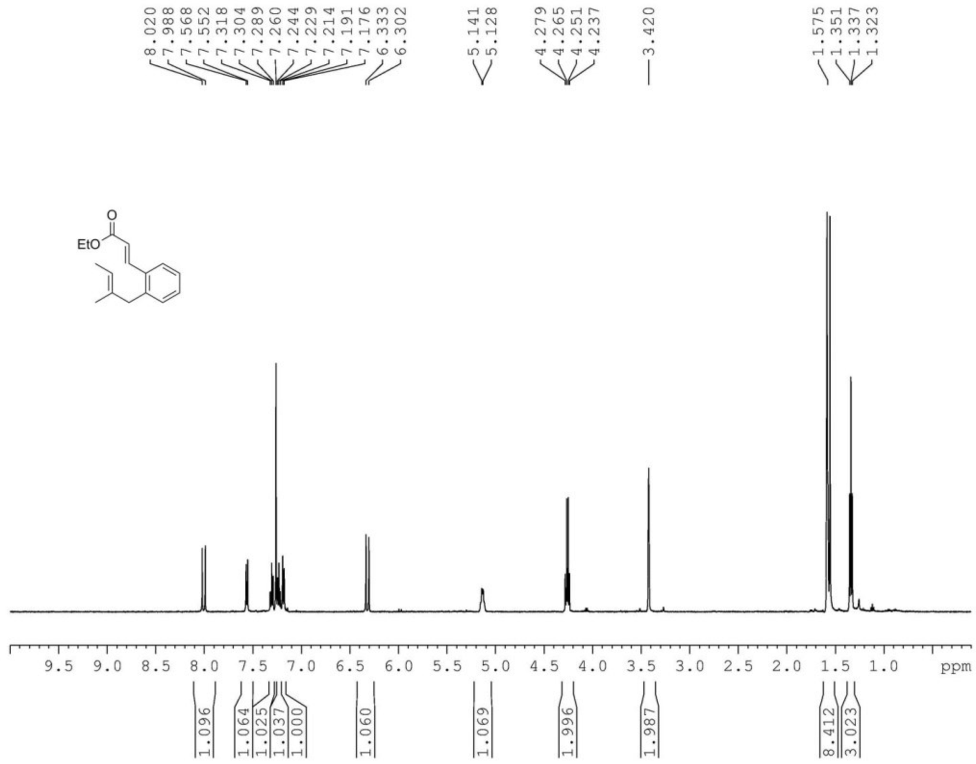
8.020
7.988
7.568
7.552
7.318
7.304
7.289
7.260
7.244
7.229
7.214
7.191
7.176
6.333
6.302
5.141
5.128
4.279
4.265
4.251
4.237
3.420
1.575
1.351
1.337
1.323
O
EtO
9.5 9.0 8.5 8.0 7.5 7.0 6.5 6.0 5.5 5.0 4.5 4.0 3.5 3.0 2.5 2.0 1.5 1.0 ppm
1.096
1.064
1.025
1.037
1.000
1.060
1.069
1.996
1.987
8.412
3.023

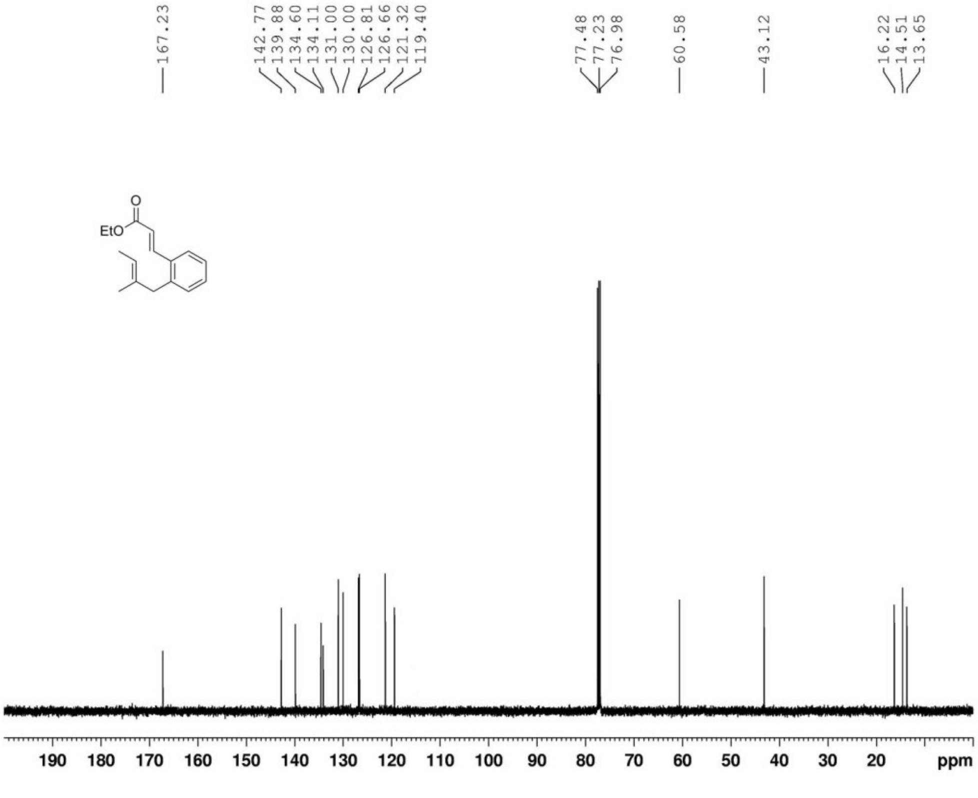
167.23
142.77
139.88
134.60
134.11
131.00
130.00
126.81
126.66
121.32
119.40
77.48
77.23
76.98
60.58
43.12
16.22
14.51
13.65
O
EtO
190 180 170 160 150 140 130 120 110 100 90 80 70 60 50 40 30 20 ppm

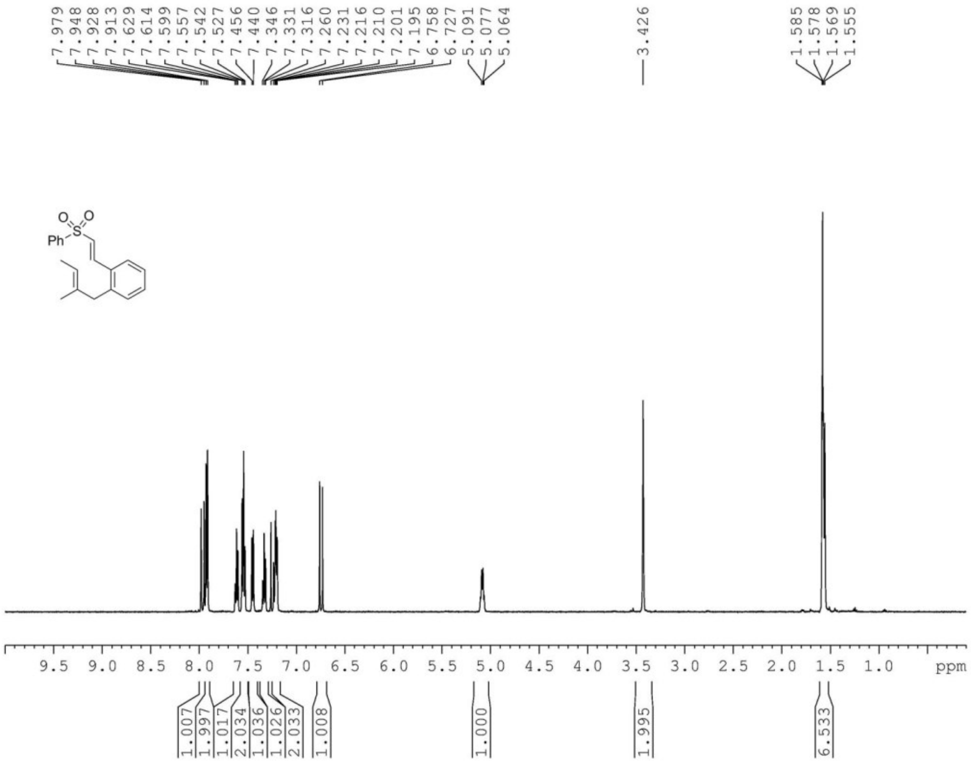
7.979
7.948
7.928
7.913
7.629
7.614
7.599
7.557
7.542
7.527
7.456
7.440
7.346
7.331
7.316
7.260
7.231
7.216
7.210
7.201
7.195
6.758
6.727
5.091
5.077
5.064
3.426
1.585
1.578
1.569
1.555
O
O
S
Ph
9.5
9.0
8.5
8.0
7.5
7.0
6.5
6.0
5.5
5.0
4.5
4.0
3.5
3.0
2.5
2.0
1.5
1.0
ppm
1.007
1.997
1.017
2.034
1.036
1.026
2.033
1.008
1.000
1.995
6.533

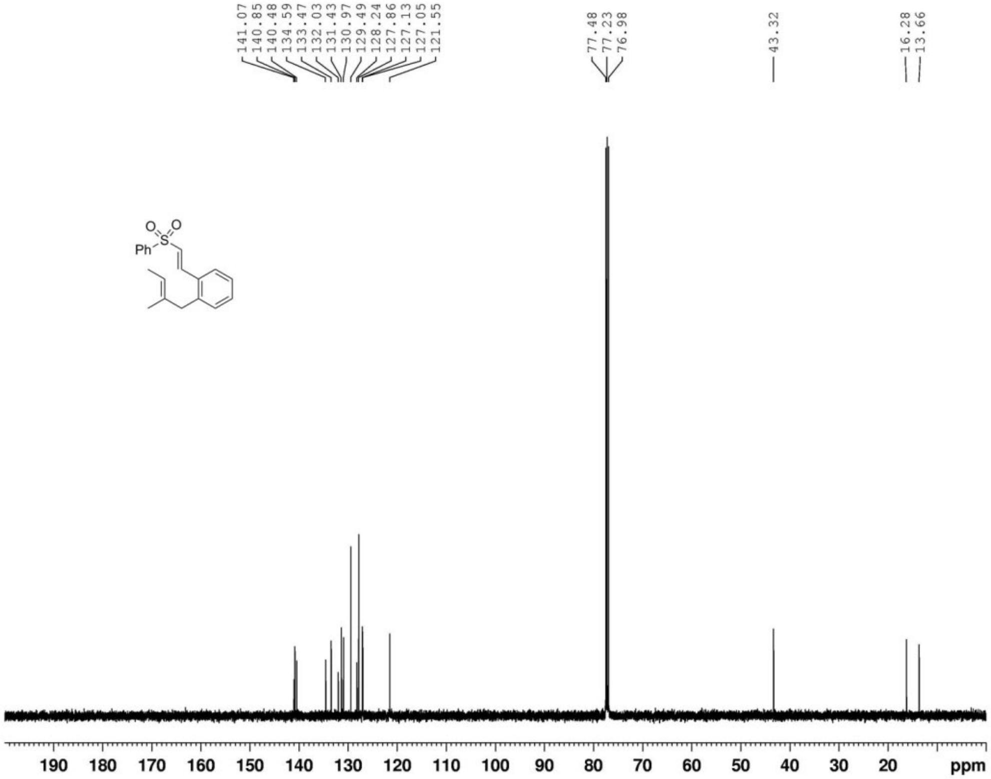
141.07
140.85
140.48
134.59
133.47
132.03
131.43
130.97
129.49
128.24
127.86
127.13
127.05
121.55
77.48
77.23
76.98
43.32
16.28
13.66
O
O
S
Ph
190
180
170
160
150
140
130
120
110
100
90
80
70
60
50
40
30
20
ppm

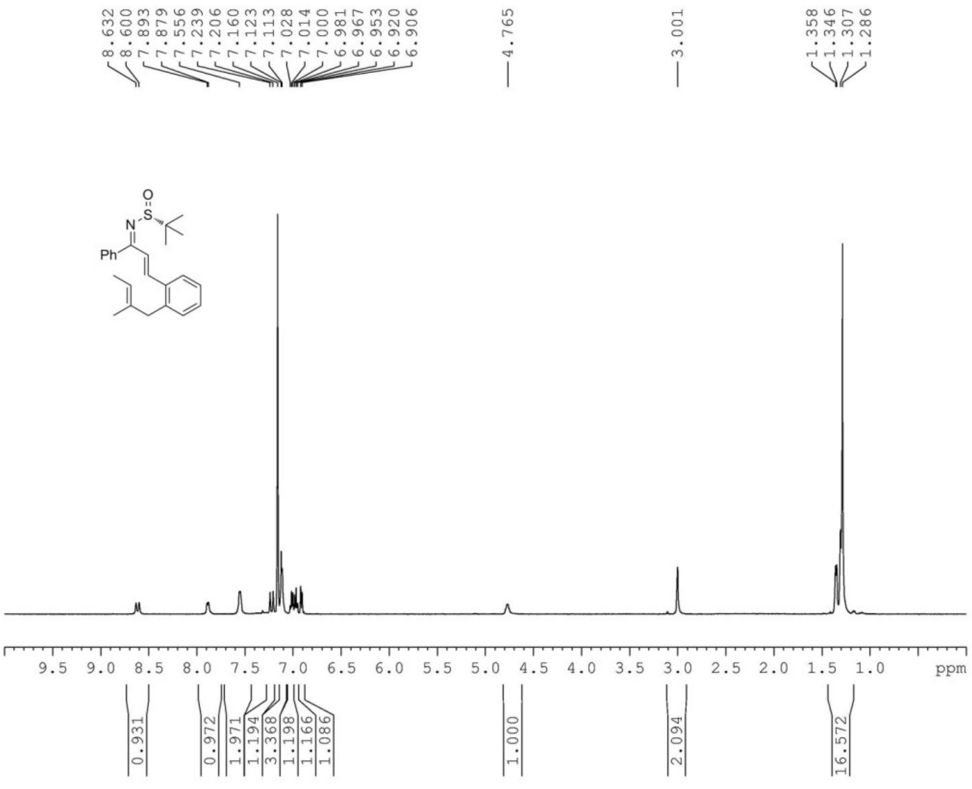
8.632
8.600
7.893
7.879
7.556
7.239
7.206
7.160
7.123
7.113
7.028
7.014
7.000
6.981
6.967
6.953
6.920
6.906
4.765
3.001
1.358
1.346
1.307
1.286
O
S
N
Ph
9.5
9.0
8.5
8.0
7.5
7.0
6.5
6.0
5.5
5.0
4.5
4.0
3.5
3.0
2.5
2.0
1.5
1.0
ppm
0.931
0.972
1.971
1.194
3.368
1.198
1.166
1.086
1.000
2.094
16.572

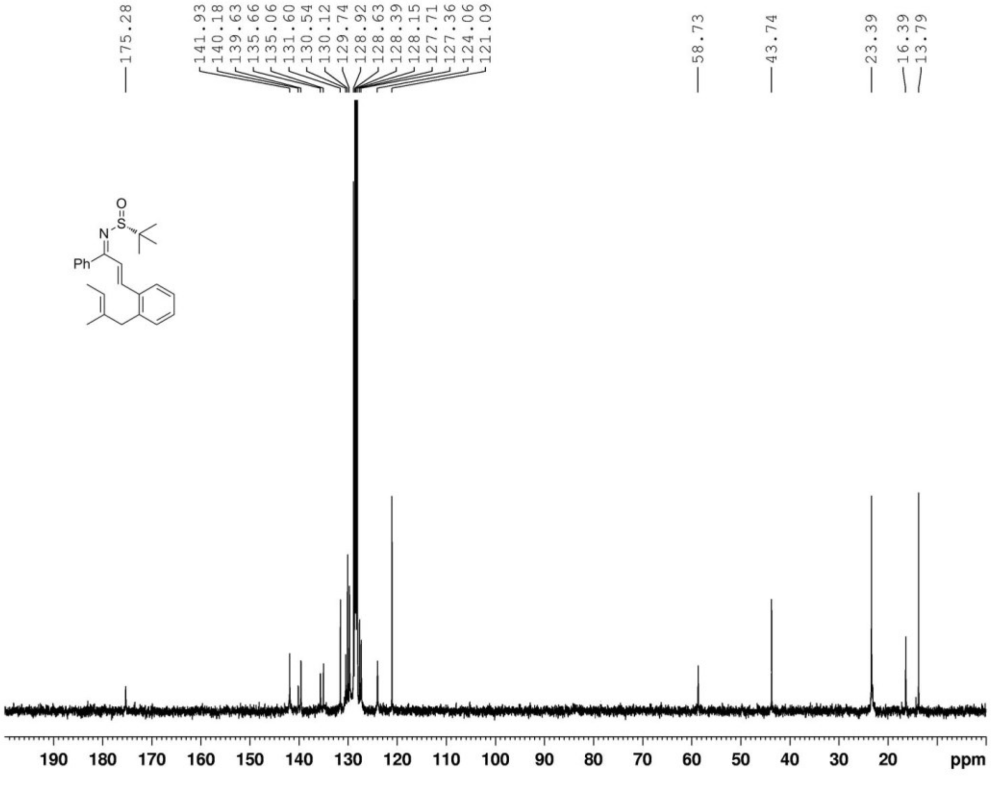
175.28
141.93
140.18
139.63
135.66
135.06
131.60
130.54
130.12
129.74
128.92
128.63
128.39
128.15
127.71
127.36
124.06
121.09
58.73
43.74
23.39
16.39
13.79
O
S
N
Ph
190
180
170
160
150
140
130
120
110
100
90
80
70
60
50
40
30
20
ppm

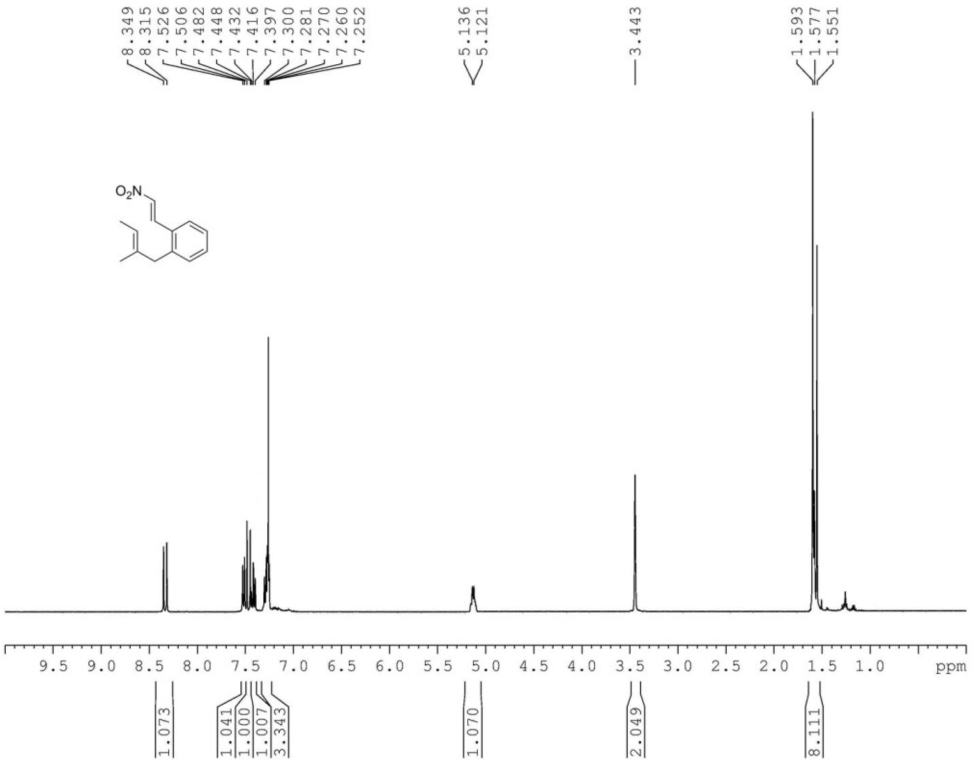
8.349
8.315
7.526
7.506
7.482
7.448
7.432
7.416
7.397
7.300
7.281
7.270
7.260
7.252
5.136
5.121
3.443
1.593
1.577
1.551
O_2N
9.5
9.0
8.5
8.0
7.5
7.0
6.5
6.0
5.5
5.0
4.5
4.0
3.5
3.0
2.5
2.0
1.5
1.0
ppm
1.073
1.041
1.000
1.007
3.343
1.070
2.049
8.111

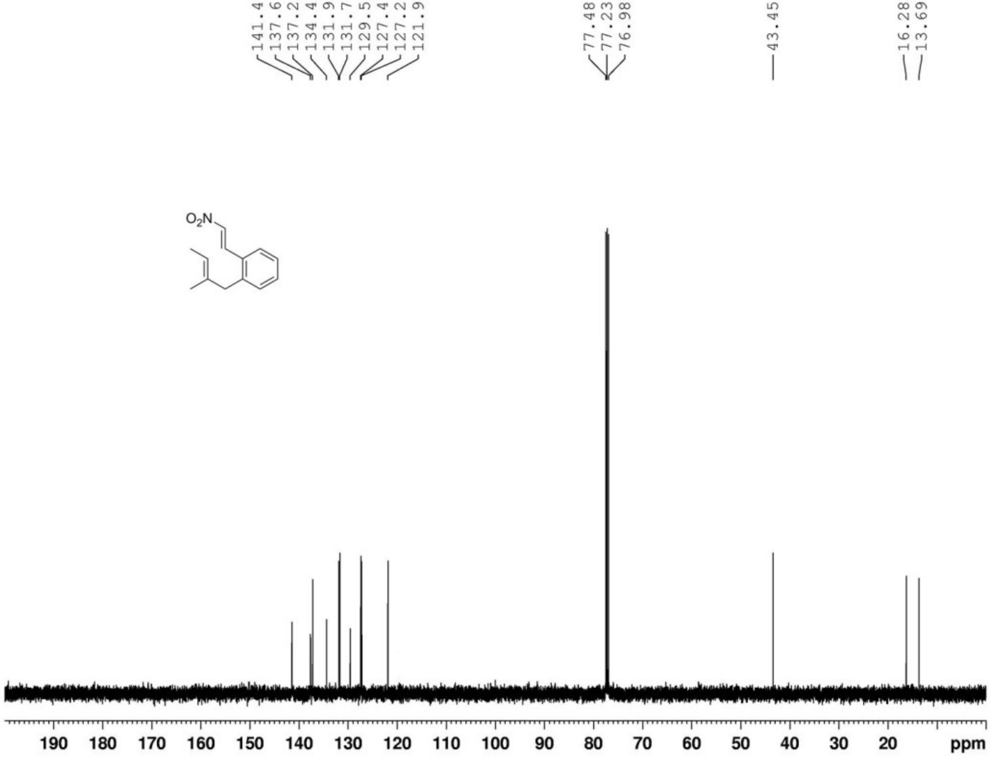
141.47
137.68
137.25
134.41
131.93
131.74
129.59
127.45
127.26
121.94
77.48
77.23
76.98
43.45
16.28
13.69
O_2N
190
180
170
160
150
140
130
120
110
100
90
80
70
60
50
40
30
20
ppm

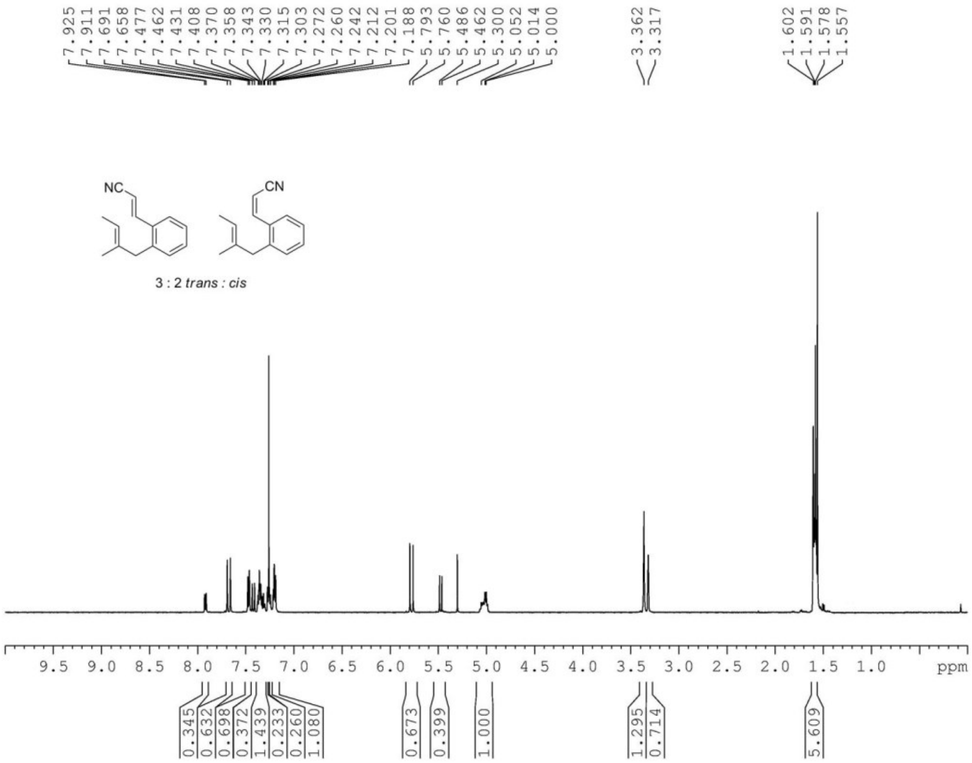
7.925
7.911
7.691
7.658
7.477
7.462
7.431
7.408
7.370
7.358
7.343
7.330
7.315
7.303
7.272
7.260
7.242
7.212
7.201
7.188
5.793
5.760
5.486
5.462
5.300
5.052
5.014
5.000
3.362
3.317
1.602
1.591
1.578
1.557
NC
CN
3 : 2 *trans* : *cis*
9.5 9.0 8.5 8.0 7.5 7.0 6.5 6.0 5.5 5.0 4.5 4.0 3.5 3.0 2.5 2.0 1.5 1.0 ppm
0.345
0.632
0.698
0.372
1.439
0.233
0.260
1.080
0.673
0.399
1.000
1.295
0.714
5.609

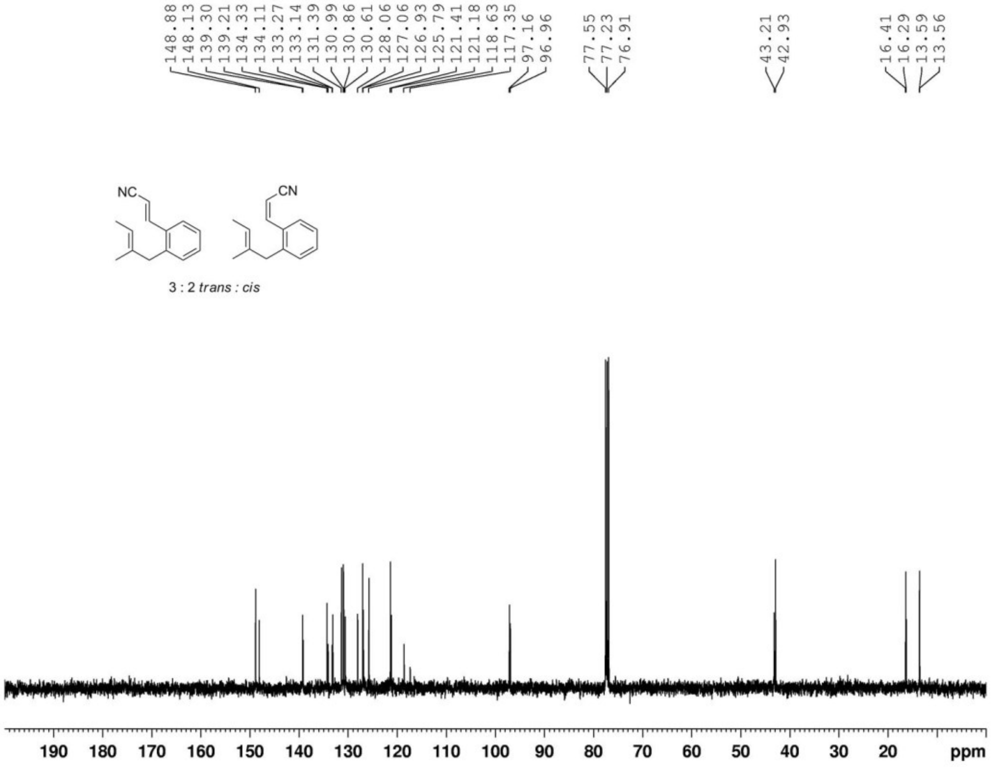
148.88
148.13
139.30
139.21
134.33
134.11
133.27
133.14
131.39
130.99
130.86
130.61
128.06
127.06
126.93
125.79
121.41
121.18
118.63
117.35
97.16
96.96
77.55
77.23
76.91
43.21
42.93
16.41
16.29
13.59
13.56
NC
CN
3 : 2 *trans* : *cis*
190 180 170 160 150 140 130 120 110 100 90 80 70 60 50 40 30 20 ppm

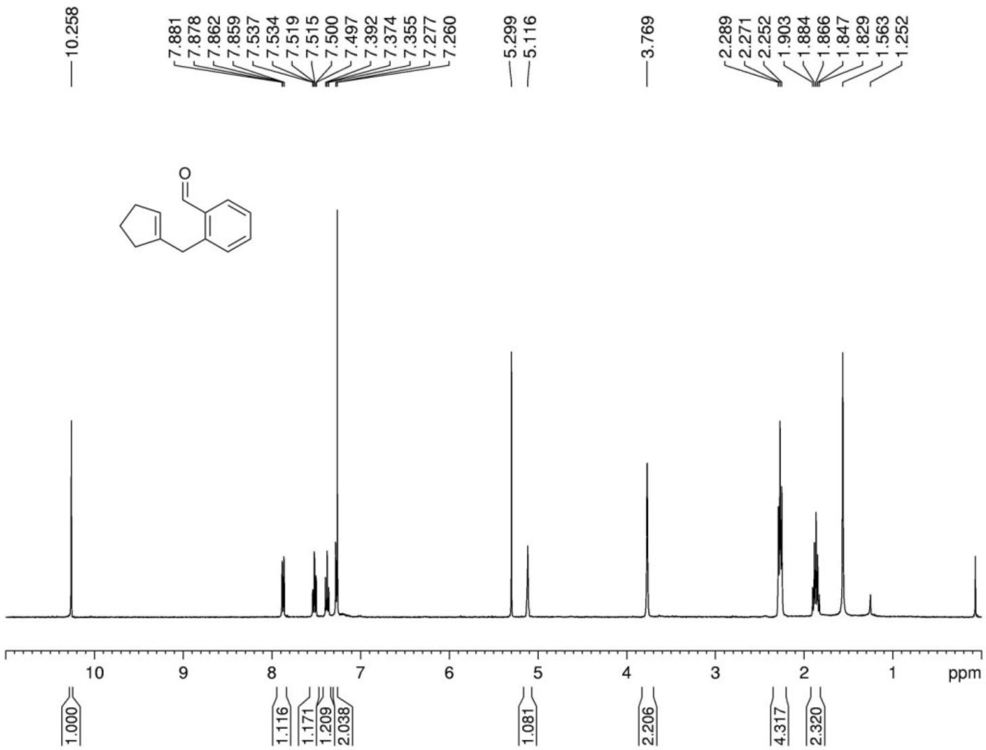
10.258
7.881
7.878
7.862
7.859
7.537
7.534
7.519
7.515
7.500
7.497
7.392
7.374
7.355
7.277
7.260
5.299
5.116
3.769
2.289
2.271
2.252
1.903
1.884
1.866
1.847
1.829
1.563
1.252
O
10
9
8
7
6
5
4
3
2
1
ppm
1.000
1.116
1.171
1.209
2.038
1.081
2.206
4.317
2.320

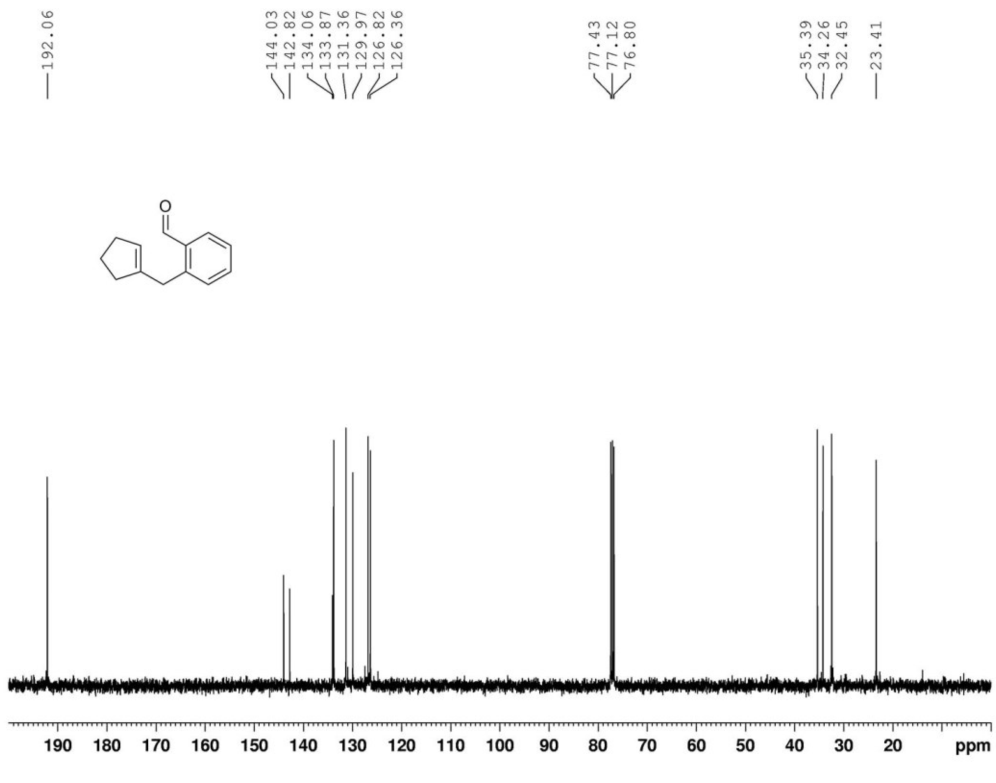
192.06
144.03
142.82
134.06
133.87
131.36
129.97
126.82
126.36
77.43
77.12
76.80
35.39
34.26
32.45
23.41
O
190
180
170
160
150
140
130
120
110
100
90
80
70
60
50
40
30
20
ppm

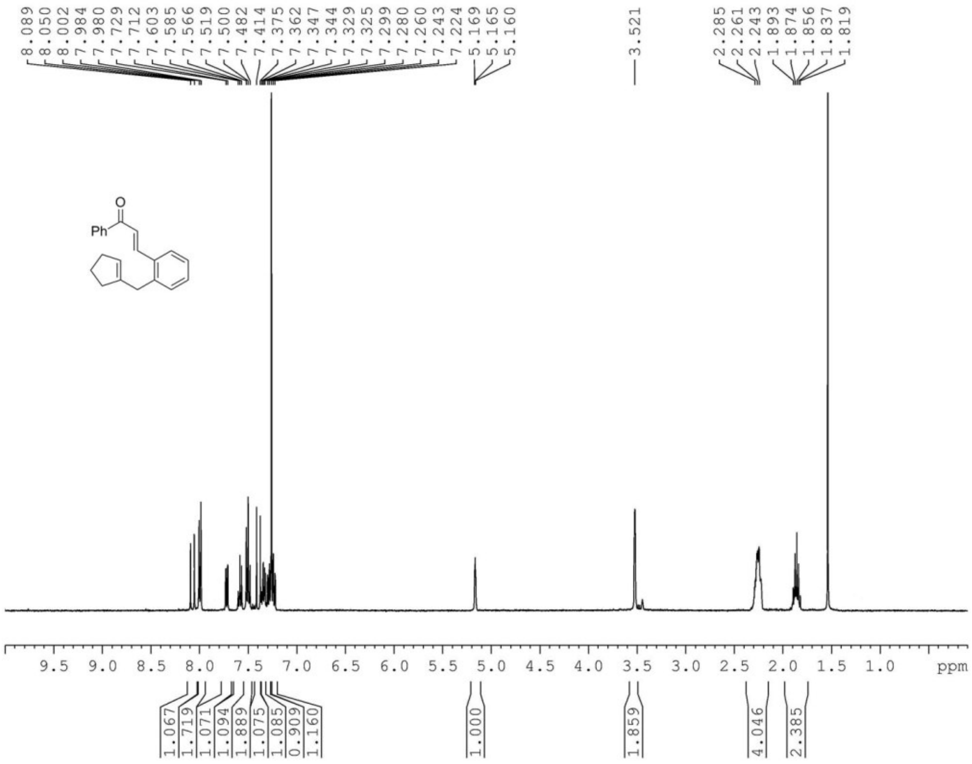
8.089
8.050
8.002
7.984
7.980
7.729
7.712
7.603
7.585
7.566
7.519
7.500
7.482
7.414
7.375
7.362
7.347
7.344
7.329
7.325
7.299
7.280
7.260
7.243
7.224
5.169
5.165
5.160
3.521
2.285
2.261
2.243
1.893
1.874
1.856
1.837
1.819
O
Ph
9.5 9.0 8.5 8.0 7.5 7.0 6.5 6.0 5.5 5.0 4.5 4.0 3.5 3.0 2.5 2.0 1.5 1.0 ppm
1.067
1.719
1.071
1.094
1.889
1.075
1.085
0.909
1.160
1.000
1.859
4.046
2.385

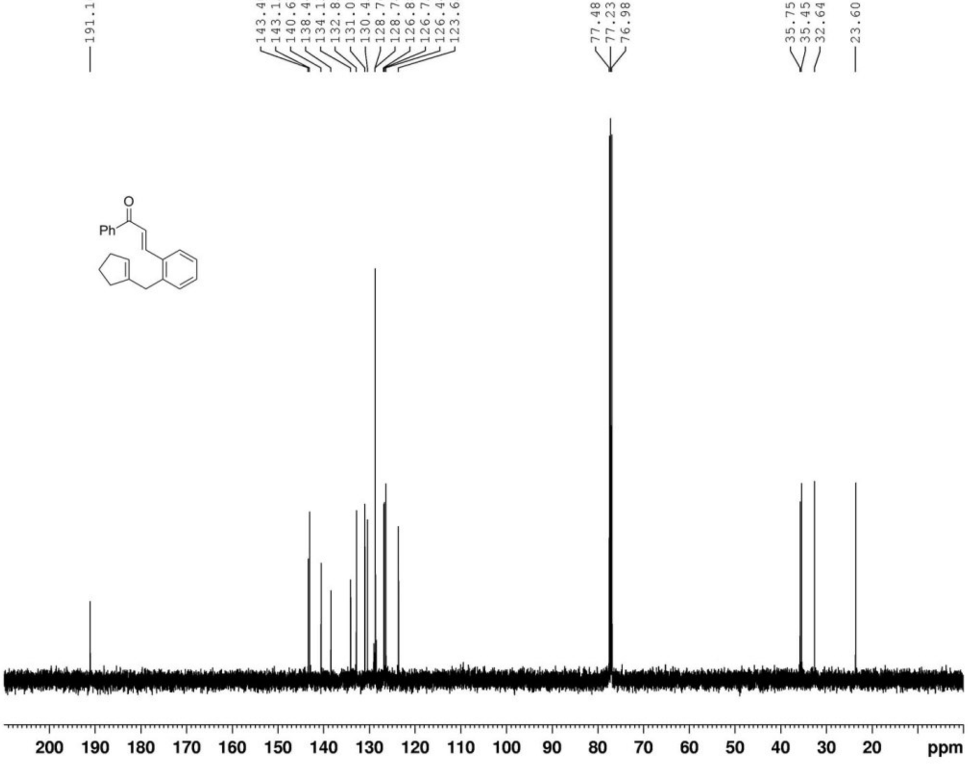
191.16
143.40
143.13
140.61
138.44
134.13
132.85
131.01
130.43
128.76
128.74
126.88
126.73
126.44
123.65
77.48
77.23
76.98
35.75
35.45
32.64
23.60
O
Ph
200 190 180 170 160 150 140 130 120 110 100 90 80 70 60 50 40 30 20 ppm

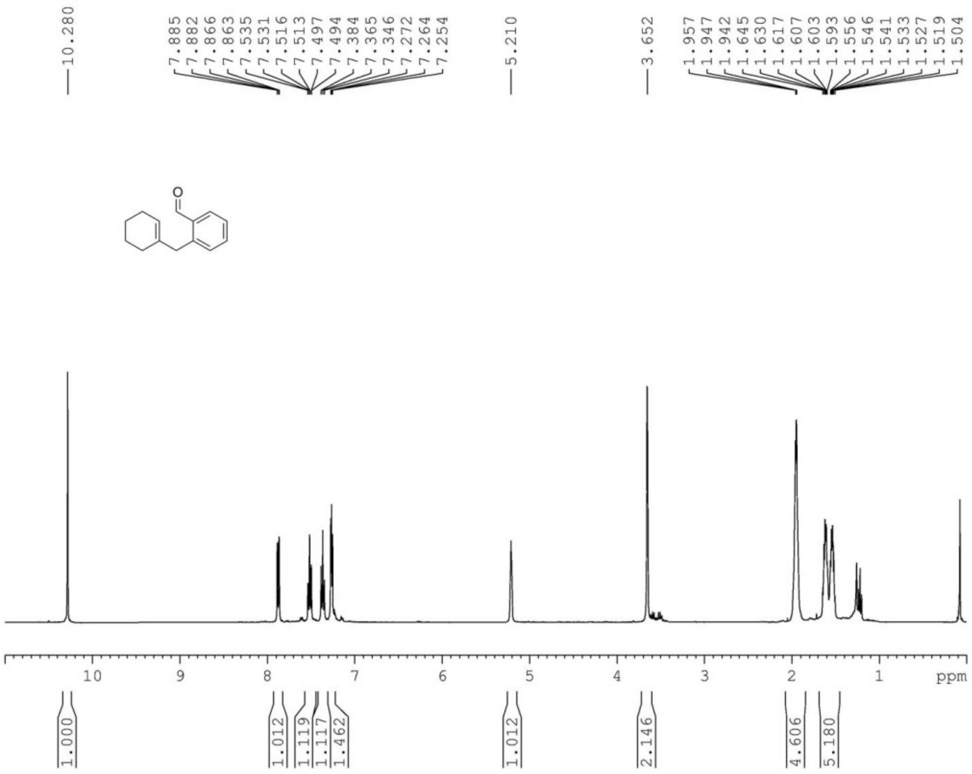
10.280
7.885
7.882
7.866
7.863
7.535
7.531
7.516
7.513
7.497
7.494
7.384
7.365
7.346
7.272
7.264
7.254
5.210
3.652
1.957
1.947
1.942
1.645
1.630
1.617
1.607
1.603
1.593
1.556
1.546
1.541
1.533
1.527
1.519
1.504
O
10
9
8
7
6
5
4
3
2
1
ppm
1.000
1.012
1.119
1.117
1.462
1.012
2.146
4.606
5.180

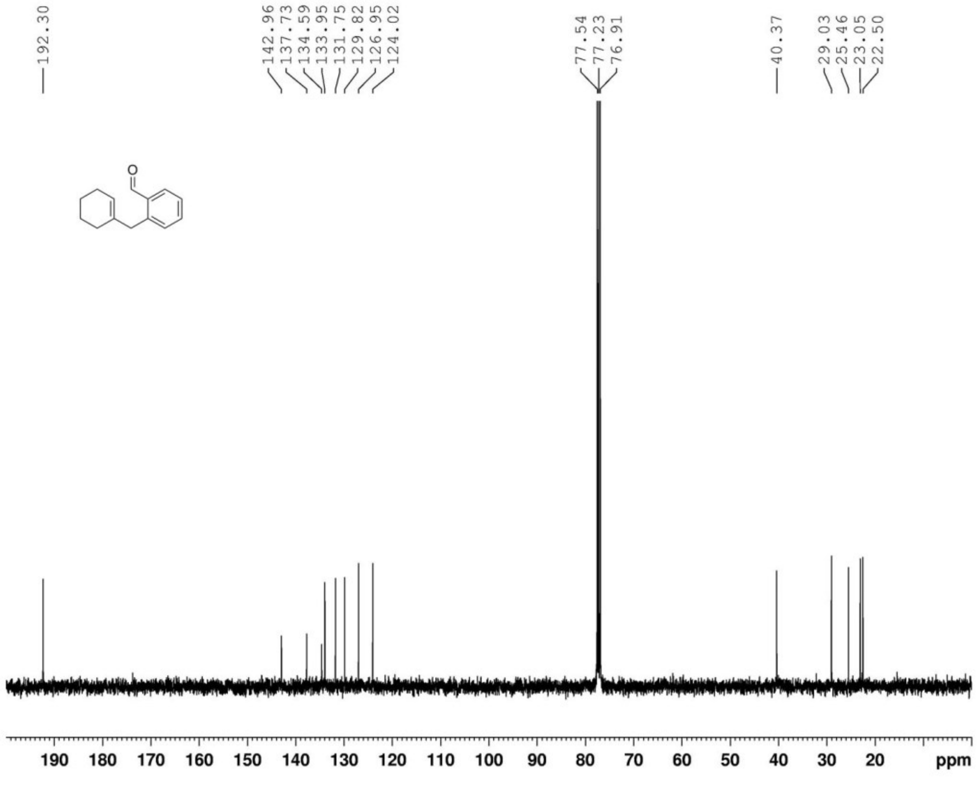
192.30
142.96
137.73
134.59
133.95
131.75
129.82
126.95
124.02
77.54
77.23
76.91
40.37
29.03
25.46
23.05
22.50
O
190
180
170
160
150
140
130
120
110
100
90
80
70
60
50
40
30
20
ppm

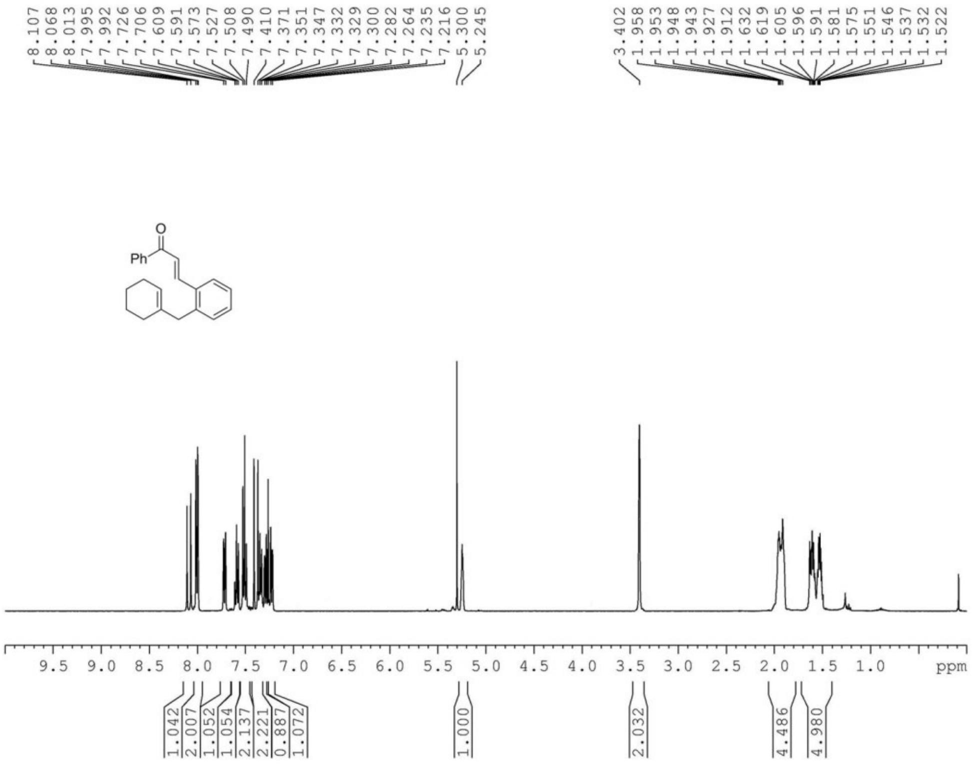
8.107
8.068
8.013
7.995
7.992
7.726
7.706
7.609
7.591
7.573
7.527
7.508
7.490
7.410
7.371
7.351
7.347
7.332
7.329
7.300
7.282
7.264
7.235
7.216
5.300
5.245
3.402
1.958
1.953
1.948
1.943
1.927
1.912
1.632
1.619
1.605
1.596
1.591
1.581
1.575
1.551
1.546
1.537
1.532
1.522
O
Ph
9.5 9.0 8.5 8.0 7.5 7.0 6.5 6.0 5.5 5.0 4.5 4.0 3.5 3.0 2.5 2.0 1.5 1.0 ppm
1.042
2.007
1.052
1.054
2.137
2.221
0.887
1.072
1.000
2.032
4.486
4.980

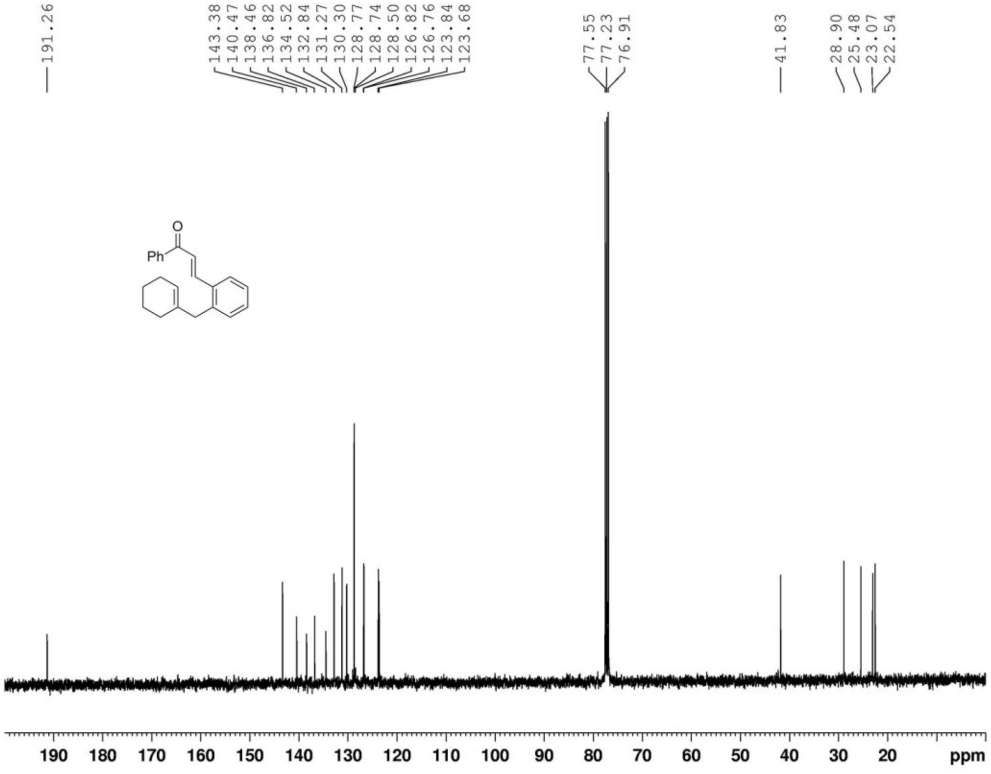
191.26
143.38
140.47
138.46
136.82
134.52
132.84
131.27
130.30
128.77
128.74
128.50
126.82
126.76
123.84
123.68
77.55
77.23
76.91
41.83
28.90
25.48
23.07
22.54
O
Ph
190 180 170 160 150 140 130 120 110 100 90 80 70 60 50 40 30 20 ppm

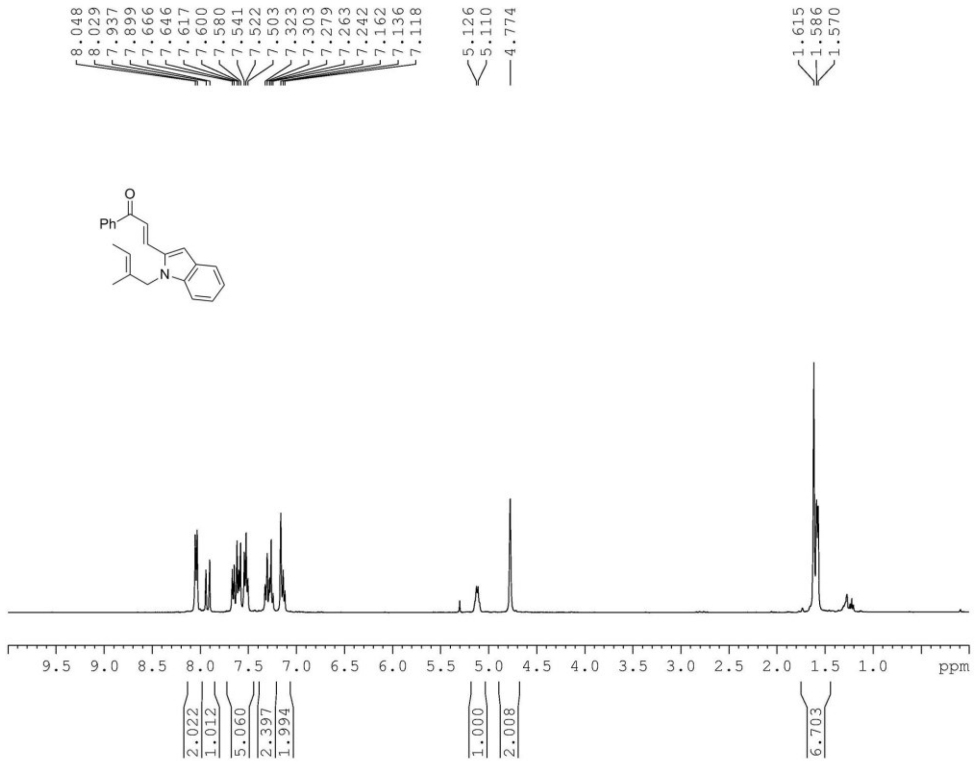
8.048
8.029
7.937
7.899
7.666
7.646
7.617
7.600
7.580
7.541
7.522
7.503
7.323
7.303
7.279
7.263
7.242
7.162
7.136
7.118
5.126
5.110
4.774
1.615
1.586
1.570
Ph
O
N
9.5 9.0 8.5 8.0 7.5 7.0 6.5 6.0 5.5 5.0 4.5 4.0 3.5 3.0 2.5 2.0 1.5 1.0 ppm
2.022
1.012
5.060
2.397
1.994
1.000
2.008
6.703

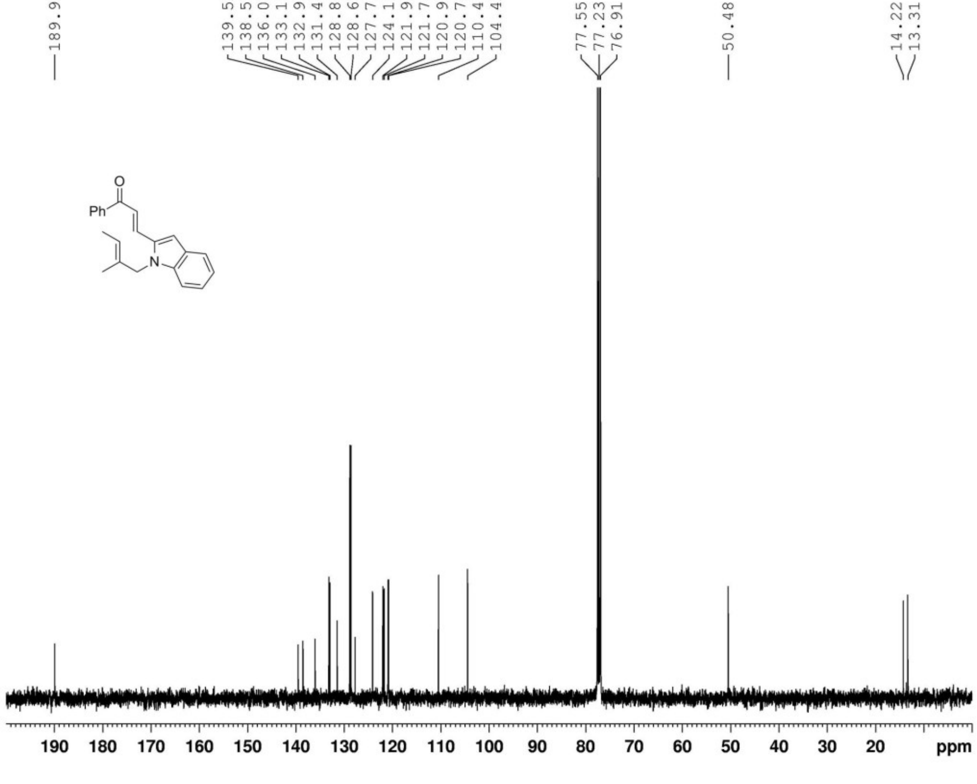
189.91
139.52
138.51
136.00
133.15
132.93
131.44
128.84
128.60
127.71
124.10
121.98
121.70
120.91
120.79
110.44
104.42
77.55
77.23
76.91
50.48
14.22
13.31
Ph
O
N
190 180 170 160 150 140 130 120 110 100 90 80 70 60 50 40 30 20 ppm

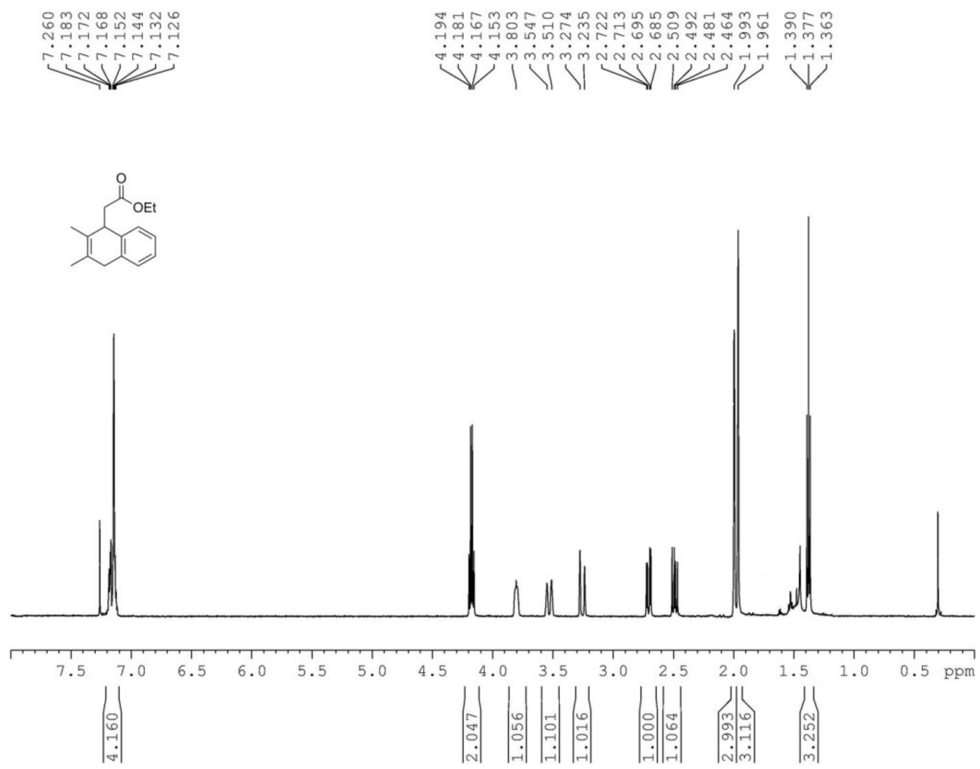
7.260
7.183
7.172
7.168
7.152
7.144
7.132
7.126
4.194
4.181
4.167
4.153
3.803
3.547
3.510
3.274
3.235
2.722
2.713
2.695
2.685
2.509
2.492
2.481
2.464
1.993
1.961
1.390
1.377
1.363
O
OEt
7.5
7.0
6.5
6.0
5.5
5.0
4.5
4.0
3.5
3.0
2.5
2.0
1.5
1.0
0.5
ppm
4.160
2.047
1.056
1.101
1.016
1.000
1.064
2.993
3.116
3.252

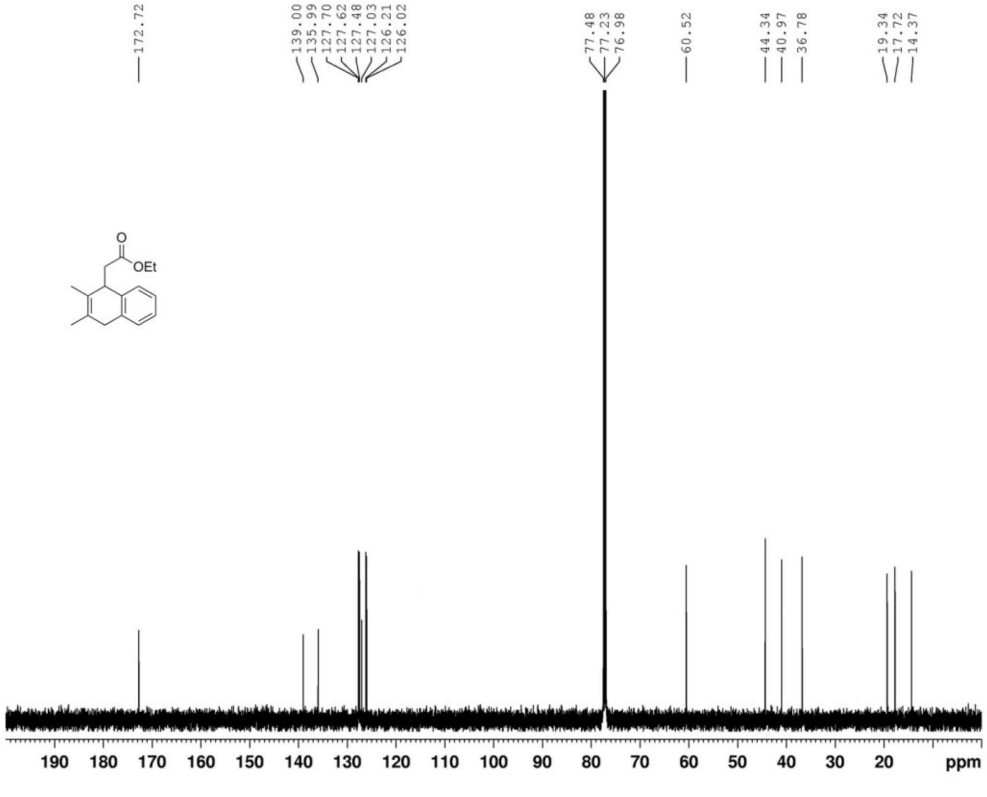
172.72
139.00
135.99
127.70
127.62
127.48
127.03
126.21
126.02
77.48
77.23
76.98
60.52
44.34
40.97
36.78
19.34
17.72
14.37
O
OEt
190
180
170
160
150
140
130
120
110
100
90
80
70
60
50
40
30
20
ppm

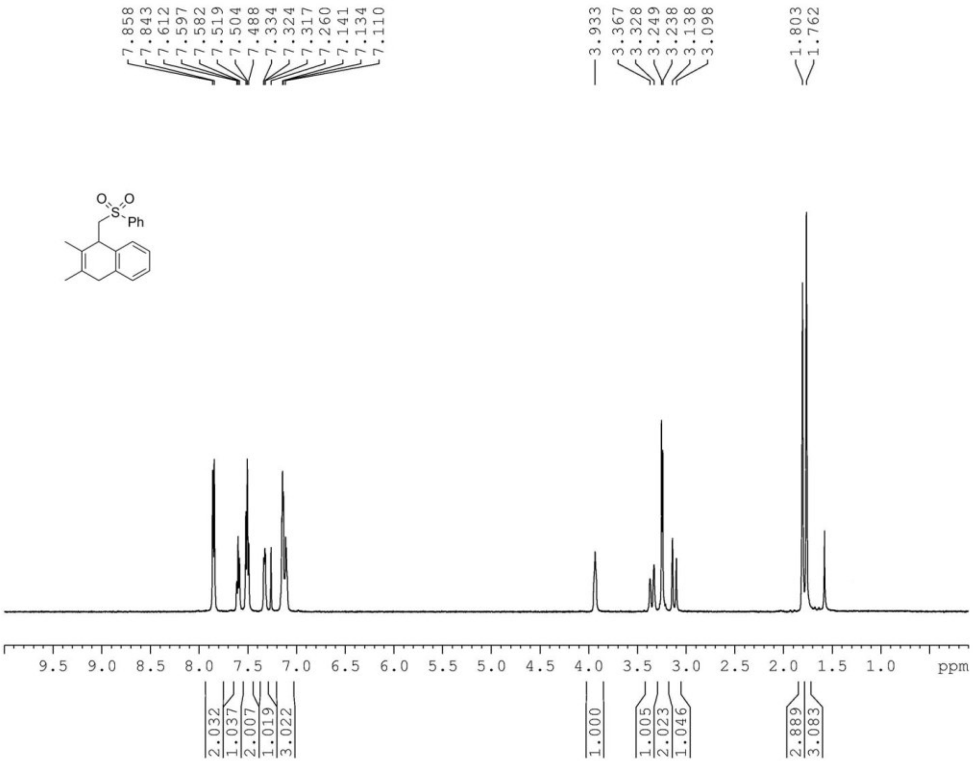
7.858
7.843
7.612
7.597
7.582
7.519
7.504
7.488
7.334
7.324
7.317
7.260
7.141
7.134
7.110
3.933
3.367
3.328
3.249
3.238
3.138
3.098
1.803
1.762
O
O
S
Ph
9.5
9.0
8.5
8.0
7.5
7.0
6.5
6.0
5.5
5.0
4.5
4.0
3.5
3.0
2.5
2.0
1.5
1.0
ppm
2.032
1.037
2.007
1.019
3.022
1.000
1.005
2.023
1.046
2.889
3.083

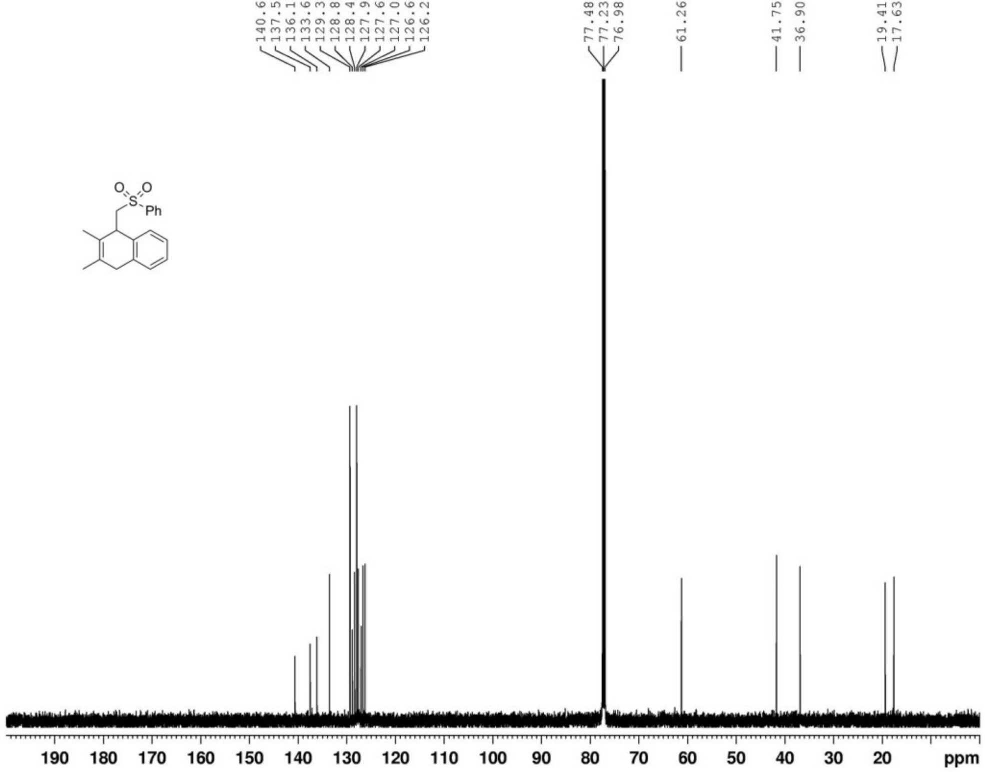
140.68
137.52
136.16
133.60
129.35
128.89
128.41
127.95
127.62
127.06
126.69
126.27
77.48
77.23
76.98
61.26
41.75
36.90
19.41
17.63
O
O
S
Ph
190
180
170
160
150
140
130
120
110
100
90
80
70
60
50
40
30
20
ppm

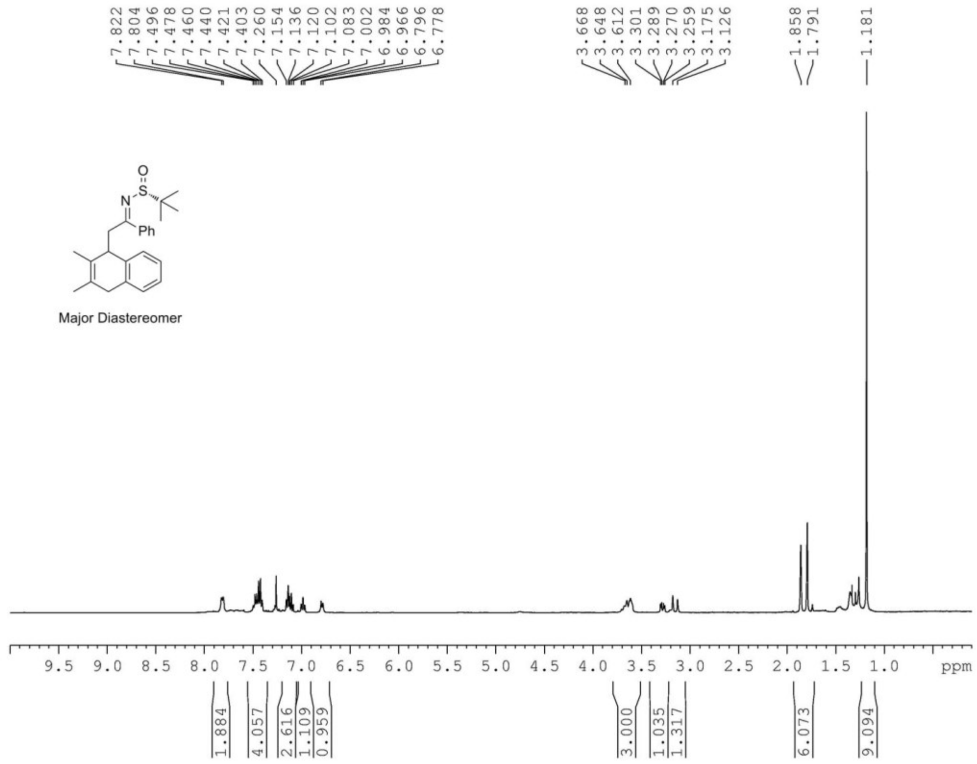
7.822
7.804
7.496
7.478
7.460
7.440
7.421
7.403
7.260
7.154
7.136
7.120
7.102
7.083
7.002
6.984
6.966
6.796
6.778
3.668
3.648
3.612
3.301
3.289
3.270
3.259
3.175
3.126
1.858
1.791
1.181
O
N
S
Ph
Major Diastereomer
9.5
9.0
8.5
8.0
7.5
7.0
6.5
6.0
5.5
5.0
4.5
4.0
3.5
3.0
2.5
2.0
1.5
1.0
ppm
1.884
4.057
2.616
1.109
0.959
3.000
1.035
1.317
6.073
9.094

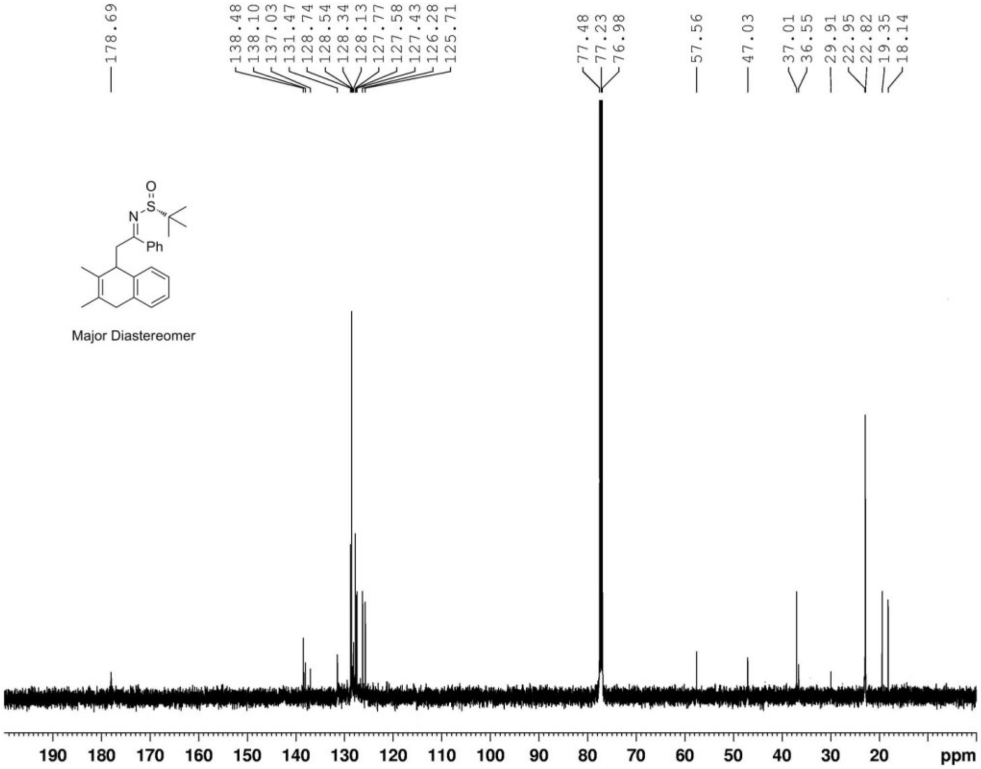
178.69
138.48
138.10
137.03
131.47
128.74
128.54
128.34
128.13
127.77
127.58
127.43
126.28
125.71
77.48
77.23
76.98
57.56
47.03
37.01
36.55
29.91
22.95
22.82
19.35
18.14
O
N
S
Ph
Major Diastereomer
190
180
170
160
150
140
130
120
110
100
90
80
70
60
50
40
30
20
ppm

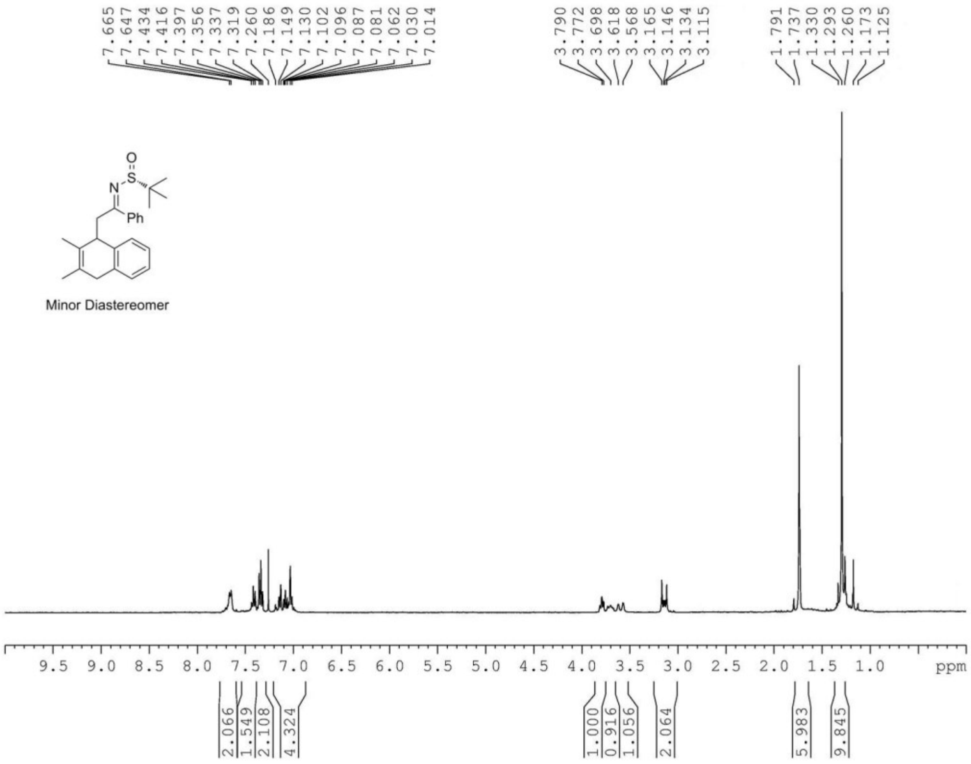
7.665
7.647
7.434
7.416
7.397
7.356
7.337
7.319
7.260
7.186
7.149
7.130
7.102
7.096
7.087
7.081
7.062
7.030
7.014
3.790
3.772
3.698
3.618
3.568
3.165
3.146
3.134
3.115
1.791
1.737
1.330
1.293
1.260
1.173
1.125
O
S
N
Ph
Minor Diastereomer
9.5
9.0
8.5
8.0
7.5
7.0
6.5
6.0
5.5
5.0
4.5
4.0
3.5
3.0
2.5
2.0
1.5
1.0
ppm
2.066
1.549
2.108
4.324
1.000
0.916
1.056
2.064
5.983
9.845

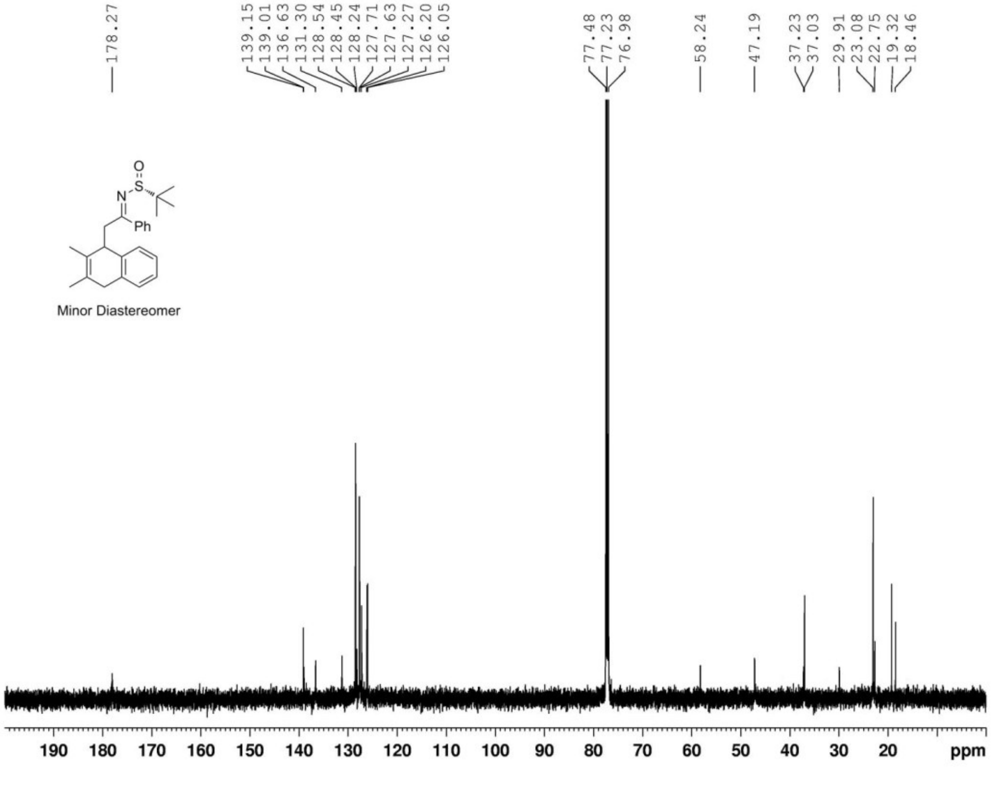
178.27
139.15
139.01
136.63
131.30
128.54
128.45
128.24
127.71
127.63
127.27
126.20
126.05
77.48
77.23
76.98
58.24
47.19
37.23
37.03
29.91
23.08
22.75
19.32
18.46
O
S
N
Ph
Minor Diastereomer
190
180
170
160
150
140
130
120
110
100
90
80
70
60
50
40
30
20
ppm

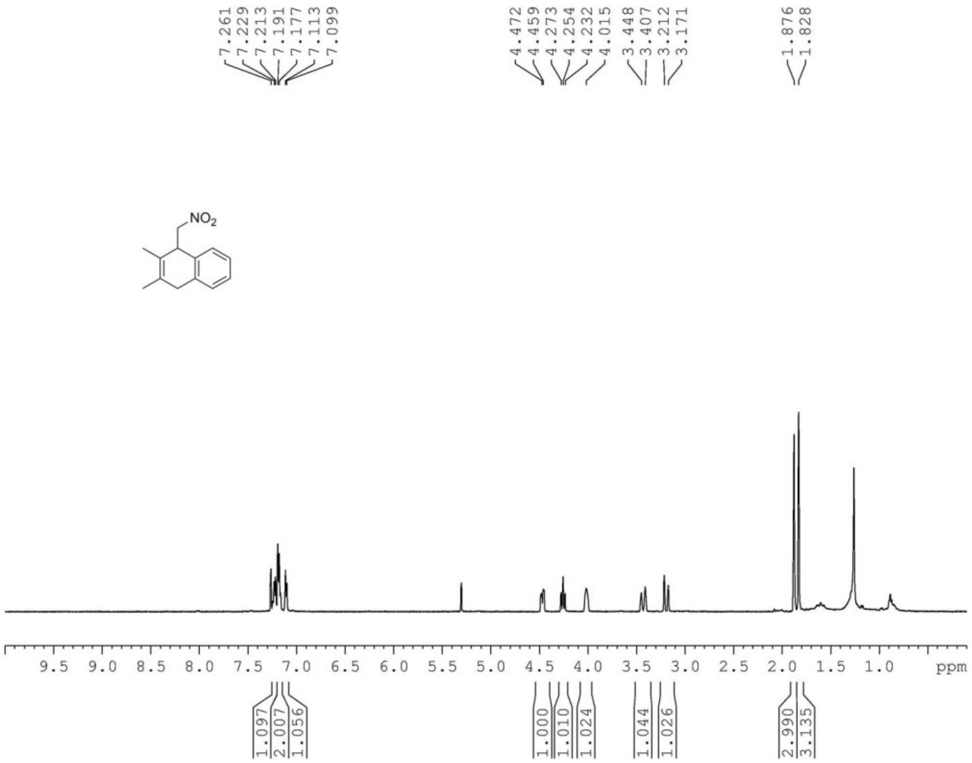

7.261
7.229
7.213
7.191
7.177
7.113
7.099
4.472
4.459
4.273
4.254
4.232
4.015
3.448
3.407
3.212
3.171
1.876
1.828
NO2
9.5 9.0 8.5 8.0 7.5 7.0 6.5 6.0 5.5 5.0 4.5 4.0 3.5 3.0 2.5 2.0 1.5 1.0 ppm
1.097
2.007
1.056
1.000
1.010
1.024
1.044
1.026
2.990
3.135

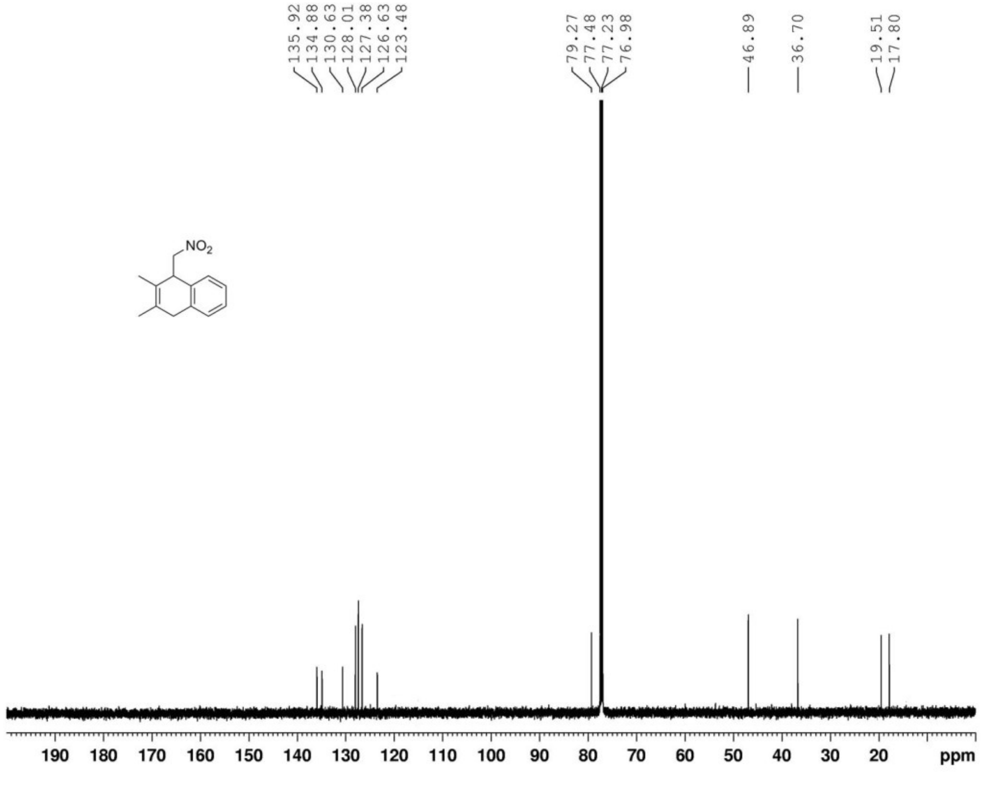

135.92
134.88
130.63
128.01
127.38
126.63
123.48
79.27
77.48
77.23
76.98
46.89
36.70
19.51
17.80
NO2
190 180 170 160 150 140 130 120 110 100 90 80 70 60 50 40 30 20 ppm

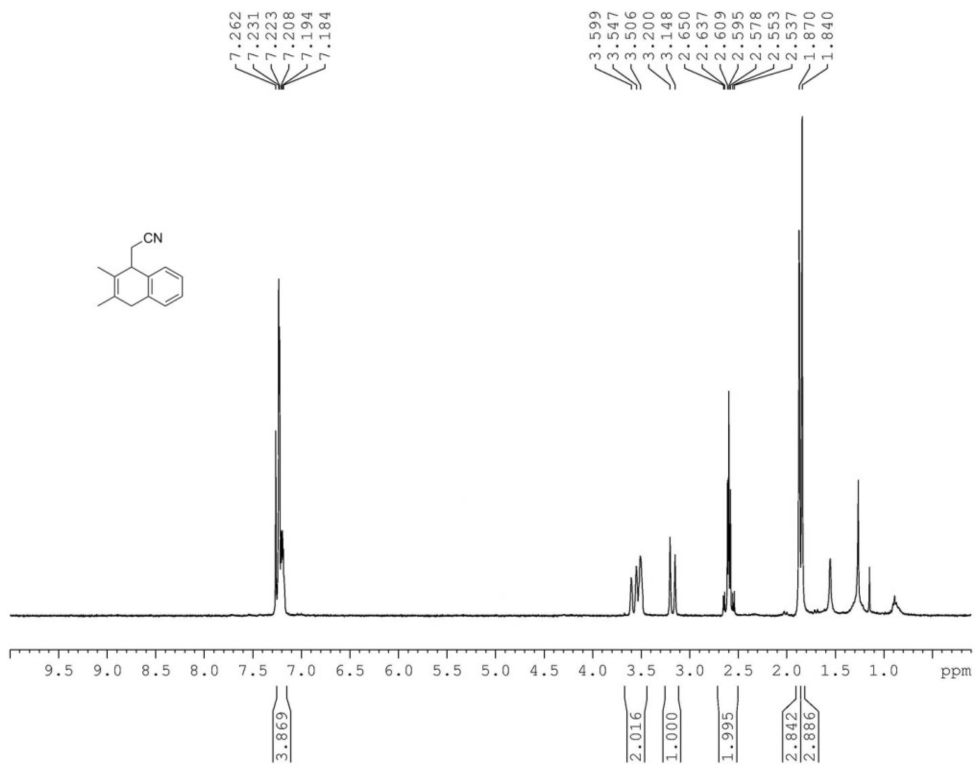
7.262
7.231
7.223
7.208
7.194
7.184
3.599
3.547
3.506
3.200
3.148
2.650
2.637
2.609
2.595
2.578
2.553
2.537
1.870
1.840
CN
9.5
9.0
8.5
8.0
7.5
7.0
6.5
6.0
5.5
5.0
4.5
4.0
3.5
3.0
2.5
2.0
1.5
1.0
ppm
3.869
2.016
1.000
1.995
2.842
2.886

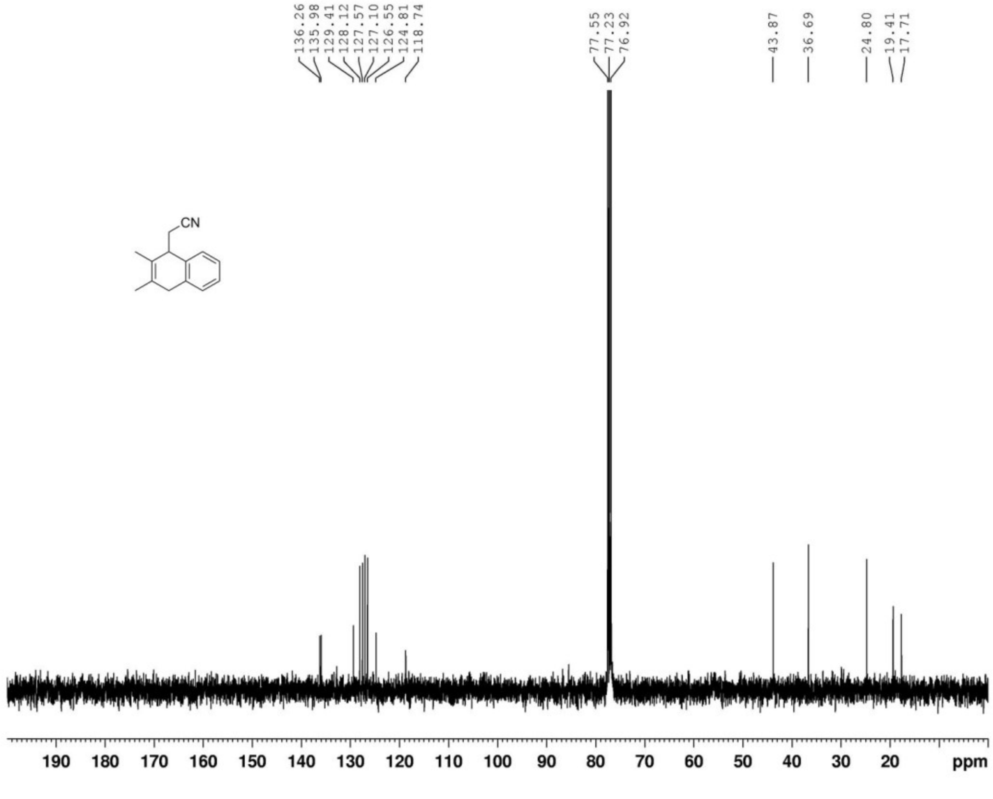
136.26
135.98
129.41
128.12
127.57
127.10
126.55
124.81
118.74
77.55
77.23
76.92
43.87
36.69
24.80
19.41
17.71
CN
190
180
170
160
150
140
130
120
110
100
90
80
70
60
50
40
30
20
ppm

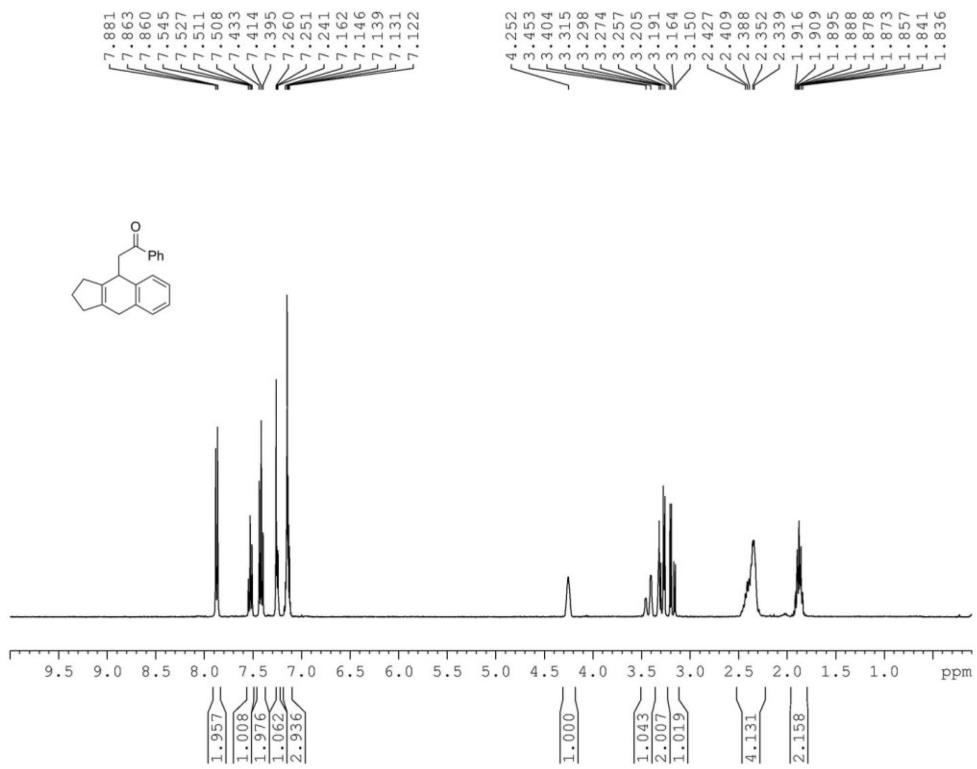
7.881
7.863
7.860
7.545
7.527
7.511
7.508
7.433
7.414
7.395
7.260
7.251
7.241
7.162
7.146
7.139
7.131
7.122
4.252
3.453
3.404
3.315
3.298
3.274
3.257
3.205
3.191
3.164
3.150
2.427
2.409
2.388
2.352
2.339
1.916
1.909
1.895
1.888
1.878
1.873
1.857
1.841
1.836
O
Ph
9.5
9.0
8.5
8.0
7.5
7.0
6.5
6.0
5.5
5.0
4.5
4.0
3.5
3.0
2.5
2.0
1.5
1.0
ppm
1.957
1.008
1.976
1.062
2.936
1.000
1.043
2.007
1.019
4.131
2.158

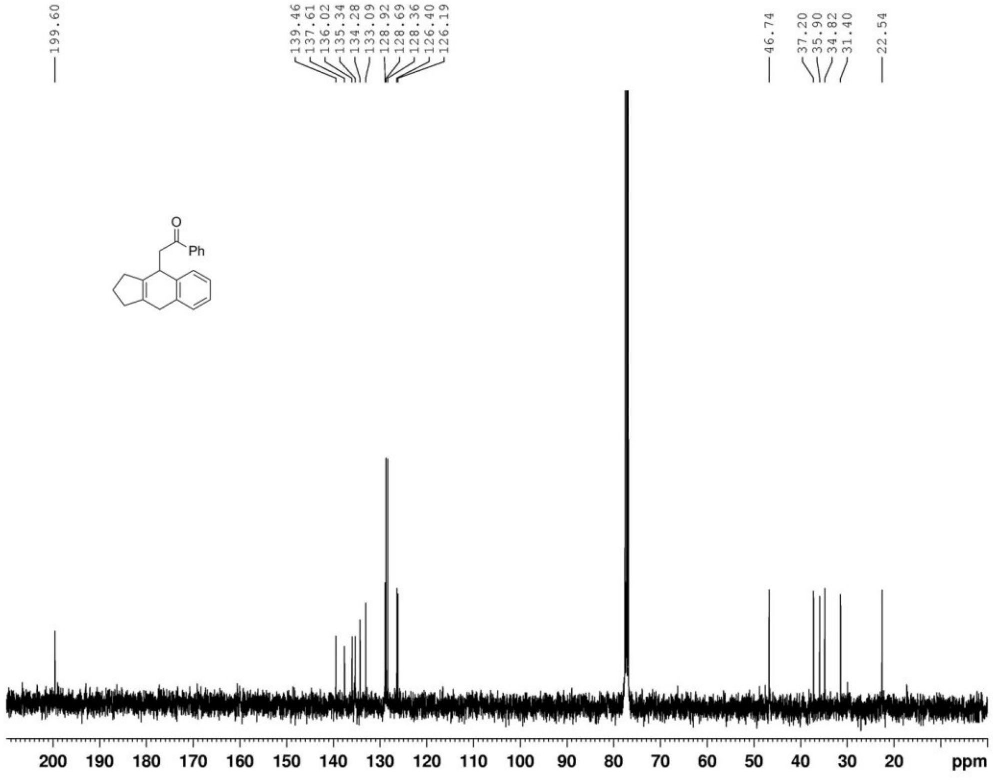
199.60
139.46
137.61
136.02
135.34
134.28
133.09
128.92
128.69
128.36
126.40
126.19
46.74
37.20
35.90
34.82
31.40
22.54
O
Ph
200
190
180
170
160
150
140
130
120
110
100
90
80
70
60
50
40
30
20
ppm

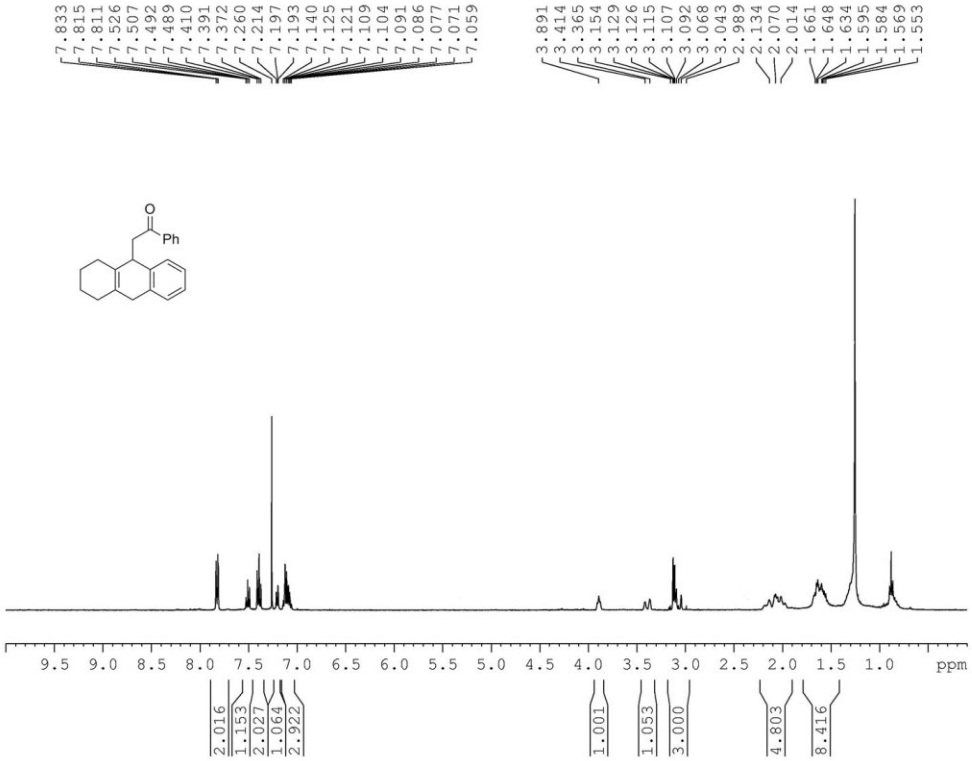
7.833
7.815
7.811
7.526
7.507
7.492
7.489
7.410
7.391
7.372
7.260
7.214
7.197
7.193
7.140
7.125
7.121
7.109
7.104
7.091
7.086
7.077
7.071
7.059
3.891
3.414
3.365
3.154
3.129
3.126
3.115
3.107
3.092
3.068
3.043
2.989
2.134
2.070
2.014
1.661
1.648
1.634
1.595
1.584
1.569
1.553
O
Ph
9.5
9.0
8.5
8.0
7.5
7.0
6.5
6.0
5.5
5.0
4.5
4.0
3.5
3.0
2.5
2.0
1.5
1.0
ppm
2.016
1.153
2.027
1.064
2.922
1.001
1.053
3.000
4.803
8.416

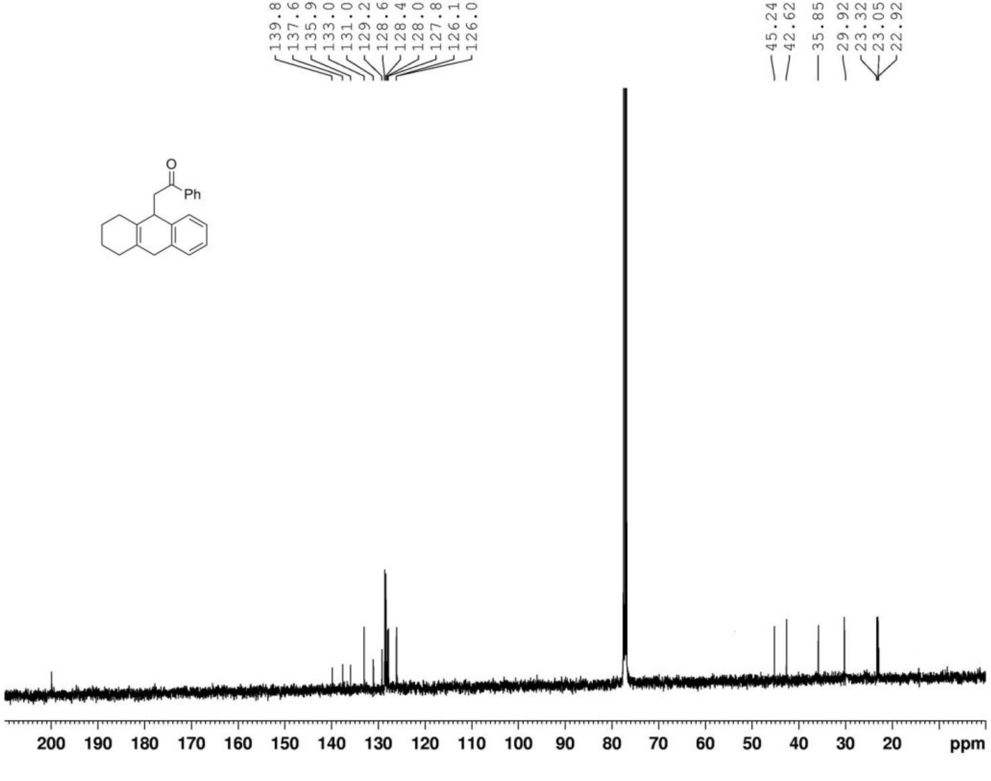
139.89
137.63
135.94
133.06
131.07
129.23
128.64
128.41
128.09
127.86
126.11
126.08
45.24
42.62
35.85
29.92
23.32
23.05
22.92
O
Ph
200
190
180
170
160
150
140
130
120
110
100
90
80
70
60
50
40
30
20
ppm

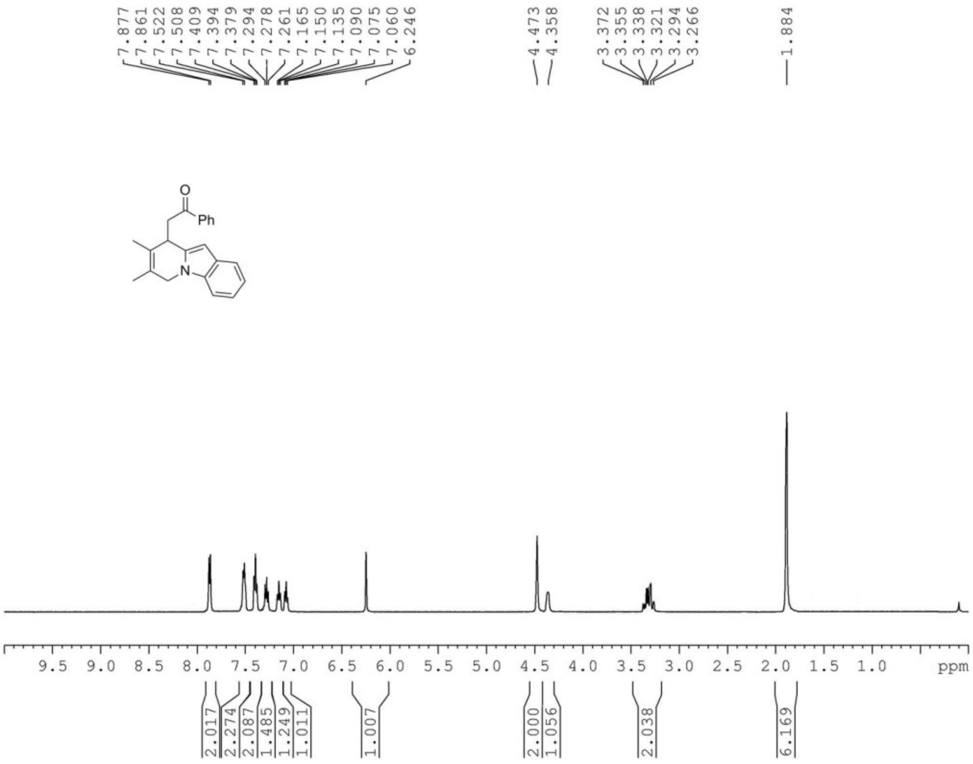
7.877
7.861
7.522
7.508
7.409
7.394
7.379
7.294
7.278
7.261
7.165
7.150
7.135
7.090
7.075
7.060
6.246
4.473
4.358
3.372
3.355
3.338
3.321
3.294
3.266
1.884
O
Ph
N
9.5
9.0
8.5
8.0
7.5
7.0
6.5
6.0
5.5
5.0
4.5
4.0
3.5
3.0
2.5
2.0
1.5
1.0
ppm
2.017
2.274
2.087
1.485
1.249
1.011
1.007
2.000
1.056
2.038
6.169

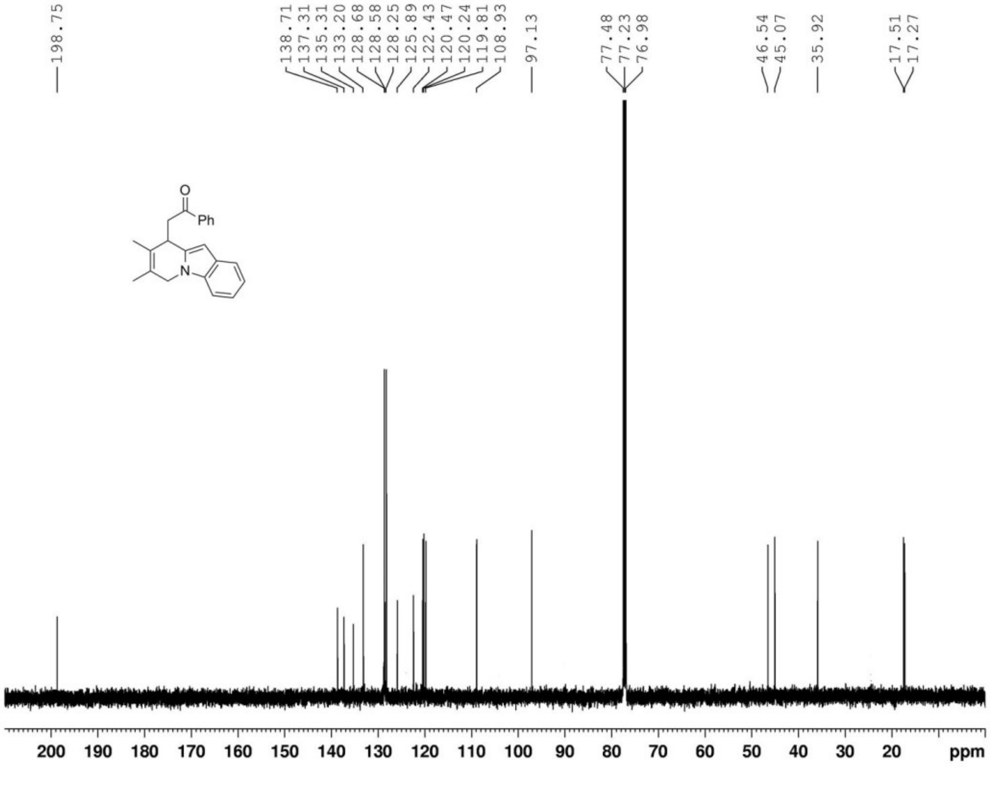
198.75
138.71
137.31
135.31
133.20
128.68
128.58
128.25
125.89
122.43
120.47
120.24
119.81
108.93
97.13
77.48
77.23
76.98
46.54
45.07
35.92
17.51
17.27
O
Ph
N
200
190
180
170
160
150
140
130
120
110
100
90
80
70
60
50
40
30
20
ppm

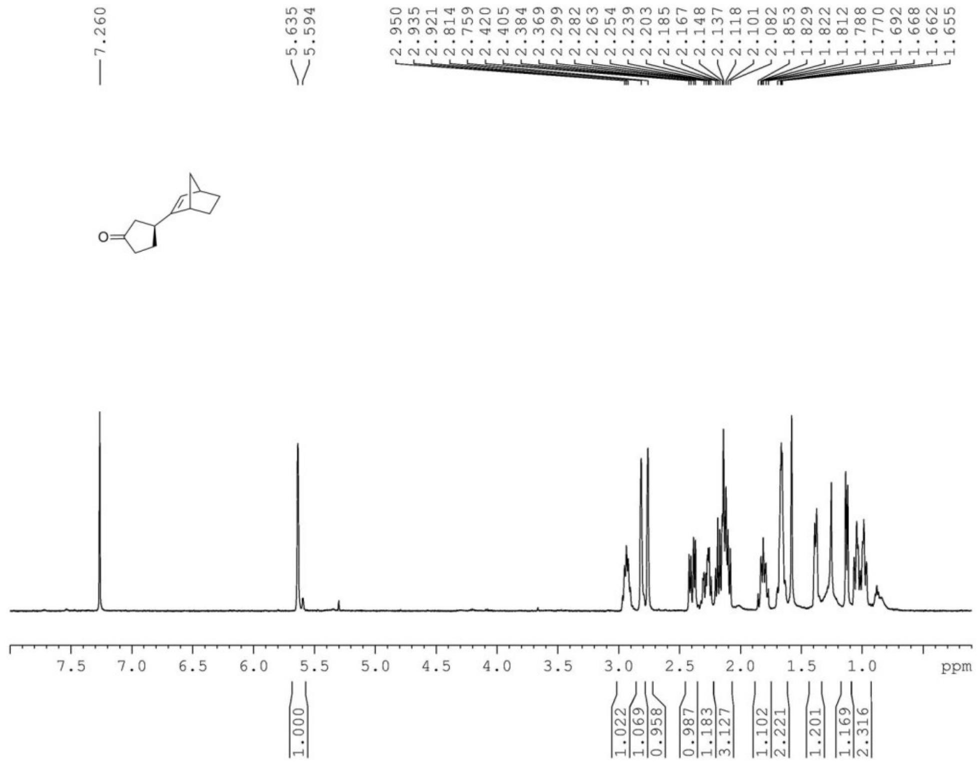
7.260
5.635
5.594
2.950
2.935
2.921
2.814
2.759
2.420
2.405
2.384
2.369
2.299
2.282
2.263
2.254
2.239
2.203
2.185
2.167
2.148
2.137
2.118
2.101
2.082
1.853
1.829
1.822
1.812
1.788
1.770
1.692
1.668
1.662
1.655
O
7.5
7.0
6.5
6.0
5.5
5.0
4.5
4.0
3.5
3.0
2.5
2.0
1.5
1.0
ppm
1.000
1.022
1.069
0.958
0.987
1.183
3.127
1.102
2.221
1.201
1.169
2.316

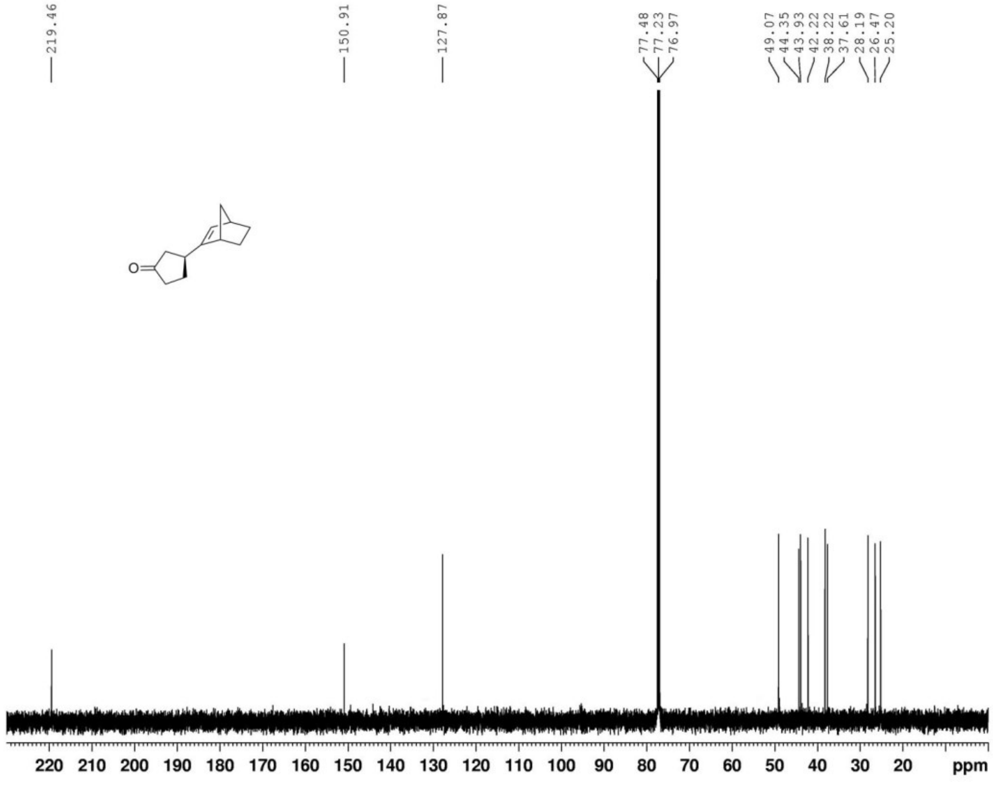
219.46
150.91
127.87
77.48
77.23
76.97
49.07
44.35
43.93
42.22
38.22
37.61
28.19
26.47
25.20
O
220
210
200
190
180
170
160
150
140
130
120
110
100
90
80
70
60
50
40
30
20
ppm

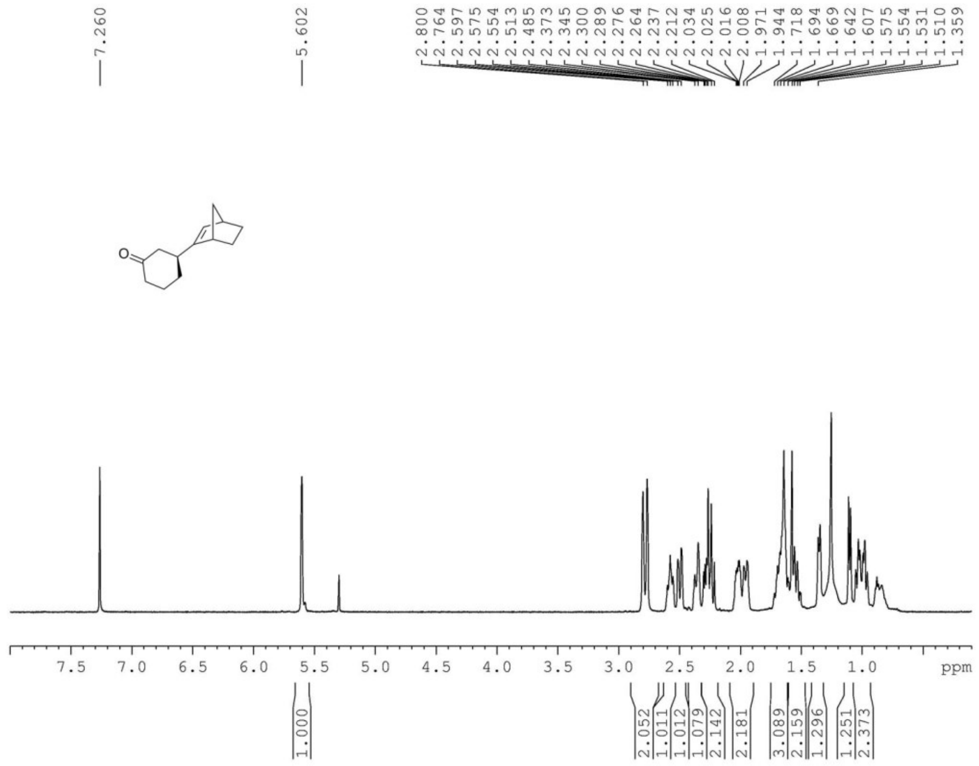
7.260
5.602
2.800
2.764
2.597
2.575
2.554
2.513
2.485
2.373
2.345
2.300
2.289
2.276
2.264
2.237
2.212
2.034
2.025
2.016
2.008
1.971
1.944
1.718
1.694
1.669
1.642
1.607
1.575
1.554
1.531
1.510
1.359
O
7.5
7.0
6.5
6.0
5.5
5.0
4.5
4.0
3.5
3.0
2.5
2.0
1.5
1.0
ppm
1.000
2.052
1.011
1.012
1.079
2.142
2.181
3.089
2.159
1.296
1.251
2.373

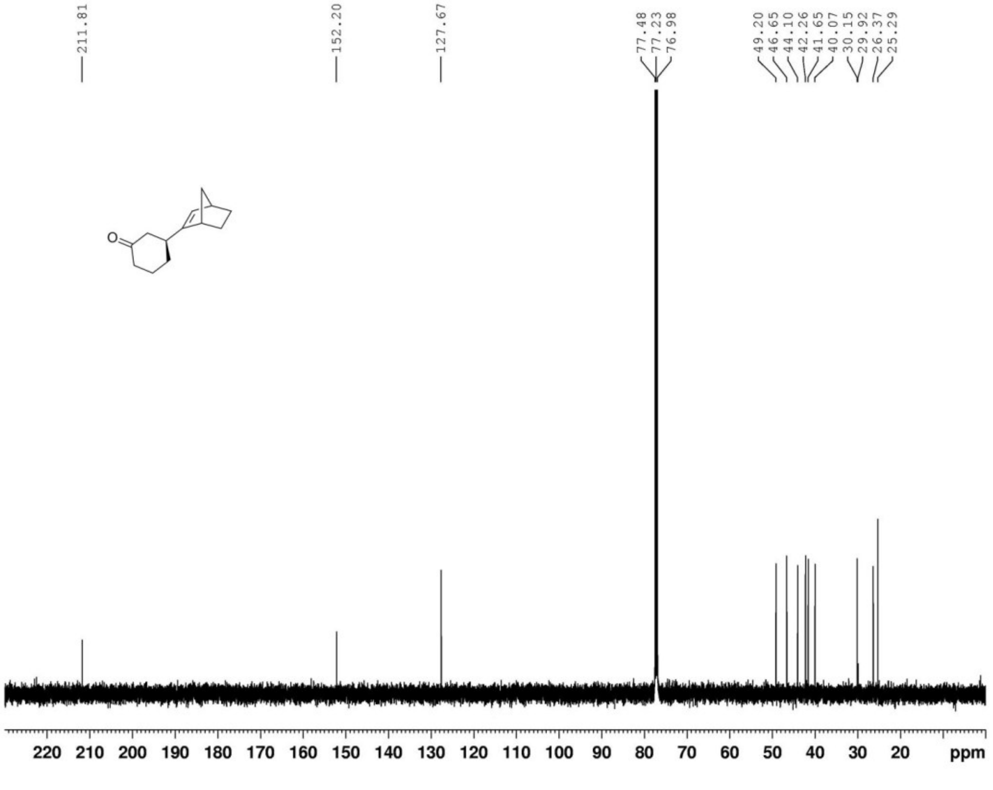
211.81
152.20
127.67
77.48
77.23
76.98
49.20
46.65
44.10
42.26
41.65
40.07
30.15
29.92
26.37
25.29
O
220
210
200
190
180
170
160
150
140
130
120
110
100
90
80
70
60
50
40
30
20
ppm

Chapter 3. The Application of a Ruthenium Dinitrosyl Complex to the Vinylic C-H Functionalization Reaction of Simple Alkenes and A Comparison of the Cobalt and Ruthenium Systems

Portions of this chapter have been previously published in:
Chen Zhao, Mark R. Crimmin, F. Dean Toste, and Robert G. Bergman. "Ligand-Based Carbon–Nitrogen Bond Forming Reactions of Metal Dinitrosyl Complexes with Alkenes and their Application to C–H Bond Functionalization," *Acc. Chem. Res.* **2014**, *47*, 517-529.

3.1. Introduction

In 2011, our groups reported the synthesis of ruthenium dinitrosyl complex **1** from the reaction of NO and dichloro-(*p*-cymene)ruthenium(II) dimer in 88% yield (eq 1).[1] Unlike the cobalt dinitrosyl complex [CpCo(NO)$_2$], ruthenium complex **1** is a stable and isolable complex. A single-crystal X-rray diffraction study demonstrated that **4** is a five-coordinate complex possessing a linear nitrosyl ligand in the basal-plane of square-based pyramidal geometry and a bent nitrosyl occupying the apical position. Hence complex **4** may be described as a neutral, 16-electron complex with a vacant coordination site opposite the apical nitrosyl. A related ruthenium complex, [RuCl(NO)$_2$(PPh$_3$)$_2$]PF$_6$, bearing both a linear and bent NO ligand, was reported by Eisenberg and co-workers in 1970.[2,3]

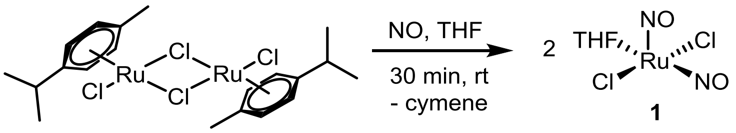

(eq 3.1)

Alkenes have been shown to bind ruthenium complex **1** in a fashion similar to that of the analogous cobalt dinitrosyl complex (see Chapter 1). For example, when **1** and 5 equivalents of norbornadiene were combined in either CD$_3$CN or THF-d_8, a putative bis-solvent coordinated ruthenium dinitrosoalkane complex was observed by NMR spectroscopy, but could not be isolated (Scheme 3.1). Addition of a bidendate ligand, such as TMEDA, to the solution of the bis-solvent (solvent = CD$_3$CN or THF-d_8) complex led to the formation of the octahedral complex **2**, which was purified and isolated by silica-gel chromatography in 61% yield. Furthermore, ruthenium dinitrosoalkane complexes of simple alkenes, such as **2** and **3**, can also be synthesized directly from commercially available dichloro-(*p*-cymene)ruthenium(II) dimer in the presence of alkenes, TMEDA and NO in one pot (eq 3.1).

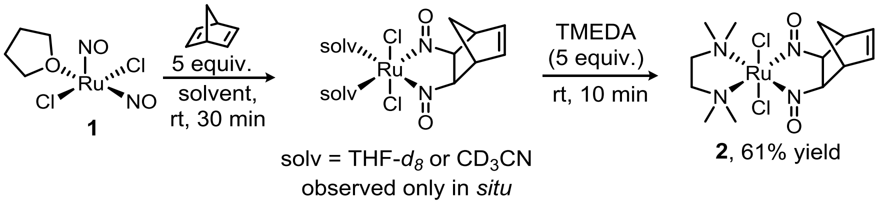

Scheme 3.1. Alkene Binding Reaction of Complex **1**, Norbornadiene and TMEDA

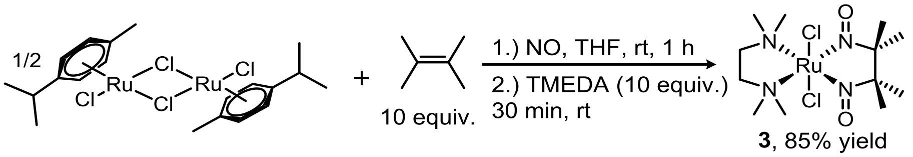
1/2
Ru
Cl
Ru
Cl
Cl
Cl
+
10 equiv.
1.) NO, THF, rt, 1 h
2.) TMEDA (10 equiv.)
30 min, rt
N
N
Cl
Ru
Cl
N
N
O
O
3, 85% yield

(eq 3.2)

The scope of the binding reaction between **4** and simple alkenes has also been surveyed and reported previously.[1] Generally, 10-30 equivalents of alkene and 10-20 equivalents of TMEDA were required to obtain the octahedral complexes in good yields (Scheme 3.2). Interestingly, following workup and purification, reactions of alkenes containing at least one vinylic C–H bond, including 1,1-disubstituted and 1,1,2-trisubstituted alkenes (e.g. 2-methyl-1-butene), resulted in the isolation of mono-oxime ruthenium complexes.

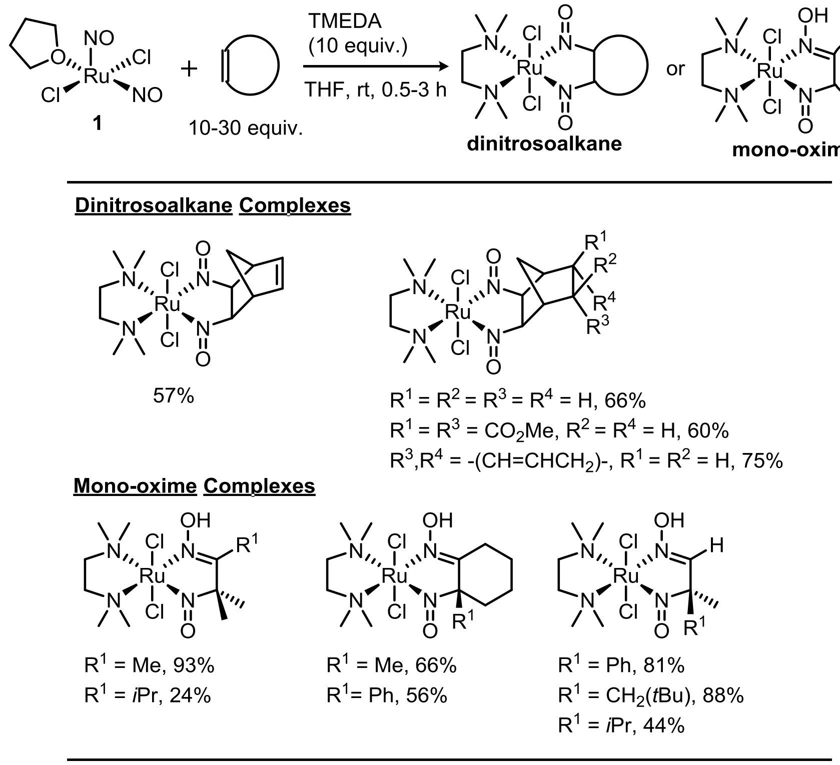
NO
O
Cl
Ru
Cl
NO
1
+
10-30 equiv.
TMEDA
(10 equiv.)
THF, rt, 0.5-3 h
dinitrosoalkane
or
OH
mono-oxime
Dinitrosoalkane Complexes
57%
R1
R2
R4
R3
R1 = R2 = R3 = R4 = H, 66%
R1 = R3 = CO2Me, R2 = R4 = H, 60%
R3,R4 = -(CH=CHCH2)-, R1 = R2 = H, 75%
Mono-oxime Complexes
R1 = Me, 93%
R1 = iPr, 24%
R1 = Me, 66%
R1= Ph, 56%
H
R1 = Ph, 81%
R1 = CH2(tBu), 88%
R1 = iPr, 44%

Scheme 3.2. Scope of Binding Reaction Between **1** and Simple Alkenes

Attempts to convert the mono-oxime complexes, such as **4** to the dinitroso complex thermally with and without tertiary amine bases, gave the isomerized *cis*-chloro-mono-oxime complex **5** as the major product. Furthermore, methylation of **4** gave the O-alkylated complex **6** as the major product and no isomerization to the dinitroso complex was observed; prolonged heating (6 days at 80 °C) only led to decomposition of **4** (Scheme 4).

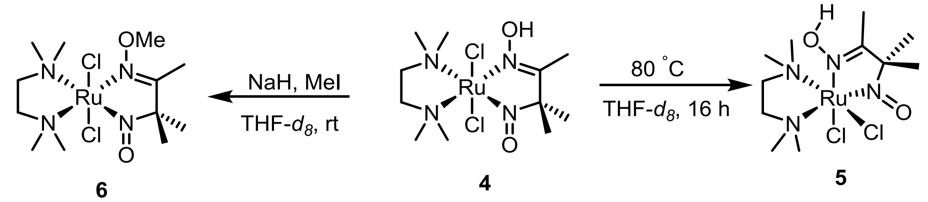

Scheme 3.3. Isomerization and O-Alkylation of Oxime Complex **4**

In contrast to the cobalt system, alkene exchange between norbornadiene and ruthenium complex **3** did not proceed cleanly under thermal conditions, and only proceeded photochemically (Scheme 10). The scope of this reaction is currently limited to norbornadiene and norbornene. Furthermore, the retention of stereochemistry upon alkene exchange seen with the analogous cobalt complexes^4 has not been proven in the ruthenium system.

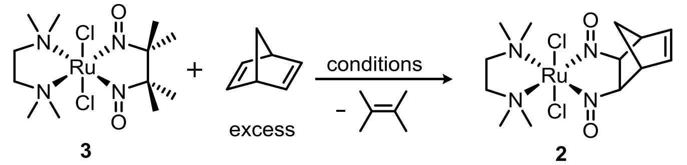

condition A: C_6D_6, 80 °C, 6 days; NMR yield - 38%
condition B: CD_3CN, ***hv***, 8 h; Isolated yied - 92%

Scheme 3.4. Alkene Exchange Reactions Between Complex **3** and Norbornadiene

In terms of C–H functionalization, however, intermolecular reactions with external electrophiles, such as enones and ynones, in the presence of base have not been realized. Thus we envisioned an intramolecular system analogous to the chemistry of cobalt dinitrosyl mediated C–H functionalization reaction to test the viability of ruthenium complex **1** to mediate vinylic C–H functionalization of alkenes.

3.2. Results and Discussion

3.2.1. Development of C-H Functionalization Reaction Mediated by Ruthenium Complex 1

We began our studies by first examining the individual steps of the overall transformation, namely substrate binding, functionalization and retrocycloaddition. It has previously been shown that $[CpCo(NO)_2]$ selectively binds electron-rich alkenes in the presence of other conjugated π-systems. Similarly, substrates **7a-f** reacted with ruthenium compelx **1** to give the corresponding dinitrosoalkane complexes **8a-f**. Using a modified procedure presented in Table 2, complexes **8a-f** were isolated and purified by silica gel chromatography in moderate to good yields (Scheme 3.5). It is noteworthy that although aldehyde-containing substrate **7d** reacted with **1** smoothly, this and similar substrates did not bind to the cobalt dinitrosyl complex. Substrate **7e**, synthesized from **7c** and enantiopure (*R*)-(+)-2-methyl-2-propanesulfinamide, gave complex **8e** as a 1:1 mixture of diastereomers. This modified procedure reduces the amounts of alkenes and ligands used and prevents isomerization of the nitroso ligand to the oxime even when the substrates contain a 1,1,2-trisubstituted alkene.

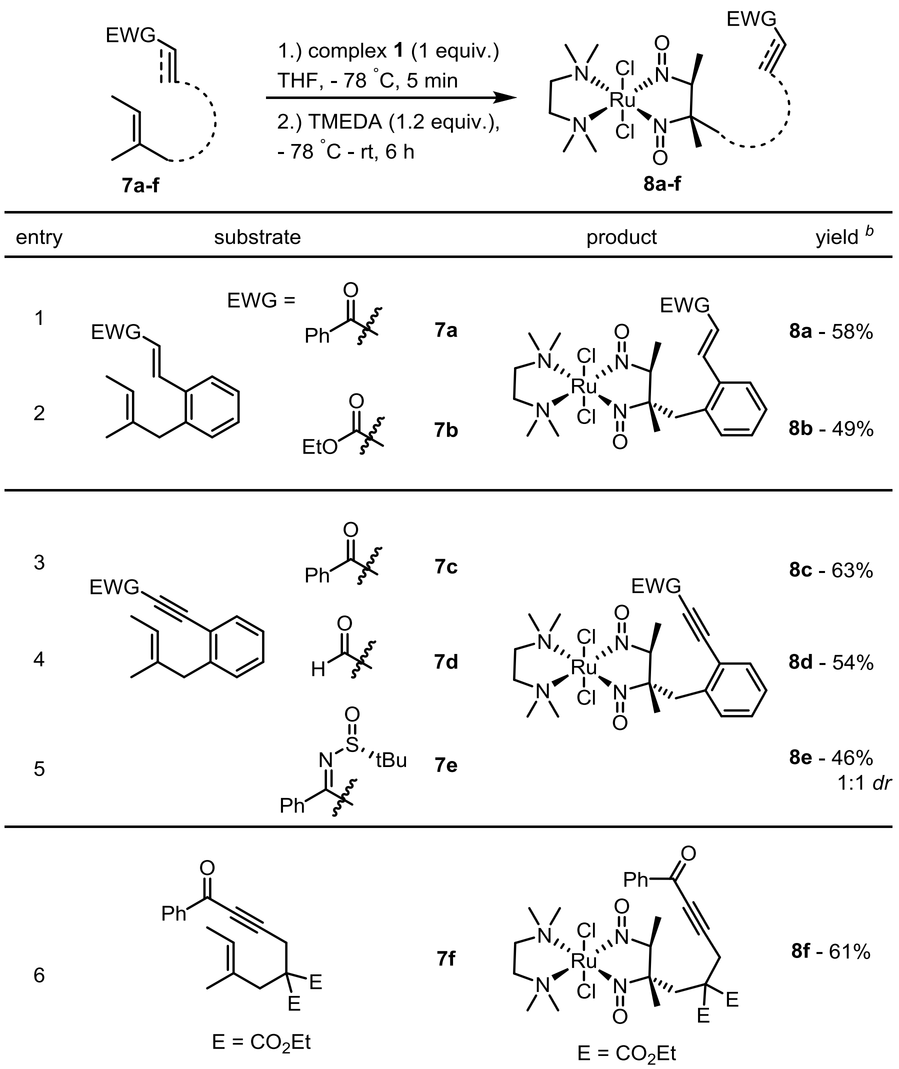
EWG
7a-f
1.) complex 1 (1 equiv.)
THF, - 78 °C, 5 min
2.) TMEDA (1.2 equiv.),
- 78 °C - rt, 6 h
Cl
Ru
N
O
8a-f
entry
substrate
product
yield b
1
2
EWG =
Ph
EtO
7a
7b
8a - 58%
8b - 49%
3
4
5
H
tBu
S
7c
7d
7e
8c - 63%
8d - 54%
8e - 46%
1:1 dr
6
E
E = CO2Et
7f
8f - 61%

[a] General condition: 2 equiv. of **7a-f**, 1 equiv. of **1**, 1.2 equiv. of TMEDA, - 78 °C - rt, 6 h. [b] Isolated yields.

Scheme 3.5. Synthesis of Ruthenium Dinitrosoalkane Complexes **8a-f** from Substrates **7a-f**

Treatment of **8a** with 20 mol% of TMEDA in CD_3CN at room temperature, with no external Lewis acid, gave complex **9** in 93% yield (Scheme 3.6). However, when the reaction was performed in THF, quantitative conversion to the oxime complex **10** was observed and **9** was not detected. Further heating of the oxime complex with and without the addition of strong bases, such as NaH, Verkade's base or P_1-*t*Bu phosphazene, led to only decomposition and no trace of either **8a** or **9** was detected. These data are consistent with the results shown in Scheme 3.3. Complex **8b** failed to cyclize in CD_3CN even when heated at 80 °C with an additional equivalent of TMEDA, giving the corresponding oxime complex **11** instead. Heating of **9** with 5 equivalents of norbornadiene at 80 °C for 1 h gave **12** and **2** in 93% and 95% isolated yields respectively (Scheme 3.6c). This stepwise sequence of substrate binding, cyclization and retrocycloaddition represents the first ruthenium dinitrosyl mediated intramolecular vinylic C–H functionalization reaction.

a.) Solvent Effect on the Cyclization of Ru-complex **8a**

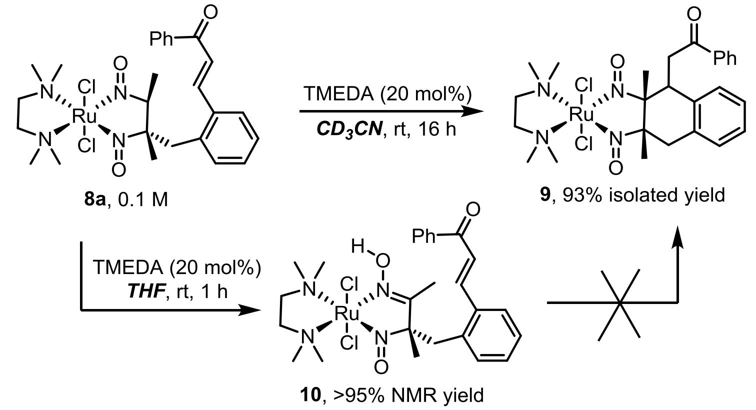

b.) Attempted Cyclization to an Enoate Electrophile

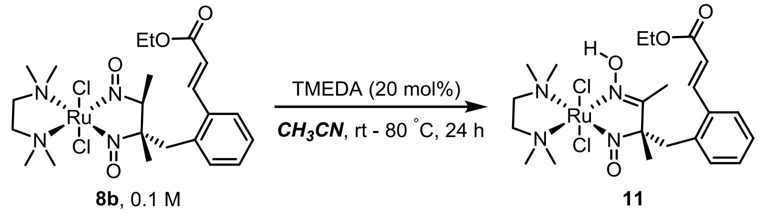

c.) Thermal alkene exchange of **9** to give **12** and **2**

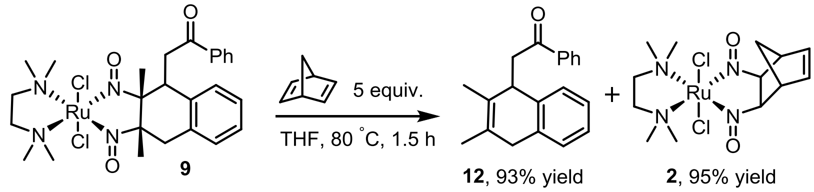

Scheme 3.6. Ruthenium Dinitrosyl Mediated Intramolecular *6-exo-trig* Addition to Enone and Enoate Groups

In addition to cyclizations with electrophilic enone functionality, ruthenium dinitrosyl mediated intramolecular ynone addition also proceeded in acetonitrile under mild reaction conditions, as shown in Scheme 3.7. In contrast to complex **8a**, **8c** cyclized to give only the corresponding organic product **13a** in quantitative yield and no organometallic product was observed. It is noteworthy that although **13d** was initially obtained as a mixture of *E* and *Z* isomers, it fully isomerized at room temperature in CD_2Cl_2 over 5 days to give exclusively the *Z* isomer. Compared to the addition to an enone, cyclization with the ynone electrophiles proceeded more facilely and retrocycloaddition of the organic product occurred readily at room temperature.

We also attempted to carry out the intramolecular C–H functionalization reaction with ruthenium complex **1** in one step. As shown in Scheme 3.8, when **7a** and **1** were reacted in the presence of TMEDA at room temperature for 24 h, **9** was obtained in 17% yield. Repeating this reaction at 80 °C gave **12** in 19% NMR yield. On the other hand, ynone substrate **7c** reacted with **1** to give only the organic product **13a** in 15% isolated yield, demonstrating the lability of the ruthenium dinitrosyl fragment in electron-deficient alkene molecule adducts such as **13a-d**. Furthermore, when substrate **7c** and 20 mol% of complex **8c** (substrate-bound dinitrosoalkane complex of **7c**) were treated with catalytic amount of TMEDA, only 18% of **13a** was obtained. Despite extensive screening of reaction parameters, we have yet to find optimized conditions for ruthenium complex **1** mediated one-pot vinylic C–H functionalization in high yields, and intermolecular functionalization attempts have yet to give promising results.

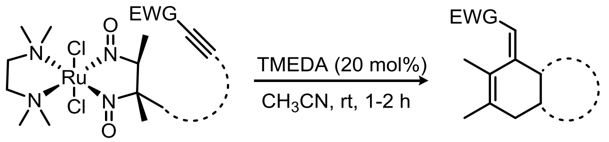
EWG
Cl
Ru
N
O
TMEDA (20 mol%)
CH$_3$CN, rt, 1-2 h
EWG

8c-f, 0.1 M

13a-d

entry	substrate complex			product	isolated yield
1	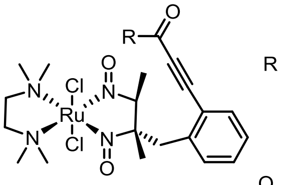	R = Ph	**8c**	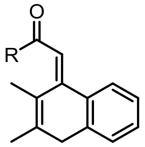	**13a** - 98%
2		= H	**8d**		**13b** - 95%
3	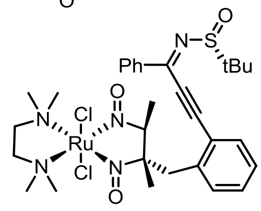		**8e**	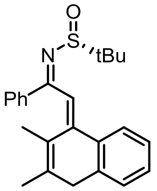	**13c** - 92%
4	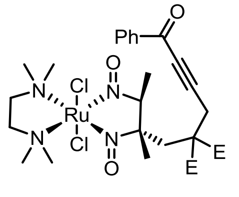		**8f**	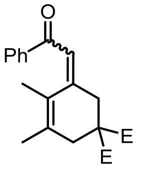	**13d** - 98% 1.3:1 *E*:*Z* ratio

E = CO$_2$Et

Scheme 3.7. Ruthenium-Dinitrosyl Mediated *6-exo-dig* Conjugate Addition to Ynone Functionality

a.) *Enone*

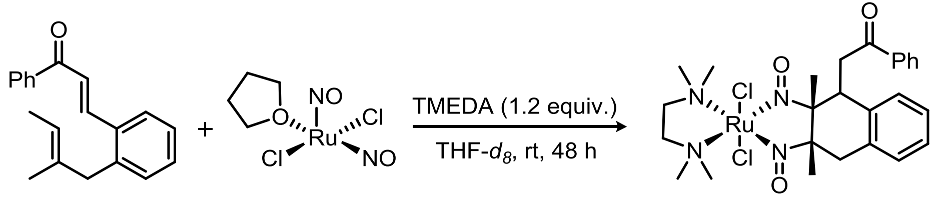
Ph
O
NO
Cl
Ru
NO
TMEDA (1.2 equiv.)
THF-d_8, rt, 48 h
Ph

7a, 2 equiv.

1, 1 equiv.

9, 17% isolated yield

b.) *Ynone*

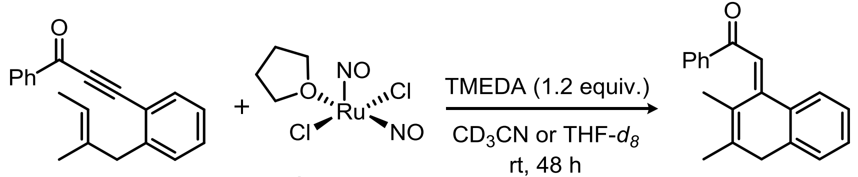
Ph
O
NO
Cl
Ru
NO
TMEDA (1.2 equiv.)
CD$_3$CN or THF-d_8
rt, 48 h
Ph

7c, 2 equiv.

1, 1 equiv.

13a, 15% NMR yield

Scheme 3.8. Ruthenium Complex **1** Mediated One-Pot Intramolecular C–H Functionalization

3.2.2. Comparison of Cobalt and Ruthenium Dinitrosyl Systems

Alkene Binding and Exchange. The experimental data on alkene binding and alkene exchange of [CpCo(NO)$_2$] and [RuCl$_2$(NO)$_2$] to form metal dinitrosoalkane complexes demonstrate some interesting parallels and contrasts.

In the simplest terms, nitrosyl ligands may be described by conformations either possessing a linear (3-electron) or bent (1-electron) mode upon coordination to transition metals. Increasing the electron density on the metal center is assumed to destabilize the linear coordination mode. In the absence of an exogenous ligand, alkene coordination to the five-coordinate [RuCl$_2$(NO)$_2$] in hydrocarbon or chlorinated solvents at room temperature is not observed. Furthermore, several thermodynamically stable four-coordinate cobalt-nitrosyl complexes have been synthesized and under the conditions examined do not undergo ligand-based alkene binding.

Formally, if the five-coordinate transient intermediate [CpCo(NO)$_2$] possessed linear nitrosyl ligands, it would be described as a 20-electron complex, while the one-linear one-bent nitrosyl and both-bent nitrosyl complexes are described as 18- and 16-electron complexes respectively (Figure 3.1). The ruthenium complex [RuCl$_2$(NO)$_2$] is isolable and a single-crystal X-ray diffraction study has demonstrated that it is a five-coordinate complex possessing a linear nitrosyl ligand in the basal-plane of square-based pyramidal geometry and a bent nitrosyl occupying the apical position, making complex [RuCl$_2$(NO)$_2$] a 16-electron complex with a vacant coordination site opposite the apical nitrosyl.

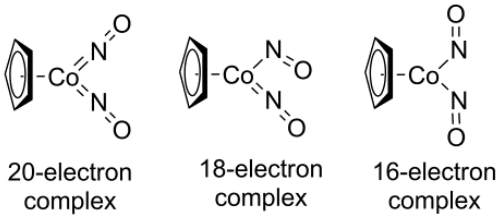

Figure 3.1. Possible Isomers of [CpCo(NO)$_2$]

Based upon these experimental observations, it is tempting to speculate that alkene binding may be ligand-accelerated. Thus, coordination of an exogenous ligand to [RuCl$_2$(NO)$_2$] may be responsible for lowering the Gibbs free activation energy of alkene binding. While four-coordinate cobalt dinitrosyl complexes have yet to be shown to bind alkenes, five coordinate analogues react readily with alkenes at and below room temperature.

Cobalt dinitrosoalkane complexes of styrene, cyclohexenes and mono- and di-substituted alkenes have only been generated and studied *in situ*, and attempts at isolation led to only decomposition. Other unsaturated functional compounds, such as alkynes, allenes, carbonyls and α,β-unsaturated enones and ynones, do not react with [CpCo(NO)$_2$] to form dinitrosoalkane complexes under the conditions that we have examined. Experimentally we observed that electron- rich and strained alkenes, such as tri- and tetra-alkyl-substituted alkenes, norbornadiene and cyclopentene, bind to [CpCo(NO)$_2$] readily and allow the isolation of the corresponding cobalt dinitrosoalkane complexes.

These findings may be rationalized by considering the microscopic reverse of alkene binding, alkene release. Alkene binding to [CpCo(NO)$_2$] is reversible and stereospecific, proceeding under either thermal or photochemical conditions.

Attempts to synthesize cobalt complexes **6a-c** from Chapter 1 *via* the methods other than alkene exchange led to deleterious side reactions (Scheme 2.1). While in the latter instance the reversibility of alkene binding is synthetically useful, we propose that this reaction provides the origin of the instability of cobalt dinitrosoalkane complexes derived from simple unstrained alkenes. The binding of [CpCo(NO)$_2$] to alkenes results in rehybridization of the *sp*^{2}-alkene to *sp*^{3}-dinitrosoalkane centers. In the case of strained alkenes, this rehybridization process is accompanied by the loss of ring strain. As a result, the *exo*-selective alkene binding of norbornene to [CpCo(NO)$_2$] is expected to be more exothermic than the analogous addition of ethylene to [CpCo(NO)$_2$]. The reactive intermediate [CpCo(NO)$_2$] is thermally unstable and decomposes to form a complex mixture, including [CpCo(μ-NO)]$_2$. The instability of, and difficulty in isolating, cobalt dinitrosoalkane complexes of unstrained alkenes may be rationalized in terms of the equilibrium between the products and reactants lying further towards the side of the reactants than with strained alkenes.

On the other hand, alkenes that do not yield isolable cobalt dinitrosoalkane complexes of [CpCo(NO)$_2$] (*e.g.* 1-phenylcyclohexene and alpha-methylstyrene) participate in alkene binding with [RuCl$_2$(NO)$_2$] to give the corresponding mono-oxime ruthenium complexes under mild reaction conditions (Scheme 3.2). These oxime complexes, however, do not isomerize back to the dinitrosoalkane complexes, or alkylate at the carbon atom, suggesting they are thermodynamically stable. In order to avoid this tautomerization process, ruthenium dinitrosoalkane complexes can be obtained when the reaction is carried out at low temperature with only slight excess (1.2 equiv.) of TMEDA (Scheme 3.5). Oxime compounds have not been observed to form from cobalt dinitrosoalkane complexes even in the presence of strong bases. We propose that the difference in reactivity of the two systems is due to the coupling of two steps, namely alkene binding and tautomerization. In the case of ruthenium, facile tautomerization stabilizes the alkene bound products and prevents alkene de-coordination, as discussed above for the cobalt system.

In contrast to the cobalt system, alkene exchange between norbornadiene and ruthenium complex **3** did not proceed cleanly under thermal conditions, and only proceeded photochemically (Scheme 3.4). On the other hand, thermal alkene exchange reaction between **9** and norbornadiene (Scheme 3.4) proceeded much more smoothly to give both products in quantitative yields. This provides another demonstration of the lability of the metal dinitrosyl fragment in dinitrosoalkane complexes of cyclohexene and its derivatives.[4-9]

A Diradical Mechanism for Alkene Binding? The ligand-based reaction between metal dinitrosyl complexes and alkenes resembles that between osmium tetroxide and alkenes. The substrates do not interact directly with the metal center, but rather with the ligands to form two covalent carbon-heteroatom bonds. In 1986, Hoffmann and co-workers reported a comparative study of the reactions of [CpCo(NO)$_2$] and OsO$_4$ with alkenes. Using extended Hückel computational methods, Hoffmann rationalized the reaction of cobalt complex **1** with alkenes in terms of a symmetry-allowed, concerted [3+2] cycloaddition of the metal fragment with the alkene, in which both 16- and 18-electron conformations of complex [CpCo(NO)$_2$] (Figure 3.1) possess HOMOs and LUMOs of the correct orbital symmetry to overlap with the LUMO and HOMO of ethylene, respectively.[10]

In recent years, closed-shell bonding models in metal nitrosyl complexes have come under increasing scrutiny. The covalent bonding picture invoked to describe the ground-state structures of [CpCo(NO)$_2$] and [RuCl$_2$(NO)$_2$] has been questioned in a series of joint spectroscopic and computational studies investigating the electronic structure of biologically relevant metal nitrosyls.[11] The comparable energy of the π*-NO and metal dπ orbitals can potentially result in a covalent bonding model in which the NO ligand is redox non-innocent and anti-ferromagnetic coupling occurs between electrons localized on metal and ligand fragments.[11]

Selected limiting bonding descriptions of [CpCo(NO)$_2$] are represented in Figure 3.2. Notably these ground-state bonding pictures possess ligand-based diradical character, and suggest a radical cyclization mechanism upon reaction with alkenes. The diradical character of cobalt dinitrosoalkane complexes was suggested as early as 1977 by Bernal and co-workers based upon the comparison of the M–N and N–O bond lengths from single crystal X-ray diffraction data upon [CpCo(μ-NO)$_2$(C$_7$H$_8$)] to those in nitroxyl free radicals and metal complexes possessing bridging nitrosyl ligands.[12] Related metal dithiolene complexes are known to bind alkenes *via* a ligand-based reaction of the thiolene moiety.[13,14] For example, the *tris*dithiolene [Mo(tfd)$_2$(bdt)] (tfd = S$_2$C$_2$(CF$_3$)$_2$; bdt = S$_2$C$_6$H$_4$) binds ethylene at the sulfur centers of the bdt ligand. It is noteworthy that *mono-*, *bis- and tris*dithiolene transition metal complexes have also recently become the subject of correlated spectroscopic and computational studies that have provided evidence for the redox non-innocence of these ligands.[15]

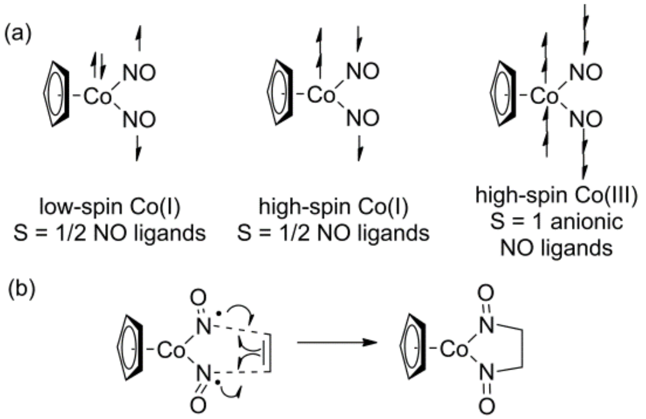

Figure 3.2. (a) Selected Limiting Valence Bond Description of [CpCo(NO)$_2$] and (b) Diradical Mechanism for Alkene Binding

Vinylic C–H Functionalization. The α-nitroso C–H bonds of metal dinitrosoalkane complexes closely resemble those of nitroalkanes, and the resulting anion can be considered to be analogous to a classical organic enolate functional group.[8] Epimerization at the carbon center has been observed previously in the reduction of a cobalt dinitrosoalkane complex of norbornadiene with LiAlH$_4$, suggesting the hydrogen at the carbon *alpha* to the nitroso group might be acidic enough to form a carbanion in the presence of a base. We confirmed this hypothesis by demonstrating carbon–carbon bond forming reactions of cobalt dinitrosoalkane complexes with a variety of Michael acceptors both inter- and intramolecularly. Although strong bases are generally required to generate the desired carbanion in the cobalt system, attempts to isolate the α-nitroso anion have not been successful. Nevertheless, a variety of alkenes and Michael acceptors, both enone and its derivatives and ynones, are tolerated for obtaining the overall vinylic C–H functionalized products using either the step-wise procedure or in a one-pot fashion.

C–H functionalization in the ruthenium system proved to be more challenging. Despite considerable efforts, intermolecular functionalization has not been achieved with either enone or ynone electrophiles. Intramolecular addition, however, to both enone and ynone functional groups has been developed (Scheme 3.6 and Scheme 3.7). Unlike the cobalt system, no strong bases are required and simple tertiary amine bases are sufficient for cyclization to occur, suggesting that the α-nitroso C–H bond of ruthenium dinitroalkane complexes is more acidic than that of the cobalt complexes. However, the p*K*a's of the α-nitroso C–H bond in either the cobalt or ruthenium dinitrosoalkane complexes have not been measured. Furthermore, it is possible that carbon–carbon bond formation in either system is reversible. This could account for the observation that the *ee* of product cobalt complex **9** (Chapter 2) decreases with longer reaction time in the enantioselective, intramolecular 5-exo-trig cyclization of cobalt complex **6a** (Chapter 2).

3.3. Conclusion

Presented in this chapter, we have developed the first example of a ruthenium dinitrosyl mediated vinylic C–H functionalization reaction. All intermediates of the reaction sequence have been isolated and characterized, and the overall vinylic C–H functionalization can be achieved in two or three steps with good to excellent yields. Along with the chemistry of the cobalt dinitrosyl system, this ruthenium dinitrosyl mediated reaction represents a rare class of ligand-based reactivity that allows for the chemoselective generation of carbon nucleophiles directly from vinyl C–H bonds. While catalysis with [(TMEDA)$RuCl_2(NO)_2$] remains elusive, if a reactive metal dinitrosyl fragment could be discovered that effected catalytic, vinylic C–H activation with a broader substrate scope, it would not only represent a significant breakthrough in ligand-based catalysis of transition metal complexes but also in the chemistry of vinyl anion equivalents.

3.4. Experimental

3.4.1. General Information. Unless otherwise noted, all reagents were obtained commercially and used without further purification. All air- and moisture-sensitive compounds were manipulated using standard Schlenk techniques. Reactions were carried out under a nitrogen atmosphere in glassware that was either oven-dried at 150 ºC overnight or flame-dried under nitrogen immediately prior to use. Pentane, hexane, diethyl ether, benzene, toluene, tetrahydrofuran and methylene chloride were dried and purified by passage through a column of activated alumina (type A2, 12 x 32, UOP LLC) under a stream of dry nitrogen. Unless otherwise specified, all other reagents were purchased from Acros, Aldrich or Fisher and were used without further purification.

Reaction solutions were magnetically stirred with the exception of those reactions performed in sealed NMR tubes. The majority of experiments were monitored by thin layer chromatography (TLC) using 0.25 mm pre-coated silica gel plates from Silicycle (TLGR10011B-323) containing a fluorescent indicator for visualization by UV light. Various stains were used to visualize reaction products, including *p*-anisaldehyde, $KMnO_4$ and phosphomolybdic acid in ethanol. Flash chromatography was performed using MP Biomedicals SiliTech silica gel 32-63D, 60 Å.

A specially designed gas cabinet was built by the College of Chemistry at University of California, Berkeley for the storage and use of nitric oxide gas cylinders. This set-up allows for direct connection between gas cylinders and manifolds for safe and controlled manipulation of harmful gases. For more details of this set-up, please contact the corresponding authors.

All NMR spectra were obtained at ambient temperature using Bruker AVQ-400, AVB-400 or DRX-500 spectrometers. ^1H NMR chemical shifts are reported relative to residual solvent peaks (7.26 ppm for $CDCl_3$, 7.16 ppm for C_6D_6). ^{13}C NMR chemical shifts were also reported with reference to residual solvent peaks (77.23 ppm for $CDCl_3$, 128.06 ppm for C_6D_6). Infrared (IR) spectra were recorded on a Nicolet Avatar FT-IR spectrometer. Low-resolution mass spectral data were obtained on an Agilent 6890N/5973 GC/MS equipped with a J&W Scientific DB-5MS capillary column (30 m x 0.25 mm, 0.50 micron). Both low- and high-resolution mass spectral data were obtained from the Micromass/Analytical Facility operated by the College of Chemistry, University of California, Berkeley.

3.4.2. Synthesis of Ruthenium Dinitrosyl 1

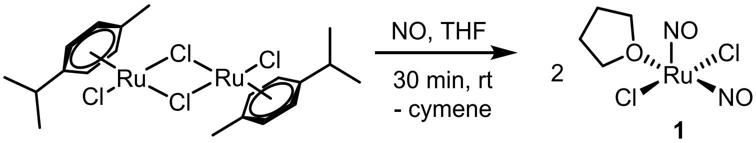

A three-neck round-bottom flask containing a suspension of $[RuCl_2\text{-(cymene)}]_2$ (1.00 g, 1.63 mmol) in THF (25 mL) was attached to a manifold fitted with nitric oxide inlet. The reaction mixture was degassed with argon and the apparatus isolated under partial vacuum. Nitric oxide was then introduced and the reaction mixture stirred under 1 atm of NO. The solution turned deep brown within the first 10 minutes at room temperature, with ruthenium starting material being consumed after about 30 minutes. After another hour, the solvent was removed *in vacuo* and the resulting crystalline brown solid was washed with pentane and dried under vacuum overnight. $[RuCl_2(NO)_2THF]$ (872mg, 2.86 mmol, 87%) was isolated as brown solid. Compelx **4**'s spectroscopic properties are in agreement with literature reported values.[1]

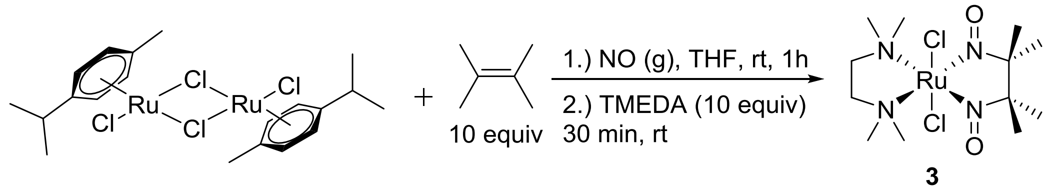

A three-neck round-bottom flask containing a suspension/solution of [$RuCl_2$-(cymene)]$_2$ (500 mg, 0.82 mmol, 1 equiv.) and tetramethylethylene (685 mg, 8.15 mmol, 0.97 mL, 10 equiv.) in THF (15 mL) was attached to a manifold fitted with nitric oxide inlet. The reaction mixture was degassed with argon and the apparatus isolated under partial vacuum. Nitric oxide was then introduced and the reaction mixture stirred under 1 atm of NO. The solution turned deep dark red/brown within the first 30 minutes at room temperature, with ruthenium starting material being consumed after about 45 minutes. TMEDA (947 mg, 8.15 mmol, 1.22 mL, 10 equiv.) was then added to the reaction mixture. After another hour, the solvent was removed *in vacuo* and the resulting crude mixture was purified by silica chromatography (10% EtOAc in hexanes) to give **10** as a dark red/brown crystalline solid. Complex **3** (598 mg, 1.39 mmol, 85%) was isolated as brown solid. Compelx **3**'s spectroscopic properties are in agreement with literature reported values.[1]

3.4.3. Substrates Synthesis (7c-f)

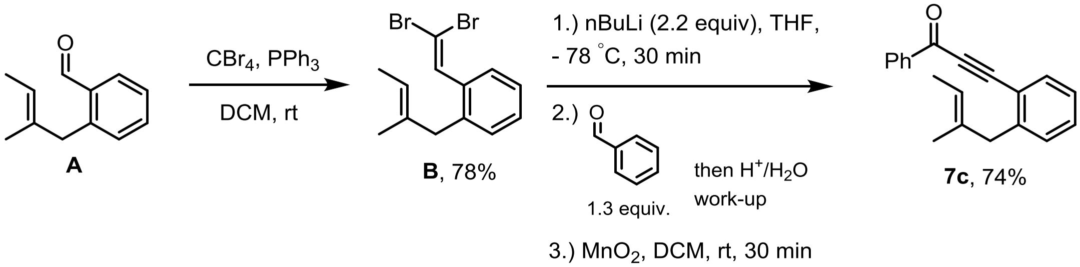

The aldehyde **A** was synthesized according to known procedure.[9]

Aldehyde **A** (1.0 g, 5.74 mmol, 1 equiv.) and CBr_4 (2.28 g, 6.86 mmol, 1.2 equiv.) were dissolved in dichloromethane (20 mL) and cooled to 0 °C. To this solution was then added triphenylphosphine (3.0 g, 11.5 mmol, 2 equiv.) as a DCM solution (10 mL) dropwise at 0 °C. The resulting solution was then warmed to room temperature and the reaction progress was followed by TLC. After 2 h, the reaction was quenched by dilution with petroleum ether (40 mL) and the resulting heterogeneous solution was filtered through a silica plug. The filtrate was then concentrated and the crude residue was purified by silica chromatography to give dibromide **B** (1.47 g, 4.46 mmol) as a pale yellow oil in 78% yield.

The dibromide **B** (736 mg, 2.23 mmol, 1 equiv.) was dissolved in THF (10 mL) and cooled to – 78 °C, followed by addition of nBuLi (2.5 M solution in hexane, 1.9 mL, 4.48 mmol, 2.1 equiv.) and the resulting solution was stirred for 1 hour. Benzaldehyde (354 mg, 3.35 mmol, 1.5 equiv.) was then added and the cold bath was removed. After 1 hour, the reaction mixture was diluted with 0.1 M HCl solution (10 mL) and the resulting mixture was extracted with diethyl ether (3x20 mL). The organic layers were combined, washed with brine, dried with $MgSO_4$ and filtered. Solvent was then removed and the resulting residue was dissolved in DCM (10 mL), followed by addition of MnO_2 (2 g, 23 mmol, 10 equiv.). The resulting heterogeneous solution was stirred for 30 minuntes at room temperature and then filtered. The resulting solution was then concentrated *in vacuo* and the residue was purified by silica chromatography (2% to 5% EtOAc in hexanes) to give the desired compound **7c** in 75% yield as a pale yellow oil. ^{1}H NMR (500 MHz, $CDCl_3$) δ(ppm) 8.22 (d, *J* = 7.7 Hz, 2H), 7.65 (m, 2H), 7.52 (t, *J* = 7.7 Hz, 2H), 7.41 (t, *J* = 7.6 Hz, 1H), 7.30 – 7.24 (m, 3H), 5.24 (q, *J* = 6.7 Hz, 1H), 3.60 (s, 2H), 1.64 (s, 3H), 1.58 (d, *J* = 6.7 Hz, 3H). ^{13}C NMR (125 MHz, $CDCl_3$) δ (ppm) 178.0, 144.4, 137.1, 134.0, 133.9, 130.8, 129.7, 129.6, 128.7, 128.1, 126.3, 121.3, 120.3, 92.4, 90.4, 44.1, 16.1, 13.6. IR [neat, νmax (cm^{-1})]: 2191, 1638, 1597, 1448, 1315, 1286, 1213, 1009, 698. HRMS (m/z): calculated for $C_{20}H_{18}O$, 274.1358 found 274.1353.

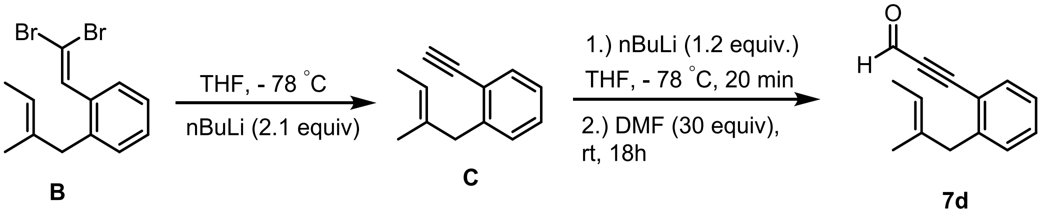

To a flame-dried flask was added a THF solution containing dibromide **B** (736 mg, 2.23 mmol, 1 equiv.) and cooled to – 78 °C. nBuLi (2.5 M solution in hexane, 1.9 mL, 4.48 mmol, 2.1 equiv.) was then added and the resulting solution was slowly warmed to room temperature. After 1 h, the solution was diluted with water (20 mL), layers were separated and the aqueous layer was extracted with diethyl ether (3x20 mL). Organic fractions were combined, dried with $MgSO_4$, filtered and concentrated. The crude residue was purified by silica chromatography to give alkyne **C** (348 mg, 2.05 mmol) as a pale yellow oil in 92% yield.

To a flame-dried round-bottom flask was charged a THF solution of the alkyne **C** (170 mg, 1.0 mmol, 1 equiv.) and cooled to – 78 °C, followed by addition of nBuLi (2.5 M solution in hexane, 0.5 mL, 1.2 mmol, 1.2 equiv.). The resulting solution was then stirred for 20 minutes and then DMF (2 mL) was added. The reaction mixture was warmed slowly to room temperature and stirred overnight. Solvent was then removed and the resulting residue was purified by chromatography (5% EtOAc in hexanes) to give **7d** (134 mg, 0.68 mmol) as a pale yellow oil in 68% yield. ^{1}H NMR (400 MHz, $CDCl_3$) δ 9.49 (s, 1H), 7.62 (d, *J* = 7.7 Hz, 1H), 7.45 (t, *J* = 7.6 Hz, 1H), 7.28 (m, 3H), 5.33 (q, *J* = 6.9 Hz, 1H), 3.56 (s, 3H), 1.72 – 1.54 (m, 6H). ^{13}C NMR (100 MHz, $CDCl_3$) δ (ppm) 176.7, 145.0, 134.1, 133.8, 131.3, 129.6, 126.3, 121.6, 119.5, 94.5, 92.1, 44.0, 15.7, 13.5. IR [neat, νmax (cm^{-1})]: 2923, 1659, 1384, 983, 760, 737. HRMS (m/z): calculated for [$C_{14}H_{14}O$], 198.1045, found 198.1041.

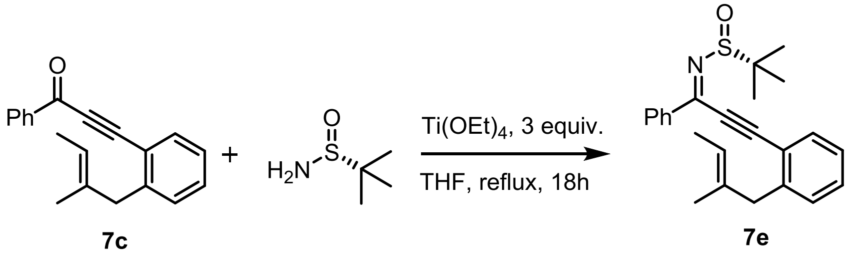

To a flamed-dried round-bottom flask was charged with a THF solution containing **7c** (178 mg, 0.65 mmol, 1 equiv.), (*R*)-(+)-2-methyl-2-propanesulfinamide (121 mg, 1.00 mmol, 1.5 equiv.) and $Ti(OEt)_4$ (444 mg, 1.95 mmol, 3 equiv.). The resulting mixture was then heated to reflux and the reaction progress was followed by TLC. After 18h, the reaction was quenched with 5 mL of saturated aqueous $NaHCO_3$ and the resulting mixture was filtered through Celite with ethyl acetate. The aqueous layer was separated and extracted with ethyl acetate. The combined organic layers were washed with brine, dried with $MgSO_4$, filtered and concentrated *in vacuo*. The resulting residue was purified by silica chromatography (5-10% EtOAc in hexanes) to give **7e** (210 mg, 0.56 mmol) as a yellow oil in 86% yield. ^{1}H NMR (500 MHz, $CDCl_3$) δ 8.21 (d, *J* = 7.7 Hz, 2H), 7.69 (d, *J* = 7.6 Hz, 1H), 7.55 (m, 1H), 7.47 (t, *J* = 7.6 Hz, 2H), 7.40 (t, *J* = 7.6 Hz, 1H), 7.27 (m, 2H), 5.18 (q, *J* = 6.9 Hz, 1H), 3.61 (m, 2H), 1.64 (s, 3H), 1.60 (d, *J* = 6.9 Hz, 3H), 1.34 (s, 9H). ^{13}C NMR (125 MHz, $CDCl_3$) δ (ppm) 159.2, 144.1, 136.4, 134.5, 133.9, 132.8, 130.9, 129.9, 128.9, 128.7, 126.5, 121.2, 121.0, 103.8, 86.2, 58.2, 44.1, 22.6, 16.4, 13.7. IR [neat, vmax (cm^{-1})]: 2919, 1529, 1445, 1315, 1175, 1088, 1016, 777, 757, 689 cm^{-1}. HRMS (m/z): calculated for $C_{24}H_{27}NOSNa$ 400.1706, found 400.1702.

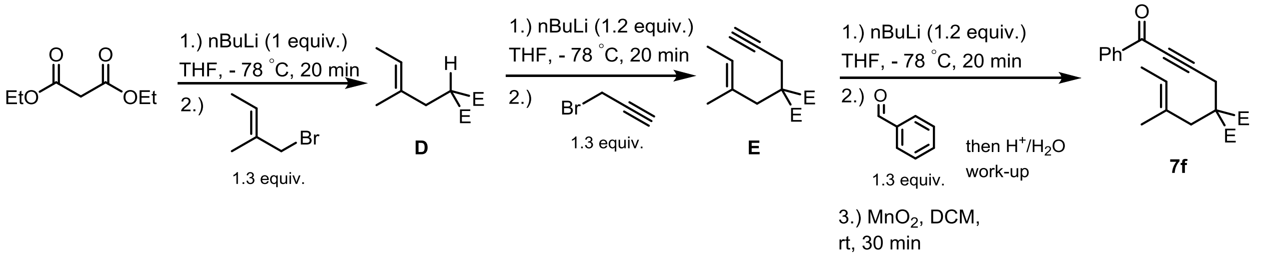

To a flame-dried round-bottom flask was added a THF solution (25 mL) of diethyl malonate (1.6 g, 10 mmol, 2 equiv.) and cooled to – 78 °C. nBuLi (2.5 M solution in hexane, 2.0 mL, 5 mmol, 1 equiv. was then added and the resulting solution was stirred at – 78 °C for 20 minutes. The allylic bromide (805 mg, 5.0 mmol, 1 equiv.) was then added and the resulting solution was warmed up to room temperature and stirred overnight. Solvent was then removed and the crude residue was purified by silica chromatography to give compound **D** (981 mg, 4.3 mmol) as a pale yellow oil in 86% yield.

Compound **E** was synthesized using the same experimental procedure for compound **D**, with propargyl bromide as the electrophile to give **E** as a pale yellow oil in 78% yield.

To a flame-dried round-bottom flask was added a THF (10 mL) solution of compound **E** (532 mg, 2.0 mmol, 1 equiv.) and cooled to –78 °C for 20 minutes. nBuLi (2.5M solution in hexane, 0.8 mL, 2.0 mmol, 1 equiv.) was then added and the resulting solution was stirred at –78 °C for 1 h. Benzaldehyde (318 mg, 3.0 mmol, 1.5 equiv.) was then added as a solution in THF (3 mL), and the resulting solution was warmed to room temperature. After 1h, the reaction mixture was diluted with 0.1 M HCl solution (10 mL) and the resulting mixture was extracted with diethyl ether (3x20 mL). The organic layers were combined, washed with brine, dried with $MgSO_4$ and filtered. Solvent was then removed and the resulting residue was dissolved in DCM (10 mL), followed by addition of MnO_2 (2 g, 23 mmol, 10 equiv.). The resulting heterogeneous solution was stirred for 30 minutes at room temperature and then filtered. The resulting solution was concentrated *in vacuo* and the crude residue was purified by silica chromatography (2% to 5% EtOAc in hexanes) to give the desired compound **7f** (533 mg, 1.44 mmol) as a pale yellow oil in 72% yield. ^{1}H NMR (400 MHz, $CDCl_3$) δ (ppm) 8.12 (d, *J* = 7.6 Hz, 2H), 7.61 (t, *J* = 7.3 Hz, 1H), 7.49 (t, *J* = 7.6 Hz, 2H), 5.43 (q, *J* = 6.6 Hz, 1H), 4.23 (m, 4H), 3.30 (s, 2H), 2.88 (s, 2H), 1.57 (m, 6H), 1.27 (t, *J* = 7.1 Hz, 6H). ^{13}C NMR (120 MHz, $CDCl_3$), 177.8, 170.2, 136.9, 134.2, 129.9, 129.8, 128.7, 125.9, 91.3, 82.2, 62.1, 56.8, 42.4, 23.7, 16.7, 14.2, 13.9. IR [neat, vmax (cm^{-1})]: 1731, 1645, 1449, 1263, 1183, 1059, 920, 700 cm^{-1}. HRMS (m/z): calculated for $C_{22}H_{26}O_5Na$, 393.1672, found 393.1678.

3.4.4. Synthesis of Ruthenium Dinitrosoalkane Complexes 8a-f

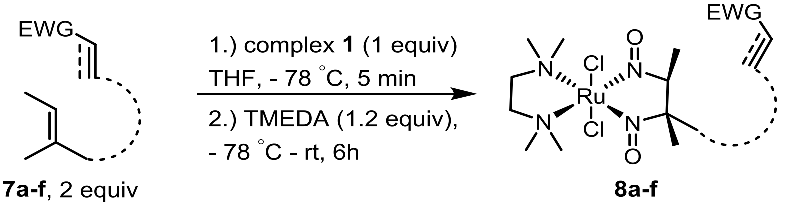

General procedure: In a flame-dried microwave tube fitted with a stir bar inside a glove-box filled with N_2, [$RuCl_2(NO)_2THF$] (30.5 mg, 0.10 mmol, 1 equiv.) and substrate **12a** (52.3 mg, 0.20 mmol, 2 equiv.) were dissolved in THF (0.2 mL) and sealed. The vessel was then taken to a dry-ice/acetone bath and cooled to – 78 °C. After 15 minutes, TMEDA (14.0 mg, 0.12 mmol, 1.2 equiv.) in THF (0.1 mL) was added to the reaction vessel and the resulting solution was warmed up to room temperature slowly over approximately 6 hours. Solvent was then removed and the unreacted substrate and the desired substrate-bound ruthenium dinitrosoalkane complexes were isolated and purified by silica chromatography (10-30% EtOAc in hexanes) as dark purple/brown solids.

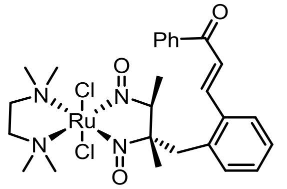

Complex **8a** was isolated as a dark brown solid in 58% yield. ^{1}H NMR (400 MHz, CD_2Cl_2) δ (ppm) 8.14 (d, *J* = 15.4 Hz, 1H), 8.01 (d, *J* = 7.6 Hz , 2H), 7.75 (dd, *J* = 5.6, 3.7 Hz, 1H), 7.59 (t, *J* = 7.6 Hz, 1H), 7.53-7.47 (m, 3H), 7.32 (dd, *J* = 5.7, 3.3 Hz, 2H), 7.21 (dd, *J* = 5.4, 3.7 Hz, 1H), 4.18 (q, *J* = 6.6 Hz, 1H), 3.53 (m, 2H), 2.78 (s, 3H), 2.73 (s, 3H), 2.62 (s, 3H), 2.50 (s, 3H), 2.64 – 2.57 (m, 4H), 1.09 (s, 3H), 1.07 (d, J = 6.6 Hz, 3H). ^{13}C NMR (101 MHz, CD_2Cl_2) δ (ppm) 189.8, 142.5, 138.5, 136.7, 135.6, 133.7, 133.2, 130.3, 129.0, 128.8, 128.2, 127.5, 124.3, 102.6, 98.7, 60.1, 54.2, 51.5, 51.0, 50.9, 50.7, 39.5, 19.2, 13.0. IR [neat, ν_{max} (cm^{-1})]: 2922, 1687, 1475, 1408, 1379, 1362, 978, 698. HRMS (*m/z*): calculated for $C_{26}H_{36}Cl_2N_4O_3RuNa$ 647.1106, found 647.1100.

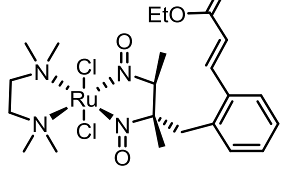

Complex **8b** was isolated as a dark brown solid in 49% yield, with small amount of the corresponding cis-isomer (about 2% by NMR) as a result of the substrate being present in the starting material. ^{1}H NMR (500 MHz, $CDCl_3$) δ (ppm) δ 8.04 (d, *J* = 15.7 Hz, 1H), 7.57 (d, *J* = 9.0 Hz, 1H), 7.33 – 7.27 (t, *J* = 3.7 Hz, 3H), 7.25 – 7.16 (m, 2H), 6.35 (d, *J* = 15.7 Hz, 1H), *cis isomer*: 6.04 (d, *J* = 12.1 Hz), 4.33 – 4.16 (m, 3H), *cis isomer*: 4.14 – 3.99 (m), 3.51 (d, *J* = 18.0 Hz, 1H), 3.54 (d, *J* = 18.0 Hz, 1H), *cis isomer*: 3.35 – 3.28 (m), 2.85 (s, 3H), 2.81 (s, 3H), 2.69 (s, 3H), 2.64 – 2.32 (m, 8H), 1.39 (t, *J* = 7.2 Hz, 3H), 1.13 (s, 3H), 1.05 (d, *J* = 6.4 Hz, 3H). ^{13}C NMR (125 MHz, $CDCl_3$) δ (ppm) 166.8, 142.3, 135.7, 134.7, 133.2, 130.0, 128.1, 127.2, 120.6, 102.6, 95.6, 60.8, 60.0, 59.9, 51.5, 51.0, 50.9, 50.8, 39.5, 19.1, 14.6, 12.9. IR [neat,

ν_{max} (cm^{-1})]: 2160, 1709, 1461, 1418, 1368, 1266, 1177, 958, 803, 701. HRMS (*m/z*): calculated for $C_{22}H_{36}O_4N_4Cl_2RuNa$ 615.1049, found 615.1044.

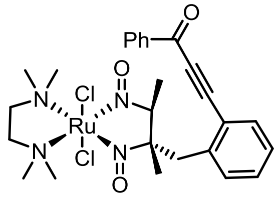

Complex **8c** was isolated as a dark brown solid in 63% yield. ^{1}H NMR (500 MHz, CD_2Cl_2): δ (ppm) 8.19 (d, 2H, *J* = 8.5 Hz), 7.68-7.63 (m, 2H), 7.55 (t, 2H, *J* = 7.5 Hz), 7.39 (t, 1H, *J* = 7.5 Hz), 7.32 (t, 1H, *J* = 7.5 Hz), 7.27 (d, 1H, *J* = 7.5 Hz), 4.27 (q, 1H, *J* = 6.5 Hz), 3.65 (dd, 2H, *J* = 17, 6.5 Hz), 2.79 (s, 3H), 2.73 (s, 3H), 2.64 (s, 3H), 2.45 (s, 3H), 2.54-2.31 (m, 4H), 1.22 (d, 3H, *J* = 6.5 Hz), 1.18 (s, 3H). ^{13}C NMR (125 MHz, CD_3CN): δ (ppm) 128.5, 140.6, 137.8, 135.4, 135.1, 133.9, 131.9, 130.5, 129.9, 128.7, 122.1, 103.1, 99.5, 92.5, 91.6, 60.5, 60.4, 51.7, 51.3, 51.2, 50.9, 41.6, 19.3, 13.5. IR [neat, ν_{max} (cm^{-1})]: 2916, 1638, 1447, 1414, 1368, 1286, 1213, 1009, 802, 699. HRMS (*m/z*): calculated for $[M+H]^+$ $C_{26}H_{35}O_3N_4Cl_2Ru$ 623.1124, found 623.1124.

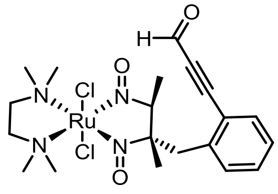

Complex **8d** was isolated as a dark brown solid in 54% yield. ^{1}H NMR (400 MHz, CD_3CN) δ 9.43 (s, 1H), 7.62 (d, *J* = 7.6 Hz, 1H), 7.47 (t, *J* = 7.5 Hz, 1H), 7.36 (d, *J* = 7.5 Hz, 2H), 4.38 (q, *J* = 6.6 Hz, 1H), 3.63 (m, 1H), 3.52 (m, 1H), 2.79 (s, 3H), 2.75 (s, 3H), 2.64 (s, 3H), 2.54 (s, 3H), 2.61 – 2.38 (m, 4H), 1.18 (s, 3H), 1.14 (d, *J* = 6.6 Hz, 3H). ^{13}C NMR (125 MHz, CD_3CN): δ (ppm) 178.6, 141.1, 135.2, 133.7, 132.3, 128.7, 121.3, 102.9, 99.3, 93.6, 92.9, 60.5, 60.4, 51.6, 51.2, 51.1, 50.9, 41.2, 19.0, 13.4. IR [neat, ν_{max} (cm^{-1})]: 2922, 1655, 1417, 1368, 1264, 981, 739. HRMS (*m/z*): calculated for $C_{20}H_{30}O_3N_4Cl_2RuNa$ 569.0631, found 569.0621.

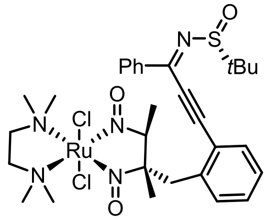

Complex **8e** was isolated as a mixture of diastereomers in 1:1 ratio in 46% yield; dark brown solid. ^{1}H NMR (500 MHz, CD_2Cl_2) δ 8.19 (d, *J* = 7.6 Hz, 2H), 7.68 (dd, *J* = 11.0, 7.5 Hz, 1H), 7.61 – 7.45 (m, 3H), 7.32 (dt, *J* = 13.7, 7.8 Hz, 2H), 7.20 (t, *J* = 9.0 Hz, 1H), diastereomer A: 4.30 (q, *J* = 6.6 Hz, 0.5H), diastereomer B: 4.19 (q, *J* = 6.6 Hz, 0.5H), 3.89 – 3.64 (m, 2H), 2.87 and 2.75 (s, 3H total), 2.75 – 2.63 (m, 6H), 2.54 (s, 3H), 2.50 (s, 3H), 2.47 – 2.35 (m, 4 H), 1.31 and 1.30 (s, 9H total), 1.30 – 1.18 (m, 6H total). ^{13}C NMR (125 MHz, CD_3CN): δ (ppm) 158.3, 157.9, 139.5, 136.6, 136.5, 134.3, 134.1, 133.3, 133.0, 132.8, 130.8, 130.7, 128.9, 128.8, 128.7, 127.6, 122.2, 122.1, 103.5, 103.4, 99.1, 98.6, 87.1, 86.9, 60.0, 59.9, 58.5, 58.3, 51.5, 51.1, 51.0, 50.9, 40.6, 40.5, 32.1, 29.9, 29.8, 29.6, 23.4, 22.9, 22.8, 22.7, 19.6, 19.3, 14.3, 13.3, 13.1. IR [neat, ν_{max} (cm^{-1})]: 2920, 1531, 1448, 1413, 1086, 1012, 753, 692. HRMS (*m/z*): calculated for $[M+H]^+$ $C_{30}H_{44}N_5O_3SRuNa$ 726.1580, found 726.1572.

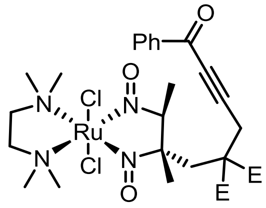

E = CO_2Et

Complex **8f** was isolated as a dark brown solid in 61% yield. ^{1}H NMR (600 MHz, CD_3CN) δ 8.24 (d, *J* = 7.6 Hz, 2H), 7.72 (t, *J* = 7.5 Hz, 1H), 7.59 (t, *J* = 7.6 Hz, 2H), 4.30 (m, 1H), 4.23 (q, *J* = 7.2 Hz, 2H), 4.16 (m, 2H), 3.33 (m, 3H), 2.76 (s, 3H), 2.72 (s, 3H), 2.62 (s, 3H), 2.57 (s, 3H), 2.54 – 2.41 (m, 4H), 1.38 (d, *J* = 6.3 Hz, 3H), 1.24 (t, *J* = 7.1 Hz, 6H), 1.09 (s, 3H). ^{13}C NMR (125 MHz, CD_3CN): δ (ppm) 178.4, 170.6, 170.3, 137.8, 135.4, 130.3, 129.8, 100.8, 98.2, 92.2, 82.6, 63.5, 63.4, 60.6, 60.5, 56.2, 51.6, 51.5, 51.2, 51.1, 38.4, 25.4, 21.3, 14.3, 14.1, 12.4. IR [neat, ν_{max} (cm^{-1})]: 2923, 1733, 1647, 1449, 1416, 1269, 1180, 703. HRMS (*m/z*): calculated for $[M+H]^+$ $C_{28}H_{43}Cl_2N_4O_7Ru$ 719.1547 found 719.1562.

3.4.5. Ruthenium Dinitrosyl Mediated C–H Functionalization

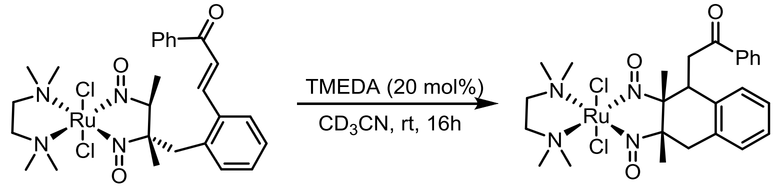

8a **9**

Complex **8a** (31.2 mg, 0.05 mmol, 1 equiv.) and TMEDA (1.16 mg, 0.01 mmol, 20 mol%) were dissolved in CD_3CN and loaded into a J-Young tube inside the glove-box. The reaction progress was monitored by ^{1}H NMR and after 18h, **8a** was completely consumed. Solvent was then removed and the resulting residue was purified by silica chromatography (15% EtOAc in hexanes) to give **9** (29 mg, 0.047 mmol) in 93% yield as dark red/brown solid. ^{1}H NMR (500 MHz, $CDCl_3$) δ 8.02 (d, *J* = 7.5 Hz, 2H), 7.58 (t, *J* = 7.5 Hz, 1H), 7.49 (t, *J* = 7.6 Hz, 2H), 7.18 – 7.07 (m, 3H), 6.87 (d, *J* = 7.3 Hz, 1H), 4.61 (dd, *J* = 11.0, 2.5 Hz, 1H), 3.72 (d, *J* = 18 Hz, 1H), 3.62 (dd, *J* = 17, 10 Hz, 1H), 3.35 (dd, *J* = 20.8, 5.4 Hz, 1H), 3.04 (d, *J* = 14.3 Hz, 1H), 2.83-2.73 (m, 8H), 2.71 (s, 3H), 2.68-2.59 (m, 2H), 2.40-2.34 (m, 2H), 1.32 (s, 3H), 1.19 (s, 3H). ^{13}C NMR (125 MHz, $CDCl_3$): 197.0, 137.4, 137.1, 134.7, 133.3, 128.9, 128.4, 128.1, 127.6, 127.3, 125.5, 105.3, 104.6, 60.6, 59.9, 51.5, 51.2, 50.9, 50.6, 41.6, 39.1, 35.7, 18.4, 14.4. IR [neat, ν_{max} (cm^{-1})]: 2920, 1688, 1461, 1407, 959, 803, 733. HRMS (*m/z*): calculated for $[C_{26}H_{36}ClN_4O_3RuNa]^+$ 589.1514, found 589.1516.

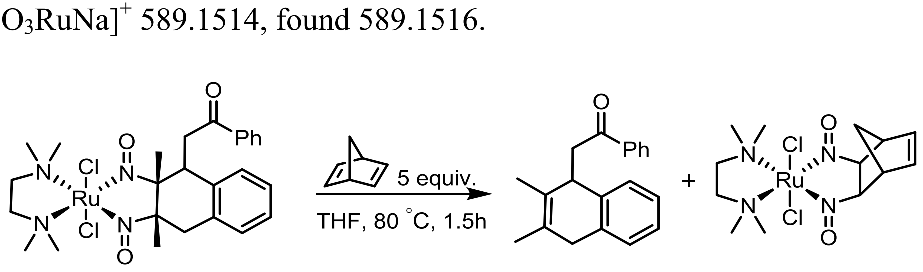

9 **12** **2**

Complex **9** (29 mg, 0.046 mmol, 1 equiv.) and norbornene (43 mg, 0.46 mmol, 10 equiv.) were dissolved in THF and loaded into a vial. The resolution was then heated to 80 °C and reaction progress was monitored by TLC. After 1.5 h, solvent was removed and the resulting residue was purified by silica chromatography to give compound **12** (12 mg, 93% yield) and **2** (19 mg, 95% yield). Compounds **12** and 2's spectroscopic properties are in agreement with literature reported values.[1,9]

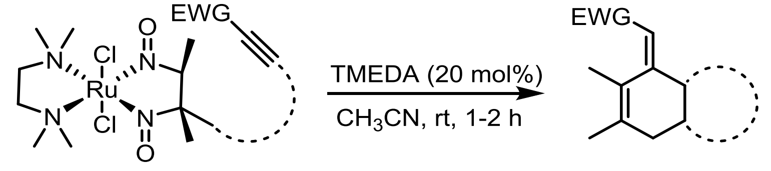

8c-f, 0.1 M

13a-d

General procedure: Complex **8c-f** (0.05 mmol, 1 equiv.) was dissolved in CD_3CN (0.5 mL) to which was added TMEDA (1.16 mg, 0.01 mmol, 20 mol%) and the resulting solution was loaded into J-Young tube and sealed inside the glove-box. The reaction progress was monitored by ^1H NMR until no starting material was observed. After 1.5h, the solvent was removed and the resulting residue was purified by silica chromatography (15-25% EtOAc in hexanes) to give compound **13a-d** in good yields.

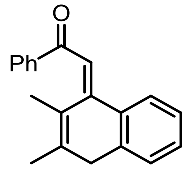

Compound **13a** was isolated as a white solid in 98% yield. ^1H NMR (500 MHz, CD_2Cl_2): δ (ppm) 8.14 (d, 2H, J = 7.0 Hz), 7.75 (d, 1H, J = 7.5 Hz), 7.65 (t, 2H, J = 7.0 Hz), 7.63 (s, 1H), 7.55 (t, 2H, J = 7.5 Hz), 7.35 (m, 2H), 4.85 (s, 2H), 2.47 (s, 3H), 2.30 (s, 3H). ^{13}C NMR (125 MHz, CD_2Cl_2): δ (ppm) 197.6, 137.7, 136.1, 135.6, 133.8, 132.8, 132.1, 129.4, 129.3, 128.7, 128.4, 127.9, 125.9, 125.3, 123.9, 39.6, 21.9, 16.9. IR [neat, ν_{max} (cm^{-1})]: 2922, 1727, 1672, 1273, 1211, 742. HRMS (m/z): calculated for $C_{20}H_{18}O$ 274.1358, found 274.1360.

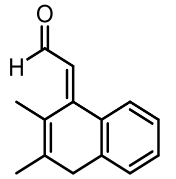

Compound **13b** was isolated as a white solid in 95% yield. ^1H NMR (600 MHz, CD_2Cl_2): δ (ppm) 9.73 (s, 1H), 7.86 (d, 1H, J = 7.8 Hz), 7.77 (d, 1H, J = 7.8 Hz), 7.64 (s, 1H), 7.45 (m, 2H), 4.22 (s, 2H), 2.49 (s, 3H), 2.42 (s, 3H). ^{13}C NMR (150 MHz, CD_2Cl_2): δ (ppm) 199.5, 135.7, 132.6, 131.7, 128.4, 128.2, 126.1, 125.5, 125.4, 123.3, 44.4, 21.8, 16.8. IR [neat, ν_{max} (cm^{-1})]:2920, 1736, 1670, 1268, 1214, 1072, 756, 736. HRMS (m/z): calculated for $C_{14}H_{14}ONa$ 221.0937, found 221.9037.

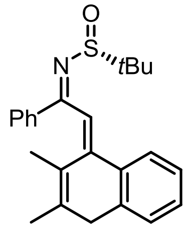

Compound **13c** was isolated as a pale yellow solid in 92% yield. The compound exists as mixture of rotomers in solution at room temperature. ^1H NMR (500 MHz, $CDCl_3$): δ (ppm) δ 7.99 – 7.88 (m, 1H), 7.82 – 7.73 (m, 3H), 7.62 (m, 1H), 7.49 – 7.40 (m, 4 H), 6.29 – 6.26 (m, 1H), 7.35 – 7.26 (m, 2H), 2.50 – 2.40 (m, 6H), 0.87 (m, 9 H). ^{13}C NMR (150 MHz, CDCl$_3$): δ (ppm) 141.7, 141.6, 137.9, 137.2, 136.1, 135.4, 135.3, 135.1, 132.5, 132.4, 129.2, 129.1, 128.9, 128.7, 128.5, 128.2, 127.8, 127.7, 127.6, 125.9, 125.6, 125.5, 125.3, 111.4, 110.8, 56.3, 29.9, 22.3, 22.1, 21.4, 21.3, 17.7, 17.6 IR [neat, ν_{max} (cm^{-1})]: 2921,1473, 1447, 1378, 1359, 1051, 759, 743, 700, 592. HRMS (*m/z*): calculated for $C_{24}H_{27}NOSNa$ 400.1706, found 400.1704.

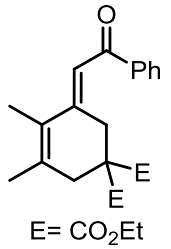

Compound **13c** was isolated as a pale yellow oil in 98% yield. Initially isolated as a mixture of *E* and *Z* isomers in 1.3:1 ratio, respectively, the mixture isomerized exclusively to the *Z* isomer at room temperature in CD_2Cl_2 over 5 days. Following data are only for the *Z* isomer. ^{1}H NMR (500 MHz, CDCl$_3$): δ (ppm) 7.93 (d, *J* = 7.5 Hz, 2H), 7.53 (t, *J* = 7.5 Hz, 1H), 7.45 (t, *J* = 7.6 Hz, 2H), 6.84 (s, 1H), 4.11 (dtt, *J* = 10.8, 7.2, 3.7 Hz, 4H), 3.52 (s, 2H), 2.78 (s, 2H), 1.94 (s, 3H), 1.90 (s, 3H), 1.07 (t, *J* = 10.6, 7.4 Hz, 6H). ^{13}C NMR (125 MHz, CDCl$_3$): δ (ppm) 192.1, 171.0, 151.5, 140.3, 140.0, 139.7, 132.4, 128.7, 128.3, 127.5, 117.6, 61.7, 54.1, 38.1, 33.2, 21.9, 14.5, 14.2. IR [neat, ν_{max} (cm^{-1})]: 2920, 1722, 1678, 1644, 1268, 1215, 746. HRMS (*m/z*): calculated for $C_{22}H_{27}O_5$ 371.11853, found 371.1855.

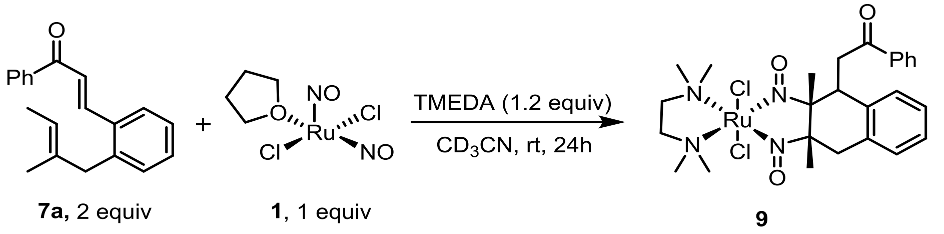

Substrate **7a** (54.5 mg, 0.2 mmol, 2 equiv.) and complex **1** (30.5 mg, 0.1 mmol, 1 equiv.) were dissolved in THF-*d8* and loaded into a J-Young tube. TMEDA (14 mg, 0.12 mmol, 1.2 equiv.) was then added and the tube was sealed inside a glove-box and reaction progress was monitored by ^{1}HNMR. After 24h, the reaction stopped, and the reaction solution was subjected to silica chromatography to give **9** in 17% yield; 70% of **7a** was also recovered.

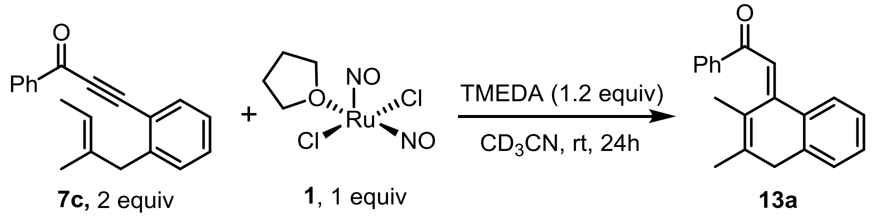

Substrate **7c** (52.8 mg, 0.2 mmol, 2 equiv.) and complex **1** (30.5 mg, 0.1 mmol, 1 equiv.) were dissolved in CD_3CN and loaded into an NMR tube. TMEDA (23 mg, 0.2 mmol, 2 equiv.) was then added and the tube was sealed inside a glovebox and reaction progress was monitored by NMR. After 24h, the reaction solution was then subjected to silica chromatography to give **13a** in 18% yield; 67% of **7c** was also recovered.

3.4.6. “Delayed” Alkene Binding with Ruthenium Complex 1

General procedure: In a N_2 filled glovebox, ruthenium complex **1** (30 mg, 0.10 mmol, 1 equiv.) and chelating-L_2 ligand (0.50 mmol, 5 equiv.) were dissolved in either THF or CH_3CN (0.5 mL) and stirred at rt for 1 h. Norbornadiene (92 mg, 1.0 mmol, 10 equiv.) were then added, as a solution in THF or CH_3CN (0.3 mL), and the resulting solution was stirred at rt for another hour. Solvent was then removed and the crude was dissolved in $CDCl_3$ and analyzed by ^1H NMR spectroscopy. In the experiments using ligands **L1-L15**, no desired ruthenium dinitrosoalkane complexes were observed by NMR. Ligand **L16, L17** and **L18** gave the corresponding ruthenium dinitrosoalkane complex in 15%, 19% and 14% NMR yields respectively, with 1,3,5-trimethoxybenzene used as internal standard. However, attempts to isolate the desired complexes led to decomposition of ruthenium species and only recovery of the ligands used.

Attempts at intramolecular C-H functionalization with **L16-18** (2 equiv.), ruthenium complex **1** (1 equiv.) and substrate **7a** and **7c** (2 equiv.) either in the presence or absence of added base (triethylamine or Hunig’s base) failed to give any trace amount of the desired organic products.

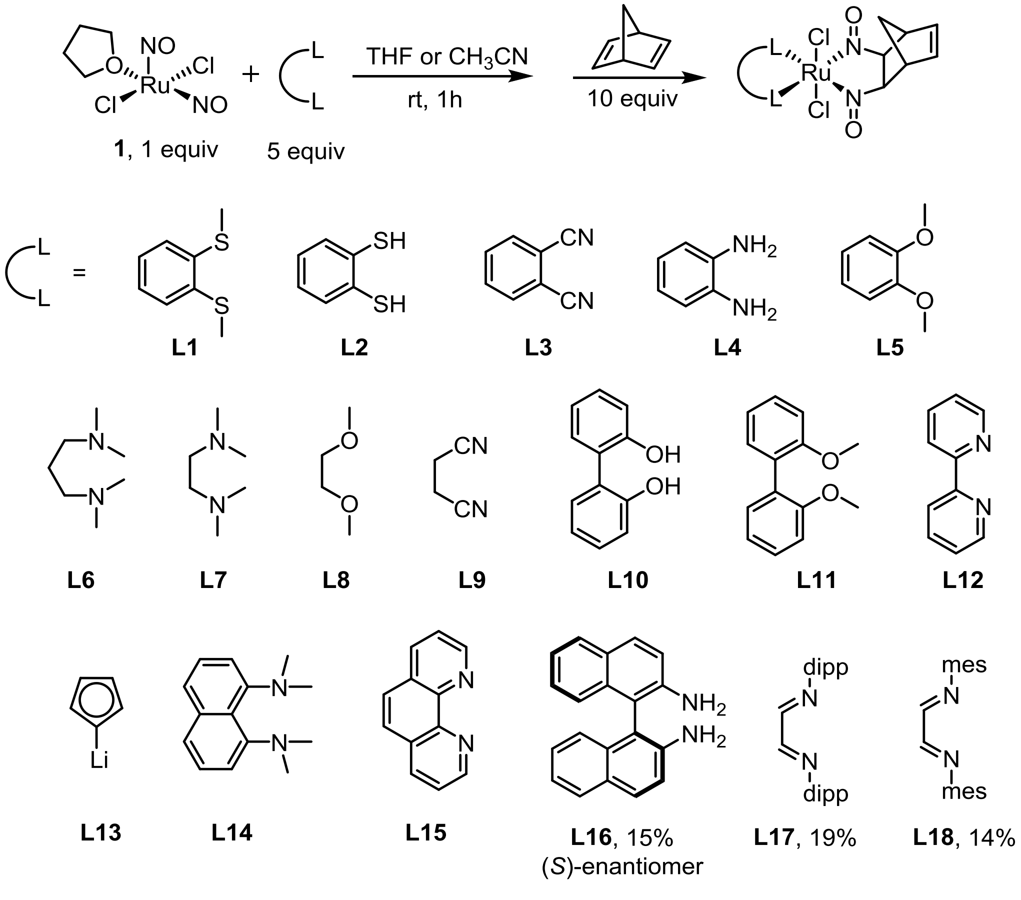

3.5. References

(1) Crimmin, M. R.; Bergman, R. G.; Toste, F. D. *Angew. Chem., Int. Ed.* **2011**, *50*, 4484-4487.
(2) Pierpont, C. G.; Eisenberg, R. *Inorg. Chem.* **1972**, *11*, 1088-1094.
(3) Pierpont, C. G.; Van Derveer, D. G.; Durland, W.; Eisenberg, R. *J. Am. Chem. Soc.* **1970**, *92*, 4760-4762.
(4) Becker, P. N.; Bergman, R. G. *J. Am. Chem. Soc.* **1983**, *105*, 2985-2995.
(5) Brunner, H. *J. Organomet. Chem.* **1968**, *12*, 517-522.
(6) Brunner, H.; Loskot, S. *J. Organomet. Chem.* **1973**, *61*, 401-414.
(7) Brunner, H.; Loskot, S. *Angew. Chem., Int. Ed.* **1971**, *10*, 515-516.
(8) Becker, P. N.; White, M. A.; Bergman, R. G. *J. Am. Chem. Soc.* **1980**, *102*, 5676-5677.
(9) Zhao, C.; Toste, F. D.; Bergman, R. G. *J. Am. Chem. Soc.* **2011**, *133*, 10787-10789.
(10) Joergensen, K. A.; Hoffmann, R. *J. Am. Chem. Soc.* **1986**, *108*, 1867-1876.
(11) Tomson, N. C.; Crimmin, M. R.; Petrenko, T.; Rosebrugh, L. E.; Sproules, S.; Boyd, W. C.; Bergman, R. G.; DeBeer, S.; Toste, F. D.; Wieghardt, K. *J. Am. Chem. Soc.* **2011**, *133*, 18785-18801.
(12) Evrard, G.; Thomas, R.; Davis, B. R.; Bernal, I. *J. Organomet. Chem.* **1977**, *124*, 59-70.
(13) Harrison, D. J.; Fekl, U. *Chem. Commun.* **2009**, *0*, 7572-7574.
(14) Harrison, D. J.; Lough, A. J.; Nguyen, N.; Fekl, U. *Angew. Chem., Int. Ed.* **2007**, *46*, 7644-7647.
(15) Eisenberg, R. *Coordination Chemistry Reviews* **2011**, *255*, 825-836.

3.6. Appendix – ^{1}H and ^{13}C NMR Spectra

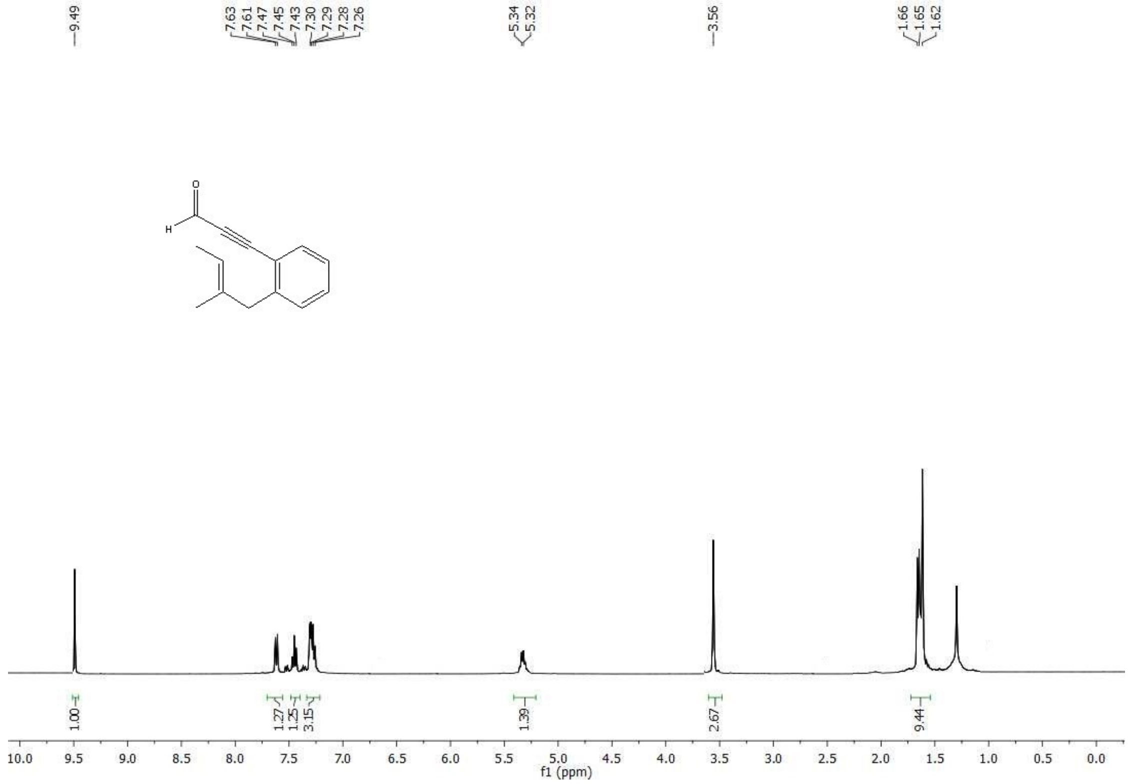

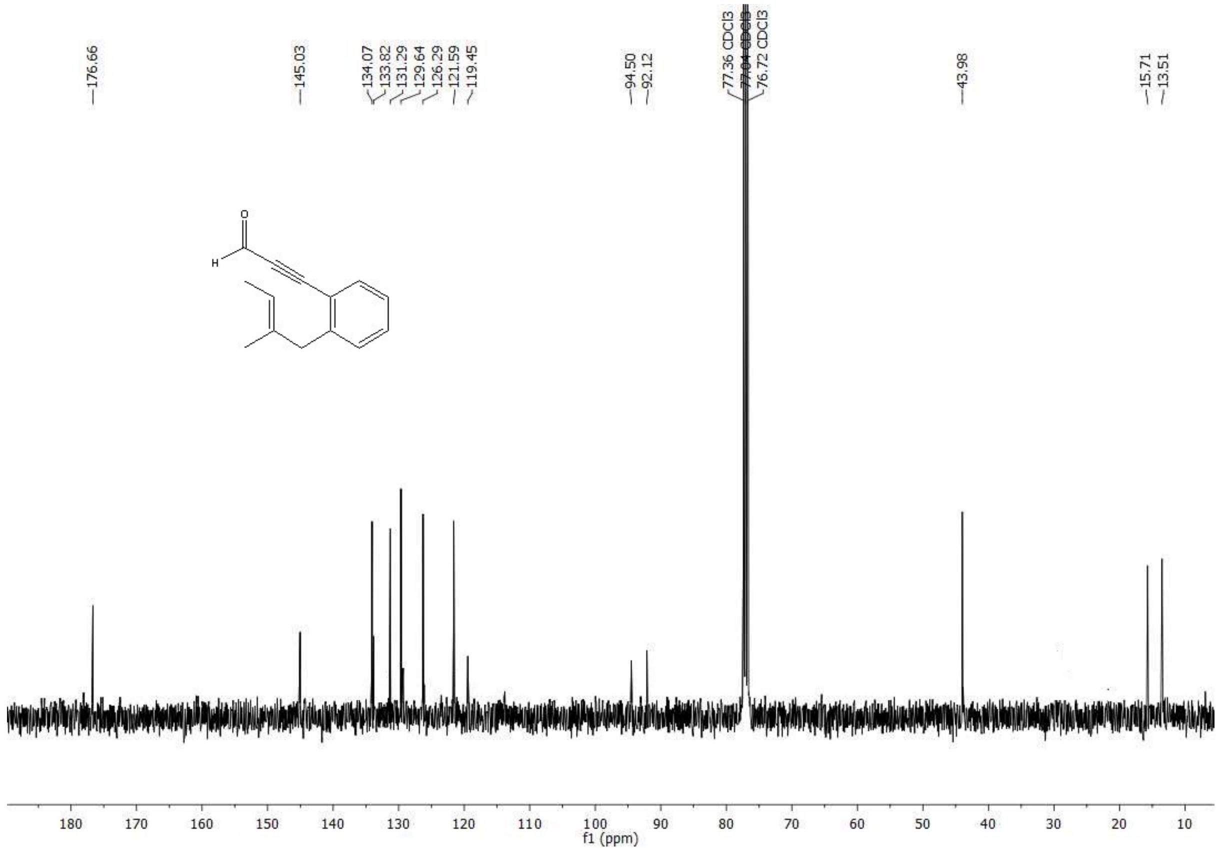

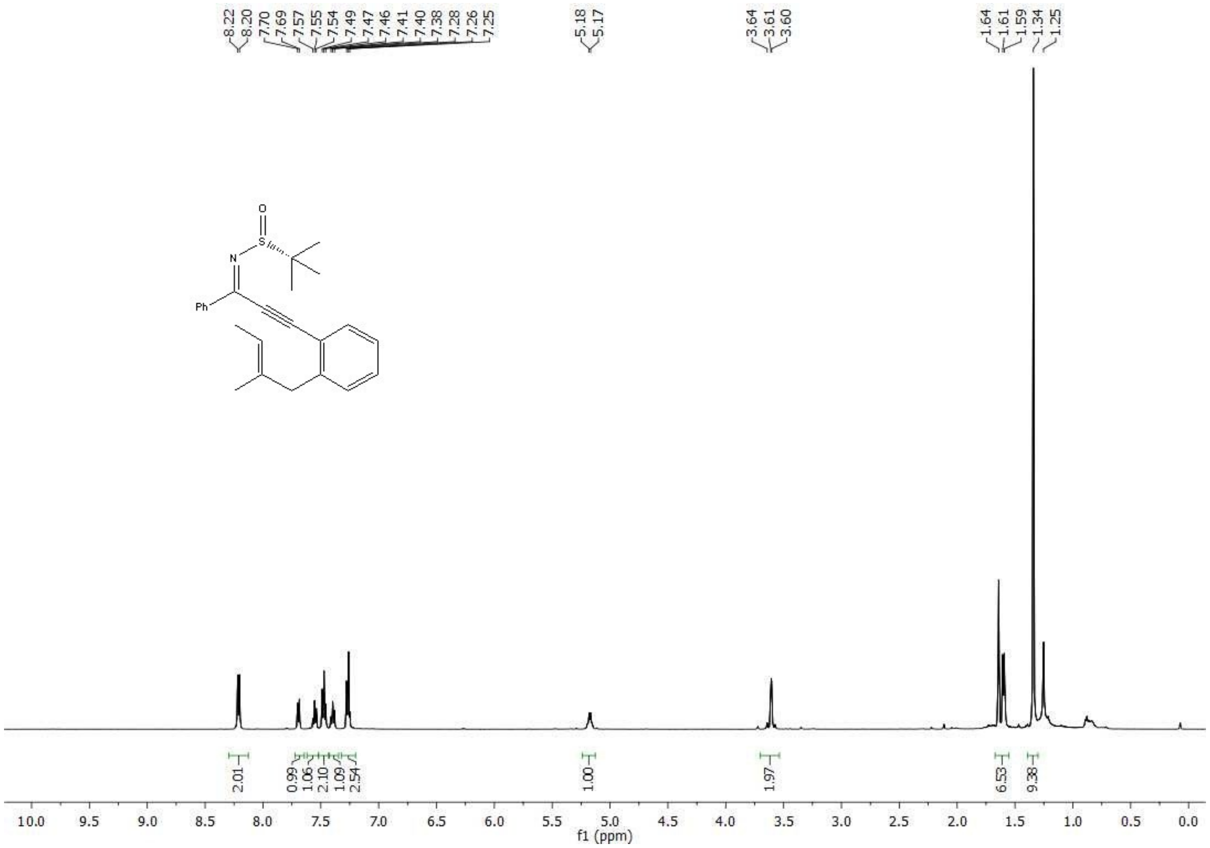
8.22
8.20
7.70
7.69
7.57
7.55
7.54
7.49
7.47
7.46
7.41
7.40
7.38
7.28
7.26
7.25
5.18
5.17
3.64
3.61
3.60
1.64
1.61
1.59
1.34
1.25
O
S
N
Ph
2.01
0.99
1.06
2.10
1.09
2.54
1.00
1.97
6.53
9.38
10.0
9.5
9.0
8.5
8.0
7.5
7.0
6.5
6.0
5.5
5.0
4.5
4.0
3.5
3.0
2.5
2.0
1.5
1.0
0.5
0.0
f1 (ppm)

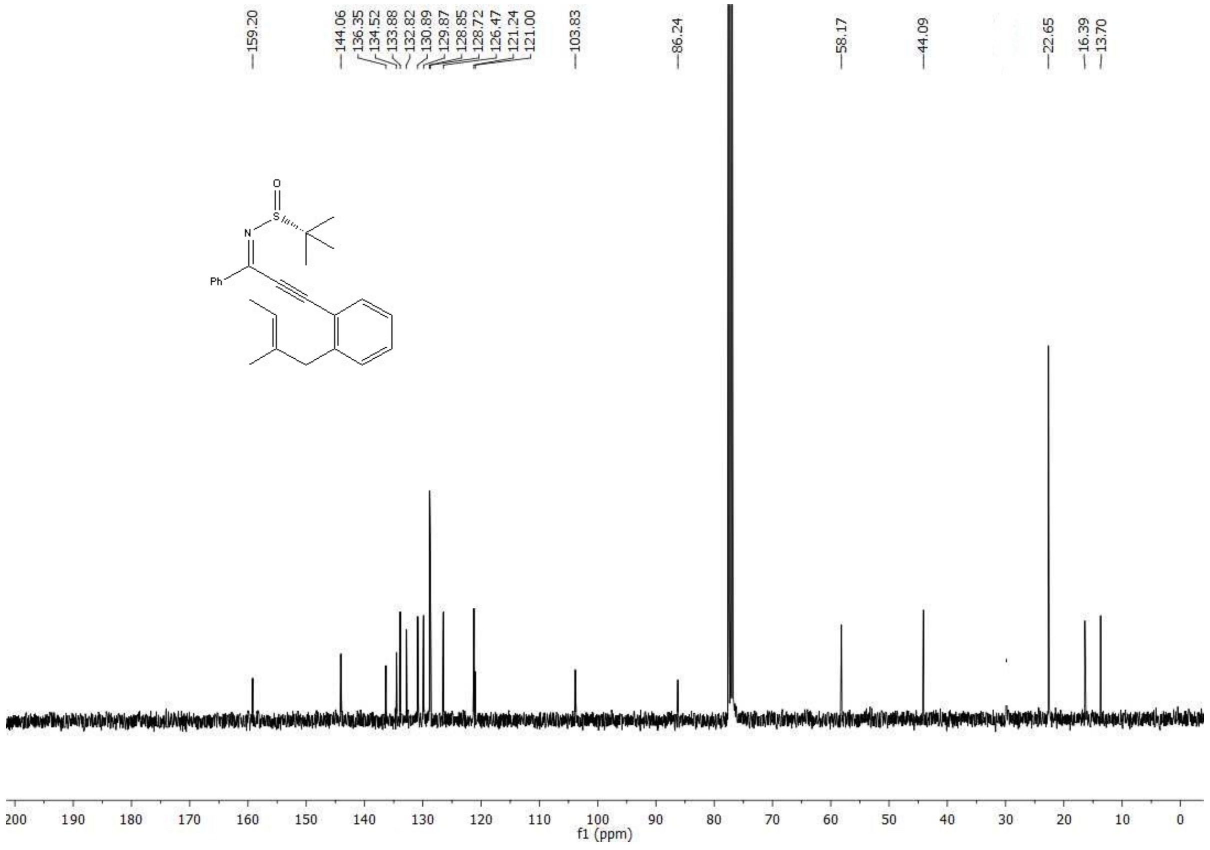
159.20
144.06
136.35
134.52
133.88
132.82
130.89
129.87
128.85
128.72
126.47
121.24
121.00
103.83
86.24
58.17
44.09
22.65
16.39
13.70
O
S
N
Ph
200
190
180
170
160
150
140
130
120
110
100
90
80
70
60
50
40
30
20
10
0
f1 (ppm)

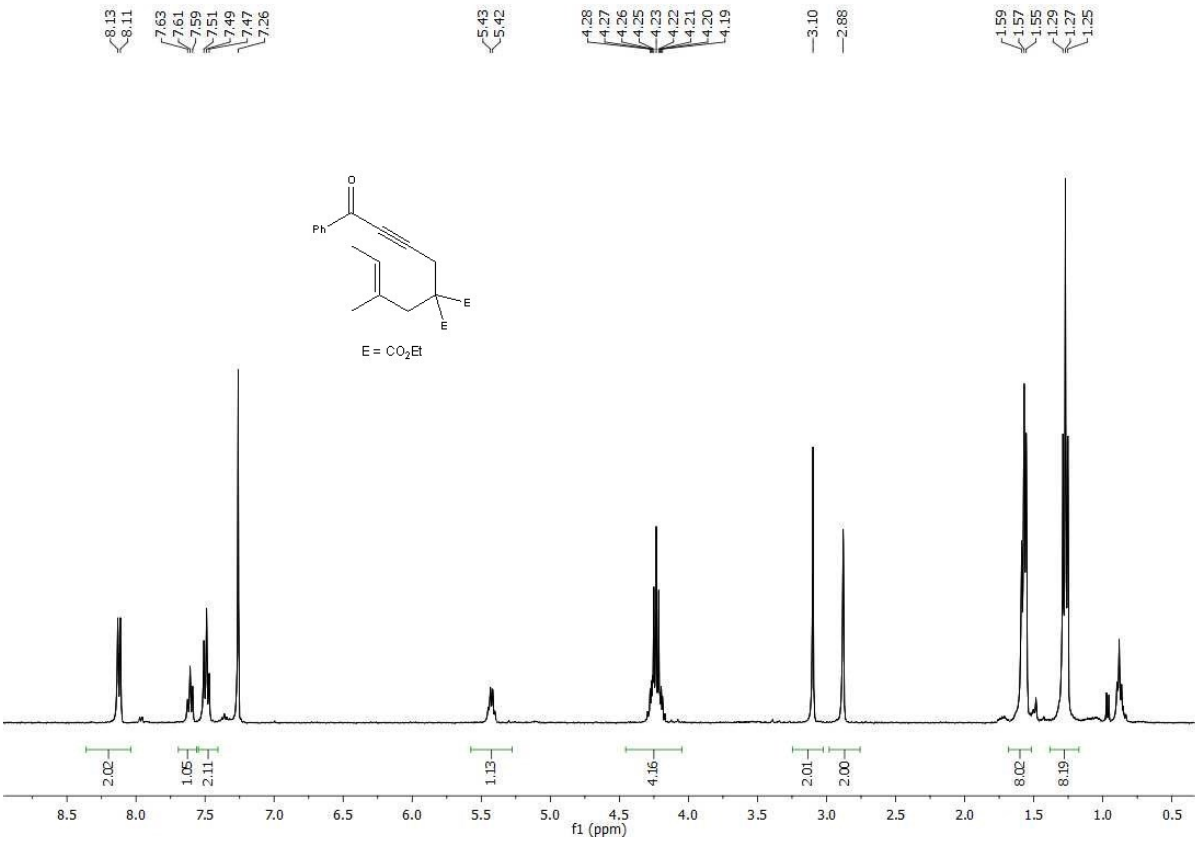
8.13
8.11
7.63
7.61
7.59
7.51
7.49
7.47
7.26
5.43
5.42
4.28
4.27
4.26
4.25
4.23
4.22
4.21
4.20
4.19
3.10
2.88
1.59
1.57
1.55
1.29
1.27
1.25
O
Ph
E
E
E = CO₂Et
2.02
1.05
2.11
1.13
4.16
2.01
2.00
8.02
8.19
8.5
8.0
7.5
7.0
6.5
6.0
5.5
5.0
4.5
4.0
3.5
3.0
2.5
2.0
1.5
1.0
0.5
f1 (ppm)

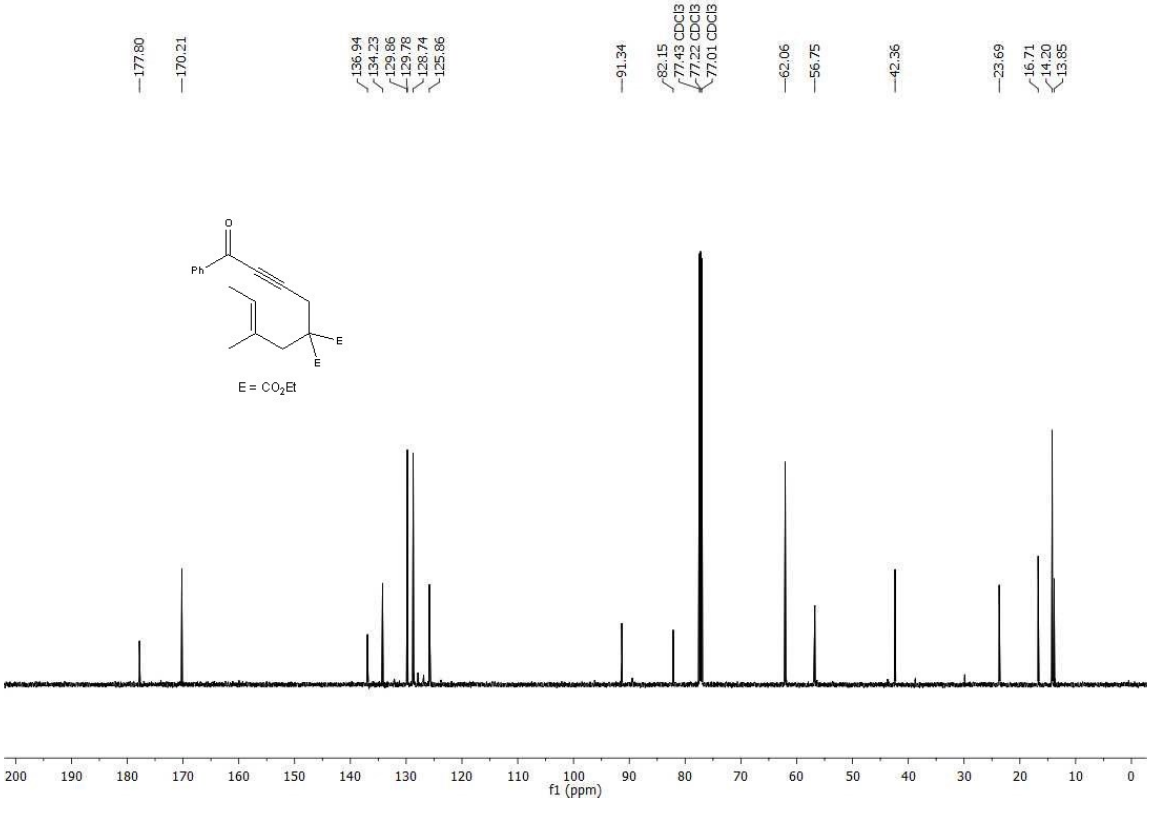
177.80
170.21
136.94
134.23
129.86
129.78
128.74
125.86
91.34
82.15
77.43 CDCl3
77.22 CDCl3
77.01 CDCl3
62.06
56.75
42.36
23.69
16.71
14.20
13.85
O
Ph
E
E
E = CO₂Et
200
190
180
170
160
150
140
130
120
110
100
90
80
70
60
50
40
30
20
10
0
f1 (ppm)

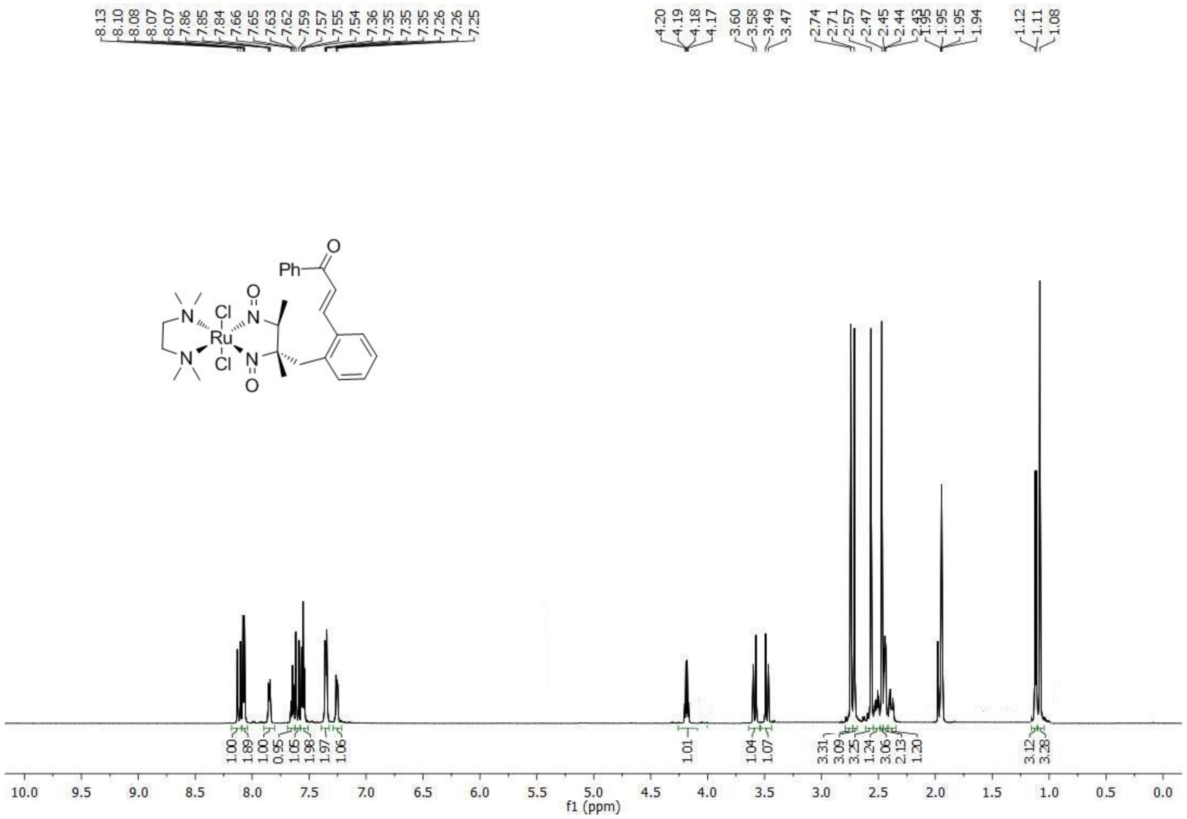
8.13
8.10
8.08
8.07
7.86
7.85
7.84
7.66
7.65
7.63
7.62
7.59
7.57
7.55
7.54
7.36
7.35
7.35
7.35
7.26
7.26
7.25
4.20
4.19
4.18
4.17
3.60
3.58
3.49
3.47
2.74
2.71
2.57
2.47
2.45
2.44
2.43
1.95
1.95
1.95
1.94
1.12
1.11
1.08
Ph
O
N
Cl
Ru
N
O
N
Cl
N
O
1.00
1.89
1.00
0.95
1.05
1.98
1.97
1.06
1.01
1.04
1.07
3.31
3.09
3.25
1.24
3.06
2.13
1.20
3.12
3.28
10.0
9.5
9.0
8.5
8.0
7.5
7.0
6.5
6.0
5.5
5.0
4.5
4.0
3.5
3.0
2.5
2.0
1.5
1.0
0.5
0.0
f1 (ppm)

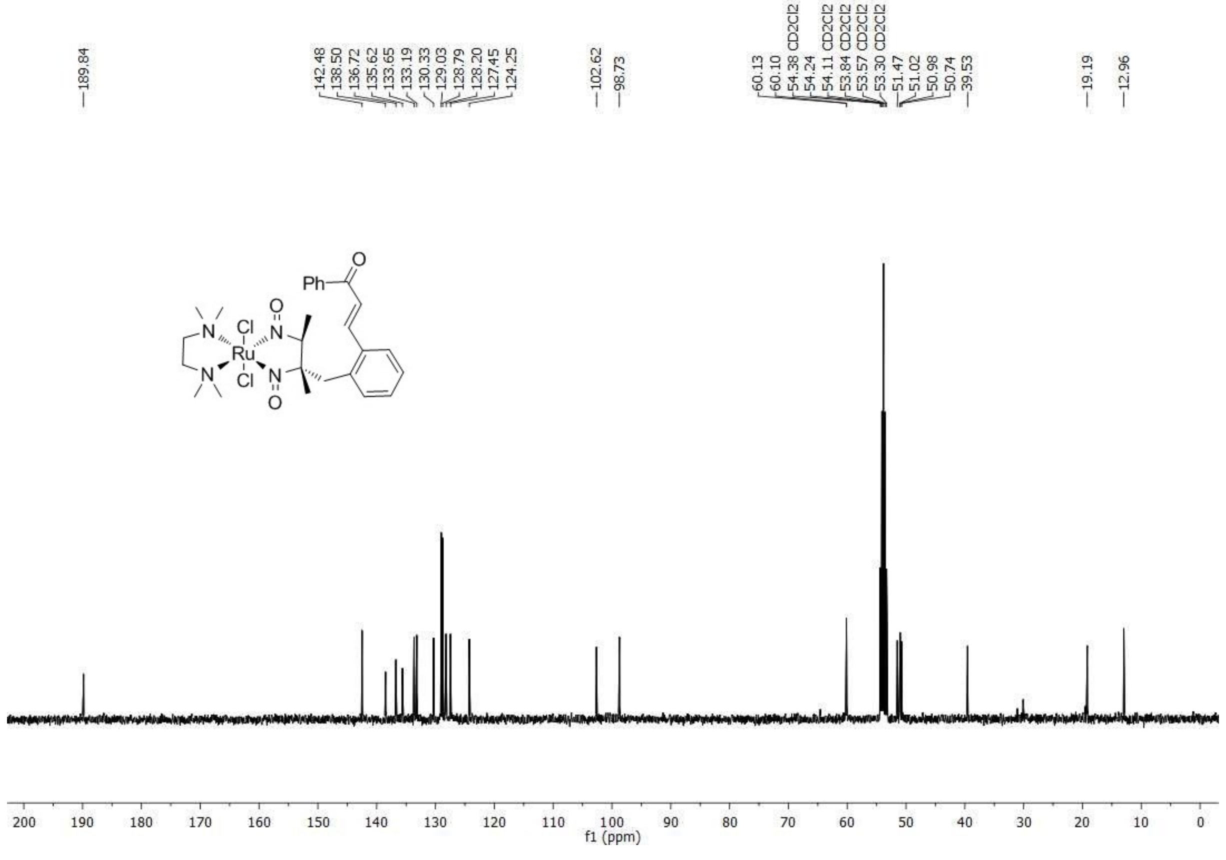
189.84
142.48
138.50
136.72
135.62
133.65
133.19
130.33
129.03
128.79
128.20
127.45
124.25
102.62
98.73
60.13
60.10
54.38 CD2Cl2
54.24
54.11 CD2Cl2
53.84 CD2Cl2
53.57 CD2Cl2
53.30 CD2Cl2
51.47
51.02
50.98
50.74
39.53
19.19
12.96
Ph
O
N
Cl
Ru
N
O
N
Cl
N
O
200
190
180
170
160
150
140
130
120
110
100
90
80
70
60
50
40
30
20
10
0
f1 (ppm)

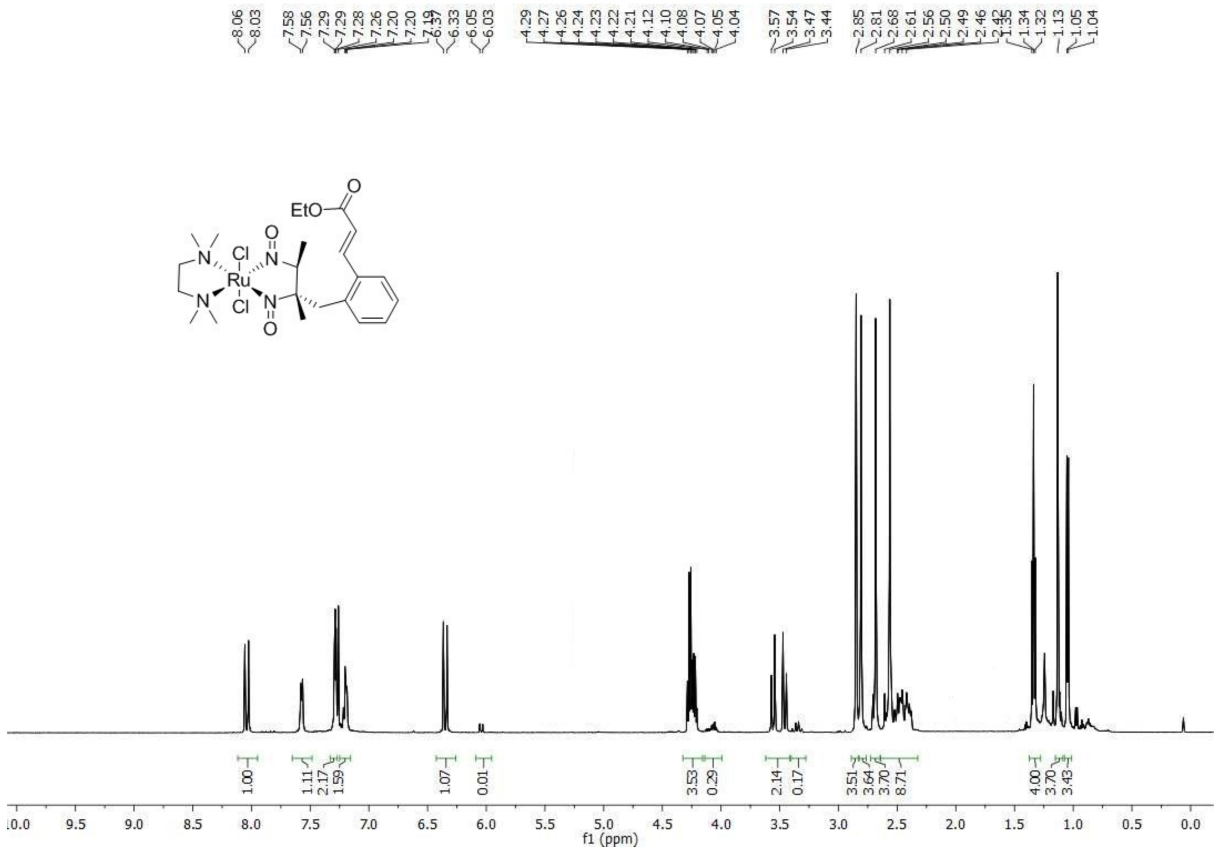
8.06
8.03
7.58
7.56
7.29
7.29
7.28
7.26
7.20
7.20
7.19
6.37
6.33
6.05
6.03
4.29
4.27
4.26
4.24
4.23
4.22
4.21
4.12
4.10
4.08
4.07
4.05
4.04
3.57
3.54
3.47
3.44
2.85
2.81
2.68
2.61
2.56
2.50
2.49
2.46
2.42
1.35
1.34
1.32
1.13
1.05
1.04
EtO
O
Cl
Cl
Ru
N
N
N
N
O
O
1.00
1.11
2.17
1.59
1.07
0.01
3.53
0.29
2.14
0.17
3.51
3.64
3.70
8.71
4.00
3.70
3.43
10.0
9.5
9.0
8.5
8.0
7.5
7.0
6.5
6.0
5.5
5.0
4.5
4.0
3.5
3.0
2.5
2.0
1.5
1.0
0.5
0.0
f1 (ppm)

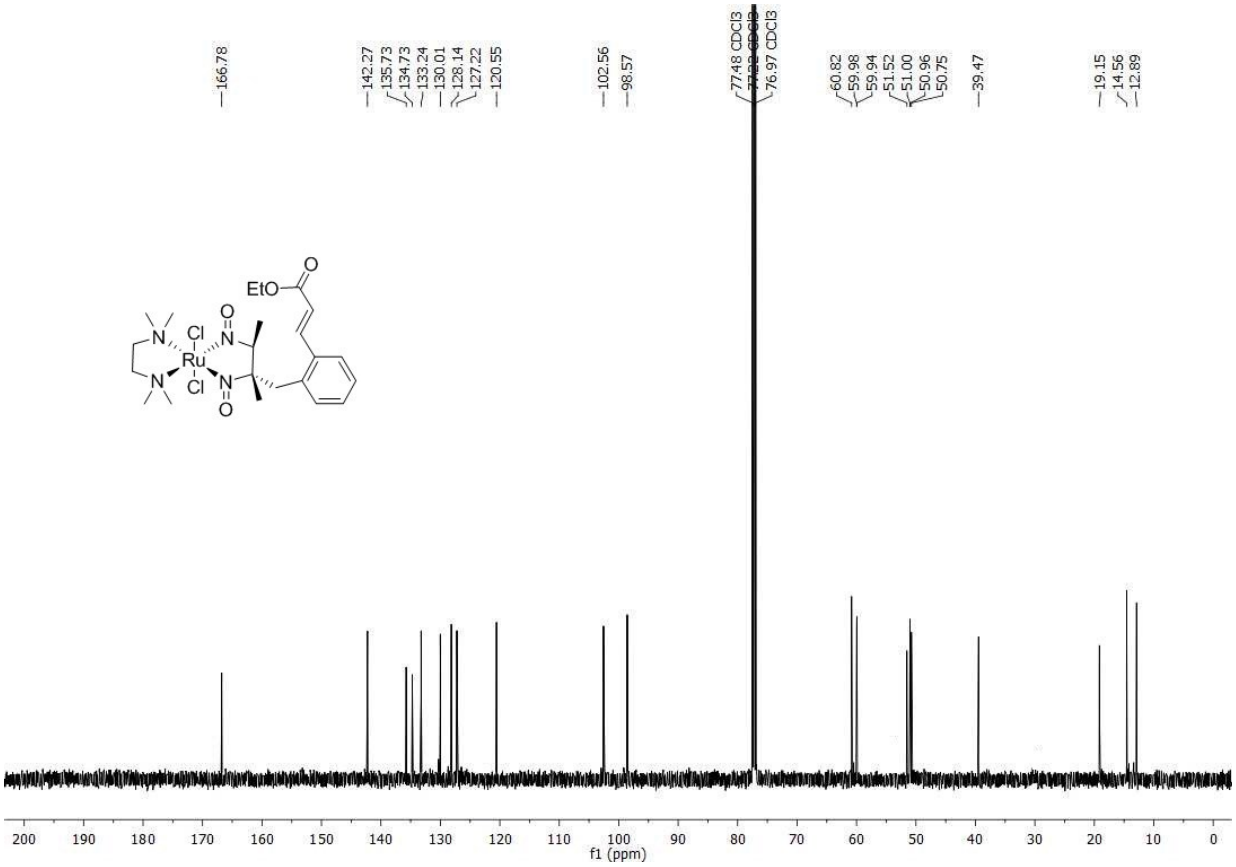
166.78
142.27
135.73
134.73
133.24
130.01
128.14
127.22
120.55
102.56
98.57
77.48 CDCl3
77.22 CDCl3
76.97 CDCl3
60.82
59.98
59.94
51.52
51.00
50.96
50.75
39.47
19.15
14.56
12.89
EtO
O
Cl
Cl
Ru
N
N
N
N
O
O
200
190
180
170
160
150
140
130
120
110
100
90
80
70
60
50
40
30
20
10
0
f1 (ppm)

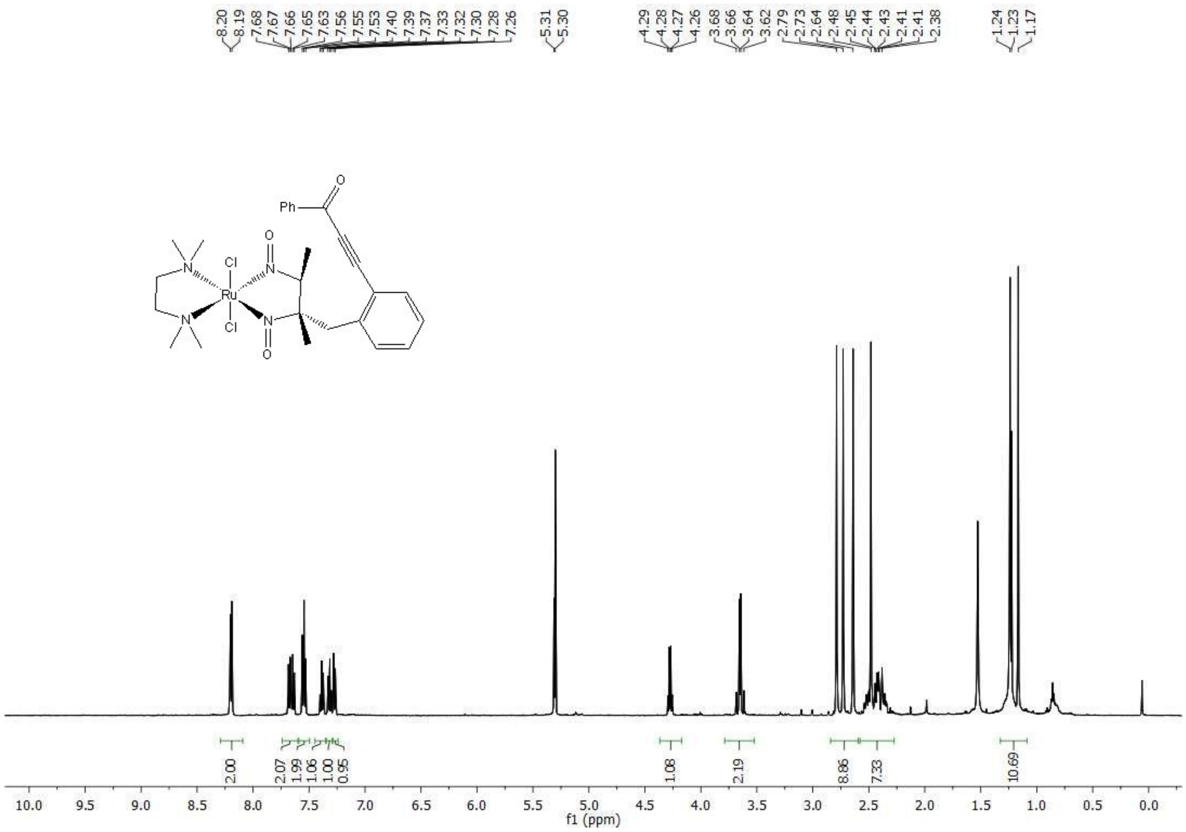
8.20
8.19
7.68
7.67
7.66
7.65
7.63
7.56
7.55
7.53
7.40
7.39
7.37
7.33
7.32
7.30
7.28
7.26
5.31
5.30
4.29
4.28
4.27
4.26
3.68
3.66
3.64
3.62
2.79
2.73
2.64
2.48
2.45
2.44
2.43
2.41
2.41
2.38
1.24
1.23
1.17
Ph
O
Cl
N
Ru
2.00
2.07
1.99
1.06
1.00
0.95
1.08
2.19
8.86
7.33
10.69
10.0 9.5 9.0 8.5 8.0 7.5 7.0 6.5 6.0 5.5 5.0 4.5 4.0 3.5 3.0 2.5 2.0 1.5 1.0 0.5 0.0
f1 (ppm)

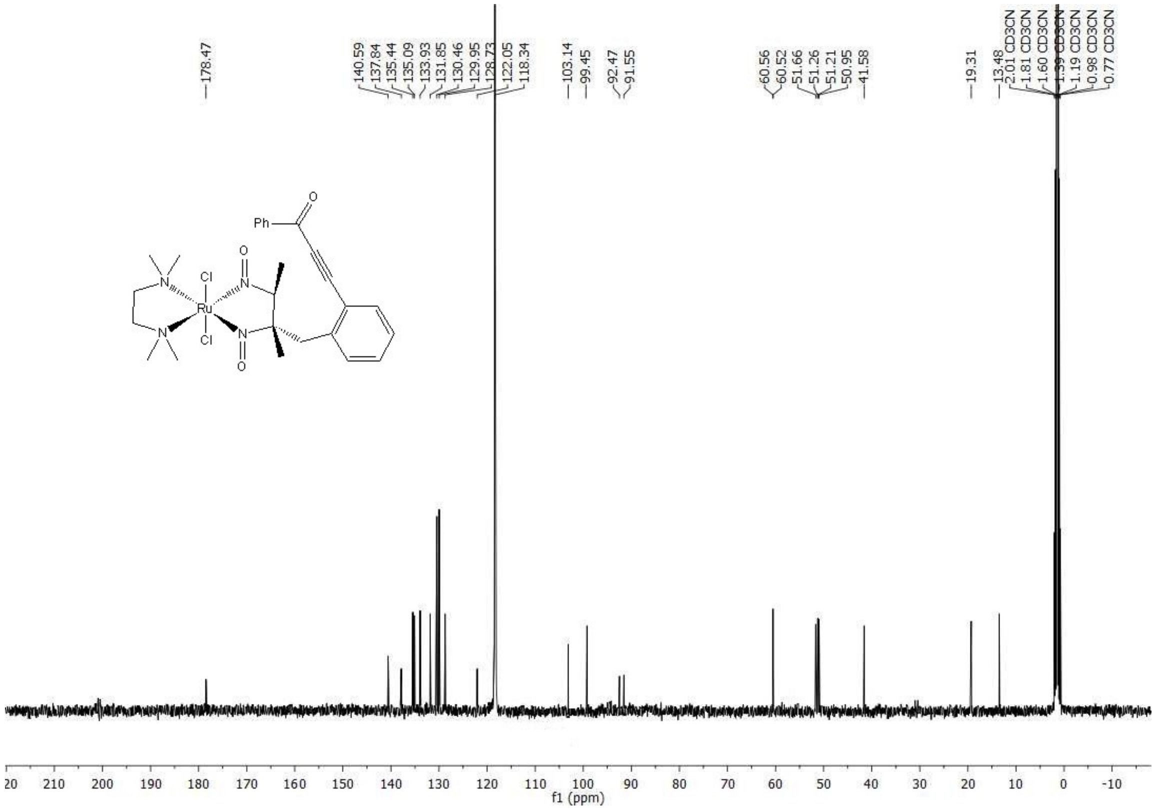
178.47
140.59
137.84
135.44
135.09
133.93
131.85
130.46
129.95
128.73
122.05
118.34
103.14
99.45
92.47
91.55
60.56
60.52
51.66
51.26
51.21
50.95
41.58
19.31
13.48
2.01 CD3CN
1.81 CD3CN
1.60 CD3CN
1.39 CD3CN
1.19 CD3CN
0.98 CD3CN
0.77 CD3CN
Ph
O
Cl
N
Ru
20 210 200 190 180 170 160 150 140 130 120 110 100 90 80 70 60 50 40 30 20 10 0 -10
f1 (ppm)

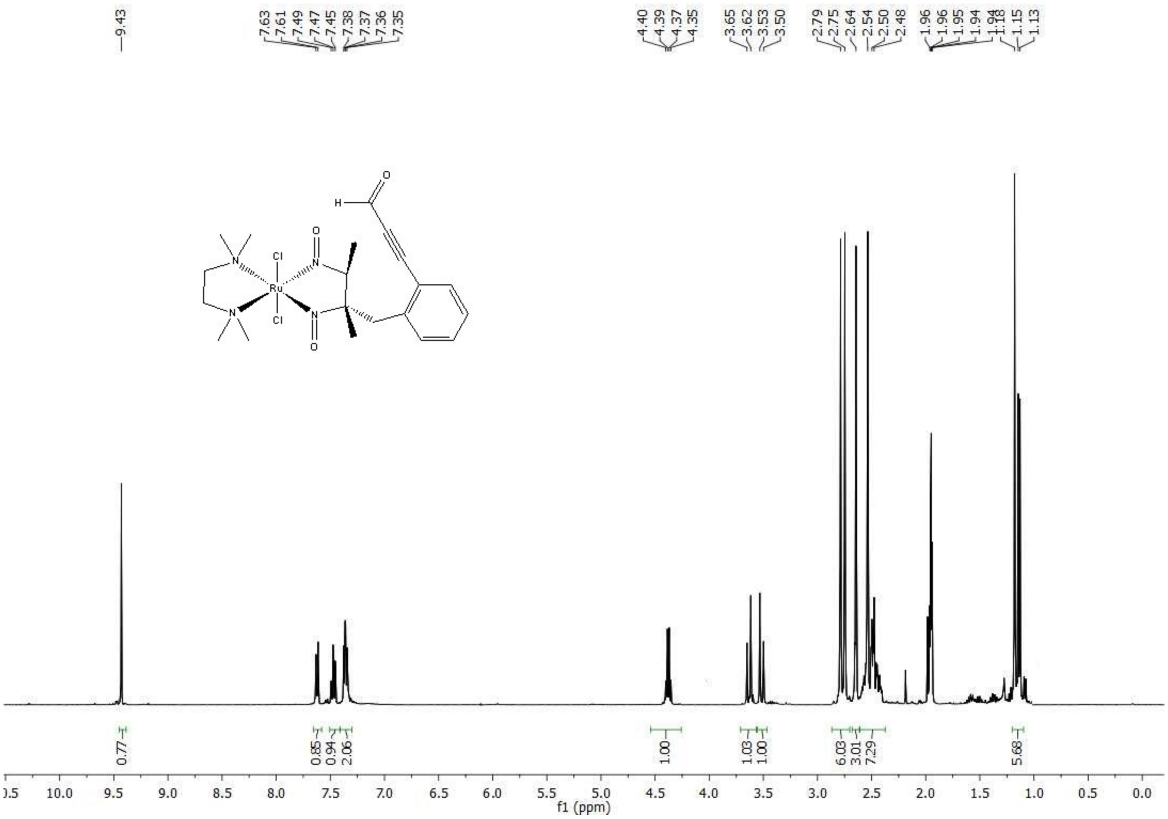
9.43
7.63
7.61
7.49
7.47
7.45
7.38
7.37
7.36
7.35
4.40
4.39
4.37
4.35
3.65
3.62
3.53
3.50
2.79
2.75
2.64
2.54
2.50
2.48
1.96
1.96
1.95
1.94
1.94
1.18
1.15
1.13
H
O
Cl
Ru
N
O
0.77
0.85
0.94
2.06
1.00
1.03
1.00
6.03
3.01
7.29
5.68
10.0
9.5
9.0
8.5
8.0
7.5
7.0
6.5
6.0
5.5
5.0
4.5
4.0
3.5
3.0
2.5
2.0
1.5
1.0
0.5
0.0
f1 (ppm)

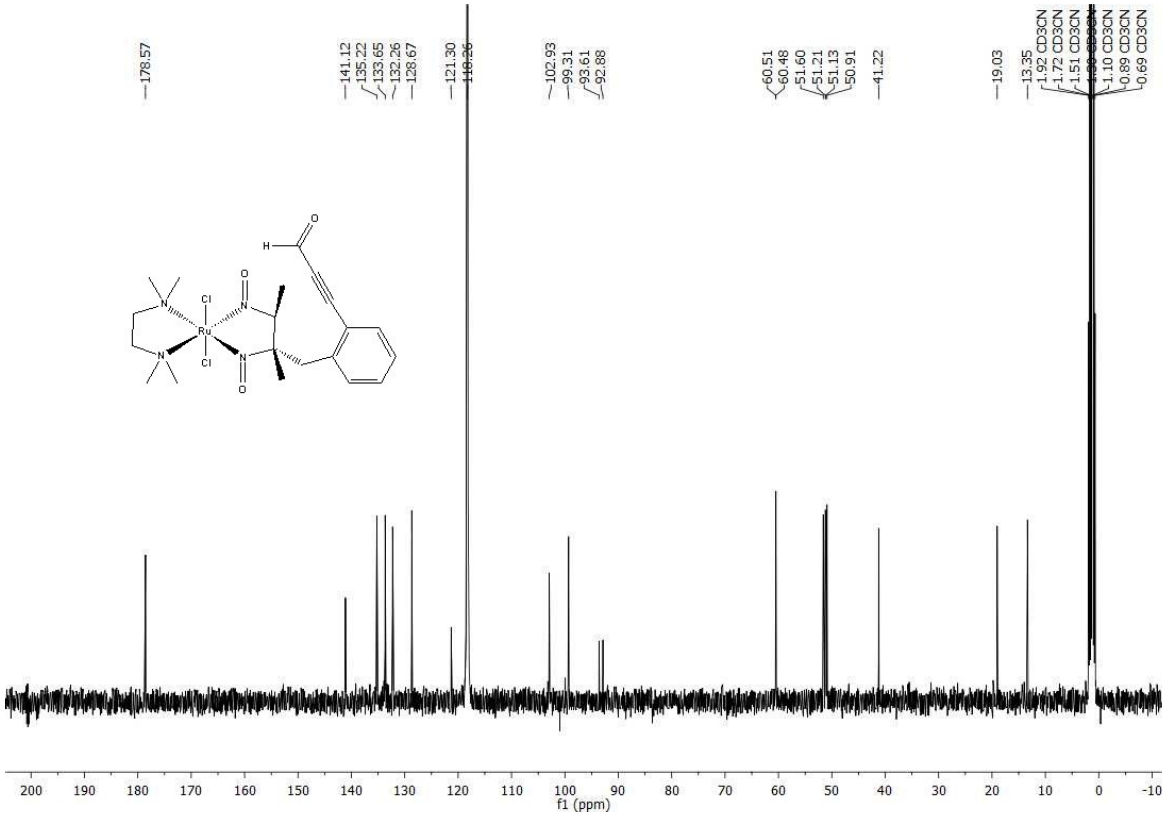
178.57
141.12
135.22
133.65
132.26
128.67
121.30
118.26
102.93
99.31
93.61
92.88
60.51
60.48
51.60
51.21
51.13
50.91
41.22
19.03
13.35
1.92 CD3CN
1.72 CD3CN
1.51 CD3CN
1.30 CD3CN
1.10 CD3CN
0.89 CD3CN
0.69 CD3CN
H
O
Cl
Ru
N
O
200
190
180
170
160
150
140
130
120
110
100
90
80
70
60
50
40
30
20
10
0
-10
f1 (ppm)

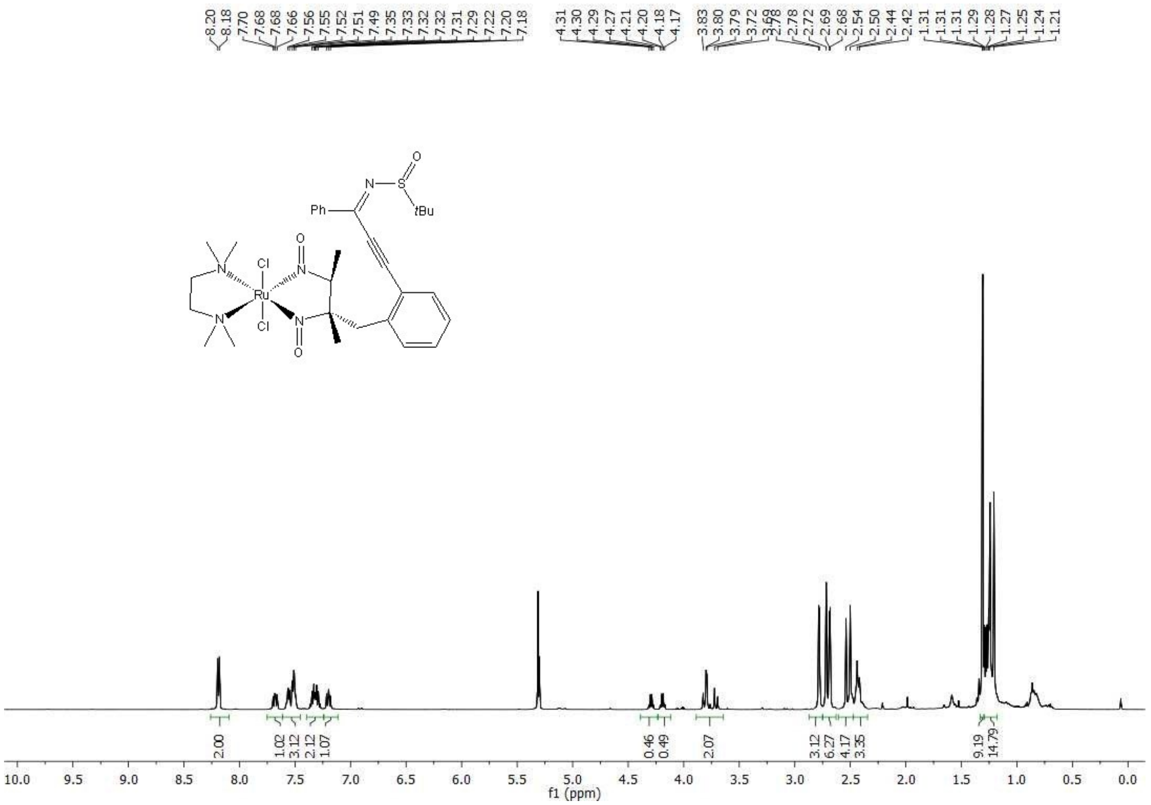
8.20
8.18
7.70
7.68
7.68
7.66
7.56
7.55
7.52
7.51
7.49
7.35
7.33
7.32
7.32
7.31
7.29
7.22
7.20
7.18
4.31
4.30
4.29
4.27
4.21
4.20
4.18
4.17
3.83
3.80
3.79
3.72
3.69
2.78
2.78
2.72
2.69
2.68
2.54
2.50
2.44
2.42
1.31
1.31
1.31
1.29
1.28
1.27
1.25
1.24
1.21
O
N
S
Ph
tBu
N
Cl
Ru
N
Cl
N
O
N
O
2.00
1.02
3.12
2.12
1.07
0.46
0.49
2.07
3.12
6.27
4.17
3.35
9.19
14.79
10.0
9.5
9.0
8.5
8.0
7.5
7.0
6.5
6.0
5.5
5.0
4.5
4.0
3.5
3.0
2.5
2.0
1.5
1.0
0.5
0.0
f1 (ppm)

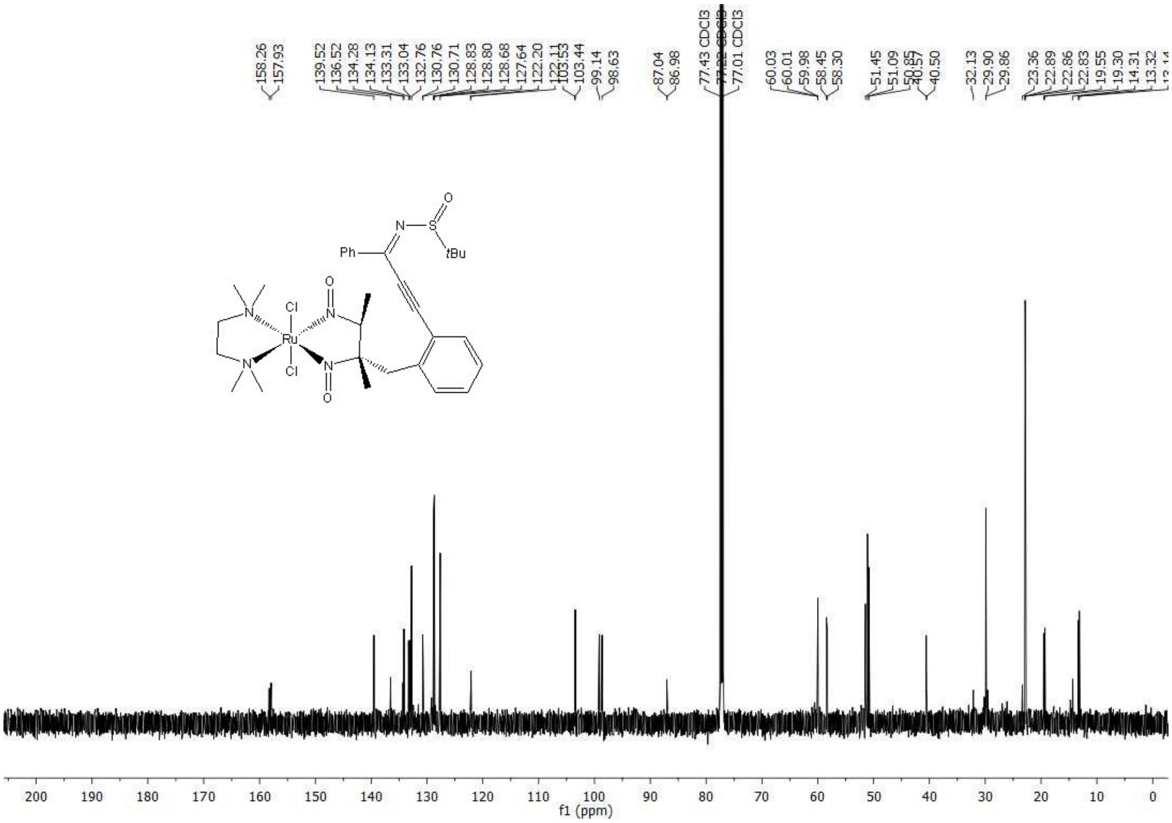
158.26
157.93
139.52
136.52
134.28
134.13
133.31
133.04
132.76
130.76
130.71
128.83
128.80
128.68
127.64
122.20
122.11
103.53
103.44
99.14
98.63
87.04
86.98
77.43 CDCl3
77.22 CDCl3
77.01 CDCl3
60.03
60.01
59.98
58.45
58.30
51.45
51.09
50.85
50.57
40.50
32.13
29.90
29.86
23.36
22.89
22.86
22.83
19.55
19.30
14.31
13.32
O
N
S
Ph
tBu
N
Cl
Ru
N
Cl
N
O
N
O
200
190
180
170
160
150
140
130
120
110
100
90
80
70
60
50
40
30
20
10
0
f1 (ppm)

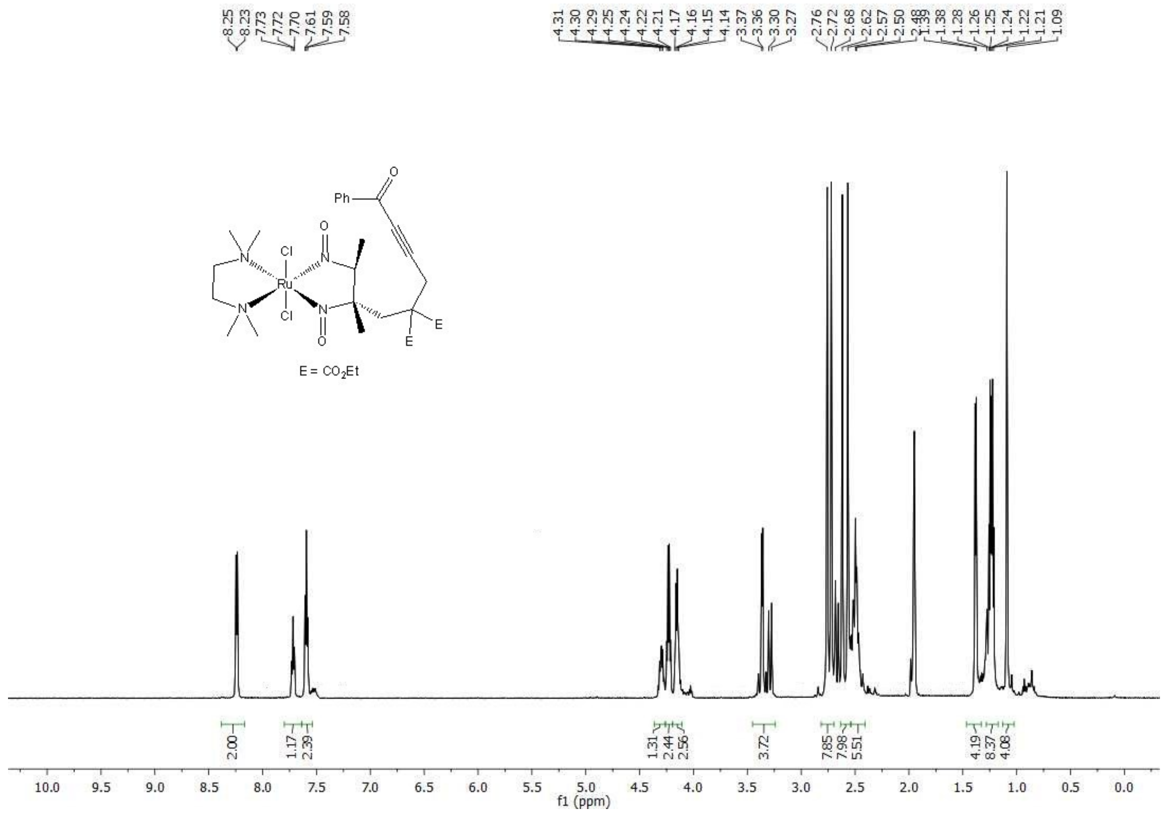
8.25
8.23
7.73
7.72
7.70
7.61
7.59
7.58
4.31
4.30
4.29
4.25
4.24
4.22
4.21
4.17
4.16
4.15
4.14
3.37
3.36
3.30
3.27
2.76
2.72
2.68
2.62
2.57
2.50
2.48
1.39
1.38
1.28
1.26
1.25
1.24
1.22
1.21
1.09
Ph
O
Cl
N
Ru
Cl
N
O
N
O
N
E
E
E = CO2Et
2.00
1.17
2.39
1.31
2.44
2.56
3.72
7.85
7.98
5.51
4.19
8.37
4.08
10.0
9.5
9.0
8.5
8.0
7.5
7.0
6.5
6.0
5.5
5.0
4.5
4.0
3.5
3.0
2.5
2.0
1.5
1.0
0.5
0.0
f1 (ppm)

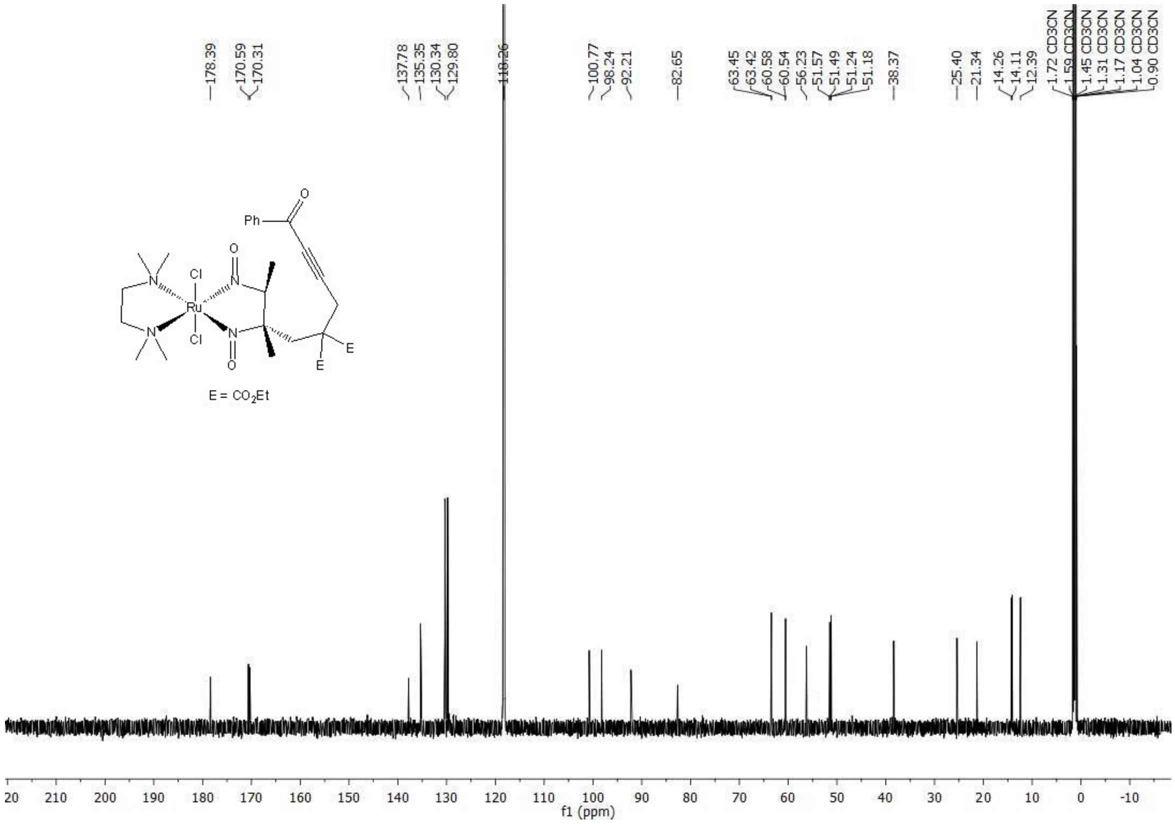
178.39
170.59
170.31
137.78
135.35
130.34
129.80
118.26
100.77
98.24
92.21
82.65
63.45
63.42
60.58
60.54
56.23
51.57
51.49
51.24
51.18
38.37
25.40
21.34
14.26
14.11
12.39
1.72 CD3CN
1.59 CD3CN
1.45 CD3CN
1.31 CD3CN
1.17 CD3CN
1.04 CD3CN
0.90 CD3CN
Ph
O
Cl
N
Ru
Cl
N
O
N
O
N
E
E
E = CO2Et
20
210
200
190
180
170
160
150
140
130
120
110
100
90
80
70
60
50
40
30
20
10
0
-10
f1 (ppm)

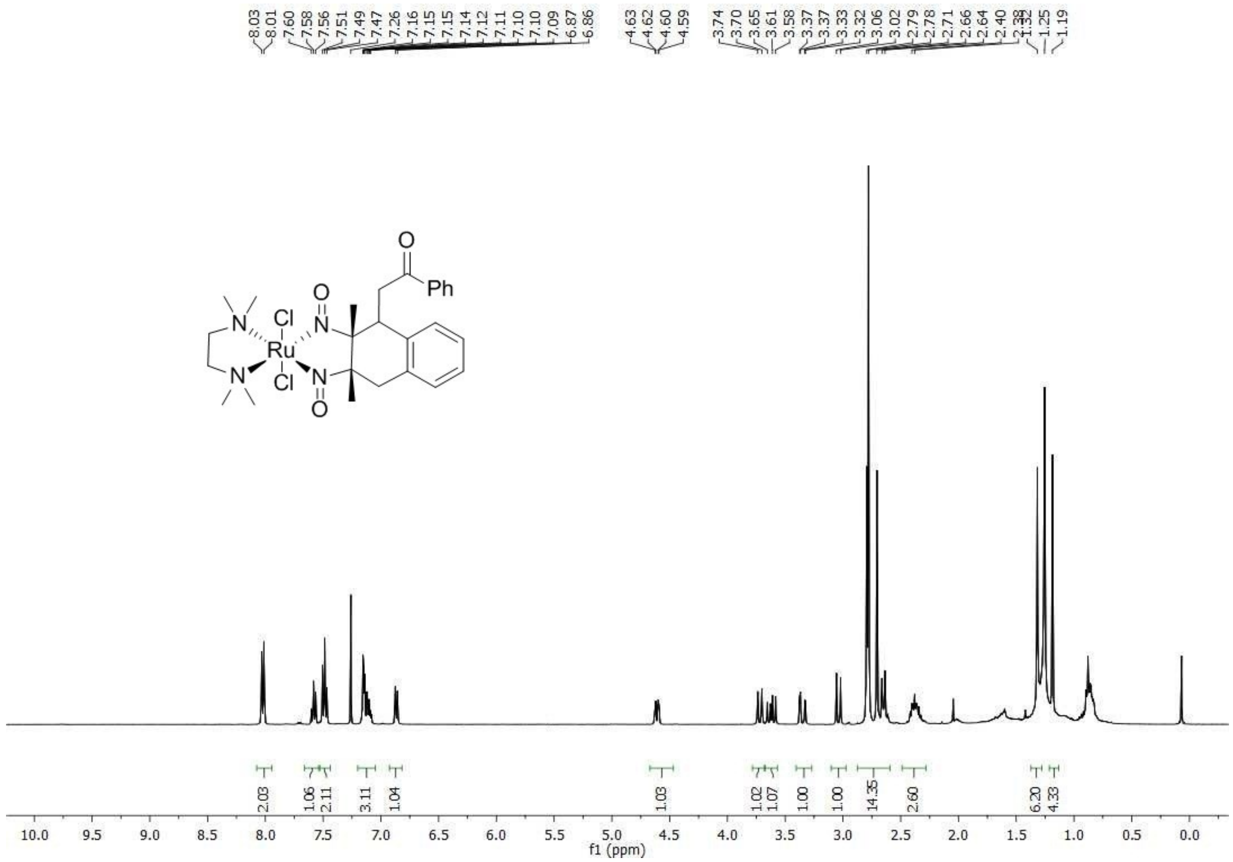
8.03
8.01
7.60
7.58
7.56
7.51
7.49
7.47
7.26
7.16
7.15
7.15
7.14
7.12
7.11
7.10
7.10
7.09
6.87
6.86
4.63
4.62
4.60
4.59
3.74
3.70
3.65
3.61
3.58
3.37
3.37
3.33
3.32
3.06
3.02
2.79
2.78
2.71
2.66
2.64
2.40
2.38
1.32
1.25
1.19
O
Ph
N
Cl
Ru
N
O
N
Cl
N
O
2.03
1.06
2.11
3.11
1.04
1.03
1.02
1.07
1.00
1.00
14.35
2.60
6.20
4.33
10.0
9.5
9.0
8.5
8.0
7.5
7.0
6.5
6.0
5.5
5.0
4.5
4.0
3.5
3.0
2.5
2.0
1.5
1.0
0.5
0.0
f1 (ppm)

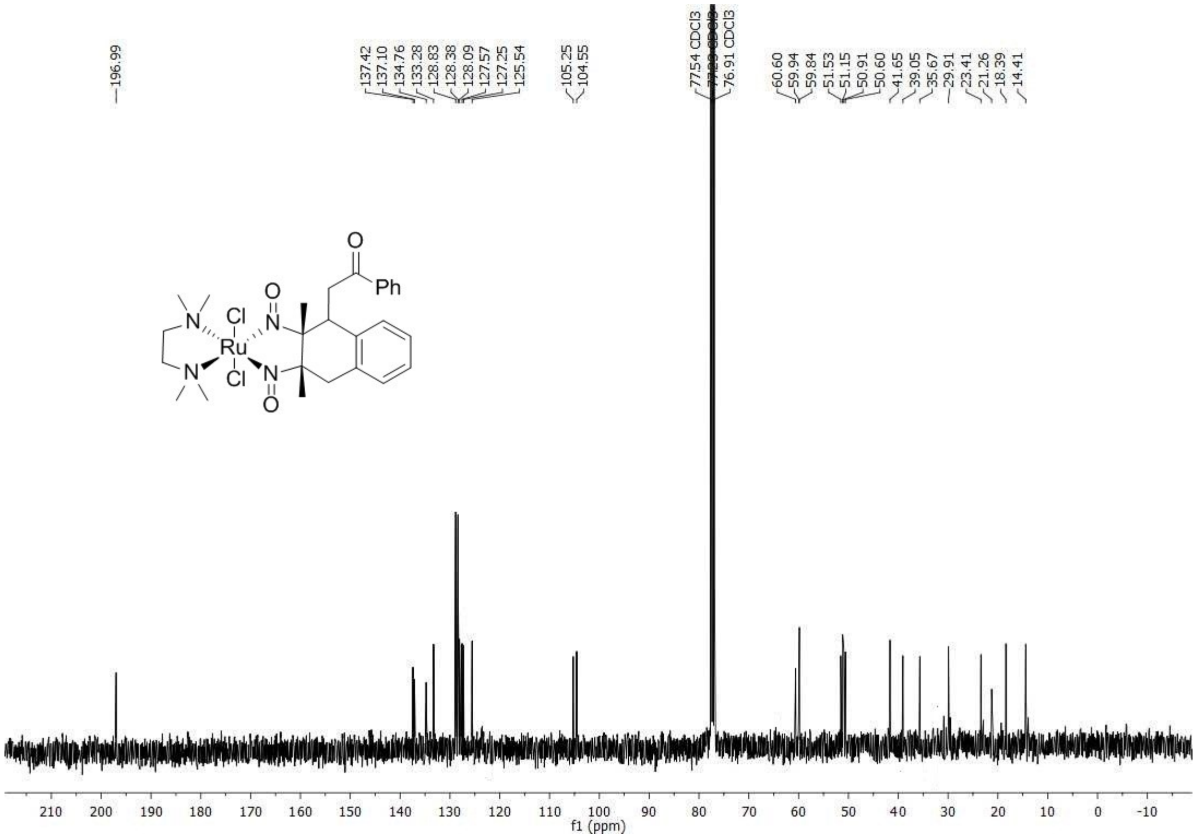
196.99
137.42
137.10
134.76
133.28
128.83
128.38
128.09
127.57
127.25
125.54
105.25
104.55
77.54 CDCl3
77.23 CDCl3
76.91 CDCl3
60.60
59.94
59.84
51.53
51.15
50.91
50.60
41.65
39.05
35.67
29.91
23.41
21.26
18.39
14.41
O
Ph
N
Cl
Ru
N
O
N
Cl
N
O
210
200
190
180
170
160
150
140
130
120
110
100
90
80
70
60
50
40
30
20
10
0
-10
f1 (ppm)

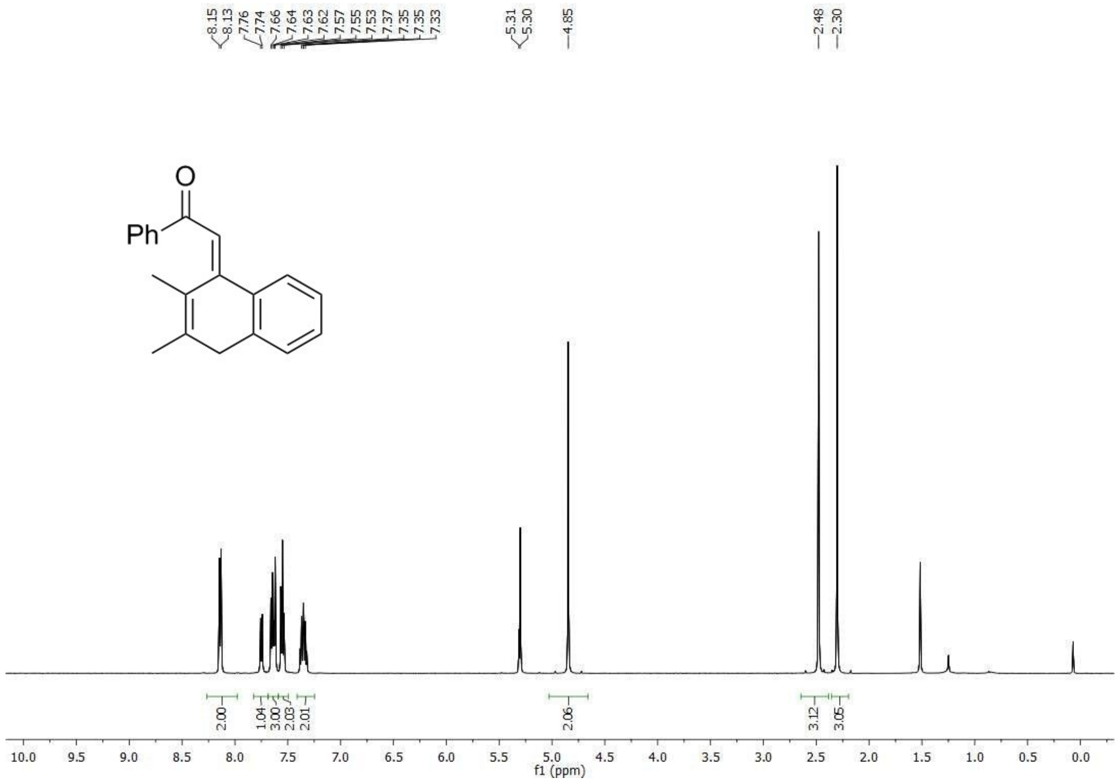
8.15
8.13
7.76
7.74
7.66
7.64
7.63
7.62
7.57
7.55
7.53
7.37
7.35
7.35
7.33
5.31
5.30
4.85
2.48
2.30
O
Ph
2.00
1.04
3.00
2.03
2.01
2.06
3.12
3.05
10.0 9.5 9.0 8.5 8.0 7.5 7.0 6.5 6.0 5.5 5.0 4.5 4.0 3.5 3.0 2.5 2.0 1.5 1.0 0.5 0.0
f1 (ppm)

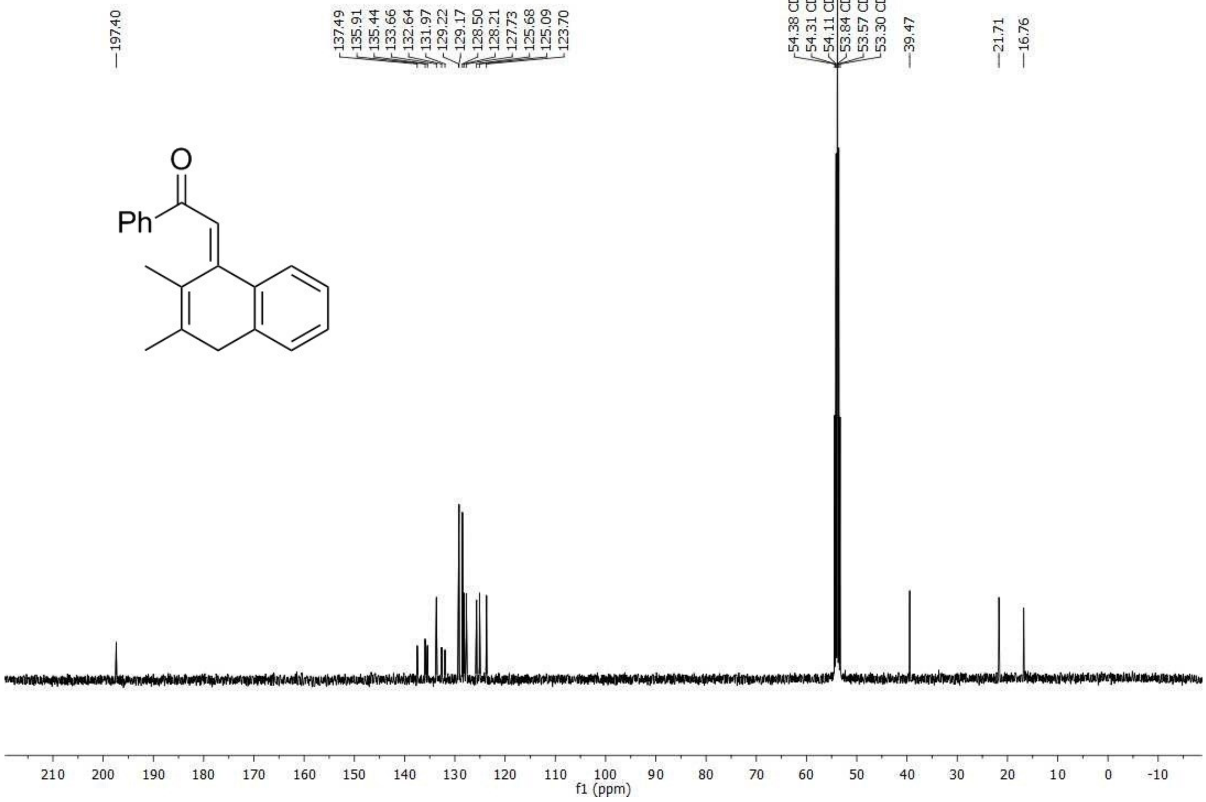
197.40
137.49
135.91
135.44
133.66
132.64
131.97
129.22
129.17
128.50
128.21
127.73
125.68
125.09
123.70
54.38 CD2Cl2
54.31 CD2Cl2
54.11 CD2Cl2
53.84 CD2Cl2
53.57 CD2Cl2
53.30 CD2Cl2
39.47
21.71
16.76
O
Ph
210 200 190 180 170 160 150 140 130 120 110 100 90 80 70 60 50 40 30 20 10 0 -10
f1 (ppm)

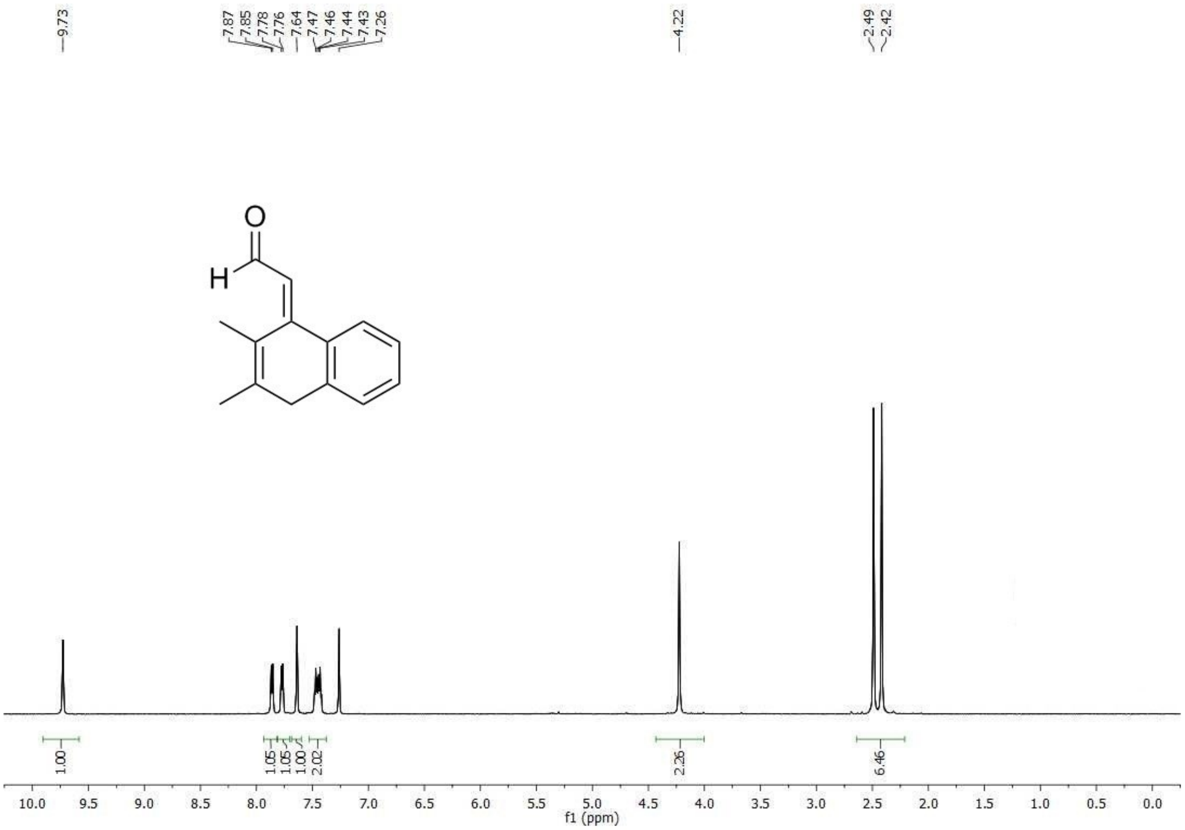
9.73
7.87
7.85
7.78
7.76
7.64
7.47
7.46
7.44
7.43
7.26
4.22
2.49
2.42
O
H
1.00
1.05
1.05
1.00
2.02
2.26
6.46
10.0
9.5
9.0
8.5
8.0
7.5
7.0
6.5
6.0
5.5
5.0
4.5
4.0
3.5
3.0
2.5
2.0
1.5
1.0
0.5
0.0
f1 (ppm)

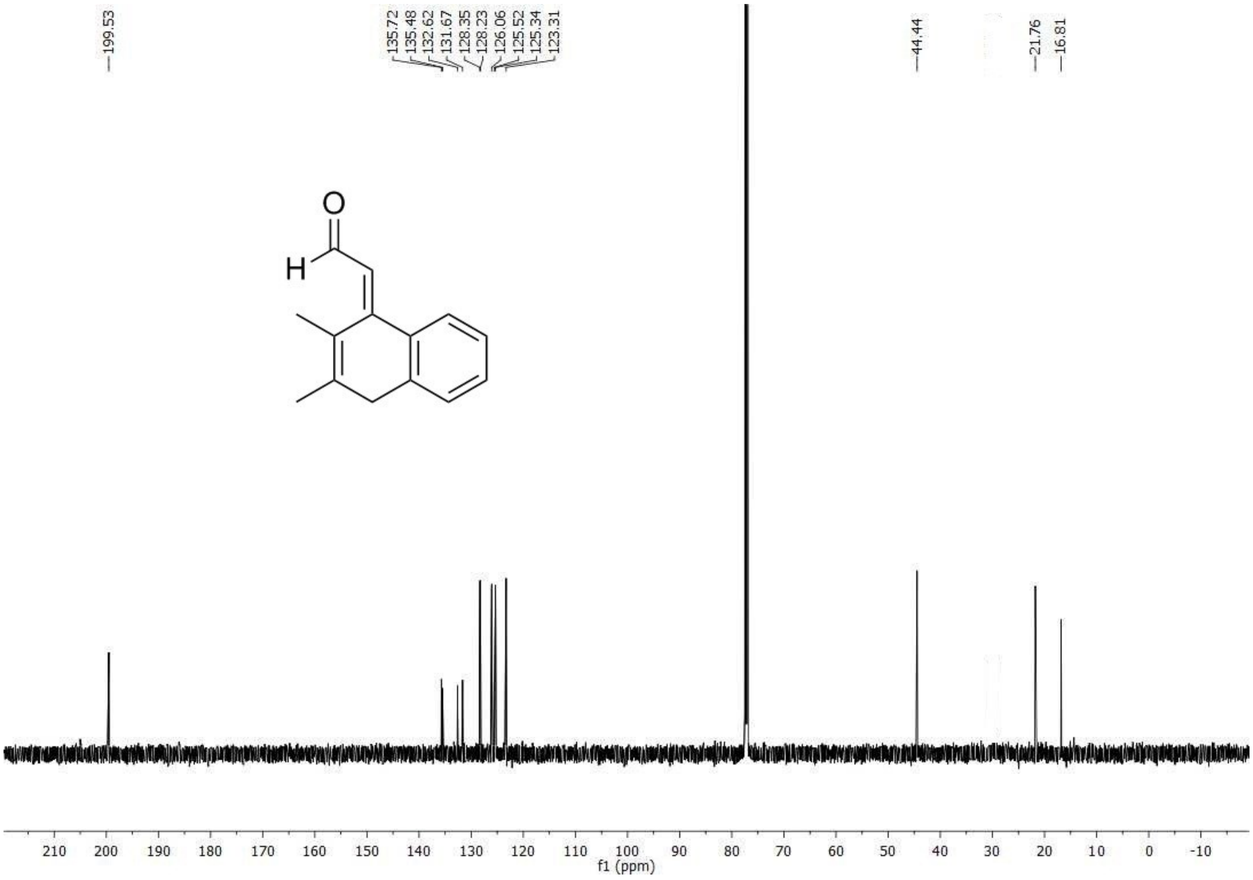
199.53
135.72
135.48
132.62
131.67
128.35
128.23
126.06
125.52
125.34
123.31
44.44
21.76
16.81
O
H
210
200
190
180
170
160
150
140
130
120
110
100
90
80
70
60
50
40
30
20
10
0
-10
f1 (ppm)

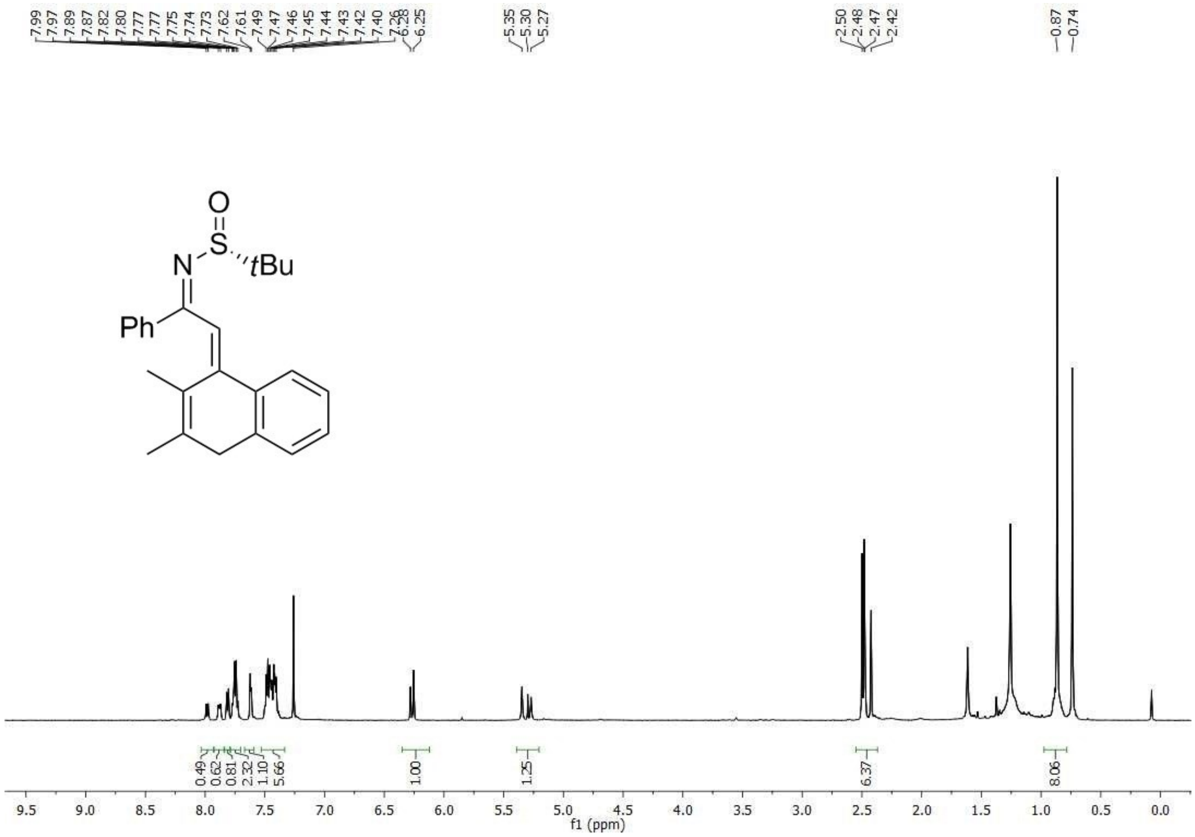
7.99
7.97
7.89
7.87
7.82
7.80
7.77
7.77
7.75
7.74
7.73
7.62
7.61
7.49
7.47
7.46
7.45
7.44
7.43
7.42
7.40
7.26
6.28
6.25
5.35
5.30
5.27
2.50
2.48
2.47
2.42
0.87
0.74
O
S
N
tBu
Ph
0.49
0.62
0.81
2.32
1.10
5.66
1.00
1.25
6.37
8.06
9.5
9.0
8.5
8.0
7.5
7.0
6.5
6.0
5.5
5.0
4.5
4.0
3.5
3.0
2.5
2.0
1.5
1.0
0.5
0.0
f1 (ppm)

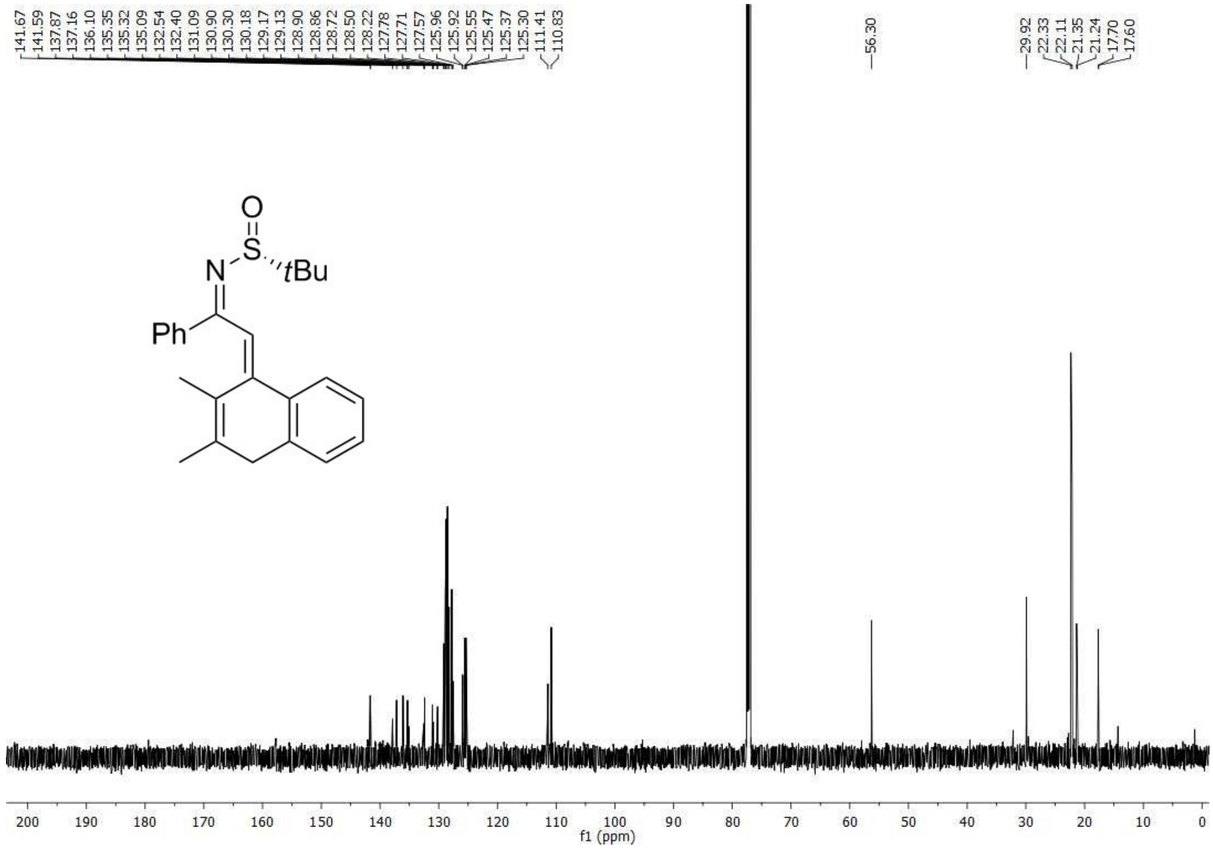
141.67
141.59
137.87
137.16
136.10
135.35
135.32
135.09
132.54
132.40
131.09
130.90
130.30
130.18
129.17
129.13
128.90
128.86
128.72
128.50
128.22
127.78
127.71
127.57
125.96
125.92
125.55
125.47
125.37
125.30
111.41
110.83
56.30
29.92
22.33
22.11
21.35
21.24
17.70
17.60
O
S
N
tBu
Ph
200
190
180
170
160
150
140
130
120
110
100
90
80
70
60
50
40
30
20
10
0
f1 (ppm)

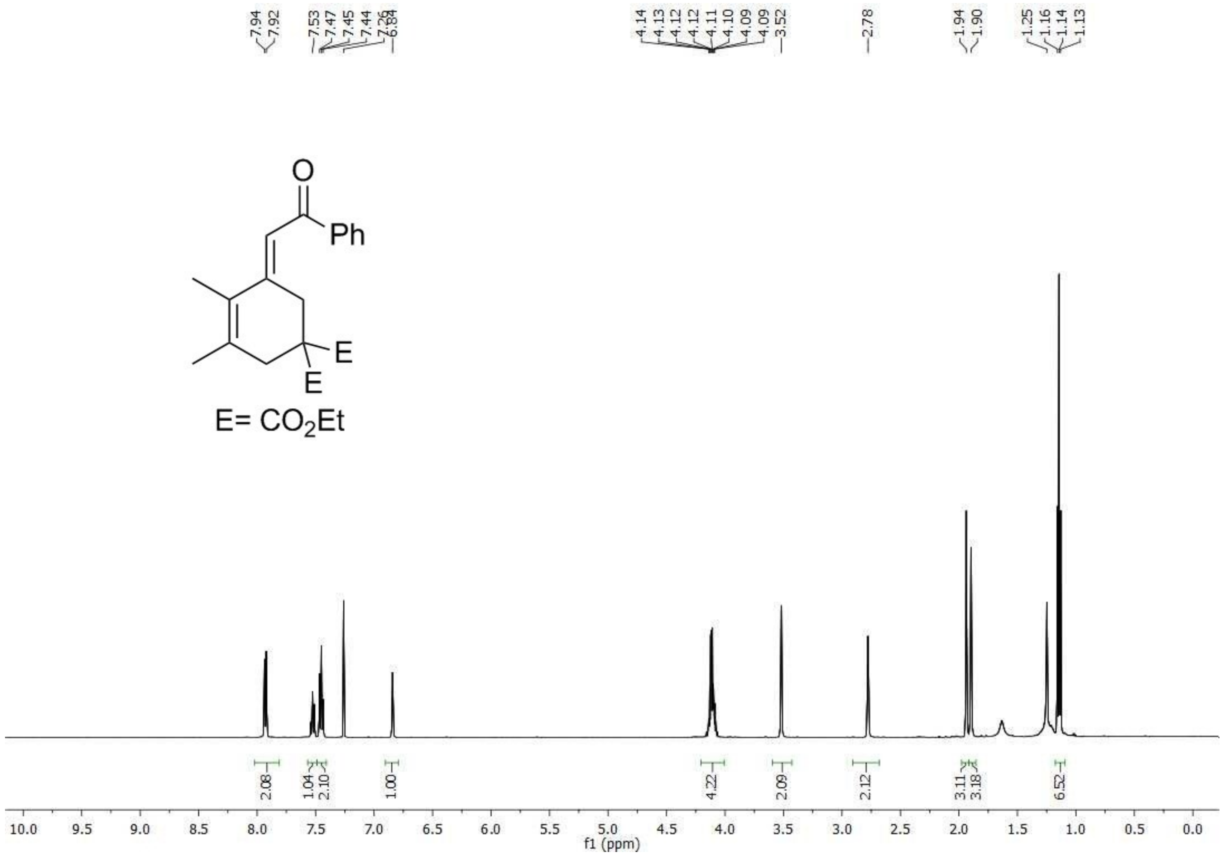
7.94
7.92
7.53
7.47
7.45
7.44
7.26
6.84
4.14
4.13
4.12
4.12
4.11
4.10
4.09
4.09
3.52
2.78
1.94
1.90
1.25
1.16
1.14
1.13
O
Ph
E
E
E= CO2Et
2.08
1.04
2.10
1.00
4.22
2.09
2.12
3.11
3.18
6.52
10.0
9.5
9.0
8.5
8.0
7.5
7.0
6.5
6.0
5.5
5.0
4.5
4.0
3.5
3.0
2.5
2.0
1.5
1.0
0.5
0.0
f1 (ppm)

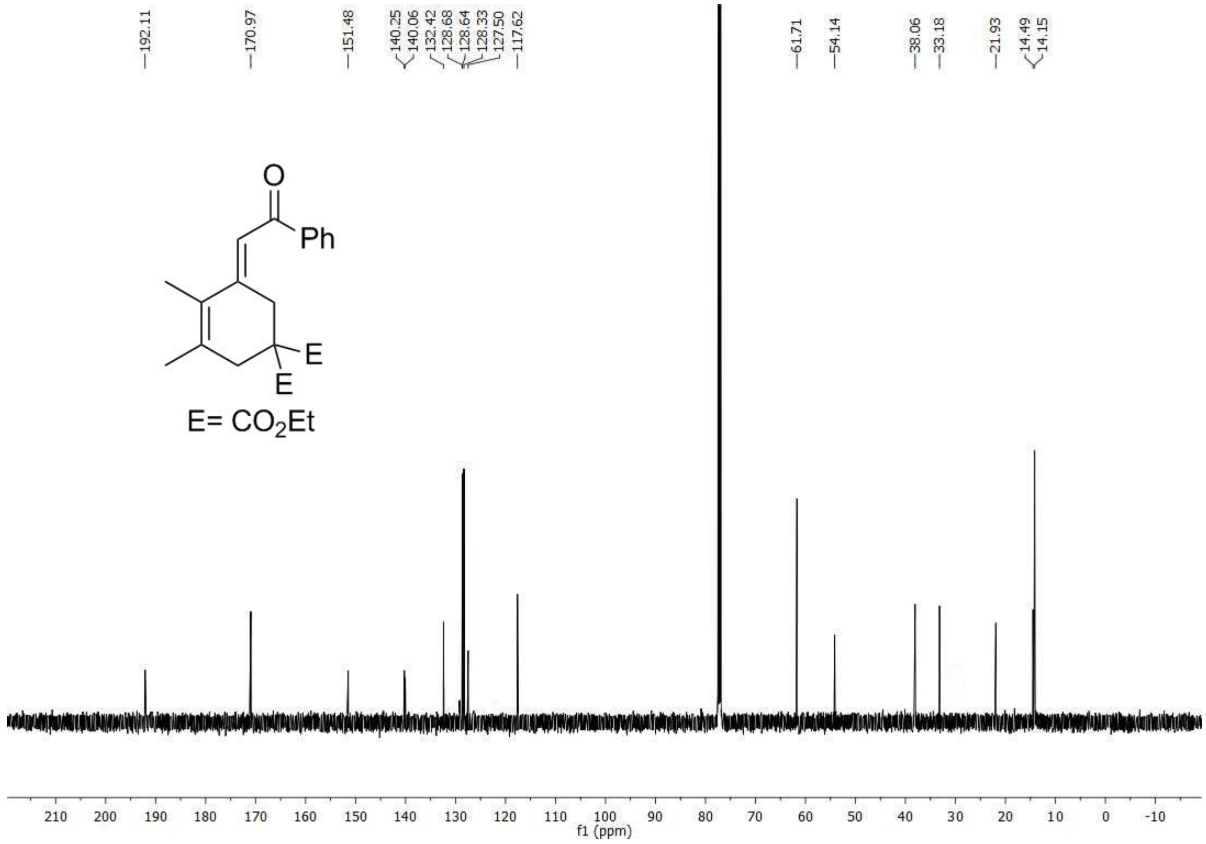
192.11
170.97
151.48
140.25
140.06
132.42
128.68
128.64
128.33
127.50
117.62
61.71
54.14
38.06
33.18
21.93
14.49
14.15
O
Ph
E
E
E= CO2Et
210
200
190
180
170
160
150
140
130
120
110
100
90
80
70
60
50
40
30
20
10
0
-10
f1 (ppm)

Chapter 4. Enantiopure Supramolecular Host Assemblies and their Application to Asymmetric Organic Catalysis

4.1. Introduction

The field of supramolecular chemistry has long endeavored to mimic the properties of enzymes and their ability to catalyze chemical transformations by providing reactive “active sites”.[1] The reaction pockets of many enzymes often endow the biocatalyst with the ability to select substrates based on size, shape and chirality, and induce reactions different from those observed in bulk solution.[2-4] In contrast to the vast majority of traditional organic catalytic systems that rely on covalent bond-breaking and bond-forming reactions to control molecular structure, supramolecular chemistry takes advantage of reversible non-covalent interactions that produce strongly associated and well-defined macromolecular complexes. Thus, supramolecular chemistry provides an alternative approach toward molecular construction and diversity complementary to traditional organic catalysis.[5,6]

Crown ethers, one of the earliest and simplest examples of supramolecular complexes, are cyclic polyethers that coordinate with alkali metal cations *via* their oxygen atoms and form strongly-associated species as illustrated in eq. 4.1.[7,8] While a single oxygen-metal interaction is relatively weak, the combination of multiple coordinating atoms with a single K^+ cation has been shown to produce binding constants on the order of 10^6, demonstrating the ability of supramolecular structures to exhibit the type of high affinity often needed to support host-guest chemistry.[9]

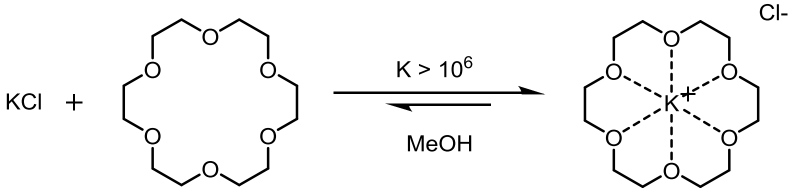

eqn 4.1

In 1997, Rebek and co-workers reported an organic-soluble supramolecular complex, or sometime referred to as a “molecular flask”, comprised of two subunits held together by intermolecular hydrogen bonds (eq. 4.2). This complex is capable of catalyzing the Diels-Alders reaction of *p*-benzoquinone and cyclohexadiene (Figure 4.1).[10] While product inhibition limited catalytic turnover of the supramolecular host, when the reaction was performed with 2,5-dimethylthiophene dioxide as the diene, up to 7 turnovers of the active catalyst were observed.[11] This report is regarded by many as the first example of organic catalysis by a supramolecular nanovessel.

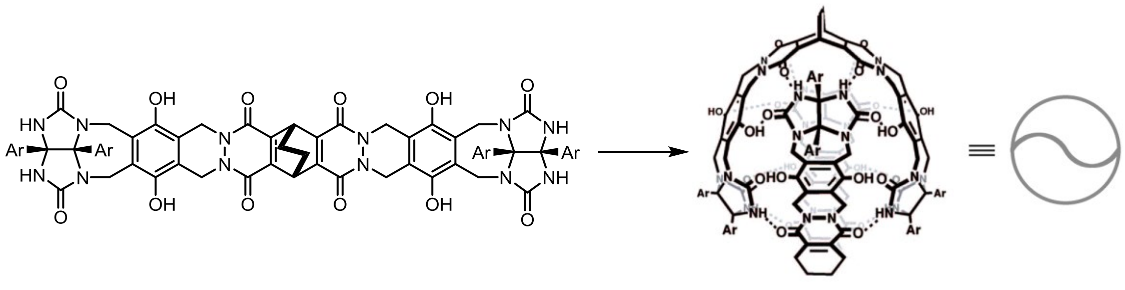

complex **1**

eqn 4.2

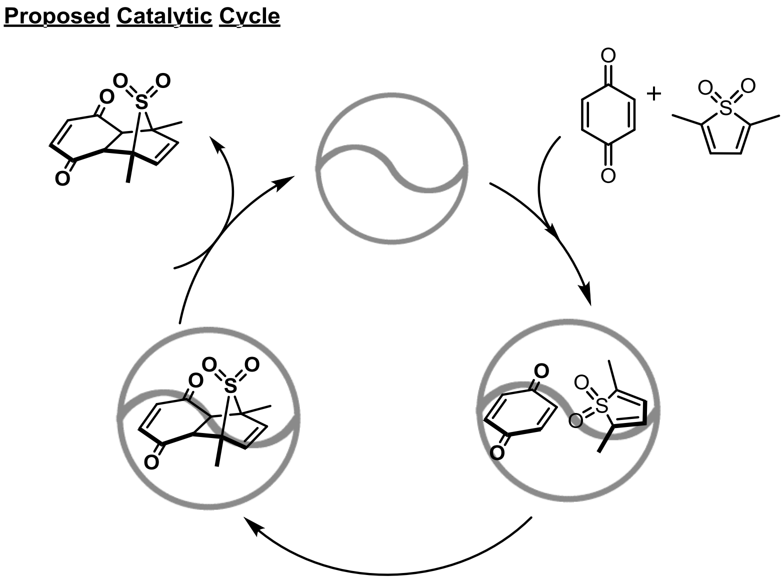

Figure 4.1. Supramolecular host complex **1** catalyzed Diels-Alders reaction of *p*-benzoquinone and 2,5-dimethylthiophene dioxide.

Since these seminal reports, synthetic chemists have become interested in designing supramolecular complexes, particularly enantiopure host assemblies, that can operate as catalysts for chemical reactions. This chapter describes an overview of enantiopure supramolecular complexes and their use in asymmetric organic transformations. Related examples of reactions induced or driven by encapsulation inside a macromolecule, such as metal-organic frameworks and polymers, have also been reported but are beyond the scope of this dissertation and will not be discussed. This chapter provides the context for which Chapters 5-7 can be viewed.

4.2. Chiral Supramolecular Host Complexes

Initially reported in 1998, the Raymond group synthesized supramolecular host complex **2** having $K_{12}Ga_4L_6$ stoichiometry, where L = *N,N'*-bis(2,3-dihydroxybenzoyl)-1,5-diaminonaphthalene, with chiral metal ions occupying the vertices and bridging ligands spanning each wall.[12] Mechanical coupling of the ligands enforces chirality transfer between the metal vertices, thus leading to the exclusive formation of a racemic mixture of homochiral enantiomers, namely $\Delta\Delta\Delta\Delta$-**2** and $\Lambda\Lambda\Lambda\Lambda$-**2** (Figure 4.2).[13] The tetra-anionic catecholate ligand, in combination with the trivalent metal centers, generates an overall -12 charged assembly, while its naphthalene walls give rise to a hydrophobic interior with an approximate volume of 300 to 500 Å^3. The well-defined internal cavity has been demonstrated to preferentially encapsulate monocationic molecules, consequently cause pK_a shifts of up to four units for amines and phosphines, and stabilize reactive intermediates such as a phosphine-acetone adduct, a phosphine-gold cation, and imminium cations that would otherwise decompose. Nanovessel **2** has also been shown to be an effective catalyst that enhances the rate and selectivity of a variety of organic and organometallic reactions, including the Nazarov cyclization[14,15] and a hydroalkoxylation reaction catalyzed by an encapsulated Au(I) complex.[16]

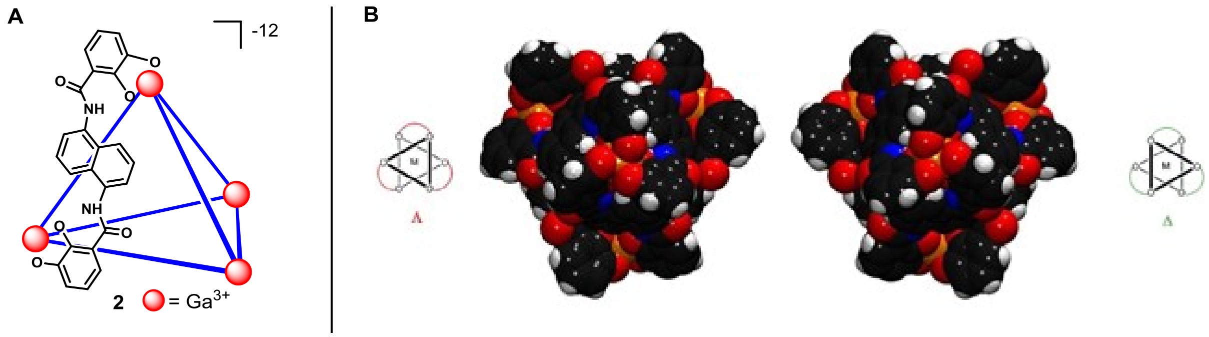
A
-12
O
O
O
NH
NH
O
O
O
2
= Ga3+
B
Λ
Δ

Figure 4.2. (A) Schematic representation of Ga_4L_6 supramolecular assembly **2**. (B) The homochiral **ΛΛΛΛ** and **ΔΔΔΔ** enantiomers of assembly **2**.

The enantiomeric pair of complexes **2** can be easily resolved with a chiral guest, such as a nicotinium salt, as shown in Figure 4.3. It was found that the chiral salt is responsible for the resolution via external association to the host assembly since resolution of $[\mathrm{NEt_4} \subset \mathbf{2}]$ can also be achieved by using excess (*S*)-nicotinium iodide. Since (*S*)-nic is a rather strongly-binding guest molecule, subsequent ion exchange chromatography with excess NMe_4Cl, a weakly-binding guest, has been utilized to give ΛΛΛΛ-$[\mathrm{NMe_4} \subset \mathbf{2}]$. However, the use enantiopure ΛΛΛΛ- and ΔΔΔΔ-$[\mathrm{NMe_4} \subset \mathbf{2}]$ complexes as catalyst for asymmetric organic transformations is limited to guest molecules that bind more strongly to the cavity of **2** than does NMe_4. While further ion-exchange of ΛΛΛΛ-$[\mathrm{NMe_4} \subset \mathbf{2}]$ with potassium iodide gives the desired "empty" or solvent-filled hosts in 40% yield, these hosts prove to be unstable in solution at room temperature.[13]

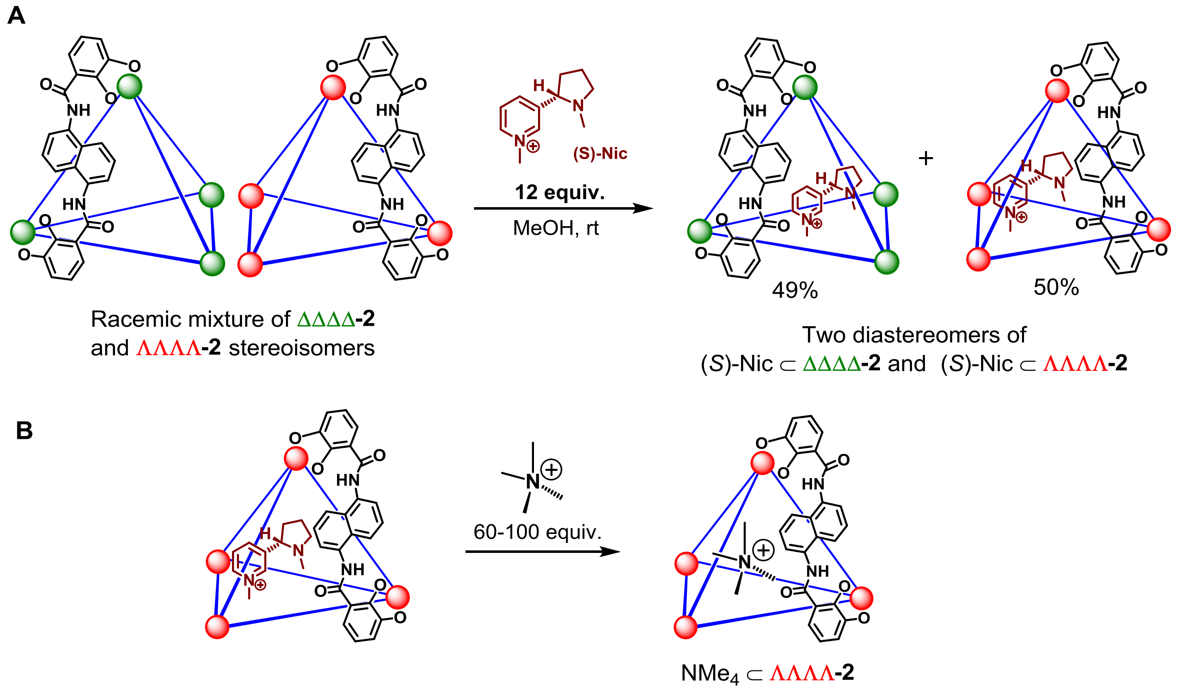
A
H
N
N⊕
(S)-Nic
12 equiv.
MeOH, rt
+
49%
50%
Racemic mixture of ΔΔΔΔ-2
and ΛΛΛΛ-2 stereoisomers
Two diastereomers of
(S)-Nic ⊂ ΔΔΔΔ-2 and (S)-Nic ⊂ ΛΛΛΛ-2
B
N⊕
60-100 equiv.
NMe4 ⊂ ΛΛΛΛ-2

Figure 4.3. (A) Resolution of assembly **2** using (*S*)-nicotinium salt. (B) Ion-exchange of [(*S*)-Nic ⊂ ΛΛΛΛ-**2**] with NMe_4Cl to give $[\mathrm{NMe_4} \subset$ ΛΛΛΛ-**2**]

In 2010, Cui and coworkers reported the synthesis of tetrahedral complex **3** composed of 1,1-biphenyl-derived ligands with gallium or iron metal centers.[17] Like the Raymond cluster **2**, the host assembly is homochiral, giving rise to ΛΛΛΛ and ΔΔΔΔ enantiomers. The complex ΛΛΛΛ-**3** was demonstrated to be a highly selective assembly capable of resolving a racemic mixture of 2-butanol to give one enantiomer of the alcohol in an enantiopure fashion.

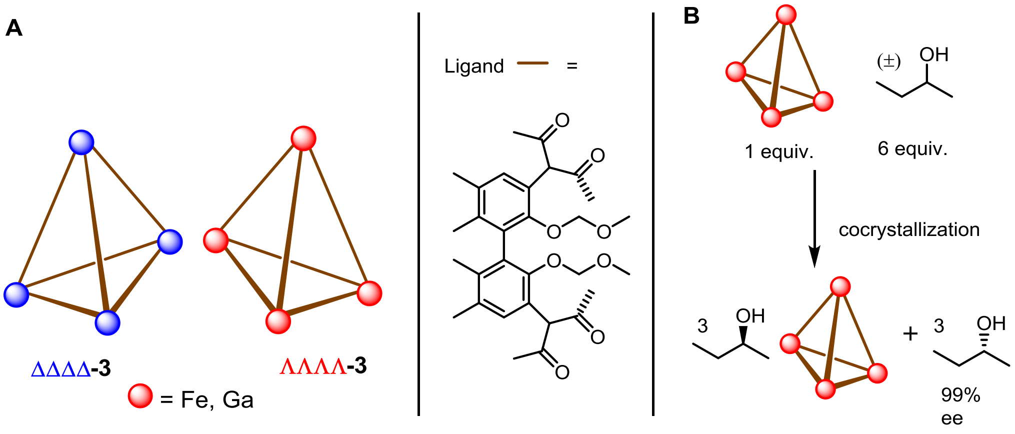
A
Ligand =
ΔΔΔΔ-3
ΛΛΛΛ-3
= Fe, Ga
O
O
O
O
B
(±) OH
1 equiv.
6 equiv.
cocrystallization
3 OH
+ 3 OH
99% ee

Figure 4.4. (A) Synthesis of enantiopure tetrahedron **3** with 1,1-biphenyl-derived chiral ligands and Fe or Ga atoms. (B) Enantioselective association of one enantiomer of a chiral alcohol that results in the enantiopure co-crystallization of 2-butanol.

Lusby and coworkers reported in 2012 the synthesis of an octahedral molecular capsule **4**, shown in Figure 4.5, in which an enantiopure iridium unit occupies the cluster vertices [18]. The multitopic nitrile ligand, in combination with the phenylpyridine-iridium complex, gives the desired host assembly with luminescence that is much more intense than that of the corresponding mononuclear complex. Furthermore, the overall +6 complex **4** readily encapsulates anionic guest molecules, such as triflate and tetrafluoroborate anions.

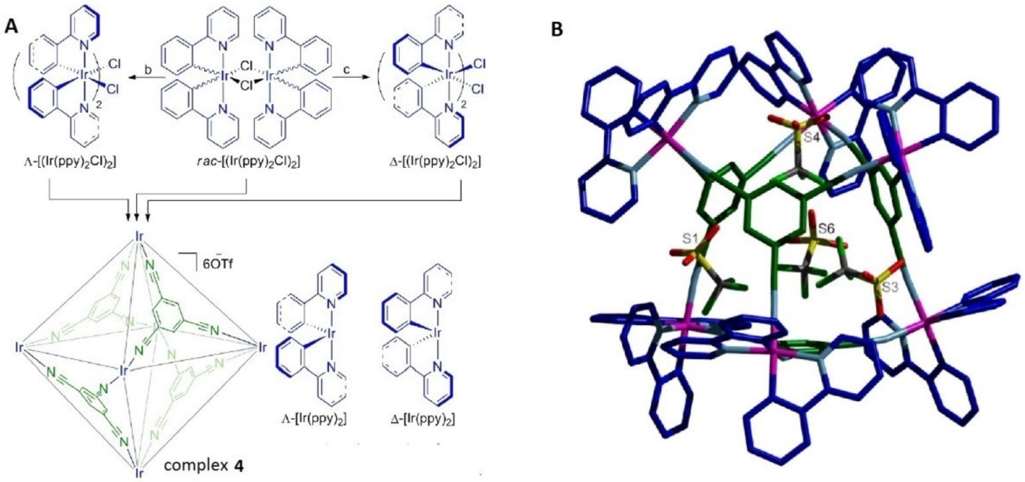
A
b
c
Λ-[(Ir(ppy)2Cl)2]
rac-[(Ir(ppy)2Cl)2]
Δ-[(Ir(ppy)2Cl)2]
6OTf
complex 4
Λ-[Ir(ppy)2]
Δ-[Ir(ppy)2]
B
S4
S6
S1
S3

Figure 4.5. (A) Synthesis of homochiral hexanuclear iridium assemblies.
(B) X-ray crystal structure of complex **3** (figure adapted from reference 18).

The Nitschke group presented another example of an enantiopure tetrahedral cluster in 2013. Assembly **5**, shown in Figure 4.6, was observed to bind a wide range of organic guests and was able to distinguish between the enantiomers of a chiral molecule.[19]

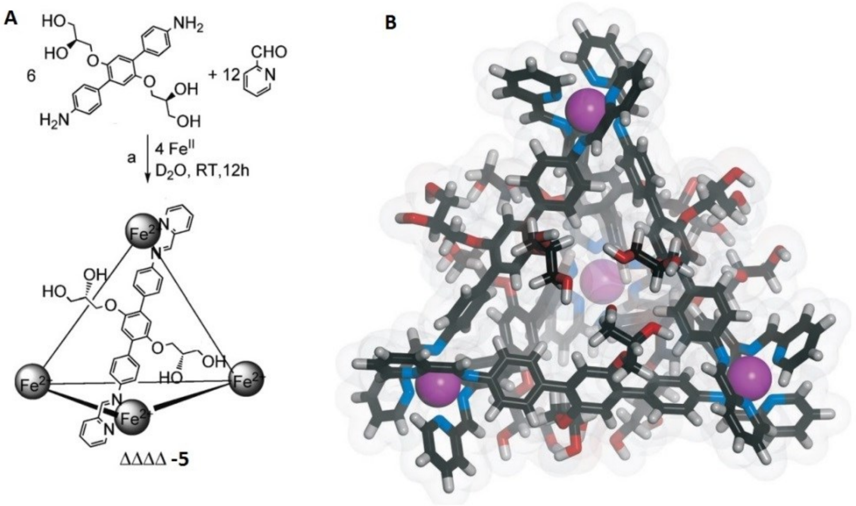

Figure 4.6. (A) The synthesis of an enantiopure tetrahedral cluster **ΔΔΔΔ-5**.
(B) X-ray crystal structure of complex **2** (figure adapted from reference 19).

4.3. Asymmetric Organic Reactions Mediated and Catalyzed by Chiral Nanovessels

While many enantiopure supramolecular assemblies have been synthesized, effective asymmetric organic synthesis using these host complexes as chiral catalysts remains elusive. To date, only a few examples of such reactivity have been demonstrated. For example, the Fujita group utilized their octahedral complex **6** (Figure 4.7A), capped with chiral diamine ligands, as an enantioselective host assembly for the asymmetric [2+2] photoaddition of fluoranthene and maleimide derivatives to give products in good yields with up to 50% enantiomeric excess.[20] Although used in stoichiometric amounts, complex **6** proved to possess a chiral pocket capable of controlling the enantioselectivity of a photochemical cycloaddition through purely non-covalent and electrostatic interactions.

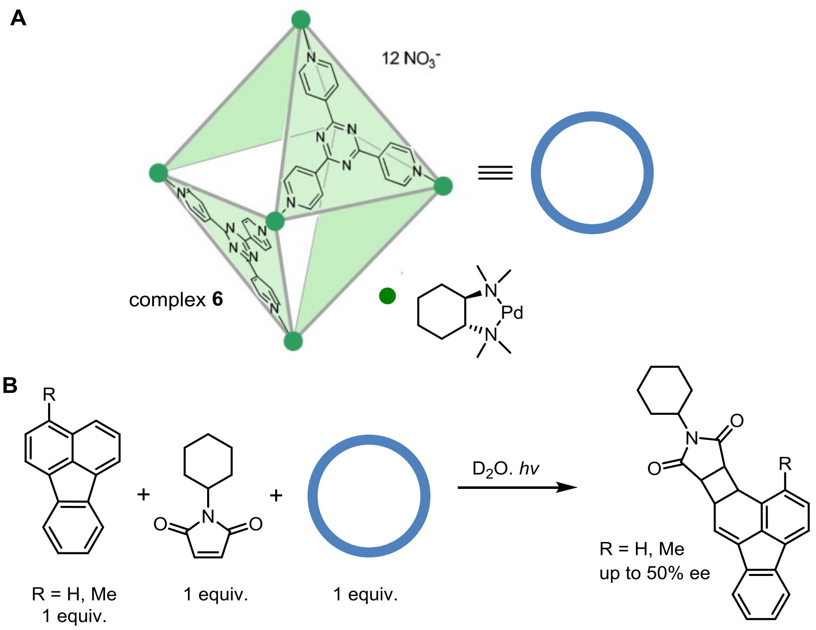

Figure 4.7. (A) Schematic representation of an enantiopure octahedral assembly. (B) Application of **6** as a chiral reaction pocket for the enantioselective [2+2] photoaddition of fluoranthene and maleimide.

More recently, the Raymond and Bergman groups in collaboration demonstrated the application of enantiopure assembly **5** as a catalyst for the enantioselective Aza-Cope rearrangement of enammonium substrates.[21,22] The reaction proceeds through encapsulation of the cationic substrate inside complex **5**, followed by rearrangement to produce a chiral imminium compound that is readily hydrolyzed in bulk solution, thus allowing turnover of the active catalyst. While this report served as the first example of a *catalytic* enantioselective transformation mediated by a chiral supramolecular host, the requirement of cationic substrates (due to the resolution of **5** that results in NMe_4-templated enantiopure ΛΛΛΛ-5) limits the application of host **5** since neutral substrates cannot compete for the cavity of the host. Thus, enantiopure host complexes that are "empty" or only filled with solvent molecules would make possible the asymmetric transformations of both charged and neutral molecules.

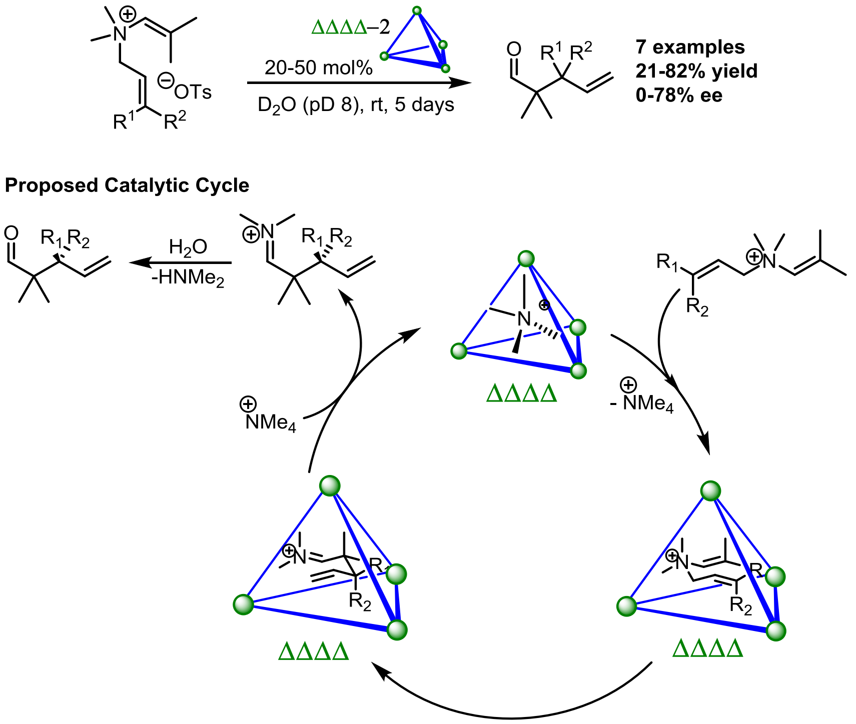
OTs
R1
R2
ΔΔΔΔ–2
20-50 mol%
D2O (pD 8), rt, 5 days
O
R1 R2
7 examples
21-82% yield
0-78% ee
Proposed Catalytic Cycle
O
R1 R2
H2O
-HNMe2
N
R1 R2
NMe4
ΔΔΔΔ
N
R1
R2
- NMe4
ΔΔΔΔ
ΔΔΔΔ

Figure 4.8. Enantioselective Aza-Cope rearrangement reaction catalyzed by enantiopure host **5**.

The research presented in Chapters 5 through 7 builds upon the supramolecular host-guest chemistry presented in this chapter. In particular, the design and synthesis of a new family of terephthalamide-based Ga_4L_6 clusters will be described. The newly designed chiral ligand exhibits stereochemical control during cluster formation to give highly diastereo- and enantiomerically enriched cationic guest-free complexes. The development of enantioselective organic transformations of neutral substrates catalyzed by the new host assemblies will also be discussed. Finally, Chapter 7 presents a nucleophilic substitution reaction of secondary benzylic substrates that proceeds with overall high levels of retention of stereochemistry when the reaction proceeds inside the cavity of Ga_4L_6 assemblies.

4.4. References

(1) Breslow, R.; Dong, S. D. *Chem. Rev.* **1998**, *98*, 1997-2011.

(2) Oshovsky, G. V.; Reinhoudt, D. N.; Verboom, W. *Angew. Chem., Int. Ed.* **2007**, *46*, 2366-2393.

(3) Smit, B.; Maesen, T. L. M. *Nature* **2008**, *451*, 671-678.

(4) Takezawa, H.; Murase, T.; Fujita, M. *J. Am. Chem. Soc.* **2012**, *134*, 17420-17423.

(5) Lehn, J.-M. *Science* **1985**, *227*, 849-856.

(6) Cram, D. J. *Angewandte Chemie International Edition in English* **1988**, *27*, 1009-1020.

(7) Pedersen, C. J. *J. Am. Chem. Soc.* **1967**, *89*, 2495-2496.

(8) Pedersen, C. J. *J. Am. Chem. Soc.* **1967**, *89*, 7017-7036.

(9) Izatt, R. M.; Bradshaw, J. S.; Nielsen, S. A.; Lamb, J. D.; Christensen, J. J.; Sen, D. *Chem. Rev.* **1985**, *85*, 271-339.

(10) Kang, J. M.; Rebek, J. *Nature* **1997**, *385*, 50-52.

(11) Kang, J. M.; Santamaria, J.; Hilmersson, G.; Rebek, J. *J. Am. Chem. Soc.* **1998**, *120*, 7389-7390.

(12) Caulder, D. L.; Powers, R. E.; Parac, T. N.; Raymond, K. N. *Angew. Chem., Int. Ed.* **1998**, *37*, 1840-1843.

(13) Davis, A. V.; Fiedler, D.; Ziegler, M.; Terpin, A.; Raymond, K. N. *J. Am. Chem. Soc.* **2007**, *129*, 15354-15363.

(14) Hastings, C. J.; Pluth, M. D.; Bergman, R. G.; Raymond, K. N. *J. Am. Chem. Soc.* **2010**, *132*, 6938-6940.

(15) Hastings, C. J.; Backlund, M. P.; Bergman, R. G.; Raymond, K. N. *Angew. Chem., Int. Ed.* **2011**, *123*, 10758-10761.

(16) Wang, Z. J.; Brown, C. J.; Bergman, R. G.; Raymond, K. N.; Toste, F. D. *J. Am. Chem. Soc.* **2011**, *133*, 7358-7360.

(17) Liu, T.; Liu, Y.; Xuan, W.; Cui, Y. *Angew. Chem., Int. Ed.* **2010**, *49*, 4121-4124.

(18) Chepelin, O.; Ujma, J.; Wu, X.; Slawin, A. M. Z.; Pitak, M. B.; Coles, S. J.; Michel, J.; Jones, A. C.; Barran, P. E.; Lusby, P. J. *J. Am. Chem. Soc.* **2012**, *134*, 19334-19337.

(19) Bolliger, J. L.; Belenguer, A. M.; Nitschke, J. R. *Angew. Chem., Int. Ed.* **2013**, *52*, 7958-7962.

(20) Nishioka, Y.; Yamaguchi, T.; Kawano, M.; Fujita, M. *J. Am. Chem. Soc.* **2008**, *130*, 8160-8161.

(21) Fiedler, D.; Bergman, R. G.; Raymond, K. N. *Angew. Chem., Int. Ed.* **2004**, *116*, 6916-6919.

(22) Brown, C. J.; Bergman, R. G.; Raymond, K. N. *J. Am. Chem. Soc.* **2009**, *131*, 17530-17531.

Chapter 5. The Synthesis of Terephthalamide-based Diastereo- and Enantiopure Ga$_4$L$_6$ Supramolecular Nanovessels

Portions of this chapter have been previously published in:
Chen Zhao, Qing-Fu Sun, William M. Hart-Cooper, Antonio G. DisPasquale, F. Dean Toste, Robert G. Bergman, Kenneth N. Raymond. "Chiral Amide Directed Assembly of a Diastereo- and Enantiopure Supramolecular Host and its Application to Enantioselective Catalysis of Neutral Substrate," *J. Am. Chem. Soc.* **2013**, *135*, 18802-18805.

5.1. Introduction

Raymond and co-workers have developed tetrahedral supramolecular assembly **1** of $K_{12}Ga_4\mathbf{2}_6$ stoichiometry, where **2** = *N,N*-bis(2,3-dihydroxybenzoyl)-1,5-diaminonaphthalene,[1] as shown in Figure 5.1. Complex **1** is a chiral species because the three catecholates coordinated to a given gallium atom can form either a right (Δ)- or a left (Λ)-handed helicity at each of the metal centers. Enforced by mechanical coupling and chirality transfer of the four vertices,[2] complex **1** is formed as a racemic mixture of two homochiral enantiomeric forms, namely ΛΛΛΛ-**1** and ΔΔΔΔ-**1**. Resolution of the racemate was realized using (-)-N'-methylnicotinium iodide as a resolving agent, giving access to enantiopure ΛΛΛΛ-(S-nic $\subset$ **1**) and ΔΔΔΔ-(S-nic $\subset$ **1**) stereoisomers.[3] Sequential ion exchange chromatography with large excess amounts of tetramethylammonium and potassium iodides salts then afforded "empty" and enantiopure clusters. However, the low yield and generally wasteful nature of this process coupled with the instability of the isolated "empty" or solvent-filled ΛΛΛΛ-**1** and ΔΔΔΔ-**1** clusters warrant improvements.[3]

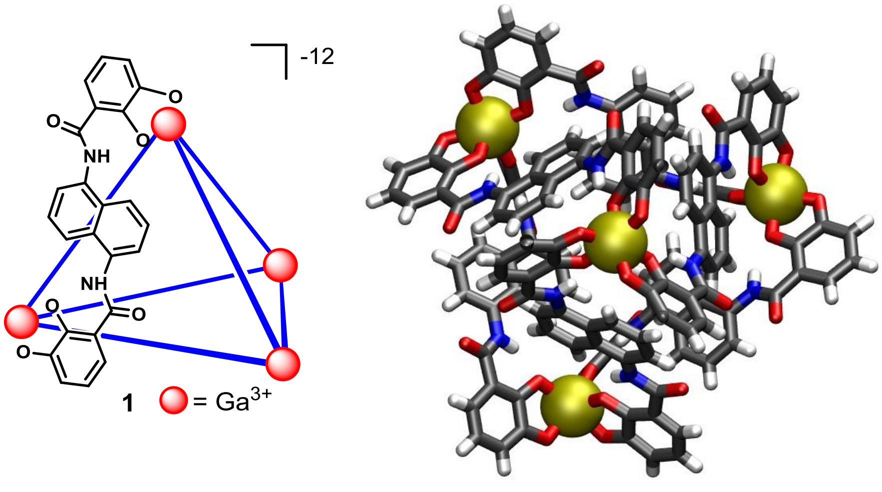

Figure 5.1. Supramolecular Ga$_4$L$_6$ assembly (left) Schematic view of **1** (right) Stick model of **1** (along C$_3$ axis)

In this chapter, we describe the design and synthesis of a new class of Ga$_4$L$_6$ supramolecular nanovessels based on terephthalamide-derived C_2-symmetric catechol ligands with a main focus on the chiral amide directed assembly of a diastereo- and enantiopure cluster. This chiral assembly can be prepared without the need of strong-binding templates or guest molecules, giving rise to "empty" assemblies.

5.2. Results and Discussion

5.2.1. Synthesis and Characterization of Enantiopure Ga_4L_6 Supramolecular Host Complex

Our strategy for achieving an enantiopure supramolecular Ga_4L_6 assembly without resolution involves the addition of an amide-containing chiral directing group at the vertex of ligand **2**, as shown in Scheme 5.1. We envisioned that this chiral source would control the helical configuration of the proximal metal center during cluster formation and direct a highly diastereoselective process in which the desired Ga_4L_6 supramolecular assemblies would be formed in a stereoselective fashion. We also anticipated that this additional amide functional group would stabilize the resulting assembly via hydrogen bonding with the catecholates and could prevent ligand oxidation and decomposition due to its electron withdrawing nature.

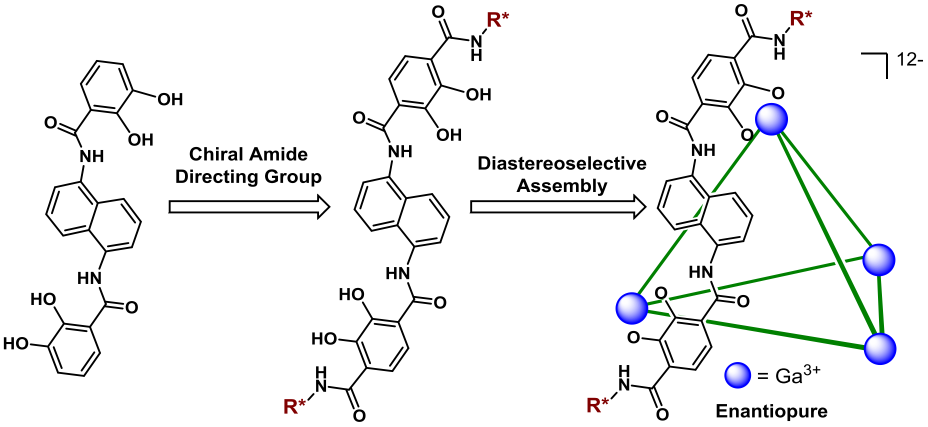

Scheme 5.1. Ligand Design for the Diastereoselective Assembly of an Enatiopure Cluster

We began our studies by synthesizing ligand **(*R*)-5** as shown in Scheme 5.2. The terephthalate sodium salt was converted to the corresponding acyl chloride. This was followed by amide bond formation with commercially available chiral amine (*R*)-(-)-3,3-dimethyl-2-butylamine and subsequent saponification with KOH in methanol to afford the desired intermediate **(*R*)-3**. Next, reaction between **(*R*)-3** and 1.2 equivalents of HATU, (O-(7-azabenzotriazol-1-yl)-*N,N,N',N'*-tetramethyluronium hexafluorophosphate), in THF for 1h at room temperature followed by addition of 1,5-diaminonapthalene gave the desired methyl-protected chiral ligand **(*R*)-4**. Methyl group deprotection of **(*R*)-4** was achieved by treatment with BBr_3 and hydrolysis of the resulting borate to produce the desired terephthalamide-based chiral ligand (*R*)-5 in 52% yield over 5 steps. The corresponding enantiomer **(*S*)-5** was also synthesized according to the procedures shown in Scheme 5.2 by using (*S*)-(-)-3,3-dimethyl-2-butylamine instead.

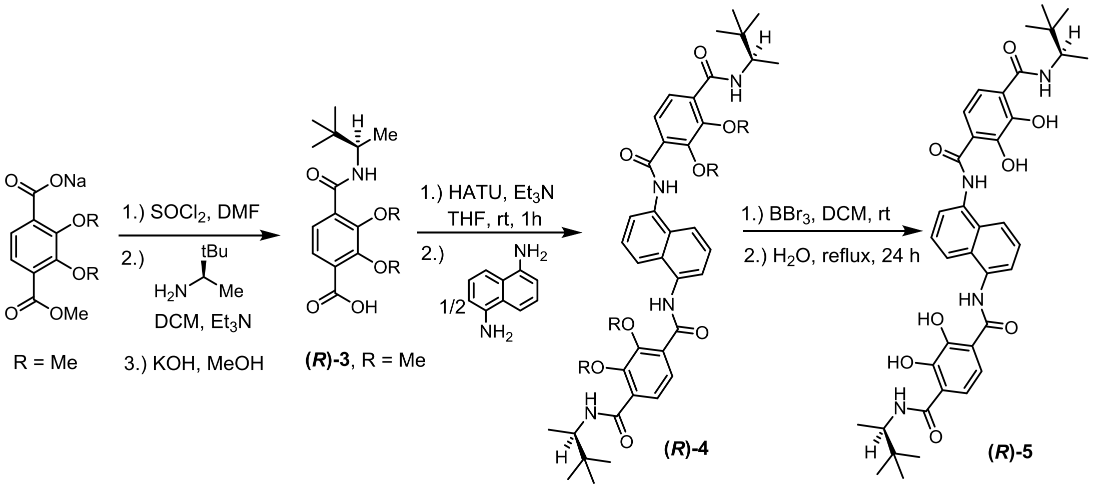
ONa
OR
OR
OMe
R = Me
1.) SOCl2, DMF
2.) tBu H2N Me
DCM, Et3N
3.) KOH, MeOH
H
Me
NH
OR
OR
OH
(R)-3, R = Me
1.) HATU, Et3N
THF, rt, 1h
2.) NH2 1/2 NH2
H
N
H
OR
OR
NH
HN
RO
RO
O
(R)-4
1.) BBr3, DCM, rt
2.) H2O, reflux, 24 h
OH
OH
HO
HO
(R)-5

Scheme 5.2. Synthesis of Ligand (***R***)-**5**

We next investigated whether ligand (***R***)-**5** was viable for the synthesis of the desired tetrahedral supramolecular assembly. The initial reaction between 4 equivalents of $Ga(acac)_3$, 6 equivalents of ligand (***R***)-**5**, and 12 equivalents of KOH in methanol at room temperature, without the use of any cationic species as a template, gave a mixture of products as analyzed by ^{1}H NMR spectroscopy (See Experimental Section). However when the reaction was repeated at 50°C for 1 h, highly symmetric complex **6**, as suggested by the simplicity of its ^{1}H NMR spectrum (Figure 5.1), was isolated as a yellow solid. When 5 equivalents of PEt_4I was added to a D_2O solution of **6**, encapsulation of PEt_4^+ was observed as indicated by the proton resonances at $\delta = -1.45$ and -1.78 ppm (Figure 5.3). This observation can also be taken as an indication of the successful formation of the desired tetrahedral assembly **6**-$K_{12}Ga_4$(***R***)-**5**$_6$. Further analysis of **6** by ESI mass spectrometry confirmed its stoichiometry as $K_{12}Ga_4$(***R***)-**5**$_6$. More importantly, **6**-$K_{12}Ga_4$(***R***)-**5**$_6$ was synthesized without the use of any cationic species as a template, and was found to be bench-top stable, whereas complex **1** was sensitive to oxidation. Complex **6**-$K_{12}Ga_4$(***S***)-**5**$_6$, the enantiomer of **6**-$K_{12}Ga_4$(***R***)-**5**$_6$, was also synthesized by using ligand (***S***)-5, $Ga(acac)_3$ and KOH following a procedure directly analogous to that outlined in Scheme 5.3.

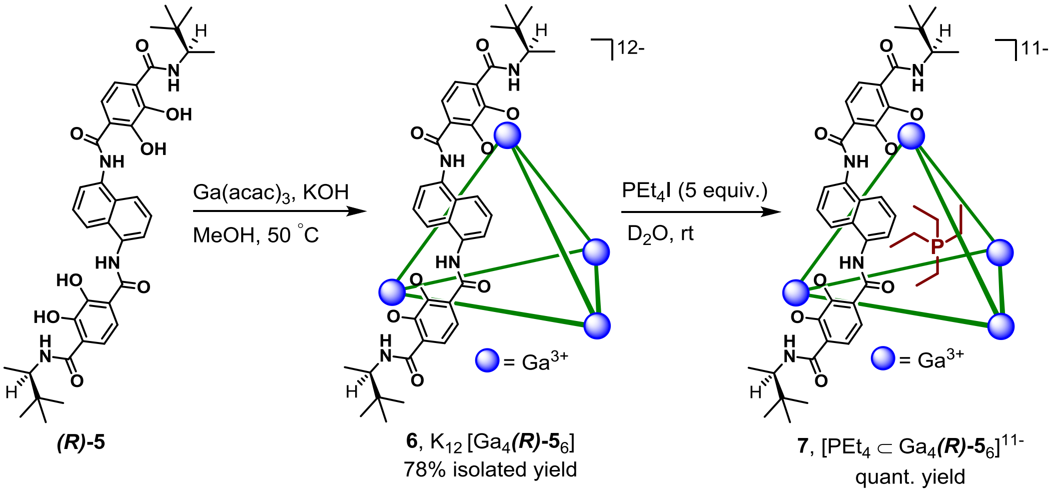
H
N
H
OH
OH
NH
HN
HO
HO
(R)-5
Ga(acac)3, KOH
MeOH, 50 °C
12-
= Ga3+
6, K12 [Ga4(R)-56]
78% isolated yield
PEt4I (5 equiv.)
D2O, rt
11-
P
= Ga3+
7, [PEt4 ⊂ Ga4(R)-56]11-
quant. yield

Scheme 5.3. Synthesis of Supramolecular Assembly **6** and its Encapsulation of PEt_4 Cation

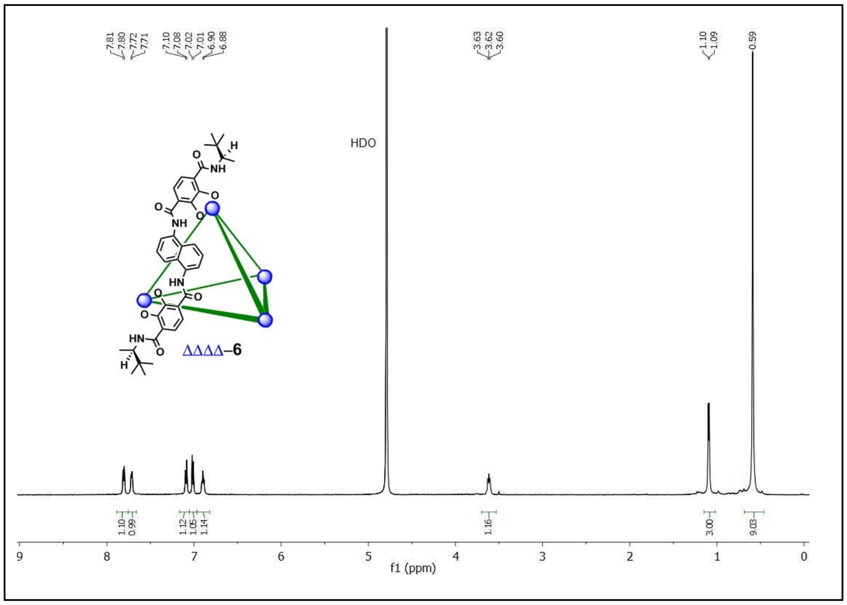

Figure 5.2. ^{1}H NMR Spectra of **6**-$K_{12}Ga_4$(***R***)-**5**$_6$

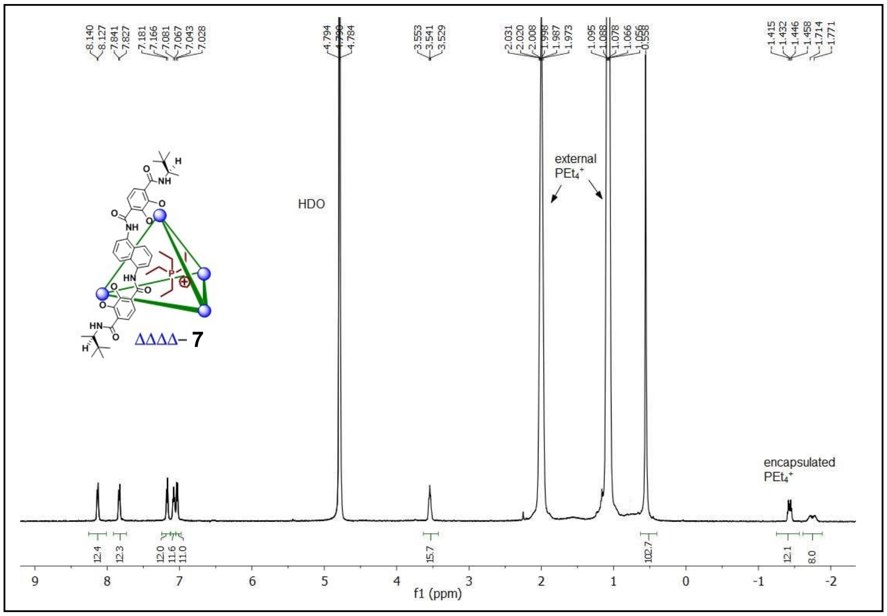

Figure 5.3. ^{1}H NMR Spectra of **7**

It was reported previously that the UV π–π^* transitions of the catechol moiety of assembly **1** produced a strong and distinct exciton couplet.[4] This property allowed for the determination of absolute configuration of the resolved enantioenriched parent assembly **1** by circular dichroism (CD) spectroscopy.[3] The UV-Vis absorption spectrum of complex **6** shows two absorption peaks at 275 and 348 nm respectively (Figure 5.4). When assemblies **6-**$K_{12}Ga_4$**(*R*)-5**$_6$ and **6-**$K_{12}Ga_4$(***S***)**-5**$_6$ were examined by CD spectroscopy, the spectra of the two enantiomers proved to be perfect mirror images of each other and contain a shape and sign of the Cotton effect at the Ga-to-catecholates charge transfer transition similar to those of ΔΔΔΔ-**1** and ΛΛΛΛ-**1** (Figure 5.4). We infer by comparison and assign complex **6-**$K_{12}Ga_4$**(*R*)-5**$_6$ as the

ΔΔΔΔ stereoisomer and **6-**K$_{12}$Ga$_4$**(S)-5**$_6$ as the ΛΛΛΛ stereoisomer.

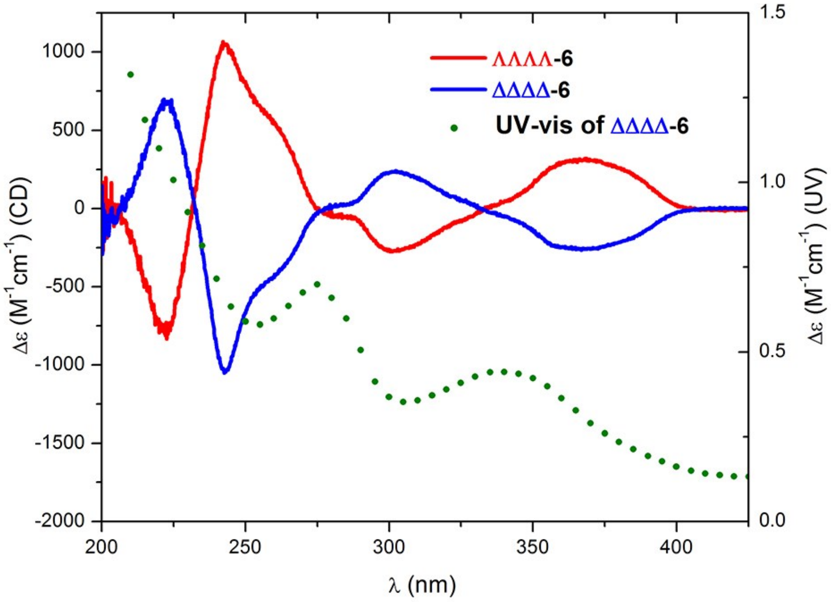

Figure 5.4. CD and UV-Vis Absorption Spectra of **ΔΔΔΔ-6** and **ΛΛΛΛ-6**

The CD spectra of the enantiomeric pair of ΔΔΔΔ-[$\mathrm{NEt_4} \subset$ **6**] and ΛΛΛΛ-[$\mathrm{NEt_4} \subset$ **6**], and the diastereomeric pair of ΔΔΔΔ-[S-nic $\subset$ **6]** and ΛΛΛΛ-[S-nic $\subset$ **6**] (Figure 5.5) show similar shape and sign of the Cotton effect as compared to that of the "empty" ΔΔΔΔ-**6** and ΛΛΛΛ-**6**. Such observations confirm that the origin of the CD signals comes from the catecholate-gallium interactions rather than from the ligand or the encapsulated guest molecules, and are consistent with data obtained from the previous system.[3]

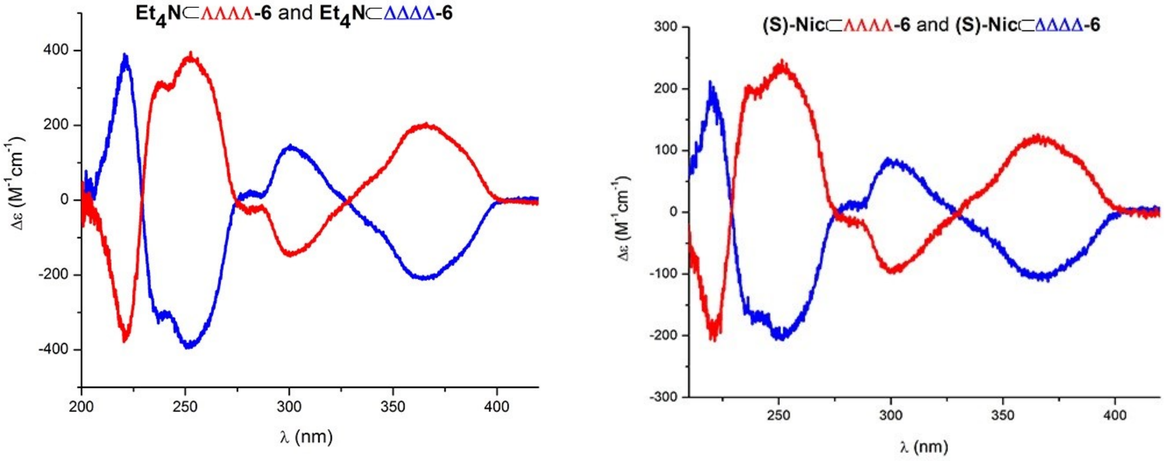
Et$_4$N⊂ΛΛΛΛ-6 and Et$_4$N⊂ΔΔΔΔ-6

(S)-Nic⊂ΛΛΛΛ-6 and (S)-Nic⊂ΔΔΔΔ-6

Figure 5.5. CD Absorption Spectra of ΔΔΔΔ-[$\mathrm{NEt_4} \subset$ **6**] and ΛΛΛΛ-[$\mathrm{NEt_4} \subset$ **6**] (left) and ΔΔΔΔ-[*S*-nic $\subset$ **6**] and ΛΛΛΛ-[*S*-nic $\subset$ **6**]

The absolute stereochemical assignment of ΔΔΔΔ-**6** was further supported by X-ray crystallographic analysis. Single crystals were obtained by slow diffusion of THF vapor into a water solution of ΔΔΔΔ-**6**. The complex crystallized in the chiral space group R3 with three molecules of the enantiopure complex in the unit cell, each with crystallographic 3-fold symmetry. As shown in Figure xx, all four gallium centers adopted the Δ configurations, with an average Ga–Ga distance of 12.6 Å, similar to that found in the resolved parent assembly **1**. The chiral directing groups bury the metal vertices of the cage with additional intramolecular hydrogen bonds between the amide proton and catecholate oxygen, which could be responsible for the observed stability of this new cluster. By crystal packing, each cage is part of a larger network of 12 neighboring cages, forming a 3-dimensional molecular organic framework. A large solvent accessible void of 24558.8 Å^3 was also calculated for the unit cell (65% of total unit cell volume), as a result of the large channels found along both the a and b axes of the crystal.

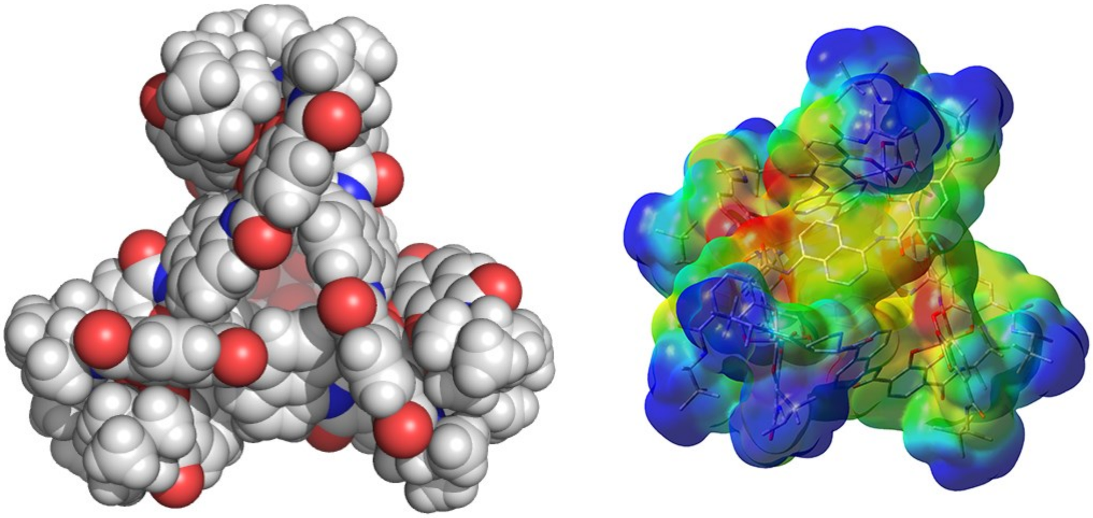

Figure 5.6. X-Ray Structure of ΔΔΔΔ-**6**

As a further probe of the stereochemistry of ΔΔΔΔ-**6** and ΛΛΛΛ-**6**, we investigated their host-guest chemistries individually with both enantiomers of ammonium salt **8**. As illustrated in Figure 5.7, complex **9**, or ΔΔΔΔ-[**(*S*)-8** $\subset$ **6**], should have different and distinguishable properties from complex **10**, ΔΔΔΔ-[(***R***)-**8** $\subset$ **6**], due to their diastereomeric relationship. ^{1}H NMR spectroscopy (Figure. 3) reveals that the two complexes are indeed different, most notably in the encapsulation region of the spectra. On the other hand, complex **11**, ΛΛΛΛ-[**(*R*)-8** $\subset$ **6**], and complex **9** are enantiomers, and exhibit exactly the same spectroscopic behaviors when analyzed by ^{1}H NMR; the same result was also observed for complexes **10** and **12**. This evidence, combined with results from X-ray crystallography and CD spectroscopy, demonstrate that complex **6** is both diastereo- and enantiopure. The chiral group of ligand **5** exhibits control during cluster formation to give the desired Ga_4**5**$_6$ cluster as a single diastereomer.

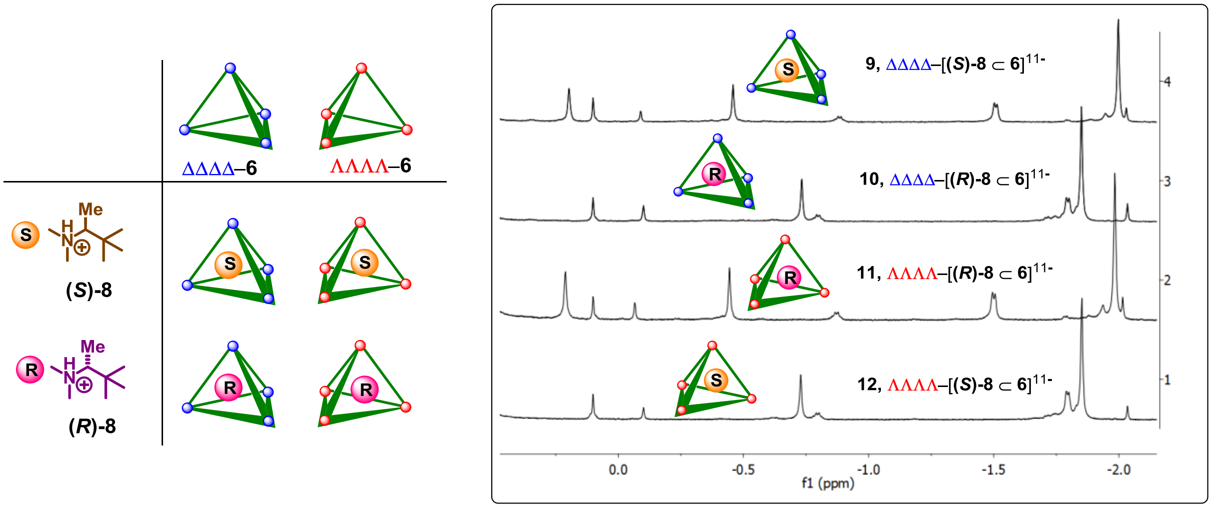

Figure 5.7. ^{1}H NMR spectra (encapsulation region) of complexes from host-guest chemistry of **ΔΔΔΔ-6** and **ΛΛΛΛ-6** individually with chiral ammonium salts **(*S*)-8** and **(*R*)-8**

5.2.2. Synthesis and Characterization of Racemic and Terephthalamide-based Ga$_4$L$_6$ Clusters

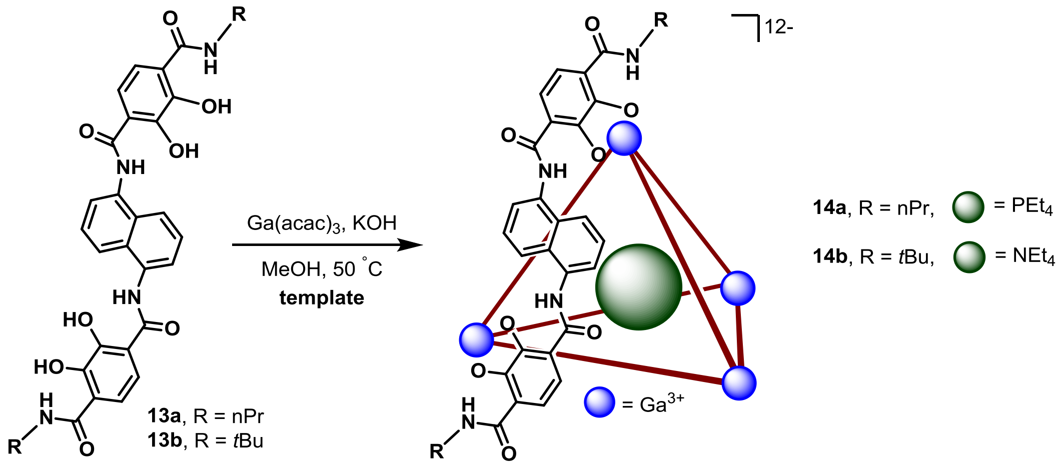

Scheme 5.4. Synthesis of chiral and racemic terephthalamide-based Ga$_4$L$_6$ clusters

By applying synthetic routes similar to that outlined in Scheme 5.2, we also synthesized terephthalamide-based ligands containing simple and achiral amide functional groups analogous to ligand (***R***)-**5**. In the presence of a strong binding guest, such as PEt$_4$I or NEt$_4$Cl, ligands **13a-b** both led to the formation of the desired Ga$_4$L$_6$ supramolecular complexes **14a-b** respectively. In the absence of templates, ligand **13b** reacted with Ga(acac)$_3$ with base to give the corresponding "empty" cluster **14b** after reaction at 50 °C for 5 days, and the isolated complex readily encapsulates PEt$_4$ cation in solution (Figure 5.10). However, attempts to synthesize hosts **14a** without templates have not led to clean formation of the desired host complexes, even on prolonged heating. Further efforts could be made aimed at accessing "empty" terephthalamide-based Ga$_4$L$_6$ supramolecular host complexes with ligands **13a** and its related analogues.

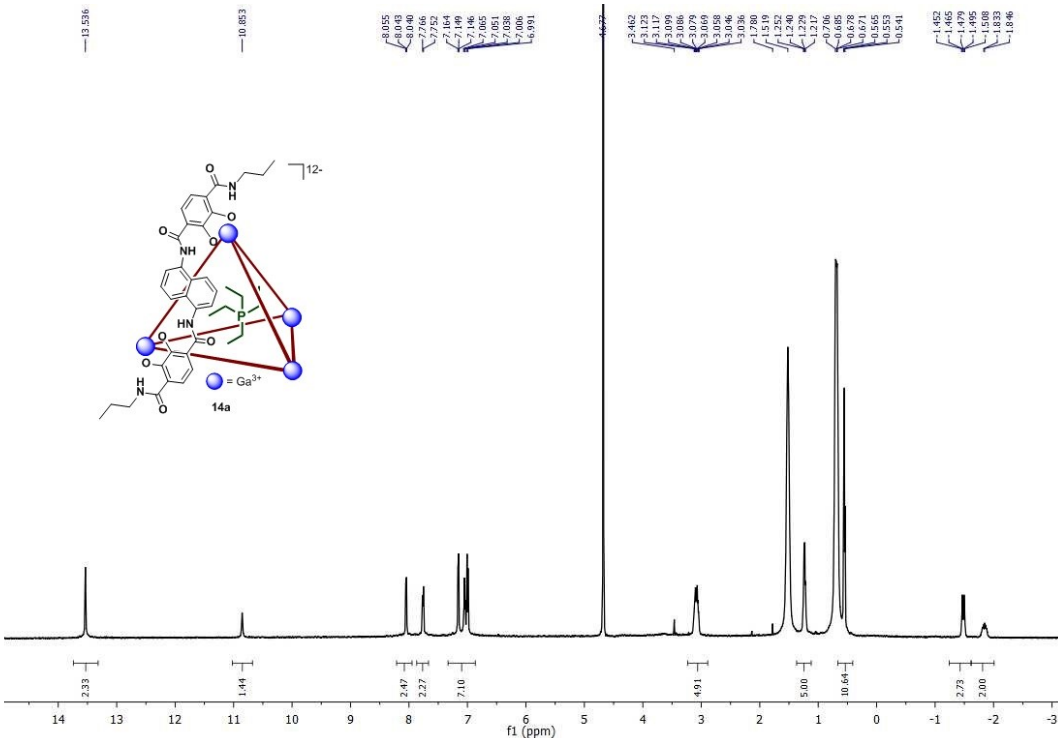

Figure 5.8 ^{1}H NMR Spectrum of **14b**

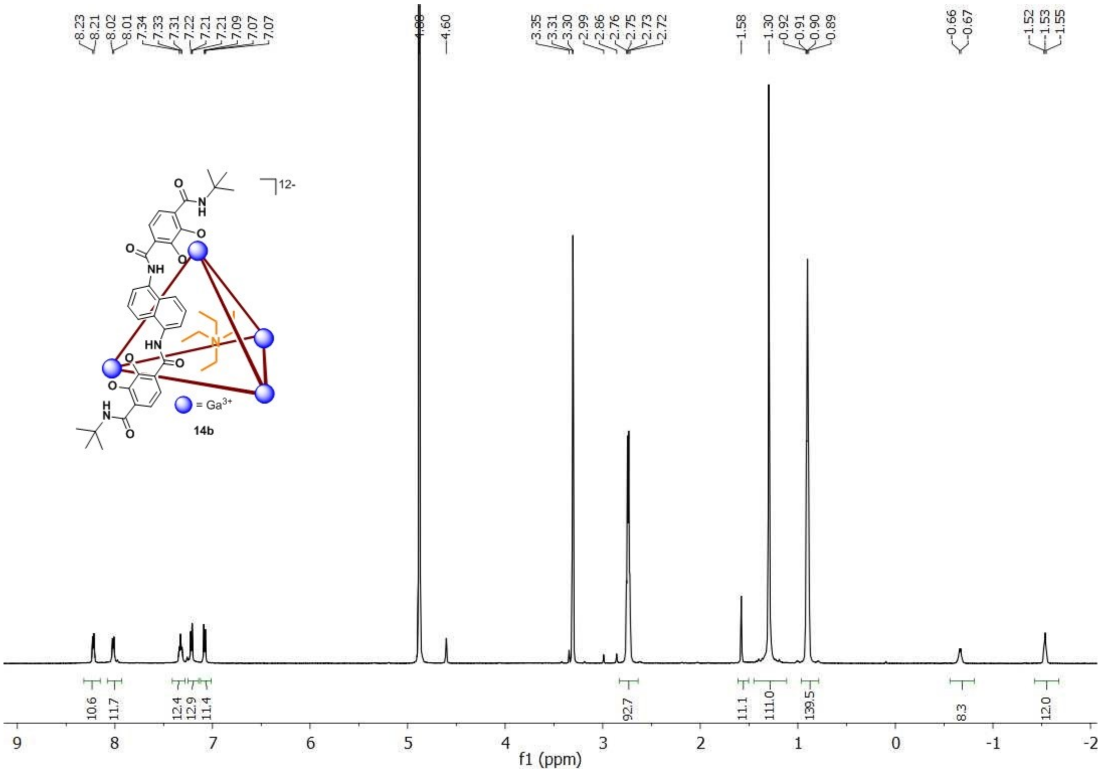

Figure 5.9. ^{1}H NMR Spectrum of **14b**

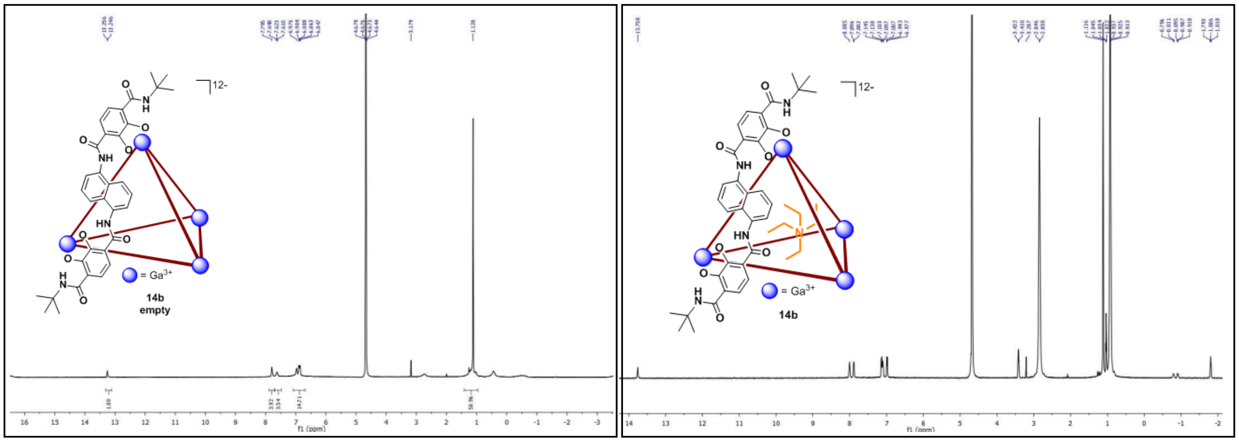

Figure 5.10. ^{1}H NMR spectra of "empty" **14b** and its encapsulation of NEt_4 cation

5.3. Conclusion

Described in this chapter, a new class of Ga_4L_6 supramolecular host complexes based on terephthalamide-derived catecholate ligands have been synthesized and fully characterized. With chiral amide functional groups, the corresponding ligand directs cluster formation to afford highly diastereo- and enantiomerically pure complexes. The self-assembled chiral host complex can be synthesized without the use of any template to give "empty" or solvent-filled clusters, which allows encapsulation of neutral molecules inside a chiral pocket. Compared to the parent assembly **1**, complexes ΔΔΔΔ-**6** and ΛΛΛΛ-**6** proved to be more stable to air oxidation in both the solid and solution states. Chiral but racemic terephthalamide-based host complexes **14a-b** have also been synthesized with achiral ligands in the presence of achiral templates.

5.4. Experimental

5.4.1. General Methods. Unless otherwise noted, all reagents were obtained commercially and used without further purification. All air- and moisture-sensitive compounds were manipulated using standard Schlenk techniques. Reactions were carried out under a nitrogen atmosphere in glassware that was either oven-dried at 150 °C overnight or flame-dried under nitrogen immediately prior to use. Diethyl ether, tetrahydrofuran and methylene chloride were dried and purified by passage through a column of activated alumina (type A2, 12 x 32, UOP LLC) under a stream of dry nitrogen. Unless otherwise specified, all other reagents were purchased from Acros, Aldrich or Fisher and were used without further purification.

Reaction solutions were magnetically stirred with the exception of those reactions performed in NMR tubes. The majority of experiments were monitored by thin layer chromatography using 0.25 mm pre-coated silica gel plates from Silicycle (TLGR10011B-323) containing a fluorescent indicator for visualization by UV light. Various stains were used to visualize reaction products, including *p*-anisaldehyde, $KMnO_4$ and phosphomolybdic acid in ethanol. Flash chromatography was performed using MP Biomedicals SiliTech 32-63D.

All NMR spectra were obtained at ambient temperature using Bruker AVB-400, DRX-500, AV-500 and AV-600 spectrometers. ^1H NMR chemical shifts are reported relative to residual solvent peaks (7.26 ppm for $CDCl_3$, 5.30 ppm for CD_2Cl_2, 3.31 ppm for CD_3OD, 4.80 for D_2O, 2.50 for DMSO-d_6). ^{13}C NMR chemical shifts were also reported with reference to residual solvent peaks (77.23 ppm for $CDCl_3$, 53.84 for CD_2Cl_2, 49.00 for CD_3OD, 39.52 for DMSO-d_6) Multiplicities of ^1H NMR resonances are reported as s = singlet, d = doublet, t = triplet, m = multiplet and br = broad). X-ray crystallographic data was collected on MicroSTAR-H APEX II Cu-Ka Rotating Anode X-ray Diffractometer. Chiral GC analyses were conducted using HP 6850 series GC system fitted with a chiral column, BetaDex 120 Fused Silica Capillary Column (30m x 0.25mm x 0.25um film thickness). UV-Vis absorption spectra were recorded on a Hewlett-Packard 8450A UV/Vis diode array spectrophotometer. Circular dichroism (CD) spectra were measured with a Jasco J-500C spectropolarimeter equipped with an IF-500 II A/D converter. Both low- and high-resolution mass spectral data were obtained from the Micromass/Analytical Facility operated by the College of Chemistry, University of California, Berkeley.

5.4.2. Synthesis of chiral ligand (*R*)-5

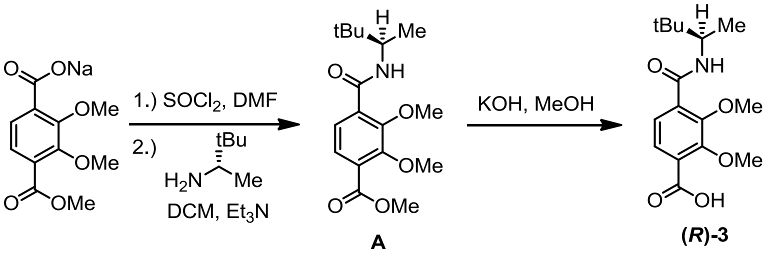

The known sodium-terephthalate salt[5] (1.00 g, 4.16 mmol, 1 equiv.) was dissolved in thionyl chloride (10 mL), followed by the addition of 2 drops of DMF at room temperature. The reaction mixture was then heated at 50 °C for 1 hour. The excess $SOCl_2$ was removed *in vacuo* and the resulting residue was then dissolved in DCM and filtered to remove any salts. The solvent was then removed again *in vacuo* and the resulting residue was used without any purification. The acid chloride was dissolved in DCM (15 mL) and treated with *(R)*-3,3-

dimethyl-2-butylamine (504 mg, 5.0 mmol, 1.2 equiv.) and Et_3N (0.40 mL) at 0 °C. The resulting solution was allowed to warm to rt and monitored by TLC analysis (solvent 30% EtOAc in hexanes). After 4 h, acid chloride appeared to be consumed, and the reaction was quenched by addition of water (10 mL) and DCM (20 mL). The organic layer was then washed with 1 N HCl (aq) (2 x 20 mL), followed by 1 N NaOH (aq) (2 x 20 mL), brine (20 mL), and dried with $MgSO_4$, filtered, and concentrated to yield the chiral ester **A** as a yellow oil (1.17 g, 3.62 mmol) in 87% yield. ^{1}H NMR (600MHz, $CDCl_3$): δ (ppm) 7.90 (d, 1H, *J* = 9.6 Hz), 7.87 (d, 1H, *J* = 7.8 Hz), 7.55 (d, 1H, *J* = 7.8 Hz), 4.06 (dq, 1H, *J* = 5.4, 6.8 Hz), 3.95 (s, 3H), 3.91 (s, 3H), 3.90 (s, 3H), 1.15 (d, 3H, *J* = 6.8 Hz), 0.96 (s, 9H). ^{13}C NMR (150MHz, $CDCl_3$): δ (ppm) 165.6, 163.2, 153.2, 152.1, 130.6, 128.6, 126.0, 125.8, 61.8, 61.6, 53.2, 52.4, 34.2, 26.3, 16.0. IR [neat, ν_{max} (cm^{-1})]: 1731, 1650, 1525, 1454, 1400, 1280, 1237, 1040, 1013, 817, 756 cm^{-1}. HRMS (*m/z*): calculated for $[C_{17}H_{26}NO_5]^+$, 324.1805; observed, 324.1807.

The ester **A** (586 mg, 1.81 mmol) was dissolved in MeOH (4.0 mL) and then treated with 4 M KOH (aq) (4 mL) dropwise. The resulting yellow biphasic solution was stirred vigorously at rt. After 1 h, 6 M HCl (aq) (3 mL) was added dropwise to form a white precipitate. To the resulting heterogenous solution was added DCM (20 mL). The mixture was extracted with CH_2Cl_2 (3 x 10 mL). The organic layer was washed with brine, dried (Na_2SO_4), filtered and concentrated to give chiral acid **(*R*)-3** as a white foam in 88% yield (503 mg, 1.62 mmol), and used without further purification. ^{1}H NMR (600 MHz, $CDCl_3$): δ (ppm) 7.98 (d, 1H, *J* = 8.3 Hz,), 7.88 (d, 1H, *J* = 8.4 Hz), 7.81 (d, 1H, *J* = 9.5 Hz), 4.10-4.13 (m, 1H) 4.10 (s, 3H), 4.01 (s, 3H), 1.21 (d, 3H, *J* = 7.2 Hz), 1.01 (s, 9H). ^{13}C NMR (150 MHz, $CDCl_3$): δ (ppm) 165.9, 163.0, 152.8, 151.3, 132.2, 127.4, 126.7, 126.0, 62.3, 61.8, 53.5, 34.2, 26.3, 16.0. IR [neat, ν_{max} (cm^{-1})]: 1714, 1633, 1537, 1455, 1401, 1277, 1238, 1038, 1008, 731 cm^{-1}. HRMS (*m/z*): calculated for $[C_{16}H_{24}NO_5]^+$, 310.1649; observed, 310.1648.

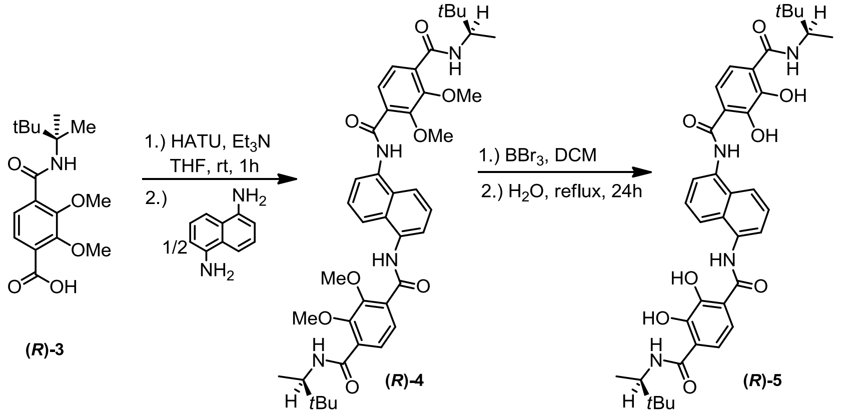

Chiral acid **(*R*)-3** (503 mg, 1.62 mmol, 1 equiv.), Et_3N (163 mg, 1.62 mmol, 2 equiv.) and HATU (1.23 g, 3.24, 2 equiv.) were dissolved/suspended in THF (20 mL) and stirred at room temperature for 1 h. To the heterogenous solution was added a THF solution (5 mL) containing 1,5-diaminonapthalene (128 mg, 0.81 mmol, 0.5 equiv.) and the resulting solution was stirred at room temperature for 14 h. The reaction mixture was then diluted with diethyl ether (20 mL) and extracted with 1 N HCl (15 mL). The organic layer was washed with 1 N NaOH (15 mL), brine (20 mL), dried with $MgSO_4$, filtered and concentrated. The resulting residue was purified by silica chromatography (30-50% EtOAc in hexanes) to give a yellow powder. This solid was then dissolved in minimal amount of DCM (~ 5 mL) and precipitated by slow addition of diethyl ether (100 mL). The fine powder was then collected by filtration and the desired compound **(*R*)-**

4 was isolated in 71% yield (420 mg, 0.57 mmol). ^{1}H NMR (600 MHz, $CDCl_3$): δ (ppm) 10.5 (s, 2H), 8.54 (d, *J* = 7.8 Hz, 2H), 8.13 (d, *J* = 8.4 Hz, 2H), 8.05 (d, *J* = 8.4 Hz, 2H), 7.87 (d, *J* = 8.6 Hz, 2H), 7.81 (d, *J* = 9.6 Hz, 2H), 7.67 (d, *J* = 7.8 Hz, 2H), 4.19 (s, 6H), 4.15 (sept, *J* = 6.5 Hz, 2H), 4.09 (s, 6H), 1.22 (d, *J* = 6.5 Hz, 6H), 1.02 (s, 18H). ^{13}C NMR (125 MHz, $CDCl_3$): δ (ppm) 163.4, 162.6, 151.6, 151.5, 134.0, 131.3, 129.7, 127.3, 127.1, 126.9, 119.6, 116.9, 62.6, 62.2, 53.6, 34.5, 26.6, 16.3. IR [neat, ν_{max} (cm^{-1})]: 1650, 1530, 1455, 1335, 1276, 956, 767 712 cm^{-1}. HRMS (*m/z*): calculated for $[C_{42}H_{53}N_4O_8,]^+$,741.3858; observed,741.3854.

Compound **(*R*)-4** (420 mg, 0.57 mmol, 1 equiv.) was dissolved in DCM (10 mL), followed by addition of BBr_3 (neat, 857 mg, 3.42 mmol, 6 equiv.) and the resulting solution was stirred at rt for 14 h. The solution was then poured into an ice bath and allowed to warm to rt slowly. The resulting slurry was filtered to give a yellow solid, which was then suspended in water (10 mL) and heated at reflux for 24 h. The suspension was cooled to rt and filtered to give a fine yellow powder which was dried under vacuum for 24 h and used without further purification. Ligand **(*R*)-5** (360 mg, 0.52 mmol) was isolated as a fine yellow powder in 92% yield. ^{1}H NMR (600 MHz, DMSO-*d*$_6$): δ (ppm) 12.9 (br s, 2H), 12.1 (br s, 2H), 11.0 (s, 2H), 8.49 (d, *J* = 9.6 Hz, 2H), 7.98-7.94 (m, 4H), 7.66-7.63 (m, 6H), 4.06 (sept, *J* = 7.8 Hz, 2H), 1.51 (d, *J* = 7.8 Hz, 6H), 0.94 (s, 18H). ^{13}C NMR (125 MHz, DMSO-*d*$_6$): δ (ppm) 168.2, 167.3, 150.2, 148.9, 133.8, 129.3, 126.6, 123.2, 120.9, 119.7, 118.6, 117.6, 52.9, 35.1, 26.8, 15.8. IR [neat, ν_{max} (cm^{-1})]: 1636, 1548, 1276, 1223, 1159, 1130, 945, 779, 703 cm^{-1}. HRMS (*m/z*): calculated for $[C_{38}H_{43}N_4O_8]^-$, 683.3086; observed, 683.3110.

5.4.3. Synthesis of Complex 6

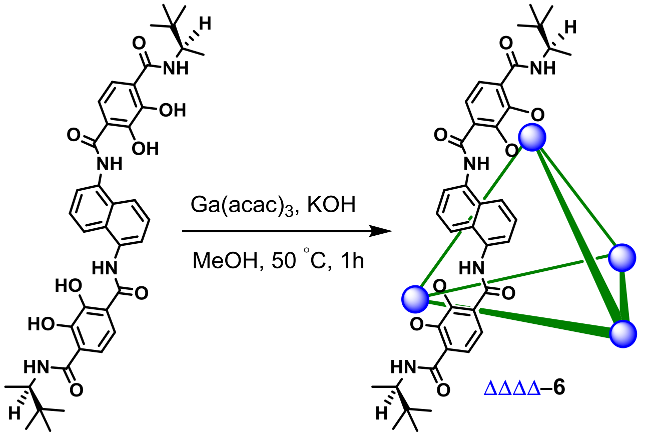

Ligand **(*R*)-5** (102 mg, 0.15 mmol, 6 equiv.) and Ga(acac)$_3$ (36.7 mg, 0.10 mmol, 4 equiv.) were dissolved/suspended in degassed methanol (8 mL) and the resulting mixture was heated to 50 °C. After 15 minutes, KOH (17.2 mg, 0.30 mmol, 12 equiv.) as a solution in methanol (1 mL) was added slowly to the hetereogeneous reaction. Upon complete addition of KOH, the yellow reaction mixture became a homogeneous solution. After 1 h, the reaction mixture was cooled to room temperature and concentrated to about 1 mL of solution. To this solution, diethyl ether (~30 mL) was added dropwise and the desired product precipitated . The yellow solid was then collected by filtration and washed with diethyl ether (20 mL) to give the desired supramolecular complex **6** (94.1 mg, 0.02 mmol) in 78% yield. ^{1}H NMR (500 MHz, D$_2$O): δ (ppm) 7.80 (d, *J* = 8.4 Hz, 12H), 7.71 (d, *J* = 7.8 Hz, 12H), 7.01 (d, *J* = 9.0 Hz, 12H), 7.01 (d, *J* = 9.0 Hz, 12H), 6.88 (t, *J* = 7.8 Hz, 12H), 3.62 (sept, *J* = 7.2 Hz, 12H), 1.09 (d, *J* = 7.2 Hz, 36H), 0.59 (s, 108H). ESI-MS (anion detection, CH$_3$OH): m/z: 1169.96 [Ga$_4$**(*R*)-5**$_6$ + 8K$^+$]$^{4-}$, 927.19 [Ga$_4$**(*R*)-5**$_6$ + 7K$^+$]$^{5-}$, 911.57 [Ga$_4$**(*R*)-5**$_6$ + 5K$^+$ + 2H$^+$]$^{5-}$, 903.57 [Ga$_4$**(*R*)-5**$_6$ + 4K$^+$ + 3H$^+$]$^{5-}$, 895.99 [Ga$_4$**(*R*)-5**$_6$ + 3K$^+$ + 4H$^+$]$^{5-}$, 766.14 [Ga$_4$**(*R*)-5**$_6$ + 6K$^+$ + 1H$^+$]$^{6-}$, 740.16 [Ga$_4$**(*R*)-5**$_6$ + 2K$^+$ + 4H$^+$]$^{6-}$.

5.4.4. Mass Spectrum of ΔΔΔΔ-6

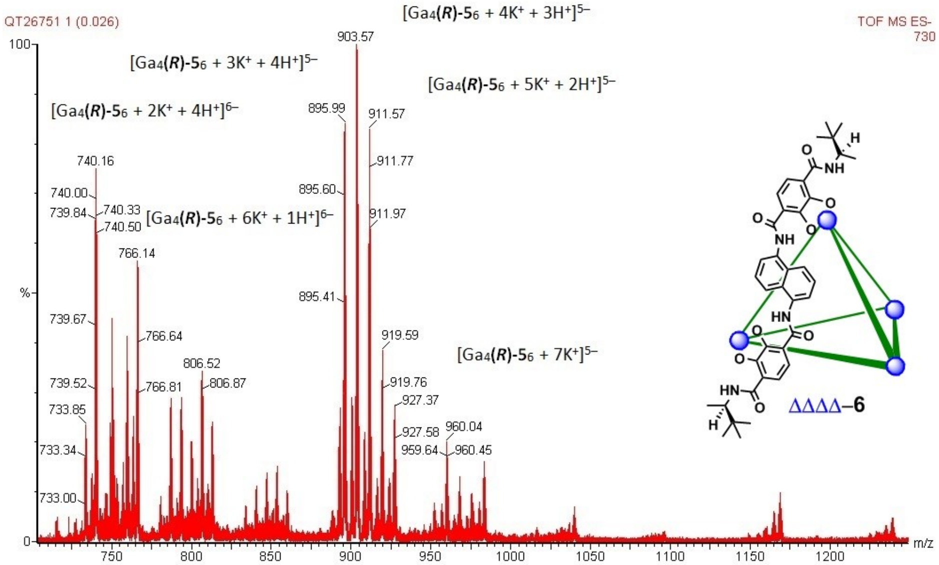

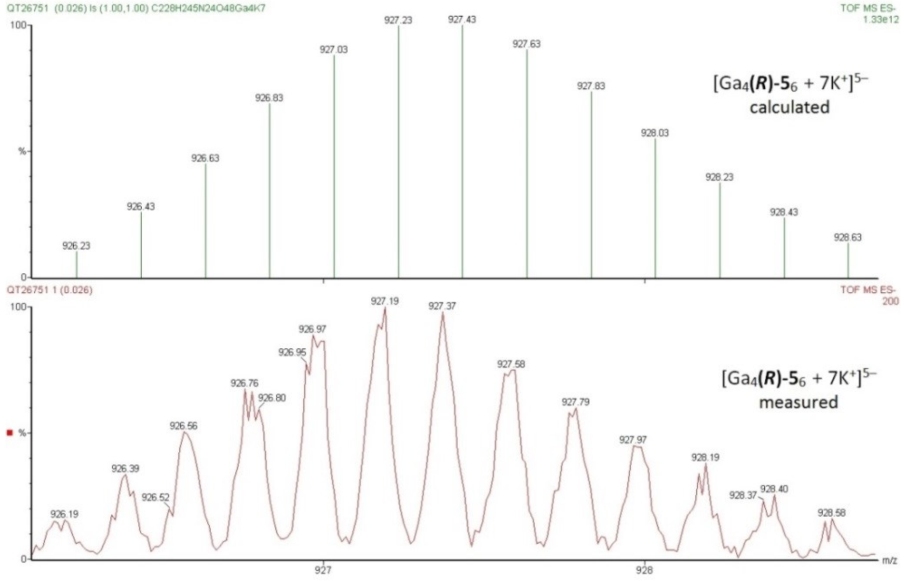

5.4.5. Encapsulation of PEt_4^+ by Assembly 6 to give 7

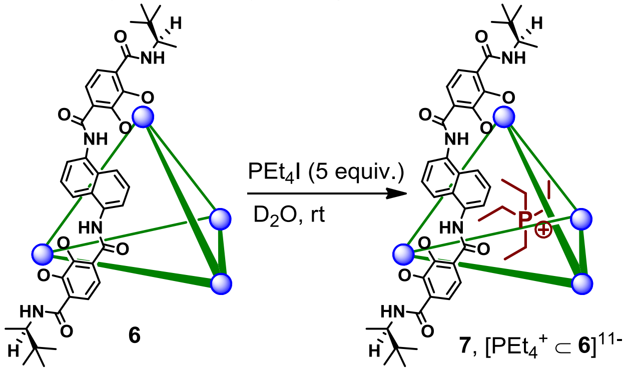
PEt4I (5 equiv.)
D2O, rt
O
NH
H
HN
P
⊕

6

7, $[PEt_4^+ \subset \mathbf{6}]^{11-}$

To a D_2O solution (0.5 mL) containing complex **6** (9.64 mg, 0.002 mmol, 1 equiv.) was added PEt_4I (3.0 mg, 0.01 mmol, 5 equiv.) and the resulting solution was analyzed by ^1H NMR spectroscopy. ^1H NMR (500 MHz, D_2O): δ (ppm) 8.13 (d, J = 7.8 Hz, 12H), 7.83 (d, J = 8.4 Hz, 12H), 7.17 (d, J = 9.0 Hz, 12H), 7.08 (t, J = 8.4 Hz, 12H), 7.03 (d, J = 9.0 Hz, 12H), 3.54 (sept, J = 7.2 Hz, 12H), 2.30-1.96 (m, external PEt_4^+), 1.11-1.03 (m, external PEt_4^+ and methyl group signals overlap), 0.56 (s, 108H), -1.43 (dt, J = 17.0, 7.6 Hz, 12H), -1.75 (m, 8H).

5.4.6. Synthesis of Chiral Salts (*R*)-8

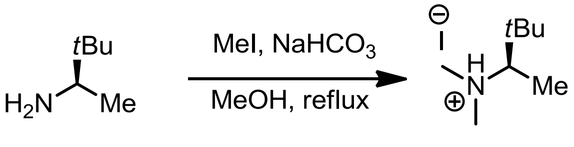

(*R*)-8

(R)-3,3-dimethyl-2-butylamine (101 mg, 1.0 mmol, 1 equiv.), methyl iodide (570 mg, 4.0 mmol, 4 equiv.) and sodium bicarbonate (252 mg, 3.0 mmol, 3 equiv.) were dissolved/suspended in methanol (5 mL). The suspension was then heated at reflux for 14h. The mixture was then cooled to room temperature and filtered to give a white powder, which was then recrystallized from absolute ethanol. The desired ***(R)*-8** was isolated as the iodide salt (236 mg, 0.92 mmol) in 92% yield. ^1H NMR (500 MHz, DMSO-d_6): δ (ppm) 3.23 (q, J = 7.0 Hz, 1H), 2.83 (d, J = 5.0 Hz, 3H), 2.65 (d, J = 5.0 Hz, 3H), 1.12 (d, J = 7.0 Hz, 3H), 0.99 (s, 9H) ^{13}C NMR (125 MHz, DMSO-d_6): δ (ppm) 70.2, 45.5, 38.6, 34.2, 26.3, 7.9. HRMS, ESI positive mode (*m/z*): calculated for $[C_8H_{20}N]^+$, 130.1590; observed, 130.1589.

5.4.7. Host-guest chemistry of ΔΔΔΔ-6 and ΛΛΛΛ-6 individually with chiral salts *(R)*-8 and (*S*)-8

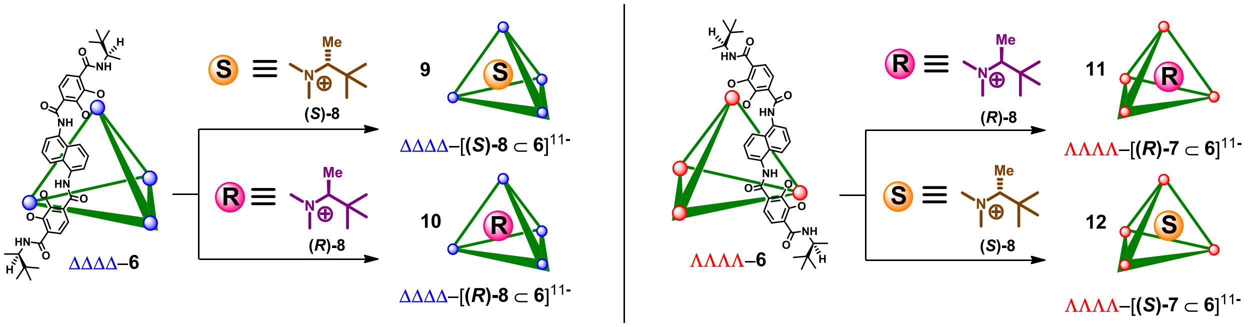

Representative procedure: Complex **ΔΔΔΔ-6** (9.7 mg, 0.002 mmol, 1 equiv.) and salt ***(S)*-8** (2.36 mg, 0.01 mmol, 5 equiv.) were combined and dissolved in 0.5 mL of a solvent mixture of $CD_3OD:D_2O$ (1:1). The solution was then transferred to a NMR tube fitted with a plastic cap and analyzed by ^1H NMR spectroscopy.

5.4.8. Appendix – ^{1}H and ^{13}C NMR Spectra

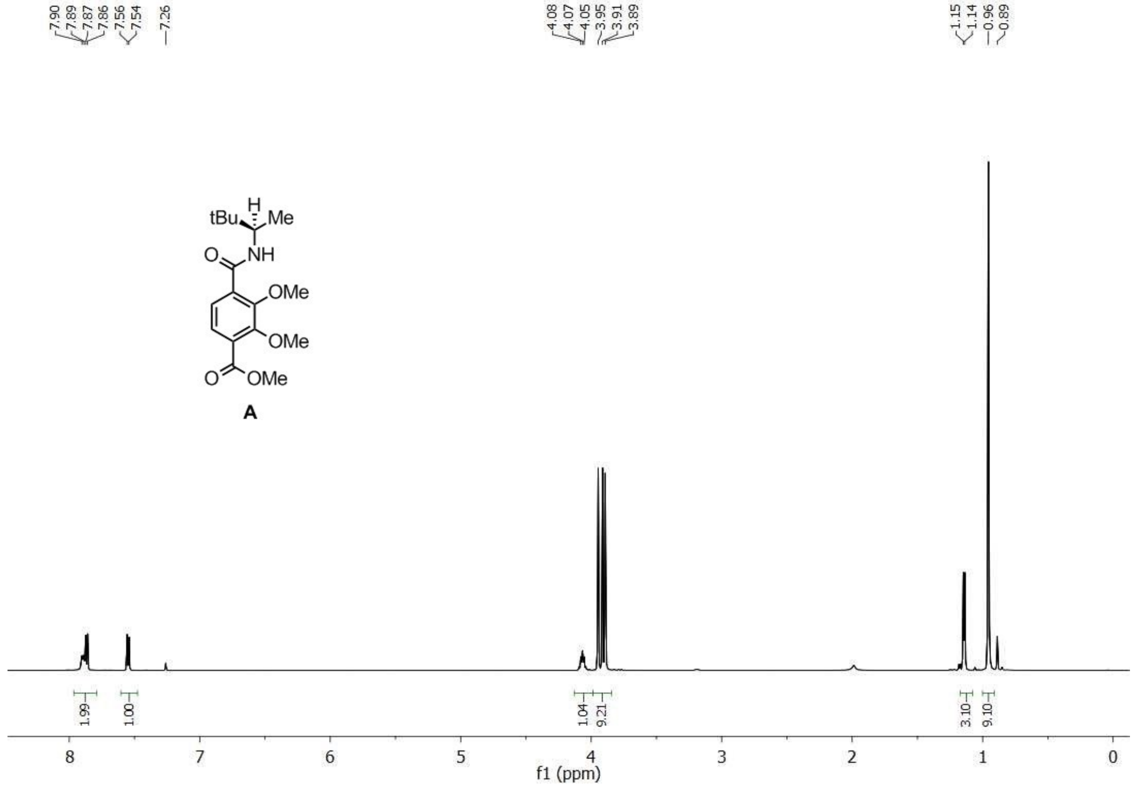

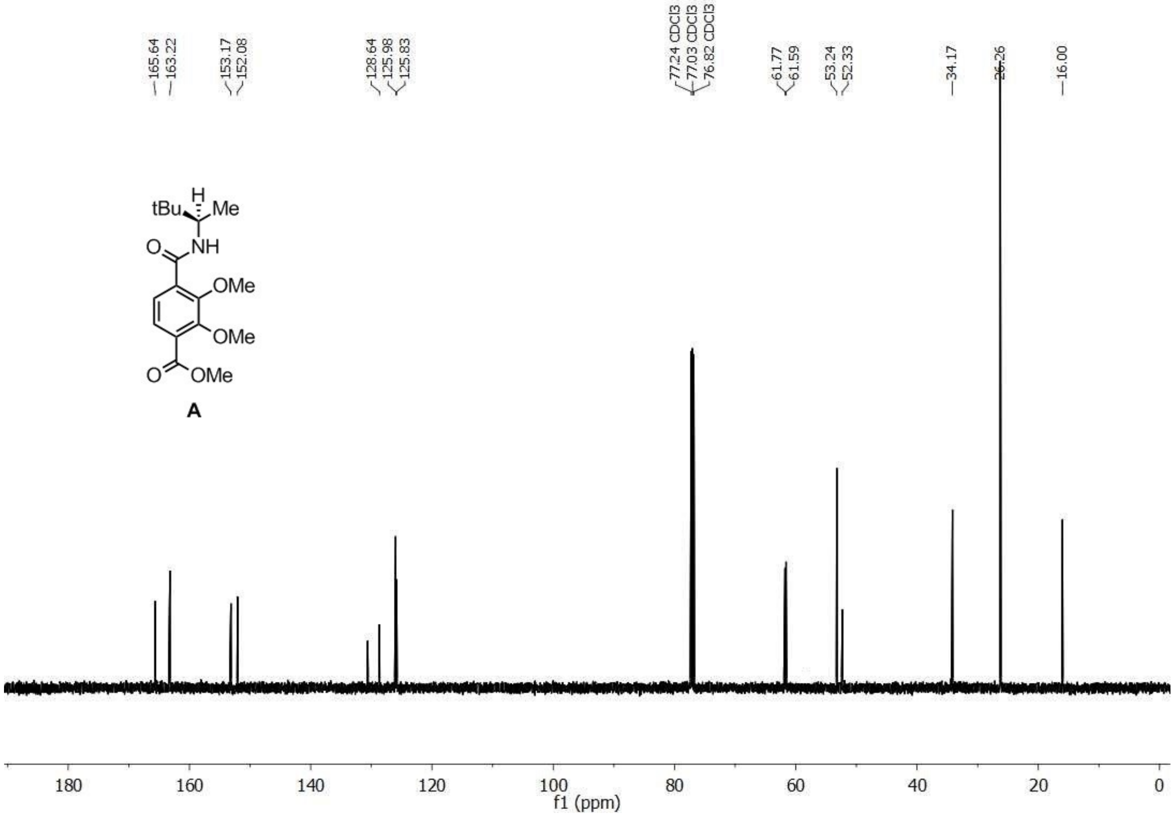

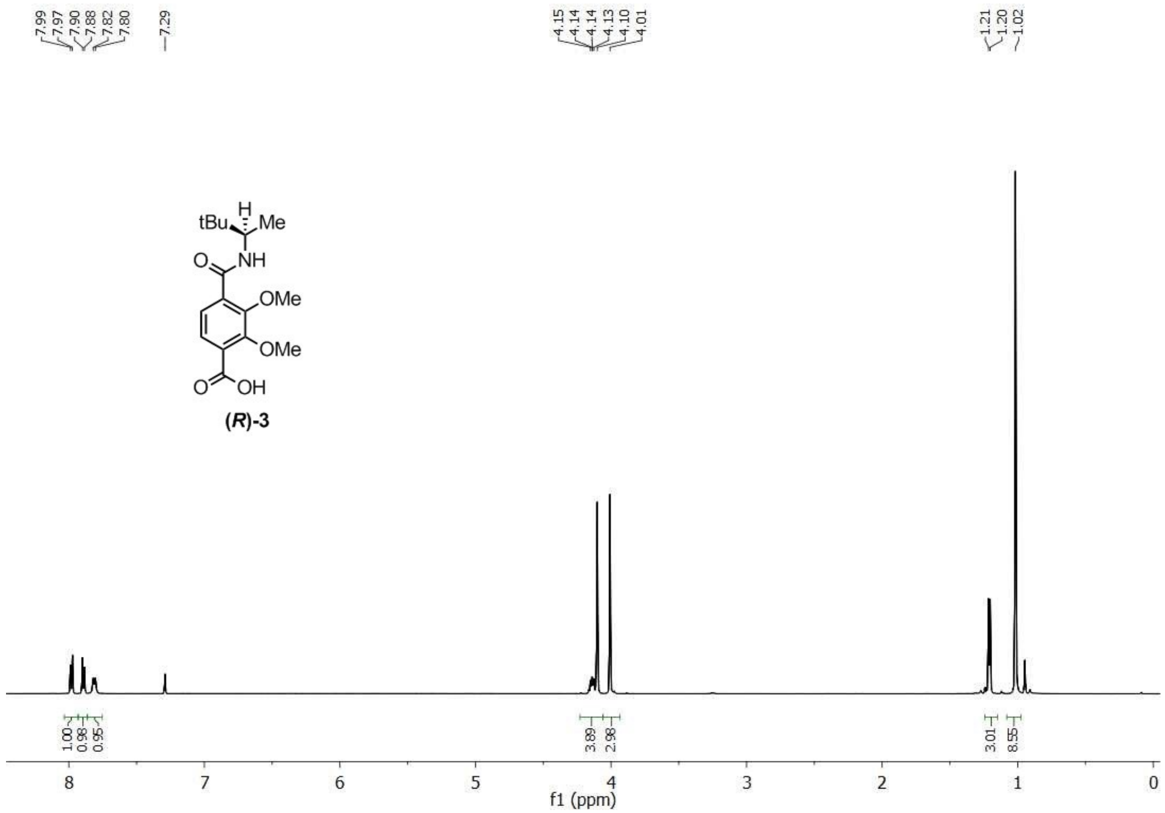
7.99
7.97
7.90
7.88
7.82
7.80
7.29
4.15
4.14
4.14
4.13
4.10
4.01
1.21
1.20
1.02
tBu
H
Me
O
NH
OMe
OMe
O
OH
(R)-3
1.00
0.98
0.95
3.89
2.98
3.01
8.55
8
7
6
5
4
3
2
1
0
f1 (ppm)

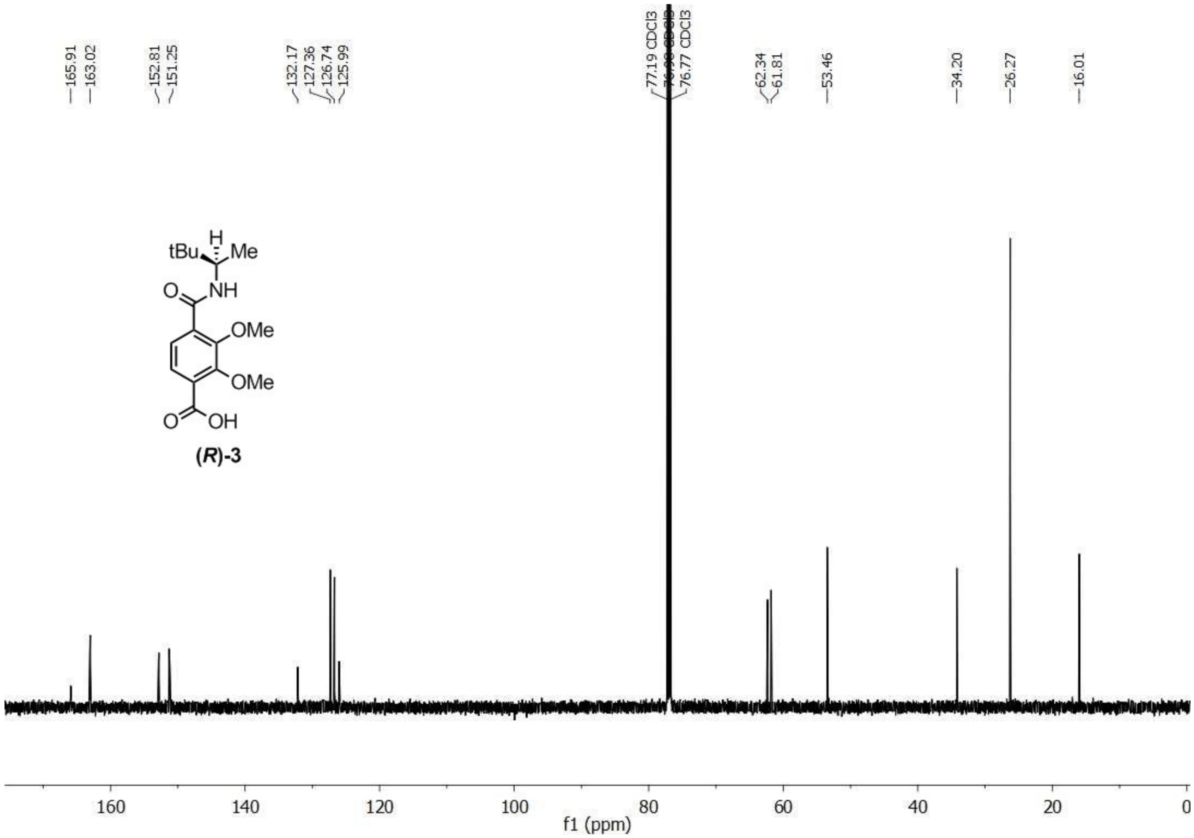
165.91
163.02
152.81
151.25
132.17
127.36
126.74
125.99
77.19 CDCl3
76.98 CDCl3
76.77 CDCl3
62.34
61.81
53.46
34.20
26.27
16.01
tBu
H
Me
O
NH
OMe
OMe
O
OH
(R)-3
160
140
120
100
80
60
40
20
0
f1 (ppm)

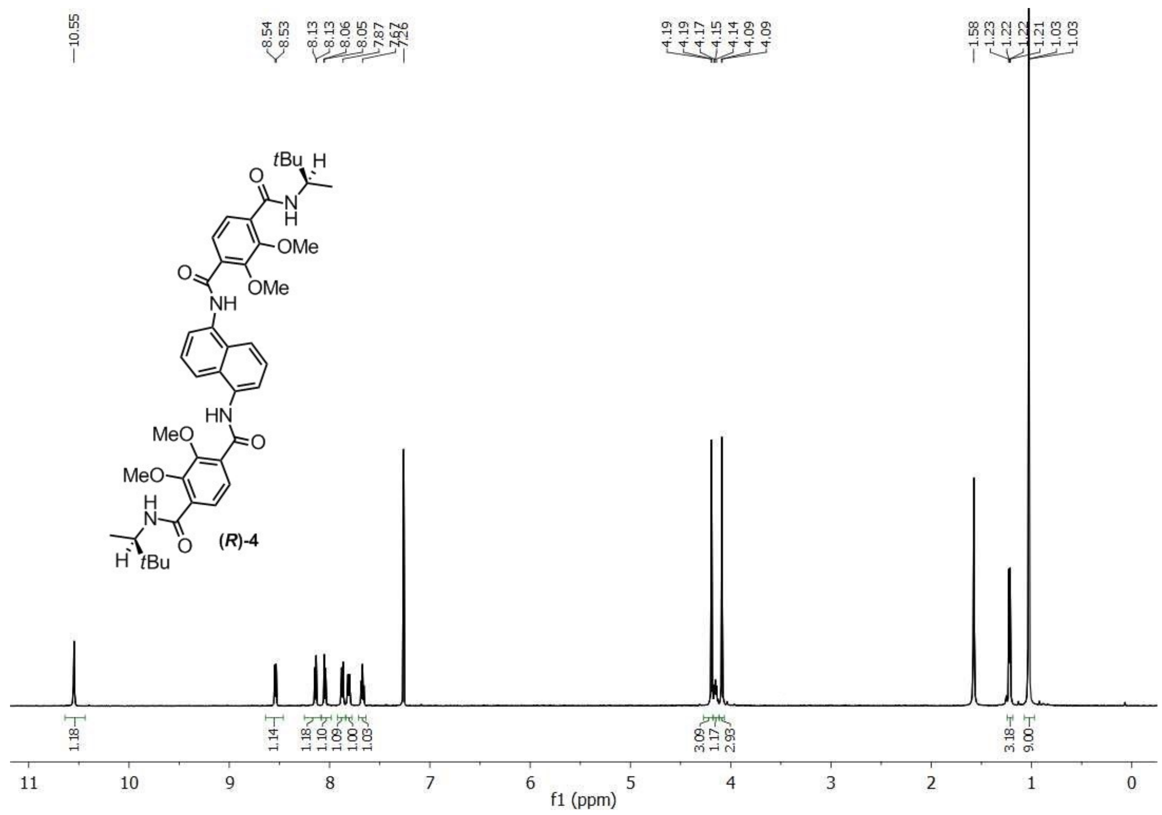
10.55
8.54
8.53
8.13
8.13
8.06
8.05
7.87
7.67
7.26
4.19
4.19
4.17
4.15
4.14
4.09
4.09
1.58
1.23
1.22
1.22
1.21
1.03
1.03
tBu
H
O
N
H
OMe
O
OMe
NH
HN
MeO
O
MeO
H
N
O
H
tBu
(R)-4
1.18
1.14
1.18
1.10
1.09
1.00
1.03
3.09
1.17
2.93
3.18
9.00
11
10
9
8
7
6
5
4
3
2
1
0
f1 (ppm)

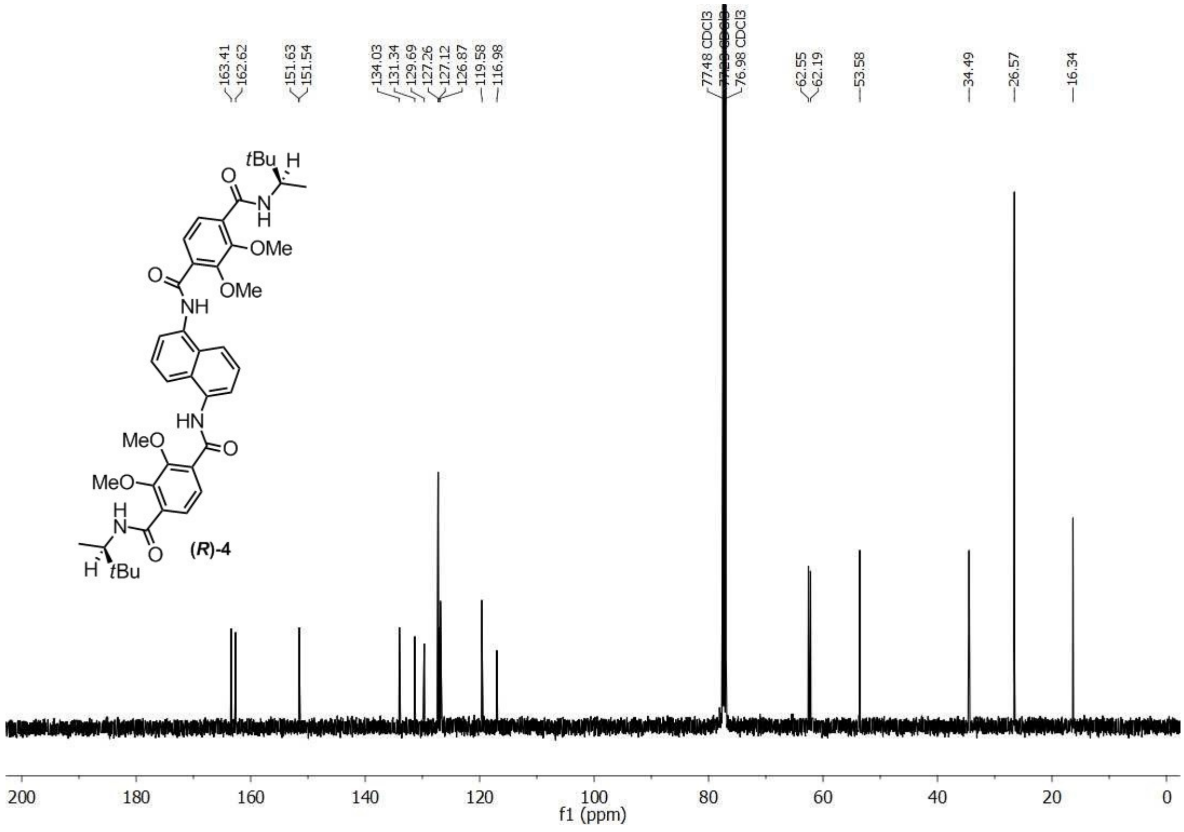
163.41
162.62
151.63
151.54
134.03
131.34
129.69
127.26
127.12
126.87
119.58
116.98
77.48 CDCl3
77.23 CDCl3
76.98 CDCl3
62.55
62.19
53.58
34.49
26.57
16.34
tBu
H
O
N
H
OMe
O
OMe
NH
HN
MeO
O
MeO
H
N
O
H
tBu
(R)-4
200
180
160
140
120
100
80
60
40
20
0
f1 (ppm)

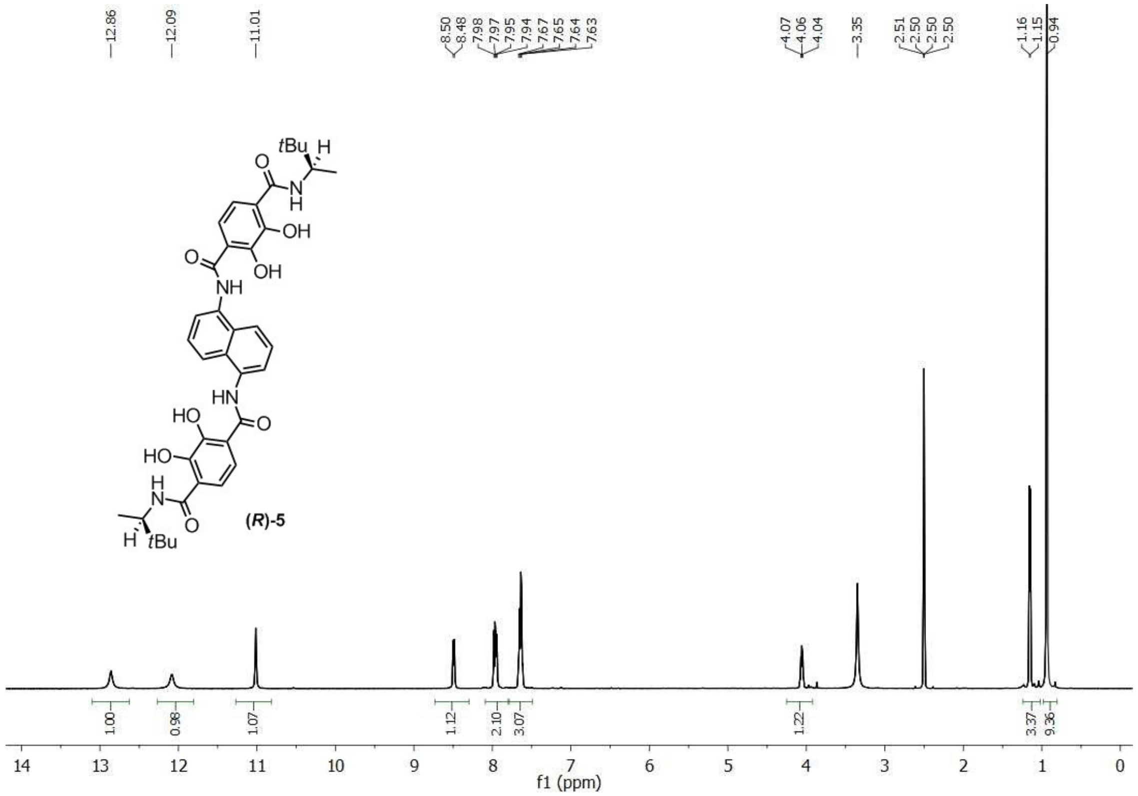
12.86
12.09
11.01
8.50
8.48
7.98
7.97
7.95
7.94
7.67
7.65
7.64
7.63
4.07
4.06
4.04
3.35
2.51
2.50
2.50
2.50
1.16
1.15
0.94
tBu
H
O
N
H
OH
OH
O
NH
HN
O
HO
HO
H
N
O
H
tBu
(R)-5
1.00
0.98
1.07
1.12
2.10
3.07
1.22
3.37
9.36
14
13
12
11
10
9
8
7
6
5
4
3
2
1
0
f1 (ppm)

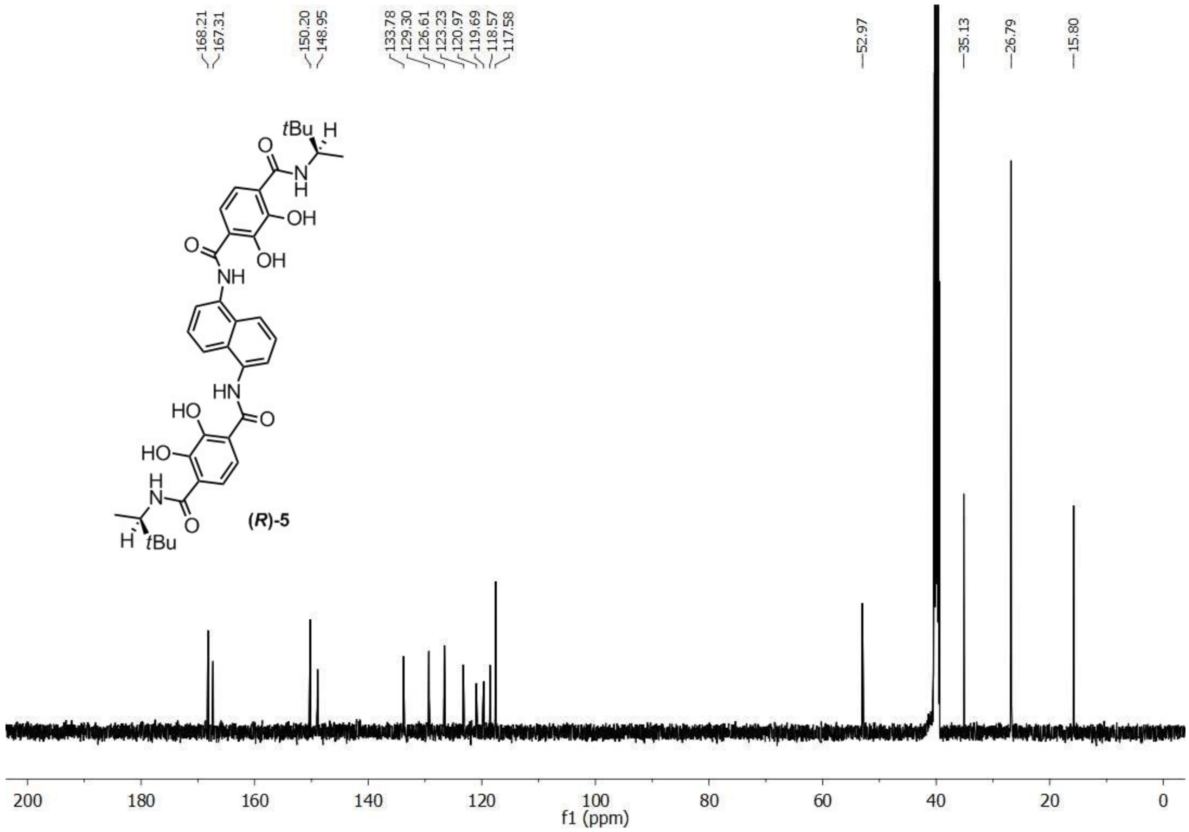
168.21
167.31
150.20
148.95
133.78
129.30
126.61
123.23
120.97
119.69
118.57
117.58
52.97
35.13
26.79
15.80
tBu
H
O
N
H
OH
OH
O
NH
HN
O
HO
HO
H
N
O
H
tBu
(R)-5
200
180
160
140
120
100
80
60
40
20
0
f1 (ppm)

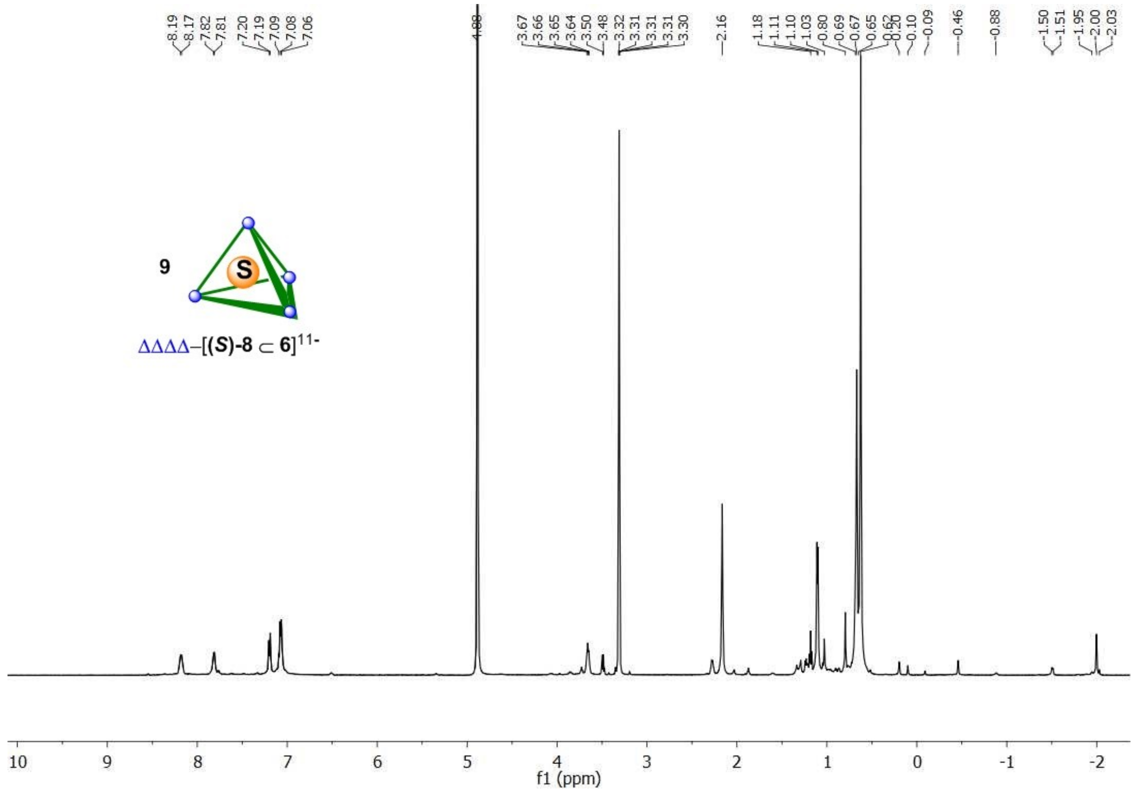

ΔΔΔΔ–[(*S*)-**8** ⊂ **6**]$^{11-}$

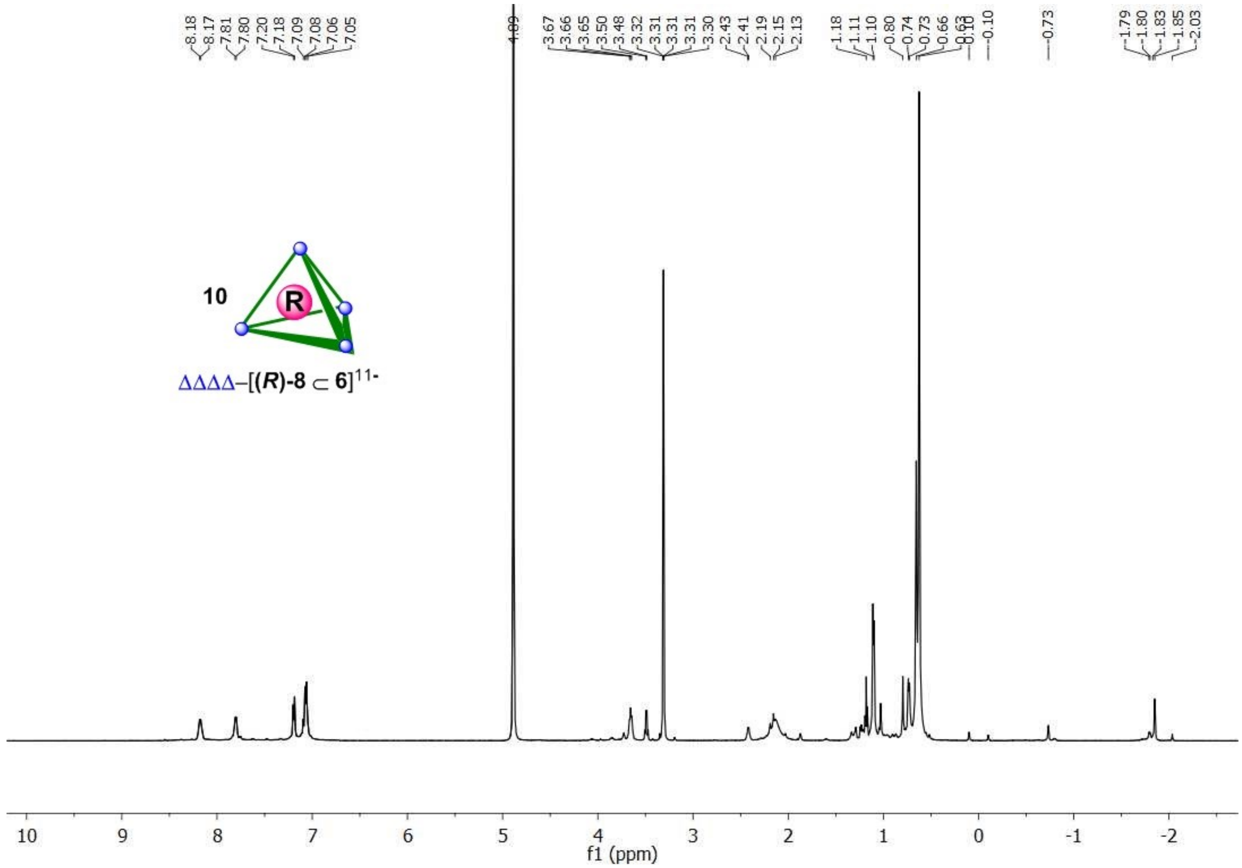

ΔΔΔΔ–[(*R*)-**8** ⊂ **6**]$^{11-}$

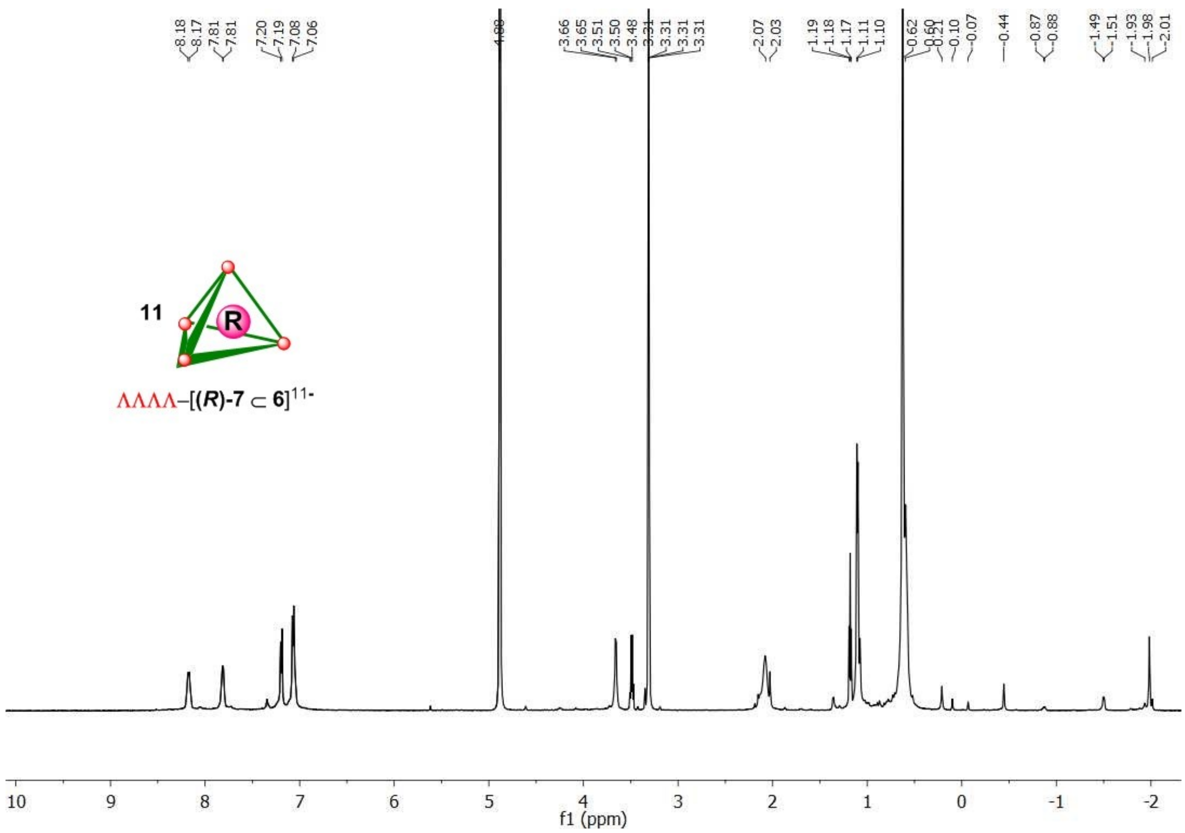
8.18
8.17
7.81
7.81
7.20
7.19
7.08
7.06
4.88
3.66
3.65
3.51
3.50
3.48
3.31
3.31
3.31
3.31
2.07
2.03
1.19
1.18
1.17
1.11
1.10
0.62
0.60
0.21
0.10
-0.07
-0.44
-0.87
-0.88
-1.49
-1.51
-1.93
-1.98
-2.01
11
R
ΛΛΛΛ–[(R)-7 ⊂ 6]11-
10
9
8
7
6
5
4
3
2
1
0
-1
-2
f1 (ppm)

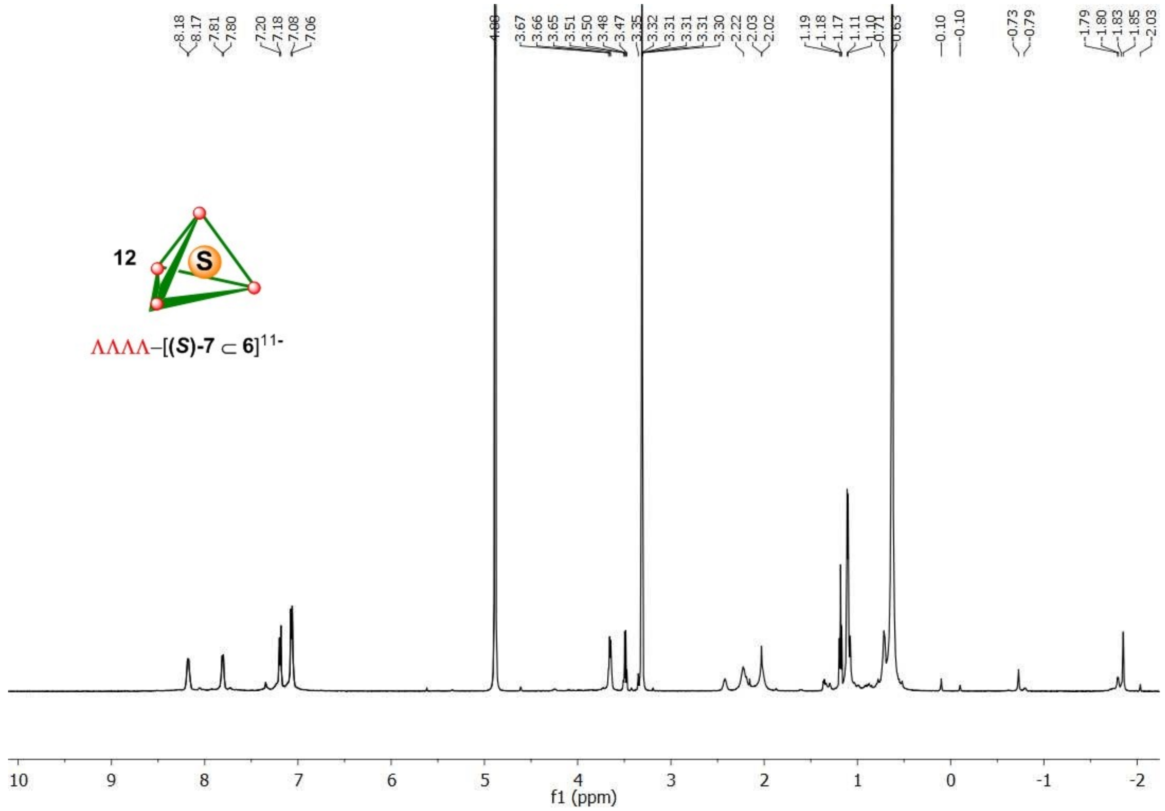
8.18
8.17
7.81
7.80
7.20
7.18
7.08
7.06
4.88
3.67
3.66
3.65
3.51
3.50
3.48
3.47
3.35
3.32
3.31
3.31
3.31
3.30
2.22
2.03
2.02
1.19
1.18
1.17
1.11
1.10
0.71
0.63
0.10
-0.10
-0.73
-0.79
-1.79
-1.80
-1.83
-1.85
-2.03
12
S
ΛΛΛΛ–[(S)-7 ⊂ 6]11-
10
9
8
7
6
5
4
3
2
1
0
-1
-2
f1 (ppm)

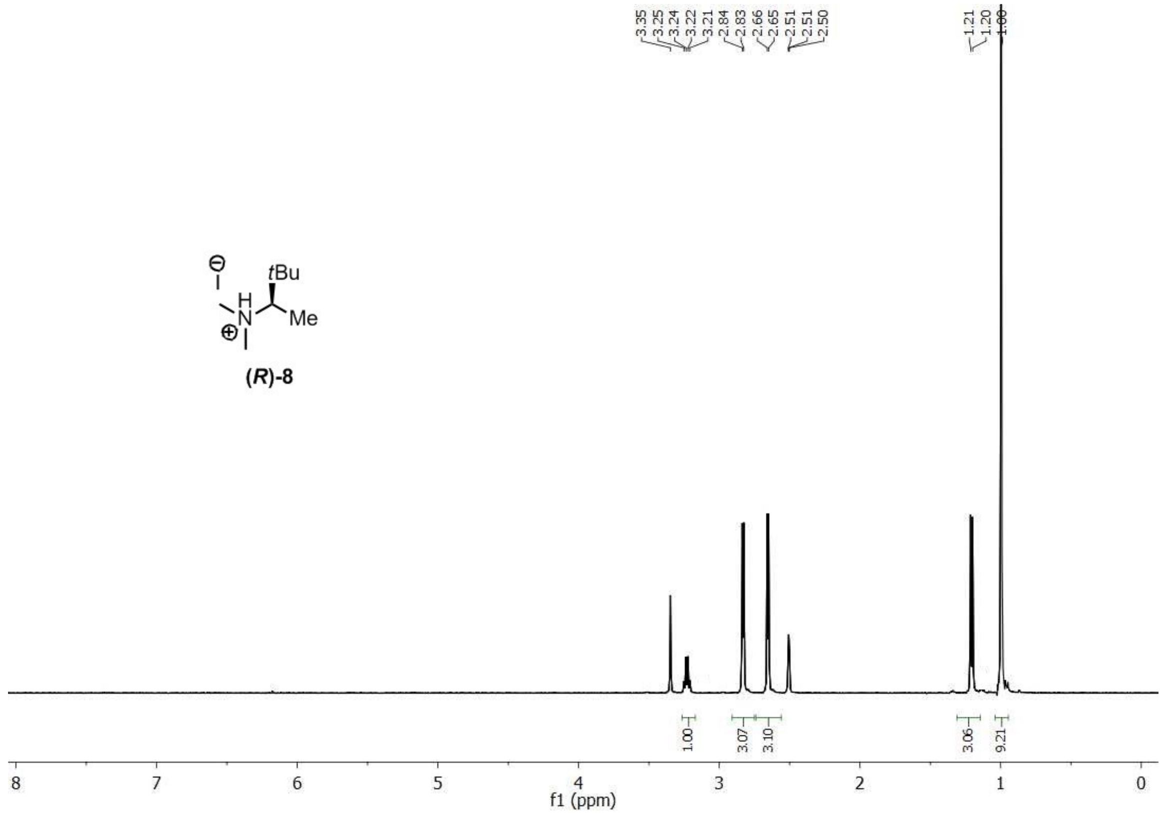
3.35
3.25
3.24
3.22
3.21
2.84
2.83
2.66
2.65
2.51
2.51
2.50
1.21
1.20
1.00
tBu
H
N
Me
(R)-8
1.00
3.07
3.10
3.06
9.21
8
7
6
5
4
3
2
1
0
f1 (ppm)

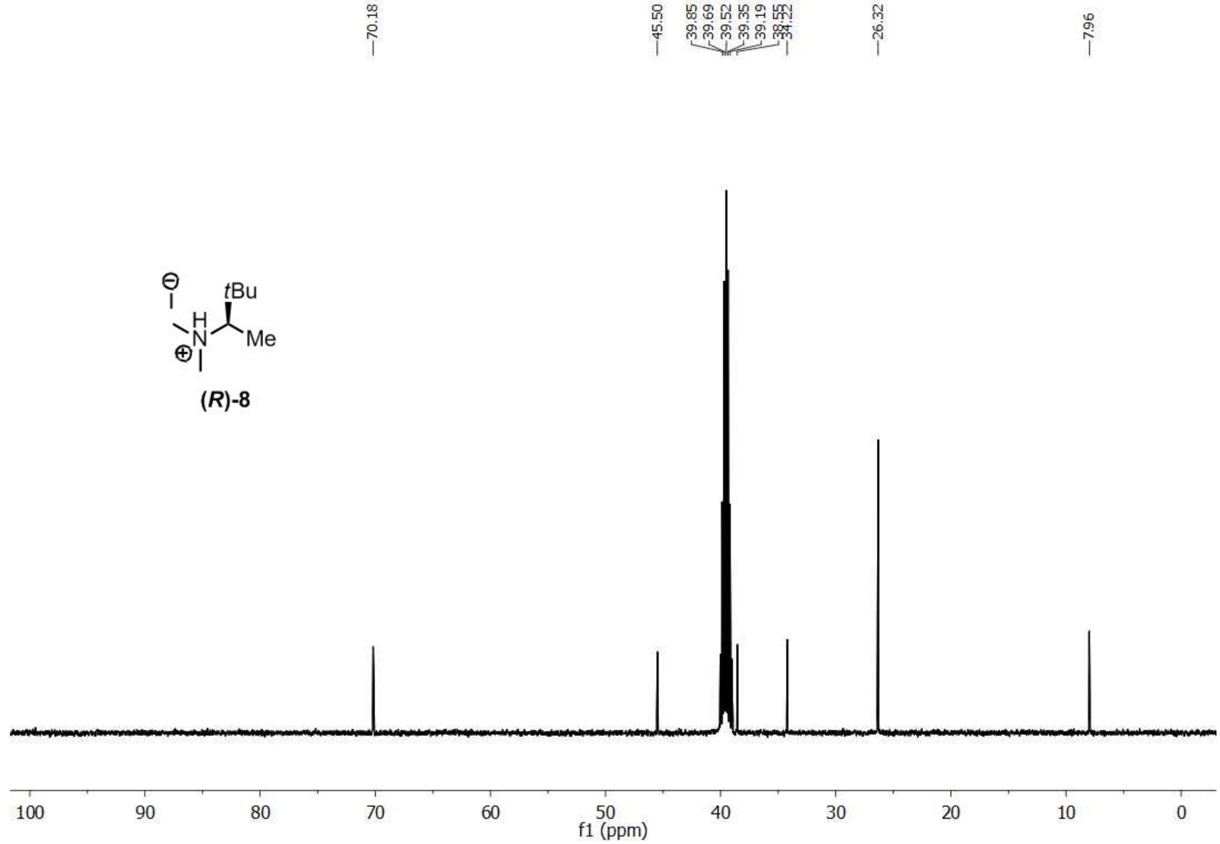
70.18
45.50
39.85
39.69
39.52
39.35
39.19
38.55
34.22
26.32
7.96
tBu
H
N
Me
(R)-8
100
90
80
70
60
50
40
30
20
10
0
f1 (ppm)

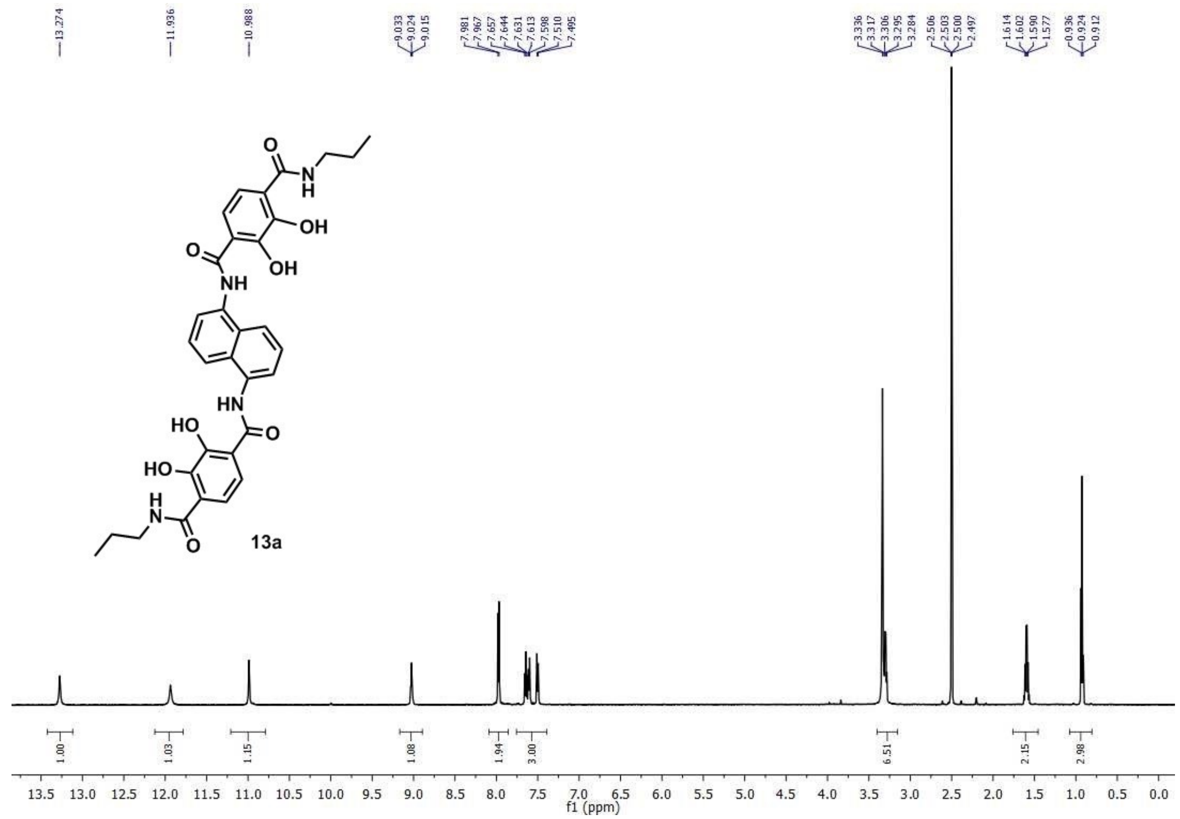
13.274
11.936
10.988
9.033
9.024
9.015
7.981
7.967
7.657
7.644
7.631
7.613
7.598
7.510
7.495
3.336
3.317
3.306
3.295
3.284
2.506
2.503
2.500
2.497
1.614
1.602
1.590
1.577
0.936
0.924
0.912
O
N
H
OH
OH
O
NH
HN
O
HO
HO
H
N
O
13a
1.00
1.03
1.15
1.08
1.94
3.00
6.51
2.15
2.98
13.5
13.0
12.5
12.0
11.5
11.0
10.5
10.0
9.5
9.0
8.5
8.0
7.5
7.0
6.5
6.0
5.5
5.0
4.5
4.0
3.5
3.0
2.5
2.0
1.5
1.0
0.5
0.0
f1 (ppm)

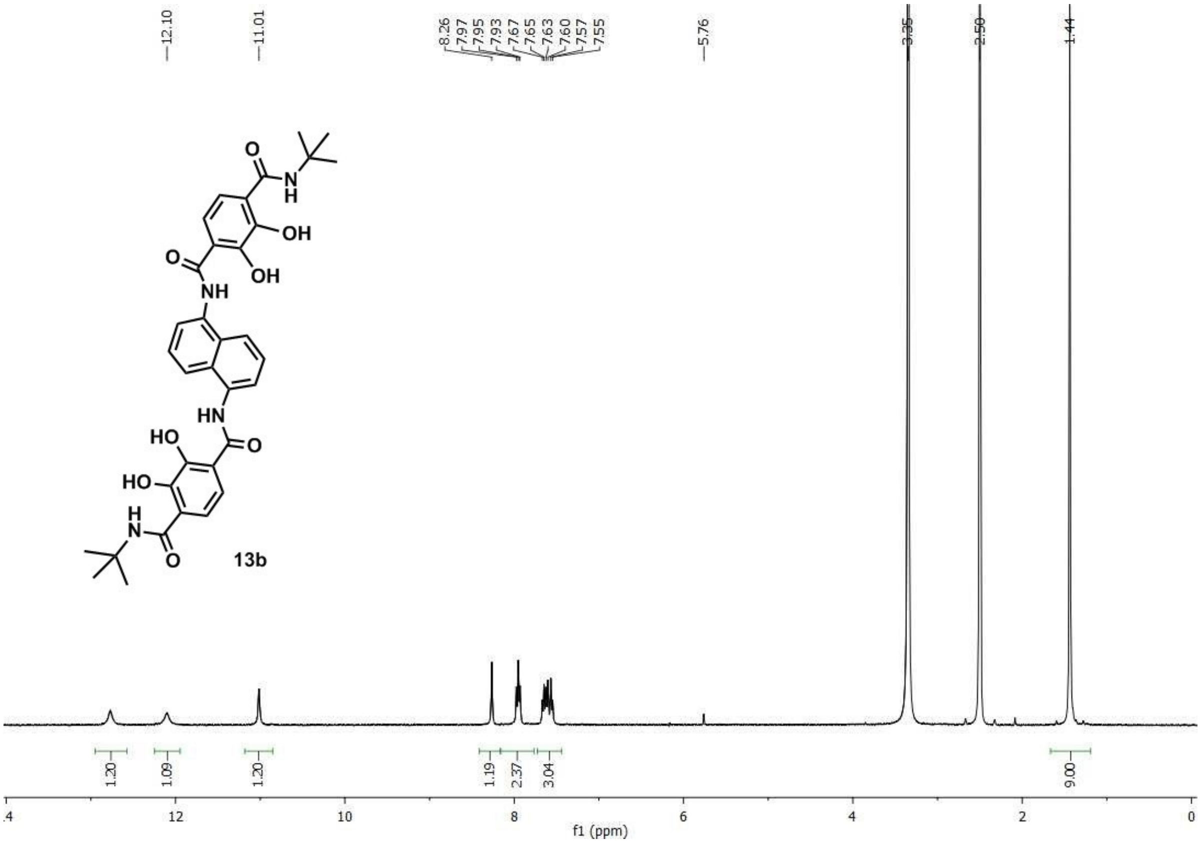
12.10
11.01
8.26
7.97
7.95
7.93
7.67
7.65
7.63
7.60
7.57
7.55
5.76
3.35
2.50
1.44
O
N
H
OH
OH
O
NH
HN
O
HO
HO
H
N
O
13b
1.20
1.09
1.20
1.19
2.37
3.04
9.00
4
12
10
8
6
4
2
0
f1 (ppm)

5.4.9. X-ray Crystallography Information for 6

A yellow prism 0.700 x 0.500 x 0.500 mm in size was mounted on a Cryoloop with Paratone oil. Data were collected in a nitrogen gas stream at 100(2) K using phi and omega scans. Crystal-to-detector distance was 60 mm and exposure time was 20 seconds per frame using a scan width of 1.0°. Data collection was 99.1% complete to 40.000° in θ. A total of 76635 reflections were collected covering the indices, -25<=*h*<=21, -25<=*k*<=25, -67<=*l*<=55. 13694 reflections were found to be symmetry independent, with an R_{int} of 0.0224. Indexing and unit cell refinement indicated a rhombohedral (obverse), trigonal lattice. The space group was found to be R 3 :H (No. 146). The data were integrated using the Bruker SAINT software program and scaled using the SADABS software program. Solution by iterative methods (SIR-2011) produced a heavy-atom phasing model consistent with the proposed structure. All Ga atoms were refined anisotropically by full-matrix least-squares (SHELXL-2013). All other non-hydrogen atoms were located from the difference map but refined isotropically. Rigid-body modeling was used for phenyl (AFIX 66) and napthyl (AFIX 116) groups and restraints, where necessary, for other groups in order to obtain convergence during refinement. All hydrogen atoms were placed using a riding model. Their positions were constrained relative to their parent atom using the appropriate HFIX command in SHELXL-2013. SQUEEZE was used to treat the diffuse electron density present in the extremely large void spaces which contain not only solvent (THF) but K^+ counterions. The empirical formula, formula weight, density, F(000), and absorption coefficient have been modified to reflect an estimate of the contents of the void space in addition to the refined cluster molecule. Crystallographic data for the structure reported in this paper have been deposited with the Cambridge Crystallographic Data Centre as supplementary publication no. CCDC-953011. These data can be obtained free of charge from the Cambridge Crystallographic Data Centre (http://www.ccdc.cam.ac.uk/data_request/cif).

Table 1. Crystal data and structure refinement for toste73.

X-ray ID	toste73	
Sample/notebook ID	R-Ga4-CZ	
Empirical formula	C444 H672 Ga4 K12 N24 O102	
Formula weight	8726.10	
Temperature	100(2) K	
Wavelength	1.54178 Å	
Crystal system	Trigonal	
Space group	R 3 :H	
Unit cell dimensions	a = 25.5125(13) Å	α= 90°.
	b = 25.5125(13) Å	β= 90°.
	c = 67.262(4) Å	γ = 120°.
Volume	37915(4) $Å^3$	
Z	3	
Density (calculated)	1.147 Mg/m^3	
Absorption coefficient	1.718 mm^{-1}	

F(000)	14016
Crystal size	0.700 x 0.500 x 0.500 mm^3
Crystal color/habit	yellow prism
Theta range for data collection	2.105 to 50.464°.
Index ranges	-25<=h<=21, -25<=k<=25, -67<=l<=55
Reflections collected	76635
Independent reflections	13694 [R(int) = 0.0224]
Completeness to theta = 40.000°	99.1 %
Absorption correction	Semi-empirical from equivalents
Max. and min. transmission	0.137 and 0.056
Refinement method	Full-matrix least-squares on F^2
Data / restraints / parameters	13694 / 23 / 315
Goodness-of-fit on F^2	1.094
Final R indices [I>2sigma(I)]	R1 = 0.0915, wR2 = 0.2541
R indices (all data)	R1 = 0.0952, wR2 = 0.2584
Absolute structure parameter	0.14(5)
Extinction coefficient	n/a
Largest diff. peak and hole	0.460 and -0.677 e.Å^{-3}

5.5. References

(1) Caulder, D. L.; Powers, R. E.; Parac, T. N.; Raymond, K. N. *Angew. Chem., Int. Ed.* **1998**, *37*, 1840-1843.
(2) Ziegler, M.; Davis, A. V.; Johnson, D. W.; Raymond, K. N. *Angew. Chem., Int. Ed.* **2003**, *42*, 665-668.
(3) Davis, A. V.; Fiedler, D.; Ziegler, M.; Terpin, A.; Raymond, K. N. *J. Am. Chem. Soc.* **2007**, *129*, 15354-15363.
(4) Ziegler, M.; von Zelewsky, A. *Coord. Chem. Rev.* **1998**, *177*, 257-300.
(5) Gramer, C. J.; Raymond, K. N. *Org. Lett.* **2001**, *3*, 2827-2830.

Chapter 6. Asymmetric Organic Transformations Catalyzed by a Diastereo- and Enantiopure Supramolecular Host Complex

Portions of this chapter have previously been published in:
Chen Zhao, Qing-Fu Sun, William M. Hart-Cooper, Antonio G. DisPasquale, F. Dean Toste, Robert G. Bergman, Kenneth N. Raymond. "Chiral Amide Directed Assembly of a Diastereo- and Enantiopure Supramolecular Host and its Application to Enantioselective Catalysis of Neutral Substrate," *J. Am. Chem. Soc.* **2013**, *135*, 18802-18805.

6.1. Introduction

The use of supramolecular host complexes as catalysts for organic transformations has become a popular topic of interest in chemical research. In recent years, many examples have been reported, such as the Diels-Alder reaction by Fujita[1] and the Nazarov cyclization reaction by Raymond and coworkers.[2] However, the use of enantiopure supramolecular host complexes as catalysts for enantioselective organic transformations remain less explored. Although some examples of chiral and enantiopure supramolecular complexes have been reported,[3-5] their use as catalysts for asymmetric organic transformations have been limited to the charged substrates of the Aza-Cope rearrangement,[6] or the stoichiometric chiral host mediated [2+2] cycloaddition of neutral guests.[7]

The recently reported complex **1** is an enantiopure supramolecular nanovessel that provides a chiral environment within which reactions can take place.[8] Since host **1**'s cavity contains only weakly binding molecules as guests, such as potassium or its solvent adducts, it allows for the encapsulation and transformation of neutral species, an area of research only made possible by complex **1**. Described in this chapter is progress made toward the development of enantioselective organic transformations of both cationic and neutral species that are catalyzed by supramolecular nanovessel **1**.

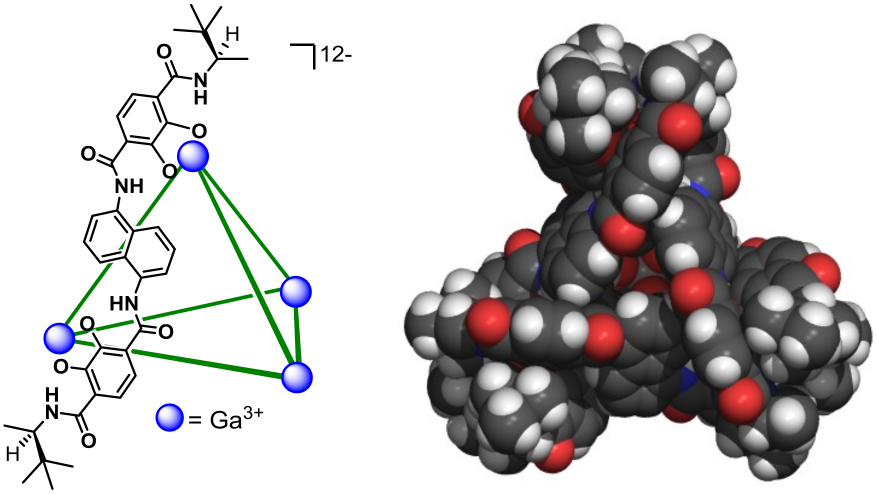

Figure 6.1. (left) Schematic representation of ΔΔΔΔ-**1** (right) X-ray crystal structure of ΔΔΔΔ-**1**

6.2. Results and Discussion

6.2.1. Asymmetric Ring-Opening Reaction of an Episulfonium Ion

The enantioselective ring-opening reactions of *meso*-episulfonium intermediates have been reported recently by both the Toste[9] and Jacobsen groups.[10] The reaction proceeds via *in situ* generation of the sulfonium intermediate, followed by ring-opening with alcohol nucleophiles in the presence of chiral counterions to give enantioenriched products. While high enantioselectivities can be achieved for *cis*-stilbene derived substrates with either catalytic system, small and non-aromatic substrates, such as **2**, only proceeded to give the desired product in low yield and low enantioselectivity (Scheme 6.1). Such poor selectivity could be the result of substrate **2**'s inability to interact with the thiourea catalyst via π-π interaction. However, the small size featured by compound **2** could be advantageous for reaction inside the cavity of **1**. Since the ability of complex **1**'s analog to stabilize otherwise unstable species via encapsulation has been well documented,[11] host **1** should also be able to catalyze the formation of episulfonium species as a guest and thereby exert control over its ring-opening reaction. Thus, we began our studies by exploring the reactivity of substrates analogous to **2** with host complex **1**.

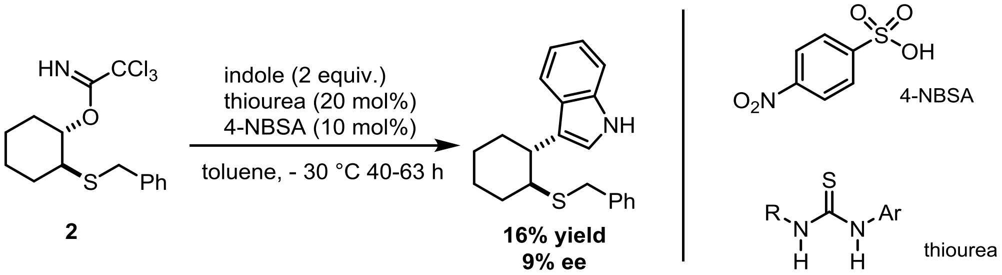

Scheme 6.1. Thiourea catalyzed ring-opening of an episulfonium ion generated from **2**

Substrates **3** were synthesized according to Scheme 6.2 in two steps from commercially available cyclohexene oxide. When **3** and 2.5 mol% of **1** were combined in a solvent mixture of CD_3OD and D_2O buffered at pD 9, the desired product **4** was obtained in quantitative NMR yield and 21% *ee* after 8h of reaction time at room temperature. Repeating the reaction with 20 mol% catalyst loading of complex **1** led to direct observation of an encapsulated species inside the cavity of **1,** as illustrated by the ^{1}H NMR spectrum shown in Scheme 6.3B. While reaction performed in 100% CD_3OD led to slight increase in enantioselectivity where product **4** was isolated with 36% ee, suggesting a solvent effect, the temperature effect on the enantioselectivity of this ring-opening reaction was found to be less significant. Control experiments between **3** and "blocked" assembly **1** ($[PEt_4 \subset$ **1**$]$) gave no product **4** after heating at 50 °C for 3 h, which strongly suggests that the desired reaction proceeds via encapsulation inside assembly **1**. Lastly, reaction between **3** and 20 mol% host complex $(NMe_4)_{12}$**5** proceeded to give no desired product **4** even after heating at 50 °C for 8h (Scheme 6.3).

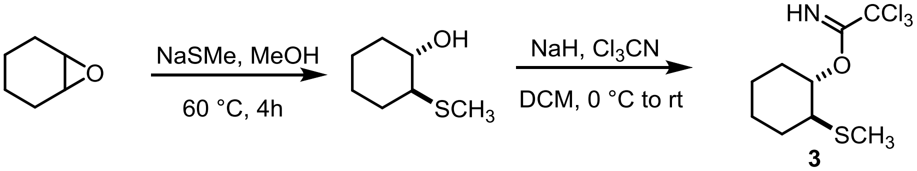

Scheme 6.2. Synthesis of substrate **3**

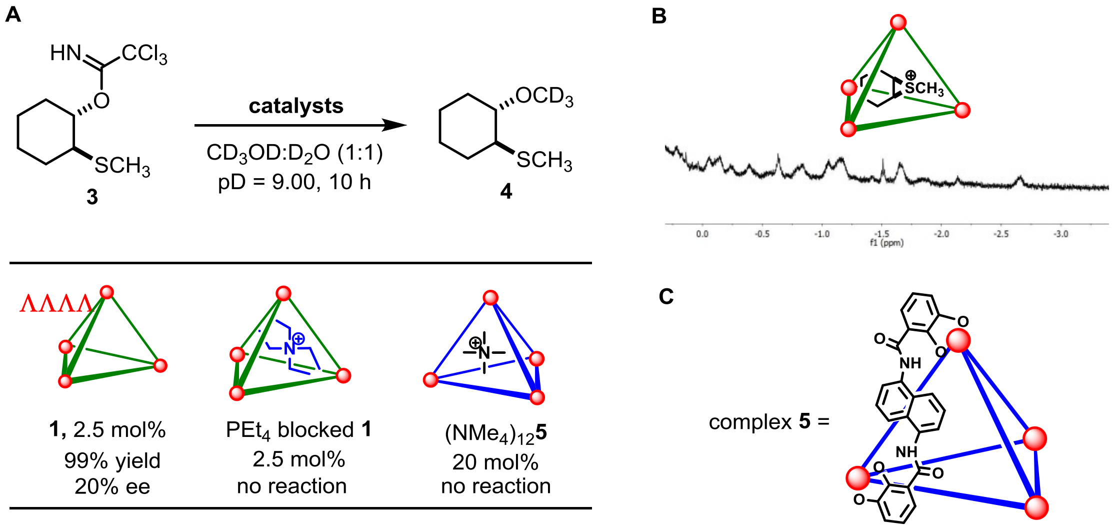
A
HN
CCl3
O
SCH3
3
catalysts
CD3OD:D2O (1:1)
pD = 9.00, 10 h
OCD3
SCH3
4
ΛΛΛΛ
1, 2.5 mol%
99% yield
20% ee
PEt4 blocked 1
2.5 mol%
no reaction
(NMe4)12 5
20 mol%
no reaction
B
SCH3
0.0
-0.5
-1.0
-1.5
-2.0
-2.5
-3.0
f1 (ppm)
C
complex 5 =
O
NH
NH
O

Scheme 6.3. (A) Reaction of **3** to **4** catalyzed by **1**, (B) ^{1}H NMR spectrum of an observed intermediate, (C) Schematic representation of complex **5**

We next surveyed the scope of this asymmetric reaction by varying the size of the chelating ring and changing the substituent on the sulfur atom. As shown in Scheme 6.4, the reaction tolerates various alkyl-substitutions on the sulfur atom to give high yields of the desired products, but with low enantioselectivity. It is difficult to establish a trend regarding what types of substitution could be ideal for high enantiodifferentiation inside the cavity of **1** based on the data presented in Scheme 6.4; therefore, further efforts could be made toward studying the effects of structure and volume size of substrates on their enantioselective reaction inside **1**.

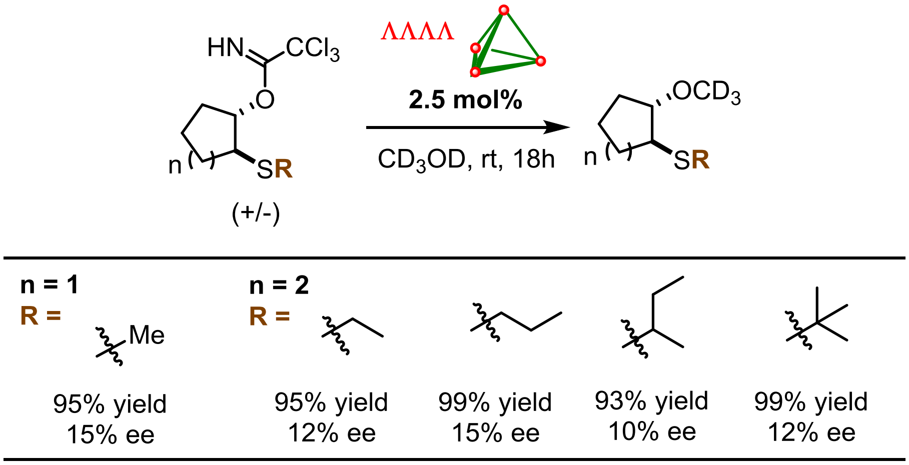
HN
CCl3
O
n
SR
(+/-)
ΛΛΛΛ
2.5 mol%
CD3OD, rt, 18h
OCD3
n
SR
n = 1
R =
Me
95% yield
15% ee
n = 2
R =
95% yield
12% ee
99% yield
15% ee
93% yield
10% ee
99% yield
12% ee

Scheme 6.4. Substrate scope of the asymmetric ring-opening reaction of *meso*-episulfonium ions catalyzed by **1**

Nevertheless, this ring-opening reaction of an episulfonium ion generated from neutral molecule **3** represents a rare example of an intermolecular asymmetric reaction catalyzed by a chiral supramolecular nanovessel. We propose the following catalytic cycle for this asymmetric ring-opening reaction catalyzed by supramolecular host **1**.

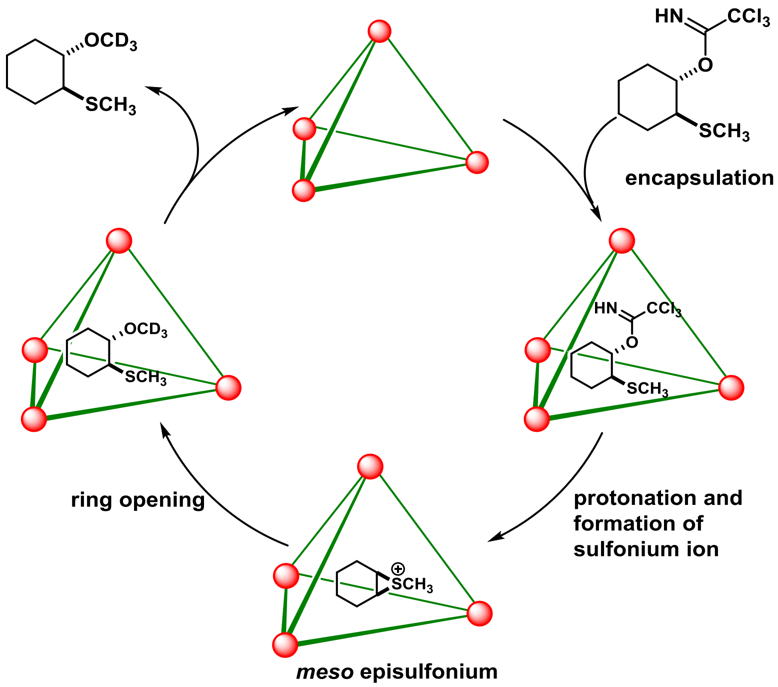

Figure 6.2. Proposed catalytic cycle for the asymmetric ring-opening reaction of *meso*-episulfonium ions catalyzed by **1**

6.2.2. Enantioselective Prins-like Carbonyl-Ene Cyclization Reaction

We recently reported the chemoselective carbonyl-ene cyclization reaction catalyzed by complex **5** (Scheme 6.5).[12] In contrast to catalysis in acidic aqueous solution, which affords cyclic diol products, host **5** catalyzed cyclizations resulted in high selectivity for alkene products due to water exclusion from the cavity of **5** because of the hydrophobic effect. This example of selectivity parallels that of terpene synthases such as limonene synthase. Specifically, cyclization of compounds **6a** catalyzed by complex **5** to give exclusively products **7a,b** respectively. Unfortunately, since the chiral and enantiopure complex **5** can only be obtained as the NMe_4-filled cluster, enantioselective cyclization of **6a** was not possible since the neutral substrate could not compete again NMe_4 for the cavity of **5**. Indeed, reaction between **6a** and 10 mol% of $(NMe_4)_{12}$**5** at 60 °C in D_2O solution buffered at pD 8 for 14h gave no desired products and only recovered starting material.

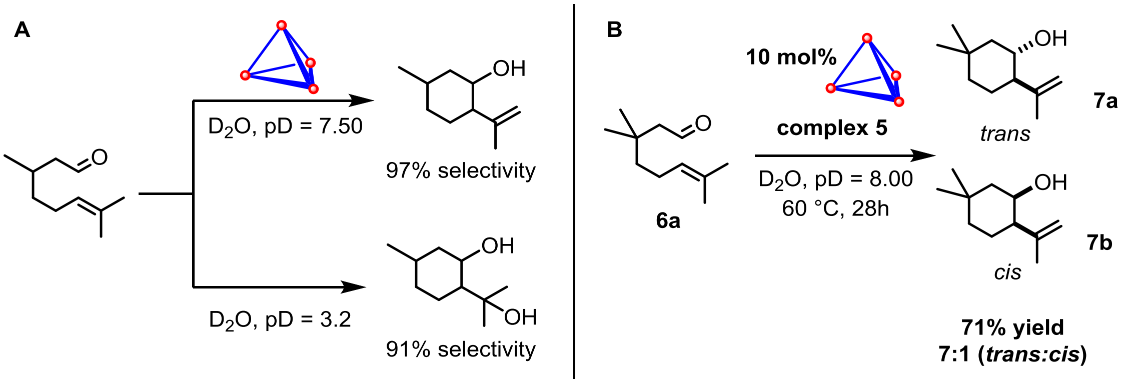

Scheme 6.5. (A) Divergent reaction pathways for the carbonyl-ene cyclization catalyzed by complex **5** and reaction in bulk acidic solution (B) Cyclization of **6a** catalyzed by **5** to give mostly *trans* product **7a**

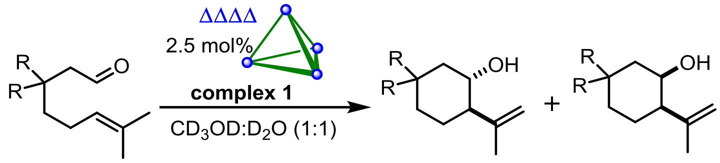

6a - R = Me
6b - R = H

7a - R = Me
7b - R = H

8a - R = Me
8b - R = H

entry	R	pD	temp (°C)	time (h)	yield (*trans:cis*)	*ee* of **7**
1	Me	8	25	50	92% (8:1)	61%
2[a]	Me	5	25	16	94% (7.5:1)	-58%
3	Me	5	-20	168	70% (8:1)	69%
4[b]	Me	5	60	24	33% (8:1)	58%
5	H	8	60	16	12% (nd)	nd
6[a]	H	5	60	16	92% (8:1)	65%

[a] Reaction performed with ΛΛΛΛ–**1** (2.5 mol%). [b] 0.3 mol% of ΔΔΔΔ–**1** was used (98 TON).

Table 6.1. Enantioselective and chemoselective Prins-like carbonyl-ene cyclization catalyzed by ΔΔΔΔ-**1**

On the other hand, complex ΔΔΔΔ-**1** catalyzed cyclization of **6a** in a solvent mixture of CD_3OD and D_2O buffered at pD 8 at room temperature gave the desired products **7a** and **8a** in 92% NMR yield with a *trans*:*cis* ratio of 8:1 and 60% ee for **7a** over two days (Table 6.1, entry 1). Compared to reaction with complex **5** as the catalyst at the same pD, cyclization of **6a** in the presence of a catalytic amount of ΔΔΔΔ-**1** proved to be faster by 7-fold (see Supporting Information). Since complex ΔΔΔΔ-**1** is stable at low pD, attempts to effect the cyclization of **6a** at pD 5 led to faster conversion compared to reaction at pD 8 (Table 6.1, entry 2). The stability and turnover capability of catalyst ΔΔΔΔ-**1** was further illustrated as only 0.3 mol% of the complex is required to achieve 33% yield of **7a** and **7a** with no loss in enantiomeric excess of **7a** (Table 6.1, entry 4), representing 98 TON of the catalyst. Interestingly, carbonyl-ene cyclization of **6b** proceeded with complex **1** at pD 8 over 16h at 60 °C to give the desired products in only 12% yield (Table 6.1, entry 5), whereas reaction at pD 5 led to much better conversion over the same reaction time to give the desired product mixture in 92% yield and 65% ee of **14b**. Although the detailed mechanism of this supramolecular host-catalyzed Prins-like cyclization of carbonyl-ene substrates are currently under investigation, we propose a preliminary catalytic cycle based on our current[13] and previously reported results.[12]

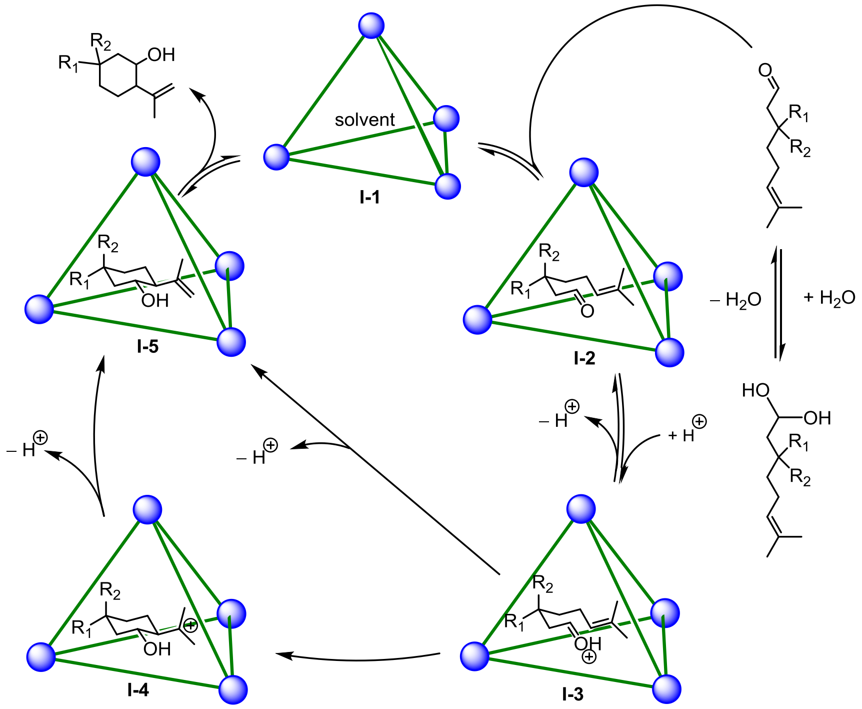

Figure 6.3. Proposed catalytic cycle for the Prins-like cyclization of carbonyl-ene substrates mediated by supramolecular nanovessel **1.**

6.2.3. Enantioselective Aza-Cope Rearrangement Reaction

As a direct comparison to reactions with host **5**, we attempted to carry out the same enantioselective reaction using the newly developed chiral supramolecular Ga_4L_6 nanovessel **1** as the active catalyst. The ammonium tosylate substrate **9a** was synthesized according to literature procedure.[6,14] As a direct comparison, we initially carried out the enantioselective Aza-Cope rearrangement reaction using 20 mol% of **1** as the catalyst in the presence of excess amount of NMe_4Cl (eq. 1). After 2 hours of reaction at 50 °C in D_2O, the reaction mixture was diluted with $CDCl_3$ and extracted to give a mixture containing both **9a** and **10a**. Analysis by ^1H NMR spectroscopy and a gas chromatograph fitted with a chiral column revealed that the reaction proceeded to give 86% yield and 36% ee of the desired aldehyde **10a**. Although these improvements are small, they demonstrate that host ΔΔΔΔ-**1** possesses a chiral pocket different from that of ΔΔΔΔ-**5**. We believe this difference is a result of both the position and existence of the additional chiral directing groups of supramolecular nanovessel **1**. The observation of external and remote modification leading to changes of cavity properties is a powerful property that is commonly found with non-active site modification of amino acid residues in enzyme and protein catalysis.[15,16]

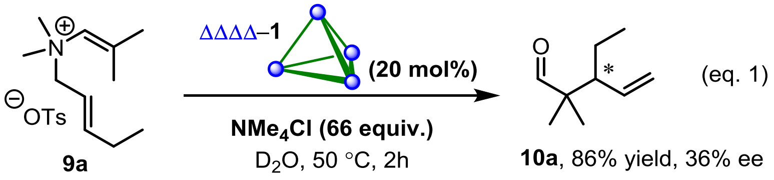
ΔΔΔΔ–1
(20 mol%)
NMe$_4$Cl (66 equiv.)
D_2O, 50 °C, 2h
$\ominus$OTs
9a
10a, 86% yield, 36% ee
(eq. 1)

When substrate **9a** and only 2.5 mol% of **1** were combined at room temperature in a 1:1 mixture of CD_3OD:D_2O buffered at pD 9.00 (eq. 2), encapsulation of **9a** was observed as analyzed by ^{1}H NMR spectroscopy (Figure 6.5A). The desired rearrangement reaction proceeded to give the product aldehyde **10a** in 95% yield and 45% ee over 200h at room temperature. When the reaction was repeated with either no catalyst or ΔΔΔΔ–[(NEt_4 ⊂ **1**], the rearrangement reaction proceeded much more slowly than the catalyzed reaction (Figure 6.5B), giving product **10a** in racemic form. Repeating the catalyzed reaction at 50 °C in the same solvent mixture gave complete conversion of **9a** to **10a** in 8h with only slight decrease in enantiomeric excess (39% ee).

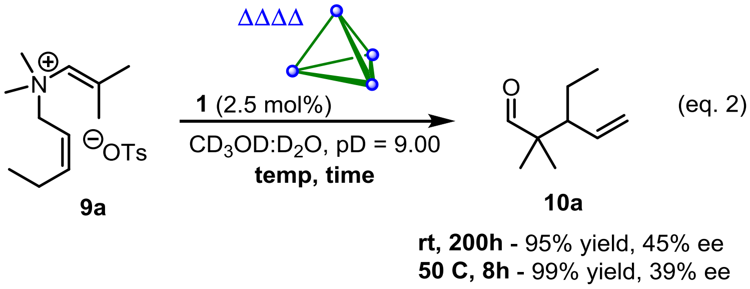
ΔΔΔΔ
1 (2.5 mol%)
CD_3OD:D_2O, pD = 9.00
temp, time
$\ominus$OTs
9a
10a
(eq. 2)
rt, 200h - 95% yield, 45% ee
50 C, 8h - 99% yield, 39% ee

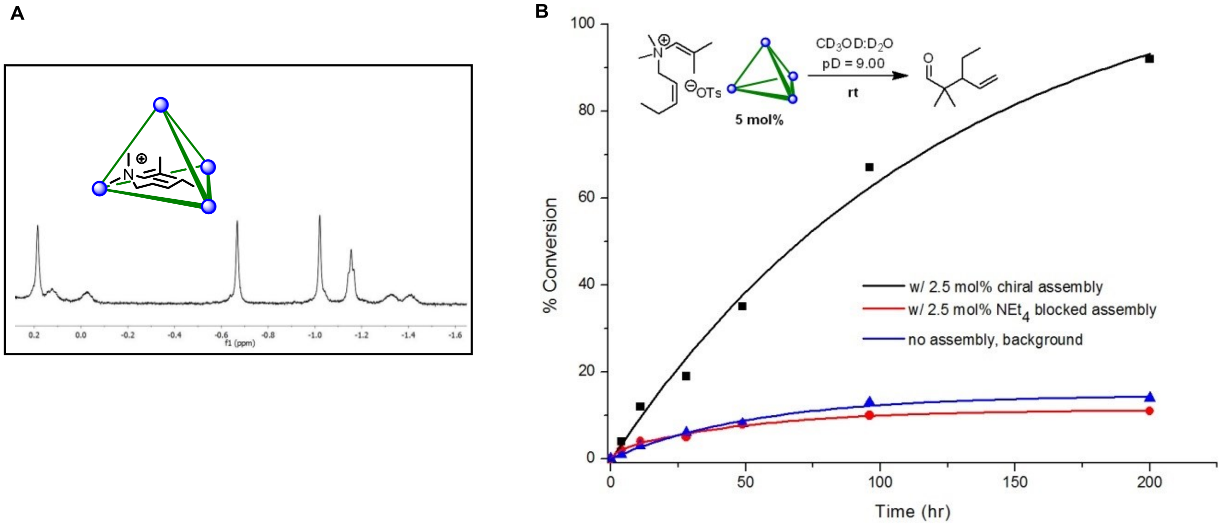

Figure 6.4. (A) ^{1}H NMR spectrum showing encapsulation of **9a**. (B) Rate acceleration of **1** catalyzed Aza-Cope rearrangement of **9a** compared to reactions with ΔΔΔΔ–[(NEt_4 ⊂ **1**] and with no catalyst

We next surveyed briefly the scope of this Aza-cope rearrangement reaction using host **1** as the catalyst. As shown by Figure 6.6, substrate **9c** cyclized in the presence of 2.5 mol% of host complex **1** to give the desired aldehyde product **10c** in high yield over 4 days at room temperature. In analogy to reactions catalyzed by ΔΔΔΔ–[$(NMe_4)^+$ ⊂ **5**], the observed enantioselectivities of products shown in Scheme 6.6 displayed large variation with small changes in size and shape of the substrates. Nevertheless, the chiral host **1** proved to be an effective and robust catalyst for this Aza-cope rearrangement reaction at very low loading (2.5 mol%) to give products in high yields and moderate to good enantioselectivities.

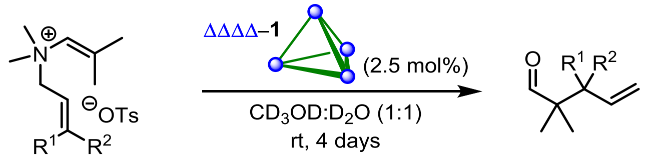

9a, R^1 = H, R^2 = Et
9b, R^1 = H, R^2 = Me
9c, R^1 = Et, R^2 = H
9d, R^1 = H, R^2 = *i*Pr

10a, 95% yield, 43% ee
10b, 90% yield, 27% ee
10c, 87% yield, 47% ee
10d, 93% yield, 53% ee

Scheme 6.6. Substrate scope of the ΔΔΔΔ-**1** catalyzed enantioselective Aza-Cope rearrangement reaction

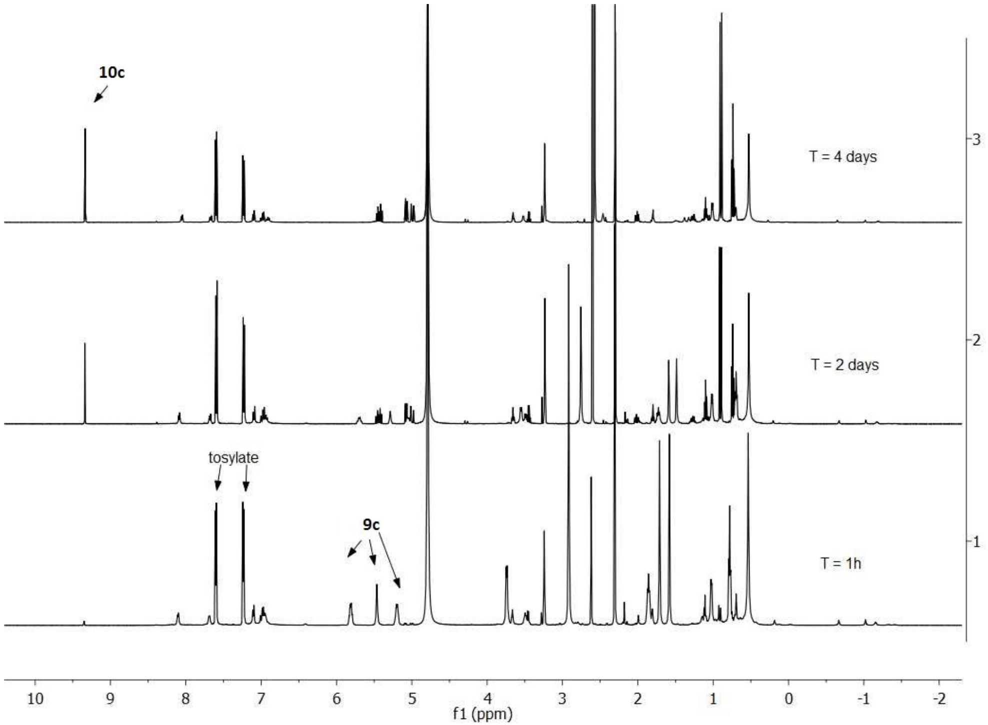

Figure 6.5. Rearrangement of **9c** to **10c** catalyzed by host **1** as monitored by ^{1}H NMR spectroscopy

6.3. Conclusion

Presented in this chapter are three examples of asymmetric organic transformations catalyzed by enantiopure supramolecular host **1**. The enantioselective ring-opening of *meso*-episulfonium intermediate derived from neutral susbtrate **3** serves as a rare example of an intermolecular asymmetric reaction catalyzed by a supramolecular nanovessel complex. We also have applied chiral assembly **1** as a catalyst for the chemo- and enantioselective monoterpene-like cyclization reaction of **6a** and **6b** to give alkene products **7a** and **7b** in high yields with good enantiomeric excess. Lastly, we re-evaluated the enantioselective Aza-Cope rearrangement reaction with chiral assembly **1** and showed that the reaction can proceed with only 2.5 mol% of the new catalyst to give high yields and comparable enantioselectivities as compared to catalysis with enantiopure **5**. In conclusion, supramolecular nanovessel **1** proves to be an efficient and robust catalyst for asymmetric organic transformations of both charged and neutral substrates.

6.4. Experimental

6.4.1. Synthesis of compound 3

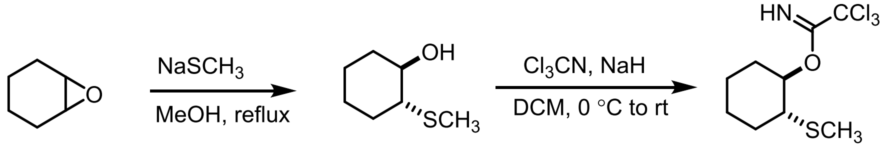

(+/-) **A** (+/-) **3**

Cyclohexene oxide (490 mg, 5.0 mmol, 1 equiv.) was dissolved in methanol (5 mL), followed by addition of sodium thiomethoxide (525 mg, 7.50 mmol 1.5 equiv.) and the resulting solution was heated at reflux for 6 h. The reaction was quenched by dilution with water (5 mL) and diethyl ether (10 mL). The bilayer solution was then extracted with water (3x10 mL), 1 N NaOH (10 mL), and brine (20 mL) and the organic layer was then separated, dried with MgSO$_4$, filtered and concentrated to give **A** (636 mg, 4.35 mmol) as a clear oil in 87% yield, which wasused without purification. ^{1}H NMR (500 MHz, CDCl$_3$) δ (ppm) 3.31 (dt, *J* = 9.8, 4.5 Hz, 1H), 2.83 (br s, 1H), 2.34 (ddd, *J* = 12.2, 9.9, 3.9 Hz, 1H), 2.17-2.11 (m, 2H), 2.07 (s, 3H), 1.80-1.70 (m, 2H), 1.46 (dd, *J* = 12.6, 3.9 Hz, 1H), 1.34-1.23 (m, 3H). ^{13}C NMR (125MHz, CDCl$_3$): δ (ppm) 71.2, 53.3, 33.9, 31.6, 26.4, 24.7, 11.5. IR [neat, ν_{max} (cm^{-1})]: 3230, 1657, 1296, 1070, 791, 643 cm^{-1}. HRMS (*m/z*): calculated for [C$_7$H$_{14}$OS]$^+$ 146.0765; observed, 146.0766.

Compound **B** (636 mg, 4.35 mmol, 1 equiv.) and trichloroacetonitrile (942 mg, 6.53 mmol, 1.5 equiv.) were dissolved in DCM (10 mL) and the resulting solution was cooled to 0 °C. NaH (60% in mineral oil, 17.4 mg, 0.435 mmol, 10 mol%) was then added and the resulting solution was stirred for 18h at 0 °C. The reaction solution was warmed to rt before dilution with water (10 mL) and diethyl ether (10 mL). The bilayer solution was then extracted with 1 N NaOH (10 mL), water (20 mL), brine (20 mL) and the organic layer was separated, dried with MgSO$_4$, filtered and concentrated. The crude residue was then purified by silica chromatography (2% Et$_3$N and 1% EtOAc in hexanes) to give the desired product **3** (960 mg, 3.31 mmol) as a pale yellow oil in 76% yield. ^{1}H NMR (500 MHz, CD$_2$Cl$_2$) δ (ppm) 8.33 (s, 1H), 4.92 (td, *J* = 8.1, 3.6 Hz, 1H), 2.80 (m, 1H), 2.25-2.07 (m, 2H), 2.14 (s, 3H), 1.80-1.62 (m, 2H), 1.62-1.50 (m, 2H), 1.48-1.28 (m, 2H). ^{13}C NMR (125 MHz, CD$_2$Cl$_2$) δ (ppm) 161.8, 91.8, 79.5, 47.7, 30.6, 28.9, 24.2, 22.9, 14.3. . IR [neat, ν_{max} (cm^{-1})]: 1657, 1296, 1070, 1016, 827, 790, 643 cm^{-1}. HRMS (*m/z*): calculated for [C$_9$H$_{14}$NOS^{35}Cl$_3$,]$^+$,288.9862; observed, 288.9865.

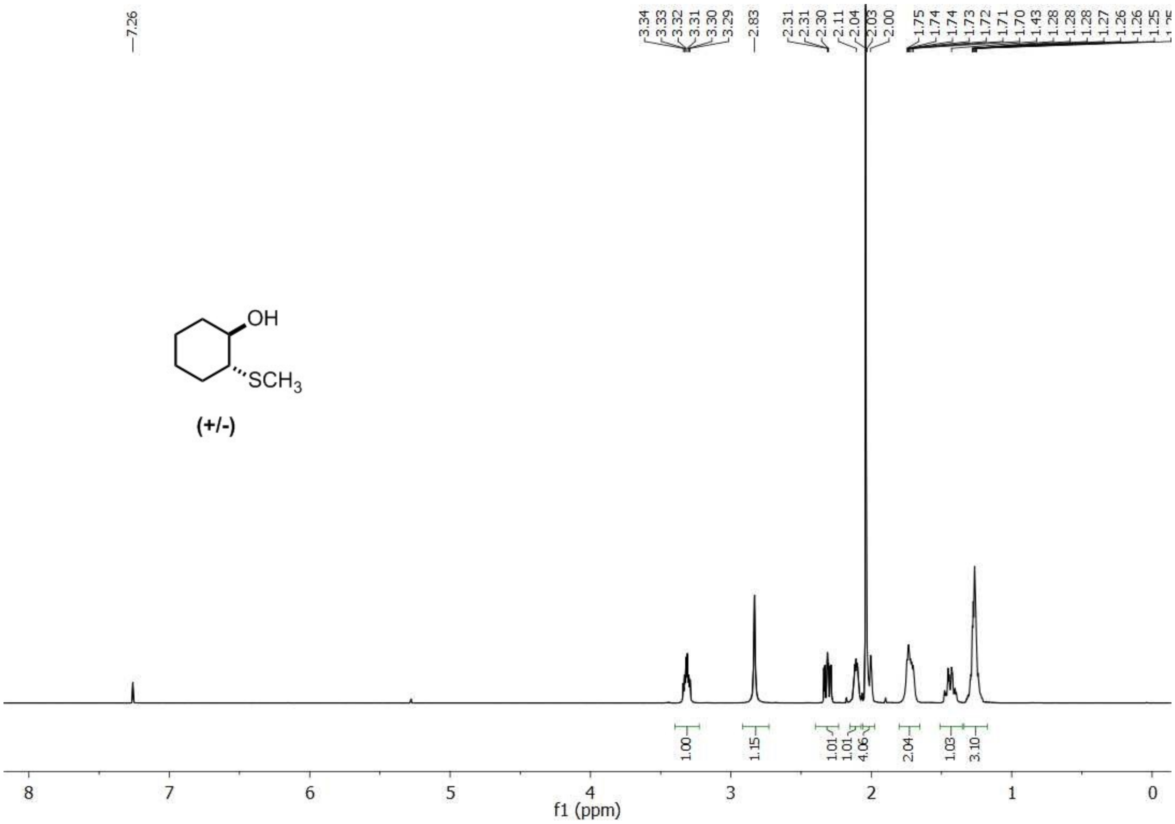
7.26
3.34
3.33
3.32
3.31
3.30
3.29
2.83
2.31
2.31
2.30
2.11
2.04
2.03
2.00
1.75
1.74
1.74
1.73
1.72
1.71
1.70
1.43
1.28
1.28
1.28
1.27
1.26
1.26
1.25
OH
SCH3
(+/-)
1.00
1.15
1.01
1.01
4.06
2.04
1.03
3.10
8
7
6
5
4
3
2
1
0
f1 (ppm)

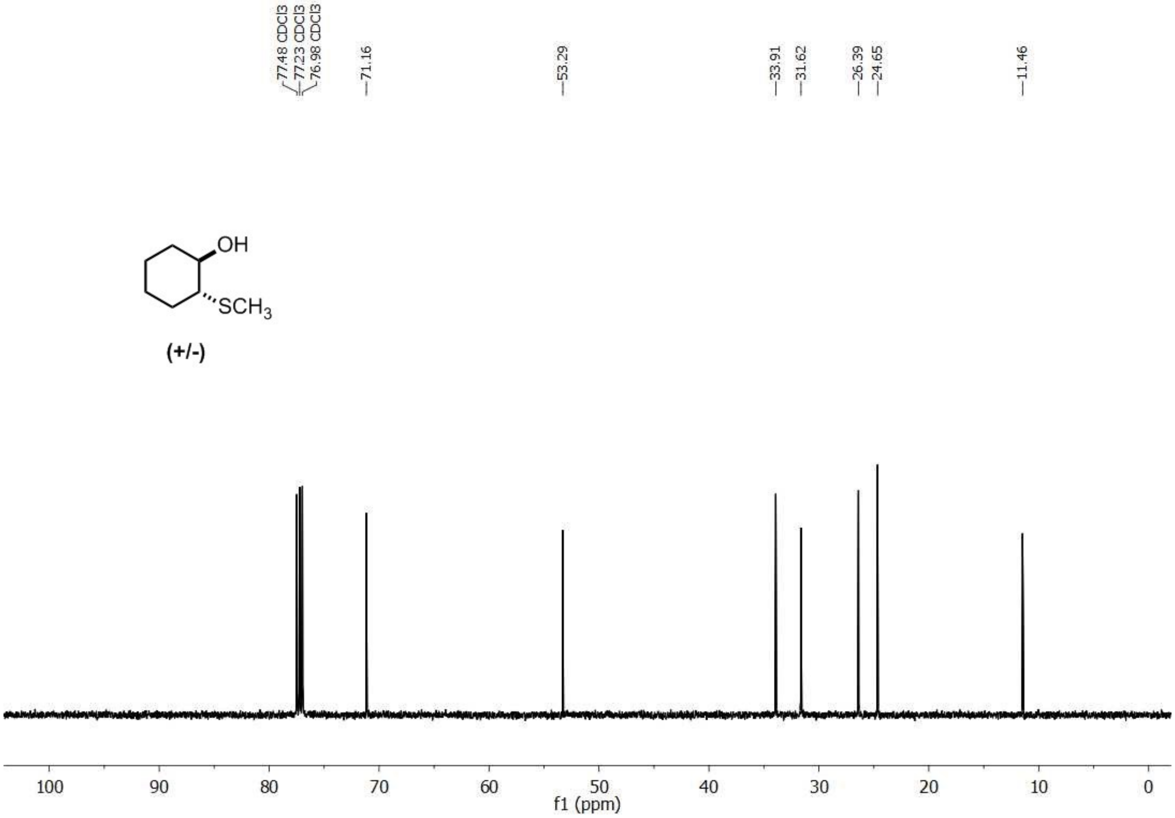
77.48 CDCl3
77.23 CDCl3
76.98 CDCl3
71.16
53.29
33.91
31.62
26.39
24.65
11.46
OH
SCH3
(+/-)
100
90
80
70
60
50
40
30
20
10
0
f1 (ppm)

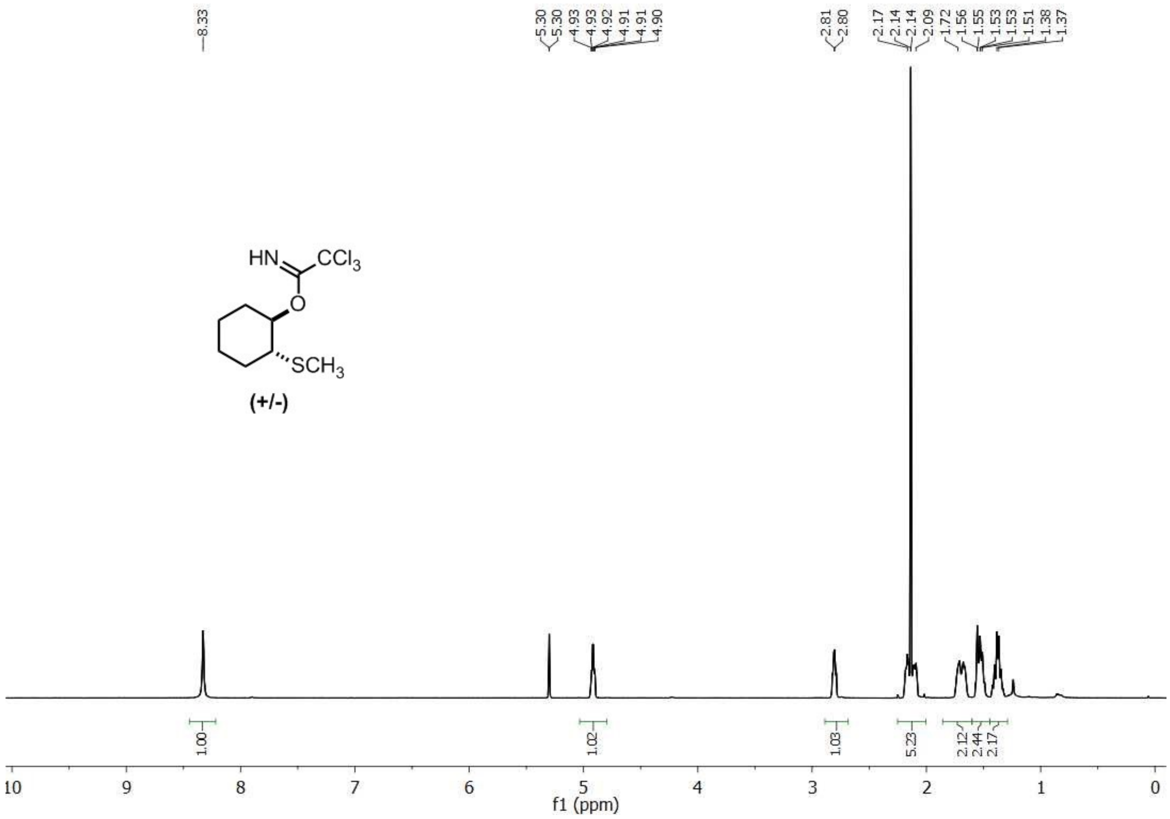
8.33
5.30
5.30
4.93
4.93
4.92
4.91
4.91
4.90
2.81
2.80
2.17
2.14
2.14
2.09
1.72
1.56
1.55
1.53
1.53
1.51
1.38
1.37
HN
CCl3
O
SCH3
(+/-)
1.00
1.02
1.03
5.23
2.12
2.44
2.17
10
9
8
7
6
5
4
3
2
1
0
f1 (ppm)

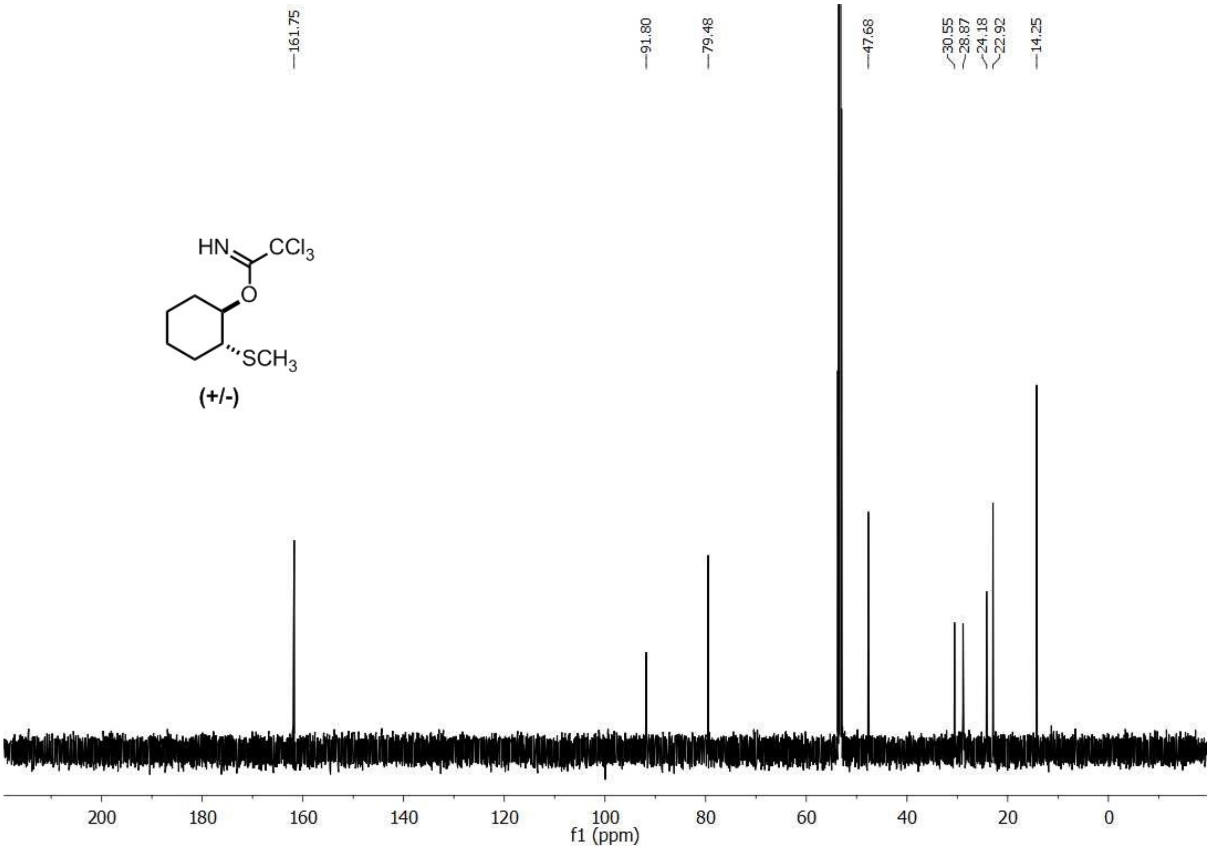
161.75
91.80
79.48
47.68
30.55
28.87
24.18
22.92
14.25
HN
CCl3
O
SCH3
(+/-)
200
180
160
140
120
100
80
60
40
20
0
f1 (ppm)

6.4.2. Asymmetric Ring Opening of an Episulfonium Ion Generated from 3 Catalyzed by Complex 1

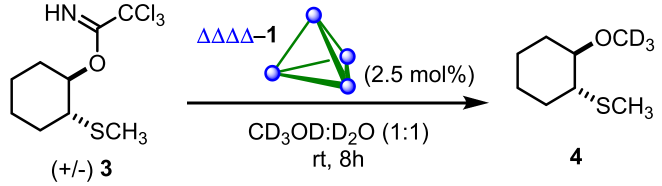

Compounds **3** (11.6 mg, 0.04 mmol, 40 equiv.) and **1** (4.83 mg, 0.001 mmol, 1 equiv.) were combined and dissolved/suspended in a solvent mixture of CD_3OD:D_2O (1:1, 0.5 mL) buffered at pD = 9.00. The resulting heterogeneous solution was then transferred to an NMR tube and capped with a plastic top. The reaction progress was then monitored by ^{1}H NMR spectroscopy (see below) and after 8 h at room temperature, complete consumption of **3** was observed. The reaction solution was then diluted with water (5 mL) and extracted with $CDCl_3$ (1.0 mL). The organic solution was then dried with $MgSO_4$ and filtered. To the resulting solution was added 1,3,5-trimethoxybenzene (6.7 mg, 0.04 mmol) as an internal standard and the yield of **4** was determined by ^{1}H NMR spectroscopy. The desired compound **4** was obtained in 98% yield and 21% ee. ^{1}H NMR (500 MHz, $CDCl_3$) δ (ppm) 3.05 (m, 1H), 2.56 (ddd, *J* = 8.1, 3.6 Hz, 1H), 2.16 (s, 3H), 2.10-2.05 (m, 2H), 1.73-1.65 (m, 2H), 1.38-1.35 (m, 1H), 1.28-1.24 (m, 3H). ^{13}C NMR (125 MHz, $CDCl_3$) δ (ppm) 83.1, 55.9 (pentet), 50.1, 31.3, 30.4, 25.3, 23.8, 14.9. IR [neat, ν_{max} (cm^{-1})]: 1726, 1447, 1126, 847, 769, 704 cm^{-1}. HRMS (*m/z*): calculated for $[C_8H_{13}D_3OS,]^+$, 163.1110; observed, 163.1109.

6.4.3. Stacked ^{1}H NMR spectra of reaction between 3 and host 1 to give 4 as monitored by ^{1}H NMR spectroscopy

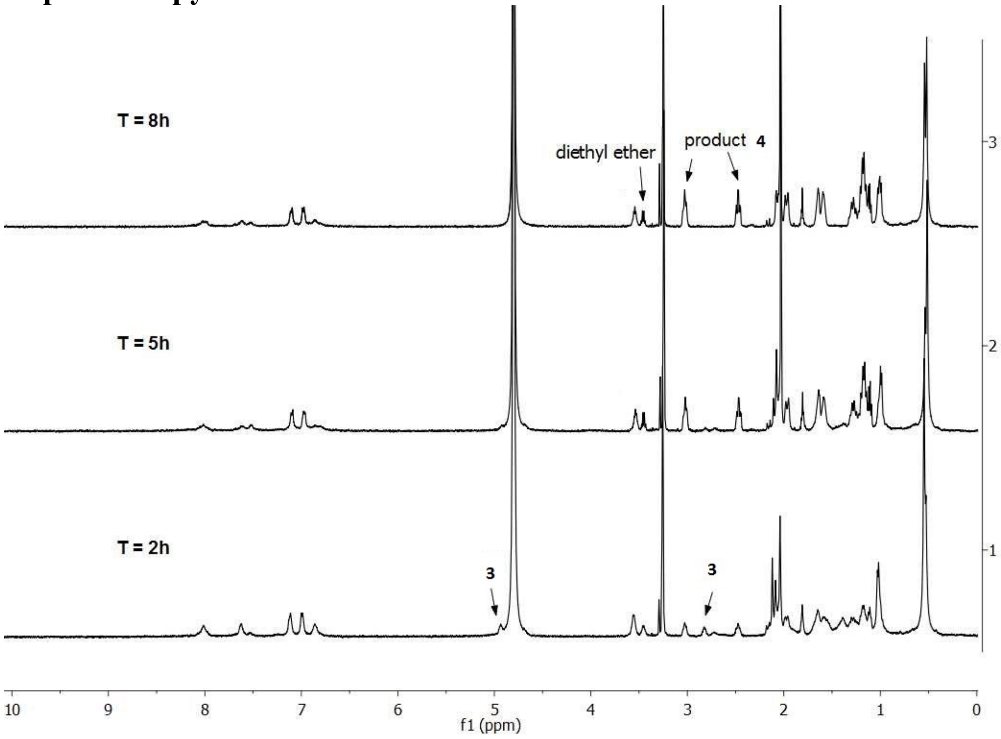

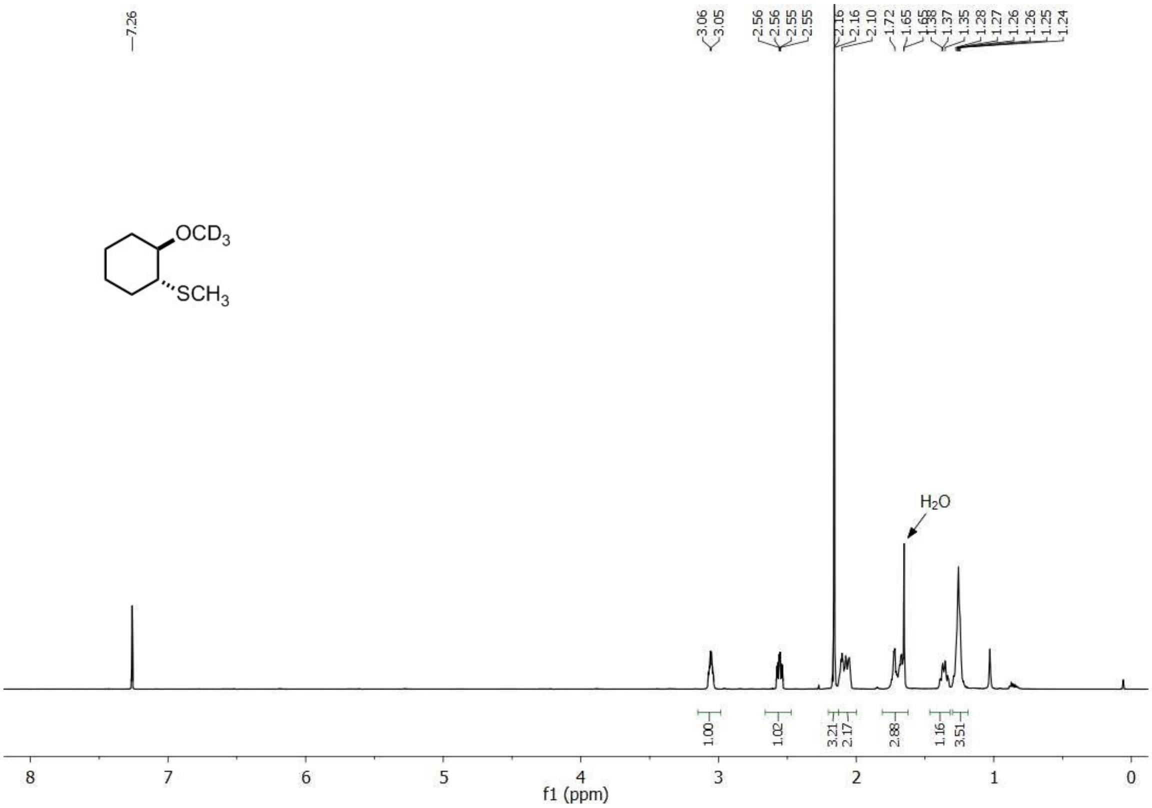
7.26
3.06
3.05
2.56
2.56
2.55
2.55
2.16
2.16
2.10
1.72
1.65
1.65
1.38
1.37
1.35
1.28
1.27
1.26
1.26
1.25
1.24
OCD3
SCH3
H2O
1.00
1.02
3.21
2.17
2.88
1.16
3.51
8
7
6
5
4
3
2
1
0
f1 (ppm)

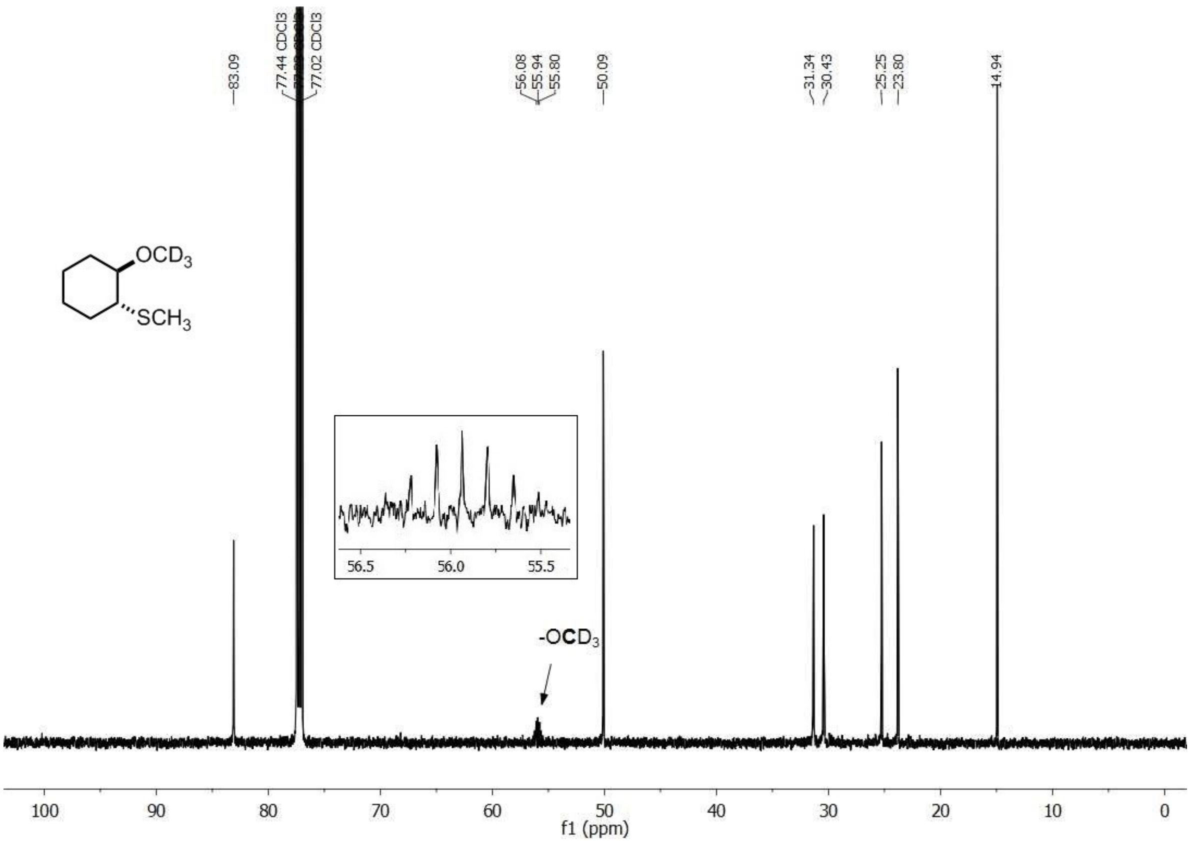
83.09
77.44 CDCl3
77.02 CDCl3
56.08
55.94
55.80
50.09
31.34
30.43
25.25
23.80
14.94
OCD3
SCH3
56.5
56.0
55.5
-OCD3
100
90
80
70
60
50
40
30
20
10
0
f1 (ppm)

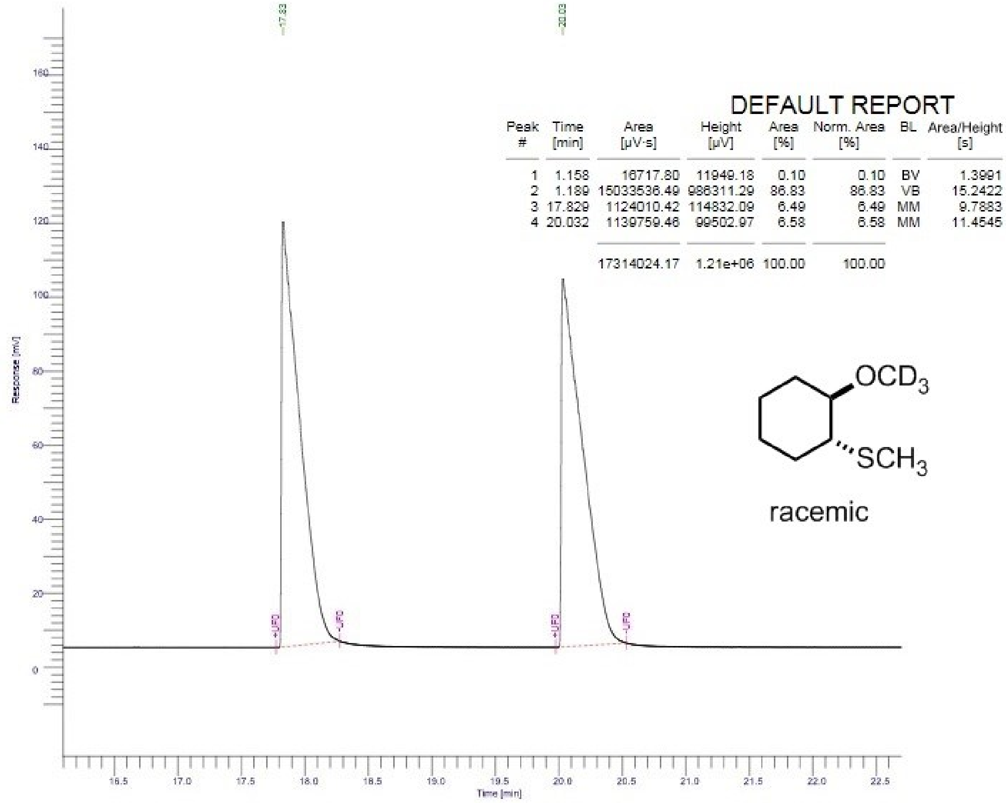

DEFAULT REPORT

Peak #	Time [min]	Area [µV·s]	Height [µV]	Area [%]	Norm. Area [%]	BL	Area/Height [s]
1	1.158	16717.80	11949.18	0.10	0.10	BV	1.3991
2	1.189	15033536.49	986311.29	86.83	86.83	VB	15.2422
3	17.829	1124010.42	114832.09	6.49	6.49	MM	9.7883
4	20.032	1139759.46	99502.97	6.58	6.58	MM	11.4545
		17314024.17	1.21e+06	100.00	100.00		

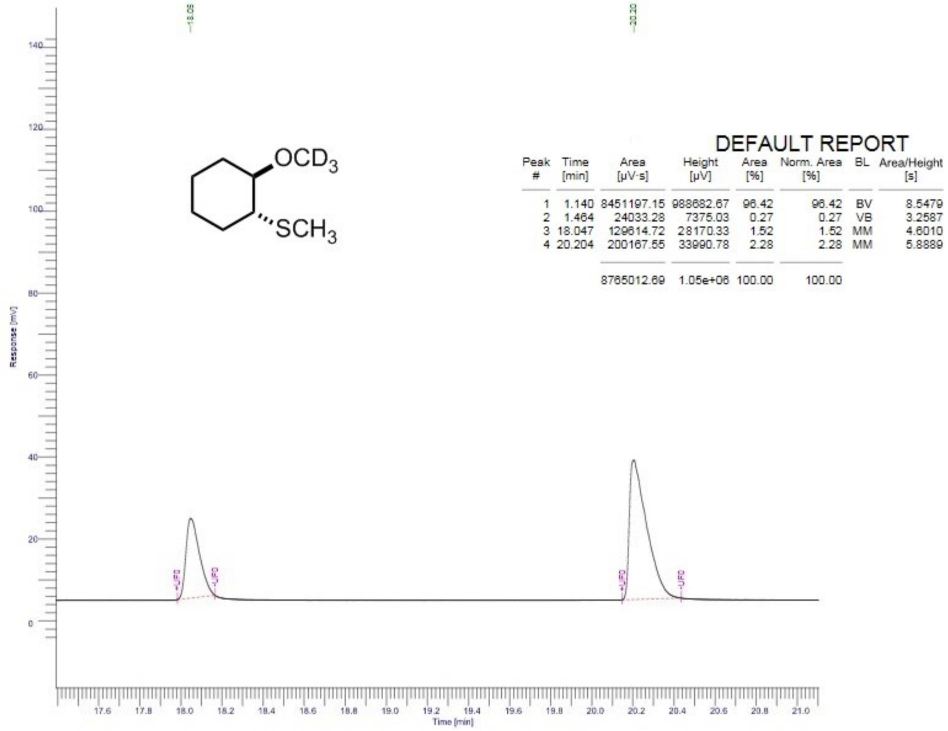

DEFAULT REPORT

Peak #	Time [min]	Area [µV·s]	Height [µV]	Area [%]	Norm. Area [%]	BL	Area/Height [s]
1	1.140	8451197.15	988682.67	96.42	96.42	BV	8.5479
2	1.464	24033.28	7375.03	0.27	0.27	VB	3.2587
3	18.047	129614.72	28170.33	1.52	1.52	MM	4.6010
4	20.204	200167.55	33990.78	2.28	2.28	MM	5.8889
		8765012.69	1.05e+06	100.00	100.00		

6.4.4. Reaction of 3, complex 5 and Me_4NCl

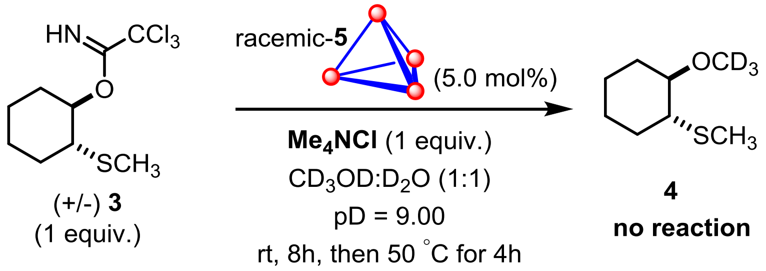
HN
CCl3
O
SCH3
(+/-) 3
(1 equiv.)
racemic-5
(5.0 mol%)
Me4NCl (1 equiv.)
CD3OD:D2O (1:1)
pD = 9.00
rt, 8h, then 50 °C for 4h
OCD3
SCH3
4
no reaction

Compound **3** (11.6 mg, 0.04 mmol, 20 equiv.), complex **5** (7.2 mg, 0.002 mmol, 1 equiv.) and Me_4NCl (4.4 mg, 0.04 mmol, 20 equiv.) were combined and dissolved/suspended in a solvent mixture of CD_3OD:D_2O (1:1, 0.5 mL) buffered at pD = 9.00. The resulting heterogeneous solution was then transferred to an NMR tube and capped with a plastic top. The reaction progress was then monitored by ^1H NMR spectroscopy, and after 8 h at room temperature, no formation of **4** was observed. The reaction mixture was then heated to 50 °C for 4h, after which time, no formation of **4** was observed as analyzed by ^1H NMR spectrum (see below).

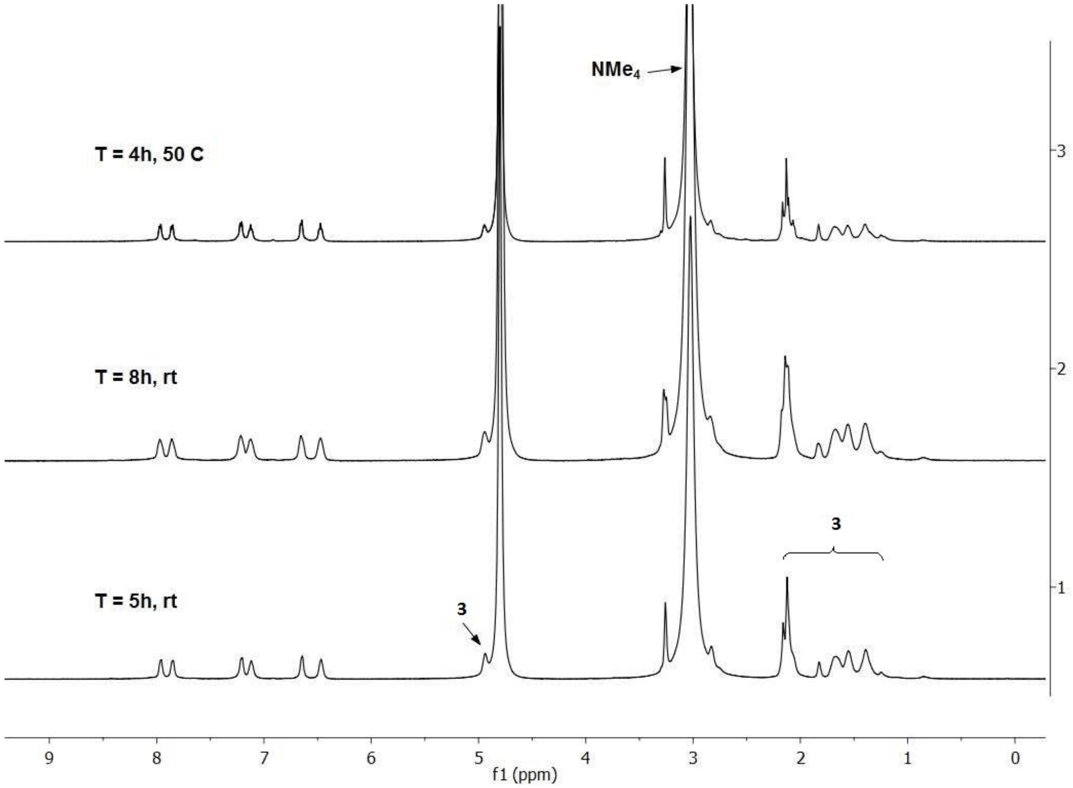

6.4.5. Enantioslective Monoterpene-like Cyclization Catalyzed by Complex 1

Substrate **6a** and **6b** were synthesized according to literature procedures.

Representative procedure: Compound **6a** (6.73 mg, 0.04 mmol, 40 equiv.) and **1** (4.83 mg, 0.001 mmol, 1 equiv.) were combined and dissolved/suspended in a solvent mixture of $CD_3OD:D_2O$ (1:1, 0.5 mL) buffered at pD = 8.00. The resulting heterogeneous solution was then transferred to an NMR tube and capped with a plastic top. The reaction progress was then monitored by ^1H NMR spectroscopy and after 50 h at room temperature, the reaction seemed to have stopped. The reaction mixture was then diluted with water (5 mL) and extracted with DCM (3 x 1.0 mL). The organic layer was then dried with $MgSO_4$ and filtered. Solvent was then removed by a gentle nitrogen stream to give 6.3 mg of the crude product mixture. The residue was dissolved in 0.5 mL of $CDCl_3$ and analyzed by ^1H NMR spectroscopy as shown below. It was previously reported that the reaction has near perfect mass balance, therefore the yield of **7a** was determined by relative integration of the starting material's and product's proton signals as analyzed by ^1H NMR spectroscopy. The enantiomeric excess of **7a** was determined by chiral GC analysis: 61% ee by chiral GC fitted with γ-TA column, 1 °C per minute from 70 °C to 110 °C, tr (minor) 24.3 min, tr (major) 24.78).

^1H NMR spectrum of the crude product mixture of reaction between 6a and complex 1

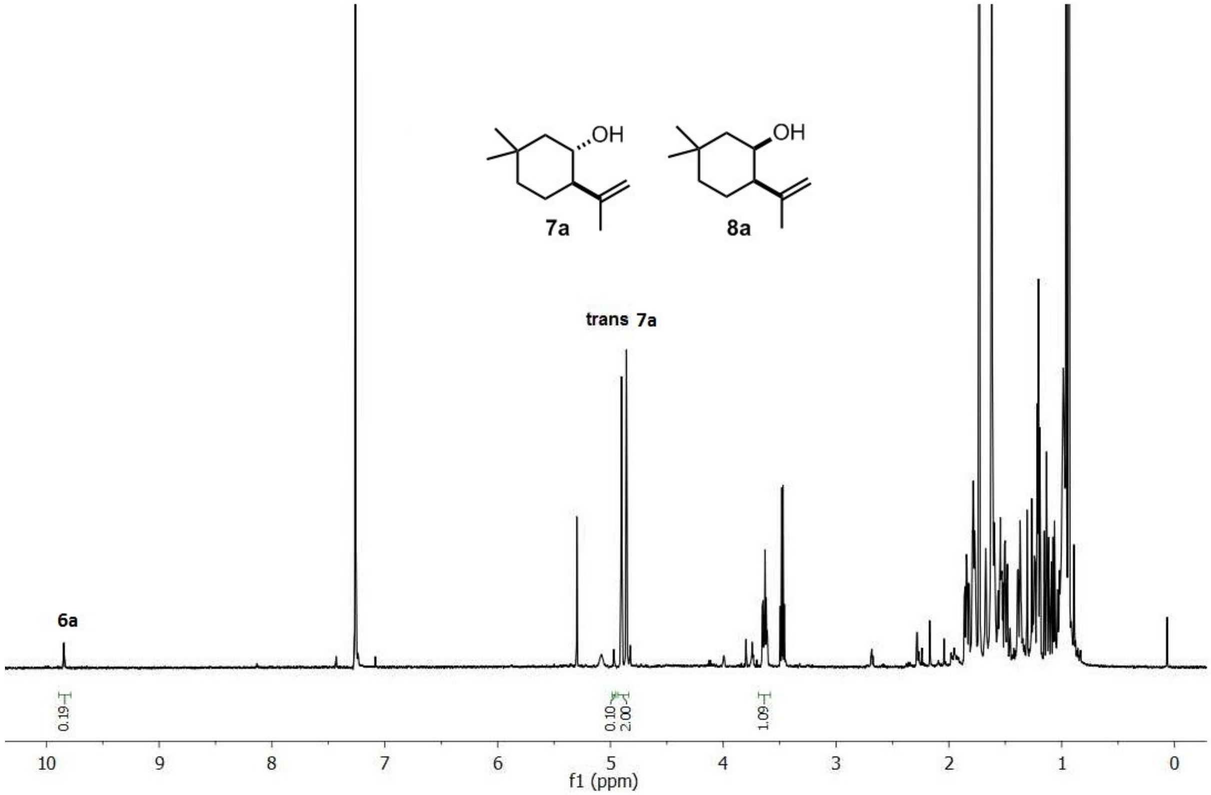

^{1}H NMR spectrum of the crude product mixture of reaction between 6b and 1 at pD 5

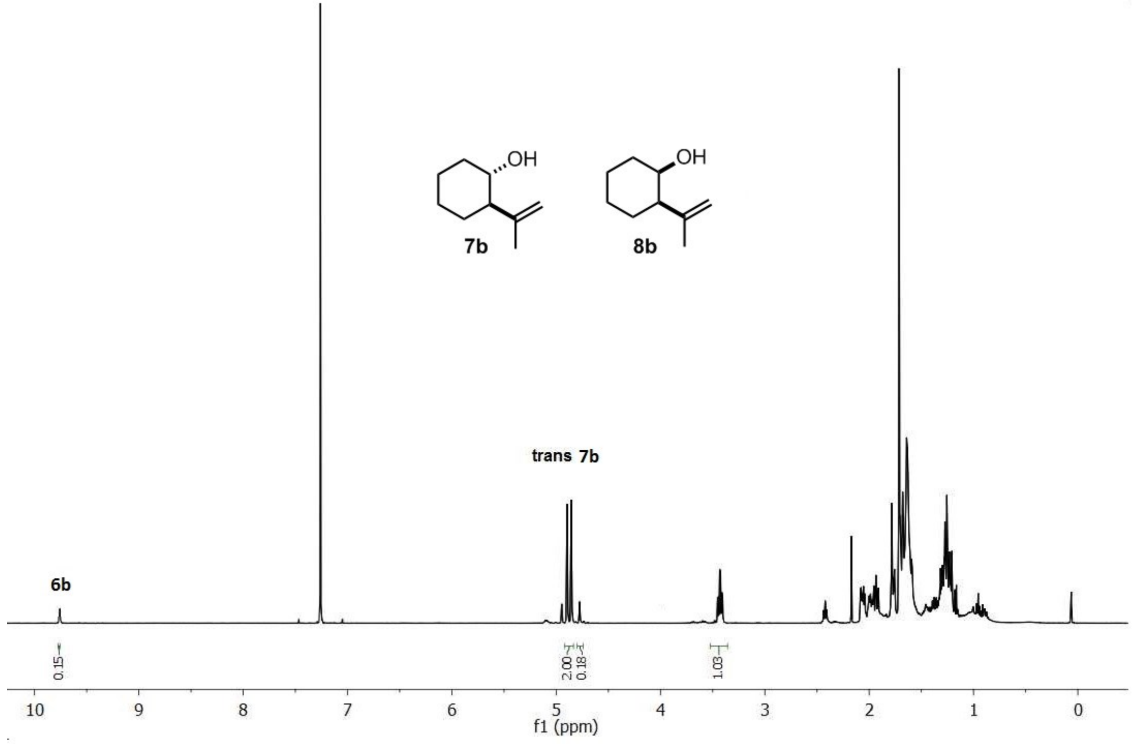

^{1}H NMR spectrum of the crude product mixture of reaction between 6b and 1 at pD 8

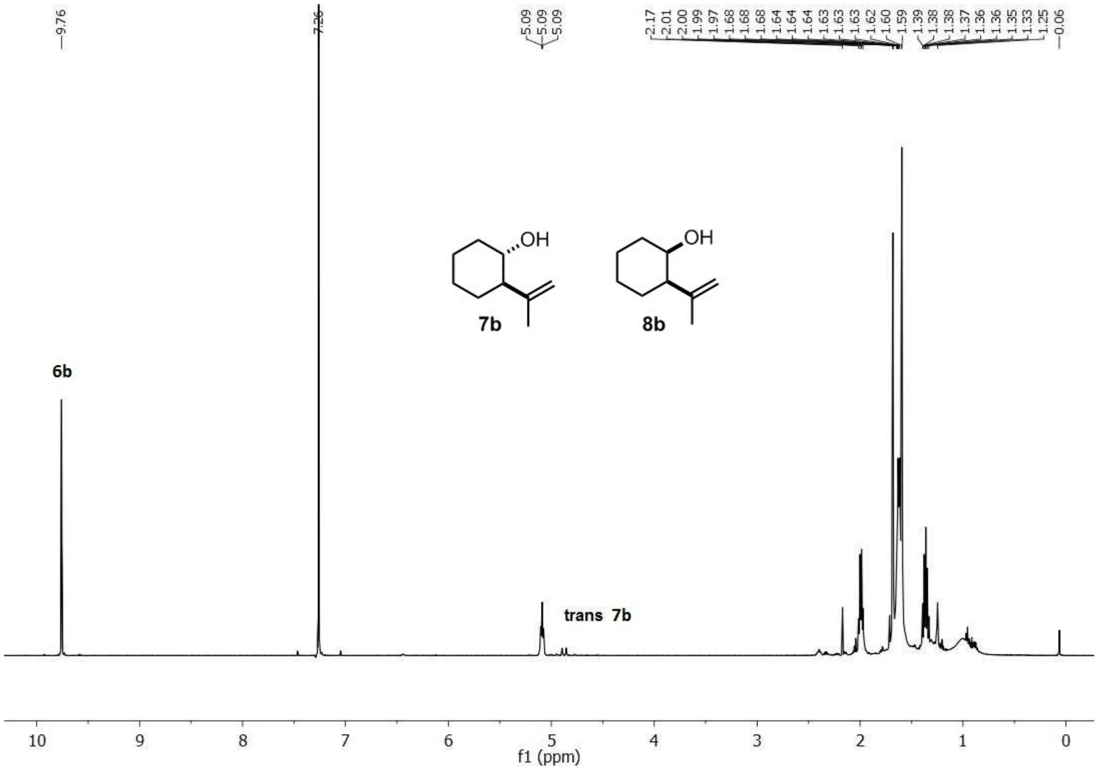

6.4.6. Rate Comparison for the Cyclization of 7a Catalyzed by Complex 1 and Complex 5

In 0.25 mL D_2O (buffered with 100 mM phosphate buffer) and 0.25 mL MeOD-d_4, complex **1** or complex **5** (1 μmol) was treated with 7 (4.8 mg, 29 μmol). The resulting solution was transferred to an NMR tube, which was inserted into a preheated NMR probe (40 °C). After a two minute temperature equilibration period, ^{1}H NMR spectra (one scan each) were acquired every 30 seconds for three hours (with complex **5**) or ten hours (with complex **1**). Starting material, product and catalyst concentrations were measured by reference to an internal standard of MeOD-d_1. The percent conversion over time is given in the plot below, from which relative first order rate constants were obtained. The reaction catalyzed by complex **1** was measured to be about 7-fold faster than reaction catalyzed by complex **5**.

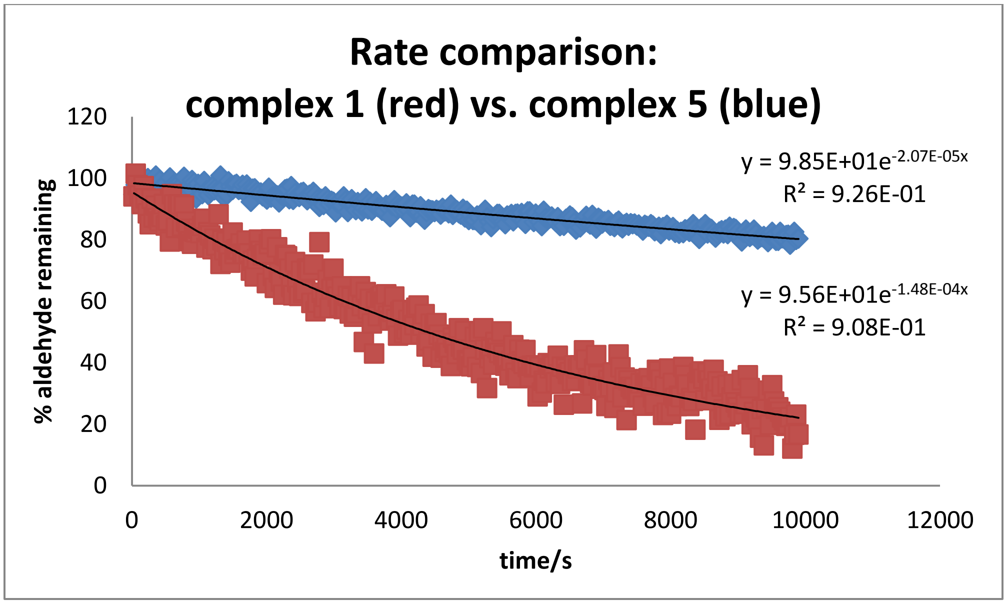

6.4.7. Enantioselective Aza-Cope Rearrangement Reactions Catalyzed by Complex 6

Substrates **9a-d** were synthesized according to literature known methods.[14]

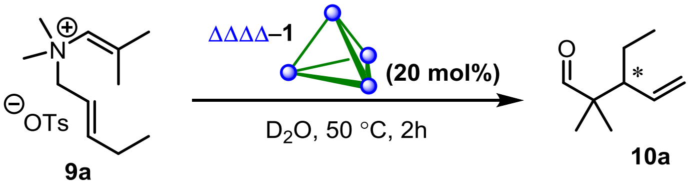

Enammonium tosylate **9a** (5.1 mg, 0.015 mmol, 5 equiv.), complex **1** (14.5 mg, 0.003 mmol, 1 equiv.) and Me_4NCl (6.6 mg, 0.06 mmol, 20 equiv.) were dissolved in D_2O (0.5 mL) and loaded into a vial fitted with a stir bar and plastic cap. The reaction vial was then heated at 50 °C for 2 h. The mixture was then cooled to room temperature and diluted with water (5 mL). The aqueous solution was then extracted with toluene-d_8 (1.0 mL) and the organic phase was dried with $MgSO_4$ and filtered. To the resulting solution was then added 1,3,5-trimethoxybenzne (2.5 mg, 0.015 mmol) as an internal standard and the yield was determined by ^{1}H NMR spectroscopy. The desired aldehyde **10a** was obtained in 86% yield and 37% ee, and its spectroscopic data are in agreement with literature reported values.[6,14]

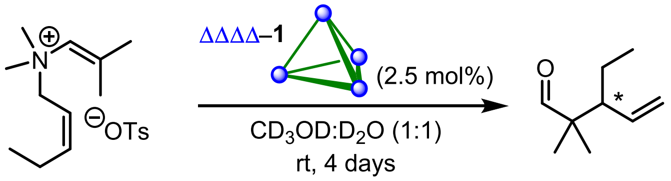

9c **10c**

Enammonium tosylate **9c** (13.5 mg, 0.04 mmol, 40 equiv.) and complex **1** (5.0 mg, 0.001 mmol, 1 equiv.) were dissolved in a solvent mixture of D_2O:CD_3OD (1:1) buffered at pD = 9.00 and loaded into a NMR tube capped with a plastic top. The reaction tube was left at room temperature and the reaction progress was monitored by ^1H NMR spectroscopy. After 96 h, **9c** was completely consumed as observed by NMR, and the reaction mixture was diluted with water and extracted with toluene-d_8 (1.0 mL). 1,3,5-trimethoxybenzene (6.7 mg, 0.04 mmol) was then added as an internal standard and the yield was determined by ^1H NMR spectroscopy. The desired aldehyde **10c** was obtained in 87% yield and 47% ee, and its spectroscopic data are in agreement with literature reported values.[6,14]

Spectroscopic data of compounds **9b, 9d, 10b** and **10d** are all in agreements with literature reported values.[6,14]

6.5. References

(1) Yoshizawa, M.; Tamura, M.; Fujita, M. *Science* **2006**, *312*, 251-254.
(2) Hastings, C. J.; Pluth, M. D.; Bergman, R. G.; Raymond, K. N. *J. Am. Chem. Soc.* **2010**, *132*, 6938-6940.
(3) Liu, T.; Liu, Y.; Xuan, W.; Cui, Y. *Angew. Chem., Int. Ed.* **2010**, *49*, 4121-4124.
(4) Bolliger, J. L.; Belenguer, A. M.; Nitschke, J. R. *Angew. Chem., Int. Ed.* **2013**, *52*, 7958-7962.
(5) Chepelin, O.; Ujma, J.; Wu, X.; Slawin, A. M. Z.; Pitak, M. B.; Coles, S. J.; Michel, J.; Jones, A. C.; Barran, P. E.; Lusby, P. J. *J. Am. Chem. Soc.* **2012**, *134*, 19334-19337.
(6) Brown, C. J.; Bergman, R. G.; Raymond, K. N. *J. Am. Chem. Soc.* **2009**, *131*, 17530-17531.
(7) Nishioka, Y.; Yamaguchi, T.; Kawano, M.; Fujita, M. *J. Am. Chem. Soc.* **2008**, *130*, 8160-8161.
(8) Zhao, C.; Sun, Q.-F.; Hart-Cooper, W. M.; DiPasquale, A. G.; Toste, F. D.; Bergman, R. G.; Raymond, K. N. *J. Am. Chem. Soc.* **2013**, *135*, 18802-18805.
(9) Hamilton, G. L.; Kanai, T.; Toste, F. D. *J. Am. Chem. Soc.* **2008**, *130*, 14984-14986.
(10) Lin, S.; Jacobsen, E. N. *Nature Chemistry* **2012**, *4*, 817-824.
(11) Dong, V. M.; Fiedler, D.; Carl, B.; Bergman, R. G.; Raymond, K. N. *J. Am. Chem. Soc.* **2006**, *128*, 14464-14465.
(12) Hart-Cooper, W. M.; Clary, K. N.; Toste, F. D.; Bergman, R. G.; Raymond, K. N. *J. Am. Chem. Soc.* **2012**, *134*, 17873-17876.
(13) Manuscript in prepreation.
(14) Fiedler, D.; van Halbeek, H.; Bergman, R. G.; Raymond, K. N. *J. Am. Chem. Soc.* **2006**, *128*, 10240-10252.
(15) Merdanovic, M.; Mönig, T.; Ehrmann, M.; Kaiser, M. *ACS Chem. Bio.* **2012**, *8*, 19-26.
(16) Kovbasyuk, L.; Krämer, R. *Chem. Rev.* **2004**, *104*, 3161-3188.

Chapter 7. Nucleophilic Substitution Catalyzed by a Supramolecular Cavity Proceeds with Retention of Absolute Stereochemistry

7.1 Introduction

As one of the fundamental transformations of organic chemistry, the nucleophilic substitution reaction can be defined as the displacement of an electron pair acceptor (leaving group) with an electron pair donor (nucleophile or entering group). When the reaction takes place at an *sp*^{3}-hybridized carbon atom, the mechanism is classified with reference to two canonical pathways (S_N1 and S_N2) that furnish products with different stereochemical outcomes.[1] One mechanism, favored with substrates where a developing carbocation can be stabilized through hyperconjugation or extensive π-delocalization from the neighboring substituents, is typically characterized by the initial generation of a planar *sp*^{2}-hybridized carbocation and subsequent attack by a nucleophile from either side of the intermediate to give highly racemized product [1-4]. In contrast, the other mechanism involving simple primary and secondary substrates is stereospecific and substitution proceeds through a transition state *via* backside attack of the carbon reaction center by nucleophile to yield products with inversion of stereochemistry.[1,5-9] This includes the overwhelming majority of solvolyses at simple secondary benzylic centers.[10-16]

In recent decades, synthetic chemists have drawn inspiration from nature to design supramolecular host complexes that mimic the properties of enzymes.[17-21] Some of these properties include the ability to induce pK_a shifts and maintain function in aqueous environments at physiological pH.[22] More importantly, many such species contain well-defined and sterically constrictive binding pockets capable of stabilizing otherwise reactive species via encapsulation.[23,24] Such complexes can thus catalyze chemical reactions with selectivity different from that observed in bulk solution reactivity.[19,25-29] We report herein an unprecedented example of a nucleophilic substitution reaction of secondary benzylic substrates catalyzed by $K_{12}Ga_4L_6$ supramolecular host complexes that proceeds with overall *stereochemical retention*.

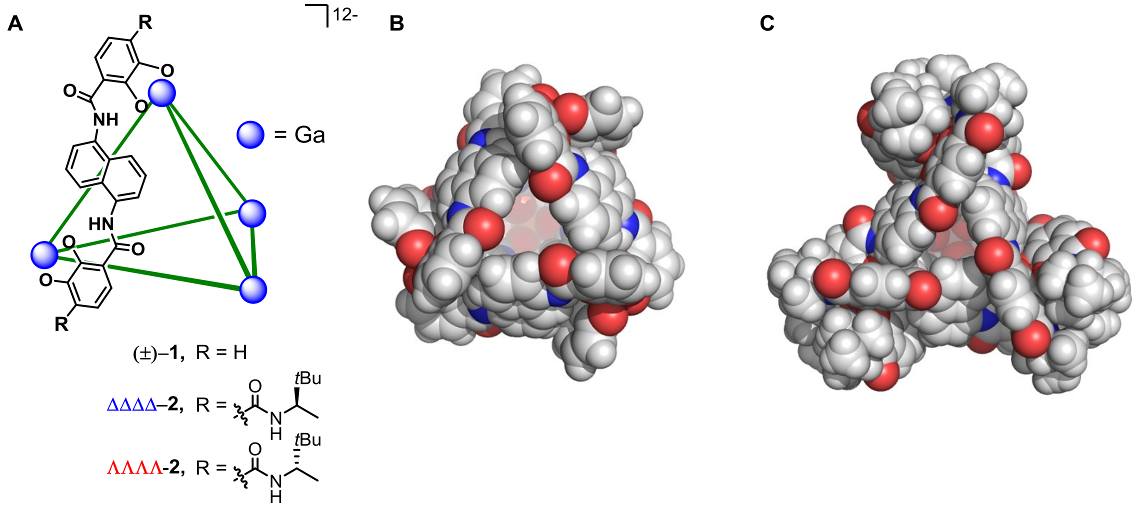

Figure 7.1. (A) Schematic representations of the Ga_4L_6 assemblies **1** and **2** with only one ligand shown for clarity. (B) X-ray crystal structure of ΛΛΛΛ-**1**. (C) X-ray crystal structure of ΔΔΔΔ-**2**.

7.2. Results and Discussion

In a continuing effort to better understand the enzyme-like behavior of our synthetic nanovessels and explore their application as catalysts for organic synthesis, we initially sought to examine the ability of **2**'s cavity to stabilize carbocations and affect their asymmetric nucleophilic addition. We envisioned that compound **3** would be a suitable substrate to test our hypothesis since the trichloroacetimidate functional group has been utilized in organic synthesis as an acid-activated leaving group. Although the activation of such a functional group in bulk solution requires the use of strong organic acids, such as 4-nitrobenzensulfonic[30] and phosphoric acids,[31] we recently showed that host **2** is capable of both encapsulating trichloroacetimidate-containing molecules as well as promoting their activation.[32] Thus, initial reaction between substrate **3** and 5 mol% of **ΔΔΔΔ-2** in CD_3OD carried out at room temperature for 124 hours gave the desired benzyl ether product **4** in high yield and 15% ee (Fig 2A). Though no encapsulated species were observed by ^1H NMR spectroscopy during the course of the reaction, experiments with either PEt_4-blocked **2** or no catalyst led to only trace amounts of product **4**, strongly suggesting that the formation of enantioenriched benzyl ether **4** from racemic **3** is catalyzed by the cavity of **2**.

The low enantioselectivity of the overall transformation prompted us to investigate the possibility of a concerted back-side attack mechanism since substitution reactions of trichloroacetimidate have been reported to proceed by such pathways in bulk solution.[30] Indeed, the reaction of enantiopure (***S***)**-3** with 5 mol% of the bulky and achiral phosphoric acid **5** in CD_3OD at room temperature gave the desired benzyl ether **4** in quantitative yield with an expected 84% inversion of stereochemistry, or a 5.25:1 ratio of (***R***)-**4** to (***S***)-**4**, at the substituted carbon atom. Surprisingly, repeating the substitution reaction of (***S***)**-3** in the presence of 5 mol% of **ΔΔΔΔ-2** proceeded at 50 ºC to give **4** in high yield with 74% *retention of stereochemistry*. Control experiments of (***S***)**-3** with either PEt_4-blocked **2** or no catalyst gave only trace amounts of product **4** with inversion of stereochemistry. Although the capacity of supramolecular host complexes to alter reactivity and selectivity via encapsulation during the course of reactions is well-documented, the ability of complex **2** to completely change the stereochemical outcome of a known S_N2 reaction to give products with high levels of overall retention is unprecedented.

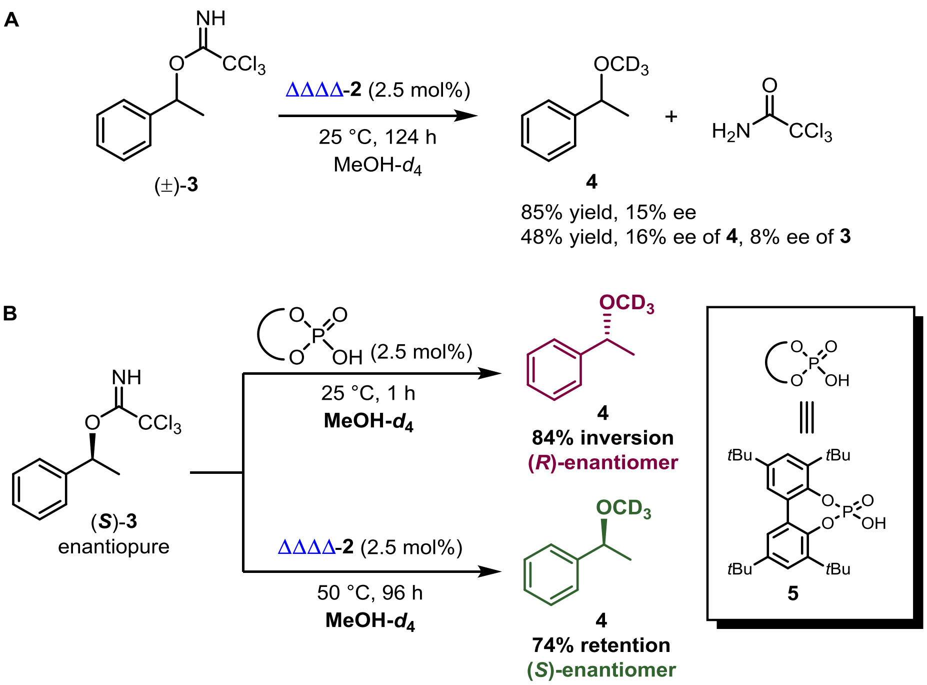
A
NH
O
CCl3
(±)-3
ΔΔΔΔ-2 (2.5 mol%)
25 °C, 124 h
MeOH-d4
OCD3
4
+
O
H2N
CCl3
85% yield, 15% ee
48% yield, 16% ee of 4, 8% ee of 3
B
NH
O
CCl3
(S)-3
enantiopure
O
O
P
O
OH (2.5 mol%)
25 °C, 1 h
MeOH-d4
OCD3
4
84% inversion
(R)-enantiomer
ΔΔΔΔ-2 (2.5 mol%)
50 °C, 96 h
MeOH-d4
OCD3
4
74% retention
(S)-enantiomer
tBu
tBu
tBu
tBu
OH
5

Figure 7.2. (A) Substitution reaction of racemic **3** catalyzed by host ΔΔΔΔ-**2**. (B) Catalyst controlled divergent stereospecific substitutions of (***S***)-**3**.

We next attempted this substitution with retention reaction in a co-solvent system of 1:1 mixture of CD_3OD/D_2O buffered at pD 8 to neutralize any potential acid that could be generated and ensure that the desired reactions take place inside the cavities of the host complexes. Although complexes **1** and **2** have been shown to exclude water from their cavities due to the hydrophobic effect, hydrolysis of **3** inside the cavity of the host catalysts to give **6** can occur. Indeed, reaction of (***S***)**-3** with either ΔΔΔΔ**-2** or ΛΛΛΛ-**2** as the catalyst at 50 ºC gave a mixture of the desired ether product **4** with improved selectivity for the retention product (***S***)**-4** (Fig. 3A, entries 1 and 2) and the corresponding alcohol **6**. When host **1** (30 mol%) was used as the catalyst, substitution of **(*S*)-3** also proceeded to give **4** with a high level of retention (90%). Longer reaction times were required for substitutions of **3** at room temperature in the presence of either racemic or enantiopure host complexes (Fig. 3A, entries 4 and 5). Similarly, reactions of enantiopure (***R***)-**3** in the presence of supramolecular assemblies **1** and **2** also gave the desired ether product with moderate to high levels of stereochemical retention (Fig. 3B). Lastly, control reactions of either (***S***)**-3** in the presence of PEt_4-blocked **2** gave low yields of product **4** with inversion of stereochemistry (Figure 3A, entry 6).

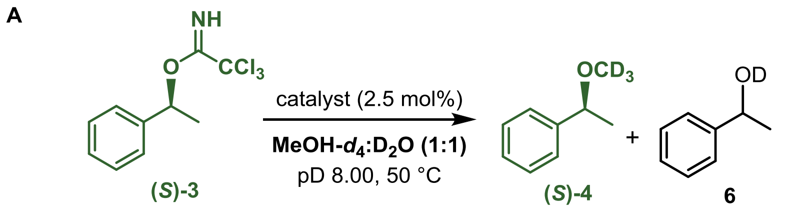

Entry	Catalyst	Time (h)	Yield (%)	Ratio of **4**:**6**[a]	*er* of **4**[b] (*S*) : (*R*)	*er* of **6**[b] (*S*) : (*R*)
1	ΛΛΛΛ–**2**	**24**	**95**	**72:28**	**85:15**	**78:22**
2	ΔΔΔΔ–**2**	**24**	**90**	**70:30**	**88:12**	**73:27**
3[c]	**(±)-1**	**16**	**99**	**78:22**	**90:10**	**75:25**
4[d,e]	**(±)-1**	96	93	67:33	64:36	53:47
5[e]	ΔΔΔΔ–**2**	96	78	68:32	74:26	42:58
6	(PEt$_4$)$_{12}$Δ$_4$**2**	24	21	50:50	19:81	10:90
7	none	24	25	50:50	24:76	27:73

[a] Product ratios were determined with ^{1}H NMR spectroscopy with an error limit estimated to be +/- 2.5%. [b] Enantiomeric ratios were determined by GC fitted with a chiral column with an error limit estimated to be about +/- 2.5%. [c] 30 mol% catalyst used. [d] 5 mol% catalyst used. [e] Reaction at 25 °C.

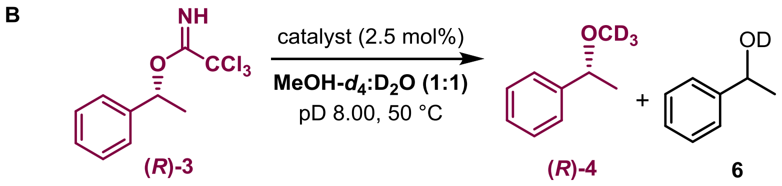

Entry	Catalyst	Time (h)	Yield (%)	Ratio of **4**:**6**[a]	*er* of **4** (*R*) : (*S*)	*er* of **6** (*R*) : (*S*)
1	ΛΛΛΛ–**2**	24	95	75:25	83:17	67:33
2	ΔΔΔΔ–**2**	24	92	70:30	87:12	72:28
3[c]	ΛΛΛΛ–**2**	**16**	**99**	**80:20**	**92:8**	**74:26**
4[d]	(±)-**1**	**24**	**94**	**81:19**	**92:8**	**88:12**
5[d,e]	**5**	1	99	95:5	15:85	--
6	none	24	22	47:53	20:80	18:82

[a] Product ratios were determined with ^{1}H NMR spectroscopy with an error limit estimated to be about +/- 2.5%. [b] Enantiomeric ratios were determined by GC fitted with a chiral column with an error limit estimated to be about +/- 2.5%. [c] 10 mol% catalyst used. [d] 30 mol% catalyst used. [e] Reaction performed at 25 °C in 100% MeOH-*d*$_4$.

Figure 7.3. Stereoretentive substitution reactions of **(*S*)-3** and **(*R*)-3** catalyzed by supramolecular Ga$_4$L$_6$ hosts **1**, **ΛΛΛΛ-2**, and **ΔΔΔΔ-2**.

We next turned our attention to the substitution reaction of benzyl chloride substrate **7** catalyzed by supramolecular host complexes. Initial reaction of racemic **7** in the presence of **ΛΛΛΛ-2** gave the desired ether product **4** with 14% ee (Fig. 4A), similar to the results obtained with racemic **3** (Fig. 2A). Repeating the reaction with the other enantiomer of the catalyst, **ΔΔΔΔ-2**, gave **4** with the same enantiomeric excess but in the opposite direction. More importantly, the substitution of enantioenriched **7** catalyzed by either **ΛΛΛΛ-2** or **ΔΔΔΔ-2** proceeded to give **4** in high yields and with high levels of stereochemical retention (Fig. 4B), and reaction without any assembly gave the ether product **4** with inversion.

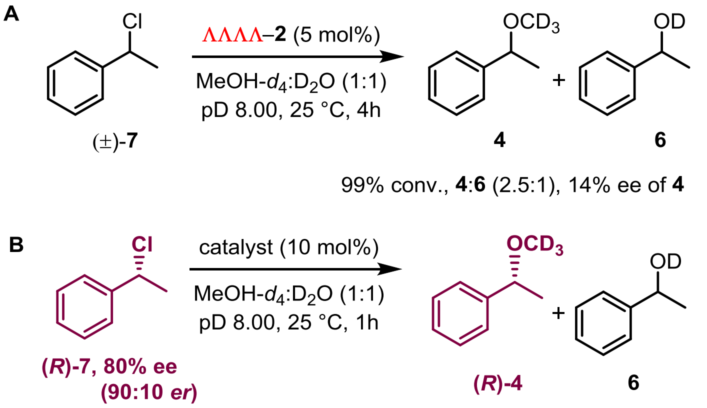
A
Cl
ΛΛΛΛ–2 (5 mol%)
MeOH-d_4:D_2O (1:1)
pD 8.00, 25 °C, 4h
OCD$_3$
OD
+
(±)-7
4
6
99% conv., 4:6 (2.5:1), 14% ee of 4
B
Cl
catalyst (10 mol%)
MeOH-d_4:D_2O (1:1)
pD 8.00, 25 °C, 1h
OCD$_3$
OD
+
(R)-7, 80% ee
(90:10 er)
(R)-4
6

Entry	Catalyst	Yield (%)	Ratio of **4**:**6**[a]	*er* of **4**[b] (*R*) : (*S*)	% retention from **7** to **4**	*er* of **6**[b] (*R*) : (*S*)
1	ΔΔΔΔ–**2**	94	75:25	82:18	**91**	71:29
2	ΛΛΛΛ–**2**	96	72:28	84:16	**93**	76:24
3	none	84	55:45	32:68	**35**	36:64
4[c]	ΛΛΛΛ–**2**	99	75:25	72:28	**92**	76:24

[a] Product ratios were determined by ^1H NMR spectroscopy with an error limit estimated to be about 5%. [b] Enantiomeric ratios were determined by GC fitted with a chiral column with an error limit estimated to be about 5%. [c] Reaction was performed with substrate **7** with an enantiomeric ratio (*er*) of 78:22 for (*R*):(*S*).

Figure 7.4. (A) Nucleophilic substitution of racemic benzyl chloride **7** catalyzed by **ΔΔΔΔ-2**. (B) Retentive substitution of enantioenriched **7** catalyzed by either **ΛΛΛΛ-2** or **ΔΔΔΔ-2**.

We also wanted to demonstrate the encapsulation of a benzyl ammonium compound **8** that has a size similar to that of the reactive substrates in the presence of supramolecular host complex **1** (eq. 1). Under stoichiometric conditions, compound **8** was readily encapsulated by **1** as observed by ^1H NMR spectroscopy to give host-guest complex **9**. While no further reaction was observed when **9** was heated at 50 ºC to 80 ºC for 4 days, the encapsulation of **8** suggests that such substrate, along with **3** and **7**, are suitable guest molecules for the cavities of supramolecular hosts **1** and **2** in term of their size and volume.

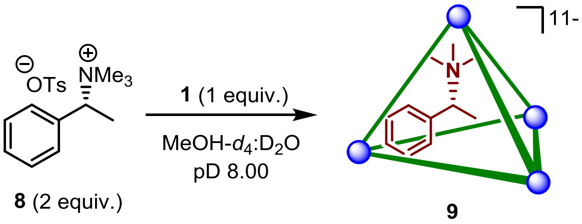
⊖
OTs
⊕
NMe$_3$
1 (1 equiv.)
MeOH-d_4:D_2O
pD 8.00
11-
N
8 (2 equiv.)
9

(eq. 1)

Though the detailed mechanism of this supramolecular host-catalyzed substitution with retention reaction of simple benzylic molecules remains under investigation, the experimental results obtained thus far provide some insights into the origin of such unique reactivity. The same level of enantioselectivity obtained from reactions with racemic **3** and **7** catalyzed by enantiopure **2** suggest that a common intermediate was accessed during the course of reaction. We propose a benzylic carbocation to be this intermediate. Since the cavity of $K_{12}Ga_4L_6$ hosts has been shown to increase the basicity of encapsulated guests, especially nitrogen-containing species, the protonation of the trichloroacetimidate functional group of **3** and its subsequent ionization to give the corresponding carbocation should be considered favorable. Furthermore, we have also reported that PMe_3AuCl can undergo ionization and chloride loss without any added silver source in the presence of host complex **1** to generate the cationic species PMe_3Au^+, which can readily be encapsulated inside **1**.[33] The strong driving force for the formation of $[PMe_3Au^+ \subset \mathbf{1}]$ host-guest complex from PMe_3AuCl could be operative for the analogous encapsulation and ionization of neutral **7** in the presence of host complex **2**.

More importantly, the substitution reactions of enantiopure **3** and enantioenriched **7** catalyzed by **1** or **2** proceed with stereochemical retention regardless of the absolute configuration or enantiopurity of the host complexes. This suggests that the intermediate maintains a strong stereointegrity inside the cavity of the host complexes. We propose that during the course of reaction inside the host catalyst, the electron density of the naphthalene walls stabilizes the developing positive charge on the benzylic carbon in the transition state through cation-π interaction (Fig. 5).[34-38] This results in one face of the intermediate being blocked from nucleophilic attack, and the complexed cation can then be trapped by an external nucleophile faster than the cation can rotate inside the cavity, thus giving product with overall retention of stereochemistry.

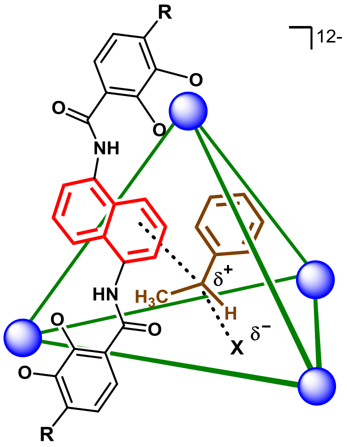

Figure 7.5. A proposed intermediate showing a transient carbocation interacting with only one of the six naphthalene walls through cation-π interactions (where X represents the leaving group).

With the trichloroacetimidate leaving group, an alternative two step mechanism could involve the rearrangement of the trichloroacetimidate functional group to give the corresponding benzylic trichloroacetamide with inversion of stereochemistry, followed by a S_N2-type nucleophilic attack by methanol to afford the overall product with stereochemical retention. However, the acidic environment offered by the cavities of host complexes **1** and **2** should eliminate the nitrogen atom's nucleophilicity by protonation, and the strained nature of the four-membered transition state for the rearrangement is likely too energetically costly even inside the cavity of **1** or **2**. Furthermore, reaction of the isomeric benzylic trichloroacetamide **10**[39] in the presence of 10 mol% of host **1** gave no substitution after heating at 80 ºC for 3 days, and in any case this mechanism is not available to the corresponding chloride.

7.3. Conclusion

Solvolytic displacement reactions that normally undergo inversion of stereochemistry in bulk hydroxylic solvent have their stereochemistry reversed when the substitution takes place within the cavity of $K_{12}Ga_4L_6$ nanovessels. To interpret these results, we propose that the cavity of the host assembly not only can stabilize the developing positively charged intermediate in the transition state through cation-π interaction, but the naphthalene walls of the complex blocks the backside of the carbocation and thereby controls the stereochemical outcome of its substitution to give products with high levels of overall retention. To our knowledge, this observation is unprecedented in the field of catalysis by supramolecular host complexes.

7.4. Experimental

7.4.1. General Information. Unless otherwise noted, all reagents were obtained commercially and used without further purification. All air- and moisture-sensitive compounds were manipulated using standard Schlenk techniques. Reactions were carried out under a nitrogen atmosphere in glassware that was either oven-dried at 150 ^{o}C overnight or flame-dried under nitrogen immediately prior to use. Diethyl ether, tetrahydrofuran and methylene chloride were dried and purified by passage through a column of activated alumina (type A2, 12 x 32, UOP LLC) under a stream of dry nitrogen. Unless otherwise specified, all other reagents were purchased from Acros, Aldrich or Fisher and were used without further purification.

Reaction solutions were magnetically stirred with the exception of those reactions performed in NMR tubes. The majority of experiments were monitored by thin layer chromatography using 0.25 mm pre-coated silica gel plates from Silicycle (TLGR10011B-323) containing a fluorescent indicator for visualization by UV light. Various stains were used to visualize reaction products, including *p*-anisaldehyde, $KMnO_4$ and phosphomolybdic acid in ethanol. Flash chromatography was performed using MP Biomedicals SiliTech silica gel 32-63D.

All NMR spectra were obtained at ambient temperature using Bruker AVB-400, DRX-500, AV-500 and AV-600 spectrometers. ^{1}H NMR chemical shifts are reported relative to residual solvent peaks (7.26 ppm for $CDCl_3$, 5.30 ppm for CD_2Cl_2, 3.31 ppm for CD_3OD, 4.80 for D_2O, 2.50 for DMSO-d_6). ^{13}C NMR chemical shifts were also reported with reference to residual solvent peaks (77.23 ppm for $CDCl_3$, 53.84 for CD_2Cl_2, 49.00 for CD_3OD, 39.52 for DMSO-d_6) Multiplicities of ^{1}H NMR resonances are reported as s = singlet, d = doublet, t = triplet, m = multiplet and br = broad). X-ray crystallographic data was collected on MicroSTAR-H APEX II Cu-Ka Rotating Anode X-ray Diffractometer. Chiral GC analyses were conducted using HP 6850 series GC system fitted with a chiral column, BetaDex 120 Fused Silica Capillary Column (30m x 0.25mm x 0.25um film thickness). UV-Vis absorption spectra were recorded on a Hewlett-Packard 8450A UV/Vis diode array spectrophotometer. Circular dichroism (CD) spectra were measured with a Jasco J-500C spectropolarimeter equipped with an IF-500 II A/D converter. Both low- and high-resolution mass spectral data were obtained from the Micromass/Analytical Facility operated by the College of Chemistry, University of California, Berkeley.

7.4.2. Synthesis of enantiopure (*S*)-3

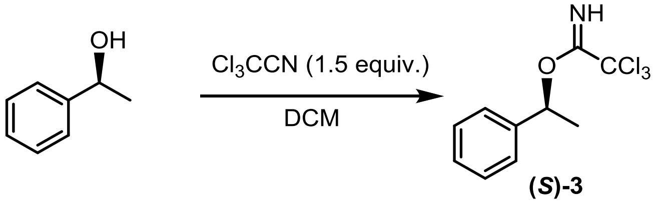

To a flame dried round bottom flask fitted with a rubber septum was added (*S*)-1-phenylethanol (99% ee, 122 mg, 1.0 mmol, 1 equiv.), trichloroacetonitrile (216 mg, 1.5 mmol, 1.5 equiv.), and dichloromethane (20 mL) and the resulting mixture was cooled to 0 °C. After 10 min, sodium hydride (60% oil dispersion, 8.0 mg, 20 mol%) was added and the reaction mixture was allowed to warm to room temperature and stirred overnight. After 16h, the reaction mixture was diluted with water (20 mL), extracted with dichloromethane (2 x 15 mL), and the organic layer was washed with brine. The organic layer was then separated, dried with MgSO4, filtered and concentrated under vacuum. The crude residue was then purified by chromatography with triethylamine-treated silica gel using a solvent system composed of 3% triethylamine in hexanes to give the desired compound in 92% yield (225 mg, 0.92 mmol) as a clear oil that solidifies at low temperature. ^{1}H NMR (600MHz, $CDCl_3$): δ (ppm) 8.42 (s, 1H), 7.48 (d, 2H, J = 7.2 Hz), 7.42 (t, 2H, J = 7.8 Hz), 7.35 (t, 1H, J = 7.8 Hz), 6.43 (q, 1H, J = 6.6 Hz), 1.70 (d, 3H, J = 6.6 Hz). ^{13}C NMR (150MHz, CD_2Cl_2): δ (ppm) 162.0, 142.1, 129.0, 128.4, 126.4, 92.4, 77.8, 22.5. HRMS (*m/z*): calculated for $[C_{10}H_{10}{}^{35}Cl_3NO]$, 264.9828; observed 264.9892.

7.4.3. Synthesis of enantioenriched benzyl chloride 7

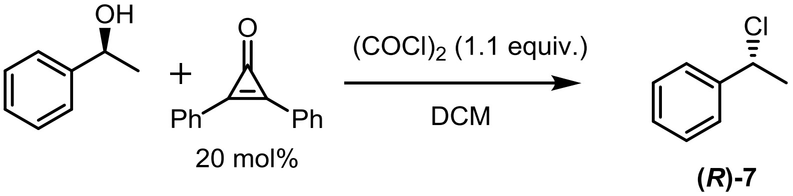

(*R*)-7

Enantioenriched benzylic chloride **7** was synthesized according to a modified procedure adopted from the literature.[40] To a three-necked round bottom flask fitted an additional funnel and rubber septa was added (*S*)-1-phenylethanol (99% ee, 122 mg, 1.0 mmol, 1 equiv.), diphenylcyclopropenone (41 mg, 0.2 mmol, 20 mol%), and dichloromethane (20 mL) and the resulting mixture was cooled to 0 °C. After 10 min, oxalyl chloride (140 mg, 1.1 mmol, 1.1 equiv.) was added drop-wise as a solution in DCM (5 mL) over 1 h. The reaction mixture was then concentrated to give the crude residue, which was re-dissolved in DCM (1 mL) and filtered through a plug of silica gel with petroleum ether (30 mL). The solvent was then removed in vacuo to give the desired compound as an oil in 82% yield with 80% ee. ^{1}H NMR (600MHz, $CDCl_3$): δ (ppm) 7.47 (d, 2H, J = 7.2 Hz), 7.41 (t, 2H, J = 7.2 Hz), 7.35 (t, 1H, J = 7.2 Hz), 5.14 (q, 1H, J = 7.2 Hz), 1.90 (d, 3H, J = 7.2 Hz). ^{13}C NMR (150MHz, $CDCl_3$): δ (ppm) 142.8, 128.6, 128.3, 126.5, 58.7, 26.5. HRMS (*m/z*): calculated for $[C_8H_9{}^{35}Cl]$, 140.0393; observed 140.0391.

7.4.4. Synthesis of enantiopure ammonium tosylate 8

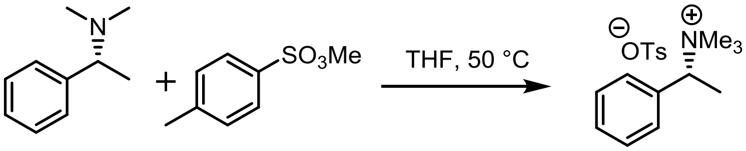

(*R*)-8

To a vial fitted with a stir bar was added (*R*)-(+)-*N,N*-dimethyl-1-phenylethylamine (99% ee, 149 mg, 1.0 mmol. 1 equiv.), methyl *p*-toluenesulfonate (200 mg, 1.2 mmol, 1.2 equiv.) and THF (5 mL). The vial was then sealed with a plastic cap and the resulting reaction mixture was heated at 50 °C. After 14h of reaction, the solvent was removed and the crude residue was washed with diethyl ether (20 mL) to give the desired compound in 93% yield. ^{1}H NMR (600MHz, $CDCl_3$): δ (ppm) 7.67 (d, 2H, J = 7.8 Hz), 7.29-7.20 (m, 5H), 7.04 (d, 2H, J = 7.8 Hz), 4.66 (q, 1H, J = 7.2 Hz), 2.94 (s, 9H), 2.20 (s, 3H), 1.52 (d, 3H, J = 6.6 Hz). ^{13}C NMR (150MHz, $CDCl_3$): δ (ppm) 143.03, 139.6, 132.9, 130.1, 128.8, 128.7, 125.8, 73.2, 50.8, 21.1, 14.7. HRMS (*m/z*): calculated for $[C_{11}H_{18}N]^+$, 164.1434; observed 164.1433.

7.4.5. Synthesis of racemic 10

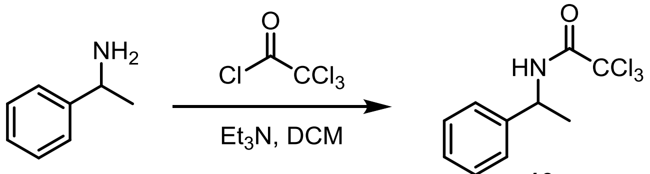

10

To a round-bottom flask fitted with a rubber septum and a stir bar was added trichloroacetyl chloride (200mg, 1.1 mmol, 1.1 equiv.), triethylamine (130 mg, 1.3 mmol, 1.3 equiv.) and DCM (20 mL), and the resulting solution was cooled to 0 °C. After 10 min, 1-phenylethylamine (121 mg, 1.0 mmol, 1 equiv.) was added as a solution in DCM (5 mL) and the resulting solution was allowed to warm up to room temperature and stirred. After 16h, the reaction solution was diluted with water (20 mL) and the resulting mixture was extracted with DCM (3 x 20 mL). The organic layer was then separated, washed with brine (20 mL), dried with $MgSO_4$, filtered and concentrated to give the crude residue, which was purified by chromatography on silica gel (5-10 % EtOAc in hexanes) to give the desired compound as a white solid in 85% yield. ^{1}H NMR (600MHz, $CDCl_3$): δ (ppm) 7.42-7.32 (m, 5H), 6.93 (broad s, 1H), 5.08 (p, 1H, *J* = 7.2 Hz), 1.59 (d, 3H, *J* = 7.2 Hz). ^{13}C NMR (150MHz, CD_2Cl_2): δ (ppm) 161.3, 142.3, 129.4, 128.4, 126.5, 93.3, 51.8, 21.8. HRMS (*m/z*): calculated for $[C_9H_7{}^{35}Cl_3NO]^+$ or $[M-CH_3]^+$ 249.9593; observed 249.9591.

7.4.6. Appendix – ^{1}H and ^{13}C NMR, and Chiral GC Spectra

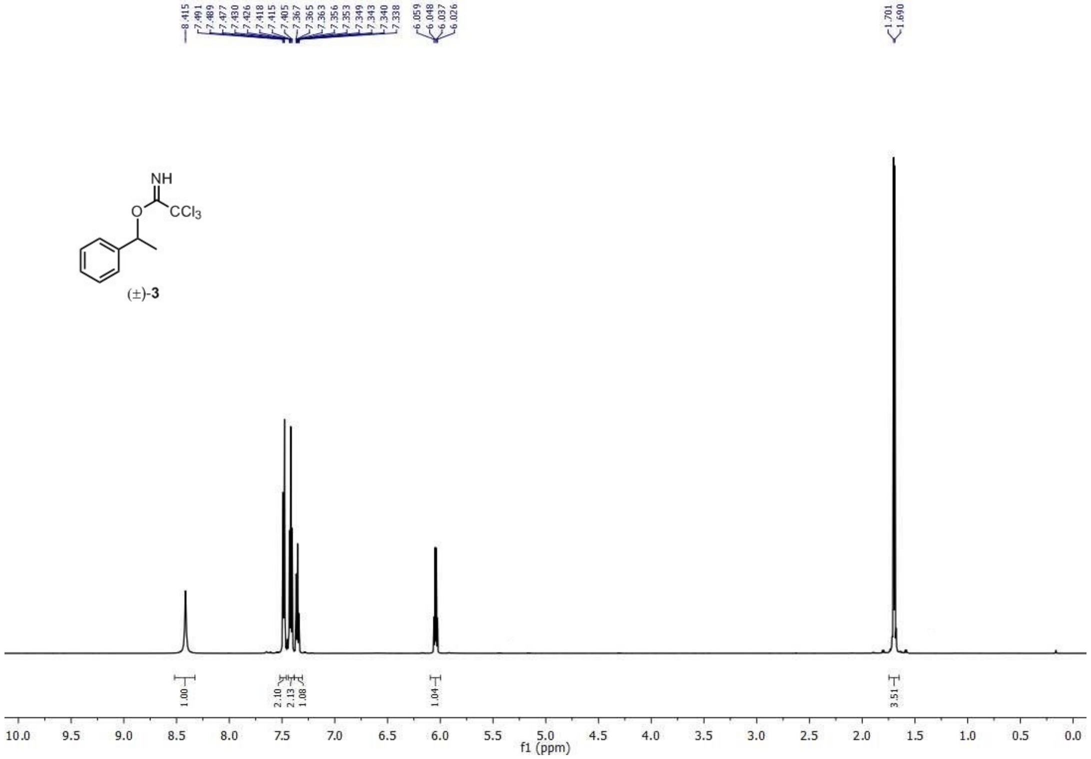

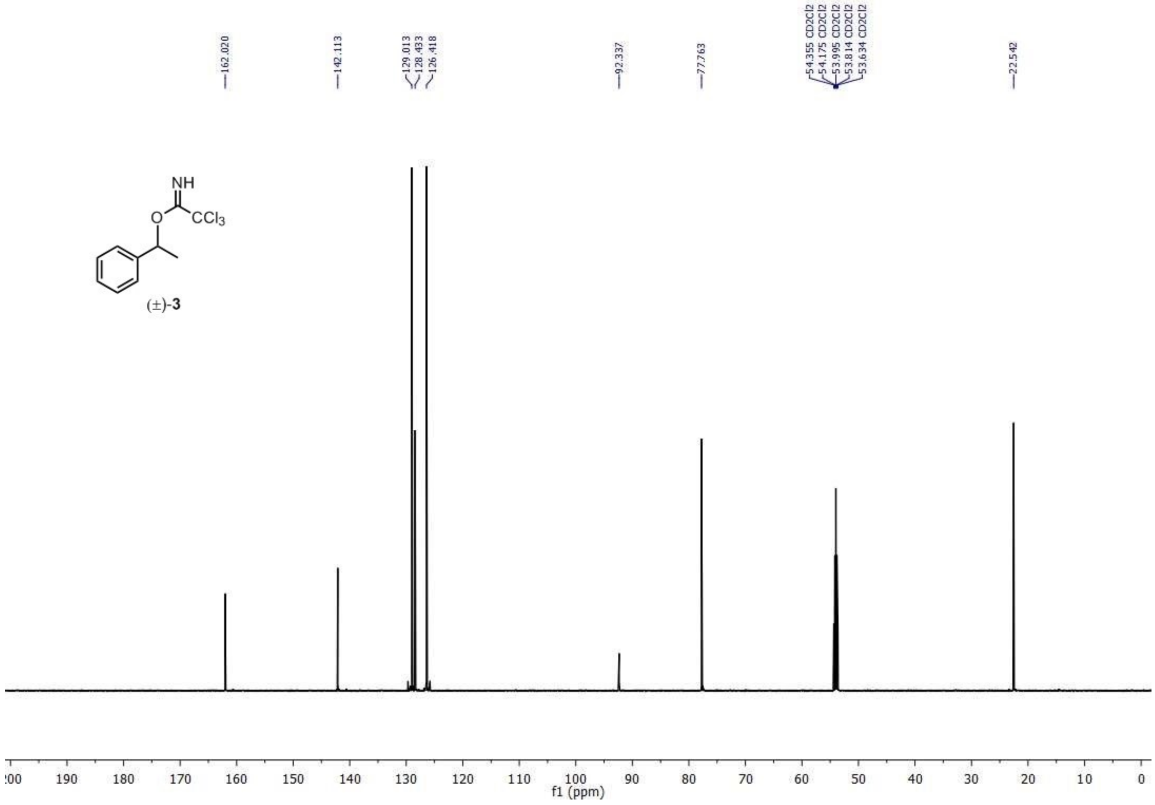

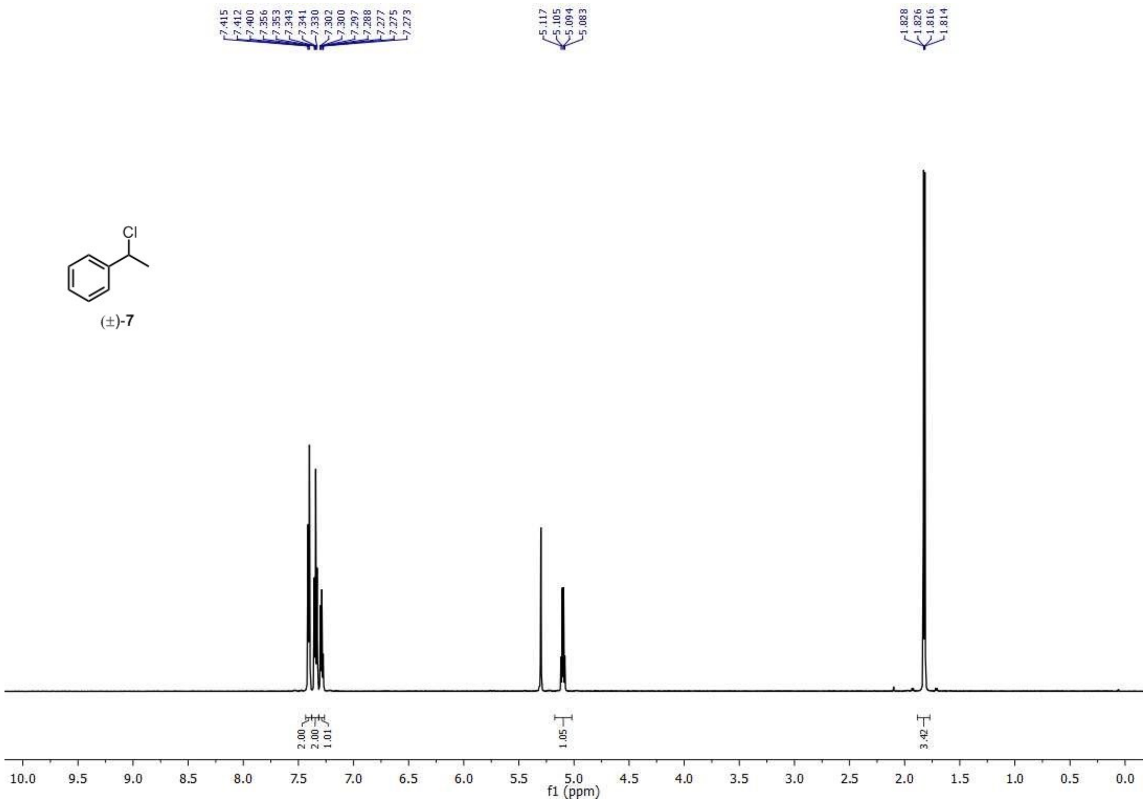
7.415
7.412
7.400
7.356
7.353
7.343
7.341
7.330
7.302
7.300
7.297
7.288
7.277
7.275
7.273
5.117
5.105
5.094
5.083
1.828
1.826
1.816
1.814
Cl
(±)-7
2.00
2.00
1.01
1.05
3.42
10.0
9.5
9.0
8.5
8.0
7.5
7.0
6.5
6.0
5.5
5.0
4.5
4.0
3.5
3.0
2.5
2.0
1.5
1.0
0.5
0.0
f1 (ppm)

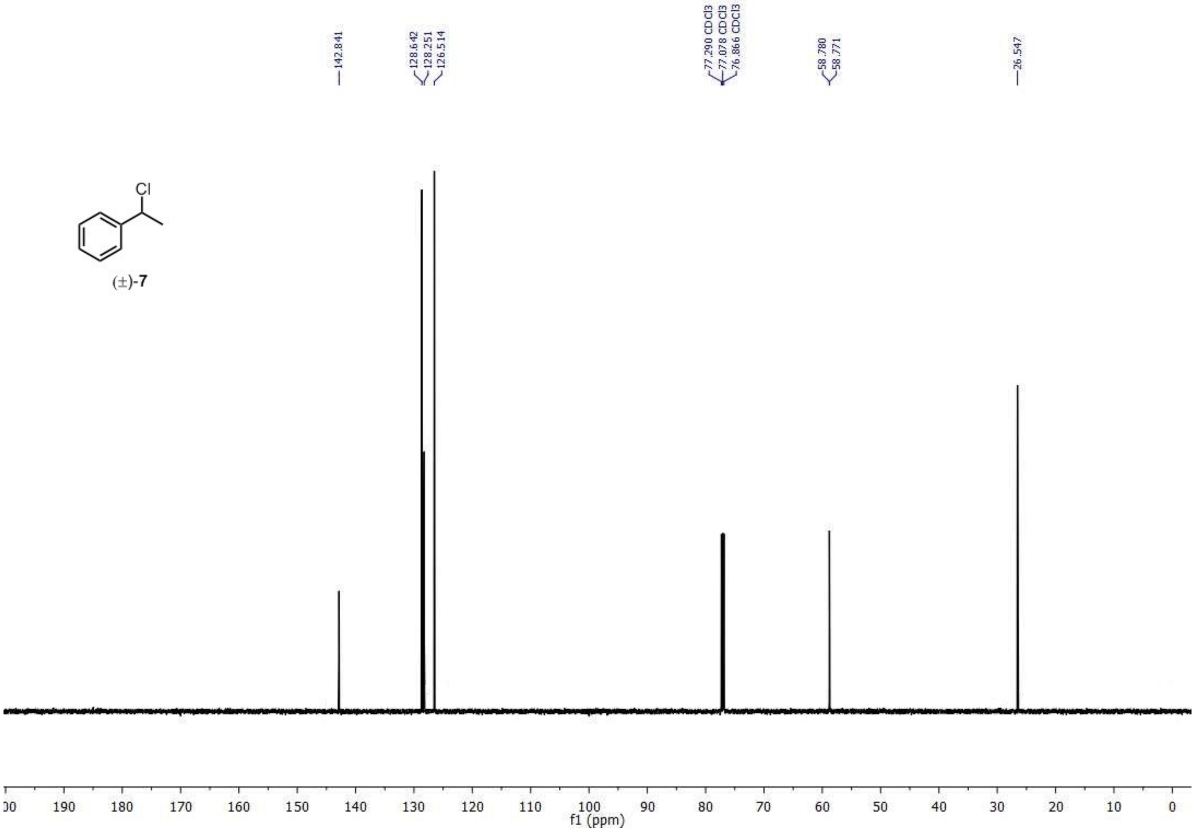
142.841
128.642
128.251
126.514
77.290 CDCl3
77.078 CDCl3
76.866 CDCl3
58.780
58.771
26.547
Cl
(±)-7
00
190
180
170
160
150
140
130
120
110
100
90
80
70
60
50
40
30
20
10
0
f1 (ppm)

Chiral GC spectrum of racemic **7**

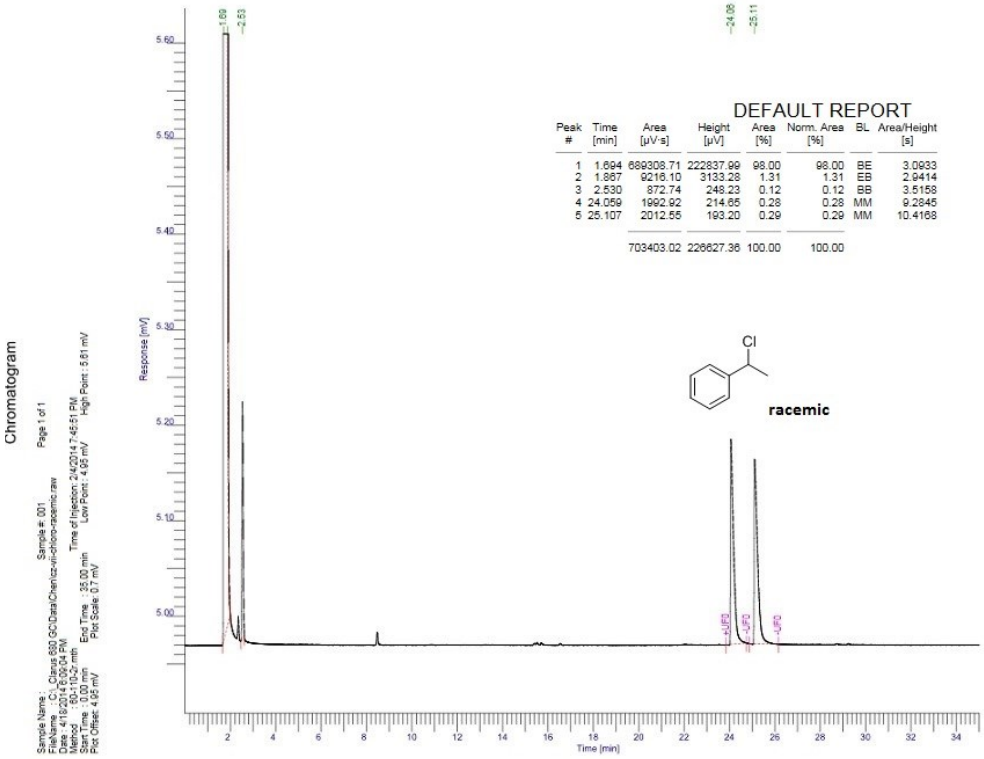

DEFAULT REPORT

Peak #	Time [min]	Area [µV·s]	Height [µV]	Area [%]	Norm. Area [%]	BL	Area/Height [s]
1	1.694	689308.71	222837.99	98.00	98.00	BE	3.0933
2	1.867	9216.10	3133.28	1.31	1.31	EB	2.9414
3	2.530	872.74	248.23	0.12	0.12	BB	3.5158
4	24.059	1992.92	214.65	0.28	0.28	MM	9.2845
5	25.107	2012.55	193.20	0.29	0.29	MM	10.4168
		703403.02	226627.36	100.00	100.00		

Chiral GC spectrum of enantioenriched ***(R)*-7**

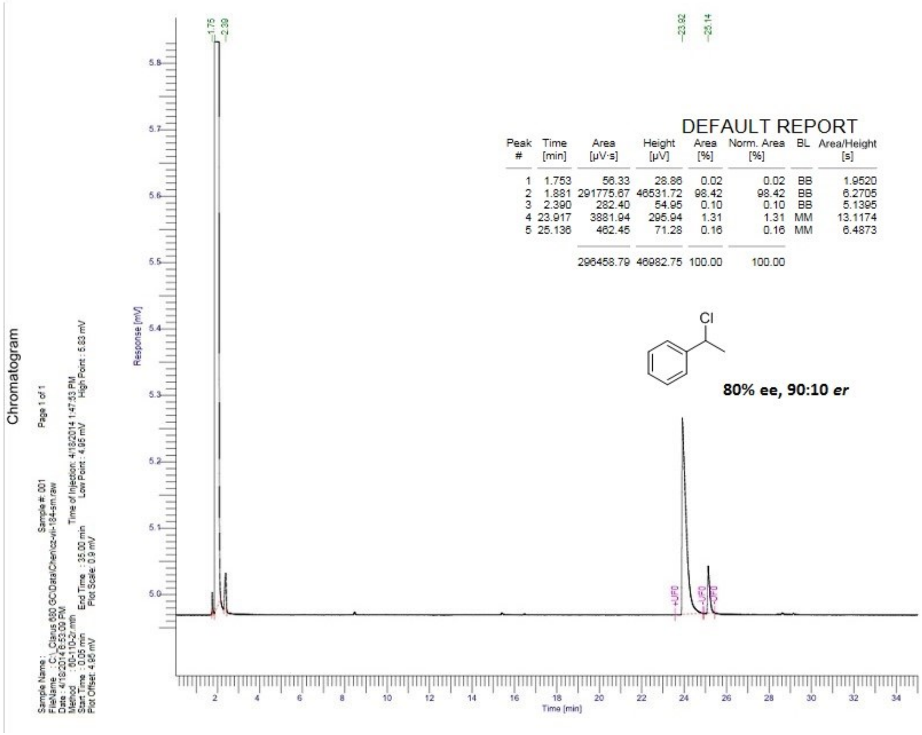

DEFAULT REPORT

Peak #	Time [min]	Area [µV·s]	Height [µV]	Area [%]	Norm. Area [%]	BL	Area/Height [s]
1	1.753	56.33	28.86	0.02	0.02	BB	1.9520
2	1.881	291775.67	46531.72	98.42	98.42	BB	6.2705
3	2.390	282.40	54.95	0.10	0.10	BB	5.1395
4	23.917	3881.94	295.94	1.31	1.31	MM	13.1174
5	25.136	462.45	71.28	0.16	0.16	MM	6.4873
		296458.79	46982.75	100.00	100.00		

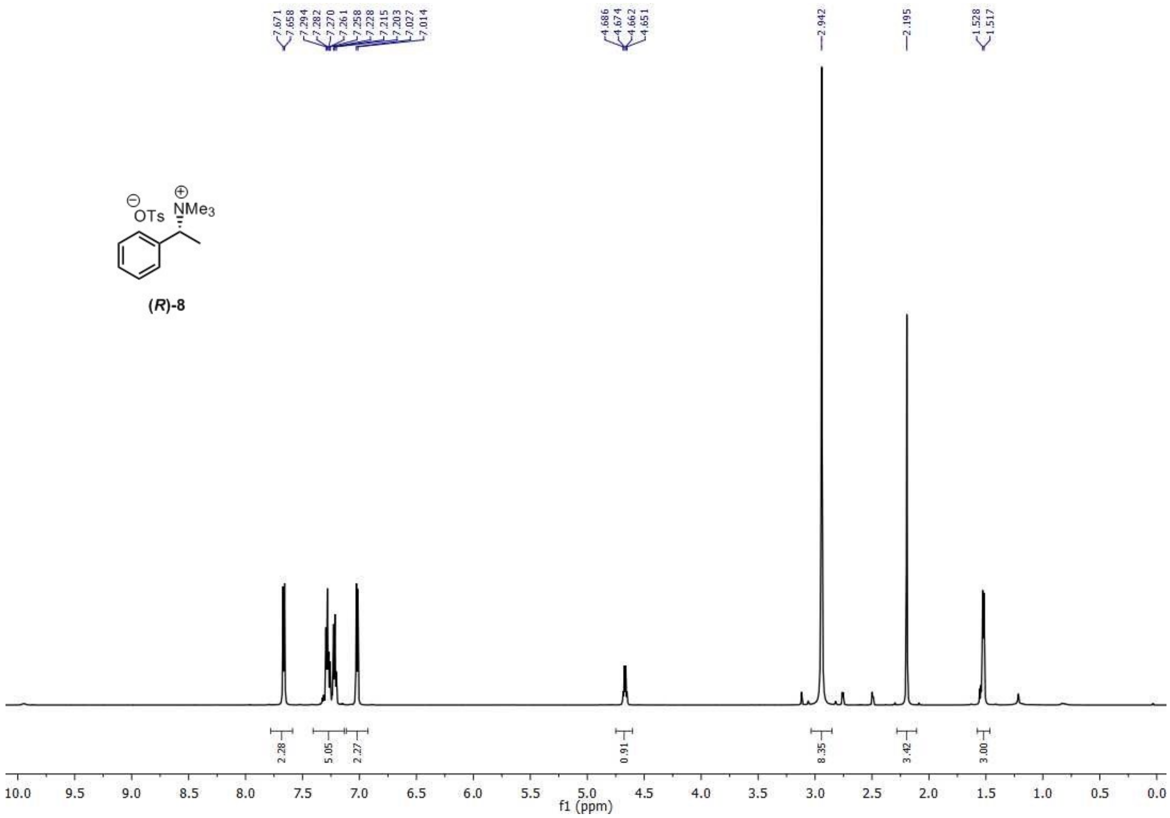
7.671
7.658
7.294
7.282
7.270
7.261
7.258
7.228
7.215
7.203
7.027
7.014
4.686
4.674
4.662
4.651
2.942
2.195
1.528
1.517
OTs
NMe3
(R)-8
2.28
5.05
2.27
0.91
8.35
3.42
3.00
10.0
9.5
9.0
8.5
8.0
7.5
7.0
6.5
6.0
5.5
5.0
4.5
4.0
3.5
3.0
2.5
2.0
1.5
1.0
0.5
0.0
f1 (ppm)

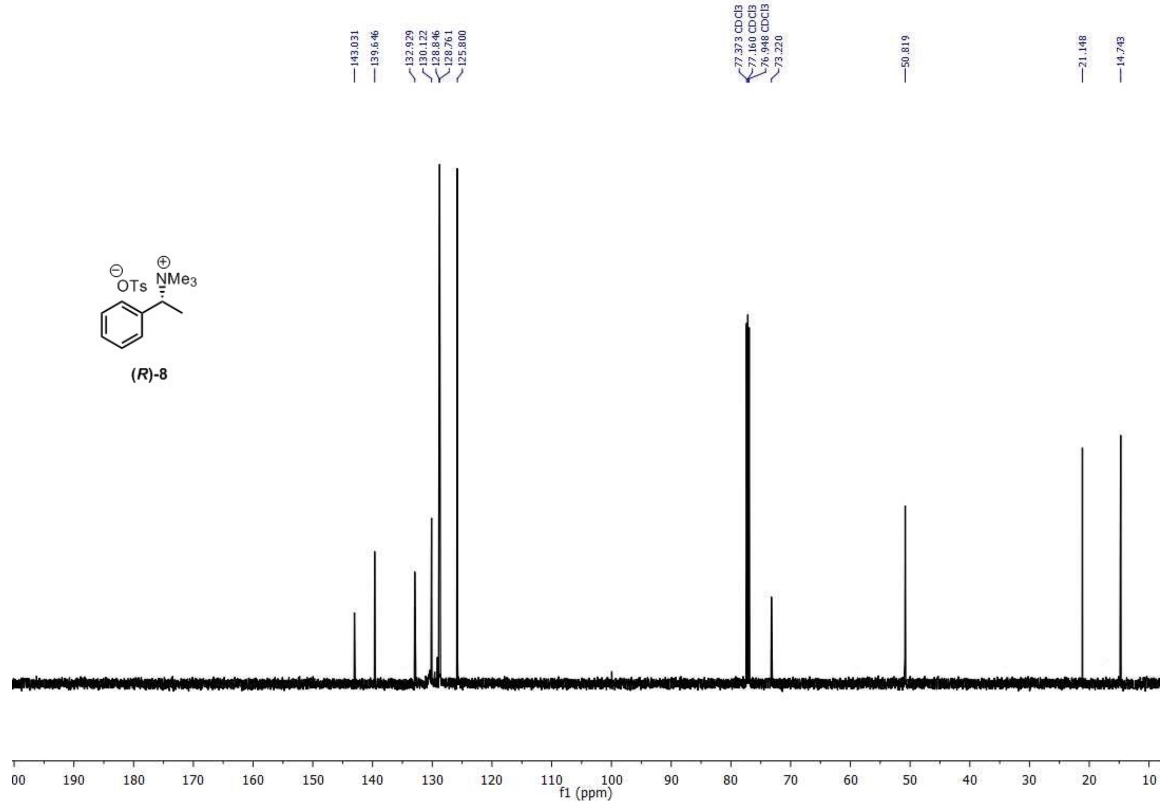
143.031
139.646
132.929
130.122
128.846
128.761
125.800
77.373 CDCl3
77.160 CDCl3
76.948 CDCl3
73.220
50.819
21.148
14.743
OTs
NMe3
(R)-8
00
190
180
170
160
150
140
130
120
110
100
90
80
70
60
50
40
30
20
10
f1 (ppm)

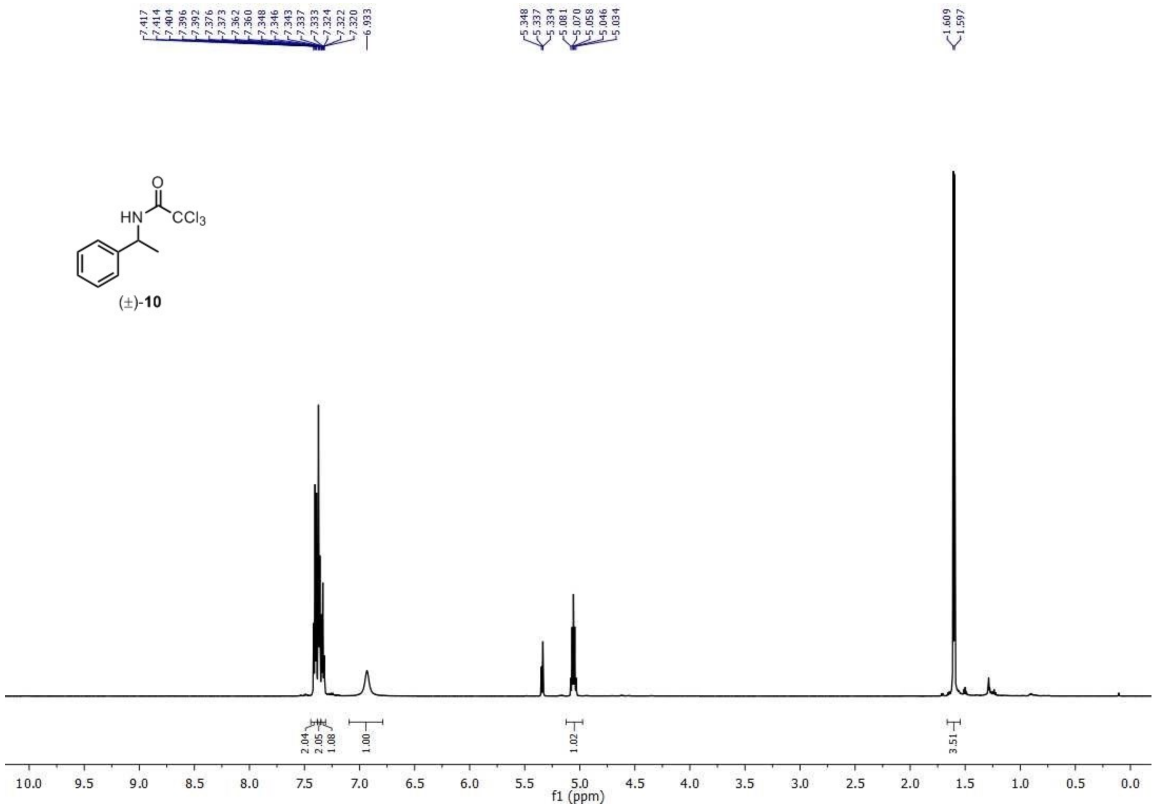
7.417
7.414
7.404
7.396
7.392
7.376
7.373
7.362
7.360
7.348
7.346
7.343
7.337
7.333
7.324
7.322
7.320
6.933
5.348
5.337
5.334
5.081
5.070
5.058
5.046
5.034
1.609
1.597
HN
O
CCl3
(±)-10
2.04
2.05
1.08
1.00
1.02
3.51
10.0
9.5
9.0
8.5
8.0
7.5
7.0
6.5
6.0
5.5
5.0
4.5
4.0
3.5
3.0
2.5
2.0
1.5
1.0
0.5
0.0
f1 (ppm)

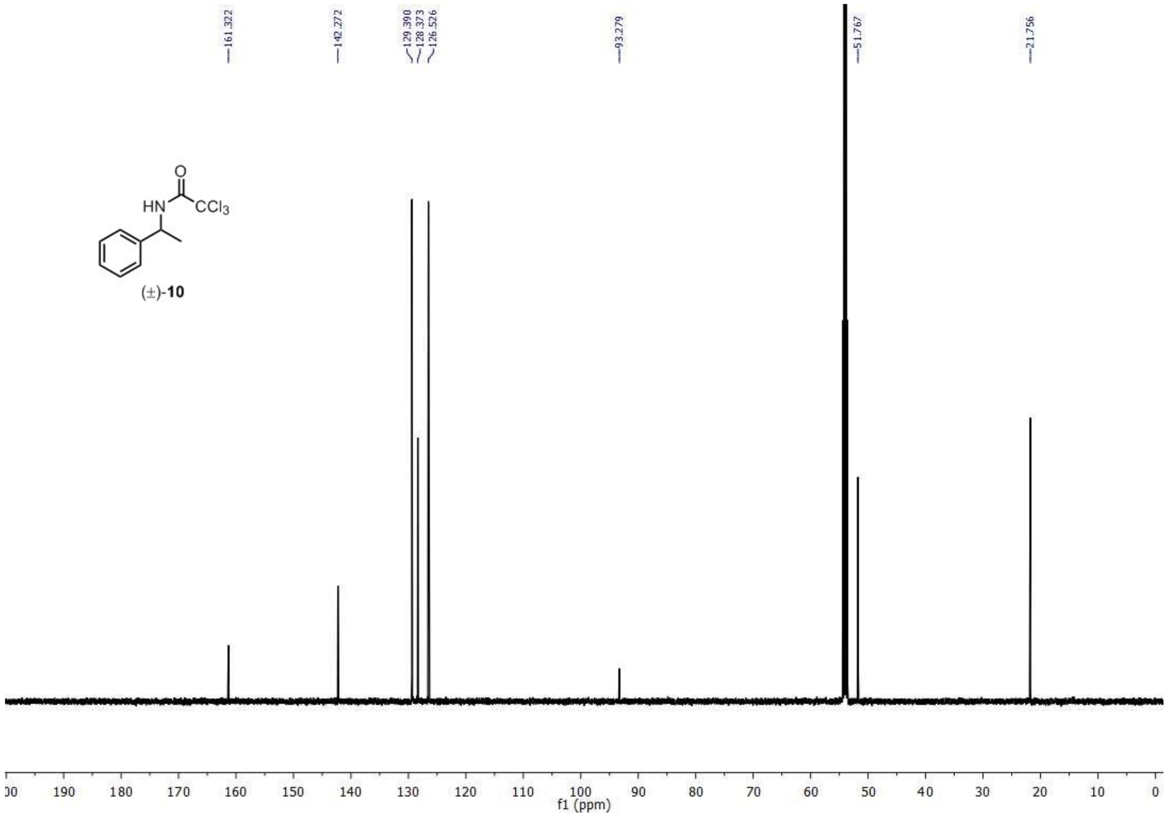
161.322
142.272
129.390
128.373
126.526
93.279
51.767
21.756
HN
O
CCl3
(±)-10
190
180
170
160
150
140
130
120
110
100
90
80
70
60
50
40
30
20
10
0
f1 (ppm)

7.4.7. Independently synthesized enantiopure (*S*)-3 from (*S*)-6

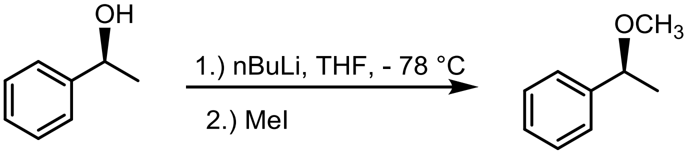

To a flame dried round-bottom flask fitted with a rubber septum and a stir bar was added **(*S*)-6** (122 mg, 1.0 mmol) and THF (10 mL, 0.1 M) and the resulting solution was cooled to –78 °C for 10 min. This was followed by the addition of nBuLi (2.5 M, 0.5 mL, 1.2 mmol, 1.2 equiv.), and the resulting solution was then stirred at –78 °C for another 10 min, after which methyl iodide (neat, 300 mg, 2.11 mmol, 2.11 equiv.) was added. The resulting reaction mixture was then allowed to warm to room temperature and subsequently stirred for 1 h. The reaction mixture was then diluted with water (10 mL) and extract with diethyl ether (2 x 10 mL). The organic layer was then separated, dried with MgSO4, filtered and concentrated to give a mixture containing (*S*)-**4** and (*S*)-**6**. Compound **4**'s spectroscopic properties are consistent with literature values.[41] See ^{1}H NMR and chiral GC spectra below.

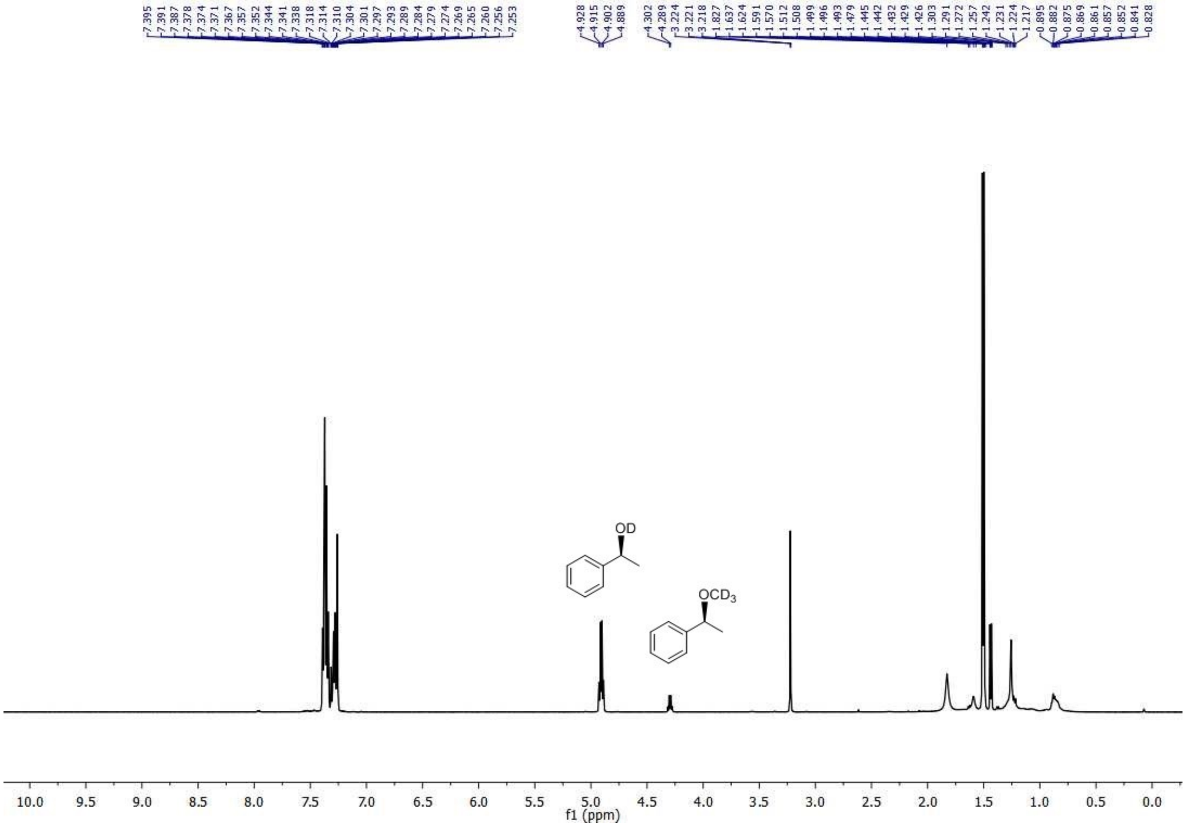

Chiral GC spectrum of enantiopure **(*S*)-4** and **(*S*)-6**

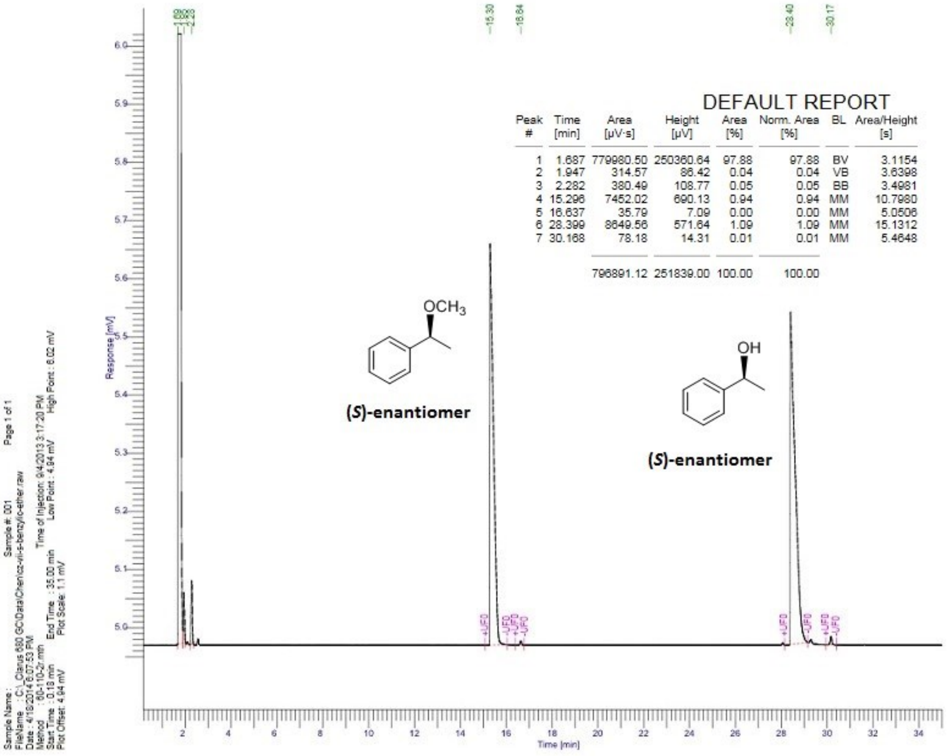

DEFAULT REPORT

Peak #	Time [min]	Area [µV·s]	Height [µV]	Area [%]	Norm. Area [%]	BL	Area/Height [s]
1	1.687	779980.50	250360.64	97.88	97.88	BV	3.1154
2	1.947	314.57	86.42	0.04	0.04	VB	3.6398
3	2.282	380.49	108.77	0.05	0.05	BB	3.4981
4	15.296	7452.02	690.13	0.94	0.94	MM	10.7980
5	16.637	35.79	7.09	0.00	0.00	MM	5.0506
6	28.399	8649.56	571.64	1.09	1.09	MM	15.1312
7	30.168	78.18	14.31	0.01	0.01	MM	5.4648
		796891.12	251839.00	100.00	100.00		

Chiral GC spectrum of racemic **4** and **6**

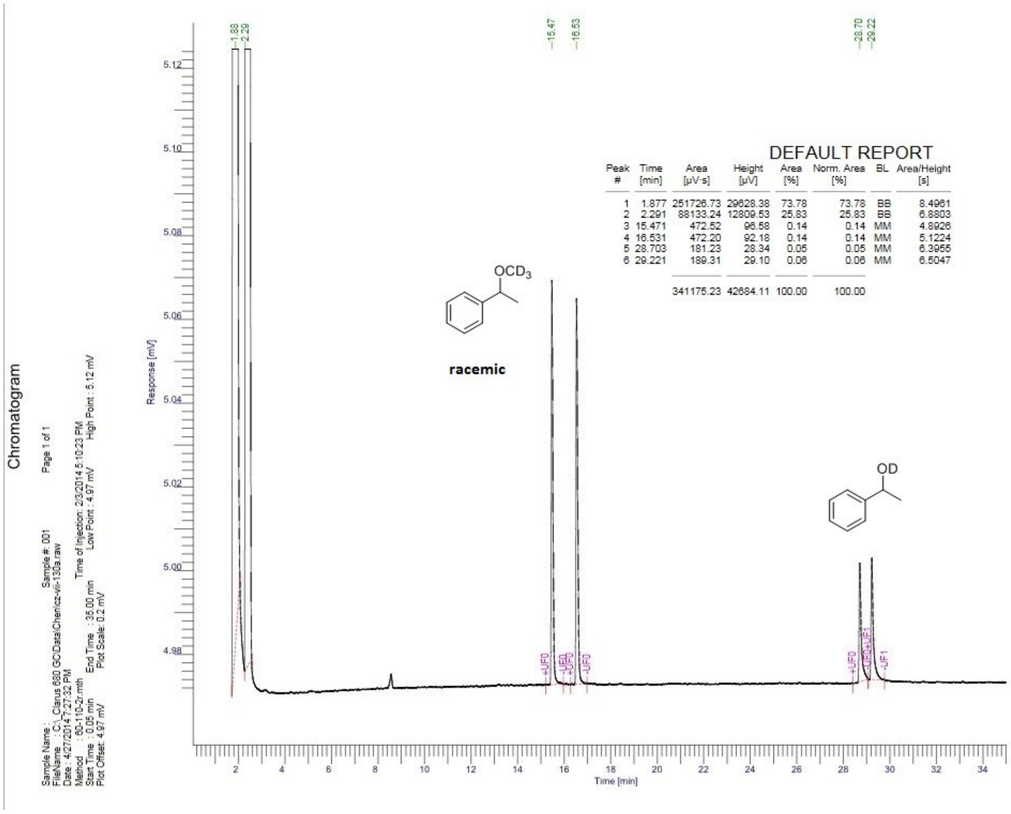

DEFAULT REPORT

Peak #	Time [min]	Area [µV·s]	Height [µV]	Area [%]	Norm. Area [%]	BL	Area/Height [s]
1	1.877	251726.73	29628.38	73.78	73.78	BB	8.4961
2	2.291	88133.24	12809.53	25.83	25.83	BB	6.8803
3	15.471	472.52	96.58	0.14	0.14	MM	4.8926
4	16.531	472.20	92.18	0.14	0.14	MM	5.1224
5	28.703	181.23	28.34	0.05	0.05	MM	6.3955
6	29.221	189.31	29.10	0.06	0.06	MM	6.5047
		341175.23	42684.11	100.00	100.00		

7.4.8. Solvolysis of (*S*)-3 in methanol catalyzed by a phosphoric acid

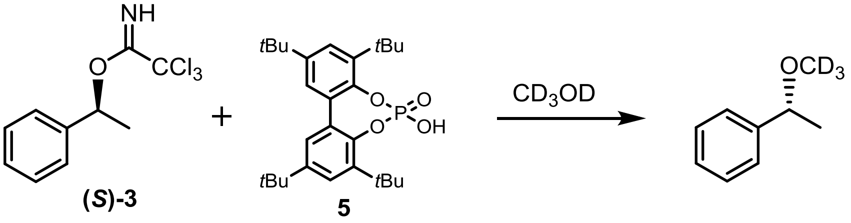

Compound **(*S*)-3** (22 mg, 0.04 mmol, 1 equiv.) and phosphoric acid **5** (1.2 mg, 0.002, 5 mol%) were dissolved in CD_3OD (0.5 mL). After one hour, analysis by ^{1}H NMR spectroscopy shows complete conversion of **(*S*)-3** to **4**. Enantiomeric ratios of **4** was then determined by chiral GC analysis: 15:85 (***S***):(***R***) with γ-TA column, 2 °C per minute from 60 °C to 110 °C, (***S***)-**4** 15.5 min, (***R***)-**4** 16.5 min.

Chiral GC spectrum of reaction between **(*S*)-3** and **5**

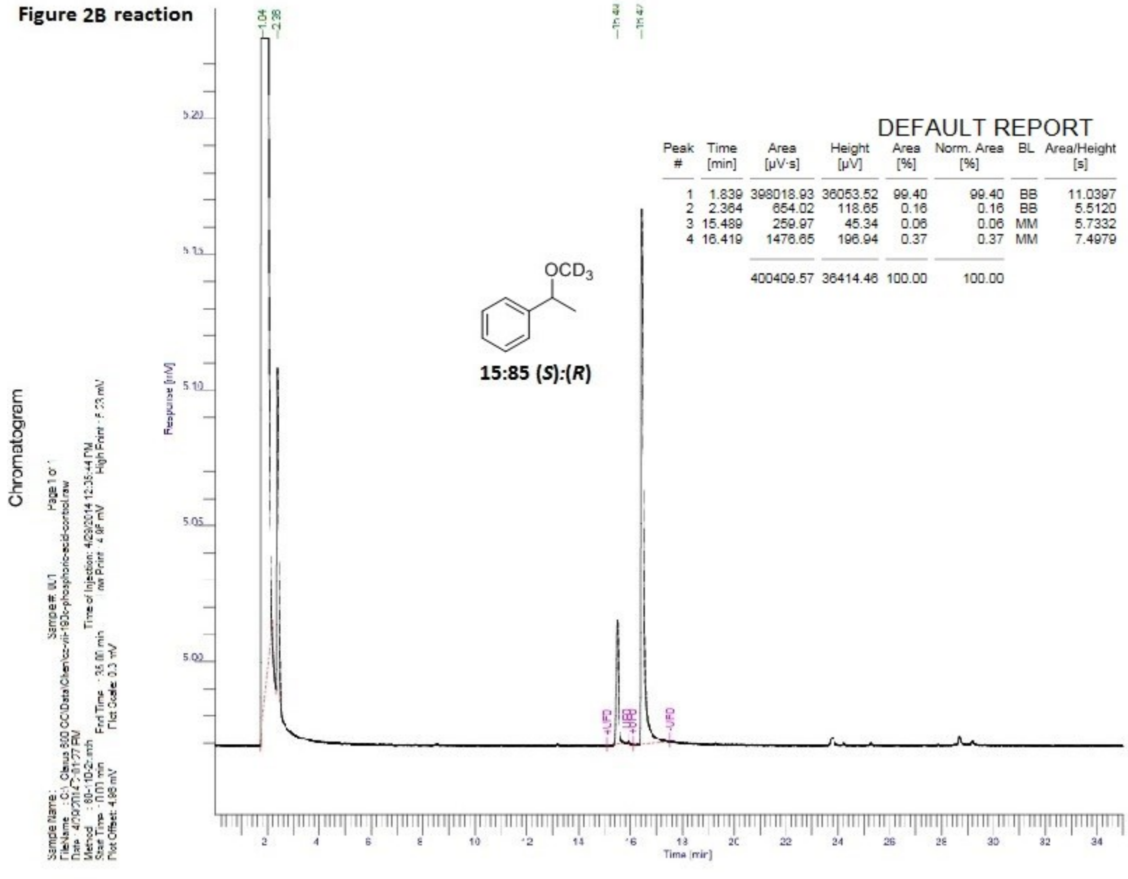

DEFAULT REPORT

Peak #	Time [min]	Area [μV·s]	Height [μV]	Area [%]	Norm. Area [%]	BL	Area/Height [s]
1	1.839	398018.93	36053.52	99.40	99.40	BB	11.0397
2	2.364	654.02	118.65	0.16	0.16	BB	5.5120
3	15.489	259.97	45.34	0.06	0.06	MM	5.7332
4	16.419	1476.65	196.94	0.37	0.37	MM	7.4979
		400409.57	36414.46	100.00	100.00		

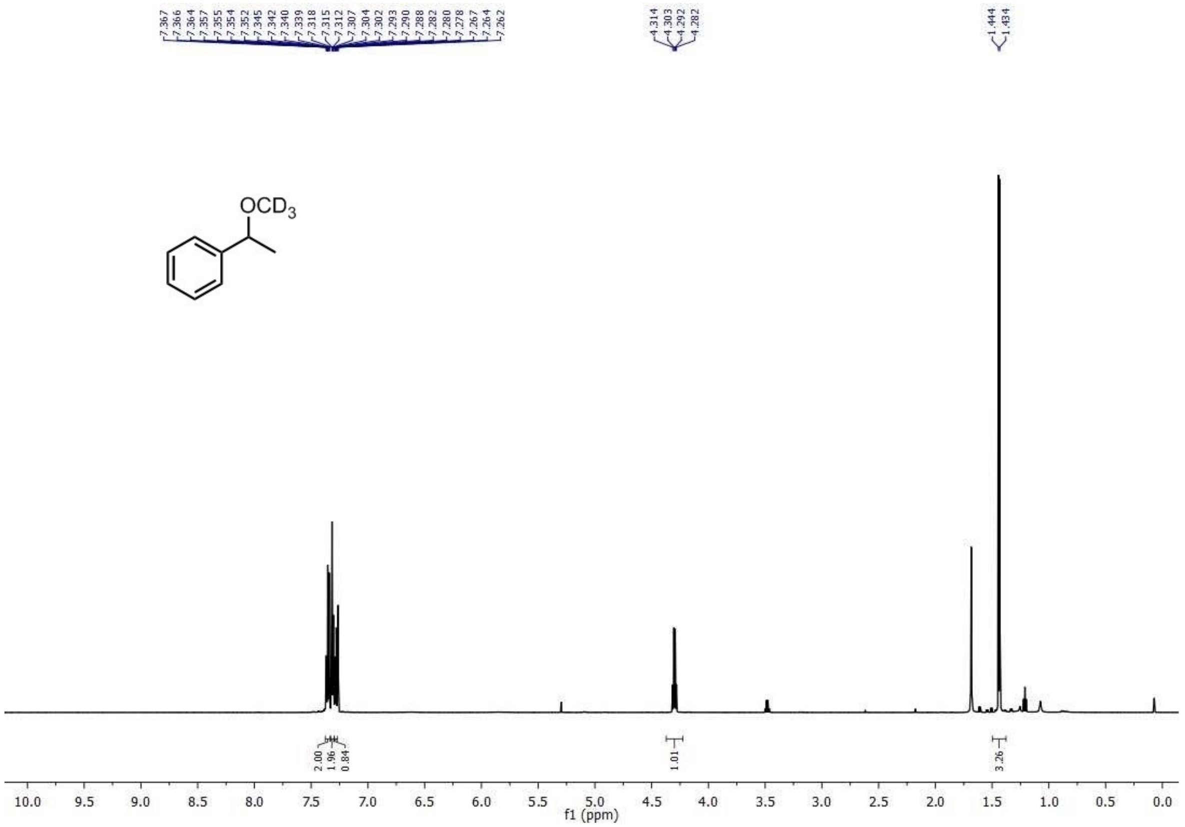
7.367
7.366
7.364
7.357
7.355
7.354
7.352
7.345
7.342
7.340
7.339
7.318
7.315
7.312
7.307
7.304
7.302
7.293
7.290
7.288
7.282
7.280
7.278
7.267
7.264
7.262
4.314
4.303
4.292
4.282
1.444
1.434
OCD3
2.00
1.96
0.84
1.01
3.26
10.0
9.5
9.0
8.5
8.0
7.5
7.0
6.5
6.0
5.5
5.0
4.5
4.0
3.5
3.0
2.5
2.0
1.5
1.0
0.5
0.0
f1 (ppm)

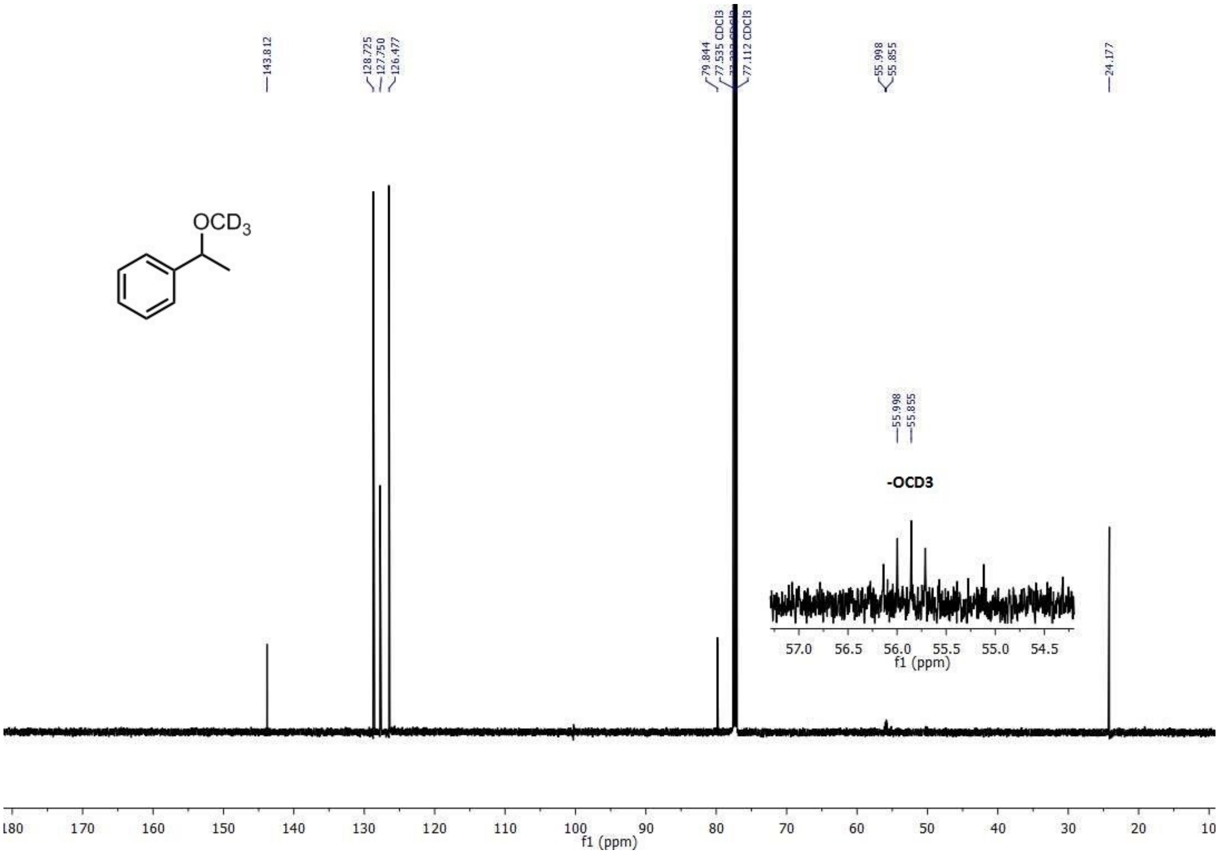
143.812
128.725
127.750
126.477
79.844
77.535 CDCl3
77.112 CDCl3
55.998
55.855
24.177
OCD3
55.998
55.855
-OCD3
57.0
56.5
56.0
55.5
55.0
54.5
f1 (ppm)
180
170
160
150
140
130
120
110
100
90
80
70
60
50
40
30
20
10
f1 (ppm)

7.4.9. Host-catalyzed substitution reaction of (*S*)-3

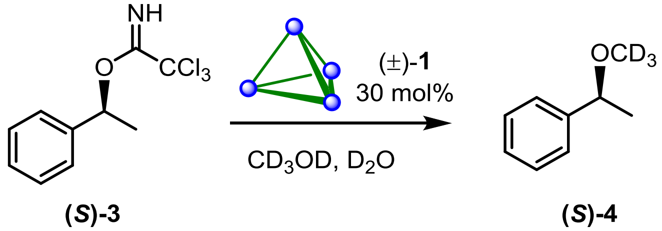

Representative procedure (Figure 3A, entry 3): The supramolecular host catalyst **1** (43 mg, 0.012 mmol, 30 mol%) was dissolved in 0.3 mL of D_2O buffered at pD 8 (100mM K_2HPO_4, pD = 8.00) and substrate **(*S*)-3** (11.0 mg, 0.04 mmol, 1 equiv.) was dissolved in 0.3 mL of CD_3OD. The two solutions were combined and loaded into an NMR tube and capped. The resulting reaction mixture was then heated at 50 °C and monitored periodically by ^{1}H NMR spectroscopy. After 16h of reaction time, the reaction mixture was diluted with water (10 mL) and the resulting mixture was extracted with $CDCl_3$ (2 x 0.6 mL). The organic portion was then separated, dried with MgSO4, filtered and loaded into an NMR tube. To this solution was then added 0.1 mL of a CDCl3 solution containing 1,3,5-trimethoxybenzene (0.13 mM, internal standard), and the resulting solution was analyzed by ^{1}H NMR spectroscopy to give overall 92% yield with a ratio of 78:22 for products **4**:**6**. Enantiomeric ratios of **4** and **6** were determined by chiral GC analysis: 90:10 (***S***):(***R***), by chiral GC fitted with γ-TA column, 2 °C per minute from 60 °C to 110 °C, (***S***)-**4** 15.4 min, (***R***)-**4** 16.5 min.

^{1}H NMR spectrum of the crude reaction extract with $CDCl_3$ (Figure 3A, entry 3)

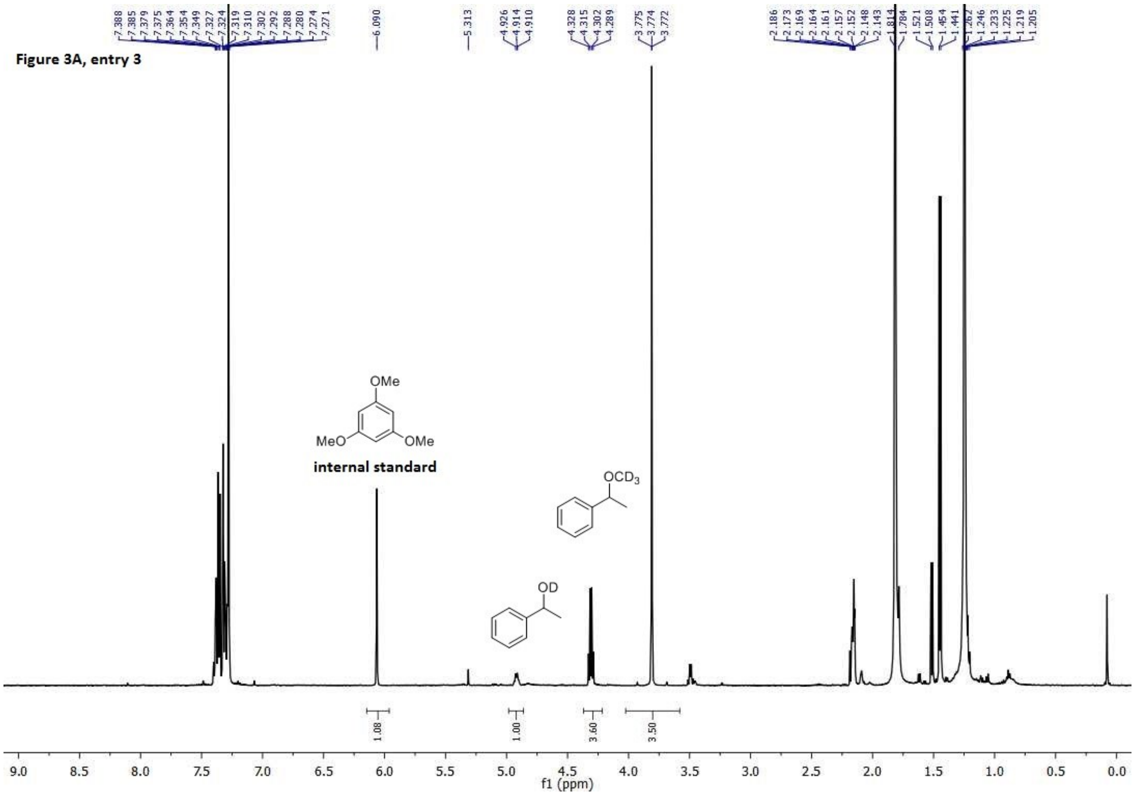

Chiral GC spectrum of the crude reaction extract with $CDCl_3$ (Figure 3A, entry 3)

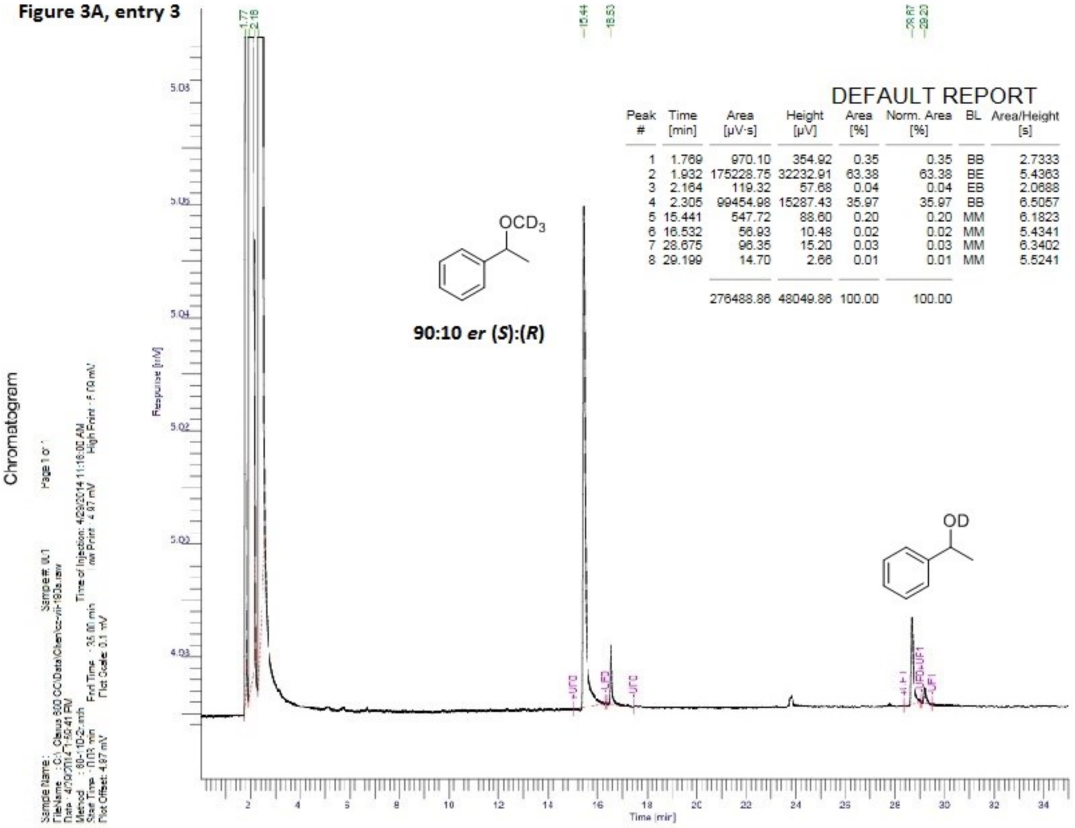

DEFAULT REPORT

Peak #	Time [min]	Area [µV·s]	Height [µV]	Area [%]	Norm. Area [%]	BL	Area/Height [s]
1	1.769	970.10	354.92	0.35	0.35	BB	2.7333
2	1.932	175228.75	32232.91	63.38	63.38	BE	5.4363
3	2.164	119.32	57.68	0.04	0.04	EB	2.0688
4	2.305	99454.98	15287.43	35.97	35.97	BB	6.5057
5	15.441	547.72	88.60	0.20	0.20	MM	6.1823
6	16.532	56.93	10.48	0.02	0.02	MM	5.4341
7	28.675	96.35	15.20	0.03	0.03	MM	6.3402
8	29.199	14.70	2.66	0.01	0.01	MM	5.5241
		276488.86	48049.86	100.00	100.00		

7.4.10. Host-catalyzed substitution reaction of (*R*)-7

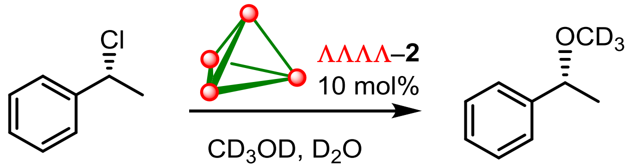

(*R*)-7, 80% ee **(*R*)-4**

Representative procedure (Figure 4B, entry 2): this reaction was carried out according to the procedure described above for the host-catalyzed reaction of **(*S*)-3**, with the exception that D_2O with 640mM K_2HPO_4 buffered at pD = 8.00 was used as co-solvent. ^1H NMR spectroscopy analysis shows overall 95% yield with a ratio of 72:28 for products **4**:**6**. Enantiomeric ratios of **4** and **6** were determined by chiral GC analysis: 16:84 (***S***):(***R***) with a chiral GC fitted with γ-TA column, 2 °C per minute from 60 °C to 110 °C, (***S***)-**4** 15.4 min, (***R***)-**4** 16.4 min.

^1H NMR spectrum of the crude reaction extract with $CDCl_3$ (Figure 4B, entry 2)

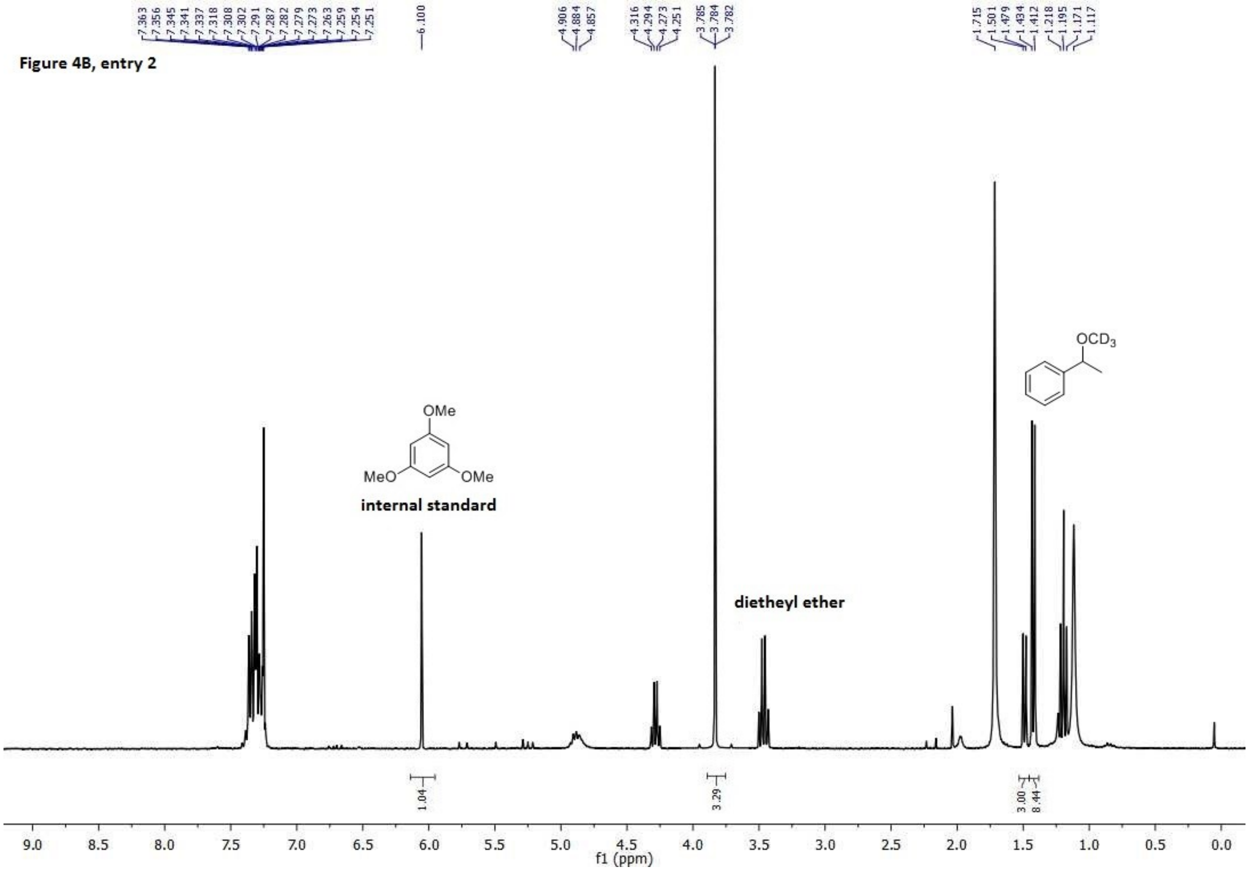

Chiral GC spectrum of the crude reaction extract with $CDCl_3$ (Figure 4B, entry 2)

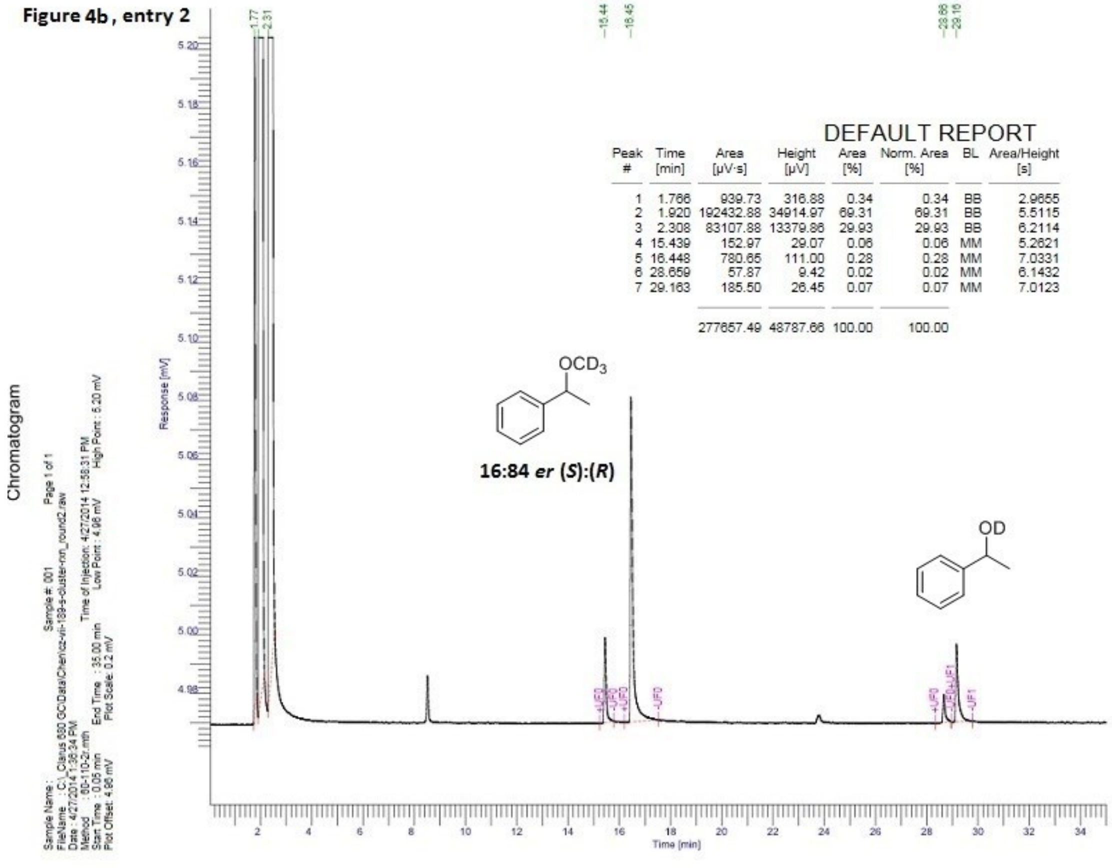

DEFAULT REPORT

Peak #	Time [min]	Area [μV·s]	Height [μV]	Area [%]	Norm. Area [%]	BL	Area/Height [s]
1	1.766	939.73	316.88	0.34	0.34	BB	2.9655
2	1.920	192432.88	34914.97	69.31	69.31	BB	5.5115
3	2.308	83107.88	13379.86	29.93	29.93	BB	6.2114
4	15.439	152.97	29.07	0.06	0.06	MM	5.2621
5	16.448	780.65	111.00	0.28	0.28	MM	7.0331
6	28.659	57.87	9.42	0.02	0.02	MM	6.1432
7	29.163	185.50	26.45	0.07	0.07	MM	7.0123
		277657.49	48787.66	100.00	100.00		

7.4.11. Encapsulation of (*R*)-8 by host complex 1

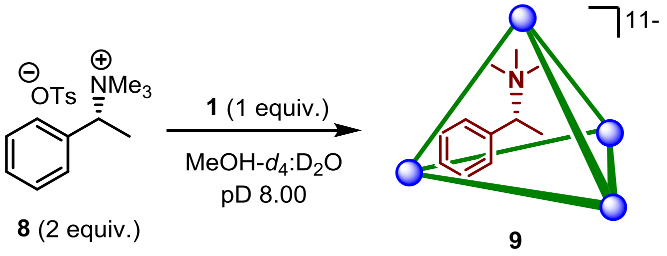

⊖ OTs
⊕ NMe3
8 (2 equiv.)
1 (1 equiv.)
MeOH-d4:D2O
pD 8.00
11-
9

Compound **8** (5.8 mg, 0.016, 2 equiv.) was dissolved in CD_3OD and complex **1** (30 mg, 0.008 mmol, 1 equiv.) was dissolved in D_2O. The two solutions were combined and analyzed by ^1H NMR spectroscopy after 10 min. Spectrum shown below.

^1H NMR spectrum of reaction between **8** and **1** obtained 10 min after mixing

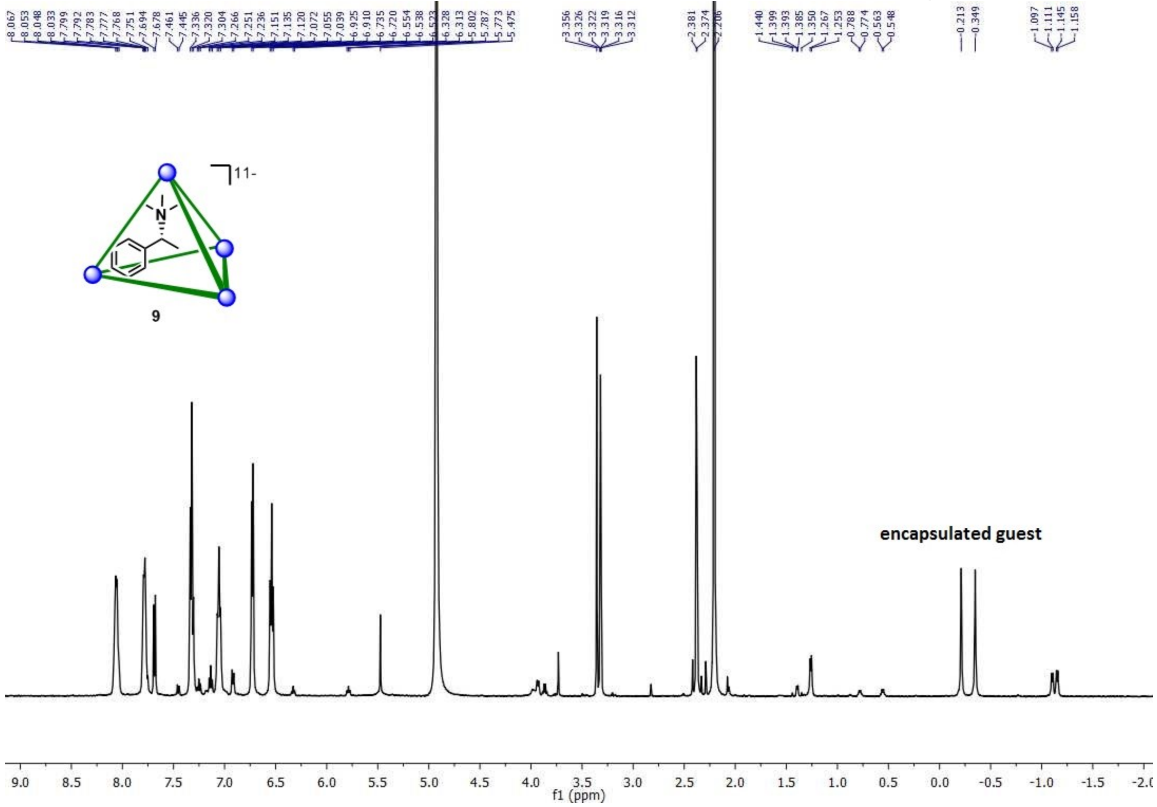

7.5. References

(1) K. P. C. Vollhardt, N. E. Schore, *Organic Chemistry* (W. H. Freeman and Company, New York, ed. 5, 2007) pp. 215-26. [5th edition].
(2) The stereochemistry of solvolysis of certain tertiary alkyl substrates and the secondary *p*-chlorobenzhydryl *p*-nitrobenzoate substrate have been found to be dependent on reaction conditions, and can lead to varying levels of retention or inversion, presumably controlled by ion pair effects. For examples, see references 3 and 4 respectively.
(3) Muller, P.; Rossier, J.-C. *J. Chem. Soc. Perkin Trans. 2* **2000**, 2232-2237.
(4) Goering, H. L.; Levy, J. F. *J. Am. Chem. Soc.* **1964**, *86*, 120-121.
(5) Pronin, S. V.; Reiher, C. A.; Shenvi, R. A. *Nature* **2013**, *503*, 300-300.
(6) Nucleophilic substitution of substrates involving backside participation of an internal group, such as migrating aryl group, the norbornyl systems or α-ferrocenyl moeity, has been observed to give products with varying levels of overall retention of stereochemistry essentially via sequential double inversion. For examples, see references 6-8 respectively.
(7) Singler, R. E.; Cram, D. J. *J. Am. Chem. Soc.* **1972**, *94*, 3512-3520.
(8) García Martínez, A.; Teso Vilar, E.; García Fraile, A.; Martínez-Ruiz, P. *Eur. J. Org. Chem.* **2001**, *2001*, 2805-2808.
(9) Gokel, G. W.; Marquarding, D.; Ugi, I. K. *J. Org. Chem.* **1972**, *37*, 3052-3058.
(10) Rare examples of simple secondary benzylic substrates have been reported to give products with low levels of overall retention of stereochemistry (10-35%), but these measurements were performed using optical rotation techniques which can be imprecise or misleading. For examples, see references 10 and 11.
(11) Okamoto, K.; Hayashi, M.; Shingu, H. *Bull. Chem. Soc. Jpn.,***1966**, *39*, 408-408.
(12) Okamoto, K.; Nitta, I.; Dohi, M.; Shingu, H. *Bull. Chem. Soc. Jpn.,***1971**, *44*, 3220-3220.
(13) For exampls of S_N2 reactions of benzylic substrates with inversion, see reference 13.
(14) A. Streitweiser, *Solvolytic Displacement Reactions*, (McGraw-Hill, New York, ed. 1, 1962).
(15) Substitution reactions proceeding with S_Ni mechanism to give products with overall retention have also been reported. For an example, see reference 16.
(16) Cram, D. J. *J. Am. Chem. Soc.* **1953**, *75*, 332-338.
(17) Breslow, R.; Dong, S. D. *Chem. Rev.* **1998**, *98*, 1997-2011.
(18) Pluth, M. D.; Bergman, R. G.; Raymond, K. N. *Acc. Chem. Res.* **2009**, *42*, 1650-1659.
(19) Yoshizawa, M.; Klosterman, J. K.; Fujita, M. *Angew. Chem., Int. Ed.* **2009**, *48*, 3418-3438.
(20) Avram, L.; Cohen, Y.; Rebek, J., Jr. *Chem. Commun.* **2011**, *47*, 5368-5375.
(21) Wiester, M. J.; Ulmann, P. A.; Mirkin, C. A. *Angew. Chem., Int. Ed.* **2011**, *50*, 114-137.
(22) Oshovsky, G. V.; Reinhoudt, D. N.; Verboom, W. *Angew. Chem., Int. Ed.* **2007**, *46*, 2366-2393.
(23) Sato, S.; Iida, J.; Suzuki, K.; Kawano, M.; Ozeki, T.; Fujita, M. *Science* **2006**, *313*, 1273-1276.
(24) Dong, V. M.; Fiedler, D.; Carl, B.; Bergman, R. G.; Raymond, K. N. *J. Am. Chem. Soc.* **2006**, *128*, 14464-14465.
(25) Hart-Cooper, W. M.; Clary, K. N.; Toste, F. D.; Bergman, R. G.; Raymond, K. N. *J. Am. Chem. Soc.* **2012**, *134*, 17873-17876.
(26) Yoshizawa, M.; Tamura, M.; Fujita, M. *Science* **2006**, *312*, 251-254.
(27) Kuil, M.; Soltner, T.; van Leeuwen, P. W. N. M.; Reek, J. N. H. *J. Am. Chem. Soc.* **2006**, *128*, 11344-11345.

(28) Iwasawa, T.; Hooley, R. J.; Rebek, J., Jr. *Science* **2007**, *317*, 493-496.
(29) Wang, Z. J.; Clary, K. N.; Bergman, R. G.; Raymond, K. N.; Toste, F. D. *Nature Chemistry* **2013**, *5*, 100-103.
(30) Lin, S.; Jacobsen, E. N. *Nature Chemistry* **2012**, *4*, 817-824.
(31) Hamilton, G. L.; Kanai, T.; Toste, F. D. *J. Am. Chem. Soc.* **2008**, *130*, 14984-14986.
(32) Zhao, C.; Sun, Q.-F.; Hart-Cooper, W. M.; DiPasquale, A. G.; Toste, F. D.; Bergman, R. G.; Raymond, K. N. *J. Am. Chem. Soc.* **2013**, *135*, 18802-18805.
(33) Wang, Z. J.; Brown, C. J.; Bergman, R. G.; Raymond, K. N.; Toste, F. D. *J. Am. Chem. Soc.* **2011**, *133*, 7358-7360.
(34) Ma, J. C.; Dougherty, D. A. *Chem. Rev.* **1997**, *97*, 1303-1324.
(35) Mecozzi, S.; West, A. P.; Dougherty, D. A. *J. Am. Chem. Soc.* **1996**, *118*, 2307-2308.
(36) Kovbasyuk, L.; Krämer, R. *Chem. Rev.* **2004**, *104*, 3161-3188.
(37) Tsuzuki, S.; Yoshida, M.; Uchimaru, T.; Mikami, M. *J. Phys. Chem. A* **2001**, *105*, 769-773.
(38) Stauffer, D. A.; Barrans, R. E.; Dougherty, D. A. *Angew. Chem., Int. Ed.* **1990**, *29*, 915-918.
(39) Reaction of racemic substrate 10 in the presence of catalytic amount (10 mol%) of host complex **1**:

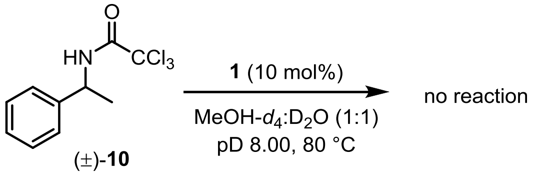

(40) Vanos, C. M.; Lambert, T. H. *Angew. Chem., Int. Ed.* **2011**, *50*, 12222-12226.
(41) Lee, S. H.; Kim, I. S.; Li, Q. R.; Dong, G. R.; Jeong, L. S.; Jung, Y. H. *J. Org. Chem.* **2011**, *76*, 10011-10019.

7.6. Additional Chiral GC Spectra

Reaction from Figure 2A

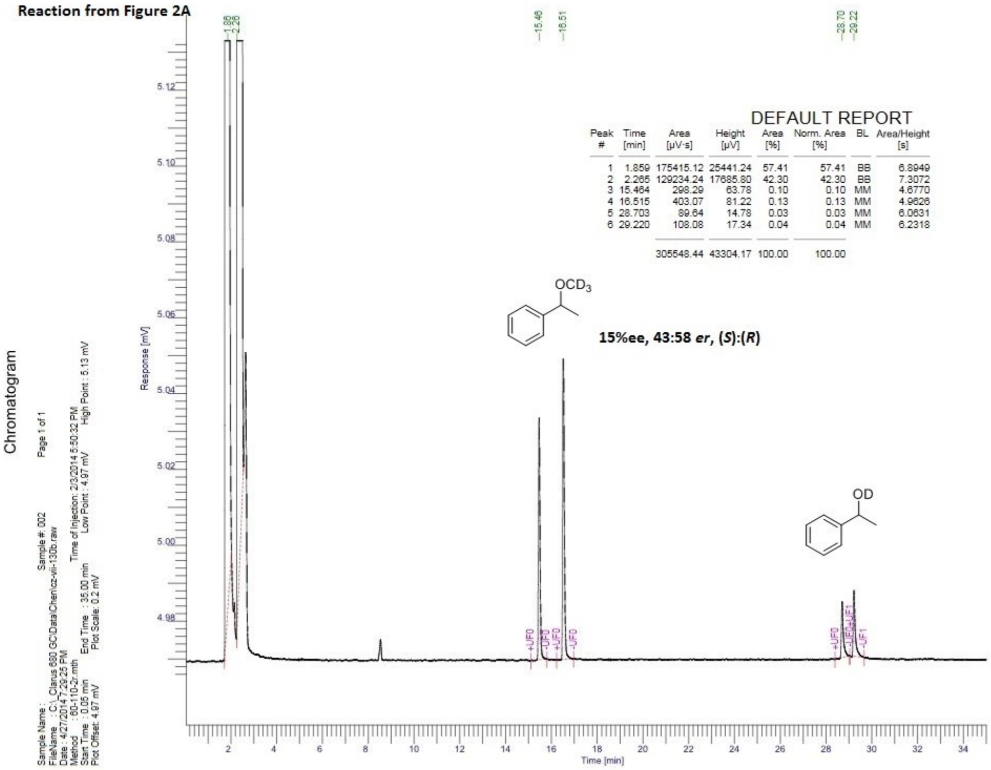

DEFAULT REPORT

Peak #	Time [min]	Area [µV·s]	Height [µV]	Area [%]	Norm. Area [%]	BL	Area/Height [s]
1	1.859	175415.12	25441.24	57.41	57.41	BB	6.8949
2	2.265	129234.24	17685.80	42.30	42.30	BB	7.3072
3	15.464	298.29	63.78	0.10	0.10	MM	4.6770
4	16.515	403.07	81.22	0.13	0.13	MM	4.9626
5	28.703	89.64	14.78	0.03	0.03	MM	6.0631
6	29.220	108.08	17.34	0.04	0.04	MM	6.2318
		305548.44	43304.17	100.00	100.00		

Figure 3A, entry 1

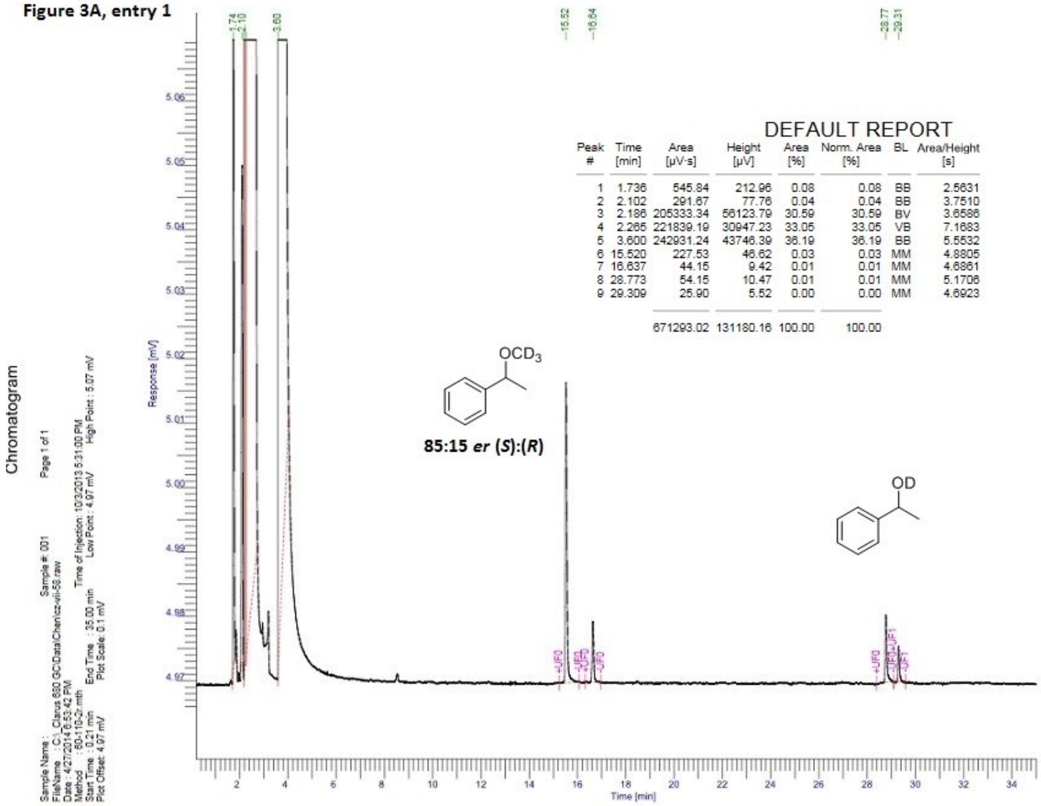

DEFAULT REPORT

Peak #	Time [min]	Area [µV·s]	Height [µV]	Area [%]	Norm. Area [%]	BL	Area/Height [s]
1	1.736	545.84	212.96	0.08	0.08	BB	2.5631
2	2.102	291.67	77.76	0.04	0.04	BB	3.7510
3	2.186	205333.34	56123.79	30.59	30.59	BV	3.6586
4	2.265	221839.19	30947.23	33.05	33.05	VB	7.1683
5	3.600	242931.24	43746.39	36.19	36.19	BB	5.5532
6	15.520	227.53	46.62	0.03	0.03	MM	4.8805
7	16.637	44.15	9.42	0.01	0.01	MM	4.6861
8	28.773	54.15	10.47	0.01	0.01	MM	5.1706
9	29.309	25.90	5.52	0.00	0.00	MM	4.6923
		671293.02	131180.16	100.00	100.00		

Figure 3A, entry 2

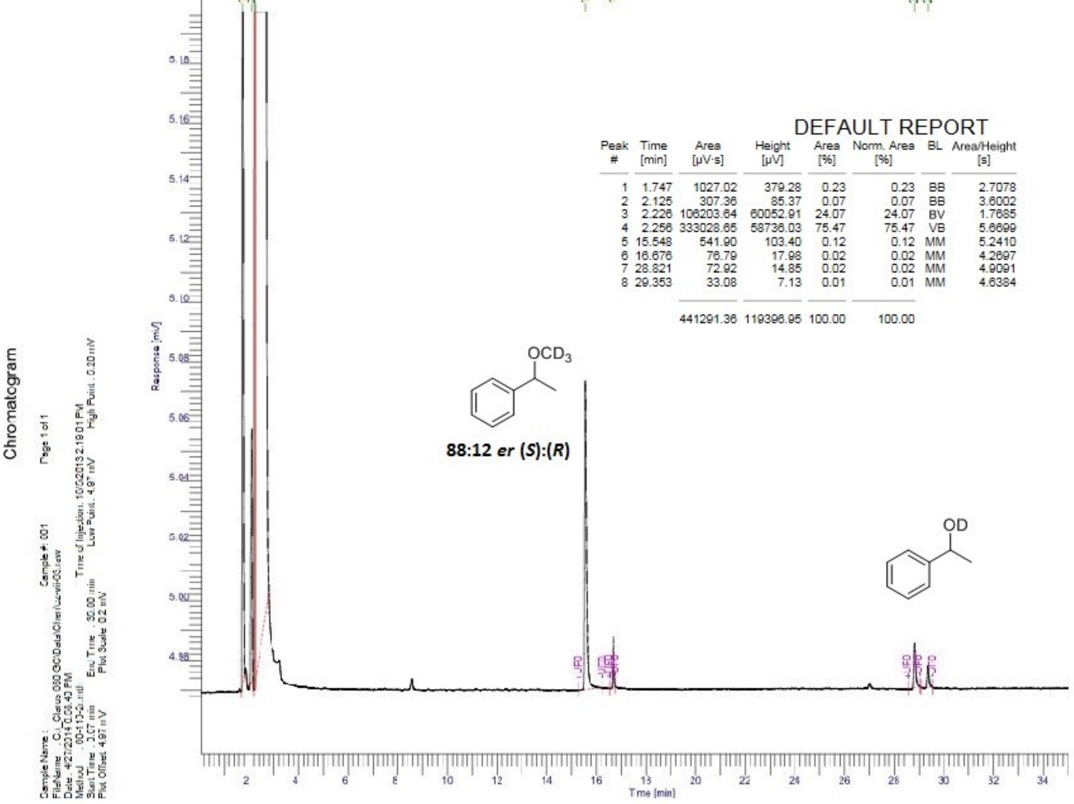

DEFAULT REPORT

Peak #	Time [min]	Area [µV·s]	Height [µV]	Area [%]	Norm. Area [%]	BL	Area/Height [s]
1	1.747	1027.02	379.28	0.23	0.23	BB	2.7078
2	2.125	307.36	85.37	0.07	0.07	BB	3.6002
3	2.226	106203.64	60052.91	24.07	24.07	BV	1.7685
4	2.256	333028.65	58736.03	75.47	75.47	VB	5.6699
5	15.548	541.90	103.40	0.12	0.12	MM	5.2410
6	16.676	76.79	17.98	0.02	0.02	MM	4.2697
7	28.821	72.92	14.85	0.02	0.02	MM	4.9091
8	29.353	33.08	7.13	0.01	0.01	MM	4.6384
		441291.36	119396.95	100.00	100.00		

Figure 3A, entry 6

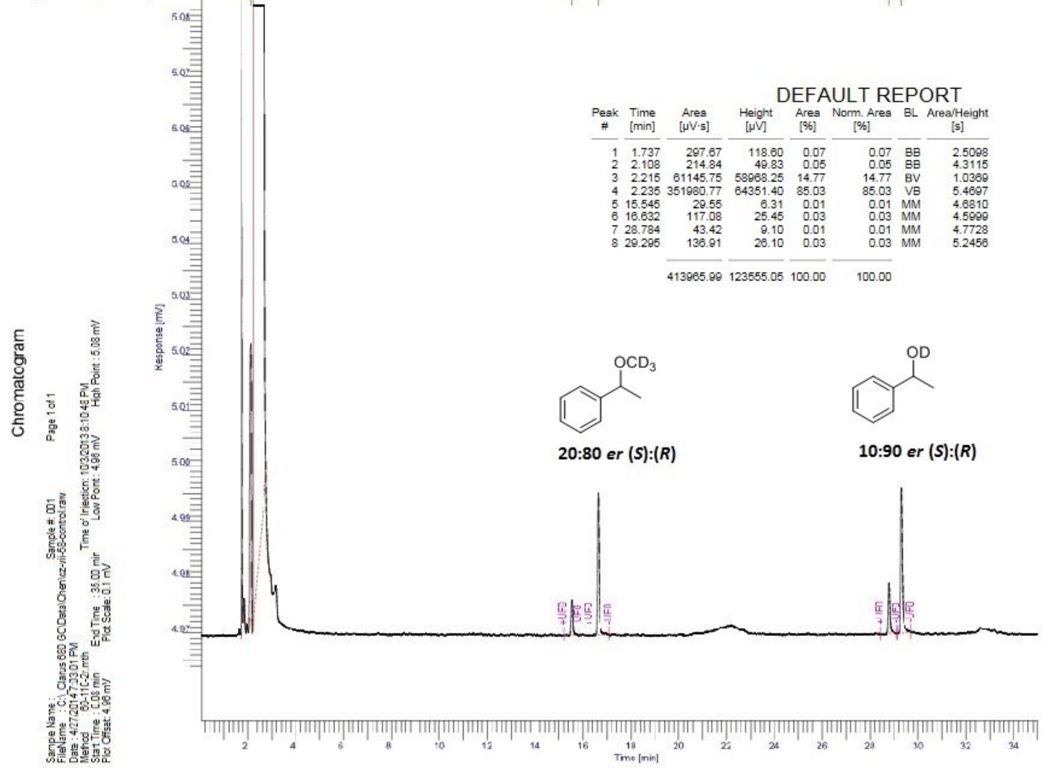

DEFAULT REPORT

Peak #	Time [min]	Area [µV·s]	Height [µV]	Area [%]	Norm. Area [%]	BL	Area/Height [s]
1	1.737	297.67	118.60	0.07	0.07	BB	2.5098
2	2.108	214.84	49.83	0.05	0.05	BB	4.3115
3	2.215	61145.75	58968.25	14.77	14.77	BV	1.0369
4	2.235	351980.77	64351.40	85.03	85.03	VB	5.4697
5	15.545	29.55	6.31	0.01	0.01	MM	4.6810
6	16.632	117.08	25.45	0.03	0.03	MM	4.5999
7	28.784	43.42	9.10	0.01	0.01	MM	4.7728
8	29.295	136.91	26.10	0.03	0.03	MM	5.2456
		413965.99	123555.05	100.00	100.00		

Figure 3B, entry 3

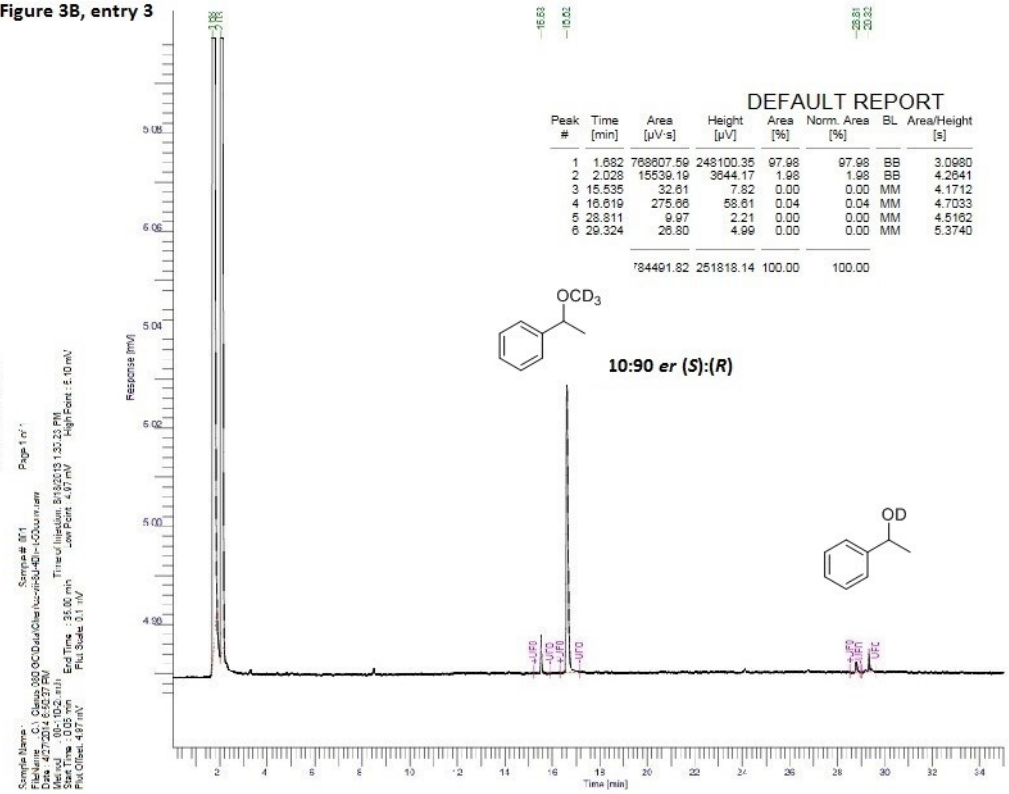

DEFAULT REPORT

Peak #	Time [min]	Area [µV·s]	Height [µV]	Area [%]	Norm. Area [%]	BL	Area/Height [s]
1	1.682	768607.59	248100.35	97.98	97.98	BB	3.0980
2	2.028	15539.19	3644.17	1.98	1.98	BB	4.2641
3	15.535	32.61	7.82	0.00	0.00	MM	4.1712
4	16.619	275.66	58.61	0.04	0.04	MM	4.7033
5	28.811	9.97	2.21	0.00	0.00	MM	4.5162
6	29.324	26.80	4.99	0.00	0.00	MM	5.3740
		784491.82	251818.14	100.00	100.00		

10:90 *er* (*S*):(*R*)

Figure 3B, entry 4

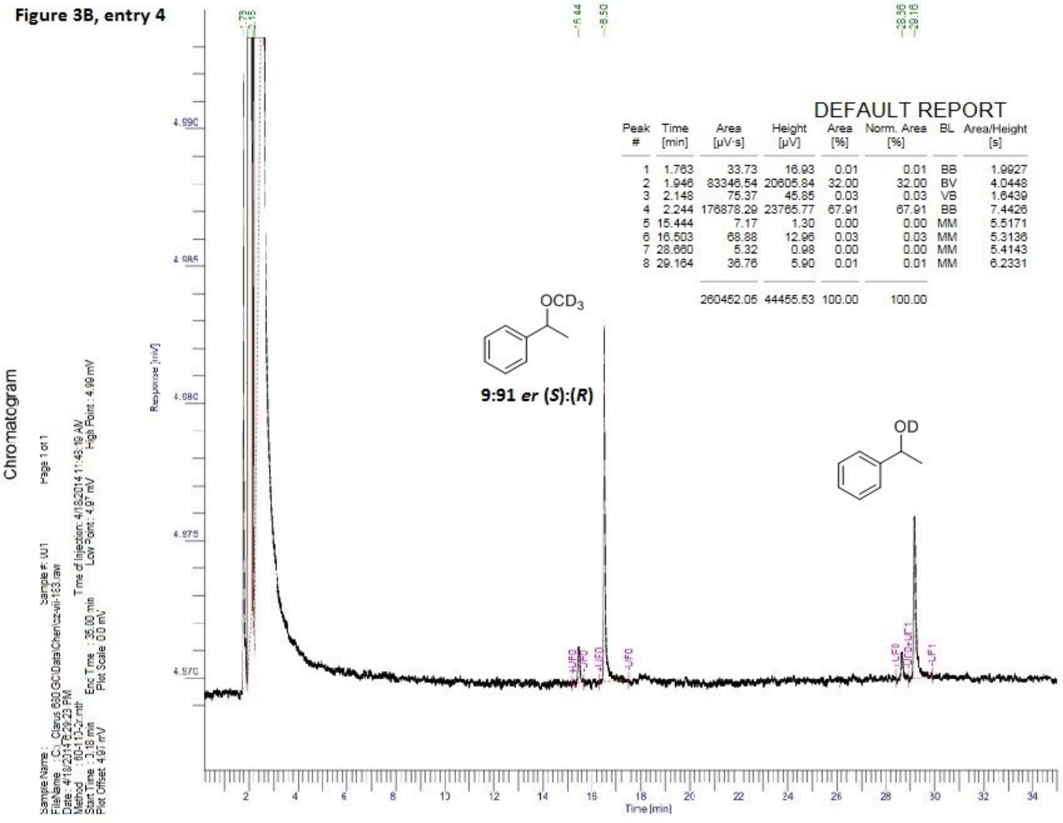

DEFAULT REPORT

Peak #	Time [min]	Area [µV·s]	Height [µV]	Area [%]	Norm. Area [%]	BL	Area/Height [s]
1	1.763	33.73	16.93	0.01	0.01	BB	1.9927
2	1.946	83346.54	20605.84	32.00	32.00	BV	4.0448
3	2.148	75.37	45.85	0.03	0.03	VB	1.6439
4	2.244	176878.29	23765.77	67.91	67.91	BB	7.4426
5	15.444	7.17	1.30	0.00	0.00	MM	5.5171
6	16.503	68.88	12.96	0.03	0.03	MM	5.3136
7	28.660	5.32	0.98	0.00	0.00	MM	5.4143
8	29.164	36.76	5.90	0.01	0.01	MM	6.2331
		260452.05	44455.53	100.00	100.00		

9:91 *er* (*S*):(*R*)

Figure 3B, entry 5

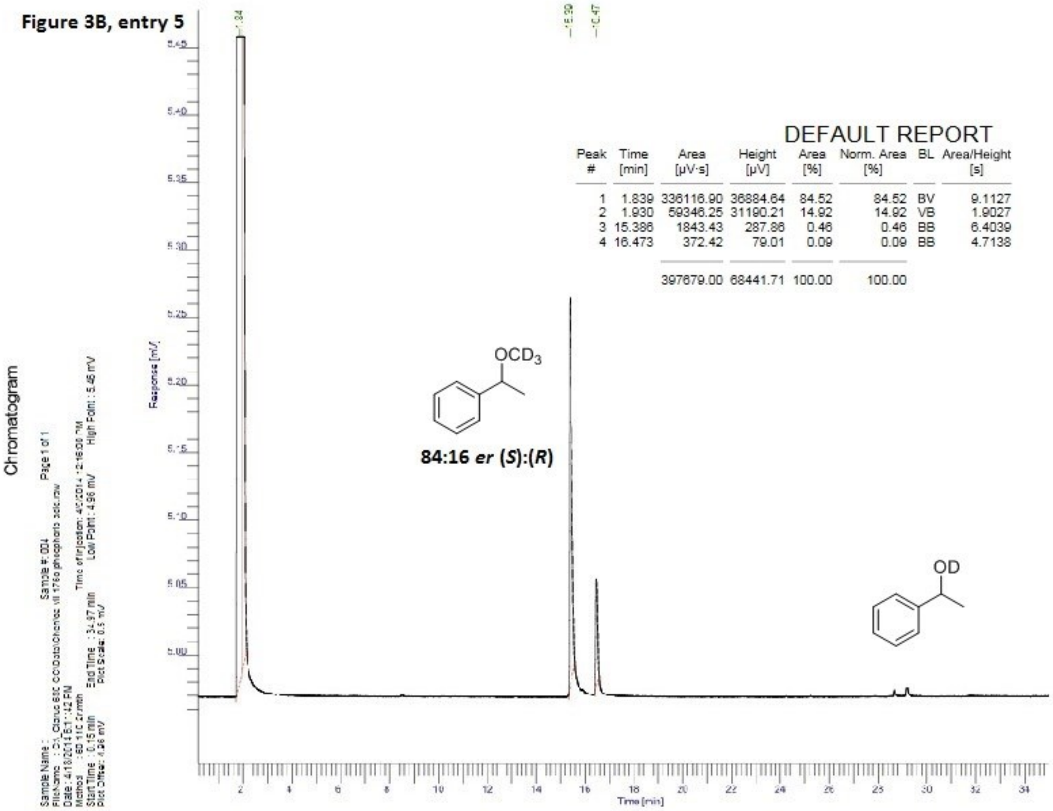

84:16 *er* (*S*):(*R*)

DEFAULT REPORT

Peak #	Time [min]	Area [µV·s]	Height [µV]	Area [%]	Norm. Area [%]	BL	Area/Height [s]
1	1.839	336116.90	36884.64	84.52	84.52	BV	9.1127
2	1.930	59346.25	31190.21	14.92	14.92	VB	1.9027
3	15.386	1843.43	287.86	0.46	0.46	BB	6.4039
4	16.473	372.42	79.01	0.09	0.09	BB	4.7138
		397679.00	68441.71	100.00	100.00		

Figure 4B, entry 3

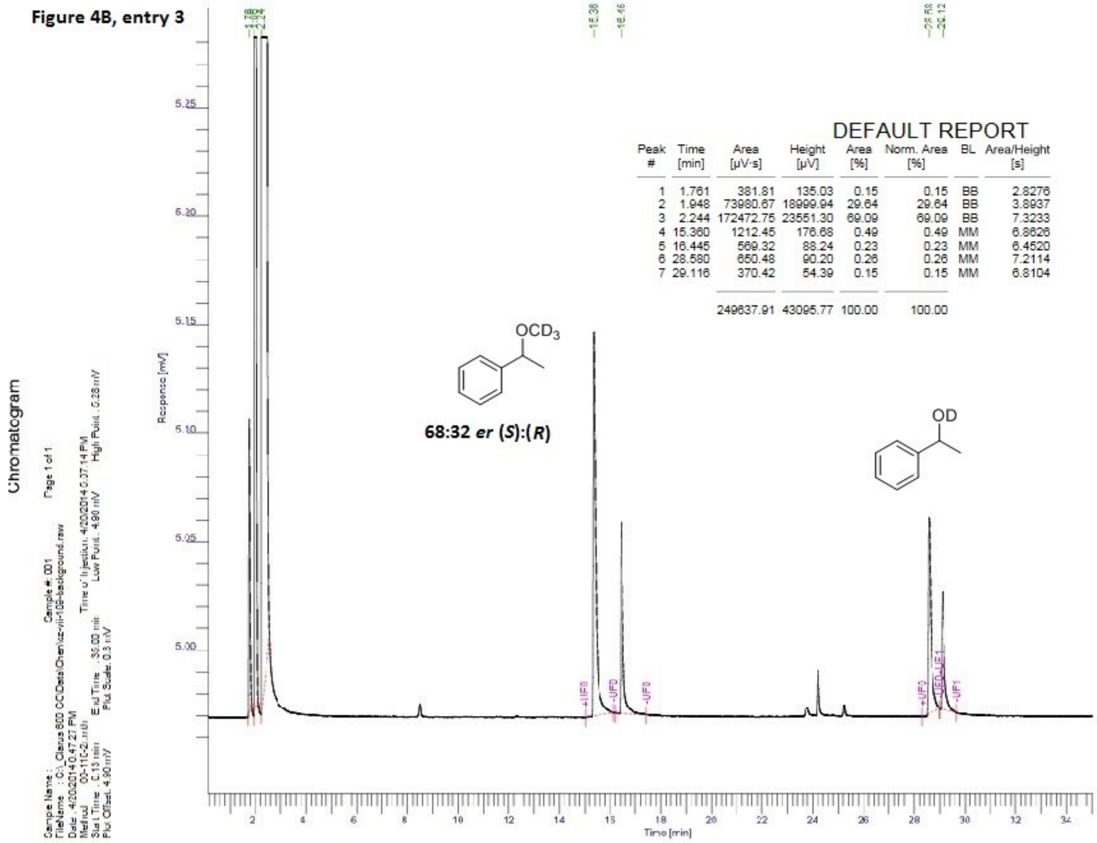

68:32 *er* (*S*):(*R*)

DEFAULT REPORT

Peak #	Time [min]	Area [µV·s]	Height [µV]	Area [%]	Norm. Area [%]	BL	Area/Height [s]
1	1.761	381.81	135.03	0.15	0.15	BB	2.8276
2	1.948	73980.67	18999.94	29.64	29.64	BB	3.8937
3	2.244	172472.75	23551.30	69.09	69.09	BB	7.3233
4	15.360	1212.45	176.68	0.49	0.49	MM	6.8626
5	16.445	569.32	88.24	0.23	0.23	MM	6.4520
6	28.580	650.48	90.20	0.26	0.26	MM	7.2114
7	29.116	370.42	54.39	0.15	0.15	MM	6.8104
		249637.91	43095.77	100.00	100.00		